

Design and synthesis of anti-tumour agents targeting Sulf2 and MDMX:p53

Annalisa Bertoli

School of Chemistry

This thesis is submitted to Newcastle University
for the degree of Doctor of Philosophy

February 2015

DECLARATION

The work described in this thesis was carried out from October 2010 to September 2014 at the Northern Institute for Cancer Research (Newcastle upon Tyne) either in the Medicinal Chemistry Laboratories (Bedson Building, School of Chemistry, Newcastle University, Newcastle upon Tyne, NE1 7RU) or in the Cancer Structural Biology Laboratories (Paul O’Gorman Building, Newcastle University, Newcastle upon Tyne, NE2 4HH).

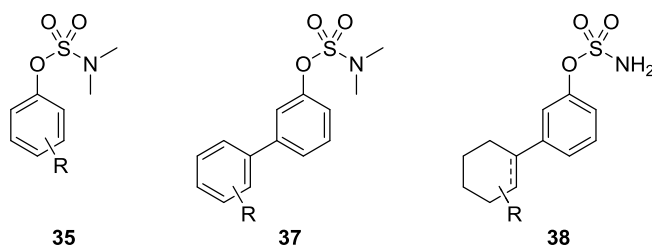
All the research described in this thesis is original and does not include any material or ideas previously presented by other authors, except where acknowledged by reference.

No part of this thesis is being, or has been previously, submitted for a degree, diploma or any qualification at any other university.

ABSTRACT

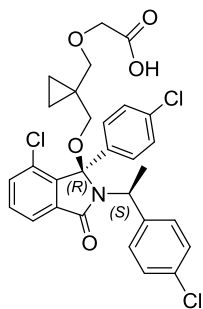
Replacement of standard chemotherapy with targeted therapy for the cure of cancer would be a desirable way to improve treatment, especially for those tumors with low survival rates, giving patients longer life expectancy and better quality of life with a reduction of the severity of side effects. Progress in the fields of genomics and proteomics and increased understanding of the mechanisms leading to cancer have allowed many potential biological targets to be identified for therapeutic intervention. The projects described herein aim to identify small molecules that interact with proteins that are relevant in pathways related to either uncontrolled proliferation or evasion of apoptosis in tumor cells.

Endosulfatases Sulf1 and Sulf2 are located in the extracellular matrix and the cell surface. They modify the sulfation state of heparan sulfate proteoglycans, which affect a number of cellular signaling events, ultimately resulting in proliferation and cell growth. Although there is evidence of the involvement of Sulf1 and Sulf2 in cancer processes, their action is not clearly understood. Therefore, the development of potent (low micromolar range) inhibitors of these endosulfatases is desirable for target validation and hit discovery purposes. Published experimental evidence suggests that sulfatases have some degree of arylsulfatase activity and that sulfamates are often efficacious for the inhibition of this enzyme class. Therefore, a range of aromatic-based tertiary (**35** and **37**) and primary (**38**) sulfamates were synthesized and tested in a biochemical assay against Sulf2 and counter-screened against ARSA and ARSB.



The tumor suppressor p53 is a transcription factor activating a number of genes responsible for cell growth arrest, senescence and apoptosis. Tumor cells evade apoptosis and proliferate by subverting the p53 pathway, either by mutation of the *TP53* gene, resulting in the expression of inactive p53 (50% of cancers), or through amplification or overexpression of proteins responsible for p53 regulation, most notably MDM2 and MDMX. As such, modulators of the interaction of MDM2 and MDMX with p53 are of potential interest as antitumor agents and are being actively pursued by many research groups.

More recently, evidence that MDMX provides a mechanism of resistance when inhibiting the MDM2:p53 interaction has focused efforts towards dual MDM2/MDMX:p53 inhibitors. Surprisingly, even though MDM2 and MDMX have a high sequence homology within the p53 binding domain (>53%), most of the small molecules designed to bind MDM2 show much lower binding affinity towards MDMX. Arising from a project aimed at developing inhibitors of the MDM2:p53 interaction, a small panel of isoindolinones showed low micromolar activity when counterscreened against MDMX. One of these compounds, **153**, containing two stereogenic centres, was utilized as the starting point for further structure-activity relationships, SAR, investigation to identify either dual inhibitors of the MDM2/MDMX:p53 or selective MDMX:p53 antagonists.



153

MDMX IC₅₀ = 16.65 μ M

MDM2 IC₅₀ = 0.0357 μ M

ACKNOWLEDGMENTS

First and foremost I would like to thank my main supervisor Prof. Roger Griffin for allowing me to join his research group and for offering me support and guidance, in science and in life, throughout my PhD. I also thank all the members of the supervisory team Prof. Bernard Golding, Dr. Ian Hardcastle and Dr. Céline Cano for helpful discussion, expertise and support.

I am extremely grateful to Cancer Research UK for funding me, my research and my professional growth over the last four years.

I thank also Prof. Herbie Newell, Prof. Steve Wedge, Prof. John Lunec and Dr. Philip Elstob. Many thanks to Prof. Martin Noble and Prof. Jane Endicott, who allowed me to do a placement in their Structural Biology group.

I would like to acknowledge Astex Pharmaceuticals (Cambridge, UK) for their support in the MDMX project, especially Dr. Pamela Williams for providing the p53₁₇₋₂₇ peptide. Many thanks also to Prof. David Lane (A*STAR Lab, Singapore) for providing the p53^{N30F}₁₇₋₃₀ peptide.

I would like to thank Dr. Ross Harrington and Dr. Ulrich Baisch of the Crystallography Service of the School of Chemistry at Newcastle University for the small molecule crystal structures and the EPSRC National Mass Spectrometry Service Centre at Swansea University for the HR-MS data.

My gratitude goes to the bio-scientists who worked on the Sulf2 project, Dr. Gary Beale and Dr. Sari Alhasan. Also, many thanks to the bio-scientists participating to the MDMX project: Dr. Yan Zhao for the ELISA data, Dr. Claire Jennings for being a wonderful teacher, Dr. Judith Reeks for offering her expertise in crystallography (for harvesting the crystals, solving and refining the co-crystal structure and for providing an extra batch of MDM2^{E69K70A}₁₇₋₁₀₈). Thanks also to all the members of the Structural Biology Laboratories who made my last months in the lab so enjoyable: Dr. Richard Heath, Dr. Mathew Martin, Dr. Julie Tucker, Dr. Martyna Pastok, Dr. Will Stanley, Dr. Martin Day, Svitlana Korolchuk, Bailey Massa, Judith Unterlass, Stephen Hallett. I thank Dr. Arnaud Baslé of the Institute for Cell and Molecular Biosciences at Newcastle

University for introducing me to the art of crystallization and related equipment.

I feel very lucky for having been part of two very different but equally wonderful teams. Thanks to the members of the Sulf2 team: Dr. Duncan Miller, for teaching me a lot about chemistry and for being ready to help at all circumstances, and Tristan Reuillon, for expert advice in chemistry and for his sense of humor. Many thanks also to my MDMX colleagues, Andrew Shouksmith for bearing with my singing in the lab and Santosh Adhikari for the science chats on the way to uni and for personal support in dark times.

My gratitude goes also to all the other members, past and present, of the Medicinal Chemistry Laboratories: Honorine Lebraud, Nick Martin, Bian Zhang, James Pickles, Elena Costa, Dr. Sarah Cully, Dr. Lauren Molyneux, Dr. David Turner, Dr. Suzannah Harnor, Dr. Stephen Hobson, Dr. Elisa Meschini, Dr. Stephanie Myers, Dr. Ruth Bawn, Dr. Benoit Carbain, Dr. Kate Smith and Dr. Timothy Blackburn. Many thanks to Dr. Karen Haggerty for HPLC analysis and purification, to Carlo Bawn for special NMR experiments and to Amy Heptinstall for her help, patience and expertise in the lab.

I am very grateful to all the friends who I got close to during my stay in Newcastle: Claudia, Alex, Honorine, Regina, Nicole, Stefania, Idria, Alina, Denise, Hilaire, Manu and Helen. Thanks to the Italians in Newcastle for the taste of Italy I could savor at each of our meetings. And I would not have gone far without the love of my friends from home. Fiora, Caterina, Chiara, Angelo, Fra, Zacchi, Erika and Elisa, despite the distance and the big changes in our lives, the bond we have stays the same. Thanks to Akis, who suddenly entered my life, made me smile again and supported me through the final stage of my PhD.

My final and most important acknowledgment goes to my family: my dad, my brother Marco and, especially, my mum. Thank you for always being there for me, since my very first moment in this world, and thank you for your unconditional love. I would have not arrived here without your support.

I dedicate this thesis to two women who strongly inspired me: nonna Leonilde and nonna Gioconda.

ABBREVIATIONS

2,4-DNP	2,4-Dinitrophenylhydrazine
4-MU	4-Methylumbelliferone
4-MUS	4-Methylumbelliferone sulfate
ARSA	Aryl Sulfatase A
ARSB	Aryl Sulfatase B
ARSC	Aryl Sulfatase C
ARSD	Aryl Sulfatase D
ARSE	Aryl Sulfatase E
ARSF	Aryl Sulfatase F
ARSG	Aryl Sulfatase G
ATM	Ataxia telangiectasia mutated
ATR	Anthrax toxine receptor
Cat Dom	Catalytic domain
CML	Chronic myelogenous leukemia
CT	C-terminal
DCE	1,2-Dichloroethane
DCM	Dichloromethane
DMA	Dimethylacetamide
DMB	Dimethoxybenzyl
DME	1,2-Dimethoxyethane
DMF	Dimethylformamide
DMSO	Dimethyl sulfoxide
DSF	Differential scanning fluorimetry
DTT	Dithiothreitol
ECM	Extra-cellular matrix
ELISA	Enzyme linked immunosorbent assay
ELSD	Evaporative light scattering detector

(ES⁺)	Electron spray positive mode
(ES⁻)	Electron spray negative mode
equiv.	Number of molar equivalents
FG	Formylglycine
FGE	Formylglycine-generating enzyme
FGF	Fibroblast growth factor
FPLC	Fast protein liquid chromatography
FRET	Fluorescence resonance energy transfer
FTIR	Fourier transform infrared
GAG	Glycosaminoglycan
GlcA	D-Glucuronic acid
GlcN	D-Glucosamine
GlcNAc	<i>N</i> -Acetylglucosamine
GlcNS6S	<i>N</i> -sulfate-glucosamine 6- <i>O</i> -sulfate
GPC3	Glypican 3
GST	Glutathione <i>S</i> -transferase
HB-GF	Heparin-bound growth factor
HCC	Hepatocellular cancer
HEPES	<i>N</i> -2-Hydroxyethylpiperazine- <i>N'</i> -2-ethanesulfonic acid
HFG	Hydroxyformylglycine
HGF	Hepatocellular growth factor
HPLC	High performance liquid chromatography
HRMS	High-resolution mass spectrometry
HRP	Horseradish peroxidase
HS	Heparan sulfate
HSPG	Heparan sulfate proteoglycan
HTRF	Homogenous time-resolved fluorescence
IdoA	L-Iduronic acid
IdoA2S	L-Iduronic acid 2- <i>O</i> -sulfate
IPTG	Isopropyl β -D-1-thiogalactopyranoside

LC-MS	Liquid chromatography-mass spectrometry
LE	Ligand efficiency
μW	Microwave
MAPK	Mitogen-activated protein kinase
MDM2	Murine double minute 2
MDMX	Murine double minute X
MeOH	Methanol
mHBS	Modified HEPES-buffered saline
MIDA	<i>N</i> -Methyliminodiacetic acid
MOMP	Mitochondrial outer membrane permeabilization
MPLC	Medium pressure liquid chromatography
m.p.	Melting point
MS	Mass spectrometry
LB	Luria-Bertani broth
OD	Optical density
ν_{\max}	Maximum vibrational frequency
N/A	Not available
NaHMDS	Sodium bis(trimethylsilyl)amide
NES	Nuclear exclusion signal
NLS	Nuclear localization signal
PAPS	3'-Phosphoadenosine 5'-phosphosulfate
PDA	Photodiode array
PPI	Protein-protein interaction
Py	Pyridine
RING	Really interesting new gene
RT	Room temperature

R_t	Retention time (HPLC)
SAR	Structure-activity relationship
SDS-PAGE	Dodecyl sulfate polyacrylamide gel electrophoresis
SLC	Secondary lymphoid tissue chemokine
STS	Steroid sulfatase
SULT	Sulfotransferase
TAD	Transactivation domain
TB	Terrific broth
TFA	Trifluoroacetic acid
THF	Tetrahydrofuran
TIPS	Triisopropylsilyl ether
TLC	Thin Layer Chromatography
TMSOTf	Trimethylsilyl trifluoromethanesulfonate
UPLC	Ultra-Performance Liquid Chromatography
v/v	Volume for volume
VEGF	Vascular endothelial growth factor

Contents

Declaration.....	ii
Abstract.....	iii
Acknowledgments	v
Abbreviations	vii
Chapter 1. Targeted cancer therapy and drug discovery	1
1.1 Cancer.....	1
1.2 Key steps in cancer pathogenesis	2
1.3 Cancer treatment.....	5
1.4 The stages of drug discovery	7
Chapter 2. Introduction to Sulf2.....	10
2.1 Sulfatases.....	10
2.2 The importance of sulfation.....	17
2.3 Steroid sulfatase inhibitors	18
2.4 Human endosulfatases (Sulf1 and Sulf2).....	20
2.4.1 Heparan sulfate: the endogenous substrate of Sulf enzymes	23
2.4.2 Proposed model for the action of Sulf1 and Sulf2	25
2.4.3 Endosulfatases and their role in signaling pathways	26
2.5 The role of Sulf1 and Sulf2 in cancer	29
2.6 Targeting Sulf1 and Sulf2 with small-molecule inhibitors	30
2.7 Project aims and design of potential novel inhibitors	33
Chapter 3. Results and discussion - Sulf2	35
3.1 Synthesis of <i>N,N</i> -dimethylsulfamates	35
3.1.1 Synthesis of a library of phenyl <i>N,N</i> -dimethylsulfamates	35
3.1.2 Attempted synthesis of a library of benzyl <i>N,N</i> - dimethylsulfamates.....	38

3.1.3	Synthesis of a library of biphenyl <i>N,N</i> -dimethylsulfamates	39
3.2	Stability studies on sample <i>N,N</i> -dimethyl sulfamates and sulfates ...	49
3.2.1	Stability of 4-(trifluoromethyl)phenyl dimethylsulfamate 51	49
3.2.2	Stability of <i>N,N</i> -dimethyl sulfamates in DMSO and MeOH	50
3.3	Suzuki-Miyaura cross-coupling of unprotected primary sulfamates	50
3.4	Synthesis of cyclohexylphenyl primary sulfamate mimics of heparan sulfate	54
3.4.1	Synthesis of the boronic esters 97 and 101	55
3.4.2	Attempted synthesis of 91 and 92 in the presence of an unprotected primary sulfamate moiety	56
3.4.3	Sulfamate-protecting strategy applied to the synthesis of 91 , 92 and 93	59
3.5	Conclusions.....	68
Chapter 4.	Summary of the biological results obtained for Sulf2 potential chemical tools	70
4.1	Activity of the synthesized sulfamates against Sulf2, ARSA and ARSB	70
4.2	Activities of a library of sulfamates against Sulf2.....	71
4.2.1	The monocyclic substituted phenyl sulfamate series.....	71
4.2.2	The substituted biphenyl sulfamate series	71
4.2.3	Compounds with a non-aromatic B-ring	72
4.3	Activities of a library of sulfamates against ARSA and ARSB.....	73
4.3.1	The monocyclic substituted phenyl sulfamate series.....	74
4.3.2	The substituted biphenyl sulfamate series	75
4.3.3	Compounds with a non-aromatic B-ring	76
4.4	Conclusions.....	77
Chapter 5.	Introduction to MDMX	78

5.1	p53, MDM2, and MDMX	78
5.1.1	The p53 tumor suppressor.....	78
5.1.2	MDM2 and MDMX.....	81
5.1.3	Cellular levels of p53 are finely tuned	87
5.2	MDMX as a target for cancer therapy	90
5.3	Protein-protein interaction inhibition.....	93
5.4	Overview of small-molecule MDMX inhibitors.....	95
5.5	Structural data on MDMX.....	97
5.6	The isoindolinone series and its potential for inhibition of MDMX...99	
5.7	Project aims and design of selective MDMX inhibitors	102
Chapter 6.	Results and discussion - MDMX.....	105
6.1	Sequential chlorine deletion.....	105
6.1.1	Rationale for the targets.....	105
6.1.2	Synthetic route to the targets.....	105
6.1.3	Determination of the absolute configuration at the isoindolinone stereocentre	109
6.1.4	Biological evaluation.....	114
6.2	Sequential chlorine deletion from 159	118
6.3	Structural minimization of the core structure.....	118
6.3.1	Biological evaluation.....	120
6.4	Variations at the 3-position.....	121
6.4.1	Removal of the side chain	121
6.4.2	Removal of the cyclopropyl motif.....	121
6.4.3	Biological evaluation.....	122
6.5	Structural minimization at the 2-position.....	124
6.5.1	Biological evaluation.....	125

6.6	Introduction of a range of substituents at the 4-benzyl position....	126
6.7	Introduction of a 5-hydroxyisoxazole moiety.....	129
6.8	Introduction of nitrogen containing heteroaromatics at the 7-position	134
6.8.1	Biological evaluation.....	137
6.9	Conclusions.....	139
Chapter 7.	Structural biology investigations with MDMX and MDM2	141
7.1	Aims.....	141
7.2	Protein crystallography and its challenges.....	141
7.2.1	Selection of protein constructs for crystallization trials	143
7.2.2	Expression and purification.....	144
7.2.3	Crystallization trials.....	147
7.2.4	Crystal formation and data collection.....	149
7.2.5	Highlights of the X-ray structure of 159 bound to MDM2	151
7.3	HTRF Assay.....	155
7.4	Differential scanning fluorimetry (DSF)	159
7.5	Conclusions drawn from the structural biology studies on MDMX	161
Chapter 8.	Conclusions	166
8.1	The Sulf2 project	166
8.2	The MDMX:p53 protein-protein interaction project.....	168
Chapter 9.	Experimental	172
9.1	Summary of generic synthetic, analytical and chromatographic conditions.....	172
9.1.1	Chemicals and solvents.....	172
9.1.2	Synthesis.....	172
9.1.3	Chromatography	172

9.1.4	Analytical techniques	173
9.2	Sulf2 project experimental procedures.....	174
9.2.1	Sulfatase Biological Assay Protocols	174
9.2.2	General synthetic procedures	175
9.2.3	Sulf2 project - Synthesized compounds	179
9.3	MDMX project experimental procedures.....	238
9.3.1	MDMX and MDM2 biological assay protocols.....	238
9.3.2	General synthetic procedures	240
9.3.3	MDMX project - Synthesized compounds.....	243
9.4	Structural biology experimental	345
9.4.1	General procedures.....	345
9.4.2	Expression from MDMX and MDM2 gene constructs	346
9.4.3	Protein purification.....	347
9.4.4	Protein preparation for crystallography.....	348
9.4.5	HTRF assay	348
9.4.6	Differential scanning fluorimetry (DSF)	349
	Appendices	351
	Appendix A - Small molecule crystal structures.....	351
	Appendix B - Crystallization conditions giving crystals.....	353
	Appendix C - Construct sequences.....	353
	References.....	357

CHAPTER 1. TARGETED CANCER THERAPY AND DRUG DISCOVERY

1.1 Cancer

There are more than two hundred disease forms that are designated as 'cancer', affecting organs or tissues in the body.¹ All are characterized by several common features, such as uncontrolled cellular replication and irregular growth with respect to normal tissues. At later stages, metastasis, the outspread and invasion of other tissues distinct from the primary site, is often observed and represents a leading cause of death from the disease.² In 2012 approximately 14.1 million cancers were diagnosed worldwide³⁻⁴ and, in the same year, it was estimated that 8.2 million people died as a consequence of the condition. According to projections, by 2030 the number of new cases worldwide will reach 20.3 million and the number of deaths will escalate to 13.2 million, with a steep rise in developing countries driven by changes in lifestyle and increasing industrialization.⁵ In the United Kingdom, cancer is the leading cause of death, mainly as a result of the increase in life expectancy observed in the last decades.⁶ Incidence rates have risen over the last four decades (Figure 1.1) and in 2011 331,487⁷ people were diagnosed with cancer in the UK, while 159,178 died as a consequence of the disease.

Primary factors triggering the development of neoplasms are genetic predisposition, a number of infectious agents, such as viruses (*e.g.* Human Papilloma Virus), occupational exposures to carcinogens, age and lifestyle. In this regard, it has been suggested that a lack of exercise, obesity, alcohol consumption, smoking and excessive exposure to UV radiation may be responsible for up to 42% of all cases.⁷ Cancer research is currently among the most prolific fields in scientific disciplines as the achievement of both a thorough understanding of the disease and more effective and safer treatments are required.

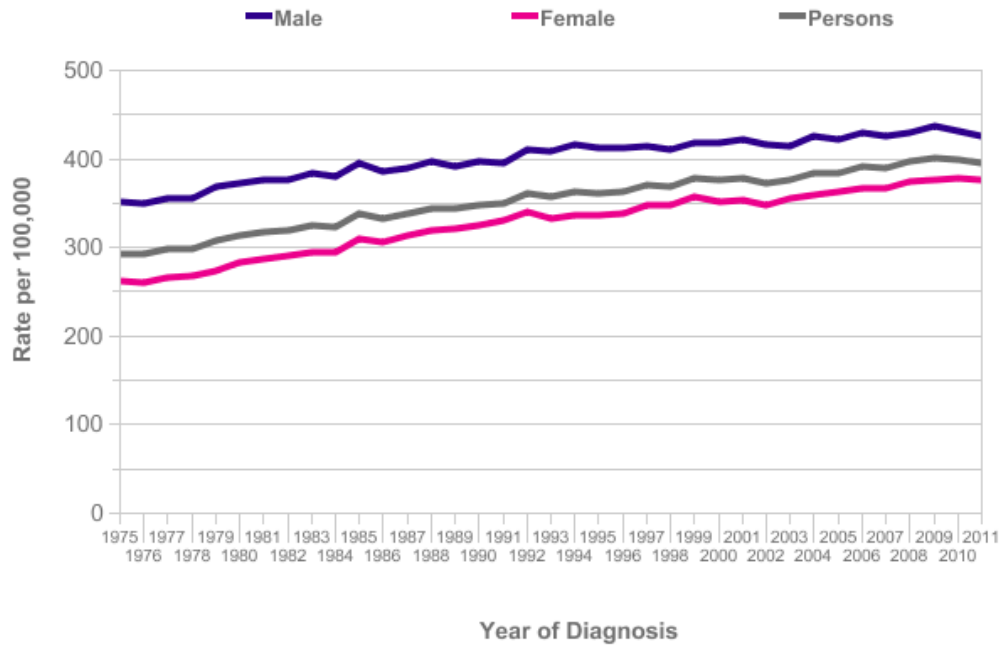


Figure 1.1 - European age-standardized incidence rates per 100,000 population, by sex, Great Britain (1975-2011).
 Reproduced from Cancer Research UK.⁷

1.2 Key steps in cancer pathogenesis

In 2000, Hanahan and Weinberg⁸ described the ‘hallmarks’ of cancer, a set of acquired features that allow the gradual evolution of normal cells to the most aggressive form of malignant tumor. In their review, they identified six characteristics acquired by cancer cells (Figure 1.2):

1. *Self-sufficiency in growth signals*: unlike normal cells, whose replication is activated by external signaling events, cancer cells may develop the ability to mimic those signals themselves.
2. *Insensitivity to antigrowth signals*: in addition to low stimulation by growth inducers, normal cells are kept in a quiescent state by the release of antiproliferative signals that tumor cells are able to avoid.
3. *Evasion of apoptosis*: programmed cell death is one of the tools used to limit the progression of neoplasms. Under physiological stress conditions, such as those found in the tumor environment, pathways leading to apoptosis should be activated but are evaded by cancer cells.

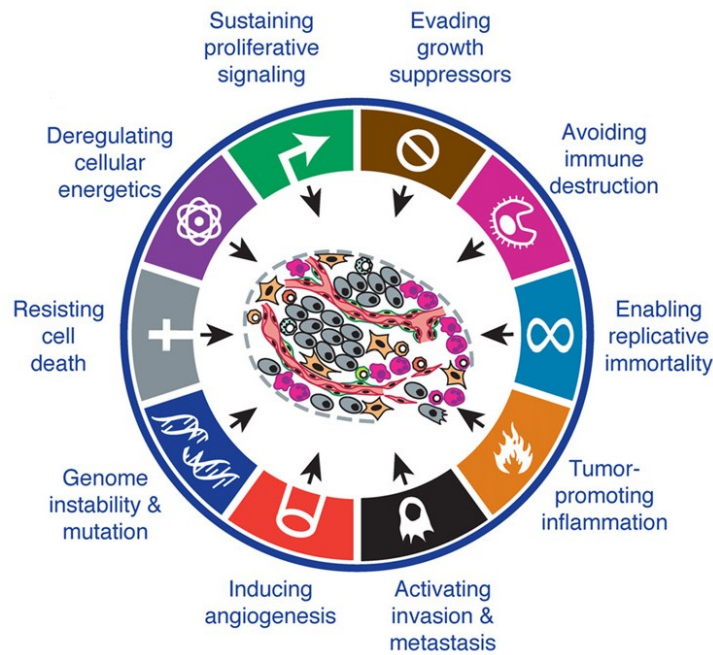


Figure 1.2 - The hallmarks of cancer.

Reproduced from Hanahan, 2011.⁹

4. *Limitless replicative potential*: normal cells are able to replicate only a limited number of times, proportional to the length of the telomeres, hexanucleotide TTAGGG repetitive units found at the end of chromosomes. To become immortalized, tumor cells overexpress the enzyme telomerase or activate an alternative lengthening of telomeres (ALT) mechanism to elongate telomere units at the end of DNA strands.
5. *Sustained angiogenesis*: tumors require a blood supply to provide oxygen and nutrients and to allow the discharge of carbon dioxide and other wastes produced during the metabolic cycle. To satisfy these requirements, tumor cells induce new blood vessels to grow from the existing quiescent ones after activation of an 'angiogenic switch'. Angiogenesis, the formation of new blood vessels, is regulated by several factors having either a positive (*e.g.* vascular endothelial growth factor-A, VEGF-A; acidic and basic fibroblast growth factors, FGF 1/2) or negative (*e.g.* thrombospondin-1, TSP-1) effect on the development of new vessels.
6. *Invasion and metastasis*: these represent the stepwise process by which tumors spread into the body and originate secondary neoplasms. Starting from the localized invasion of neighbouring tissues, malignant cells

propagate through the circulatory and lymphatic systems and form micrometastatic outgrowths that ultimately lead to the formation of secondary tumors in other organs.

In a more recent review,⁹ Hanahan and Weinberg identified two new hallmarks to be added to the six previously described (Figure 1.2):

1. *Reprogramming energy metabolism*: cancer cells undergo a metabolic switch and provide themselves with energy through alternative pathways that are not yet completely understood.
2. *Evading immune destruction*: a well-functioning immune system should detect and destroy tumors at an early stage of development and the reasons why this does not always happen are still to be elucidated.

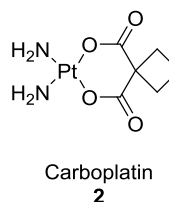
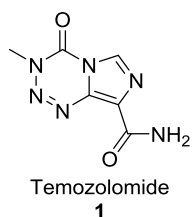
Two new features, or 'enabling characteristics', that allow tumor cells to acquire the aforementioned set of capabilities (Figure 1.2) were also introduced:

1. *Genome instability and mutation*: to acquire the hallmarks of cancer, cells need to accumulate a number of mutations. This is made possible by cell sensitization to carcinogens, impairment of DNA repair pathways and breakdown of the tumor suppressor mechanisms that should trigger senescence or apoptosis to prevent propagation of damaged DNA. This may lead to acquisition of hyper-mutated phenotypes which allow mutations conferring other hallmarks to be accumulated more rapidly.
2. *Tumor-promoting inflammation*: it has been recently found that tumor-related inflammation processes can play a role in fostering tumor progression. It has become clear that growth and proangiogenic factors, as well as other bioactive molecules, are provided to the tumor microenvironment as a consequence of the inflammatory state, thus contributing to the expansion of the malignancy. Further mutation of neoplastic cells can also be promoted by reactive oxygen species or other chemicals produced by inflammatory cells.

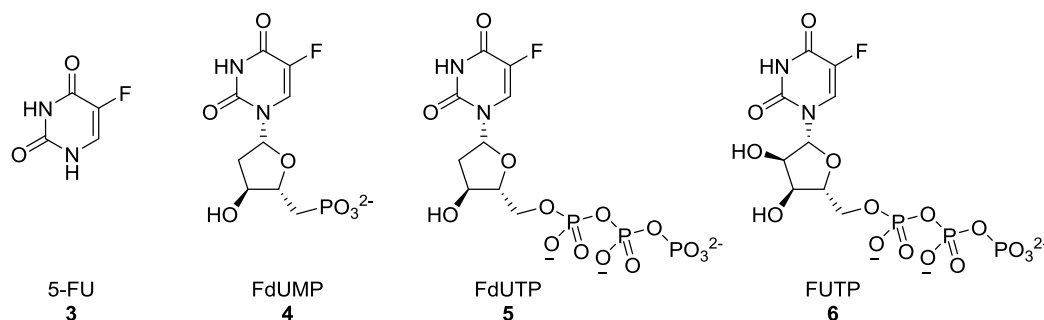
1.3 Cancer treatment

The first written record of cancer dates back 5000 years in ancient Egypt. Hippocrates (460-370 BC) in Greece and the Roman Celsus (50-28 BC), described tumors using the word 'crab', *carcinos* and *cancer* in ancient Greek and Latin, respectively. Later, Galen (130-200 AD), another Roman physician, referred to cancer with the Latin word for 'swelling', *oncos*, which is still found in medical terminology.¹⁰ One of the first attempts at treating cancer was the excision of the outgrowth that could result in deadly infections and blood loss or, if the patient survived, could end up in remanifestation of the disease, accounting for a low rate of success. It was not until the modern age that significant progress has been accomplished in the knowledge and treatment of cancer. With a deeper understanding of the mechanisms leading to the onset, development and spread of tumors, and with a larger range of techniques useful both for diagnosis (ultrasound, computer tomography, magnetic resonance imaging) and treatment (cryosurgery, radiofrequency ablation, X-rays, proton beam radiation) many are the tools currently available in the battle against cancer.¹⁰⁻¹¹

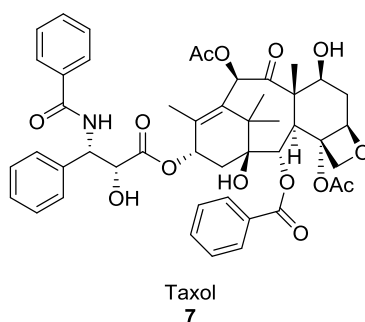
In addition to surgery and radiotherapy, pharmacotherapy has become increasingly important over the last sixty years. Following the discovery that some synthetic substances, for example nitrogen mustard, widely used during World War I, had cytotoxic effects towards rapidly-dividing cells, including cancer cells, several drugs were developed. This kind of pharmacologic approach to cancer treatment is referred to as chemotherapy and the drugs used can be classified into three main categories, depending on their mode of action. The first class includes alkylating agents, such as temozolomide **1**, and platinum-based drugs, *e.g.* carboplatin **2**, which disrupt DNA replication and induce DNA damage triggering apoptosis.¹²⁻¹³



Another strategy involves the use of antimetabolites, chemotherapeutic agents structurally similar to endogenous biomolecules, to inhibit metabolic pathways. 5-Fluorouracil **3**, a uracil and thymine mimic often used for the treatment of colorectal cancer, is converted *in vivo* to three active metabolites. 5-fluorodeoxyuridine monophosphate **4** (FdUMP) inhibits thymidylate synthase, the enzyme producing the nucleotide deoxythymidine monophosphate. 5-fluorodeoxyuridine triphosphate **5** (FdUTP) and fluorouridine triphosphate **6** (FUTP), instead, are misincorporated in RNA and DNA and lead to dysfunctional chains.¹⁴

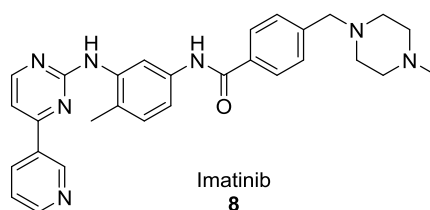


A third typology of therapeutic drugs includes natural products, such as the antimetabolic agent taxol (Paclitaxel, **7**) from *Taxus brevifolia*, which counteracts the depolymerization of microtubules during cell division by binding to the β -tubulin subunits.



Unfortunately, the administration of chemotherapeutic agents often leads to debilitating side effects (nausea, vomiting, hair loss, *etc.*) due to the lack of selectivity towards target tumor cells and their more generalized action on all rapidly dividing cells in the body, such as cells in the bone marrow, skin, hair follicles, and digestive tract. To avoid harming healthy cells, new strategies have been recently conceived, including targeted cancer therapy.¹¹ This approach exploits recent significant progress in the field of molecular biology to identify

molecular pathways directly linked to the onset and/or progression of tumors and aims to develop drugs addressing specific cellular mechanisms. Because these molecular pathways may be found in smaller subgroups of patients affected by a certain type of cancer, a stratified, or personalized, approach to the administration of drugs is required. The most remarkable success obtained with this strategy is Glivec™ (imatinib, **8**), a tyrosine kinase inhibitor approved by the Food and Drug Administration (FDA) in 2001, designed for the treatment of chronic myelogenous leukaemia (CML) and targeting a fusion tyrosine kinase originating from reciprocal translocation between the *ABL* gene (Abelson murine leukemia viral oncogene homolog 1) on chromosome 9 and the *BCR* (breakpoint cluster region protein) gene on chromosome 22¹⁵ resulting in an abnormally long chromosome 9+ and a short chromosome 22-, also known as the Philadelphia chromosome, carrying a *BCR-ABL* fusion gene.¹⁶ The fusion gene encodes for a BCR-ABL fusion oncoprotein with an elevated tyrosine kinase activity that ultimately enhances cell proliferation. After five years of treatment with Glivec, the survival rate is 89% (17% estimated relapse rates), considerably higher than the 30% achieved with treatments available before the drug entered the market.¹⁷



In most cases, the co-administration of several agents is required to overcome the heterogeneity of cancerous cells within a tumor and resistance mechanisms that are likely to arise. Combination therapies commonly include the use of both cytotoxic and targeted agents, or the administration of two drugs acting on two different targets, either in the same pathway or in parallel pathways.¹⁸

1.4 The stages of drug discovery

The modern scientific approach to drug discovery (Figure 1.3)¹⁹ starts when fundamental research provides evidence for the identification of a suitable target, a protein-protein interaction or a biomolecule, such as an enzyme or a

receptor, linked to a condition for which no efficacious cure is available or better treatments are needed. To be suitable for drug discovery, the relationship between the disease and the biological target needs to be proved and validated. Additionally, the target must be 'druggable', meaning that it must possess features, such as catalytic or allosteric pockets, likely to interact with a small-molecule modulator. The safety of addressing a particular target has to be considered and a profound knowledge of the pathways in which it might play a role is desirable.

Once a target has been identified, more studies are required to validate it, often using a tool compound active against the target. In order to minimize failure of a drug in the clinic due to the lack of desired effect, once a lot of money and effort have already been invested, target identification and target validation are crucial stages of drug discovery. In these phases, studies include both data mining of information in the literature (bioinformatics) and experimental models at all levels, starting from genetic models up to *in vivo* studies (e.g. genetic validation, cell-based systems, animal models).

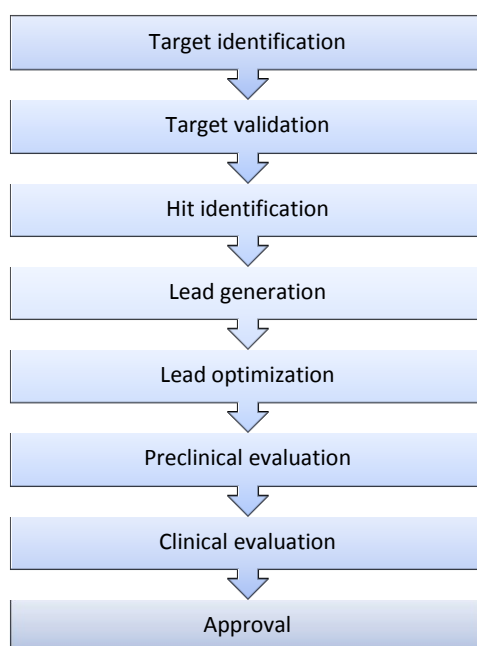


Figure 1.3 - Flow chart representing the stages of drug discovery.

The stage of hit identification for a validated target requires development of an assay to test for modulation of the target. The primary assay can be either a

cell-based assay, frequently applied for receptors and ion channels, or a cell-free biochemical assay that will only include the biochemical entity in question, more often used for enzyme targets. An efficient assay is highly reproducible, gives good quality data and is cost-effective. Common ways of identifying a hit compound include virtual screening, screening of compound libraries (either high-throughput or focused), fragment screening and structure-based drug design, if a crystal structure of the target is available.¹⁹

Once a hit has been discovered and validated, usually by re-synthesis and re-testing, further development of the active pharmacophore is carried out. During the lead generation phase, extensive structure-activity relationship (SAR) studies are carried out aiming to increase potency against the desired target and selectivity over similar biological entities. At this stage, the physicochemical (*e.g.* molecular weight, rotatable bonds, hydrogen bond donors/acceptors, ionization state, solubility) and pharmacokinetic properties (absorption, distribution, metabolism, elimination, or ADME, properties) are also evaluated. Early assessment of toxicity (*e.g.* behavioral effects, cardiotoxicity, mutagenicity) is also performed. Once a lead compound, a 'drug-like' molecule, has been selected, optimization is required for the identification of a clinical candidate satisfying all the requirements.¹⁹

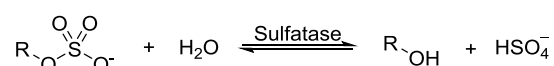
Safety and efficacy of the drug candidate are usually assessed in pre-clinical studies on animal models before administration to healthy human volunteers in phase I clinical trials, principally to assess the dose-response of the drug. Some candidates will enter Phase II for efficacy and safety studies and, if successful at this stage, larger scale Phase III clinical trials to provide data on side-effects.¹³ The entire process leading to the discovery of a drug generally can last about 12-15 years, with costs of the order of billions of pounds. Failure is possible at each stage and it is, therefore, critical to recognize the weaknesses of a drug discovery project as early as possible.

The projects discussed herein are both at the target validation stage, and medicinal chemistry efforts were started in order to provide better chemical tools for validation than the compounds available from the literature and to start building a confident SAR for hit discovery.

CHAPTER 2. INTRODUCTION TO SULF2

2.1 Sulfatases

Sulfatases are a class of hydrolase enzymes that catalyze the cleavage of sulfate esters to release the corresponding alcohol or phenol and an inorganic sulfate (Scheme 2.1).



Scheme 2.1 - Sulfatases catalyze the hydrolysis of sulfate esters.

The nature of sulfatase substrates is diverse and they are involved in many different signaling pathways within the cell. Some sulfatases are specific for the desulfation of sulfated carbohydrates, for example in the context of saccharide residues on glycosaminoproteoglycans, while others recognize and cleave the sulfate group appended to lipophilic scaffolds, such as steroidal sulfates.²⁰

Fifteen human sulfatases are currently known, in addition to further sulfatases from invertebrates, lower eukaryotes and prokaryotes.²⁰ In most cases, these enzymes are membrane bound and located in the endoplasmic reticulum or the Golgi network. Two sulfatases, Sulf1 and Sulf2, and several others found in lower eukaryotes are secreted into the extracellular matrix and exist as soluble proteins.²⁰ Studies on this class of enzymes have highlighted the high degree of conservation of primary structure across the known sulfatases (ranging from prokaryotic to human), particularly in the *N*-terminal region containing the catalytic site. As reviewed by Hanson and co-workers,²⁰ this part of the peptide chain contains two key motifs, referred to as sulfatase signature sequences I and II. The former is a consensus sequence involved in the recognition event necessary for the post-translational modification required for catalytic activity, while the latter sequence plays a role in the catalytic mechanism of the enzyme.²¹ The signature sequence I for known sulfatases is shown in Figure 2.1.²⁰⁻²¹ As highlighted in black, approximately six out of twelve residues in the motif are usually conserved in both prokaryotic and eukaryotic enzymes.

	1	2	3	4	5	6	7	8	9	10	11	12	Position of FG	Length
Human sulfatases														
ARSA	C	T	P	S	R	A	A	L	L	T	G	R	69	507
ARSB	C	T	P	S	R	S	Q	L	L	T	G	R	75	533
ARSC	C	T	P	S	R	A	A	F	M	T	G	R	83	583
ARSD	C	T	P	S	R	A	A	F	L	T	G	R	89	593
ARSE	C	T	P	S	R	A	A	F	L	T	G	R	86	589
ARSF	C	S	P	S	R	S	A	F	L	T	G	R	79	591
ARSG	C	S	P	S	R	A	S	L	L	T	G	R	82	525
GalN6S	C	S	P	S	R	A	A	L	L	T	G	R	79	522
GlcN6S	C	C	P	S	R	A	S	I	L	T	G	K	91	552
GlcN5S	C	S	P	S	R	A	S	L	L	T	G	L	70	502
IdoA2S	C	A	P	S	R	V	S	F	L	T	G	R	84	550
Sulf1	C	C	P	S	R	S	S	M	L	T	G	K	87	871
Sulf2	C	C	P	S	R	S	S	I	L	T	G	K	88	870
Invertebrate and lower eukaryotic sulfatases														
HeARS	C	T	P	S	R	S	A	I	M	T	G	R	106	559
HpArs	C	T	P	S	R	S	A	I	M	T	G	R	100	551
SARS	C	T	P	S	R	S	A	I	V	T	G	R	115	567
HpSulf1	C	T	P	T	R	S	Q	L	M	S	G	R	80	508
PGSS	C	S	P	A	R	T	A	V	L	T	G	K	70	532
CARS	C	C	P	S	R	T	N	L	C	A	A	S	73	646
NARS	C	C	P	A	R	V	S	L	W	T	G	K	89	639
VARS	C	C	P		R	T	N	L	W	R	G	Q	72	649
Prokaryotic sulfatases														
FHS2S	C	T	P	S	R	S	A	I	F	S	G	K	82	464
KARS	S	A	P	A	R	S	M	L	L	T	G	N	72	577
PARS	C	S	P	T	R	S	M	L	L	T	G	T	51	533
PMdS	S	T	P	A	R	A	C	L	L	T	G	L	79	517
SChoS	C	A	P	A	R	A	S	F	M	A	G	Q	54	512

Figure 2.1 - Conservation of sulfatase signature sequence I in the majority of known sulfatases.

Reproduced from Hanson, 2004.²⁰

The pentapeptide at the beginning of the signature sequence is almost invariable among human sulfatases and is generally well conserved in other species. The arginine residue at position 5 of the pentapeptide was found to be critical both in the formation and stabilization of a formylglycine (FG, 9; Figure 2.2) residue which is critical for the activity of all sulfatases.²⁰ During biosynthesis, sulfatases undergo extensive post-translational modifications including one conferring catalytic activity. Active sulfatases exhibit the unusual formylglycine residue, which originates from oxidation of a conserved cysteine (or, in some cases, serine) through the action of a formylglycine-generating enzyme (FGE).²⁰ Under

physiological conditions, FG may be hydrated to give hydroxyformylglycine (HFG, **10**; Figure 2.2). Sulfatases lacking the formylglycine residue are catalytically inactive.²² Organisms having non-functional FGE suffer from an autosomal recessive disorder called multiple sulfatase deficiency. This rare disorder originates from mutations on the *SUMF1* gene encoding for FGE, leading to a deficiency of this important post-translational modifying enzyme.²⁰

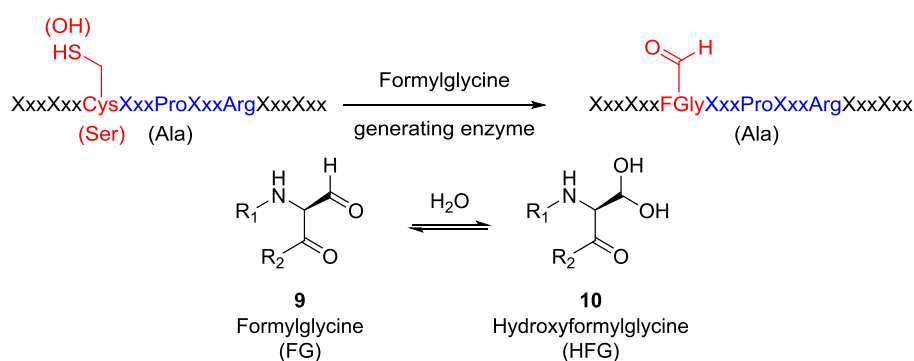


Figure 2.2 - The formylglycine residue.

a) Biosynthesis of the catalytically active formylglycine (FG) residue in the sulfatase active site; **b)** equilibrium between formylglycine and its hydrated form, hydroxyformylglycine (HFG). Adapted from Spencer, 2013.²³

The location and physiological substrate of each of the fifteen human sulfatases is described in Table 2.1.²⁰ The most extensively studied enzyme of this family is steroid sulfatase (STS), also known as aryl sulfatase C (ARSC) or estrone sulfatase, which has risen in interest over the last two decades due to its crucial role in hormone-dependent cancers, such as breast and prostate cancers.

Table 2.1 - Physiological substrate and subcellular location of known human sulfatases.

Reproduced from Hanson, 2004.²⁰

Sulfatase	Abbr.	Physiological substrate	Subcellular location
Aryl sulfatase A	ARSA	Sulfatide	Lysosome
Aryl sulfatase B	ARSB	Dermatan sulfate, chondroitin sulfate	Lysosome
Aryl sulfatase C, Steroid sulfatase	ARSC, STS	Steroid sulfates	ER
Aryl sulfatase D	ARSD	Unknown	ER
Aryl sulfatase E	ARSE	Unknown	Golgi network
Aryl sulfatase F	ARSF	Unknown	ER
Aryl sulfatase G	ARSG	Unknown	ER
Galactosamine-6-sulfatase	GalN6S	Chondroitin sulfate, keratan sulfate	Lysosome
Glucosamine-3-sulfatase	GlcN3S	Heparan sulfate	Lysosome
Glucosamine-6-sulfatase	GlcN6S	Heparan sulfate, keratan sulfate	Lysosome
Glucuronate-2-sulfatase	GlcA2S	Heparan sulfate	Lysosome
Heparan-N-sulfatase	GlcNS	Heparan sulfate	Lysosome
Iduronate-2-sulfatase	IdoA2S	Heparan sulfate, dermatan sulfate	Lysosome
Endo sulfatase 1	Sulf1	Heparan sulfate	ECM
Endo sulfatase 2	Sulf2	Heparan sulfate	ECM

ER: endoplasmic reticulum. ECM: extracellular matrix.

STS is one of four sulfatases whose X-ray crystal structure has been solved, in addition to two human sulfatases, aryl sulfatase A (ARSA) and aryl sulfatase B (ARSB), and a prokaryotic aryl sulfatase from *Pseudomonas aeruginosa* (PARS). Superposition of the four crystal structures highlights the degree of conservation of the globular domain folding (Figure 2.3).²⁴ The STS crystal structure exhibits an additional transmembrane domain not present in the other structures, consisting of two antiparallel α -helices, which anchors the enzyme to the membrane of the endoplasmic reticulum and is also believed to play a role in STS substrate recognition.²⁴

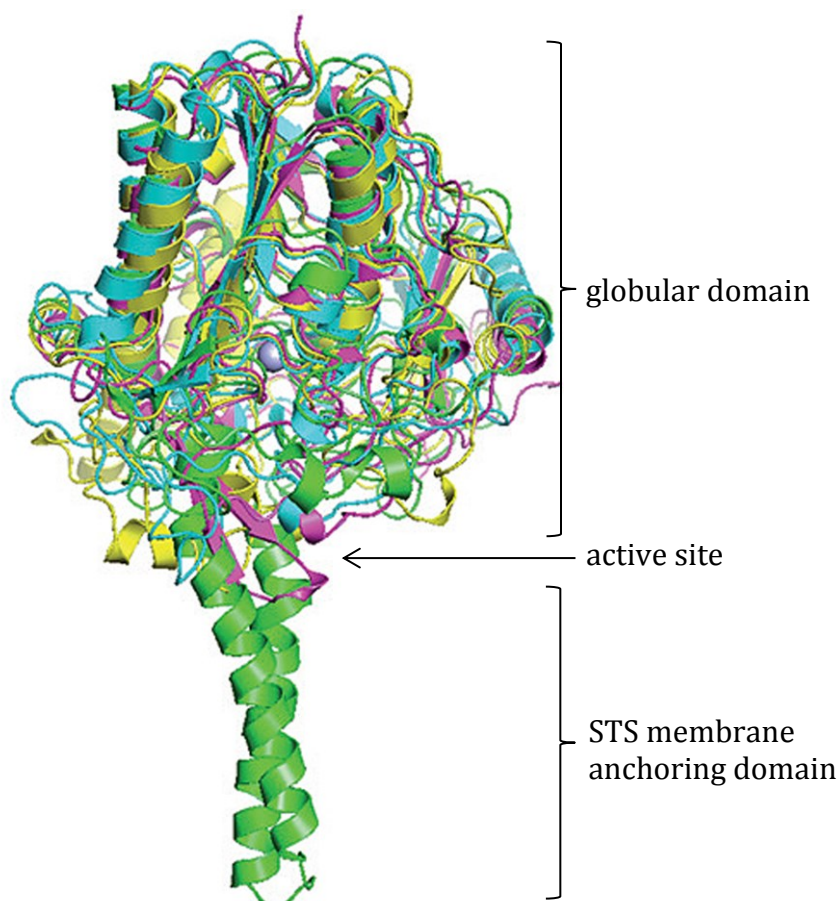


Figure 2.3 - Structural data on human sulfatases.

Superposition of the crystal structure of ARSA (blue), ARSB (magenta), STS (green) and PARS (yellow). Reproduced from Ghosh, 2007.²⁴

Despite the fact that no structures of sulfatases co-crystallized with their endogenous substrates have been reported, the available structural data and a series of mutagenesis studies are a valuable source of information to acquire an insight into the active site of these enzymes. It is postulated that the hydroxyformylglycine residue is stabilized by a number of positively charged residues (ArgA, HisA and LysA in Figure 2.4) and one of its hydroxyl groups makes an ionic interaction with a divalent metal cation (Ca^{2+} or Mg^{2+}); the metal ion is additionally coordinated by a sulfate and by the electron-donor group on the side chain of AspA, AsnA, AspB and AspC. The metal cation may play a role in stabilizing the formylglycine, in binding the substrate and in activating the substrate for sulfate hydrolysis. Studies in which the residues significant for metal coordination were mutated showed decrease in binding and catalytic activity, confirming the

importance of these active site residues.²⁵ A further set of protonated basic residues (LysB and HisB) in the active site may be involved in protonation of the alcohol leaving group of the substrate and in binding to inorganic sulfate formed during the reaction.^{20,24}

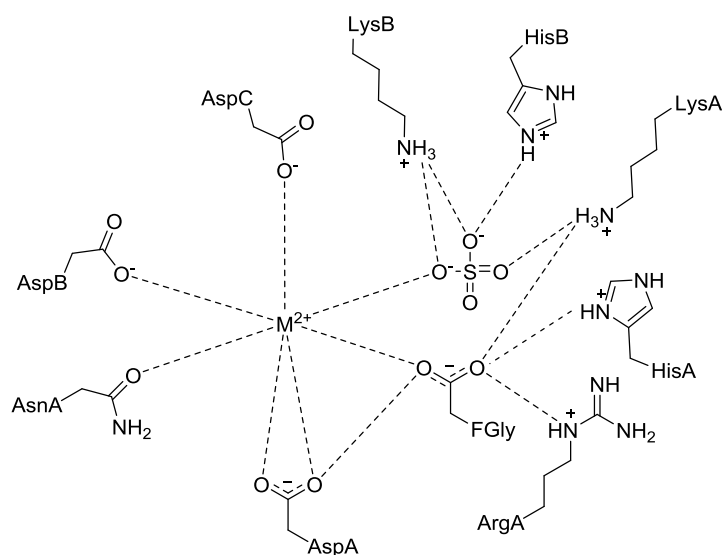
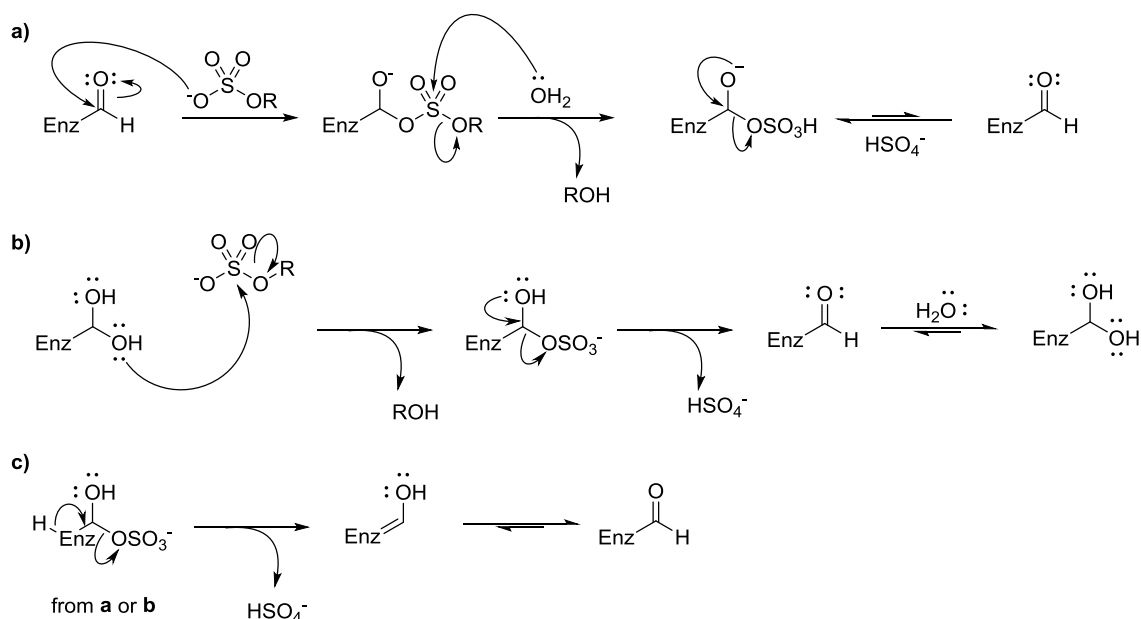


Figure 2.4 - Representation of the active site of sulfatases.

Reproduced from Hanson, 2004.²⁰

The lack of structural data for sulfatases interacting with their physiological substrates prevents a clear understanding of substrate recognition events and the enzyme domains involved. Nevertheless, since many sulfatases are able to hydrolyze small aryl sulfates, it is reasonable to infer that residues distinct from the active site may also be implicated in substrate recognition.²⁰

While it is widely agreed that the formylglycine residue is involved in the catalytic mechanisms, there has been much debate about the mechanism of the catalytic event.²⁰ Initially, an addition-hydrolysis mechanism was proposed (Scheme 2.2a). This invoked nucleophilic attack of an oxy-anion of the sulfate substrate on the carbonyl carbon of the formylglycine, followed by a second nucleophilic attack carried out by a molecule of water on the sulfur to release the desulfated substrate alcohol (ROH). Subsequent loss of bisulfate ion would restore the active site formylglycine residue for subsequent entry into the catalytic cycle.



Scheme 2.2 - Proposed mechanisms for the desulfation of substrates by sulfatases.

a) Addition-hydrolysis mechanism; **b)** transesterification-elimination mechanism; **c)** loss of sulfate and tautomerization of the enol to formylglycine. Reproduced from Hanson, 2004, and Bojarová, 2008.^{20,26}

The second proposed mechanism involves the hydration of the formylglycine to hydroxyformylglycine, whose second hydroxyl group would be necessary for sulfate cleavage. According to this theory, hydrolysis may proceed *via* a transesterification-elimination mechanism (Figure 2.2b):²⁰ one of the two hydroxyl groups of the *gem*-diol of HFG attacks the sulfur atom of the sulfate thus releasing the desulfated substrate alcohol (ROH) in an S_N2-like mechanism. Subsequently, the second hydroxyl group drives an α-elimination step that generates formylglycine and inorganic sulfate. Finally, a molecule of water re-hydrates the FG residue and regenerates the active HFG side chain. In the third proposed mechanism, after elimination of the alcohol following either pathway a or b, loss of an α-proton triggers elimination of the sulfate and subsequent tautomerization of the enol re-establishes the formylglycine moiety (Figure 2.2c).

Unlike the wild-type enzymes, when [³⁵S]-*p*-nitrocatechol sulfate is hydrolyzed by mutated ARSA and ARSB enzymes carrying a serine in place of the catalytic formylglycine, the labelled sulfur atom was not eliminated from the enzyme,

suggesting that the contribution of the oxygen lone pair of the second hydroxyl of HFG is required for the elimination step to occur. These data support the transesterification-elimination pathway.²⁰

2.2 The importance of sulfation

To understand the role of sulfatases, it is necessary to examine in more detail the process of sulfation and its relevance in biological systems.

The enzymes responsible for the sulfation of alcoholic and phenolic hydroxyl groups *in vivo* are sulfotransferases (SULTs) and, in eukaryotes, these rely on 3'-phosphoadenosine 5'-phosphosulfate (PAPS, **11**) as sulfate donor (Figure 2.5). The assertion that sulfation is a key biochemical reaction is supported by two main observations. Firstly, enzymes involved in sulfation and desulfation events (sulfotransferases and sulfatases) have been found across a wide range of (if not all) species. Secondly, PAPS is a high energy molecule requiring two molecules of ATP for its biosynthesis, making sulfation an expensive process for the cell in terms of energy balance.²⁷

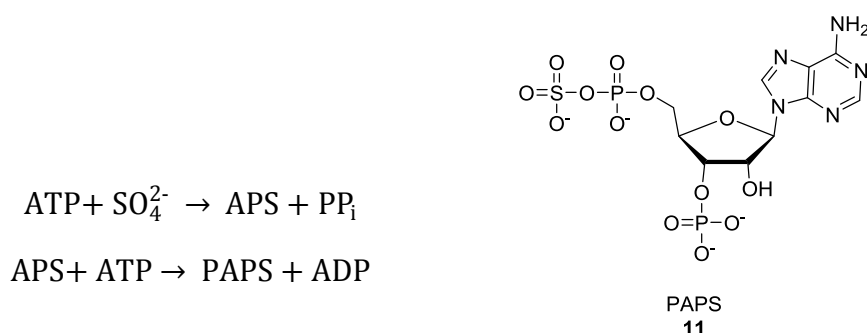


Figure 2.5 - Bioynthesis of PAPS.

In the first step, a molecule of adenosine 5'-phosphosulfate (APS) is formed from ATP and inorganic sulfate with release of pyrophosphate (PP_i). Further phosphorylation of APS by a second molecule of ATP yields 3'-phosphoadenosine 5'-phosphosulfate (PAPS, **11**) which is used as a co-enzyme by sulfotransferases.

On the basis of the current knowledge, three main roles of sulfation have been identified. First, the involvement of sulfation in the protection of organisms from xenobiotics has been long known.²⁸ Lipophilic molecules of exogenous source are rapidly sulfated in order to obtain a) a less active and potentially less harmful compound and/or b) a water soluble counterpart which is rapidly excreted *via* the

urine or the bile (phase II metabolism). In addition to its crucial role in the preservation of the cellular environment, sulfation is also an important tool used both in the biosynthesis of hormones and in the activation of biomolecules.²⁷ These aspects will be discussed in more detail below.

2.3 Steroid sulfatase inhibitors

Due to its involvement in hormone-dependent cancers, steroid sulfatase has been widely studied and considerable effort has focused on the design of small molecules that would efficiently inhibit its action. STS activates steroid hormones, for example estrone and dehydroepiandrosterone, by catalyzing the hydrolysis of the sulfate group from inactive sulfated precursors (Figure 2.6)

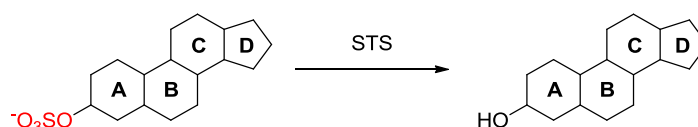
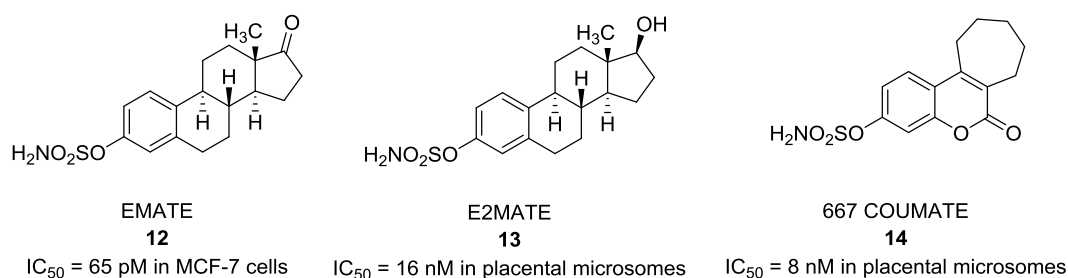


Figure 2.6 - Hydrolysis of a sulfate group from a generic steroid catalyzed by STS.

This desulfation route represents the major source of estrogen in estrogen-dependent breast cancer where STS activity is elevated. Several publications by Potter and co-workers describe the synthesis and structure-activity relationship (SAR) evaluation of STS inhibitors.²⁹⁻³⁷ In these studies the sulfate moiety on a steroid scaffold was replaced by a range of functional groups with the potential of mimic the sulfate (phosphonate, H-phosphonate, thiophosphonate, sulfonate, sulfonamide, amide, urea). The best inhibition of sulfatase activity was obtained by molecules bearing a primary sulfamate moiety on an estrogen or estrogen-mimicking fragment.^{30,33}

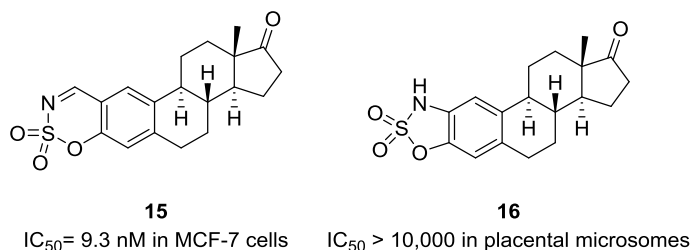
Key examples of steroid sulfatase inhibitors are estrone sulfamate (EMATE, **12**)³³ and estradiol 3-*O*-sulfamate (E2MATE or PGL2001, **13**).³⁸ EMATE shows high potency against STS ($\text{IC}_{50} < 0.1$ nM in an intact MCF-7 cell assay).³⁰ Additionally, EMATE has been shown to act as an irreversible inhibitor, with a time-dependent inhibition being observed upon formation of a covalent bond between the enzyme and the sulfamate group of the inhibitor. E2MATE **13**, which is rapidly oxidized *in*

vivo to give EMATE **12**, is also a potent inhibitor of STS (IC_{50} = 16 nM in placental microsomes).³⁸ Unfortunately, both compounds show estrogenic effects that prevented their entry into clinical trials for estrogen-dependent breast cancer. Another therapeutic application was found for E2MATE, which is currently in a phase II clinical trial for the treatment of endometriosis in pre-menopausal women.²³



Subsequently, to avoid the side effects of steroid-based drugs and to improve biological selectivity and stability to human metabolism, Potter and co-workers focused their efforts on non-steroidal cores. They identified 667-COUMATE **14** (STX 64 or irusostat) as an example of a potent coumarin-based irreversible inhibitor of STS (IC_{50} = 8 nM in placental microsomes). 667-COUMATE was unsuccessful in a number of clinical trials and is not currently under further development.²³

While primary sulfamates ($-OSO_2NH_2$) are irreversible inhibitors of STS, mono- or di- substitution on the sulfamate nitrogen to give a secondary ($-OSO_2NHR$) or tertiary sulfamate ($-OSO_2NR_2$), respectively, yields reversible inhibitors. Such substituted sulfamates were also found to be significantly less active against STS (both having 87% inhibition at 1 μ M).³³ Taken together, the findings reported by Potter and his team suggest that the primary sulfamate moiety is an efficacious pharmacophore in the inhibition of STS and is crucial for the irreversible inhibition of steroid sulfatase while secondary and tertiary sulfamates reversibly bind to the target and show lower potency.



The cyclic sulfamate **15** was a potent inhibitor of STS and gave positive results *in vivo* in mice xenograft model. In contrast, the five-membered cyclic sulfamate **16** was inactive.²³ This may be explained by postulating *in situ* hydrolysis of the imino-sulfamate **15** to generate an *ortho*-formyl primary sulfamate which may be the agent inhibiting the enzyme.²³

Due to the conserved catalytic site, it is reasonable to assume that specifically designed sulfamate-based inhibitors may also have activity against other sulfatases.

2.4 Human endosulfatases (Sulf1 and Sulf2)

Interest in the field of sulfatases was increased by the discovery of two human sulfatases,³⁹ Sulf1 and Sulf2, and their possible implication in cancer (see Section 2.5).⁴⁰ Similar to other sulfatases, Sulf1 and Sulf2 contain a cysteine residue, Cys87 and Cys88, respectively,³⁹ that is post-translationally modified to the active formylglycine counterpart. These enzymes have several characteristics that distinguish them from other known human sulfatases. Firstly, they have an amino acid sequence which is ~800 residues long, while most sulfatases have between 500 and 600 residues.²⁰ Sulf1 and Sulf2 are also the only known human sulfatases located in the extra-cellular matrix, as shown in Table 2.1.²⁰ Finally, the other sulfatases that act on unbranched polysaccharide glycosaminoglycans (*e.g.* heparan sulfate, chondroitin sulfate or keratan sulfate) are exosulfatases, preferentially removing sulfate groups from the non-reducing termini of the polysaccharide chains. In contrast, Sulf1 and Sulf2 are endosulfatases that can hydrolyze sulfate esters internal to the polysaccharide chain. The natural substrate of these endosulfatases is heparan sulfate (HS, **17**, Figure 2.7), a highly sulfated extracellular polysaccharide making up the hydrophilic part of proteoglycans. The structure and functions of heparan sulfate will be discussed in Section 2.4.1. In

their seminal work, Morimoto-Tomita and co-workers also reported low arylsulfatase activity of Sulf1 and Sulf2.³⁹ Consistent with their extracellular localization, the activity of the endosulfatase enzymes is optimal at neutral pH.³⁹

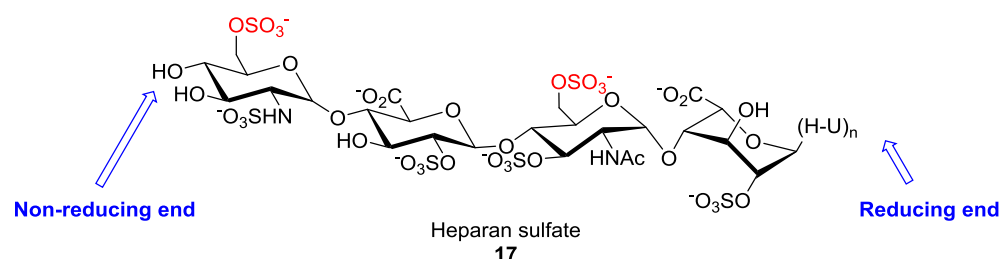


Figure 2.7 - Example of a fragment of heparan sulfate, 17.

Positions which are likely to undergo desulfation by Sulfs are marked in red.

Sulf1 and Sulf2 are closely related in structure (63-65% sequence homology)³⁹ and their roles appear to overlap.⁴¹⁻⁴² Sulf1 or Sulf2 (*Sulf1*^{-/-} or *Sulf2*^{-/-}) knock-out mice do not exhibit major abnormalities and present no phenotype when compared to the wild-type animals. Double knock-out mice lacking both Sulf1 and Sulf2 genes, on the other hand, result in perinatal lethality and low long term survival frequency (~15%). Taken together, these data suggest that Sulf1 and Sulf2 may possess mutually redundant but essential roles during development.⁴³

Consistent with other sulfatases, the primary structure of the endosulfatases can be divided into two domains: an *N*-terminal domain bearing catalytic activity and a *C*-terminal domain. The latter, highly hydrophilic, domain is unique to Sulf1 and Sulf2 and is believed to be involved in recruiting the substrate.⁴⁴ Indirect evidence that the *C*-terminal domain may be involved in recognition of the substrate heparan sulfate comes from the observation that there are several conserved sequences in this domain that are also present in the exosulfatase glucosamine 6-sulfatase (which hydrolyses glucosamine 6-sulfate residues belonging to heparan sulfate).²⁰

Human endosulfatases are initially translated as a pre-proprotein.^a A small peptide is post-translationally cleaved from the *N*-terminus generating the proprotein which is further processed by a furin-type protease. This cleaves the

^a Precursor to an inactive protein precursor, which is called proprotein.

proprotein within the hydrophilic domain to form the Sulf protein as a heterodimer. These two subunits are subsequently linked together by a disulfide bridge (Figure 2.8).⁴¹

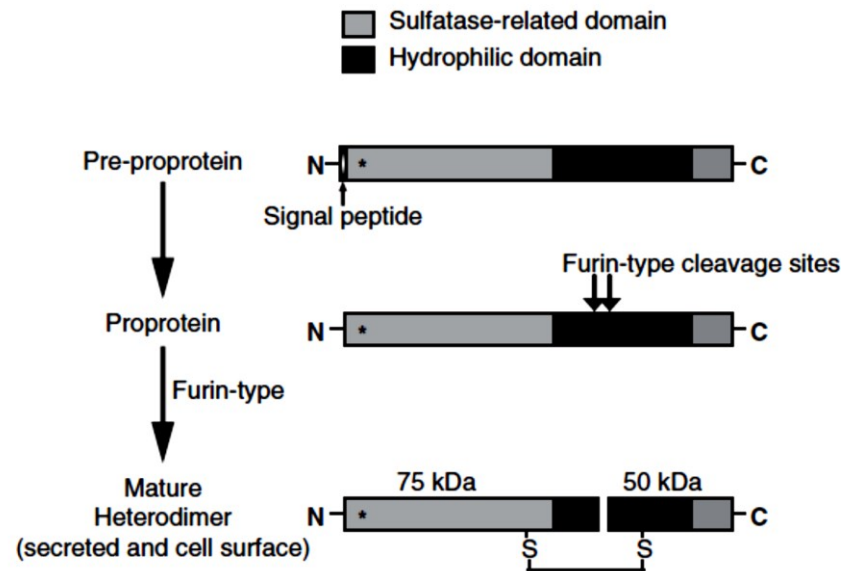


Figure 2.8 - Post-translational process that brings to mature Sulf enzymes.

A signal peptide at the *N*-terminus is cleaved from the pre-proprotein to originate the proprotein. Furin-type enzymes cleave the proprotein generating two fragments linked by a disulfide bridge. Reproduced from Rosen, 2010.⁴¹

Several splice variants of Sulf1 have been identified in quail,⁴⁵ human, dog and cat,⁴⁶ and different splice variants of Sulf2 have also been reported.⁴⁷ In both enzymes the shorter splice variants do not contain the Cys87 or Cys88 residue, respectively, and are, therefore, catalytically inactive. The splice variants of Sulf1 have been shown to have opposing effects: the active full length variant of the enzyme appeared to prevent angiogenesis, while in the embryo the shorter form is predominant and showed an angiogenic effect possibly by binding to heparan sulfate and preventing the cleavage of 6-*O*-sulfates on which VEGF and FGF signaling pathways rely. The Wnt pathway (see Section 2.4.3) is affected by Sulf1 splice variants in an opposite way: full length enzyme activates the pathway, while the shorter splice variant inhibits it.⁴⁶

2.4.1 Heparan sulfate: the endogenous substrate of Sulf enzymes

Heparan sulfate **17** (HS, Figure 2.7) is a linear polysaccharide, belonging to the family of glycosaminoglycans (GAGs), in which dimeric repetitive units consist of D-glucosamine (GlcN, **18**) residues and either a D-glucuronic acid (GlcA, **19**) or a L-iduronic acid residue (IdoA, **20**), shown in Figure 2.9.⁴¹

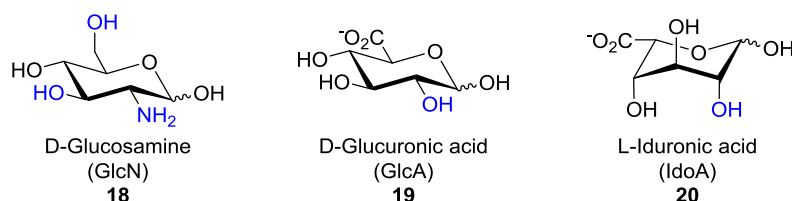


Figure 2.9 - Structures of monosaccharide monomers 18, 19, and 20 which constitute heparan sulfate chains.

Positions which are liable to sulfation are marked in blue.

A heparan sulfate chain on average contains approximately 150 disaccharides⁴⁴ and has a half-life of 4-24 h.⁴⁸ A heparan sulfate proteoglycan (HSPG) is formed when heparan sulfate is covalently associated to a protein core (syndecan, glypican, perlecan, agrin or collagen VIII). Characterization of HSPGs, both in structure and function, is complicated by their chemical heterogeneity, with the structure depending both on length and functionalization of the long polysaccharide chains and on the nature of the protein core. HSPGs are found on the outside of cell membranes or in the extra-cellular matrix.

The biosynthesis of HS is non-template driven⁴⁹ and takes place in the Golgi apparatus by elongation of a tetrasaccharide through progressive addition of glucuronic acid-*N*-acetylglucosamine (GlcA-GlcNAc) disaccharide units by glycosyl transferase.⁵⁰ The newly synthesized precursor of heparan sulfate, called heparosan,⁵¹ is edited by the action of several enzymes. The polysaccharide chain may undergo enzyme-mediated sulfation on the *N*-position of glucosamine residues, epimerization of D-glucuronic acid residues to L-iduronic acid and sulfation of the 2-*O* position of the uronic acid residues and 3-*O* and 6-*O* positions of glucosamine residues.⁵⁰ The pattern of functionalization of HS is complex and can vary depending, for instance, on the type of cell expressing the biopolymer and on the extracellular signals reaching the cell surface.⁵¹

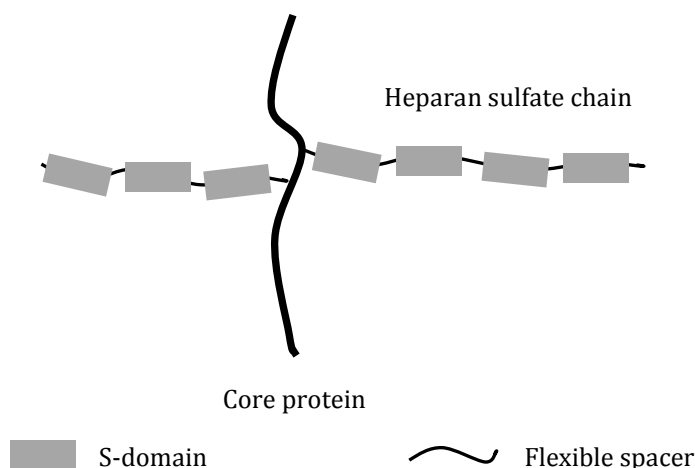


Figure 2.10 - Cartoon depicting the structure of heparan sulfate proteoglycans.

Reproduced from Rosen, 2010.⁴¹

Heparan sulfate chains alternate rigid highly sulfated regions (S-domains) and flexible regions, characterized by lower or no sulfation (*N*-acetylated domains),⁵¹ as shown in Figure 2.10.⁴¹ Heparan sulfate plays an active role in many biological processes. HSPGs are able either to bind or release a wide range of protein ligands (growth factors, cytokines, etc.), which are involved in numerous cascade events as a result of the modulation of their sulfation state by sulfatases and sulfotransferases.

The roles of HS include the mediation of protein-protein interactions, for example by stabilizing the conformation of a protein. Also, heparan sulfate acts as a co-receptor, promoting the interaction between proteins by binding them on a template glycosaminoglycan chain (*e.g.* FGF-receptor tyrosine kinase interaction).⁵² Finally, HS sequesters signaling molecules and prevents the activation of signaling cascades.⁴⁸

As mentioned above, Sulf1 and Sulf2 are endosulfatases and cleave sulfate groups from the 6-*O* position of glucosamine residues (GlcN, **18**) found in the disaccharide repetitive unit of the heparin/heparan sulfate glycosaminoglycan. The enzymes showed greatest activity towards the trisulfated disaccharide units made up of 2-*O*-sulfated L-iduronic acid and *N*-sulfate-glucosamine 6-*O*-sulfate (IdoA2S-GlcNS6S).³⁹ A recent study by Staples *et al.*, provided experimental evidence that

the pattern of heparan sulfate needs to satisfy certain structural requirements to enable binding and editing by the endosulfatases.⁴⁹ The study determined that removal of the 6-*O*-sulfates lowers the affinity of Sulf1 and Sulf2 for HS, thus allowing the substrate to be released.

2.4.2 Proposed model for the action of Sulf1 and Sulf2

At the time when this project was initiated, no information was available concerning the shape (pocket or groove), size or location of the active site of Sulf1 and Sulf2. A recent biochemical study focused on the C-terminal hydrophilic domain, which is unique to the extracellular endosulfatases. This portion of the enzyme contains a high number of basic residues regularly arranged along the primary amino acid sequence. Within the hydrophilic domain of Sulf1, the authors were able to identify at least two binding sites for heparan sulfate. Following their observations, Milz *et al.* postulate a cooperativity between the catalytic (primary binding site) and the hydrophilic domain (secondary binding site or exosite), in which the hydrophilic domain binds to the heparan sulfate chain in at least two sites, while the catalytic domain hydrolyzes the sulfate group from a proximal disaccharide. Once the sulfate has been cleaved, the hydrophilic domain presents the next 6-*O*-sulfate group to the active site while the enzyme moves along the polysaccharide chain (Figure 2.11).⁴⁴

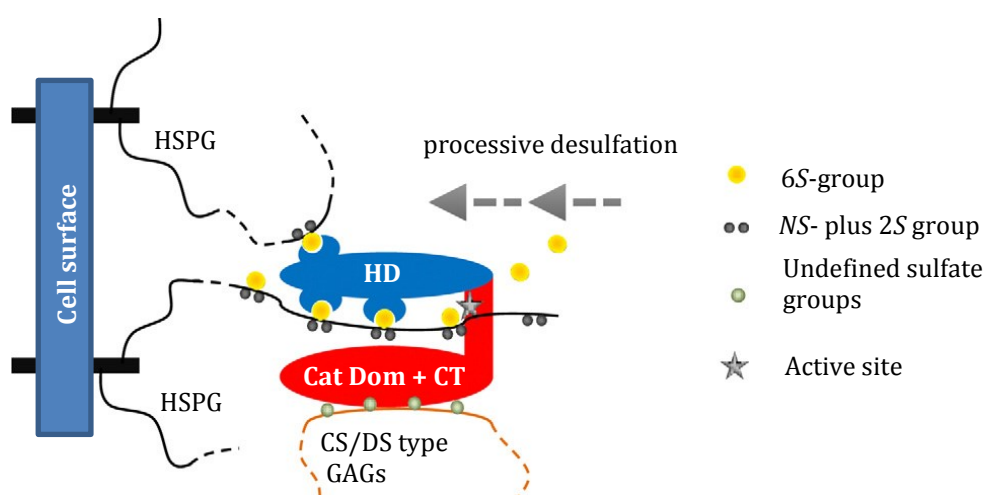


Figure 2.11 - Schematic description of the proposed processive action of Sulf1 on heparan sulfate chains.

HD: hydrophilic domain. Cat Dom: catalytic domain. CT: C-terminal domain. Endosulfatases can bind other glycosaminoglycans, such as chondroitin sulfate and dermatan sulfate, but is not able to desulfate them. Adapted from Milz, 2013.⁴⁴

The loss of sulfatase activity shown by Sulf1 when the hydrophilic domain is not present, supports the hypothesis of the binding function of the hydrophilic domain. A homology model of Sulf1 based on the structure of ARSB was reported in the same study and suggested that the hydrophilic domain could be positioned in the proximity of the active site (Figure 2.12).⁴⁴ Given the great degree of homology between Sulf1 and Sulf2, it is likely that Sulf2 could function in an analogous manner.

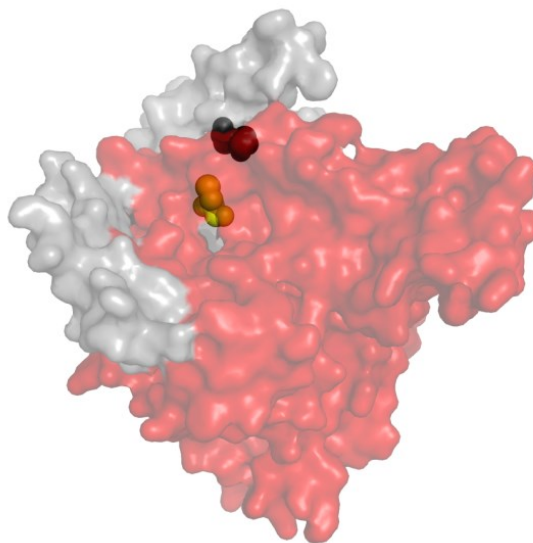


Figure 2.12 - Homology model of Sulf1.

The catalytic domain is depicted in red, the hydrophilic domain in grey; Cys87 is highlighted in yellow; the dark spheres are the amino acid residues that mark the end of the *N*-terminal domain and the beginning of the HD. This model suggests that the hydrophilic domain is close enough to the active site to participate to recognition and binding of the substrate. Reproduced from Milz, 2013.⁴⁴

2.4.3 Endosulfatases and their role in signaling pathways

By means of their sulfate groups, heparan sulfate proteoglycans interact with a variety of growth factors and cytokines modulating a number of signaling pathways, such the wingless/int (Wnt) pathway and the pathways downstream of the fibroblast growth factor (FGF) receptor (*e.g.* mitogen-activated protein kinase, MAPK, pathway).^{51,53} Because of the desulfating action exerted on HSPGs, Sulf1 and Sulf2 also have an active role in the regulation of signal transduction.

Sulf1 has been shown to repress fibroblast growth factor (FGF) receptor tyrosine kinase signaling.⁵⁴ The highly sulfated domains of heparan sulfate act as a co-

receptor and facilitate the interaction between FGF-2 and the fibroblast growth factor receptor (FGFR) by formation of a ternary complex. This promotes dimerization of FGFR and activation of the receptor tyrosine kinase activity, with consequent transphosphorylation. The signal activates a phosphorylation cascade through the MAPK pathway (Ras-Raf-MEK-ERK, Figure 2.13), leading to increased cell proliferation, angiogenesis and survival.⁵⁵⁻⁵⁶ Desulfation of the heparan sulfate chain by Sulf1 reduces affinity for its partners and disrupts the ternary complex, effectively down-regulating the MAPK signaling pathway. As a result, cell proliferation, angiogenesis and survival are also diminished.⁵⁶ With different HSPG selectivity, Sulf2 has an opposing effect to that of Sulf1, showing enhanced FGF signaling. Flow cytometry of human hepatocyte carcinoma Hep3B cells, either in the presence or in the absence of Sulf2, using biotinylated FGF-2 suggests that FGF-2 binding to the receptor is increased by the action of Sulf2.⁵⁴

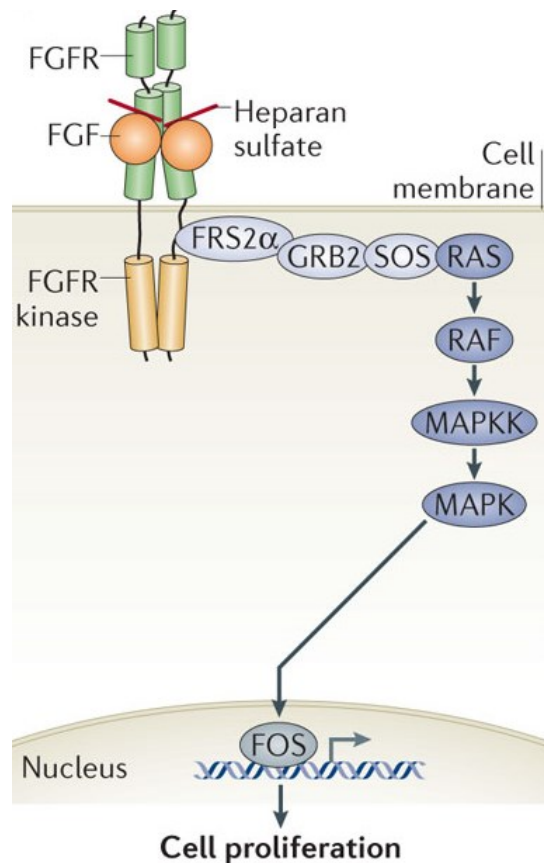


Figure 2.13 - FGF signaling pathway.

Formation of a ternary FGF:FGFR:heparan sulfate complex leads to FGFR dimerization and transphosphorylation with activation of the MAPK pathway. Reproduced from Goetz, 2013.⁵⁵

The canonical Wnt/ β -catenin pathway, which promotes cell adhesion and cell proliferation through activation of target genes, is positively regulated by endosulfatases. As depicted in Figure 2.14, heparan sulfate proteoglycans sequester Wnt ligands on the cell surface by interaction with sulfate groups and prevent binding to the trans-membrane Frizzled receptor. As a result, β -catenin is sequestered by a destruction complex, phosphorylated and degraded. However, endosulfatase-catalyzed desulfation of HS chains releases the Wnt peptide which binds to Frizzled receptor, leading to disruption of the destruction complex and stabilization of β -catenin, which enters the nucleus where it contributes to gene expression.

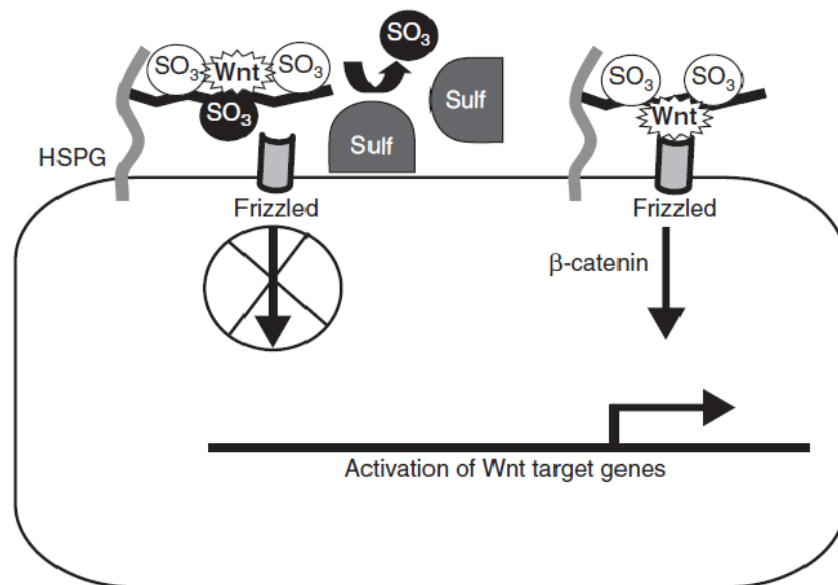


Figure 2.14 - The Wnt signaling pathway.

The desulfation of HSPG by Sulf1 and Sulf2 causes the release of Wnt ligand that binds Frizzled receptor and leads to the activation of the Wnt target genes *via* stabilization of β -catenin. Reproduced from Rosen, 2010.⁴¹

There is a wide range of growth factors and chemokines interacting with heparan sulfate with potential implications on other signaling pathways. Similar to the FGF pathway the hepatocellular growth factor (HGF), heparin-binding growth factor (HB-GF) and vascular endothelial growth factor (VEGF) signaling pathways are influenced by Sulf1.⁵⁶ ELISA studies by Uchimura *et al.* proved that Sulf2 mobilized VEGF₁₆₅ and the chemokines stromal cell-derived factor 1 (SFD-1) and secondary lymphoid tissue chemokine (SLC).⁵⁷

Recently, Sulf2 was identified as a downstream effector of p53. No comment on Sulf1 were made by the authors.⁵⁸

2.5 The role of Sulf1 and Sulf2 in cancer

As a consequence of their active role in the dynamic modulation of the sulfation state of heparan sulfate chains in the extracellular matrix and of the relevance of HS in regulating important cellular signaling pathways,⁴² Sulf1 and Sulf2 have been found to play an important role in a range of diseases, such as arthritis,⁵⁹ atherogenic dyslipidemia,⁶⁰ chronic renal fibrosis⁶¹ and cancer.⁴¹

An increasing body of literature reports altered levels of Sulf1 and Sulf2 in several subtypes of cancer, including brain cancer, breast and ovarian cancer, melanoma and cancers related to the gastro-intestinal tract, such as hepatocellular carcinoma, pancreatic adenocarcinoma, gastric and colorectal cancer.⁴¹ Despite the high sequence homology between the two enzymes and their apparently redundant functions, they may have contrasting roles in the regulation of cancer processes.⁵⁶ In the case of hepatocellular carcinoma, for example, the negative regulation exerted by Sulf1 on the FGF pathway appears to have a tumor suppressor effect reducing cell proliferation.⁵⁶ By contrast, Sulf2 activates the pathway and acts as an oncogene, resulting in proliferation and migration.⁵⁶ Immunocytochemistry and confocal microscopy experiments revealed that overexpression of Sulf2 correlates with increased levels of the heparan sulfate proteoglycan glypican 3 (GPC3), which is involved in upregulation of the Wnt pathway⁵⁴ and has been reported as an oncoprotein.⁵⁶

Consistent with opposing effects on the FGF pathways, Sulf1 is downregulated in 30% of hepatocellular carcinoma (HCC) primary tumors, while Sulf2 is overexpressed in 60% of cases. Poor prognosis was also observed in patients with HCC having high Sulf2 levels (Figure 2.15).⁴² Recurrence after surgery is also accelerated compared to patients with low Sulf2 levels.⁵⁴ In addition to hepatocellular carcinoma, up-regulation of Sulf2 protein correlates on the pathological level to onset of pancreatic⁶² and breast cancers and non-small cell lung carcinoma.⁴¹

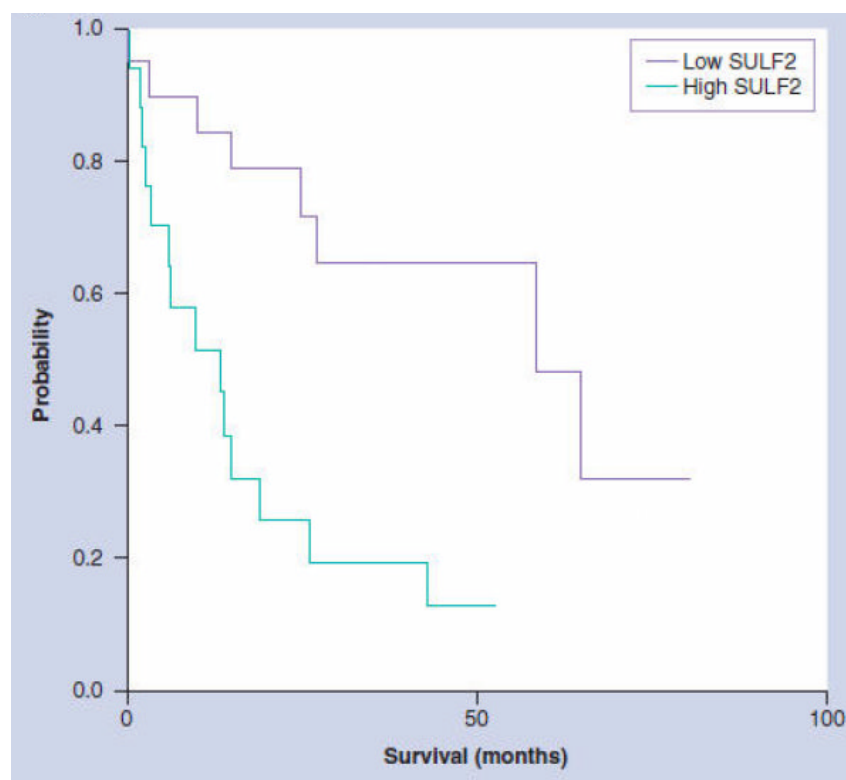


Figure 2.15 - Kaplan-Meier plots for patients affected by hepatocellular carcinoma.

High Sulf2 levels translate in poor prognosis. Reproduced from Lai, 2008.⁵⁶

The current understanding of the processes the endosulfatases participate in is limited and, to further complicate the picture, there is the possibility of different splicing variants of both enzymes being implicated. On the whole, the role of Sulf1 and Sulf2 is complex and further investigation is required to fully elucidate the roles of human endosulfatases in cancer. Such studies would be assisted by selective inhibitors of the respective enzymes. Both the endosulfatase activity and the extracellular localization of Sulf1 and Sulf2 may reduce the chances of selectivity issues against other intracellular sulfatases with exogenous inhibitors, thus making them an attractive target for drug discovery.

2.6 Targeting Sulf1 and Sulf2 with small-molecule inhibitors

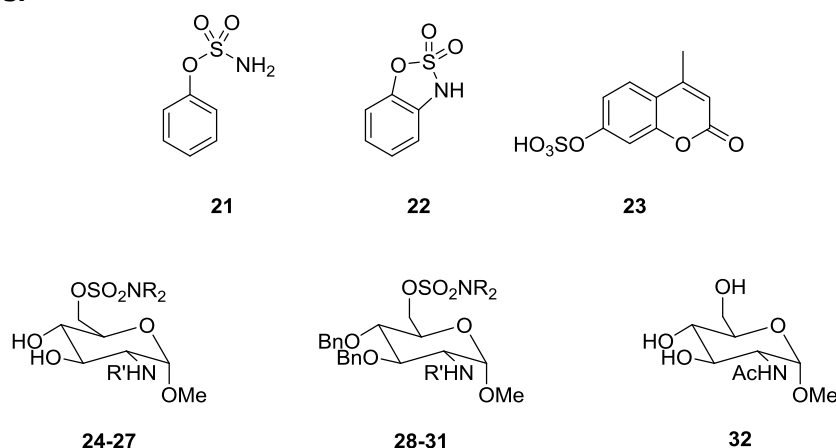
Aiming to characterize the composition of heparan sulfate, Saad and co-workers⁶³ developed an electrospray ionization-mass spectrometry (ESI-MS) based assay and tested Sulf2 activity against heparin oligomers. Little catalytic activity was observed towards digested heparin fragments smaller than a

trisulfated tetrasaccharide, suggesting that it might be difficult to inhibit these enzymes with molecular weights typical for small-molecule modulators. In 2009, Hossain *et al.*⁶⁴ reported that both Sulf1 and Sulf2 are inhibited by PI-88 (phosphomannopentose sulfate), a heparin mimetic antiangiogenic and antimetastatic agent, and gave further experimental evidence that a minimum of a tetrameric unit is required for binding to the target. Using a theoretical approach based on the structural data available on thirteen sulfatases, Lai *et al.*⁵⁶ observed that the residues in close proximity to the active formylglycine (5 Å radius) are equivalent in both Sulf1 and Sulf2. They therefore postulated that the site for substrate recognition in the endosulfatases might be located distant from the active site, in agreement with the model proposed by Milz.⁴⁴

A recent communication by Schelwies *et al.* in the context of research on inflammatory processes,⁵⁹ reported the synthesis and activity of the first small molecule saccharide-based inhibitors of Sulf1 and Sulf2. Their work was based on the incorporation of a sulfamate moiety, which had proven effective in the inhibition of the extensively studied steroid sulfatase. Schelwies and co-workers chose the small aryl sulfamates **21** and **22** as a starting point for their studies, as well as the sulfamoylated monosaccharides **24-27**, which can be regarded as heparan sulfate mimics. Finally, they tested a number of intermediates, **28-32**. The assay exploited the aryl sulfatase activity of Sulf1 and Sulf2 on 4-methylumbelliferyl sulfate (4-MUS, **23**) as a reporter substrate (see Chapter 4) to evaluate the inhibitory effect of the synthesized molecules. The resulting inhibition profiles of Sulf1 and Sulf2 (Table 2.2) did not differ considerably between the two enzymes, in agreement with what postulated by Lai *et al.*⁵⁶

Both the aryl sulfamate **21** and **22** and the monosaccharide molecules **24-32** proved to inhibit the human endosulfatases. The most potent compounds reported were the *N*-sulfated monosaccharides **24** (Sulf1: IC₅₀ = 95 µM; Sulf2: IC₅₀ = 130 µM) and **25** (Sulf1: IC₅₀ = 180 µM; Sulf2: IC₅₀ = 240 µM) which were more active than their acetamido-analogues **26** and **27**. The phenyl-based sulfamates **21** and **22** and the unsubstituted amines **28** and **29** were all less potent than the monosaccharides **24** and **25**. Interestingly, even though primary sulfamates were more potent than the *N,N*-dimethyl analogues, *N*-alkylation seemed to be well tolerated.

Table 2.2 - Structure and Sulf1/Sulf2 activities of aryl and monosaccharide sulfamates.⁵⁹



#	Compound	R	R'	Sulf1 activity	Sulf2 activity
1	21	-	-	~30% inhibition at 5 mM	~30% inhibition at 5 mM
2	22	-	-	~50% inhibition at 5 mM	~50% inhibition at 5 mM
3	24	H	SO ₃ Na	IC ₅₀ = 95 μM	IC ₅₀ = 130 μM
4	25	CH ₃	SO ₃ Na	IC ₅₀ = 180 μM	IC ₅₀ = 240 μM
5	26	H	Ac	40% inhibition at 5 mM	30% inhibition at 5 mM
6	27	CH ₃	Ac	~50% inhibition at 5 mM	~50% inhibition at 5 mM
7	28	H	H	~10% inhibition at 5 mM	~10% inhibition at 5 mM
8	29	CH ₃	H	~10% inhibition at 5 mM	~18% inhibition at 5 mM
9	30	H	SO ₃ Na	~85% inhibition at 5 mM	~65% inhibition at 5 mM
10	31	CH ₃	SO ₃ Na	~70% inhibition at 5 mM	~80% inhibition at 5 mM
11	32	-	-	~10% inhibition at 5 mM	~10% inhibition at 5 mM

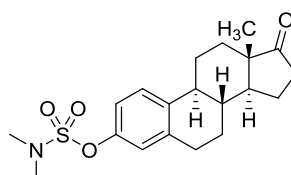
This study provides experimental evidence that inhibition of Sulf1 and Sulf2 by low molecular weight templates may be possible. It also represents the first structure-activity relationship (SAR) study on these enzymes in the literature and suggests that *N*-sulfation and 6-*O*-sulfamoylation of the monosaccharides appear to be crucial for inhibition of human endosulfatases. However, these results suggest that obtaining selectivity between Sulf1 and Sulf2 could be problematic with small molecules. The most active molecule in the series, monosaccharide **24**, was re-synthesized in the Medicinal Chemistry laboratories of the Northern Institute for Cancer Research by Duncan Miller⁶⁵ and tested in the assay developed

by Gary Beale and Sari Alhasan.⁶⁶⁻⁶⁸ The results published in the literature could not be reproduced and compound **24** proved inactive against Sulf2 (<10% inhibition at 1 mM).

2.7 Project aims and design of potential novel inhibitors

The present work is focused on the identification of a tool compound to enable target validation studies for the inhibition of the cancer-related extracellular sulfatase Sulf2, which seems to play an important role in hepatocellular carcinoma determining low survival rates and high frequency of recurrence after excision.⁵⁴ Following the communication by Schelwies *et al.*,⁵⁹ the synthesis of monosaccharide-based inhibitors was also successfully undertaken within the group.⁶⁵

Due to issues, both synthetic and pharmacokinetic, of developing and synthesizing saccharide-based inhibitors, it was desirable to undertake the development of non-saccharide inhibitors. Although no crystal structure of the target enzyme was available, a large amount of data concerning another sulfatase linked to cancer, steroid sulfatase (STS), was available in the literature demonstrating the key role of the sulfamate group as a sulfate isoster. The most potent known inhibitor of steroid sulfatase, EMATE **12** (IC_{50} <0.1 nM in an intact MCF-7 cell-based assay), bears a primary sulfamate moiety on an estrogen scaffold. In contrast, the tertiary sulfamate analogue **33** effectively inhibits STS with a reversible mode of action, but is less potent than EMATE **12** (90%, 87% and 79% inhibition at 10, 1.0 and 0.1 μ M, respectively, in MCF-7 cells).³³ In further lead discovery studies, the primary sulfamate moiety was retained while changing the estrogenic scaffold to avoid undesirable off-target effects.



33

In the current study, a similar approach was taken with the aim of understanding SARs for low molecular weight aromatic sulfamates. The design and synthesis of compounds bearing a sulfamate attached to a diversely substituted aromatic ring

(**34** and **35**) was undertaken in an attempt to investigate whether a well-designed aromatic molecule could efficiently bind to the active site of Sulf2.

Introduction of substituents onto the aryl scaffold allowed determination of SAR for steric and electronic requirements for effective inhibition of Sulf1 and Sulf2.⁶⁵ To further explore the scope of arylsulfamate-based motifs, a second set of potential tool molecules was devised based on the 3D structure of the dimeric repetitive units of heparan sulfate. As shown in Figure 2.16, the sulfamate moiety was retained at the 3-position of phenyl ring A, while incorporation of a range of substituents, such as carboxylic acids, esters, amines and *N*-sulfates, in different positions on phenyl ring B was explored to attempt to identify binding interactions that might be exploited in the further development of a tool compound (**36** and **37**). Finally, since the HS substrate consists of saturated heterocyclic rings, a non-aromatic B ring was attached to the 3-position of the aromatic ring A to explore whether this could improve inhibition. This non-aromatic B ring was further functionalized with hydroxyl and *N*-sulfate moieties in the 2- or 4-position to attempt to identify beneficial polar interactions within the enzyme active site.

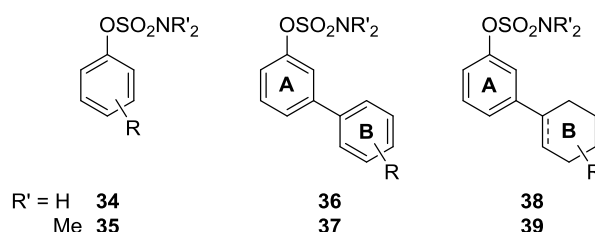


Figure 2.16 - Generation of three scaffolds of tool molecules for preliminary studies on the inhibition of Sulf2.

CHAPTER 3. RESULTS AND DISCUSSION - SULF2

No structural data were available for Sulf2 at the start of the project but a review of the literature of sulfatase inhibitors revealed that the sulfamate group is a common pharmacophoric feature in inhibitors of sulfatases.^{20,33,35,59,69} The first targets were designed as tool molecules aiming to build an understanding of structural features important for Sulf2 inhibition to direct the more focused design of potential inhibitors. Assay development was investigated in parallel with compound synthesis. Unfortunately, the isolation of catalytically active protein proved challenging, and inhibition data were generated after the synthesis of all compounds had been completed.

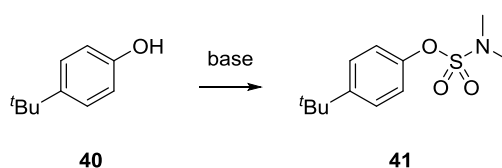
3.1 Synthesis of *N,N*-dimethylsulfamates

3.1.1 Synthesis of a library of phenyl *N,N*-dimethylsulfamates

The endogenous substrate of Sulf2 is heparan sulfate, a polysaccharide. As most sulfatases are able to catalyze desulfation of small aryl sulfate substrates, it was therefore desirable to investigate the activity of the target enzyme towards aromatic systems. Compared to carbohydrates, the chemistry of aromatic rings offers a number of advantages, such as the presence of a chromophore, ease of synthesis because of the absence of stereochemistry, commercial availability of a variety of starting materials and a wide scope of reactions for further manipulation of the building blocks. A small library of phenyl *N,N*-dimethylsulfamates was synthesized to be screened against Sulf2 for developing SARs. In parallel, Duncan Miller synthesized a similar set of primary aryl sulfamates **65**. While these works were carried out, the communication by Schelwies *et al.*⁵⁹ confirmed the hypothesis that small aryl sulfamates weakly inhibit Sulf2.

To enable the synthesis of a group of diversely substituted aromatic tertiary sulfamates the limited number of procedures available in the literature were used as a starting point. Woo *et al.*³⁶ reported the synthesis of *N,N*-dimethylsulfamates from phenols using a large excess of triethylamine (10 equiv.) and *N,N*-dimethylsulfamoyl chloride, (Me₂NSO₂Cl, 14 equiv.) in DCM. The sulfamoylating

agent, $\text{Me}_2\text{NSO}_2\text{Cl}$, is classified as a potential carcinogen and proved to be stable to an aqueous work-up (TLC monitoring; petrol ether 100%), prompting the pursuit of a safer procedure to avoid having to handle crude product and waste stream containing the toxic substance. Quasdorf and co-workers⁷⁰ were able to use just 1.2 equiv. of dimethylsulfamoyl chloride in their synthesis of aryl dimethylsulfamates, employing sodium hydride to obtain the reactive phenolate ion. In an attempt to identify safer conditions, an optimization study of the sulfamoylation reaction was undertaken prior to embarking in the synthesis of a library of aromatic dimethylsulfamates. 4-*tert*-Butylphenol **40** was chosen as a model system (Scheme 3.1).



Scheme 3.1 - Synthesis of *N,N*-dimethylsulfamates.

Addition of *N,N*-dimethylsulfamoyl chloride (1.5 equiv.) to a suspension of the phenol and K_2CO_3 in acetonitrile at 0 °C yielded the desired (4-*tert*-butyl)phenyl dimethylsulfamate **41** in 24% yield. The reaction proceeded without formation of side products and the sulfamate **41** was obtained pure after work-up without further purification. Nonetheless, the product was obtained in modest yield.

Table 3.1 - Optimization of the sulfamoylation of 4-*t*-butylphenol.

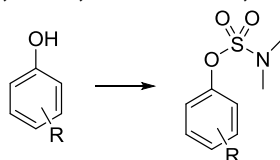
#	Base	Solvent	Phenol (equiv.)	Base (equiv.)	Heating method	Time	T (°C)	Conversion ^a %
1	K_2CO_3	MeCN	1.5	1.7	C	8 d	up to 40	65
2	NaH	DMF	1.5	1.7	C	3 d	up to 35	68
3	Cs_2CO_3	MeCN	1.5	1.7	C	22 h	18	> 99
4	Cs_2CO_3	MeCN	1.5	1.7	M	30 min	up to 150	66

C = conventional heating. M = microwave heating. ^a Determined by LC-MS UV trace.

The effect of the base was investigated for the sulfamoylation of 4-*tert*-butylphenol **40** (Table 3.1). Complete conversion of the starting material was only obtained using cesium carbonate in acetonitrile at room temperature (Table 3.1 - Entry 3) while potassium carbonate and sodium hydride did not lead to a conversion higher than 70%, even upon gentle heating over several days (Table 3.1 - Entries 1 and 2). Aiming at reducing the reaction time, microwave heating was applied to the most successful reaction conditions, but the reaction did not proceed to completion under these conditions. The conditions in Entry 3 were chosen as standard for the synthesis of the library of aryl dimethylsulfamates. Isolated yields are summarized in Table 3.2.

Table 3.2 - Summary of yields for the sulfamoylation of phenols

Reagents and conditions: phenol, base, Me₂NSO₂Cl, MeCN, 0 °C then RT, 18 h.



#	Compound	R	Yield %	#	Compound	R	Yield %
1	41	4- <i>t</i> -Bu	24 ^{a,c}	11	51	4-CF ₃	33 ^b
2	42	4-OMe	74 ^a	12	52	3-CF ₃	47 ^b
3	43	3-OMe	63 ^b	13	53	2-CF ₃	52 ^b
4	44	2-OMe	43 ^b	14	54	4-Cl	93 ^b
5	45	4-CN	71 ^b	15	55	4-Ph	90 ^a
6	46	3-CN	58 ^b	16	56	3-Ph	75 ^b
7	47	2-CN	92 ^b	17	57	2-Ph	72 ^b
8	48	4-NO ₂	49 ^b	18	58	H	27 ^b
9	49	3-NO ₂	>99 ^b	19	59	3-Br	73 ^b
10	50	2-NO ₂	94 ^b				

^a Base was potassium carbonate.

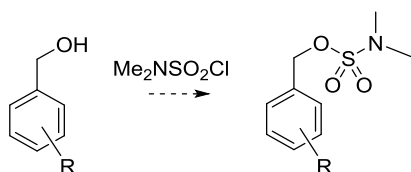
^b Base was cesium carbonate.

^c Phenol was the limiting reagent.

The optimized sulfamoylation conditions gave good yields for most compounds. Moderate yields were obtained with methoxy- at the 2-position **44** (Table 3.2 - Entry 4), nitro- at the 4- position **48** (Table 3.2 - Entry 8) and in general when a trifluoromethyl substituent was present anywhere on the ring (Table 3.2 - Entries 11-13).

3.1.2 Attempted synthesis of a library of benzyl *N,N*-dimethylsulfamates

With the purpose of mimicking the 6-*O*-sulfate group of the endogenous substrate of Sulf2, a second small library of benzylic tertiary sulfamates was targeted from benzyl alcohols using a similar synthetic approach to that described for the phenyl series (Scheme 3.2).

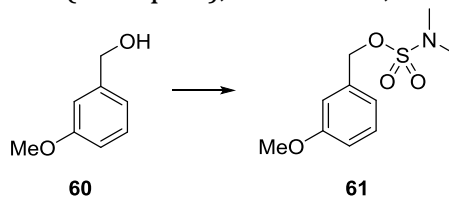


Scheme 3.2 - Approach to the synthesis of benzyl *N,N*-dimethylsulfamates.

To investigate this reaction, 3-methoxybenzyl alcohol **60** was selected as a model system to obtain the product **61**. The reaction conditions tested are summarized in Table 3.3. Using the procedure optimized for phenols described above (Table 3.3- Entry 1) no products were formed. This is likely to be explained by the Cs₂CO₃ (conjugate acid p*K*_a ~10) being too weak base to deprotonate the benzylic alcohol (conjugate acid p*K*_a ~16) required for reaction with the dimethylsulfamoyl chloride. Stronger bases, such as sodium hydride (conjugate acid p*K*_a ~35), sodium bis(trimethylsilyl)amide (conjugate acid p*K*_a ~26) and potassium *tert*-butoxide (conjugate acid p*K*_a ~17), were therefore investigated, but in each case a complex mixture was obtained with no evidence of formation of the desired product (Table 3.3 - Entries 2 to 4). A pyridine/DMAP system led to the formation of two products by LC-MS, but purification on silica led to degradation with only several minor impurities being recovered (Table 3.3 - Entry 5). Similar results were obtained following a literature procedure⁷¹ in the absence of base (Table 3.3 - Entry 6). These observations suggest that the desired benzyl dimethylsulfamate **61** may be chemically unstable and, as a consequence, these targets were not pursued further.

Table 3.3 - Screening of reaction conditions for the synthesis of 3-methoxybenzyl dimethylsulfamate 61.

Reagents and conditions: base (1.7 equiv.), Me₂NSO₂Cl, solvent, 0 °C then RT, 18 h.



#	Base	Solvent	Temperature (°C)	Result
1	Cs ₂ CO ₃	MeCN	0	Complex mixture
2	NaH (60%)	THF	-30	Complex mixture
3	NaHDMS	THF	-30	Complex mixture
4	KO ^t Bu	THF	0	Complex mixture
5	Py/DMAP	THF	0	2 main peaks
6	No base	PhCH ₃ /DMA	0	2 main peaks

3.1.3 Synthesis of a library of biphenyl *N,N*-dimethylsulfamates

The structure of the endogenous substrate of Sulf2 was used as a template to guide the design of a second round of phenyl sulfamates. The observation by Hossain *et al.*⁶⁴ (see Section 2.6) that an oligosaccharide may be required for binding to Sulf2 suggested that it may be necessary to develop higher molecular weight scaffolds to allow further interaction between the inhibitor and the Sulf2 protein in order to obtain potent Sulf2 inhibitors. With an optimized procedure for the introduction of the dimethylsulfamate group onto phenols, it was desirable to build onto the phenyl core in an attempt to incorporate features which may mimic the dimeric unit of heparan sulfate. Molecular modelling by Duncan Miller suggested that 3-substituted biphenyls of the class shown in Figure 3.1 might effectively reproduce the three-dimensional arrangement of substituents in a heparan sulfate disaccharide.

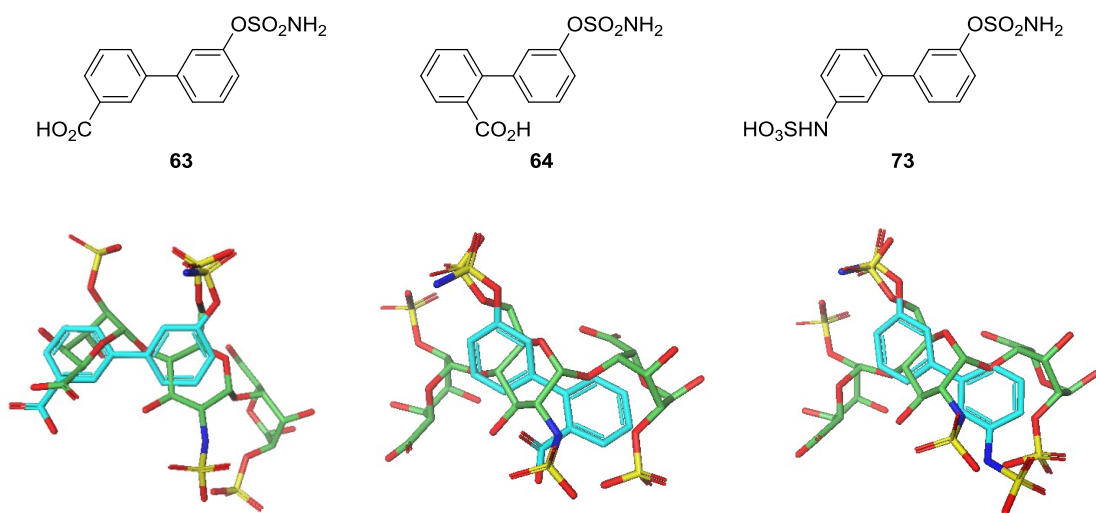
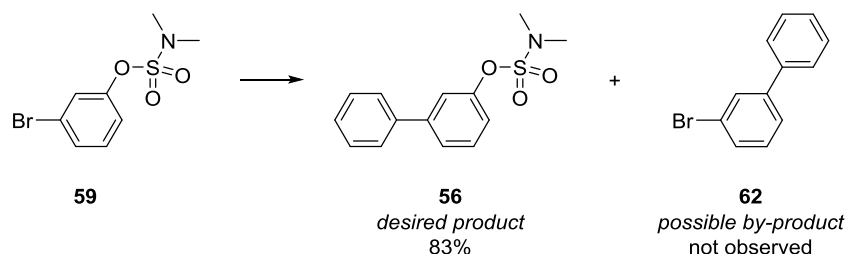


Figure 3.1 - Overlap of a heparan sulfate disaccharide unit with the primary [1,1'-biphenyl]-3-yl sulfamate analogues of 63, 64 and 73, respectively.

It was envisaged introducing the second aryl ring *via* palladium-catalyzed formation of a carbon-carbon bond under Suzuki-Miyaura conditions by coupling of 3-bromophenyl dimethylsulfamate **59** to a series of phenyl boronic acids. A publication by Macklin and Snieckus⁷² reported the coupling of bromoaryl *N,N*-diethyl sulfamates with retention of the sulfamate moiety, and reaction taking place at the bromo centre. However, a growing body of literature reported reactions in which the boronic acid coupling-partner may substitute the sulfamate group in the presence of nickel-based catalysts.^{70,73-74} More recently, examples of palladium-catalyzed Suzuki-Miyaura reaction at the sulfamate centre have also been described, using either boronic acids⁷⁵ or potassium organofluoroboranes as coupling partners.⁷⁵⁻⁷⁶ Thus, for the palladium-catalyzed reaction between sulfamate **59** and phenylboronic acid, two pathways were deemed possible, to form either biphenyl sulfamate product **56** or the bromo-biphenyl **62** (Scheme 3.3).



Scheme 3.3 - Alternative cross-coupling products.

Reagents and conditions: phenylboronic acid, Na₂CO₃ (2 M, aq.), Pd(PPh₃)₄, DME, reflux, 18 h.

The cross-coupling was attempted under reaction conditions of Macklin and Snieckus for the re-synthesis of biphenyl sulfamate **56** using 1,2-dimethoxyethane (DME) as solvent and tetrakis(triphenylphosphine)palladium as catalyst at the presence of aqueous Na₂CO₃ as base. The desired sulfamate **56** was obtained in good yield (83%) with no evidence of coupling reaction at the sulfamate centre (**62**). A library of diversely substituted biphenyl dimethylsulfamates was designed aiming to introduce polar groups such as carboxyl (**63**, **64**, **65**), amino (**69**, **70**, **71**) and aminosulfates (**72**, **73**, **74**) around the B-ring. The methyl esters (**66**, **67**, **68**) and the acetanilide (**75**, **76**, **77**) analogues were also of interest to investigate whether these groups may form stabilizing interactions with Sulf2. The introduction of polarity *via* a pyridine B-ring (**78**, **79**, **80**) was also assessed. As the boronic acids were available in-house, the 3'-cyano-, 4'-methoxy- and 4'-hydromethyl biphenyl sulfamates **81**, **82** and **83**, respectively, were included among the target compounds. The latter compound was subjected to sulfation to give the corresponding hydroxymethylsulfate **84** (Figure 3.2).

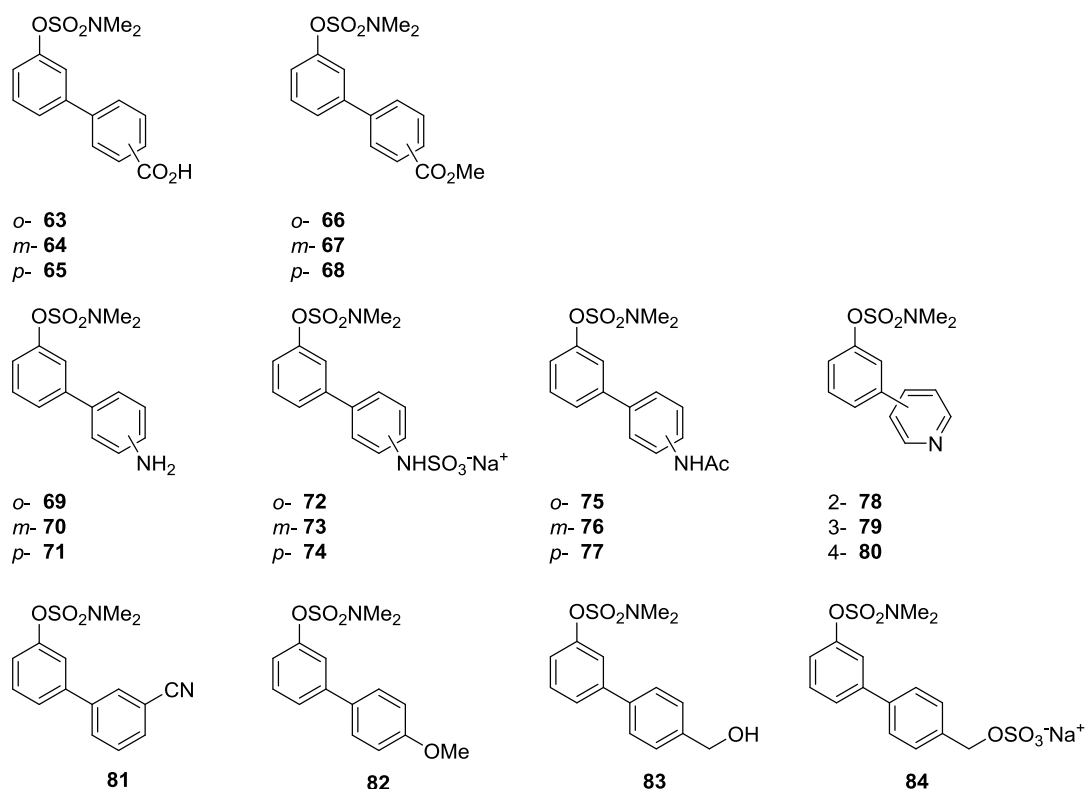


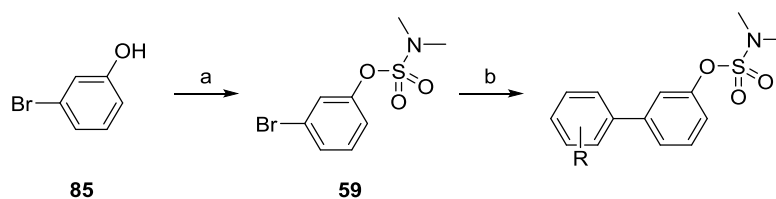
Figure 3.2 - Library of diversely substituted [1,1'-biphenyl]-3-yl dimethylsulfamates.

Synthesis of **81**, **82**, **83**

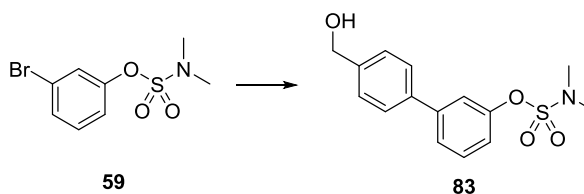
Following the literature procedure described previously and using the appropriate commercially available boronic acids, **81**, **82** and **83** were obtained in moderate yields (Table 3.4), with an overnight reaction (18 h) being required.

Table 3.4 - Summary of yields for the synthesis of a range of biphenylsulfamates.

Reagents and conditions: **a)** Cs₂CO₃, Me₂NSO₂Cl, MeCN, 0 °C then RT, 18 h, 73%; **b)** boronic acid, Na₂CO₃ (2 M, aq.), (PPh₃)₄Pd(0), DME, reflux, 18 h.



#	Compound	R	Yield %
1	81	3'-CN	38
2	82	4'-OMe	63
3	83	4'-CH ₂ OH	37



Scheme 3.4 - Model reaction for the optimization of C-C bond formation.

The coupling of *N,N*-dimethyl 3-bromophenylsulfamate **59** with 4-hydroxymethylboronic acid to give the hydroxymethylbiphenyl compound **83** (previously obtained in 37% yield) was chosen as a model system to identify conditions which would allow high yields to be obtained for further analogues (Scheme 3.4). Starting material and product were well resolved by LC-MS, offering a rapid method for monitoring the reaction and to assess the degree of conversion. In an attempt to reduce reaction time, microwave heating was investigated. All

reactions were performed on a 20 mg-scale for a fixed time and analyzed by LC-MS of the reaction mixture. To investigate the effect of temperature, a reaction mixture prepared as described in the literature⁷² was heated for 5 min under microwave irradiation at increasing temperatures.

Table 3.5 - Effect of temperature on the conversion in the Suzuki-Miyaura coupling step.

Conversion is reported as the area of the product peak in the LC-MS chromatogram normalized for the area of the peaks analyzed.

Reagents and conditions: **59** (1 equiv.), 4-hydroxymethylphenylboronic acid (1 equiv.), Na₂CO₃ (aq., 2 M, 2 equiv.), Pd (PPh₃)₄ (0.05 equiv.), DME, μ W, 5 min.

#	Temperature [°C]	Conversion [normalised product %]
1	60	0
2	80	66
3	100	54
4	120	62
5	140	62

As shown in Table 3.5, temperatures below 80 °C gave no conversion. At a temperature of 100 °C or above there was no improvement in conversion, and an increase in the number and amount of by-products was observed. For subsequent optimization reactions, the temperature was fixed at 80 °C. In the second instance, the effects of both solvent and catalyst were examined (Table 3.6). Alongside standard conditions using 1,2-dimethoxyethane and tetrakis(triphenylphosphine) palladium, dioxane and acetonitrile were evaluated as solvents and four catalyst systems commonly used in Suzuki reactions were tested, *i.e.* Pd(dba)₂/Xantphos, Pd(dppf)Cl₂, bis(tri-*tert*-butylphosphine)Pd, and Pd(dtbpf)Cl₂, thus generating an optimization matrix. The results are summarized in Table 3.6. Pd(dba)₂/Xantphos did not effectively catalyze the reaction in any of the solvents used. All the other systems gave a conversion of 53-70%. However, Pd(dppf)Cl₂ in DME gave an improved 82% conversion. As a consequence, this set of conditions was taken on to further optimization.

Table 3.6 - Effects of solvent and catalyst on the conversion in the Suzuki-Miyaura coupling step.

Conversion is reported as the area of the product peak in the LC-MS chromatogram normalized for the area of the peaks analyzed.

Reagents and conditions: **59** (1 equiv.), 4-hydroxymethylphenylboronic acid (1 equiv.), Na₂CO₃ (aq., 2 M, 2 equiv.), Pd catalyst (0.05 equiv.), solvent, μ W 80 °C, 6 min.

Catalyst Solvent	[Pd(PPh₃)₄]	Pd(dba)/ Xantphos	Pd(dppf)Cl₂	Bis(tri-<i>t</i>-Bu- phosphine)Pd	Pd-118
DME	66	0	82	54	70
Dioxane	62	0	62	66	61
Acetonitrile	53	0	58	60	63

For optimization of the base, three carbonates were investigated (Table 3.7). Potassium carbonate led to a 52% of conversion while cesium carbonate, gave 71% conversion. Sodium carbonate (Table 3.7 - Entry 1), the base used in the original procedure, resulted in the best conversion and on scale-up these conditions (DME, aq. Na₂CO₃ 2 M, Pd(dppf)Cl₂, μ W 80 °C) gave the 4-hydroxymethylbiphenyl sulfamate **83** in 76% isolated yield, which compared favorably with the 37% obtained following the literature protocol. A major advantage of the optimized procedure was the modification of the catalytic system. The use of tetrakis(triphenylphosphine)palladium, led to oxidation of the triphenylphosphine ligand to triphenylphosphine oxide and resulted in a difficult separation when isolating polar products, such as anilines and carboxylic acids. The newly optimized reaction conditions were applied to the synthesis of the majority of the compounds in the biphenylsulfamate library.

Table 3.7 - Effect of base on the conversion in the Suzuki-Miyaura coupling step.

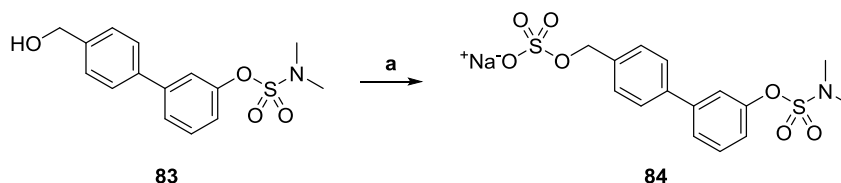
Conversion is reported as the area of the product peak in the LC-MS chromatogram normalized for the area of the peaks analyzed.

Reagents and conditions: **59** (1 equiv.), 4-hydroxymethylphenylboronic acid (1 equiv.), base (aq., 2 M, 2 equiv.), Pd(dppf)Cl₂ (0.05 equiv.), DME, μ W 80 °C, 6 min.

#	Base	Conversion [normalised product%]
1	Na ₂ CO ₃	82
2	K ₂ CO ₃	53
3	Cs ₂ CO ₃	71

Sulfation of **83**⁷⁷⁻⁷⁸

To synthesize the benzyl sulfate **84** a sulfation procedure published in a patent⁷⁷ and optimized by Tristan Reuillon⁷⁹ was employed. The method uses sulfur trioxide pyridine complex as the sulfating agent and the desired sulfate is formed in DMF at room temperature and then converted to the more stable sodium salt by addition of a large excess of aqueous sodium hydroxide (10 equiv.). The desired sulfate **84** was isolated in moderate yield (33%; Table 3.5).



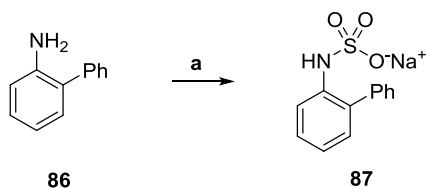
Scheme 3.5 - Sulfation of **83**.

Reagents and conditions: **a)** i) SO₃ · py, DMF, RT, 45 min; ii) aq. NaOH, RT, 1.5 h, 33%.

Synthesis of amino-[1,1'-biphenyl]-3-yl dimethylsulfamates and derivatives

In parallel with the optimization studies, the *o*- and *p*- amino-[1,1'-biphenyl]-3-yl dimethylsulfamates (**69** and **71**) were synthesized in good to excellent yield following the literature procedure of Macklin and Snieckus. However, a moderate yield (35%) was observed for the synthesis of the *meta*-substituted analogue **70**. Once the amino-compounds were available, it was intended to sulfate the aniline under the conditions described for the synthesis of **84**. Sulfation of the amino-group was first investigated using biphenyl aniline **86** as a model system lacking

the sulfamate group, with sodium [1,1'-biphenyl]-2-ylsulfamate **87** being obtained in 67% yield (Scheme 3.6).



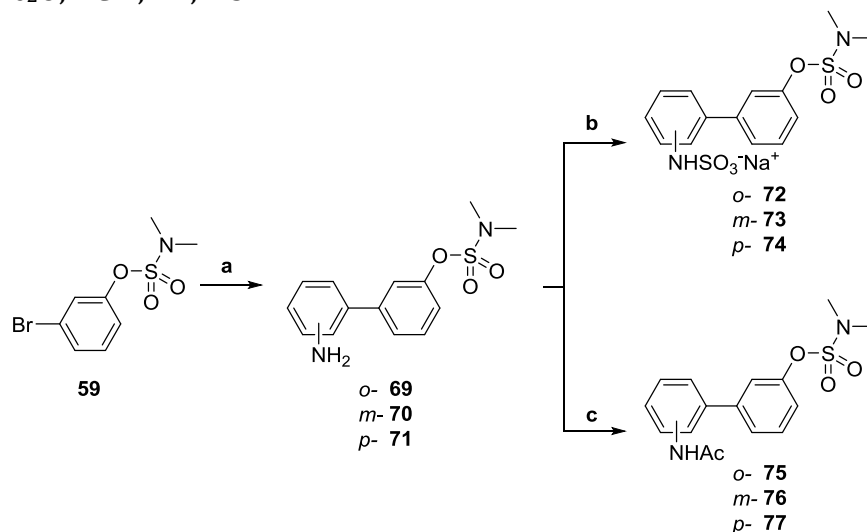
Scheme 3.6 - Synthesis of the sulfate 87.

Reagents and conditions: **a)** i) $\text{SO}_3 \cdot \text{py}$, DMF, RT, 45 min; ii) aq. NaOH, RT, 1.5 h, 67%.

Sulfation of **69**, **70** and **71** using this procedure gave high conversion for the *o*- and *p*-anilines (87% and 82%, respectively; isolated yield 73% and 58%), while conversion for **70** was lower (65%), as was the isolated yields (25%). The acetanilide analogues **75**, **76** and **77** were obtained in moderate to high yield upon treatment of the anilines with acetic anhydride.⁸⁰ Yields are summarized in Table 3.8.

Table 3.8 - Summary of yields for the synthesis of amino-[1,1'-biphenyl]-3-yl dimethylsulfamates and derivatives

Reagents and conditions: **a)** boronic acid/pinacol ester, Na_2CO_3 (aq., 2 M), $(\text{PPh}_3)_4\text{Pd}(0)$, DME, reflux, 18 h; **b)** i) $\text{SO}_3 \cdot \text{Py}$, DMF, RT, 45 min; ii) aq. NaOH, RT, 1.5 h; **c)** Ac_2O , DCM, RT, 1.5 h.



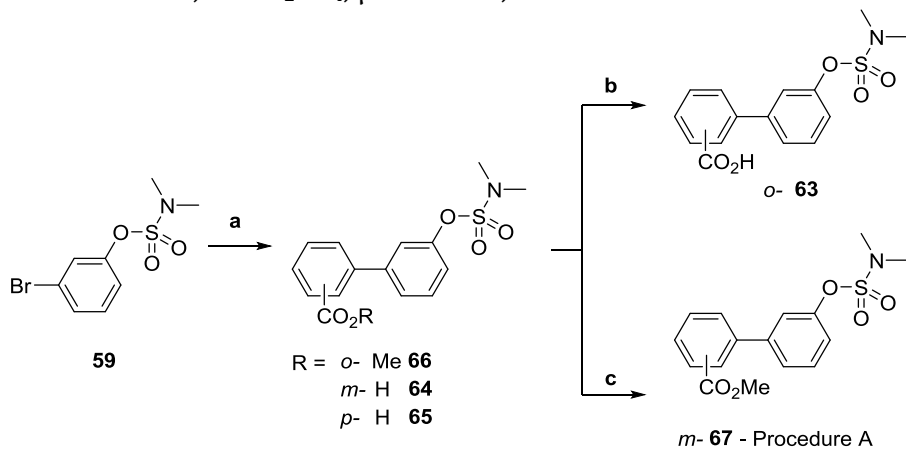
#		Product (isolated yield %) Step a	Product (isolated yield %) Step b	Product (isolated yield %) Step c
1	<i>o</i> -	69 (>99)	72 (73)	75 (>99)
2	<i>m</i> -	70 (35)	73 (76)	76 (69)
3	<i>p</i> -	71 (81)	74 (58)	77 (83)

Synthesis of a set of biphenyl carboxylic acids and their derivatives

The carboxy-functionalized biphenyl derivatives were synthesized by reaction of *N,N*-dimethyl 3-bromophenylsulfamate **59** under the optimized conditions for the microwave-assisted Suzuki-Miyaura cross-coupling. Commercially available boronic acids bearing either the free carboxy- group (*m*- and *p*-) or the corresponding methyl ester (*o*-) were used, according to availability. The methyl ester **66** was hydrolyzed using aqueous lithium hydroxide in THF at 40 °C, obtaining carboxylic acid **63** in quantitative yield. A microwave-assisted Fischer esterification (Procedure B) yielded the methyl ester **68** from acid **65** in moderate yield (57%). However, the same procedure applied to the carboxylic acid **64** gave low conversion with formation of by-products for the synthesis of **67**. An alternative method described by Brook and Chan⁸¹ (procedure A) was therefore applied to obtain the ester **67** using chlorotrimethylsilane in MeOH at room temperature. Under these conditions, complete conversion was reached and the product was isolated in good yield.⁸²⁻⁸³ Yields are summarised in Table 3.9.

Table 3.9 - Summary of yields for the synthesis of biphenyl sulfamates functionalized with a carboxylic acid or methyl carboxylate.

Reagents and conditions: **a**) boronic acid, Na₂CO₃ (aq., 2 M), Pd(dppf)Cl₂, DME, μ W 80 °C, 15 min; **b**) LiOH, H₂O/THF, 50 °C, 72 h; **c**) procedure A: TMSCl, MeOH, RT, 40 h; procedure B: MeOH, cat. H₂SO₄, μ W 100 °C, 1.5 h.



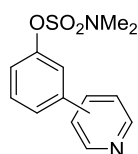
CN(C)S(=O)(=O)Oc1cccc(Br)c1 (**59**) $\xrightarrow{\text{a}}$ CN(C)S(=O)(=O)Oc1ccc(cc1)-c2ccc(cc2)C(=O)R
 R = *o*- Me **66**
 m- H **64**
 p- H **65**

CN(C)S(=O)(=O)Oc1ccc(cc1)-c2ccc(cc2)C(=O)OC (**66**) $\xrightarrow{\text{b}}$ CN(C)S(=O)(=O)Oc1ccc(cc1)-c2ccc(cc2)C(=O)O (*o*- **63**)
CN(C)S(=O)(=O)Oc1ccc(cc1)-c2ccc(cc2)C(=O)OC (**65**) $\xrightarrow{\text{c}}$ CN(C)S(=O)(=O)Oc1ccc(cc1)-c2ccc(cc2)C(=O)OC (*m*- **67** - Procedure A)
CN(C)S(=O)(=O)Oc1ccc(cc1)-c2ccc(cc2)C(=O)OC (**65**) $\xrightarrow{\text{c}}$ CN(C)S(=O)(=O)Oc1ccc(cc1)-c2ccc(cc2)C(=O)OC (*p*- **68** - Procedure B)

#		Product (isolated yield %) Step a	Product (isolated yield %) Step b	Product (isolated yield %) Step c
1	<i>o</i> -	66 (90)	63 (>99)	-
2	<i>m</i> -	64 (66)	-	67 (73)
3	<i>p</i> -	65 (68)	-	68 (57)

Synthesis of (pyridyl)phenyl sulfamates

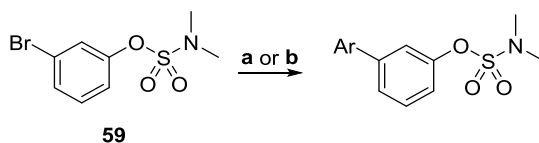
The 3-(pyridin-4-yl)phenyl and the 3-(pyridin-3-yl)phenyl dimethylsulfamates **79** and **80** were synthesized following the optimized Suzuki protocol (Table 3.10 - Entries 2 and 3). The use of thiol-functionalized polymer cartridges prior to purification was particularly important to remove all traces of catalyst which otherwise formed a complex with the pyridine nitrogen.



2- **78**
3- **79**
4- **80**

Table 3.10 - Summary of yields for the synthesis of the pyridinylphenyl dimethylsulfamates.

Reagents and conditions: a) K₂CO₃, Cu(OAc)₂, Pd(dppf)Cl₂, DMF, IPA, μ W 100 °C, 40 min; *b)* Na₂CO₃ (aq., 2 M), Pd(dppf)Cl₂, DME, μ W 80 °C, 20 min.



#	Ar	Starting material	Conditions	Product (isolated yield %)
1			a	78 (48)
2			b	79 (93)
3			b	80 (49)

The free 2-pyridylboronic acid was not commercially available because it is inherently unstable and, therefore, a different procedure was required to synthesize **78**. The stable equivalent *N*-methyliminodiacetic acid (MIDA) ester of 2-pyridylboronic acid was coupled to **59** under the conditions described by Knapp

and co-workers.⁸⁴ This procedure used isopropanol as co-solvent in place of water and involves the slow release *in situ* of 2-pyridyl boronic acid isopropyl ester in the presence of a copper(II) co-catalyst added to enhance the cross-coupling. The desired product was isolated in moderate yield (Table 3.10 - Entry 1). A recent publication by the same group suggested the use of Cu(diethanolamine)₂ in place of Cu(OAc)₂, which may allow a further improvement in yield for this reaction.⁸⁵

3.2 Stability studies on sample *N,N*-dimethyl sulfamates and sulfates

The stability of *N,N*-dimethylsulfamates to a range of different conditions was evaluated by means of HPLC and NMR analysis with a small number of the phenyl *N,N*-dimethylsulfamates synthesized.

3.2.1 Stability of 4-(trifluoromethyl)phenyl dimethylsulfamate **51**

By virtue of the destabilizing effect of the inductively electron-withdrawing trifluoromethyl group at the 4-position, 4-(trifluoromethyl)phenyl dimethylsulfamate **51** was chosen as a sample molecule for HPLC stability tests of the *N,N*-dimethyl sulfamate moiety under basic (both aqueous and anhydrous), acidic and reductive conditions. The substrate **51** was treated with sodium hydroxide in EtOH, sodium borohydride in EtOH, sodium hydride in THF and neat trifluoroacetic acid for 72 or 96 h and the residual amount of substrate **51** was monitored by HPLC. The results obtained indicated that the dimethylsulfamate moiety is stable to bases, both aqueous and anhydrous, and reducing agents, but rapidly degrades in the presence of strong acids, such as TFA (Figure 3.3).

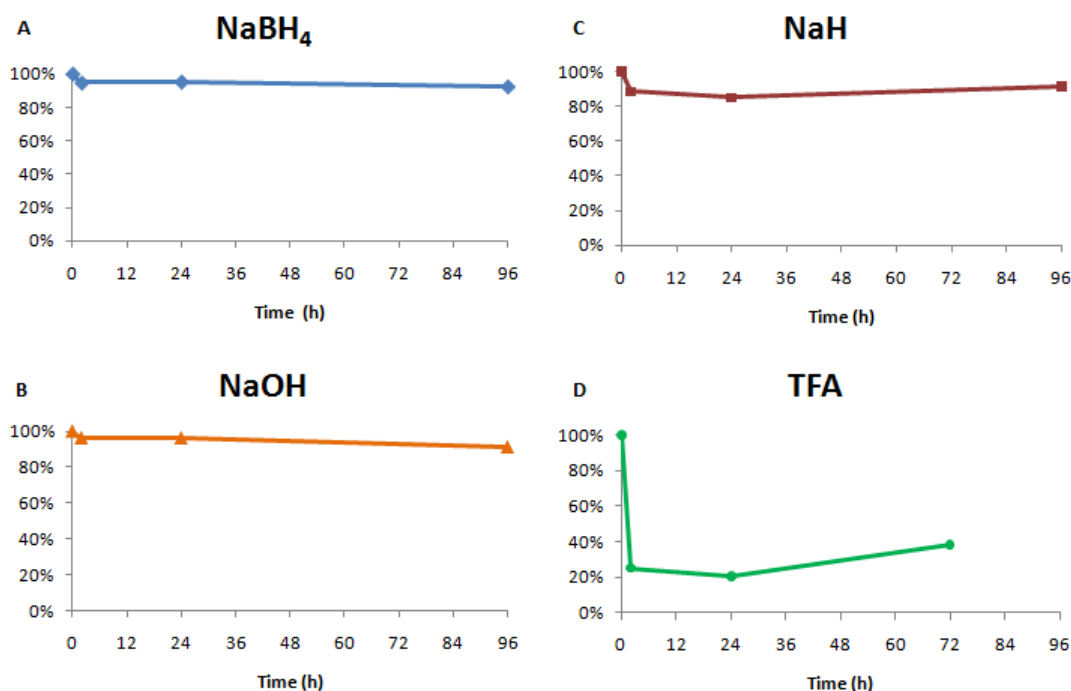


Figure 3.3 - HPLC stability studies on tertiary sulfamates.

Stability of sulfamate **51** in (A) basic anhydrous conditions; (B) basic aqueous conditions; (C) reductive conditions; (D) acidic conditions. Concentration of substrate is reported as percentage of the amount at $t = 0$ h. Replicates: $n=1$

3.2.2 Stability of *N,N*-dimethyl sulfamates in DMSO and MeOH

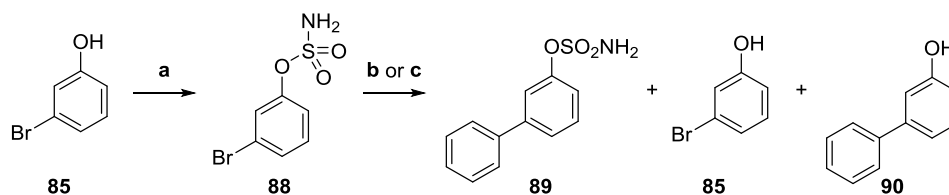
The biological evaluation requires the compounds to be stable in DMSO or, alternatively, in MeOH. Therefore, a range of dimethyl sulfamates was chosen to assess stability in d_6 -DMSO and d_4 -MeOD. The solutions were monitored periodically by ^1H -NMR spectroscopy over 24 h to assess for degradation.

Four test compounds were selected from the phenyl sulfamates bearing strongly electron-withdrawing groups: 3-cyanophenyl dimethylsulfamate **56**, 3-nitrophenyl dimethylsulfamate **49**, 2-nitrophenyl dimethylsulfamate **50**, and 3-(trifluoromethyl)phenyl dimethylsulfamate **52**. Additionally, the stabilities of the sodium sulfate salts **84**, **72** and **87** were evaluated. All molecules showed no evidence of degradation in both solvents over 24 h.

3.3 Suzuki-Miyaura cross-coupling of unprotected primary sulfamates

As described in Chapter 2, several studies on STS^{33,69} and the biological results published by Schelwies *et al.* on Sulf1 and Sulf2⁵⁹ suggested that tertiary

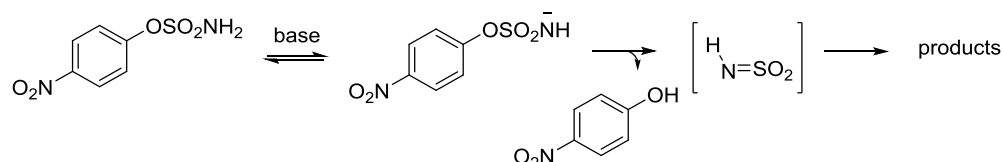
sulfamates (-OSO₂NMe₂) were less active as sulfatase inhibitors than their primary sulfamate counterparts (-OSO₂NH₂). To verify these observations and develop a SAR, matched pairs of primary and tertiary sulfamates in the phenyl and biphenyl series were required. A library of primary phenylsulfamates analogous to those discussed in Section 3.1.1 had been previously synthesized by Duncan Miller,⁶⁵ and hence the interest was focused on the synthesis of primary biphenylsulfamate analogues.



Scheme 3.7 Direct (unprotected) approach to the synthesis of biphenyl primary sulfamates.

Reagents and conditions: **a)** i) HCO₂H, ClSO₂NCO, 0 °C then RT, 3 h; ii) NH₂SO₂Cl, DMA, 0 °C then RT, 18 h, 87% over two steps; **b)** AQUEOUS CONDITIONS: base (aq., 2 M), Pd(dppf)Cl₂, DME, μ W 80 °C, 4 min; **c)** ANHYDROUS CONDITIONS: base, Pd(dppf)Cl₂, solvent, μ W 80 °C, 4 min.

Suzuki-Miyaura cross-coupling was investigated to obtain the target compounds by reaction of the 3-bromophenyl sulfamate **88**, obtained through sulfamoylation of 3-bromophenol **85** with fresh sulfamoyl chloride, NH₂SO₂Cl, with the appropriate boronic acid in the presence of palladium catalyst and base (Scheme 3.7). Unfortunately, the inherent lability of the -SO₂NH₂ group to basic conditions documented in the literature⁸⁶ was confirmed by Duncan Miller⁶⁵ by stability studies on the primary phenylsulfamate series.⁶⁵ Mechanistic studies⁸⁶ support the hypothesis that the parent phenol is generated *via* an E1Cb mechanism in the presence of base (Scheme 3.8).



Scheme 3.8 - Proposed mechanism for the decomposition of primary sulfamates in the presence of base.

In an attempt to tune the cross-coupling conditions to allow carbon-carbon bond formation to occur before degradation of the sulfamate, the 3-bromophenyl sulfamate **88** was synthesized according to the conditions optimized by Duncan Miller.⁶⁵ Thus reacting chlorosulfonyl isocyanate with formic acid generated fresh sulfamoyl chloride, which was used to sulfamoylate 3-bromophenol in DMA. Subsequently, a number of small-scale reactions of **88** with phenylboronic acid in the presence of a variety of bases were performed and the conversion of the bromosulfamate **88** into biphenyl sulfamate **89** was monitored by LC-MS (Table 3.11 - Entries 1-7). In addition to the normal aqueous conditions, the Suzuki coupling was performed in absence of water using sodium or cesium acetate as a base following a procedure from a recent publication (Table 3.11 - Entries 8-10).⁸⁷

Table 3.11 - Study on the Suzuki-Miyaura cross coupling of primary sulfamates.

#	BASE	Measured pH ^a	% 89 ^b	Yield % ^c
1	Sodium carbonate	11.9	29	22%
2	Monobasic sodium phosphate dihydrate	3.9	32	N/D
3	Monobasic sodium phosphate	4.0	0	N/D
4	Ammonium acetate	7.2	3	N/D
5	Sodium acetate	7.8	65	12%
6	Dibasic ammonium phosphate	8.5	0	N/D
7	Dibasic sodium phosphate	9.00 (0.5 M)	62	N/D
8	Sodium acetate in THF	-	67	≤5%
9	Sodium acetate in MeCN	-	28	N/D
10	Cesium acetate in THF	-	N/A	N/D

^a pH was measured for a 2 M aqueous solution of base at RT.

^b Percentages of the desired product from the LC-MS chromatogram (UV trace).

^c Isolated yield from a scale up of the reaction.

^d Water solubility 12.5 g/100 mL at 25 °C (0.88 M).

When following the reaction by LC-MS, four peaks could be identified: unconverted starting material **88**, desired product **89** and phenols **85** and **90** originating by desulfamoylation of **88** and **89**. Suzuki coupling under the

previously optimized reaction conditions using sodium carbonate reached 29% conversion and enabled isolation of the biphenylsulfamate **89** in 22% yield (Scheme 3.7). Weaker bases such as monobasic sodium phosphate and ammonium acetate did not improve conversion (Table 3.11 - Entries 2-4), while LC-MS chromatograms in the presence of slightly stronger bases, such as sodium phosphate dibasic and sodium acetate gave encouraging results (Table 3.11 - Entries 5 and 6). A scale-up of the reaction with sodium acetate was performed but difficulties in the separation of the four compounds found in the reaction mixture resulted in an isolated yield of only 12% with recovered starting material accounting for most of the remaining mass balance. Dibasic sodium phosphate also gave good conversion, but was not scaled-up as the same purification problems were foreseen.

The results obtained in anhydrous conditions were initially encouraging. The LC-MS profile of the reaction with cesium acetate suggested the formation of a 1:1 mixture of **89** and **90** (Table 3.11 - Entry 10), while sodium acetate seemed to be effective, as conversion reached 67% in THF (Table 3.11 - Entry 8) and 27% in MeCN (Table 3.11 - Entry 9). Again, a scale-up of the most successful anhydrous conditions resulted in poor isolated yield of the product **89**. To exclude the hypothesis of substrate-specific purification difficulties, the conditions reported in Table 3.11 - Entry 5 were also applied to the coupling of **88** with 4-hydroxymethylboronic acid but similar low isolated yields were obtained.

Further analysis of the experimental results highlighted that this approach was affected by several issues. The high UV absorption of the product **89** (λ_{max} 248 nm; ϵ /dm³ mol⁻¹ cm⁻¹ 49 000) compared to that of the starting material **88** (λ_{max} 256 nm; ϵ /dm³ mol⁻¹ cm⁻¹ 600) gave misleading conversion percentages. The formation of phenolic by-products made separation of the four compounds difficult due to the similar polarities of each sulfamate and its corresponding phenol.

A protecting group strategy introducing a non-polar chromophore on the primary sulfamates was therefore investigated by Tristan Reuillon⁷⁹ to improve base stability and to facilitate reaction monitoring and purification.

3.4 Synthesis of cyclohexylphenyl primary sulfamate mimics of heparan sulfate

In the attempt to access different spatial positioning of the polar groups relative to the sulfamate, three sulfated cyclohexylphenyl primary sulfamate molecules were designed: the 4-(3-(sulfamoyloxy)phenyl)cyclohexyl sulfates **91** and **92**, only differing for the relative *cis*- or *trans*- stereochemistry of the 1,4-substituents on the cyclohexyl ring, and *trans*-2-(3-(sulfamoyloxy)phenyl)cyclohexyl sulfate **93** (Figure 3.4).

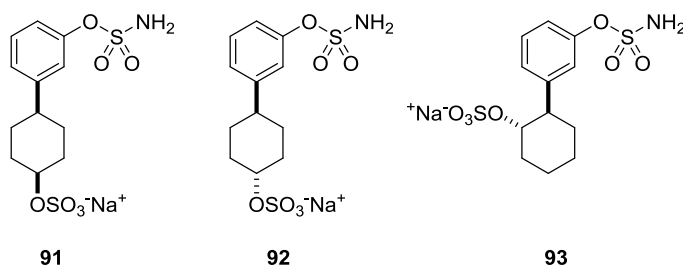


Figure 3.4 - Cyclohexylphenyl primary sulfamate mimics of heparan sulfate.

It was envisaged that sulfates **91** and **92** could be accessed, with or without dimethoxybenzyl (DMB) protection of the primary sulfamate, from the corresponding cyclohexanols *cis*- and *trans*- **95**, each obtained *via* an appropriate stereocontrolled reduction from the parent cyclohexanone **96**. The carbon-carbon bond between the aryl and the cyclohexane rings of **85** and **97** could be formed under Suzuki-Miyaura cross-coupling conditions from commercially available 3-bromophenol **85** and the easily accessible 4,4,5,5-tetramethyl-2-(1,4-dioxaspiro[4.5]dec-7-en-8-yl)-1,3,2-dioxaborolane **97** (Figure 3.5).

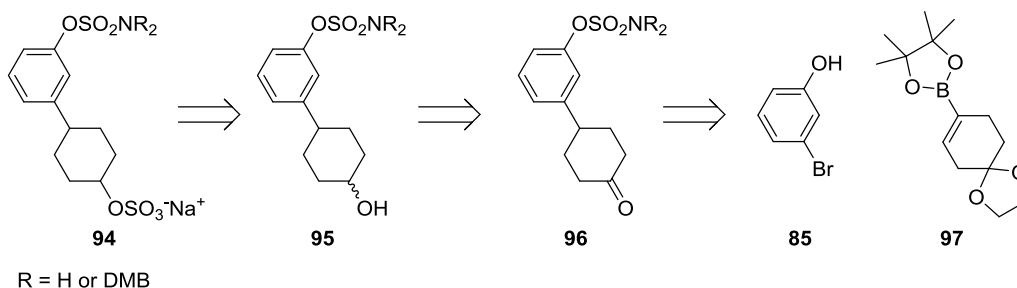


Figure 3.5 - Retrosynthetic approach to the synthesis of 91 and 92.

Similarly, a route to the 2-sulfate analogue **98** (with or without protection) was investigated by sulfation of the 3-(2-hydroxycyclohexyl)phenylsulfamate **99** obtained *via* hydroboration-oxidation of cyclohexene precursor **100** synthesized from phenol **85** and 2-(cyclohex-1-en-1-yl)-4,4,5,5-tetramethyl-1,3,2-dioxaborolane **101** (Figure 3.6).

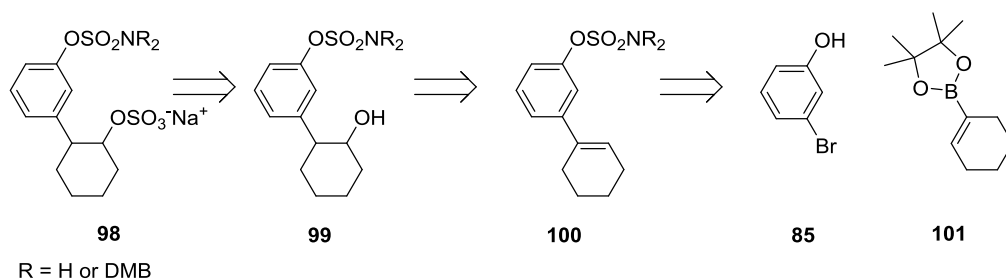
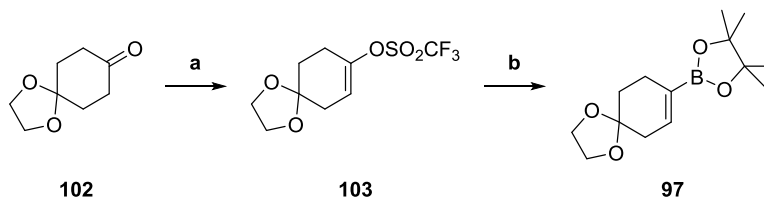


Figure 3.6 - Retrosynthetic approach to the synthesis of 93.

3.4.1 Synthesis of the boronic esters **97** and **101**

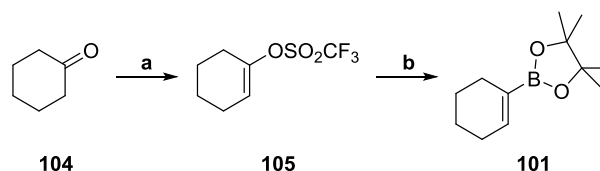
The boronic ester **97** was obtained by formation of the vinyl triflate (**103**) of the commercially available 1,4-dioxaspiro[4.5]decan-8-one **102** using KHMDS and *N*-phenylbis(trifluoromethanesulfonamide)⁸⁸ followed by Miyaura borylation⁸⁹ (Scheme 3.9).



Scheme 3.9 - Synthesis of the boronic acid 97.

Reagents and conditions: **a)** KHMDS (0.5 M in toluene), PhN(Tf)₂, THF, 96%; **b)** Pd(dppf)Cl₂, (Bpin)₂, KOAc, 1,4-dioxane, overnight, 80 °C, 94%.

The same approach was used to form the ester **101** (Scheme 3.10). An initial low yield for synthesis was related to the high volatility of vinyl triflate **105** and boronic ester **101** and was improved by avoiding heating during evaporation.

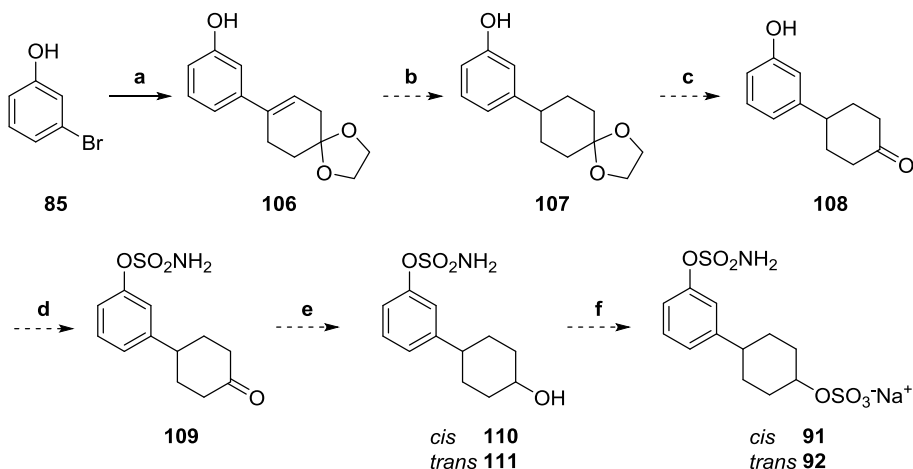


Scheme 3.10 - Synthesis of the boronic acid 101.

Reagents and conditions: **a)** KHMDS (0.5 M in toluene), PhN(Tf)₂, THF, 5 h, 65%; **b)** Pd(dppf)Cl₂, (Bpin)₂, KOAc, 1,4-dioxane, 80 °C, 3 h, 71%.

3.4.2 Attempted synthesis of 91 and 92 in the presence of an unprotected primary sulfamate moiety

The synthesis of **91** and **92** was first attempted without the use of protecting groups on the primary sulfamate. To avoid exposure of the primary sulfamate to basic conditions, the Suzuki coupling of **85** and **97** was performed in the first step of the synthesis. Catalytic hydrogenation of the double bond and acidic hydrolysis of the ketal would lead to the ketone **108**, which could be sulfamoylated on the phenolic OH to give sulfamate **109** (Scheme 3.11). The key step in the synthesis was the stereoselective reduction of the ketone to give either *cis*- stereoisomer **110** or its *trans*-alcohol **111**. Although one example of carbonyl reduction with sodium borohydride in the presence of a free primary sulfamate has been reported in a patent,⁹⁰ the reproducibility of the procedure was uncertain. Sulfation of the hydroxyl using sulfur trioxide pyridine complex followed by ion exchange chromatography to convert the sulfate into its sodium salt would yield the final targets **91** and **92** in six steps (Scheme 3.11).



Scheme 3.11 - Attempted route for the target compounds 91 and 92.

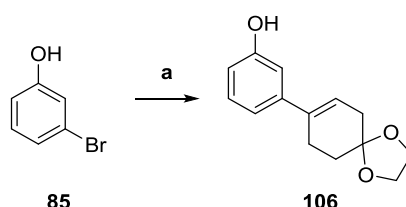
Reagents and conditions: **a)** **97**, Na₂CO₃ (aq., 2 M), Pd(dppf)Cl₂, DME, μ W 80 °C, 15 min, 28%; **b)** H₂, Pd/C 10%, EtOH, 60 °C; **c)** AcOH/H₂O/THF 20:10:3, 45 °C; **d)** i) HCO₂H, ClSO₂NCO, 0 °C then RT; ii) NH₂SO₂Cl in toluene, DMA, 0 °C then RT; **e)** NaBH₄, THF/EtOH 3:1, -78 °C to RT; **f)** i) SO₃ · py, DMF, RT; ii) ion exchange chromatography on Dowex 50W8×200 Na form, H₂O.

Suzuki-Miyaura cross-coupling of 3-bromophenol **85** was performed with the optimized conditions for bromophenylsulfamates. The reaction was difficult to monitor by both LC-MS and TLC because of the poor separation between starting material and product. After a problematic purification the desired product **106** was isolated in an unsatisfactory 28% yield.

In an attempt to obtain more synthetically useful yields at the start of the synthesis, three different approaches were undertaken.

Suzuki-coupling: approach A

Most of the examples of Suzuki coupling of phenols reported in the literature are performed with a benzyl- or methyl- protected phenol. In absence of a protecting group, yields tend to depend on reaction conditions and the nature of the coupling partners.⁹¹ Following a publication reporting the Suzuki coupling of free phenols in aqueous media using a ligandless Pd catalyst,⁹² the coupling of **85** and **97** was attempted using 10% palladium on carbon and aqueous potassium hydroxide as a base (Scheme 3.12). Although successful, the reaction yielded the desired product **106** with insufficient purity and in less than 50% yield and, therefore, this approach was not pursued further.

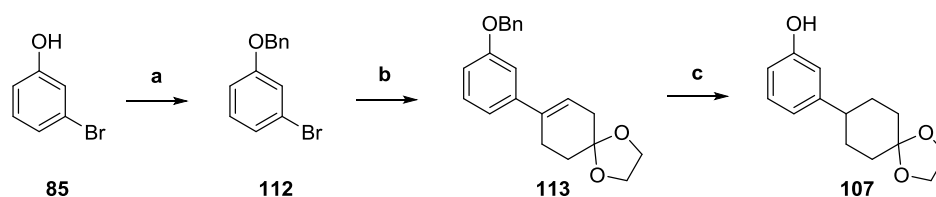


Scheme 3.12 - Suzuki coupling: approach A.

Reagents and conditions: **97**, 10% Pd/C, KOH (aq., 1 M), H₂O/EtOH, 135 °C, 3.5 h, 49%.

Suzuki-coupling: approach B

Protection of the phenolic OH of **85** with a benzyl group was investigated, as the protecting group could be removed by hydrogenation concurrently with the reduction of the alkene to give **107**, thus reducing the number of steps in the synthesis. The resulting 1-(benzyloxy)-3-bromobenzene **112** was coupled with the boronic ester **97** to give ketal **113** in good yield with straightforward purification and, finally, catalytic hydrogenation of **113** yielded the desired phenol **107**. The total yield of the desired ketal **107** was 52% over three steps (Scheme 3.13).

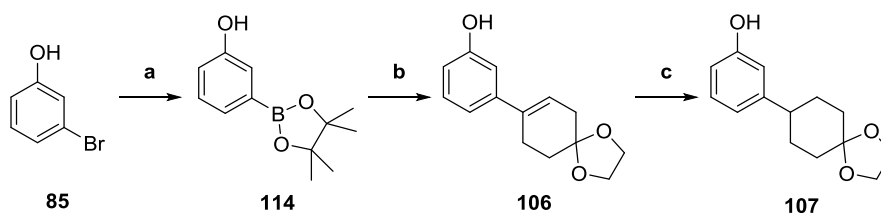


Scheme 3.13 - Suzuki coupling: approach B.

Reagents and conditions: **a)** K_2CO_3 , BnBr, acetone, 57 °C, 3 h, 89%; **b)** **97**, Na_2CO_3 (aq., 2 M), $Pd(dppf)Cl_2$, DME, μW 80 °C, 15 min, 75%, **c)** H_2 , 10% Pd/C, EtOH, 60 °C, 3.5 h, 78%.

Suzuki-coupling: approach C

The final strategy investigated (Scheme 3.14) involved reversing the coupling partners. Phenol **114**, obtained *via* Miyaura borylation from **85**, was the nucleophilic species reacting with triflate **103** (precursor of **97**) to give ketal **106**. Upon hydrogenation of the double bond, the overall yield to obtain the ketal **107** was 55%. The yield of approach C was comparable to that of approach B, but the synthesis was one step shorter (the triflate **103** was used, as starting material instead of the boronic ester **97** and no protection was needed) and, therefore, less time consuming. For this reason, approach C was chosen to continue the synthesis.



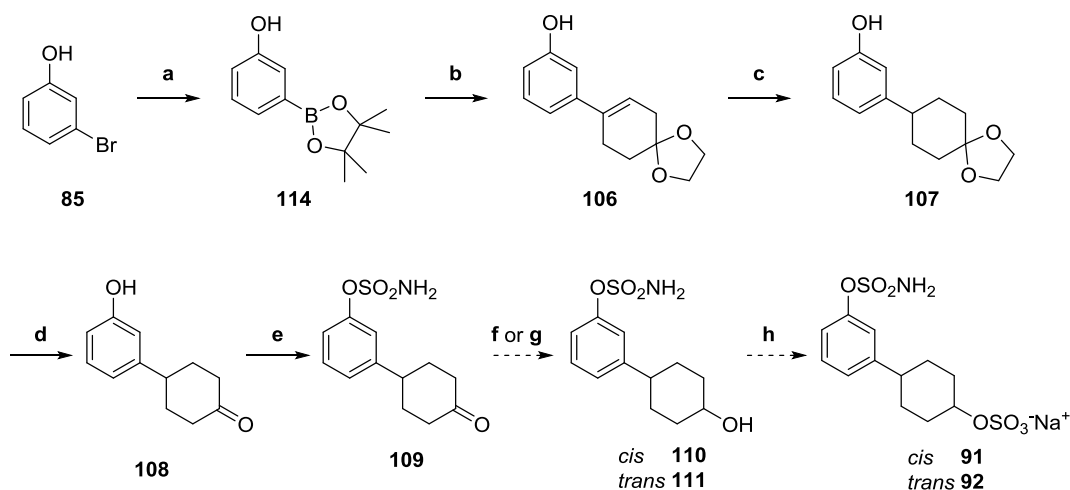
Scheme 3.14 - Suzuki coupling: approach C.

Reagents and conditions: **a)** $Pd(dppf)Cl_2$, $(Bpin)_2$, KOAc, 1,4-dioxane, 80 °C, 18 h, 91%; **b)** **103**, Na_2CO_3 (aq., 2 M), $Pd(dppf)Cl_2$, DME, μW 80 °C, 15 min, 64%; **c)** H_2 , Pd/C 10%, EtOH/THF 4:1, 40 °C, 1.5 h, 96%.

Utilizing approach C, the new route to targets **91** and **92** is depicted in Scheme 3.15. Once **107** was synthesized, the ketone was liberated under acidic conditions to obtain **108**. Despite the sulfamoylation of the phenol apparently leading to formation of sulfamate **109**, its purification proved troublesome and the product could not be isolated and fully characterized.

Once more, purification in the presence of unprotected sulfamate groups was problematic. At this point the dimethoxybenzyl (DMB) sulfamate protecting group emerged from work by Tristan Reuillon^{79,93} and efforts switched to using this

methodology to avoid the isolation issues in the synthesis of the sulfates **91**, **92** and **93**.

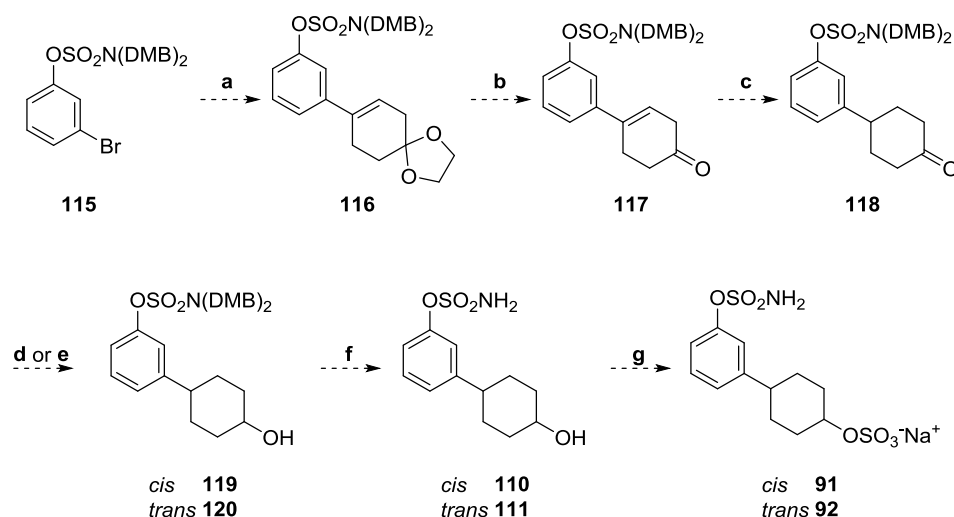


Scheme 3.15 - Revised route for the target compounds **91 and **92**.**

Reagents and conditions: **a**) (Bpin)₂, Pd(dppf)Cl₂, KOAc, 1,4-dioxane, 80 °C; **b**) **103**, Na₂CO₃ (aq., 2 M), Pd(dppf)Cl₂, DME, μ W 80 °C, 15 min, 64%; **c**) H₂, Pd/C 10%, EtOH/THF 4:1, 40 °C, 1.5 h, 96%; **d**) AcOH/H₂O/THF 20:10:3, 45 °C, 4 h, 77%; **e**) i) HCO₂H, ClSO₂NCO, 0 °C then RT, 3 h; ii) NH₂SO₂Cl in toluene, DMA, 0 °C then RT, 18 h; **f**) NaBH₄, THF/EtOH 3:1, -78 °C to RT; **g**) L-selectride, THF, -78 °C to RT; **h**) i) SO₃ · py (2 equiv.), DMF, RT; ii) ion exchange chromatography on Dowex 50W8×200 Na form, H₂O.

3.4.3 Sulfamate-protecting strategy applied to the synthesis of **91**, **92** and **93**

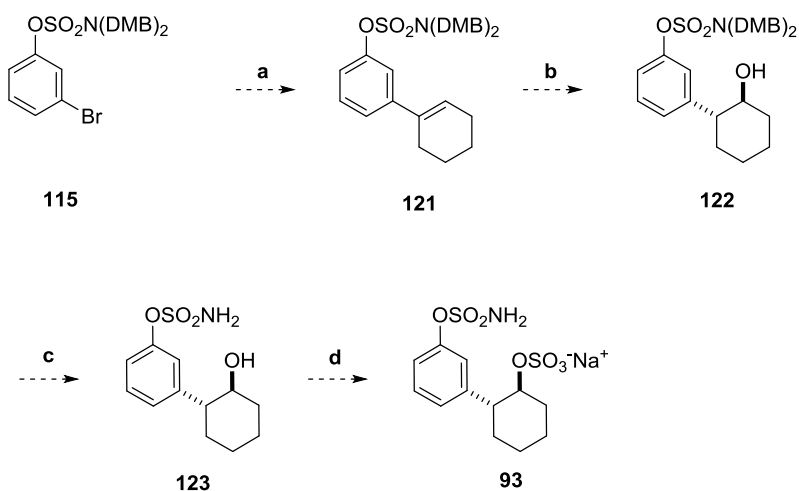
Each of the two primary sulfamate protons of the sulfamate moiety was protected with a dimethoxybenzyl (DMB) group to avoid desulfamoylation to the parent phenol. The presence of an apolar protecting group also facilitated isolation of the intermediates *via* column chromatography on silica. The protecting group can be removed at room temperature under mild acidic conditions. Upon synthesis of the common precursor **115** following the published route, Suzuki coupling with **97**⁹³ would afford the ketal **116**. Deprotection of the ketone followed by catalytic hydrogenation would generate intermediate **118**. Subsequent stereoselective reduction would yield either *trans*-alcohol **120** or *cis*-alcohol **119** that could be deprotected to give sulfamates **111** and **110**, respectively. Sulfation of the alcohol moiety would afford the desired target molecules **91** and **92** (Scheme 3.16).



Scheme 3.16 - Proposed route to the synthesis of 91 and 92.

Reagents and conditions: **a)** **97**, Na_2CO_3 (aq., 2 M), $\text{Pd}(\text{dppf})\text{Cl}_2$, DME, μW 80 °C; **b)** *p*-TSA, acetone/ H_2O , μW 60 °C; **c)** H_2 , Pd/C 10%, EtOH/THF 4:1, 40 °C; **d)** NaBH_4 , THF/EtOH 3:1, -78 °C to RT; **e)** L-selectride, THF, -78 °C to RT; **f)** TFA/DCM 9:1, RT; **g)** i) $\text{SO}_3 \cdot \text{py}$ (2 equiv.), DMF, RT; ii) ion exchange chromatography on Dowex 50W8×200 Na form, H_2O .

Similarly, coupling of **115** with the boronic ester **101** followed by hydroboration-oxidation of the cyclohexene intermediate **121** would yield the alcohol **122**. Finally, deprotection of the sulfamate group and sulfation of the 2-hydroxy group would afford the target sulfate **93** (Scheme 3.17).

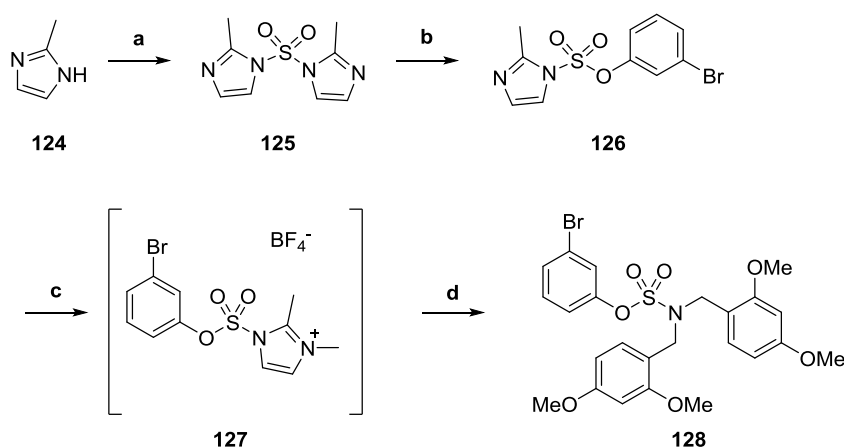


Scheme 3.17 - Proposed route to the synthesis of 93.

Reagents and conditions: **a)** **101**, Na_2CO_3 (aq., 2 M), $\text{Pd}(\text{dppf})\text{Cl}_2$, DME, μW 80 °C; **b)** i) $\text{BH}_3 \cdot \text{THF}$ (1.0 M), 0 °C; ii) NaOH , H_2O_2 , RT; **c)** TFA/DCM 9:1, RT; **d)** i) $\text{SO}_3 \cdot \text{py}$ (2 equiv.), DMF, RT; ii) ion exchange chromatography on Dowex 50W8×200 Na form, H_2O .

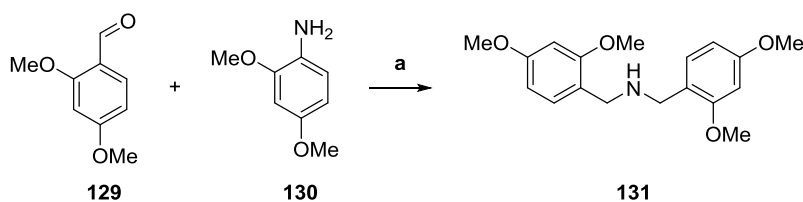
Synthesis of the protected 3-bromophenylsulfamate precursor 117

The bis(2,4-dimethoxybenzyl) protected 3-bromophenyl precursor **115** was synthesized by reaction of 2-methylimidazole **124** with sulfuryl chloride, followed by displacement of one of the imidazole groups of **125** by 3-bromophenol to obtain intermediate **126**. Methylation of the imidazole 3-nitrogen using trimethyloxonium tetrafluoroborate yielded the salt **127**, which was not isolated and was coupled directly with bis(2,4-dimethoxybenzyl)amine **131** to displace the dimethylimidazole (Scheme 3.18). The amine **131** was obtained by reductive amination from 2,4-dimethoxybenzylamine and 2,4-dimethoxybenzaldehyde (Scheme 3.19).



Scheme 3.18 - Synthesis of the bis(2,4-dimethoxybenzyl) protected 3-bromophenyl primary sulfamate 128.

Reagents and conditions: **a)** SO₂Cl₂, DCM, 0 °C to RT, 24 h, 68%; **b)** 3-bromophenol, Cs₂CO₃, MeCN, μ W 120 °C, 15 min, 90%; **c)** Me₃OBF₄, DCM, 0 °C to RT, 18 h; **d)** **131**, MeCN, RT, 8 h, 55% over two steps.

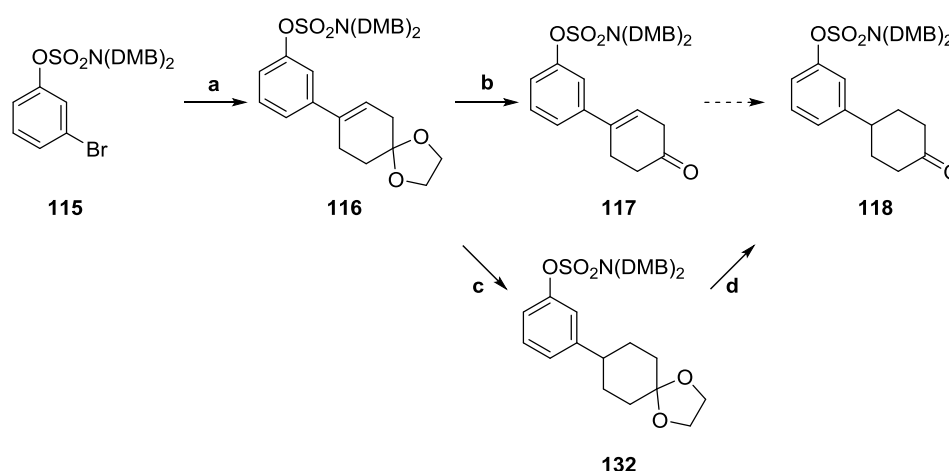


Scheme 3.19 - Synthesis of 2,4-dimethoxybenzylamine 131.

Reagents and conditions: **a)** i) EtOH, 78 °C, 5 h; ii) NaBH₄, RT, 18 h, 75%.

Synthesis of sulfates 91 and 92

The palladium-catalyzed coupling of boronic ester **97** and protected 3-bromophenylsulfamate **115** following the previously optimized Suzuki conditions led to the formation of acetal **116** in excellent yield. Deprotection of the ketone without removal of the DMB group was obtained in mild acidic conditions using an adapted literature procedure⁹⁴ to give cyclohexenone **117**. It was observed that the latter intermediate was not stable, probably because of aromatization of the cyclohexenone ring in air, and it was therefore decided to perform the catalytic hydrogenation of the double bond prior to deprotection of the ketone. Once the stable acetal **132** was obtained, a milder acid (AcOH) was utilized for the deprotection. A literature procedure using acetic acid in a mixture of water and THF at 45 °C⁹⁵ successfully afforded ketone **118** in good yield (Scheme 3.20).

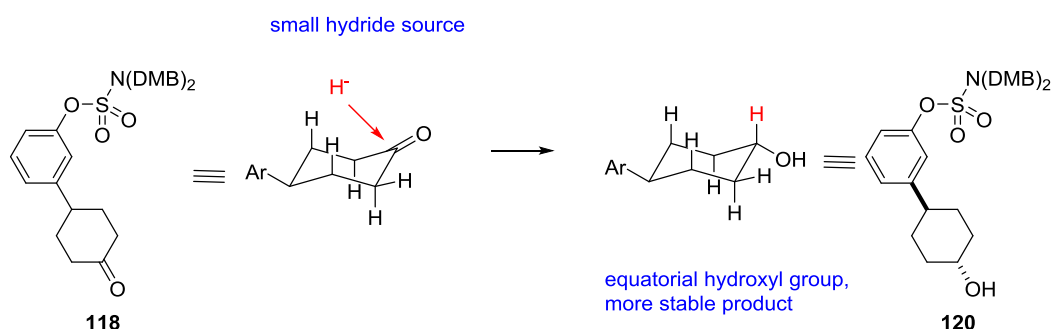


Scheme 3.20 - Synthesis of the intermediate 132.

Reagents and conditions: **a)** **97**, Na₂CO₃ (aq., 2 M), Pd(dppf)Cl₂, DME, μ W 80 °C, 15 min, 99%; **b)** *p*-TSA (1 equiv.), acetone/H₂O, μ W 60 °C, 1 h, 72%; **c)** H₂, Pd/C 10%, EtOH/THF 4:1, 40 °C, 96%; **d)** AcOH/H₂O/THF 20:10:3, 45 °C, 87%.

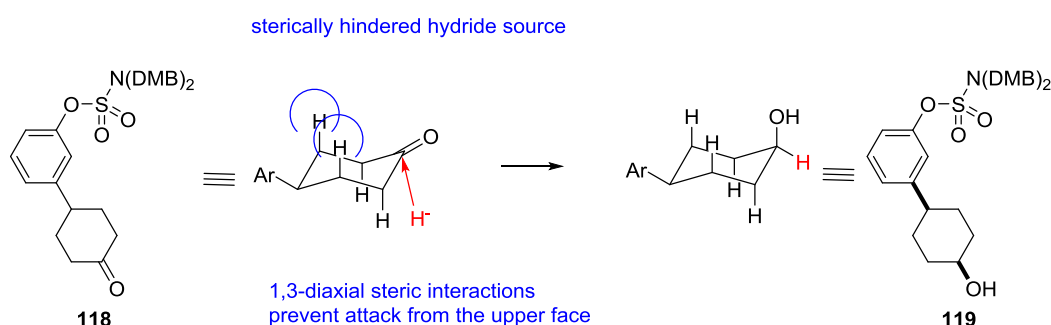
The position of the equilibrium between the two chair conformers of 4-substituted cyclohexanone **118** is such that, to minimize 1,3-diaxial interactions, the predominant form has the aryl ring occupying an equatorial position, thus facilitating the stereoselective reduction of the ketone. A hydride attacking the carbonyl from the same face of the equatorial 4-aryl group will give the *trans*-cyclohexanol (\pm)-**120** as major product, while attack coming from the opposite

face will prevalently lead to the *cis*-cyclohexanol (\pm)-**119**. When approaching the carbonyl, a small hydride source, such as NaBH₄, can overcome the unfavorable 1,3-diaxial interactions with the two hydrogens on C3 and C5 and lead to formation of the most stable *trans*-4-arylcyclohexanol (\pm)-**120** product, in which the hydroxyl is in equatorial position (Scheme 3.21). Equatorial attack is preferred by the more hindered L-Selectride to avoid 1,3-diaxial interactions resulting in *cis*-4-arylcyclohexanol (\pm)-**119** being the major product, even though it is the least favored in terms of free energy due to the hydroxyl being in an axial position (Scheme 3.22). As shown in Table 3.12, in both cases a roughly 8:1 ratio of the desired and the unwanted isomers was observed by LC-MS. The stereochemistry was confirmed by ¹H-NMR analysis of the splitting patterns (see discussion below regarding (\pm)-**92** and (\pm)-**91**).



Scheme 3.21 - Axial attack by an unhindered hydride source on a 4-arylcyclohexanone.

Reagents and conditions: NaBH₄, THF/EtOH, -78 °C to RT, 1.5 h, 78%.



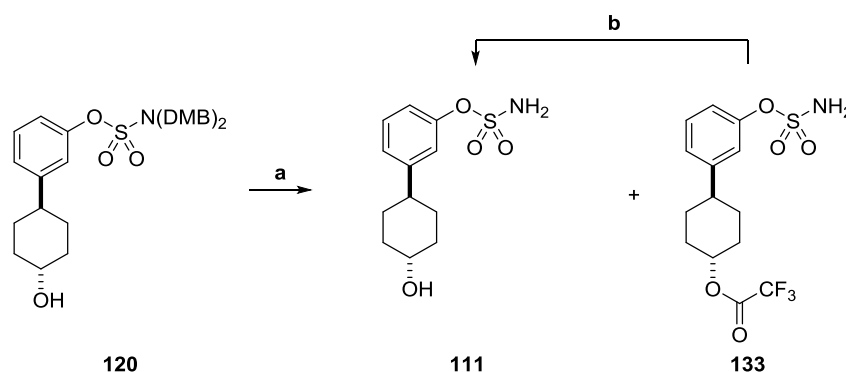
Scheme 3.22 - Equatorial attack by a hindered hydride source on a 4-arylcyclohexanone.

Reagents and conditions: L-selectride, THF, -78 °C to RT, 1 h, 69%.

Table 3.12 - Stereoselective reduction of a 4-arylcyclohexanone.

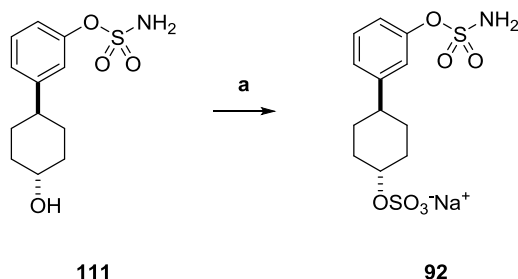
Hydride source	<i>trans/cis</i> ratio (LC-MS)	<i>trans</i> 120 isolated yield	<i>cis</i> 119 isolated yield
NaBH ₄	8.6 : 1	78%	5.5%
L-selectride	1 : 8.2	-	69%

Deprotection of the sulfamate group of (±)-**120** using 10% TFA in DCM under anhydrous conditions⁹³ led to the formation of both the desired sulfamate (±)-**111** and the corresponding trifluoroacetate side product (±)-**133**. The use of a lower concentration of TFA (5% in DCM) did not prevent esterification of the alcohol. The by-product (±)-**133** could be isolated and converted to the desired *trans*-alcohol (±)-**120** upon treatment with sodium borohydride (Scheme 3.23).

**Scheme 3.23 - Deprotection of 120.**

Reagents and conditions: **a)** TFA/DCM 9:1, RT, 2.5 h, **111**: 46%, **133**: 39%; **b)** NaBH₄, THF/EtOH 3:1, -78 °C to RT, 2.5 h, quant.

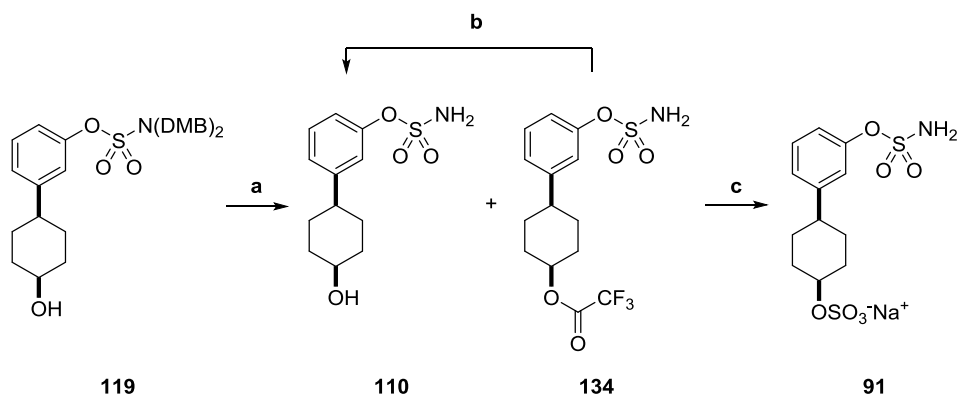
Sulfation of the hydroxyl was performed with sulfur trioxide pyridine complex in DMF using the conditions described previously. To form the more stable sodium sulfate salt (±)-**92**, ion exchange chromatography⁷⁹ at pH 7 was preferred to treatment with sodium hydroxide to avoid hydrolysis of the primary sulfamate group (Scheme 3.24).



Scheme 3.24 - Sulfation of the alcohol 111.

Reagents and conditions: **a)** i) $\text{SO}_3 \cdot \text{py}$ (2 equiv.), DMF, RT, 30 min; ii) ion exchange chromatography on Dowex 50W8 \times 200 Na form, H_2O , 84%.

The same procedure was applied to the synthesis of the *cis*-isomer (\pm)-**91** from alcohol **119** (Scheme 3.25).



Scheme 3.25 - Synthesis of 91.

Reagents and conditions: **a)** TFA/DCM 9:1, RT, 2.5 h, **110**: 53%, **134**: 25%; **b)** NaBH_4 , THF/EtOH 3:1, -78°C to RT, 2.5 h, 66%; **c)** i) $\text{SO}_3 \cdot \text{py}$, DMF, RT, 1 h; ii) ion exchange chromatography on Dowex 50W8 \times 200 Na form, H_2O , 98%.

To confirm the predicted stereochemistry the ^1H -NMR coupling constants were analyzed and compared with those expected from the Karplus equation.⁹⁶ For an axial proton, coupling constants $^3J_{\text{ax-ax}}$ are expected to be 9-13 Hz and $^3J_{\text{ax-eq}}$ should be 2-4.5 Hz. Consistent with these values, the coupling constants observed in the triplet of triplets corresponding to the axial proton H-4 of **111** were 11.0 and 4.3 Hz, respectively (Figure 3.7a). For an equatorial proton, $^3J_{\text{eq-ax}}$ and $^3J_{\text{eq-eq}}$ are expected to be in the range between 2 Hz and 4.5 Hz. Smaller coupling constants leading to the distinct multiplet observed in Figure 3.7b are consistent with the equatorial position of proton H-4 of **110**.

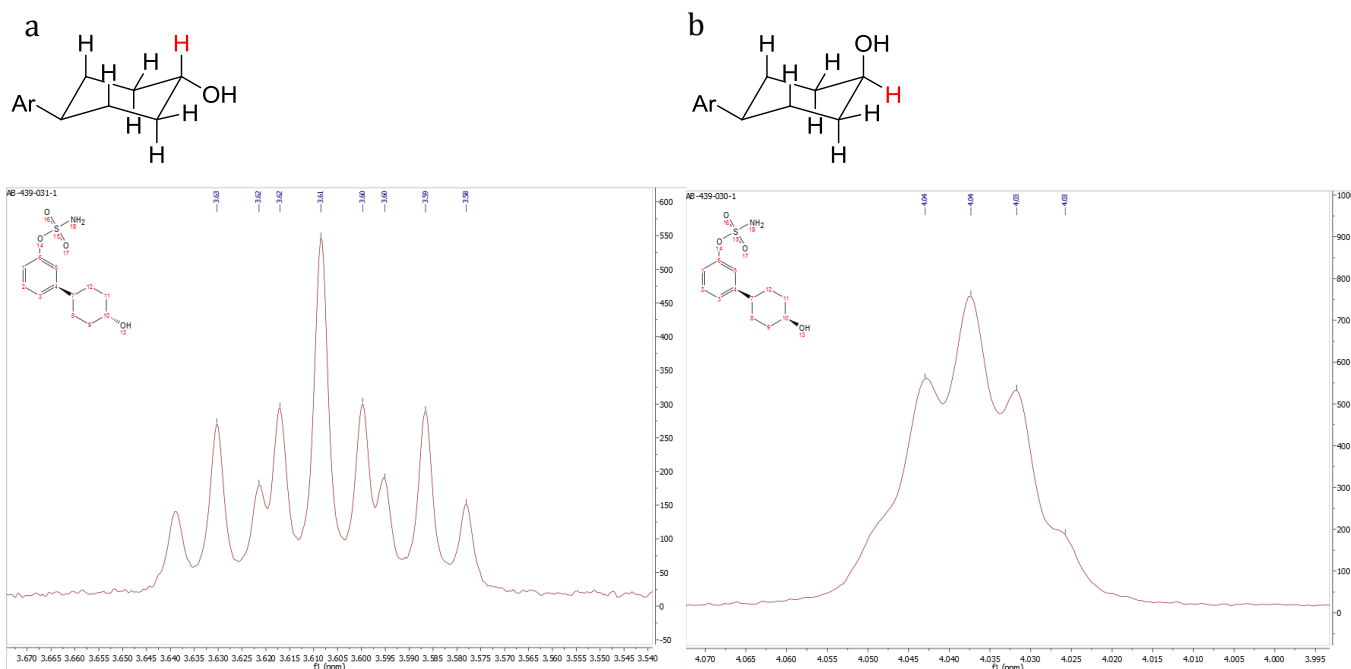
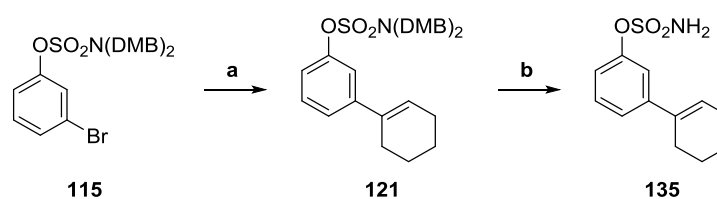


Figure 3.7 - Splitting patterns of the proton on the 4-position of the cyclohexyl ring.

Larger coupling constants are observed for the *trans*-sulfate **111** (a) while small coupling constants are found for the *cis*-product **110** (b), in agreement with the Karplus equation.

Synthesis of sulfate (\pm)-93

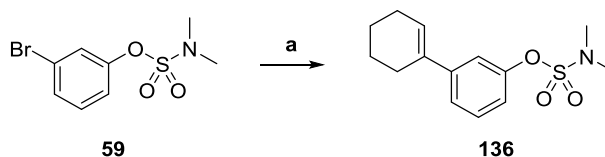
To obtain sulfate **93**, Suzuki coupling of boronic ester **101** with protected 3-bromophenylsulfamate **115** led to the formation of the 1-substituted cyclohexene **121**, which was deprotected to yield **135** (Scheme 3.26).



Scheme 3.26 - Synthesis of 135.

Reagents and conditions: **a)** **101**, Na_2CO_3 (aq., 2 M), $\text{Pd}(\text{dppf})\text{Cl}_2$, DME, μW 80 °C, 15 min, 96%; **b)** TFA/DCM 9:1, RT, 3 h, 74%.

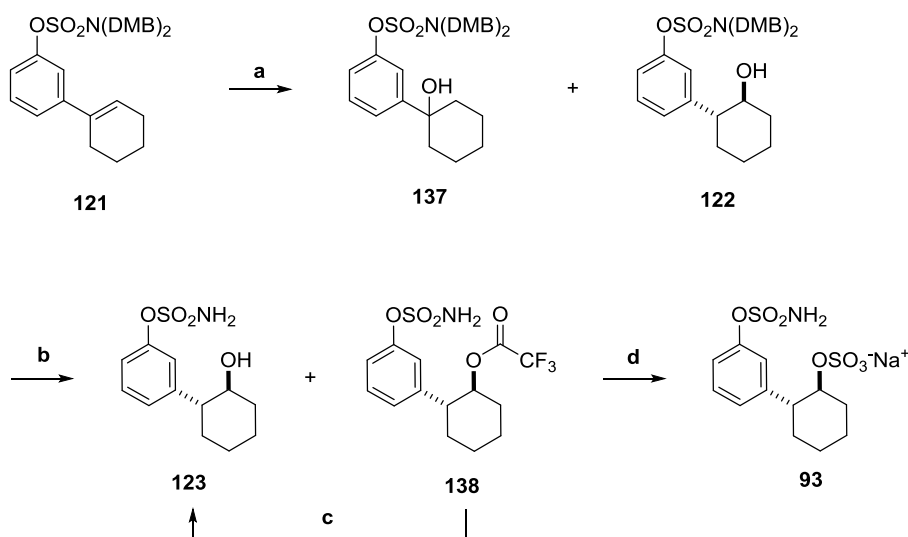
The optimized Suzuki-Miyaura conditions were also used to synthesize the tertiary sulfamate analogue **136** (Scheme 3.27).



Scheme 3.27 - Synthesis of 2',3',4',5'-tetrahydro-[1,1'-biphenyl]-3-yl dimethylsulfamate.

Reagents and conditions: a) 1-cyclohexen-1-yl boronic acid pinacol ester, Na_2CO_3 (aq., 2 M), $\text{Pd}(\text{dppf})\text{Cl}_2$, DME, μW 80 °C, 15 min, 49%.

Hydroboration-oxidation of the double bond of the cyclohexene ring of **121** gave **122** as a racemate, with attack occurring from either face of the double bond. A small amount of the regioisomer **137** was also isolated (ratio **122**:**137** 3.4:1). Deprotection of the sulfamate group of **122**, conversion of the trifluoroacetate ester side-product **138** back to the alcohol **123**, and sulfation of the latter followed by ion exchange chromatography yielded desired target **93** (Scheme 3.28). The low yield of the sulfation may be due to both steric hindrance and problematic purification.

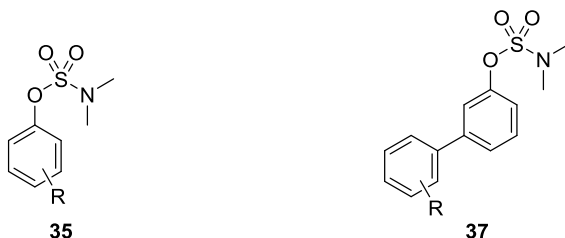


Scheme 3.28 - Synthesis of 93.

Reagents and conditions: a) i) $\text{BH}_3 \cdot \text{THF}$ (1.0 M), 0 °C, 1 h; ii) NaOH , H_2O_2 , RT, 18 h, **122** 55%; **137** 16%; **b)** TFA/DCM 9:1, RT, 18 h, **123**: 35%, **138**: 32%; **c)** NaBH_4 , THF/EtOH 3:1, -78 °C to RT, 5 h, 95%; **d)** i) $\text{SO}_3 \cdot \text{py}$, DMF, RT, 1 h; ii) ion exchange chromatography on Dowex 50W8×200 Na form, H_2O , 32%.

3.5 Conclusions

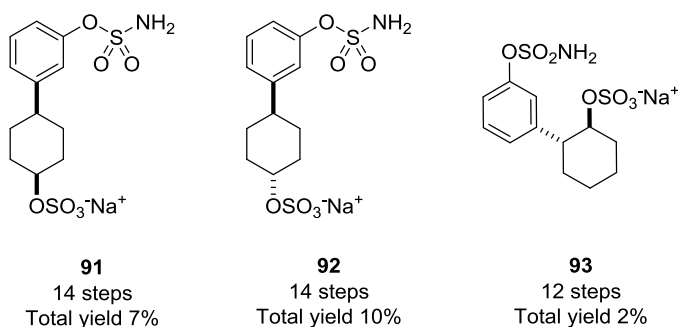
The synthesis of three small libraries of potential inhibitors of Sulf2 was reported. A library of aryl tertiary sulfamates **35** was synthesized in one step following an improved literature procedure for the sulfamoylation of appropriately substituted phenols which used an excess of phenol and base (Cs_2CO_3) with respect to the *N,N*-dimethylsulfamoyl chloride. The target compounds were obtained from commercially available starting materials in variable yields.



Subsequently, a library of 3-biaryl tertiary sulfamates **37** was designed on the model of the disaccharide unit of heparan sulfate. The B-ring was functionalized with polar moieties such as carboxylic acids, sulfates and aminosulfates. Starting from a literature procedure for the Suzuki-coupling of sulfamates with appropriate boronic acids, the optimization of the reaction conditions led to an improved yield and a reliable methodology for the formation of the C-C bond between the two aromatic rings. Further elaboration of the resulting biaryls led to the desired target molecules.

The synthesis of an analogue library of biaryl primary sulfamates following the same strategy was attempted but resulted in the partial hydrolysis of the $-\text{OSO}_2\text{NH}_2$ moiety to the parent phenol to give a complex mixture that proved difficult to purify and from which the desired product could be isolated in poor yield (20%). Several bases were tested in Suzuki-Miyaura cross coupling conditions but none of them led to an improvement, pointing out the need for a primary sulfamate protecting strategy which was therefore devised within the research group by Tristan Reuillon.

Using this protecting strategy, a third set of target molecules was synthesized which was characterized by an aryl primary sulfamate substituted at the 3-position by a cyclohexyl ring bearing an hydroxyl or a sulfate group either at the 2- or at the 4- position. Appropriate choice of the hydride source allowed the stereoselective reduction of the 4-cyclohexanone moiety to obtain either the *cis*- or the *trans*-cyclohexanol derivatives **119** and **120** which were then deprotected and sulfated to yield the target compounds **91** (14 steps; total yield 7%) and **92** (14 steps; total yield 10%), respectively. Hydroboration of the 1'-cyclohexene intermediate **121** followed by deprotection and sulfation led to primary sulfamate **93** (12 steps; total yield: 2%).



CHAPTER 4. SUMMARY OF THE BIOLOGICAL RESULTS OBTAINED FOR SULF2 POTENTIAL CHEMICAL TOOLS

4.1 Activity of the synthesized sulfamates against Sulf2, ARSA and ARSB

The compounds prepared were screened in a biochemical assay against Sulf2 at a single concentration to obtain a value of percentage inhibition of the desulfation of 4-methylumbelliferone sulfate (4-MUS, Figure 4.1a). The sulfatase-catalyzed desulfation of 4-MUS releases the parent phenol 4-methylumbelliferone (4-MU), a fluorescent indicator (Figure 4.1b). In the presence of an inhibitor, the decrease in fluorescence is proportional to the inhibitory activity (Figure 4.1c).

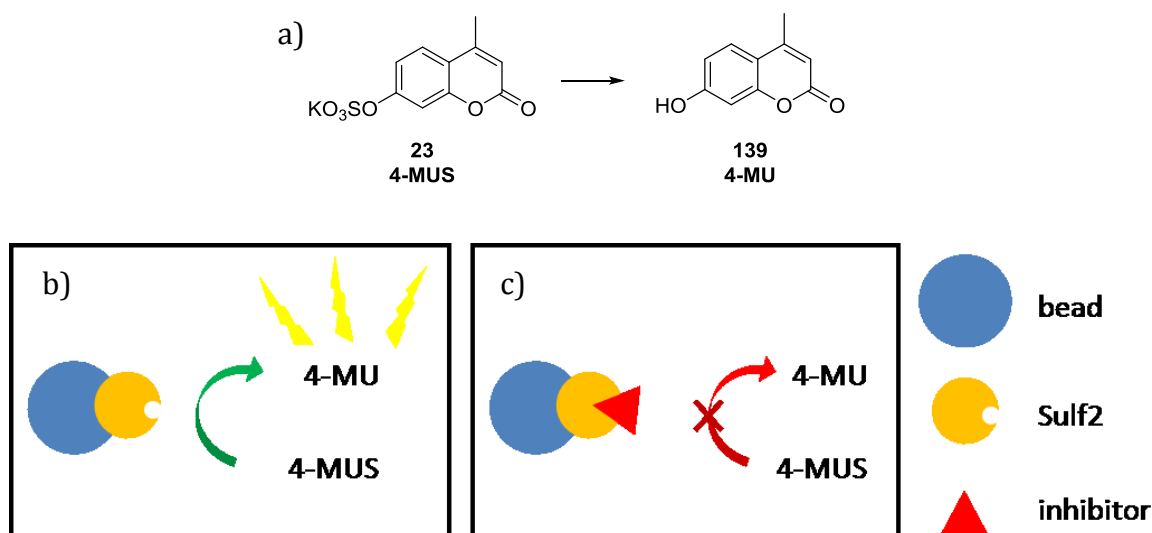


Figure 4.1 - Desulfation of 4-MUS (potassium salt).

a) Desulfation reaction of 4-methylumbelliferone sulfate; **b)** removal of the sulfate group by immobilized Sulf2 releases 4-methylumbelliferone, a fluorescent indicator; **c)** in the presence of an inhibitor, Sulf2 cannot catalyze the desulfation of 4-MUS, resulting in a decrease in fluorescence proportional to the amount of inhibited enzyme.

The assay was developed by Gary Beale⁶⁶ and Sari Alhasan⁶⁷⁻⁶⁸ who also tested all the compounds. In the Sulf2 project, the inhibitor working concentration in the assay was 1 mM, due to the low activity of the compounds analyzed. An IC_{50} was measured only for compounds with percentage inhibition higher than 50%. Initially, the benchmark compound used for assay development was the sulfated

monosaccharide **24** (lit. IC_{50} = 130 μ M; in house <10% inhibition at 1 mM), reported in the literature⁵⁹ and resynthesized by Duncan Miller.⁶⁵ At a more advanced stage, the positive and negative control compounds used were trichloromethyl {3'-(sulfamoyloxy)-[1,1'-biphenyl]-3-yl}sulfamate (IC_{50} = 156 μ M) and 3-(sulfamoyloxy)benzoic acid (16% inhibition at 1 mM), which emerged from the SAR studies conducted by Tristan Reuillon.⁷⁹

Selectivity of the compounds against sulfatases was assessed by means of a counter-screen against aryl sulfatase A (ARSA) and aryl sulfatase B (ARSB), again using 4-MUS as substrate.

4.2 Activities of a library of sulfamates against Sulf2

4.2.1 The monocyclic substituted phenyl sulfamate series

All the tertiary phenylsulfamates had no significant inhibitory activity against Sulf2.

4.2.2 The substituted biphenyl sulfamate series

In the biphenyl series (all measured at 1 mM concentration), the 3'-cyano analogue **81** was the most potent, achieving 29% inhibition. The 4'-substituted aniline **71** exhibited weak inhibition of Sulf2 (21% inhibition), while the 2'- and 3'-anilines (**69** and **70**, respectively) had no inhibitory activity. Sulfated anilines **74** (10%), **73** (17%) and **72** (11%) all showed low levels of activity. The 4'-carboxylic acid **65** (19%) and its 3'-regioisomer **64** (16%) demonstrated superior inhibition than 2'-carboxyl **63** (3%). The 4'-hydroxymethylsulfate **84** was the second most potent compound (27%) and more potent than its parent alcohol **83** (5%). The pyridyl compounds had low activity, with the most active regioisomer being 4-pyridyl **80** (13%). Apolar compounds, such as the 4'-methoxyphenyl **82**, the acetanilides **75**, **76** and **77** and the methyl esters **66**, **67**, **68** were all weakly active. Overall these results suggest that a polar group at the 4-position of the B-ring may contribute to activity against Sulf2 (Figure 4.2). However, it would appear that the biphenyl tertiary sulfamate scaffold in general does not confer good Sulf2 inhibition.

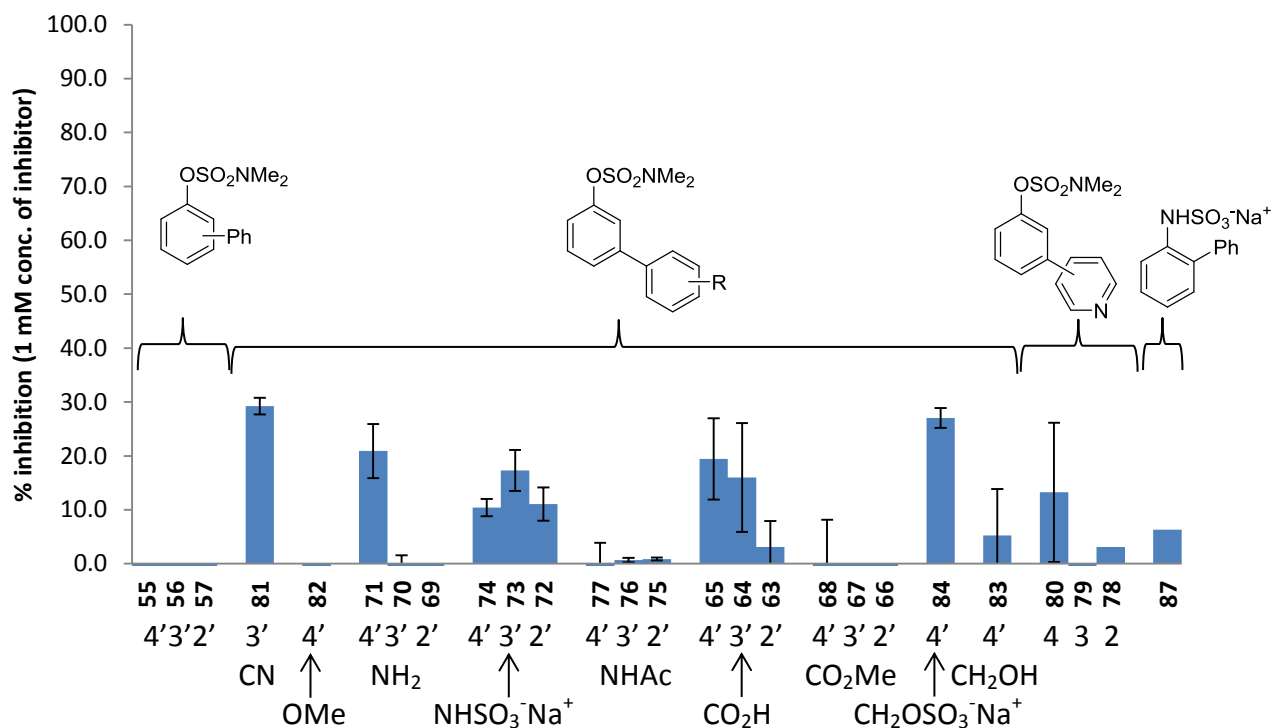


Figure 4.2 - Percentage inhibition of the substituted biphenyl sulfamate series against Sulf2. The assay was performed by Sari Alhasan.⁶⁸ Replicates: n=2. Error bars represent standard deviation.

A similar set of primary sulfamates was prepared by Tristan Reuillon⁷⁹ and found to have higher activity, again measured at 1 mM concentration. For example, the primary sulfamate analogue of **73**, had Sulf2 inhibition of 31% (compared to just 17% of **73**).

4.2.3 Compounds with a non-aromatic B-ring

The most active compound synthesized was the cyclohexene-containing primary sulfamate **135** (49% inhibition at 1 mM). Its tertiary sulfamate analogue **136** had much weaker Sulf2 activity, further supporting the superiority of primary over tertiary sulfamates. The *trans*-sulfate **92** was more active than the corresponding alcohol **111**, whereas no statistically significant difference was found between the corresponding *cis*-compounds **91** and **110**, respectively, and between **93** and **123**. The *trans*-4-cyclohexyl sulfate **92** was the most active among the sulfates (35%) followed by the *trans*-2-cyclohexyl sulfate **93** (14% at 1 mM). The results obtained with the cyclohexylsulfates initially suggest that a polar group at the 4-position

may be beneficial. It appears that a better interaction with the target is obtained when the polar substituent at the 4 position of the B-ring is equatorial and *trans* to the A-ring. Nonetheless, polarity does not seem to be a strict requirement for binding, as the most potent compound synthesized was the unsubstituted cyclohexene primary sulfamate **135** (Figure 4.3).

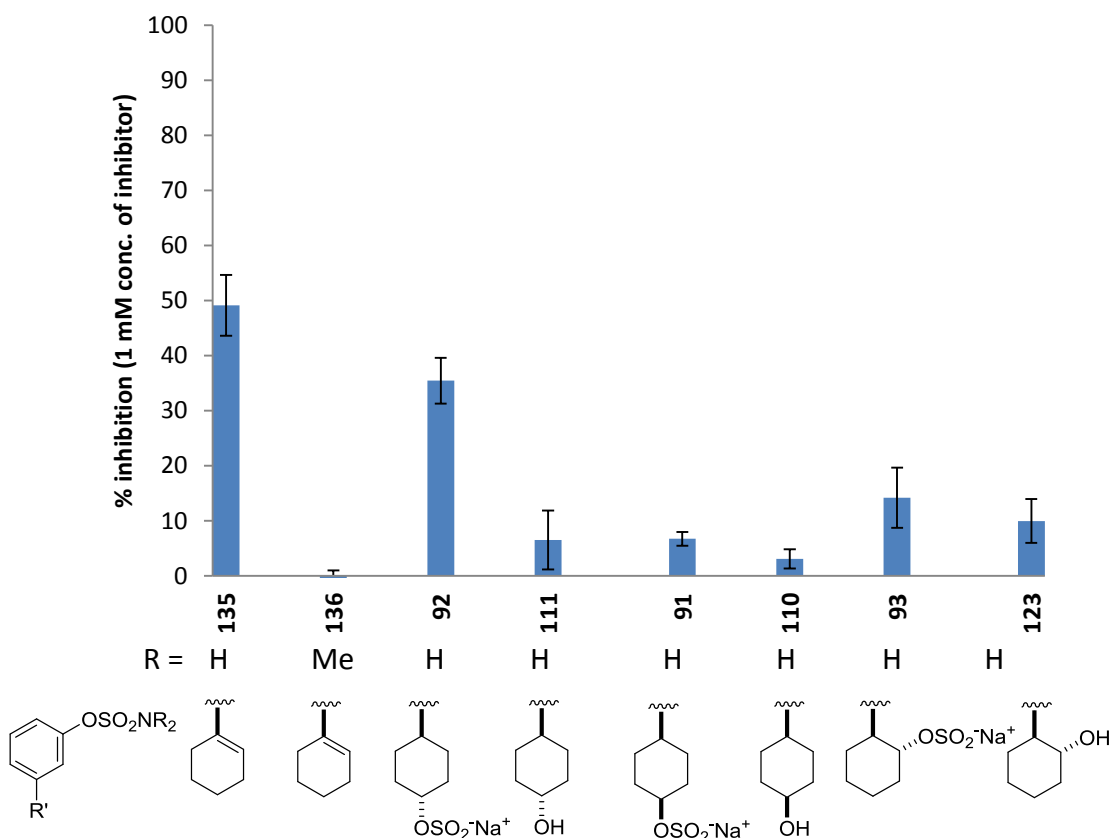


Figure 4.3 - Percentage inhibition of the non-aromatic B-ring series against Sulf2. The assay was performed by Sari Alhasan.⁶⁸ Replicates: n=2. Error bars represent standard deviation.

4.3 Activities of a library of sulfamates against ARSA and ARSB

As mentioned in Section 2.1, the active site of sulfatases is highly conserved and it is therefore necessary to probe the synthesized inhibitors against a selection of sulfatases to exclude the possibility of non-selective sulfatase inhibition. The commercially available aryl sulfatase A, ARSA, and arylsulfatase B, ARSB, were chosen for the counterscreen and, as for Sulf2, 4-MUS was used as a substrate.

4.3.1 The monocyclic substituted phenyl sulfamate series

The compounds synthesized in the phenyl series were more active against ARSA and ARSB than against Sulf2. In most cases higher activity was shown against ARSB.

Several compounds exhibited high selectivity for ARSB. For example, unsubstituted phenylsulfamate **58** only inhibited ARSB (59% inhibition at 1 mM), as did the 3-bromo analogue **59** (59%). A lipophilic substituent at the 4-position such as chloro- in **54** (ARSA: 38%; ARSB 66) or *t*-butyl- in **41** (ARSA 28%; ARSB 67%), appeared to confer some ARSA activity inhibition. Methoxy-substituted phenyls **42**, **43** and **44** were all active against ARSB (68, 71 and 68% inhibition, respectively) but much less active towards ARSA (12, 41 and 24%, respectively). The cyano- and trifluoromethyl- subgroups were also active against both enzymes. The selectivity was reversed only when nitro- was present in the 4- position of the phenyl ring, **48** (ARSA: 79%; ARSB 61%, Figure 4.4).

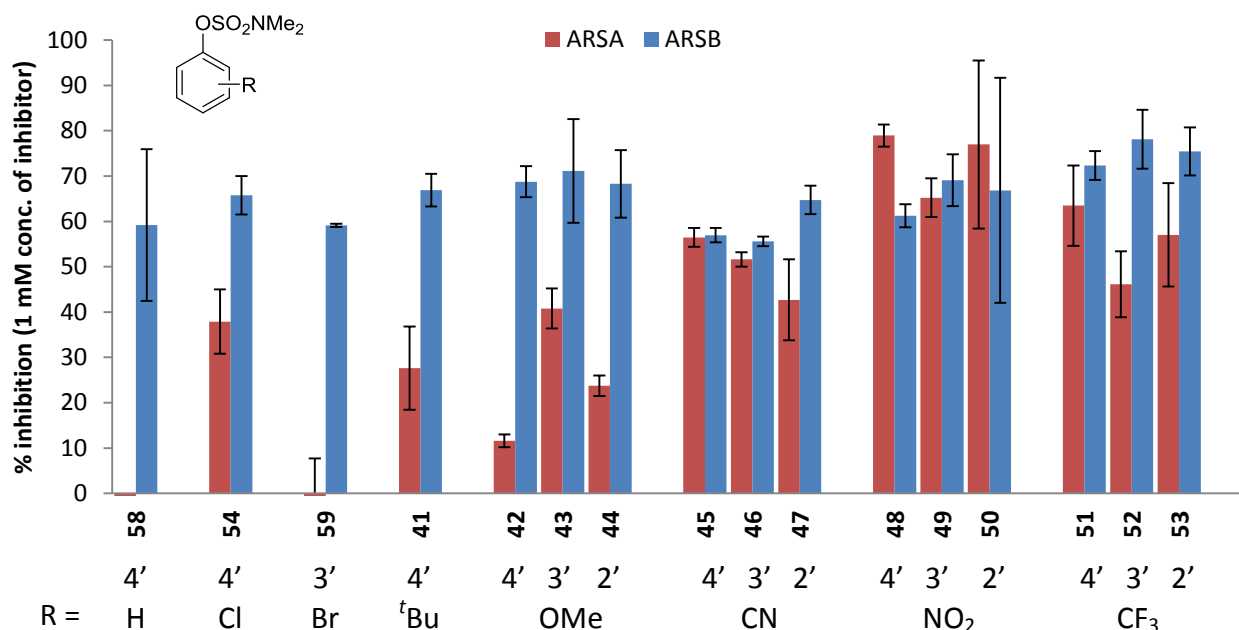


Figure 4.4 - Percentage inhibition of the monocyclic substituted phenyl sulfamate series against ARSA and ARSB. The assay was performed by Sari Alhasan.⁶⁸ Replicates: n=2. Error bars represent standard deviation.

4.3.2 The substituted biphenyl sulfamate series

In the biphenyl sulfamates, inhibitors with high selectivity for ARSA over ARSB were obtained. For example, the Sulf2-active 3'-cyano compound **81** was an effective inhibitor of ARSA at 1 mM (94%) but had low activity against ARSB (12%). A good example of the effect of regiochemistry on selectivity is observed in the case of carboxyl, where the 4'-carboxylic acid **65** (ARSA: 96%; ARSB <5%) is selective for ARSA and 2'-carboxyl **63** (ARSA: <5%; ARSB: 72%) is selective for ARSB. The corresponding methyl esters do not show such selectivity, which may indicate the establishment of interactions involving the carboxylate. 1,1'-Biphenyl 3-sulfamate **56** was active against both sulfatases (97 and 98% against ARSA and ARSB, respectively) and more active than the 2- and 4- isomers. The 4-methoxy-substituted compound was weakly active against either enzyme.

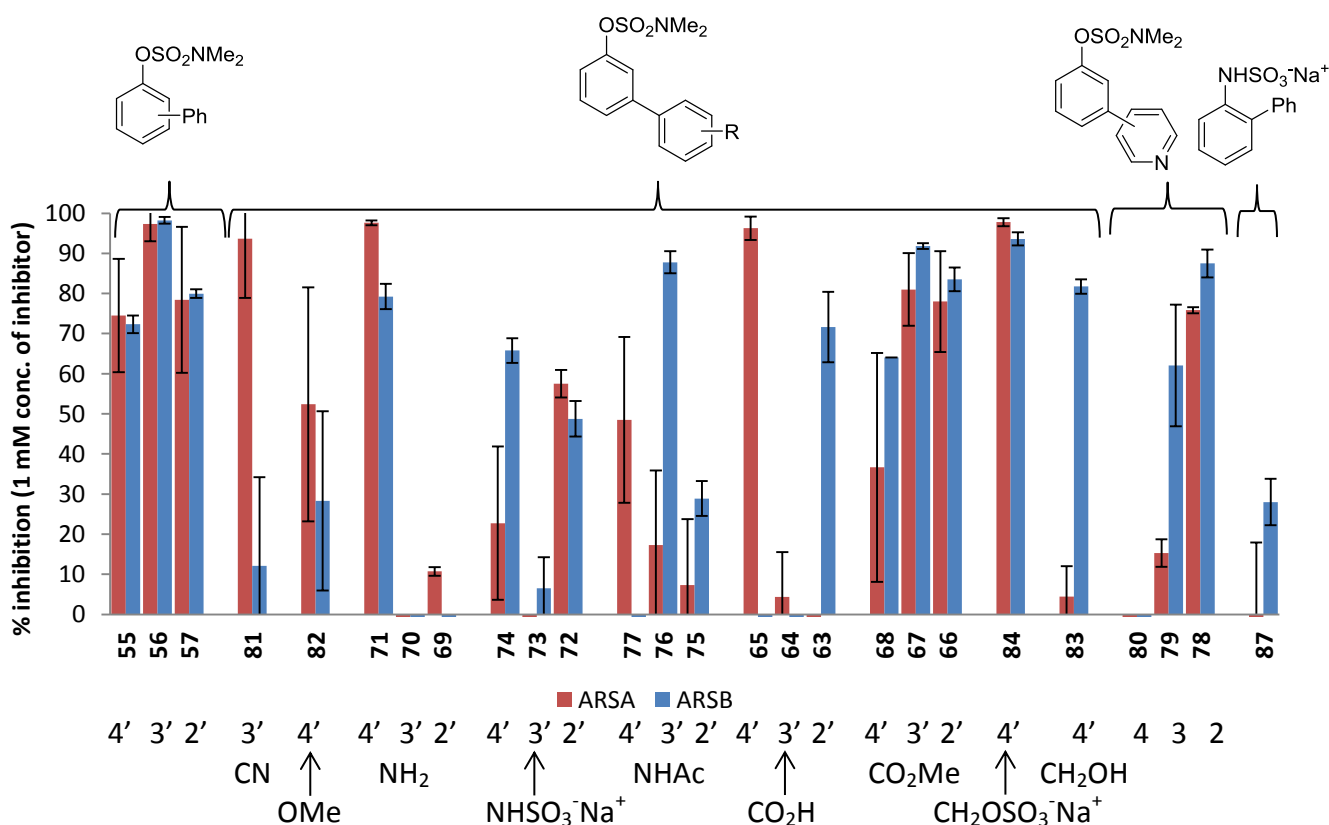


Figure 4.5 - Percentage inhibition of the substituted biphenyl sulfamate series against ARSA and ARSB. The assay was performed by Sari Alhasan.⁶⁸ Replicates: n=2. Error bars represent standard deviation.

When 4'-amino substitution was present on **71**, both ARSA (98%) and ARSB (79%) were inhibited, while the 3'- and 2'- regioisomers, **70** and **69**, respectively, were inactive. The 4'- and 2'- sulfated anilines **74** and **72** were found to be more effective inhibitors of both ARSA and ARSB than the 3'-sulfated analogue **73** (Figure 4.5). The 3'-acetanilide **76** was more active against ARSB (88%) than the other acetanilide regioisomer. The 4'-hydroxymethyl sulfate **84** was active against both enzymes, but its parent alcohol **83** (ARSA: 98%; ARSB: 94%) only inhibited ARSB (ARSA: 4%; ARSB 82%). Both targets were not affected by the 4-pyridyl **80**, but were inhibited by the 2- and 3-regioisomers **78** (ARSA: 76%; ARSB: 87%) and **79** (ARSA: 15%; ARSB: 62%), with a stronger effect observed on ARSB. Finally, the sulfated aniline **87** only weakly inhibited ARSB.

4.3.3 Compounds with a non-aromatic B-ring

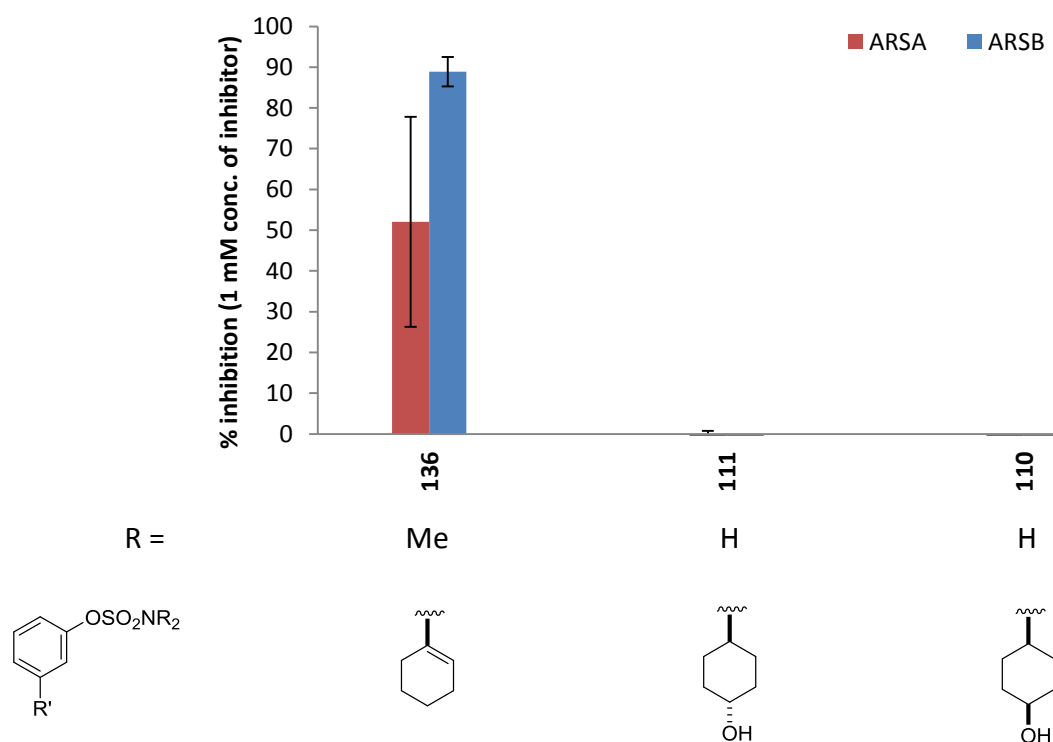


Figure 4.6 - Percentage inhibition of the non-aromatic B-ring series against ARSA and ARSB. The assay was performed by Sari Alhasan.⁶⁸ Replicates: n=2. Error bars represent standard deviation.

In this series, results were not obtained for all compounds, with data only being generated for **136**, **111** and **110**. The cyclohexenyl tertiary sulfamate **136** showed some activity against both the enzymes, whereas the primary sulfamates **111** and **110** did not show any inhibition of either ARSA or ARSB (Figure 4.6).

The results highlight that tertiary sulfamates are not good inhibitors of Sulf2 but they do exhibit greater inhibition of ARSA and ARSB. The available data are insufficient to draw definite conclusions, but replacement of the tertiary sulfamate group with a primary sulfamate appears to reduce activity towards the aryl sulfatases and improve binding to Sulf2.

4.4 Conclusions

All compounds synthesized within the Sulf2 project were tested for Sulf2, ARSA and ARSB activity using the assay developed by Gary Beale and Sary Alhasan. The results of the SAR are summarized schematically in Figure 4.7.

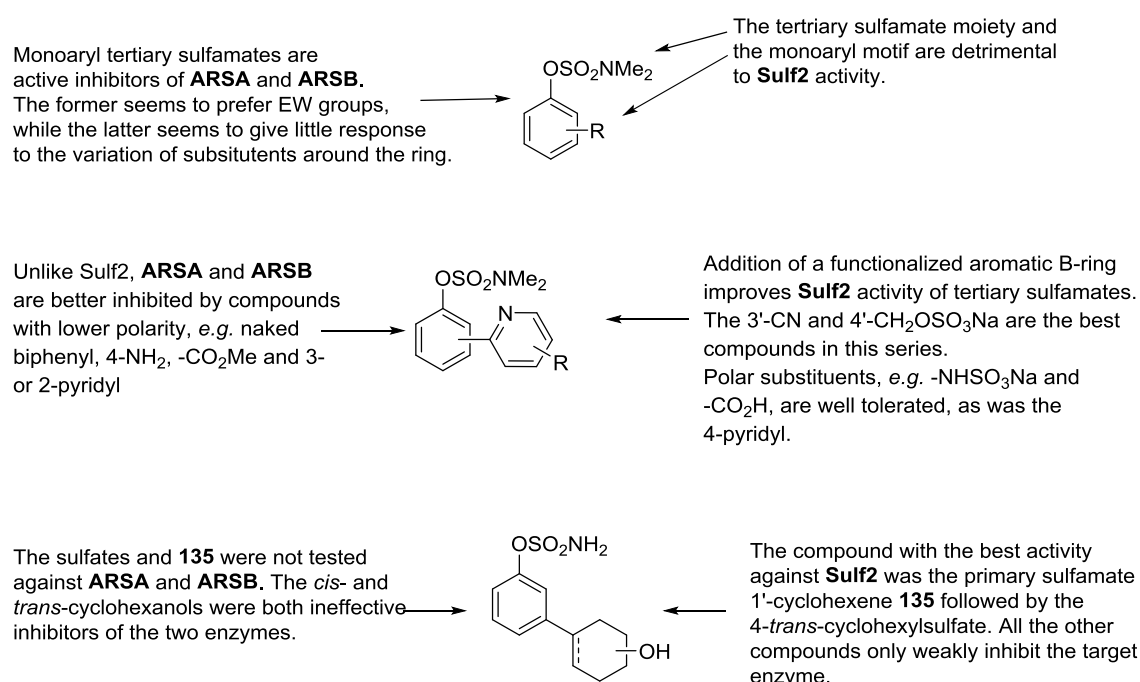


Figure 4.7 - Summary of the SAR for Sulf2, ARSA and ARSB.

CHAPTER 5. INTRODUCTION TO MDMX

5.1 p53, MDM2, and MDMX

5.1.1 The p53 tumor suppressor

In their reviews, Hanahan and Weinberg included evasion of apoptosis among the hallmarks of cancer.⁸⁻⁹ Common mechanisms by which neoplasms elude programmed cell death include the inactivation of the *TP53* gene, or the inhibition and reduction of cellular levels of p53 protein by Murine Double Minute 2 (MDM2) and Murine Double Minute X (MDMX).⁸⁻⁹ p53 mutations are found in up to 50% of human cancers (Figure 5.1); moreover, in tumors where wild-type p53 is retained, alterations in its regulation are frequently observed.⁹⁷

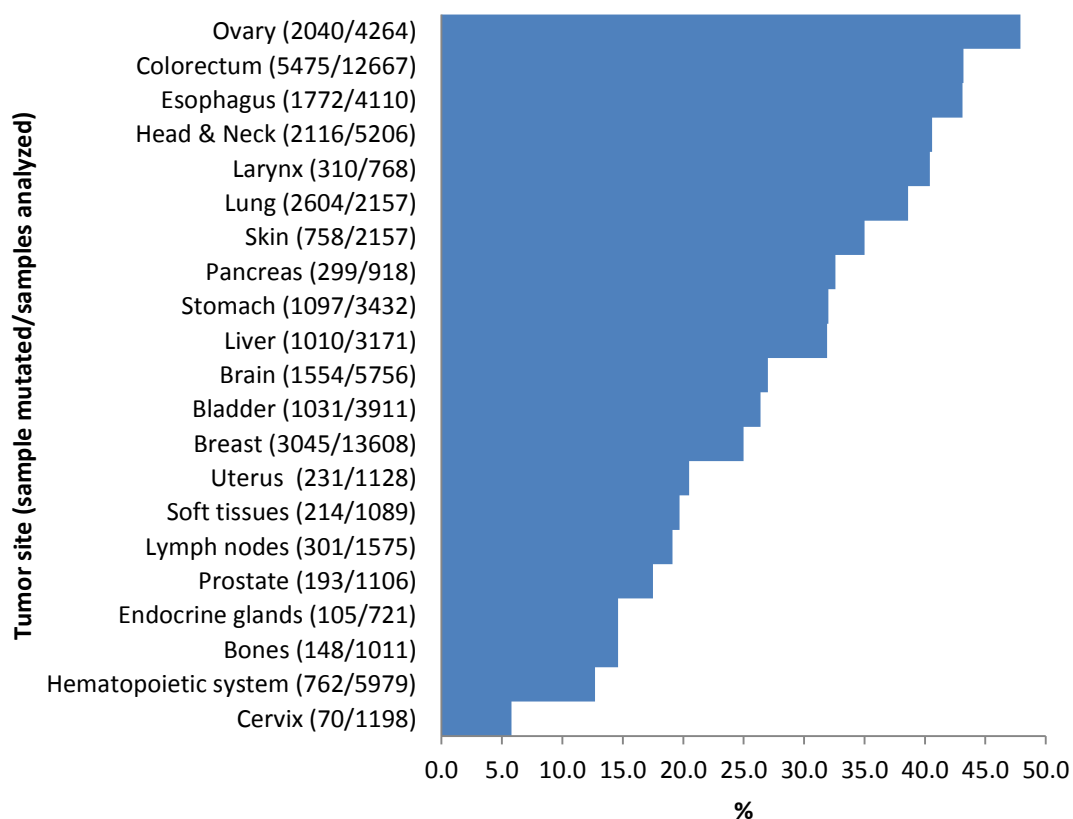


Figure 5.1 - Occurrence of p53 mutations in common cancers.

Adapted from Petitjean, 2007, last database update R17, November 2013.⁹⁸

Protein 53, or p53, is a transcription factor involved in a large number of processes including differentiation, ageing, mitochondrial respiration, angiogenesis and glycolysis. The importance of p53, also known as ‘guardian of the genome’ and ‘cellular gatekeeper’,⁹⁸⁻¹⁰¹ is linked to its ability to activate cell cycle arrest, DNA repair, senescence and apoptosis in response to cellular stress signals (Figure 5.2) with the aim of preserving the integrity of genetic information. It is, therefore, unsurprising that p53 is one of the most commonly mutated proteins in cancer.¹⁰² p53 was first reported in 1979 and was at first believed to be an oncogene.¹⁰³ It was only after establishing that the clones used to ‘prove’ tumorigenic properties of p53 were, in fact, p53 mutants and after determining the sequence of wild-type p53, that the scientific community acknowledged the tumor-suppressor role of this protein. It was formally proven in 1991 that p53 is capable of inducing apoptosis.¹⁰⁴ Subsequently, improved understanding of the p53 pathway has been achieved.

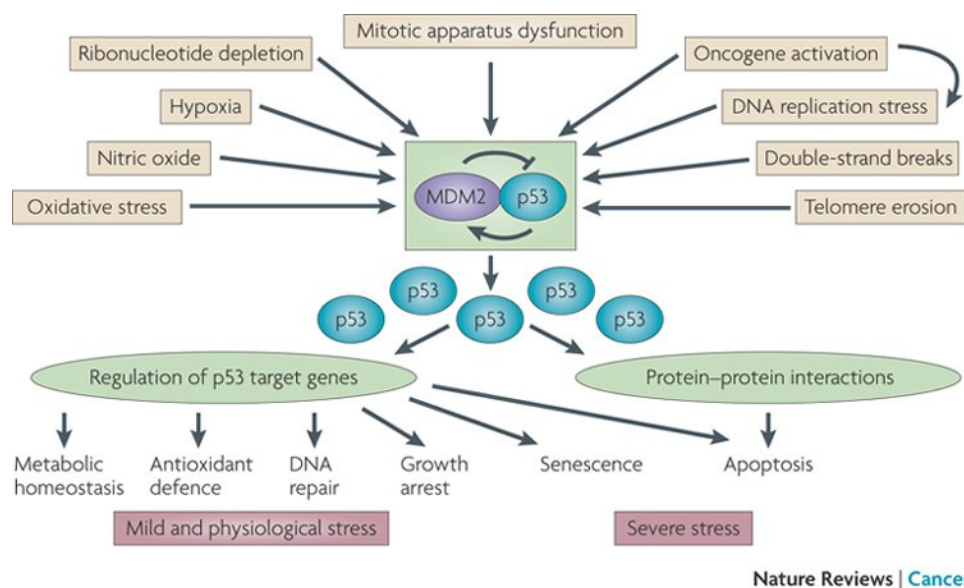


Figure 5.2 - The p53 pathway.

Upstream signals cause activation of p53 transcriptional activity leading to downstream effects according to the severity of DNA damage. Reproduced from Levine, 2009.¹⁰⁴

Consisting of 395 amino acid residues, p53 is a small protein (actually 43.7 kDa and not 53 kDa as originally claimed) undergoing several post-translational modifications including phosphorylation, acetylation and ubiquitination.¹⁰⁵⁻¹⁰⁶

Notably, active p53 binds to DNA as a homotetramer.¹⁰⁷ Together with p67 and p73, p53 belongs to a small family of transcription factors.¹⁰⁸ Functional domains in p53 include (Figure 5.3): the *N*-terminal transactivation domain, responsible for transcriptional activity, as well as for MDM2 and MDMX binding; a central DNA-binding domain which is commonly a target for mutations in cancer; a *C*-terminal domain containing a negative regulation domain and an oligomerization domain (4D), the latter comprised of a nuclear export signal (NES) and three nuclear localization signals (NLS).¹⁰⁹

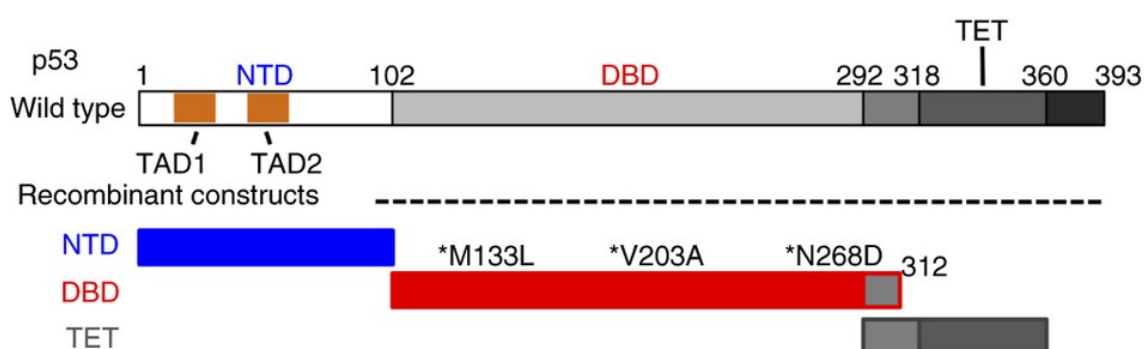


Figure 5.3 - Schematic representation of p53 primary structure.

The *N*-terminal transactivation domain, NTD, contains the two sub-domains TAD1, transactivation domain 1, TAD2, transactivation domain 2. p53 also includes a DNA binding domain, DBD, and a tetramerization domain, TET, located at the *C*-terminus. Adapted from Follis, 2014.¹¹⁰

Cellular stress conditions such as hypoxia, oxidative stress, starvation or alteration of mitochondrial and ribosomal biogenesis, trigger a number of signals which ultimately results in the activation of p53 for its nuclear and cytoplasmic functions. In the nucleus, p53 binds to specific DNA sites and promotes the transcription of target genes involved in processes designed to preserve DNA integrity, such as apoptosis (*BAX*, *NOXA*, *PUMA*), senescence (*p21*), cell-cycle arrest (*14-3-3 α* , *p21*), DNA repair (*MSH2*) and autophagy (*AMPK*, *BAX*, *PUMA*). Additionally, other downstream effects of p53 transcriptional activity are related to metabolism, antioxidant activity, angiogenesis, fertility and pigmentation. p53 is also involved in its own regulation (activation of genes such as *MDM2*, *COP1*, *CYCLIN G*, *PIRH2* and *WIP1*), establishing a negative feedback loop.^{101,111}

It has been demonstrated that p53 can induce apoptosis in cells in which the nucleus has been removed (enucleated cells). One of the most plausible explanations for this phenomenon is that alongside the transactivation of genes involved in mitochondrial-related apoptosis (*e.g. Bax, PUMA, NOXA*), cytoplasmic p53 is capable of promoting mitochondrial outer membrane permeabilization (MOMP), which is linked to the mitochondrial (or intrinsic) pathway of apoptosis through interaction with proteins of the Bcl-2 family.^{101,111}

5.1.2 MDM2 and MDMX

MDM2 and MDMX are two structurally similar proteins that are involved in the regulation of p53. Loss-of-function studies in mutant mice suggested the roles of MDM2 and MDMX to be non-redundant, as they are both necessary for embryo development.¹¹² The interplay of MDM2 and MDMX in p53 regulation is currently not fully understood but it is clear that both proteins play a crucial role in the degradation of p53 through the ubiquitin-proteasome pathway.¹¹³

The ubiquitin-proteasome pathway

The conjugation of ubiquitin, a small protein highly conserved in eukaryotic cells, is a multi-step process relying on three classes of enzymes. Initially, the adenylated carboxy-terminal residue of ubiquitin is attached to a cysteine of an ubiquitin-activating enzyme, classified as an E1 enzyme. Subsequently, ubiquitin is transferred to an ubiquitin-conjugation enzyme, E2. A third enzyme, E3, acts as a scaffold for the E2 enzyme and the target protein and catalyzes the formation of an isopeptide bond^b between the C-terminal carboxyl of ubiquitin and the lysine ϵ -amino group of the protein to be degraded. A single ubiquitin molecule is usually not sufficient to trigger degradation and, frequently, ubiquitin chains need to be formed by conjugation of multiple ubiquitin units onto lysine side chains for the target protein to be recognized by the proteasome.¹¹⁴ Ubiquitination can occur on multiple lysine residues of a protein (multi-ubiquitination) or onto ubiquitin lysine residues to form an extended ubiquitin chain (polyubiquitination).¹¹⁵

^b Peptide bond involving a side chain and resulting in a branch point from the main protein chain.

MDM2

MDM2, a 491-amino acid protein (90 kDa on SDS-PAGE), was first reported in 1992.¹¹⁶ At first believed to be an oncogene, it was shown to have E3 ligase activity towards p53, promoting its own ubiquitination¹¹⁷ and subsequent degradation by the 26S proteasome. In addition to promoting p53 degradation, MDM2 also masks the *N*-terminal transactivation domain of p53, thus preventing DNA binding and transcription promoting activity. MDM2 also promotes the export of p53 from the nucleus to the cytoplasm.¹¹⁸

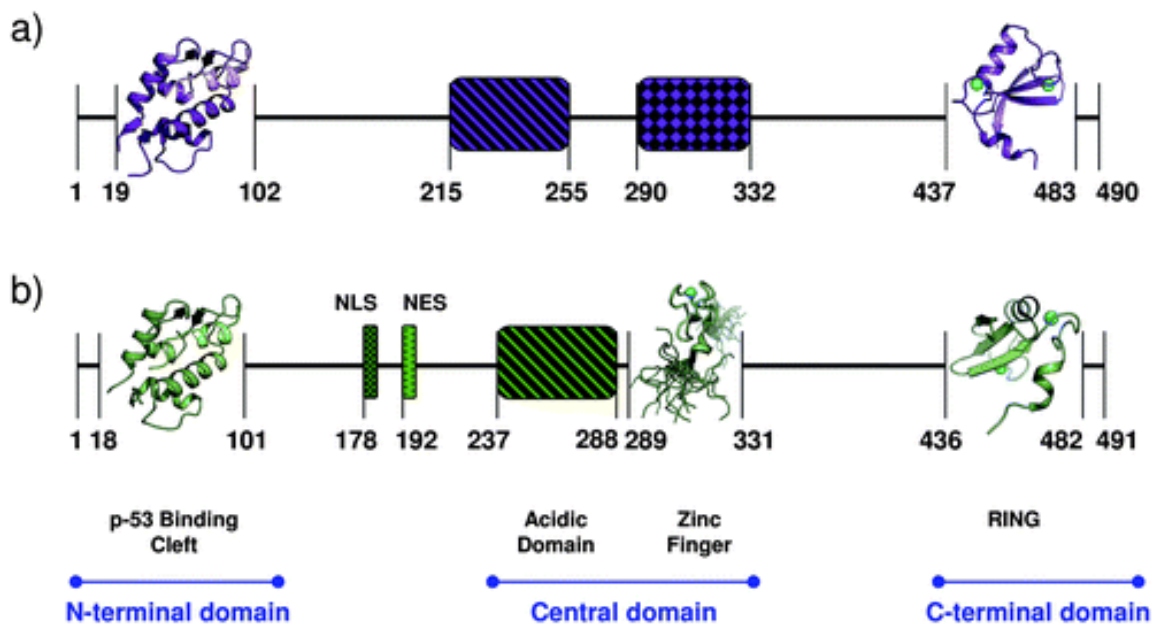


Figure 5.4 - MDMX (a) and MDM2 (b) functional domains.

Reproduced from Macchiarulo, 2011.¹¹⁹

MDM2 comprises three main functional domains (Figure 5.4.b).¹¹⁹ The *N*-terminal domain contains the p53-binding cleft, consisting of a hydrophobic region that accommodates three key residues of a p53 ligand α -helix: Phe19, Trp23 and Leu26 (Figure 5.5). This triad of amino acid residues accounts for most of the energy of binding representing the so-called 'hot spot' of the interaction (see Section 5.4). The central domain includes a zinc finger, whose function is yet to be elucidated, and a signal sequence for caspase cleavage. The *C*-terminal RING (Really Interesting New Gene) domain is responsible for both dimerization (either homodimerization, or heterodimerization with MDMX) and E3 ligase activity.¹¹⁹

The MDM2-MDMX heterodimer is more stable than the homodimer of each protein¹²⁰ and seems to promote a more effective ubiquitination of p53 than MDM2.¹²¹

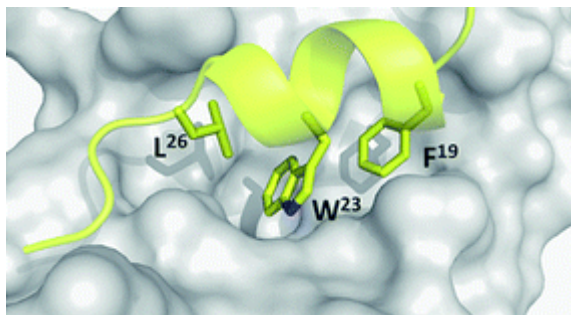


Figure 5.5 - The three key residues of p53 α -helix (green) accommodate into a hydrophobic binding cleft on MDM2.

Reproduced from Khoury, 2011.¹⁰⁸

MDMX

MDMX (also known as MDM4) is a 490 amino acid homolog of MDM2. Similarly, it has three functional domains with analogous roles, with highest sequence identity being in the p53-binding *N*-terminal domain (53.6%).¹¹⁹ Approximately 70% of the MDMX polypeptide chain is intrinsically disordered.¹²² Structural data suggests that the MDMX binding site for p53 is smaller than for MDM2. This is due to structural reasons: firstly, a leucine is replaced by a methionine in MDMX and, secondly, unlike the Tyr100 in MDM2, the MDMX Tyr99 adopts a closed conformation (see Section 5.4).¹²³ These differences may explain the large difference in binding affinity usually exhibited by MDM2 inhibitors towards these two closely related proteins.¹²⁴ More recently, Yu *et al.* showed that an opened conformation of Tyr99 (see Section 5.4 for more details) in MDMX is also possible, indicating that the binding surface is dynamic and that ligand-induced fit must be taken into account in the design of inhibitors.¹²⁵ MDMX and MDM2, through interaction of their RING domains, form a heterodimer with enhanced ubiquitination activity with respect to the MDM2 homodimer, as frequently observed for other E3 ligases.¹¹³ Although the mechanism of activation has not been elucidated, MDM2:MDMX heterodimers tend to promote polyubiquitination of the substrate, rather than its mono-ubiquitination.¹²¹

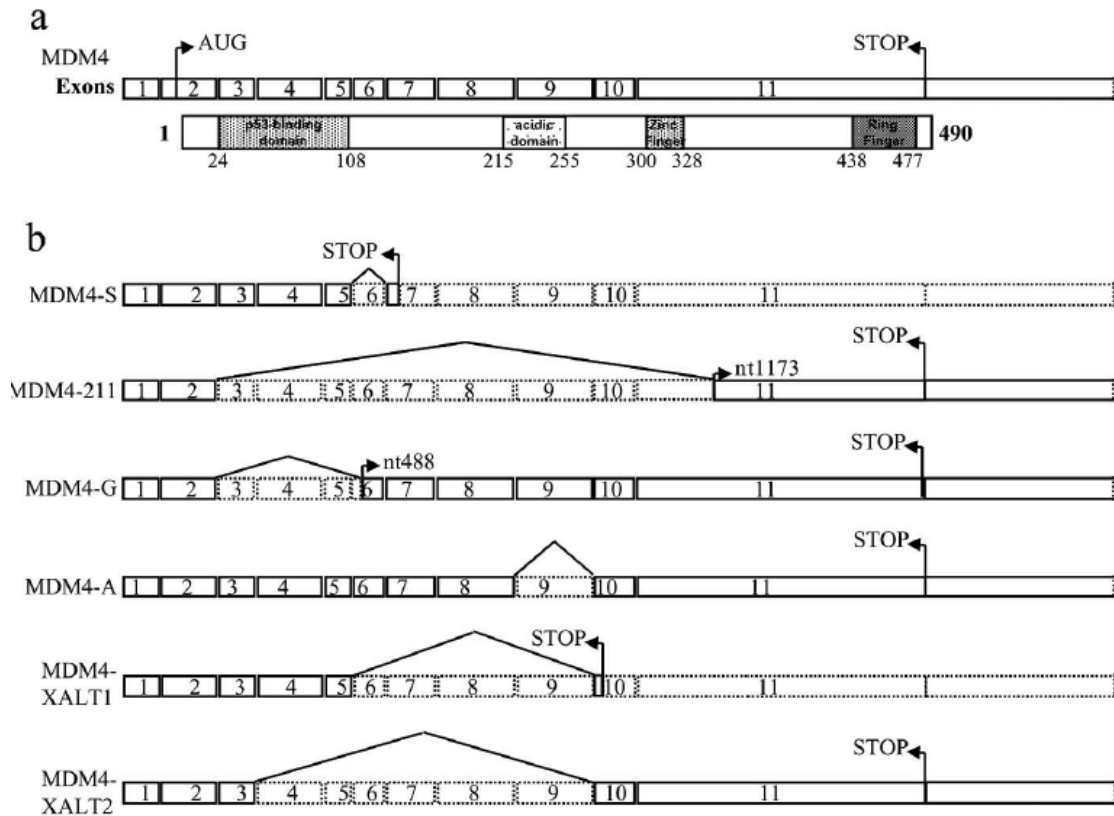


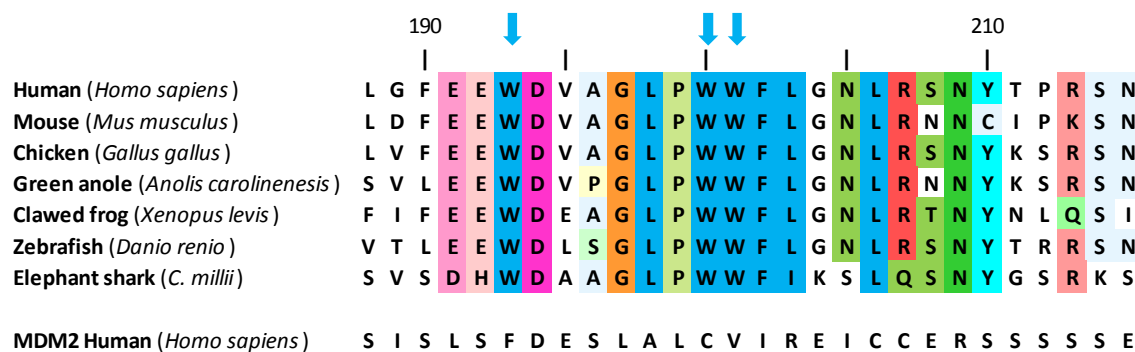
Figure 5.6 - Known splice variants of MDMX.

Reproduced from Mancini, 2009.¹²⁶

Several MDMX splice variants have been identified to date (Figure 5.6)¹²⁶⁻¹²⁸ stemming from removal of a different set of non-coding RNA sequences (introns) from the same pre-mRNA transcript by the spliceosome to generate mature mRNA. A total of seven shorter transcript variants of MDMX have been characterized, although not all are known to be translated into proteins, some being cancer-specific.¹²⁶⁻¹²⁷ Among the most interesting isoforms there is a shorter version of MDMX (MDMX-S)¹²⁸ whose estimated affinity towards the transactivation domain of p53 is approximately 70-fold higher than that of the full-length protein (Table 5.1, entries 1 and 5).

The binding affinity of the interactions between full length MDMX and both the *N*-terminal domain of p53 (entry 1) and full length p53 (entry 2) are comparable, suggesting that the association of the *N*-terminal domains drives the formation of the complex. The K_D of the association of the WWW autoinhibitory domain (MDMX 181-211) to MDMX *N*-terminal domain (1-111) is in a similar range (entry 3). Deletion of the WWW element improves binding affinity (entries 4 and 5). Adapted from Bista, 2013.¹²²

#	Complex	K_D (nM)
1	Full length MDMX + p53 17-32	$2,870 \pm 558$
2	Full length MDMX + full length p53	$1,110 \pm 101$
3	MDMX 1-111 + MDMX 181-211	$1,290 \pm 641$
4	MDMX 1-111 + p53 17-32	30.3 ± 3.9
5	MDMX-S + p53 17-32	40.3 ± 6.3



Adapted from Bista, 2013.¹²²

85

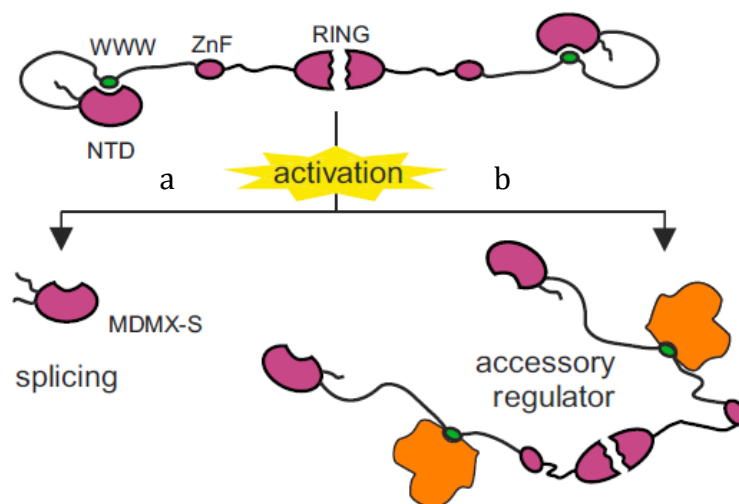


Figure 5.8 - Full-length MDMX contains an autoinhibitory sequence (WWW sequence).

The protein is activated either by a) alternative splicing giving a shorter version (MDMX-S) or b) pathway accessory regulators which bind the WWW sequence. Reproduced from Bista, 2013.¹²²

Despite the high homology with MDM2, MDMX does not have E3 ligase activity *per se*, as it lacks an essential cysteine residue in the RING domain that allegedly binds ubiquitin.¹²⁹⁻¹³⁰ The cellular localization of MDM2 and MDMX is also different, with MDM2 principally being located in the nucleolus, whereas MDMX is mainly found in the cytoplasm.¹²⁸ Furthermore, Wade and Wahl observed that the relative amount of MDMX in normal cells is only 10-20% of that of MDM2. Given that MDM2 has higher affinity for dimerizing with a molecule of MDMX rather than recruiting a second MDM2 unit, the authors suggested that most MDMX exists as MDM2:MDMX heterodimers in normal cells.¹¹³

A number of post-translational modification sites have been reported for MDMX. Multiple serine residues on the protein are phosphorylated by cyclin-dependent kinase 1 (CDK1/Cdc^{p34}), Casein Kinase 1 α (CK1 α), Checkpoint kinases 1 and 2 (Chk1/Chk2), Akt and ataxia teleangiectasia mutated (ATM).¹²⁶ Recently, AMP-activated protein kinase (AMPK) was found to phosphorylate MDMX at Ser342, thus enhancing MDMX binding to the regulatory protein 14-3-3. This pathway seems to be important for cell response to mild stress, such as glucose deprivation.¹³¹ MDMX is ubiquitinated by MDM2 to be tagged for degradation.

Another less common modification is conjugation of the protein SUMO at Lys254 and Lys379, whose effects are still to be identified.¹¹⁸

5.1.3 Cellular levels of p53 are finely tuned

Given the number and the relevance of its functions, it is not surprising that p53 transcriptional activity in normal cells is tightly regulated by a large number of enzymes, proteins and growth factors (Figure 5.9) and by a series of elegantly interconnected autofeedback loops. Regulation of p53 has been extensively studied but comprises such a complex network of signals that it is still far from fully understood.

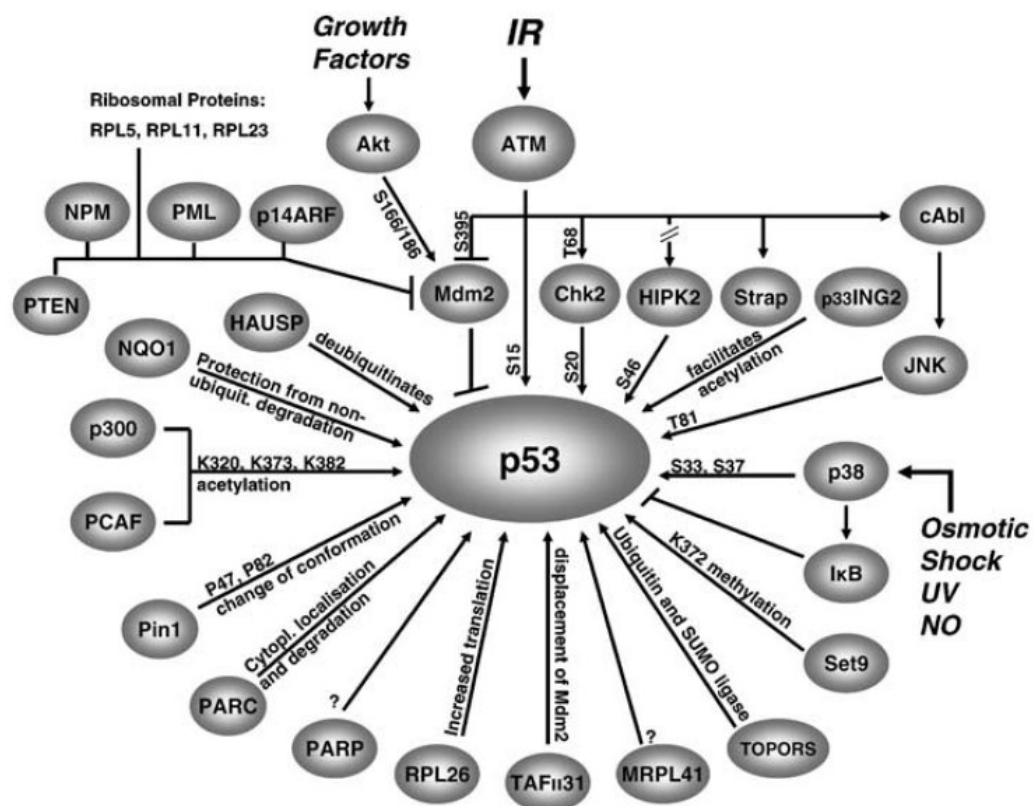


Figure 5.9 - Scheme showing the proteins known to influence p53 activity.
Reproduced from Lavin, 2006.¹⁰⁶

As anticipated, the cellular stability of p53 is prevalently influenced by MDM2 and MDMX.¹²¹ The relative amounts of p53, MDM2 and MDMX are cell-line dependent, as are the p53 regulatory processes.¹³² Under normal (*i.e.* unstressed cell) conditions, levels of p53 are kept low by MDM2 which, through its E3 ligase activity, promotes p53 degradation *via* the ubiquitin-proteasome pathway.

Additionally, ubiquitinated p53 is translocated from the nucleus to the cytoplasm, away from the target DNA. Finally, p53 transcriptional functions are inhibited by interaction of its transactivation domain with MDM2 and MDMX. The constant presence of low cellular levels of short-lived p53 (half-life ~5-20 min)¹³³ ensures a rapid response in the unfortunate event of DNA damage. When the cell is subjected to stress conditions, phosphorylation of MDM2 and MDMX¹¹³ triggers a response ranging from cell cycle arrest, to allow DNA repair, through to apoptosis, if the cell is highly compromised (Figure 5.10).

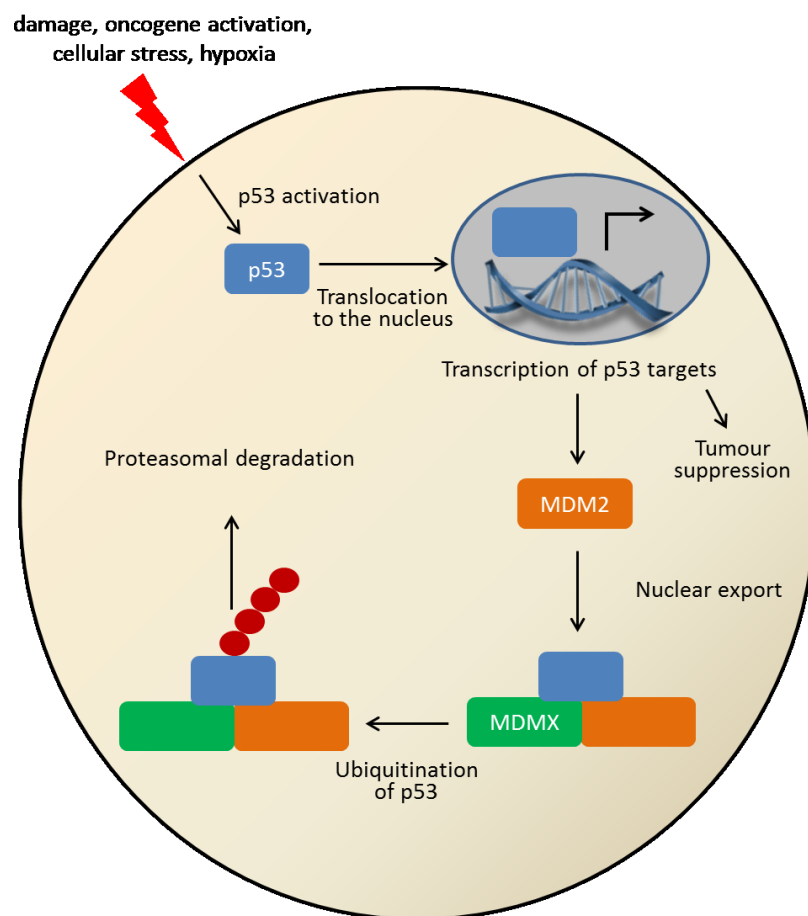


Figure 5.10 - Regulation of p53 by MDM2 and MDMX.

In response to stressors, such as hypoxia, UV radiation, activation of oncogenes, cells will activate the p53 pathway to arrest replication until the appropriate repair processes are completed. p53 is released by MDM2 and MDMX and is able to bind DNA and exert its transcriptional activity. At this point, the preferred substrates targeted for ubiquitination by MDM2 are MDM2 itself and MDMX, thus allowing p53 accumulation. The *MDM2* gene is one of the target genes induced by p53, originating a negative feedback loop and bringing p53 down to normal levels after the appropriate response has been achieved.

Early studies showed that *MDMX* is not transcriptionally activated by p53 in stressed cells.¹³⁴ Interestingly, a new promoter of the human *MDMX* gene has been recently discovered. Upon p53 binding to this new promoter, a longer version of MDMX, with reduced affinity for p53 itself, is expressed (MDMX-L isoform, containing an extra *N*-terminal 18-aminoacid sequence; Figure 5.11a). This adds another level of complexity to the network of feedback loops that regulates p53, MDM2 and MDMX, and further studies are required to fully understand the role of this isoform.¹²¹

A question may arise at this stage: what is the molecular switch which makes MDMX a better substrate for ubiquitination by MDM2:MDMX dimer? Cellular stress causes MDMX to be phosphorylated by ATM/ATR and c-Abl kinases, resulting in nuclear MDMX localization. Phosphorylated MDMX is now the preferred substrate for MDM2:MDMX E3 ligase and is quickly degraded by the 26S proteasome, leaving p53 free to exert its transcriptional function (Figure 5.11c).^{121,135} Upon stress relief, phosphatase-catalyzed dephosphorylation of MDM2 and MDMX restores normal conditions and the p53 concentration lowers to basal levels.

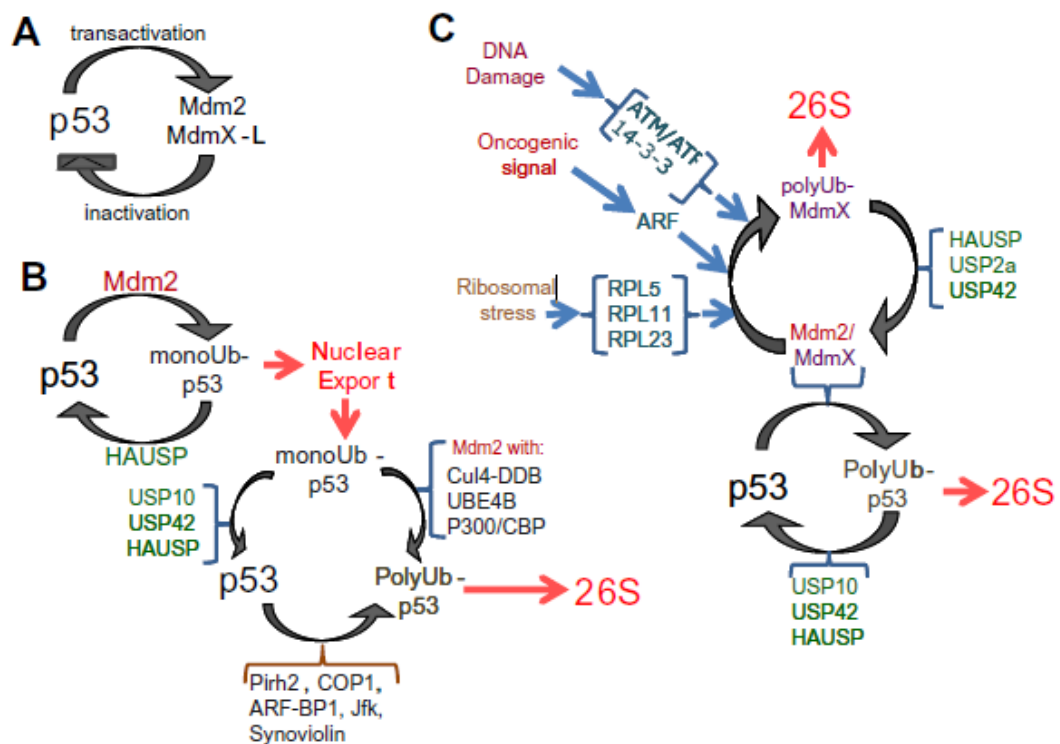


Figure 5.11 - The p53 network.

a) p53 promotes transcription of MDM2 and MDMX-L genes; p53 is inactivated upon binding to MDM2 or MDMX proteins. **b)** Mono-ubiquitinated p53 is translocated to the cytoplasm and further ubiquitinated for subsequent proteasomal degradation. There are deubiquitinases, both in the nucleus and in the cytoplasm, which are able to remove the tag. **c)** Stress signals promote polyubiquitination of p53 by MDM2/MDMX heterodimers, resulting in proteasomal degradation. The process is inverted by a panel of deubiquitinases. At the same time, MDM2/MDMX ligase leads to polyubiquitination and degradation of MDMX. Reproduced from Wang.¹²¹

5.2 MDMX as a target for cancer therapy

As previously described, tumors retaining wild-type p53 often display a severely impaired p53 regulation which can be achieved *via* either amplification or overexpression of the *MDM2* and *MDMX* genes.^{119,136} The role of MDM2 in cancer has been studied for over 20 years and it is currently well established that, in cancer cells characterized by MDM2 overexpression and wild-type p53, antagonists of the MDM2:p53 interaction lead to p53 reactivation and tumor suppression.¹⁰⁰ Although MDMX was also found to be amplified or overexpressed in many cancer types, its role is yet to be completely unravelled. As shown in Table 5.2, increased MDMX levels are found predominantly in retinoblastoma,

melanoma, breast, head and neck cancers and in hepatocellular carcinoma,¹¹³ lending support to the idea that MDMX acts as an oncogene.

Table 5.2 - Frequency of amplification or overexpression of MDMX in a panel of cancers.

Adapted from Wade, 2009.¹¹³

Tumor type	% of cases
Retinoblastoma	60
Glioblastoma	4
Colon	19
Lung	18
Breast	19
Melanoma	14
Hepatocellular carcinoma	50
Head and neck	50
Sarcoma	22
Bladder cancer	25
All cell lines	40

In MCF-7 breast cancer cells (characterized by wild-type p53), it has been shown that the knock-down of *MDMX* leads to increased levels of the p53-activated gene p21 not accompanied by a variation in p53 levels, suggesting that MDMX sequesters p53 to prevent its transcriptional activity.¹²⁰

Gembarska and co-workers showed that MDMX is highly expressed in melanomas and has an active role in the evasion of p53-induced apoptosis leading to cell proliferation.¹³⁷ In gliomas, high levels of the MDMX-S splice variant were observed¹²⁰ and a recent paper identified, within the same tumor type, a new splice variant (MDMX-B) whose expression was found to correlate directly to tumor stages.¹²⁷

The role of MDMX in cancer is still controversial, as other studies could find no correlation between MDMX overexpression and tumor development.¹³⁶ Following a recent study by Carrillo *et al.*, a p53-independent role of MDMX in genomic instability and tumorigenesis was hypothesized. The research team demonstrated

that transformation occurs in MDMX-overexpressing p53-devoid cells, suggesting an evolutionary advantage of the simultaneous increase in MDMX and decrease in active p53.¹³⁸

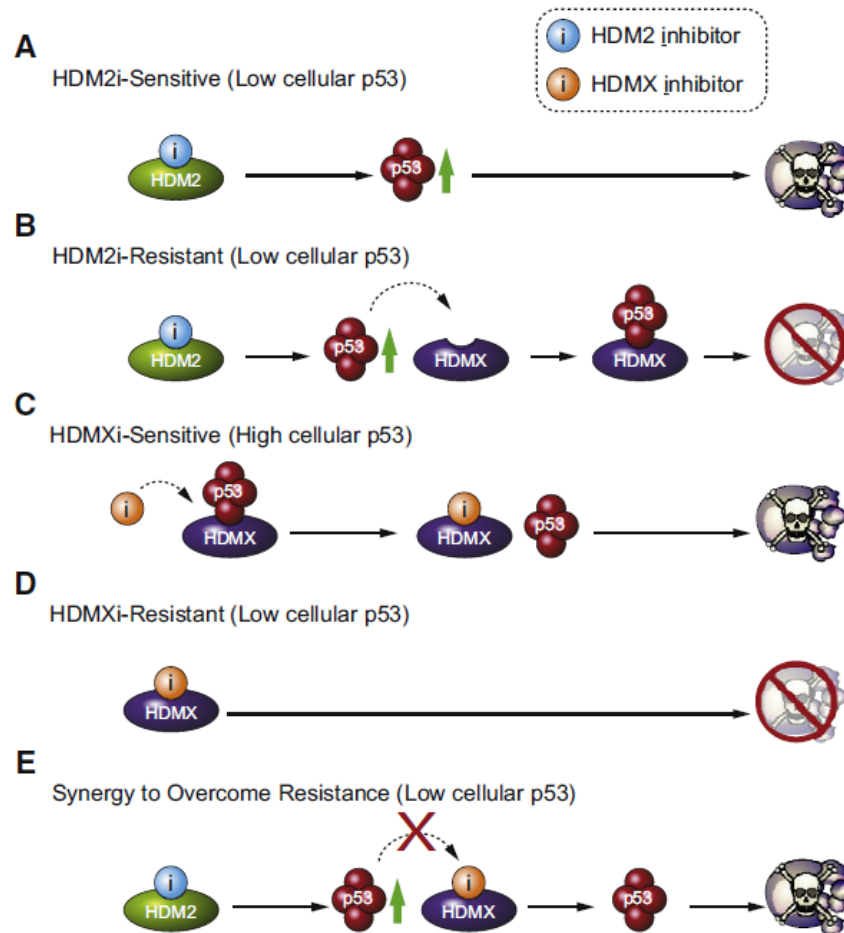


Figure 5.12 - Inhibition of MDM2 and MDMX and cancer cell susceptibility.
 Reproduced from Bernal, 2010.¹³²

The current knowledge suggests that simultaneous inhibition of MDMX and MDM2 would be more effective in the reactivation of p53.¹²⁰ In particular, dual inhibition could be advantageous when targeting cancers with pathologically low levels of p53.¹³² As shown in Figure 5.12, the cellular susceptibility to MDM2 and MDMX inhibitors seems to depend on the relative amounts of the three proteins, MDMX, MDM2 and p53. Single-agent MDM2 inhibitors successfully lead to apoptosis in the absence of MDMX (Figure 5.12a), but cells show resistance in the presence of MDMX (Figure 5.12b). If MDMX is overexpressed and there is a high

concentration of MDMX:p53, MDMX inhibition reactivates p53 (Figure 5.12c). Nonetheless, if p53 levels are not sufficiently high, no effect is observed upon inhibition of MDMX (Figure 5.12d). In a situation where MDMX levels are high and p53 levels are low, dual inhibition is thought to be the solution to the problem of resistance (Figure 5.12e).¹³²

Unfortunately, as Hu *et al.* reported in 2006,¹³⁹ MDMX binding affinity to the inhibitors designed for MDM2 is low or negligible. As a consequence, when treated with these drugs, patients who overexpress MDMX are likely to have no benefit from the treatment because p53 levels remain low. It is, therefore, very important to achieve a deeper understanding of the differences in the binding cleft of the two homolog proteins and rationally design MDMX inhibitors for combination therapy or, ideally, dual MDM2/MDMX inhibitors.

5.3 Protein-protein interaction inhibition

In recent years the importance of protein-protein interactions, PPIs, in the regulation of most physiological and pathological biological processes has become apparent, as ca. 650,000 PPIs are predicted to be involved in human cellular biology. It follows that, in the quest for new medications, interest in disrupting protein-protein associations has increased among medicinal chemists.

The effect of common drugs, developed for mimicking enzyme (or receptor) endogenous inhibitors (or antagonists/agonists), is due to the establishment of strong directional interactions with a few key residues in the target protein, such as either amino acid side chains or backbone peptide bonds, that are located in a defined cavity or active site. Such interactions include ionic binding (21-42 kJ/mol in a biological system¹⁴⁰) and hydrogen bonds (4-29 kJ/mol¹⁴⁰). By contrast, it has been an established belief in medicinal chemistry that, to prevent two proteins from coming in contact with one another, a large number of weak hydrophobic interactions, *e.g.* the interaction between two methylene groups which is as weak as 1.5 kJ/mol,¹⁴⁰ covering a broad surface is necessary (Figure 5.13). However, Clackson and Wells observed that the interaction with a few key residues, the so-called 'hot spots', accounts for most of the free energy gain in some PPIs.¹⁴¹ The interactions that are more likely to be antagonized by small molecules are those in

which recognition occurs via an α -helix, as in MDM2:p53 and MDMX:p53 interactions. Generally, this kind of PPIs involve 3-4 amino acid side chains, branching off on the same face of the helix and a suitable binding cleft on the partner protein.¹⁴²

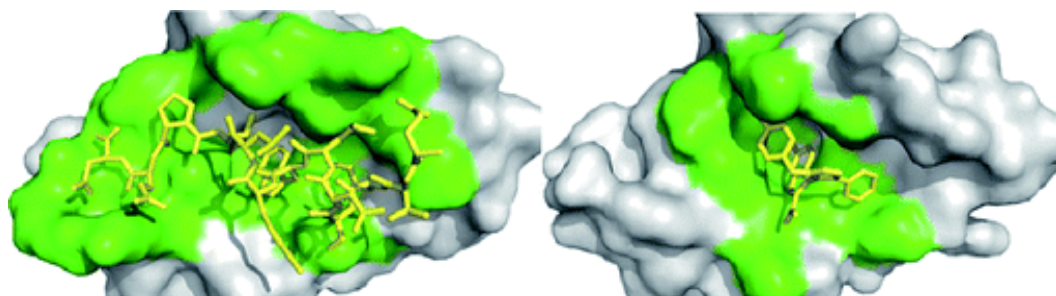


Figure 5.13 - Surface engaging interaction with p53 (left) and with a small molecule inhibitor (right).

MDM2 is shown in grey. The structure of the interacting molecule is represented in yellow sticks. The contact surface between the receptor and its ligand is highlighted in green. Reproduced from Khoury.¹⁰⁸

There are three main strategies in the development of small molecules able to engage the binding cleft competitively:

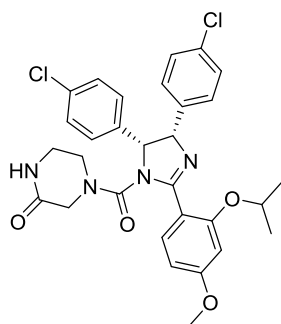
1. Type I mimetics: oligopeptides mimicking the interacting surface of the endogenous substrate, *i.e.* stapled peptides, β -peptides;
2. Type II mimetics: non-peptide small molecules engineered to fill effectively the acceptor protein binding cleft *via* a set of interactions, which are not necessarily overlapping to that of the endogenous substrate, *i.e.* Nutlins;
3. Type III mimetics: non-peptide molecules simulating the characteristic of the interacting side chains in the α -helix recognition element, *i.e.* 3,2',2''-terphenyl derivatives.

In his review on the topic,¹⁴³ Wilson stresses that, due to the particular nature of the targeted interaction, Lipinski's rule of five¹⁴⁴ is not always applicable to PPI inhibition. He also points out that ligand efficiency is constitutionally lower in PPI inhibitors compared to classic enzyme inhibitors.¹⁴³ From a drug discovery point of view, it is very important to bear in mind these two observations when targeting a PPI.

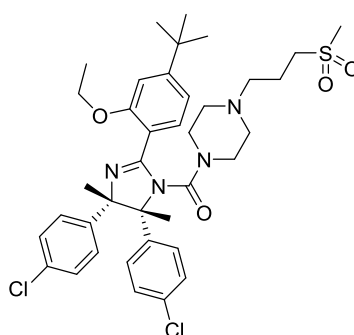
5.4 Overview of small-molecule MDMX inhibitors

In the large and growing body of literature concerning MDM2:p53 protein-protein interaction inhibitors (over 20 different chemotypes developed¹⁴⁵), only a few molecules are also active against MDMX, often with not excellent binding affinities. Here follows an overview of the most representative known small molecule inhibitors of MDMX.

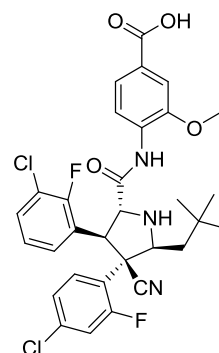
The *cis*-imidazoline Nutlin-3 (**140**), patented by Hoffman-La Roche and current benchmark compound for the inhibition of the MDM2:p53 protein-protein interaction ($K_D = 0.7 \mu\text{M}$), only weakly binds to MDMX ($K_D = 25 \mu\text{M}$) and does not reactivate p53 in MDMX-overexpressing cancer cells *in vitro*.¹³⁶ Further development in the Nutlin series led to the discovery of RG7112 (**141**) which is a very potent inhibitor of MDM2 ($\text{IC}_{50} = 18 \text{ nM}$), but has been reported as inactive against MDMX:p53.¹⁴⁶ RG7388 (**142**), a second generation MDM2 inhibitor developed by Roche and currently in phase I clinical trials, showed low micromolar activity when tested in-house (MDMX $\text{IC}_{50} = 8.04 \mu\text{M}$; MDM2 $\text{IC}_{50} = 0.4 \text{ nM}$, lit. 6 nM).¹⁴⁷



Nutlin-3a
140
MDMX $K_D = 25 \mu\text{M}$
MDM2 $K_D = 0.7 \mu\text{M}$

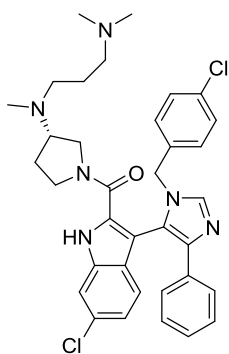


RG7112
141
MDMX *inactive*
MDM2 $\text{IC}_{50} = 0.018 \mu\text{M}$



RG7388
142
MDMX $\text{IC}_{50} = 8.04 \mu\text{M}$ (*in-house*)
MDM2 $\text{IC}_{50} = 0.006 \mu\text{M}$

In the imidazo-indole series, WK298 (**143**) is worth mentioning, as it is the only small-molecule whose co-crystal structure with MDMX has been solved and published (PDB 3LBJ; see Section 5.5).¹⁴⁸

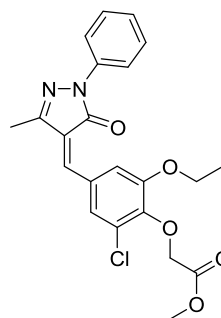


WK298

143

MDMX IC_{50} = 19.7 μ M

MDM2 IC_{50} = 0.19 μ M



SJ-172550

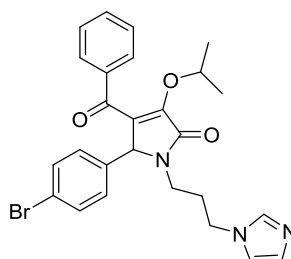
144

MDMX EC_{50} = 0.84 μ M

MDM2 *poor activity*

At St. Jude's Children Research Hospital, a selective inhibitor of MDMX was developed which enhanced the effect of Nutlin-3 in *in vitro* tests (SJ-172550, **144**: IC_{50} = 0.84 μ M).¹³⁶

Zhuang *et al.* reported pyrrolidone **145** as a nanomolar inhibitor of MDM2:p53 and a low micromolar inhibitor of MDMX:p53. To our surprise, the pyrrolidone **145** was inactive against either target in the ELISA assay available in-house (MDM2 17% inhibition at 200 μ M; MDMX no activity at 200 μ M). Consistent with the ELISA data, the pyrrolidone **145** did not show any growth-inhibitory activity against either MDM2 or MDMX overexpressing cell lines (data not shown).¹⁴⁹



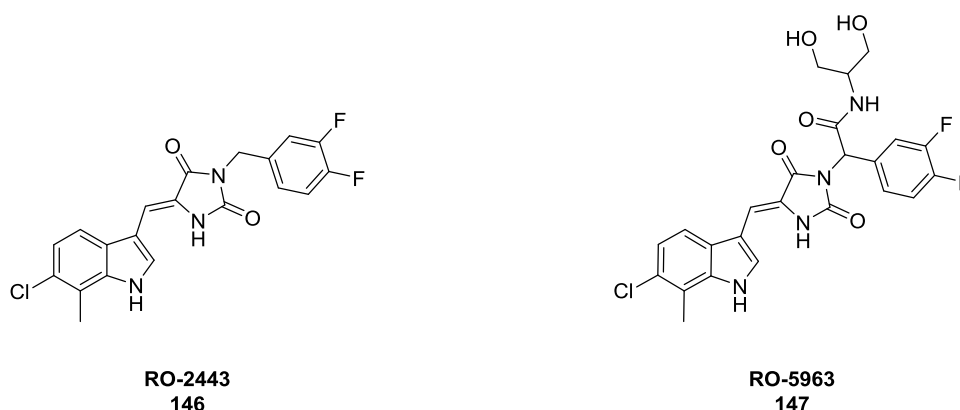
145

MDMX K_i = 2.68 μ M

MDM2 K_i = 0.26 μ M

RO-2443 (**146**) and RO-5963 (**147**) are low nanomolar inhibitors of both MDM2 and MDMX showing an unusual mechanism of action, as demonstrated by X-ray crystallography¹⁵⁰ (see Section 5.5). The compounds were synthesized and examined in our laboratories as part of the target validation process.¹⁵¹ Surprisingly, both the hydantoin compounds RO-2443 and RO-5963 were found to

be three orders of magnitude less potent in our biochemical assay compared with the values reported in the literature.¹⁵²



	MDMX IC50 (μM)	MDM2 IC50 (μM)
Published	0.041	0.033
In-house	13.7	6.9

	MDMX IC50 (μM)	MDM2 IC50 (μM)
Published	0.0247	0.0173
In-house	20.2	17.2

The most promising class of MDM2/MDMX dual inhibitors is that of stapled-peptides, short peptide sequences comprising a hydrocarbon crosslink, the ‘staple’, to promote the chain to adopt the active α -helix conformation. The most potent molecule in this series is SAH-p53-8 (MDMX K_D = 0.0023 μ M; MDM2 K_D = 0.055 μ M in a fluorescence polarization assay), whose sequence is based on that of the *N*-terminal of p53.

5.5 Structural data on MDMX

The crystal structure of zebrafish MDMX in complex with a p53 peptide (15 residues) reveals that the folding and the arrangement of the domains in MDMX are comparable to those of MDM2.¹⁵³ In MDMX, the tryptophan binding pocket seems to be less deep than in MDM2. This is due mainly to the presence of the neutral residue Met50 and to the open conformation adopted by Tyr96 (directing the hydroxyl away from the binding cleft), as opposed to the closed conformation observed in MDM2 (hydroxyl going into the binding cleft). The shallower pocket possibly results in a non-optimal interaction with one of the chlorophenyl rings of Nutlin-3a and can account for the low affinity of the inhibitor for MDMX. Although the transition of Tyr96 from an open to a closed conformation is believed to be achievable in MDMX, an energetic penalty would apply due to a steric clash with

Glu20 and the hydrophobicity requirements for an effective inhibitor may be significantly different.¹⁵³

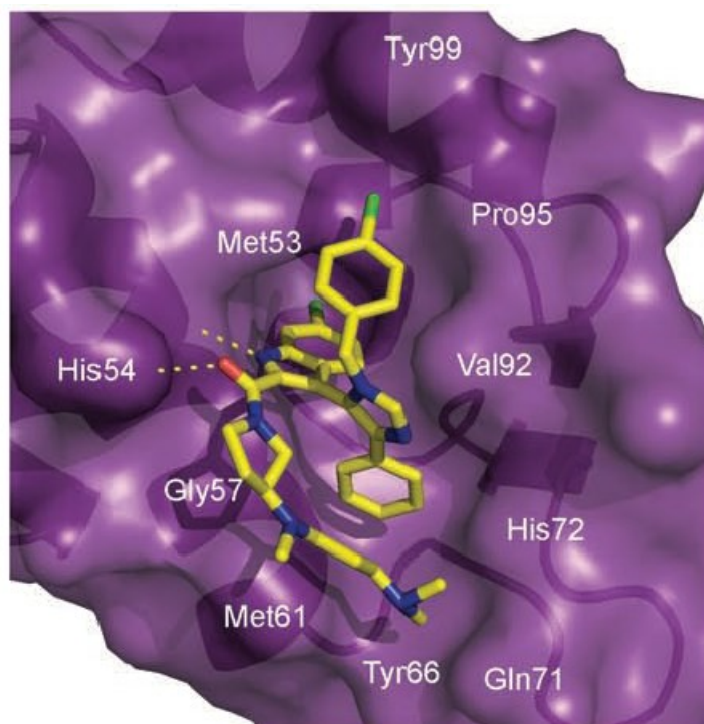


Figure 5.14 - WK298 bound to MDMX (PDB: 3LBJ).

Reproduced from Popowicz, 2010.¹⁵⁴

Although structural data of a number of peptides bound to human MDMX are available in the public domain, the co-crystal structures of only two small molecule inhibitors had been published so far. In 2010, Popowicz and co-workers obtained the crystal structure of MDMX bound to WK298 (PDB: 3LBJ).¹⁵⁴ This compound occupies the same space as the endogenous ligand p53, with the 6-chloroindole penetrating the tryptophan binding pocket, the 4-chlorobenzyl going into the leucine pocket and the phenyl ring filling the phenylalanine pocket. As shown in Figure 5.14, hydrogen bonds are established with His54 and Met53. The *N,N*-dimethylpropylamine side chain of WK298 does not point straight out to the solvent but wraps over the core and the phenyl ring. There is no significant change in the folding of the protein upon binding of the inhibitor compared to p53, although induced fit is observed, for example around the bulky 6-chloroindole. Interestingly, the Tyr99 is in a conformation, that is neither open nor closed. The interactions of the inhibitor with the other pockets, Leu26 and Phe19, are weak.

The authors also observe that the mode of binding of WK298 to MDMX is similar to that of an earlier analogue, WK23, to MDM2.

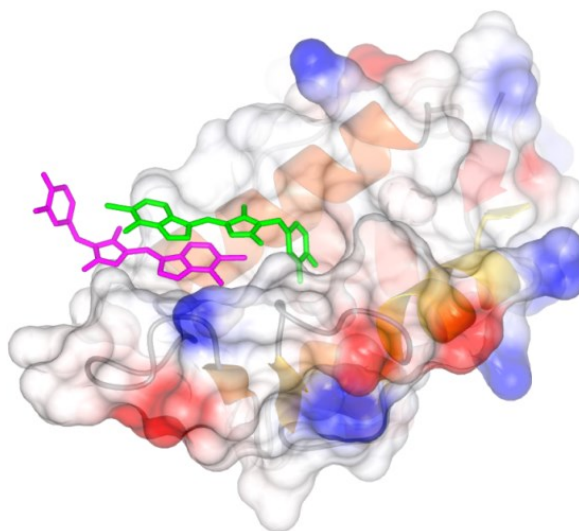


Figure 5.15 - Structure of RO-2443 inducing dimerization of MDMX.
Reproduced from PDB (3U15).¹⁵⁰

Another co-crystal structure was reported by Graves *et al.* in 2012 in which humanized-zebrafish MDMX is bound to RO-2443. As described in Section 5.4, RO-2443 displays a fairly unique binding mode (Figure 5.15), in which two molecules of inhibitor interact with one another triggering the dimerization of MDMX. The inhibitor does not interact with all three pockets. The phenylalanine pocket is occupied by the indole-hydantoin group where it can also interact with Tyr63 (π -stacking). The tryptophan binding pocket is occupied by the difluorophenyl moiety of the second inhibitor molecule and the leucine pocket is left empty. It is reasonable to assume that the same mode of binding is adopted also by the more potent RO-5963.

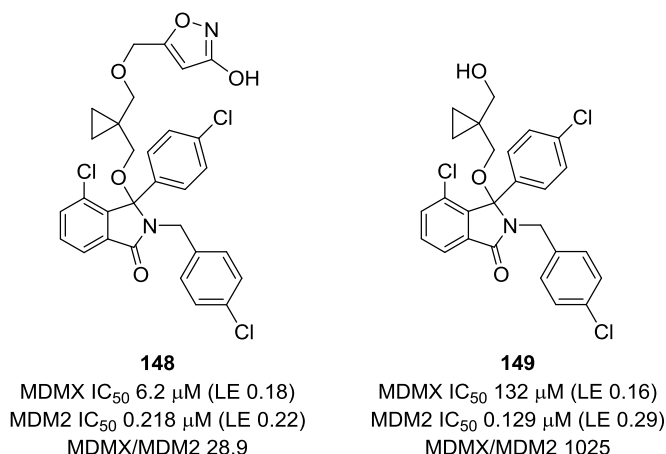
5.6 The isoindolinone series and its potential for inhibition of MDMX

In the Medicinal Chemistry Laboratories of the Newcastle Cancer Centre, within a project aimed at the inhibition of the MDM2:p53 protein-protein interaction, a series of pyrroles was developed showing dual inhibition against the target PPIs, but was discontinued because of poor solubility and off-target effects.¹⁵⁵ In a second series, a large number of diversely substituted isoindolinones were

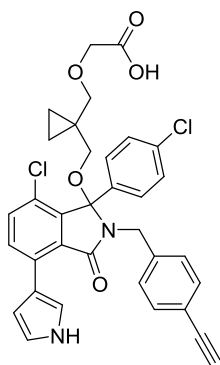
synthesized and tested against MDM2. Activity against MDMX was also measured for some of the most potent compounds in order to assess selectivity. Several compounds proved to be low micromolar inhibitors of MDMX, thus offering the chance to elucidate the differences in the binding interactions with the two proteins and, potentially, to lead to the development of selective MDMX inhibitors or dual MDM2/MDMX inhibitors.

The isoindolinones with the lowest IC_{50} against MDMX:p53 are:

1. Compound **148** (MDMX IC_{50} = 6.22 μ M; MDM2 IC_{50} = 0.218 μ M): characterized by the presence of a 3-hydroxyisoxazole as a carboxylic acid replacement at the extremity of the side chain, this isoindolinone shows a 21-fold increase in potency compared to its parent compound **149**. The enantiomers were not resolved.

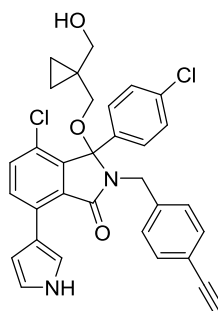


2. Compound **150** (MDMX IC_{50} = 6.54 μ M; MDM2 IC_{50} = 0.071 μ M): bears a pyrrole ring at the 7-position and a carboxylic acid moiety on the side chain. Its potency as a racemate is significantly higher than both its parent racemic alcohol **151** (MDMX IC_{50} = 55 μ M) and the correspondent active enantiomer of the latter, **152** (MDMX IC_{50} = 30 μ M).



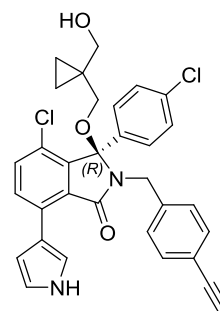
150

MDMX IC_{50} = 6.5 μ M (LE 0.17)
MDM2 IC_{50} = 71.4 nM (LE 0.23)
MDMX/MDM2 92



151

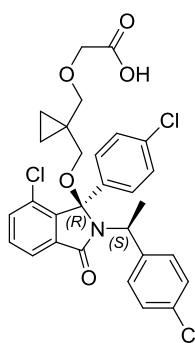
MDMX IC_{50} = 55 μ M (LE 0.15)
MDM2 IC_{50} = 27.6 nM (LE 0.27)
MDMX/MDM2 1990



152

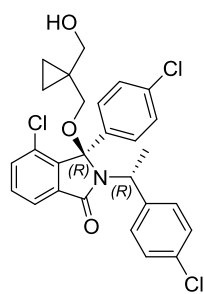
MDMX IC_{50} = 30 μ M (LE 0.16)
MDM2 IC_{50} = 57.5 nM (LE 0.25)
MDMX/MDM2 517

3. Compound **153** (MDMX IC_{50} = 16.7 μ M; MDM2 IC_{50} = 0.036 μ M): a methyl group was added at the benzylic position, alpha to the isoindolinone nitrogen, to enable the separation of diastereoisomers by traditional column chromatography using an enantiopure starting material α -methylbenzylamine. This approach was advantageous compared to time-consuming chiral HPLC for separating enantiomers. As already seen for **150**, the potency of each of the four diastereoisomers bearing the free alcohol moiety **154-157** is not excellent (ranging from 60 to 130 μ M), but when the carboxylic acid is introduced, an increase in activity is observed for the (3*R*,1'*S*) isomer (**153**). The latter compound was chosen as a benchmark in the context of the development of MDMX inhibitors (see Section 5.7).



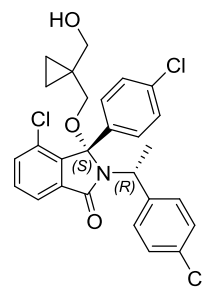
153

MDMX IC_{50} = 16.65 μ M (LE 0.17)
MDM2 IC_{50} = 0.0357 μ M (LE 0.27)
MDMX/MDM2 467



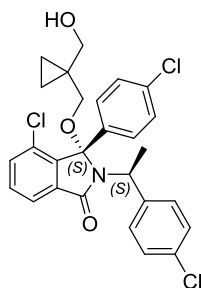
154

MDMX IC_{50} = 102 μ M (LE 0.16)
MDM2 IC_{50} = 1.71 μ M (LE 0.23)
MDMX/MDM2 60



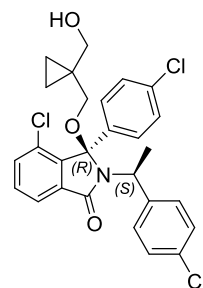
155

MDMX IC_{50} = 132 μ M (LE 0.16)
MDM2 IC_{50} = 1.15 μ M (LE 0.24)
MDMX/MDM2 115



156

MDMX 40% @ 200 μ M
MDM2 IC_{50} = 11.4 μ M (LE 0.20)
MDMX/MDM2 N/A



157

MDMX IC_{50} = 59.6 μ M (LE 0.17)
MDM2 IC_{50} = 0.0394 μ M (LE 0.30)
MDMX/MDM2 1512

Structural data¹⁵⁶ show that isoindolinones bind to MDM2 so that the core is accommodated in the Phe19 pocket, the 4-chlorophenyl occupies the Trp23 pocket and the 4-chlorobenzyl enters the Leu26 pocket, while the cyclopropyl side chain points out towards the solvent. In the light of the results published by Popowicz *et al.* regarding the imidazolyl-indole scaffold,¹⁵⁴ it is reasonable to assume that the mode of binding of the isoindolinones with MDMX is similar to the one observed with MDM2.

5.7 Project aims and design of selective MDMX inhibitors

The current literature suggests that inhibition of the MDM2:p53 interaction alone may not be enough to treat wild-type p53 cancer effectively. In addition to its low nanomolar potency against MDM2, the isoindolinone scaffold would become more valuable if dual inhibition could be achieved. The objective of the work described herein was to identify an isoindolinone with a submicromolar IC_{50} against both MDMX and MDM2. Key to this was the achievement of a deeper understanding of

the interaction of the isoindolinones with MDMX through SAR studies and/or a co-crystal structure.

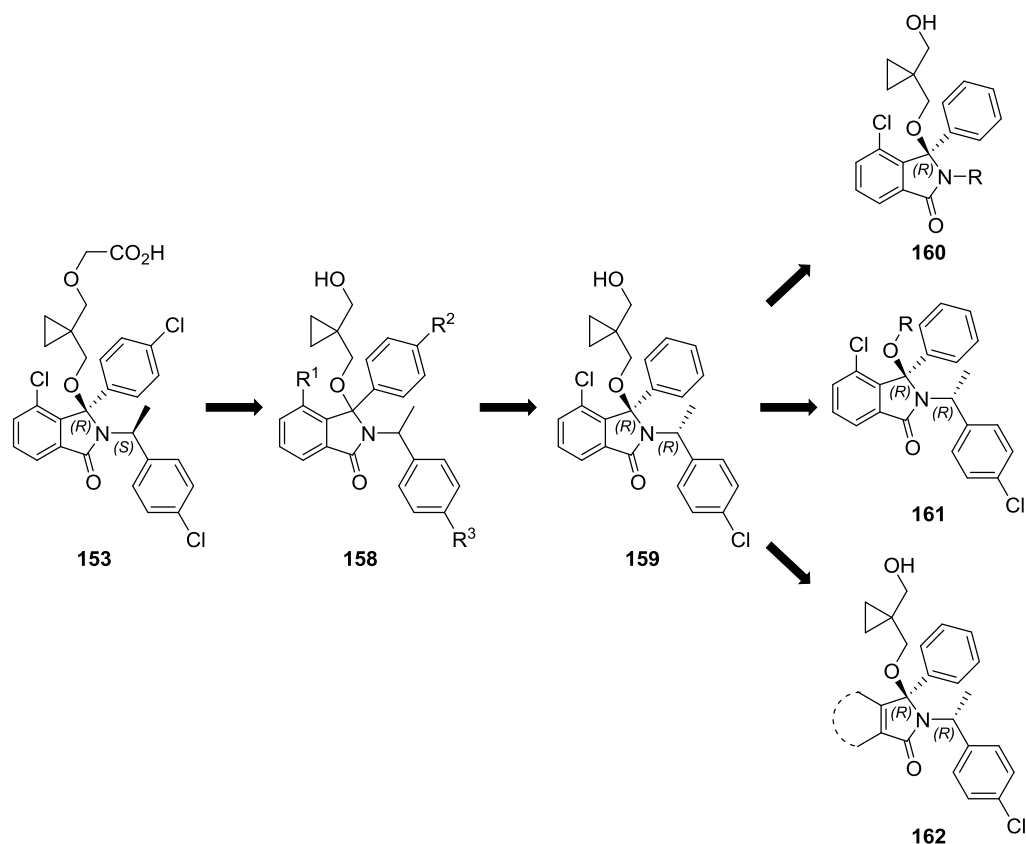


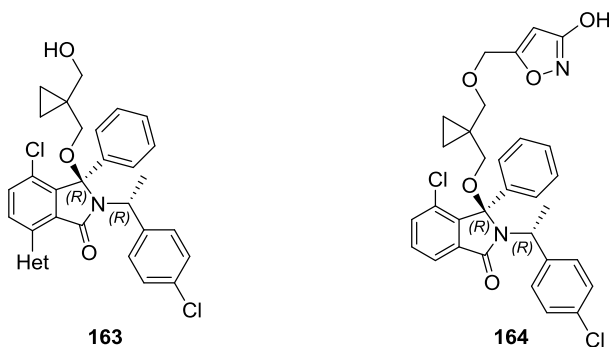
Figure 5.16 - SAR studies of the isoindolinone scaffold against MDMX:p53.

For the SAR studies, a structural minimization approach was undertaken to quickly and effectively assess what parts of the molecule are necessary for binding. The 1'-methyl isoindolinone **153** was chosen as a starting point, offering the opportunity to investigate both the contribution to binding of each one of the three chloro substituents and the stereochemical preference of the two proteins. Compound **159**, with its (3*R*,1'*R*) configuration at the stereocentres and lack of the 4-chloro substituent on the 3-phenyl ring, showed selectivity towards MDMX and was therefore selected as a benchmark compound for further studies. The contribution to binding of each part of the molecule was assessed by sequential removal of the benzyl (**160**), simplification of the cyclopropane side chain (**161**) and by minimization of the isoindolinone core (**162**).

Following some promising inhibition data against MDMX in the library of compounds designed to target MDM2, nitrogen-containing heterocycles were

introduced at the 7-position of **159**. For the same reason, the side chain was extended with a 3-hydroxyisoxazole (**164**), trying to achieve the same 20-fold jump in potency observed in the *des*-methyl series. Exploration of the Leu26 pocket was attempted by replacement of the chlorine at the 4-benzyl position with a variety of substituents with different electronic and steric requirements.

When possible, the synthesized compounds were tested against both MDMX:p53 and MDM2:p53.



With regard to the structural biology aspects of the project, a group of isoindolinones having either good potency (low micromolar range) or good selectivity against MDMX was selected from the available library to perform co-crystallization trials with three constructs of both MDMX and MDM2.

CHAPTER 6. RESULTS AND DISCUSSION - MDMX

6.1 Sequential chlorine deletion

6.1.1 Rationale for the targets

The first aims of the project were to investigate a) the contribution to binding of each one of the chlorine atoms present in **153** and b) the absolute configuration preferred by MDMX at the two stereocentres. Although previous results obtained in the MDM2:p53 project showed that a terminal carboxylic acid on the side chain improves potency against both MDMX and MDM2, the synthesis was stopped at the (1-hydroxymethyl-cyclopropyl)methoxy side chain for the purposes of this study. Twelve analogues of **157**, a precursor of **153**, in which a single chloro-group was replaced with a hydrogen atom were synthesised in all four diastereomeric forms (Figure 6.1 – **165-167**). The set of diastereoisomers lacking all three chlorines was also synthesized (Figure 6.1 – **168**).

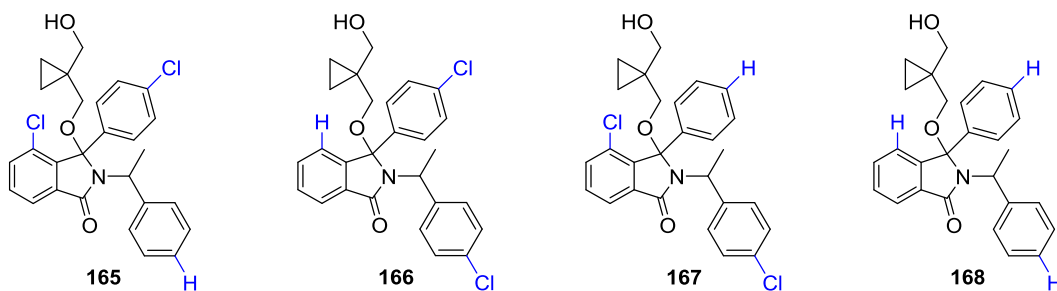
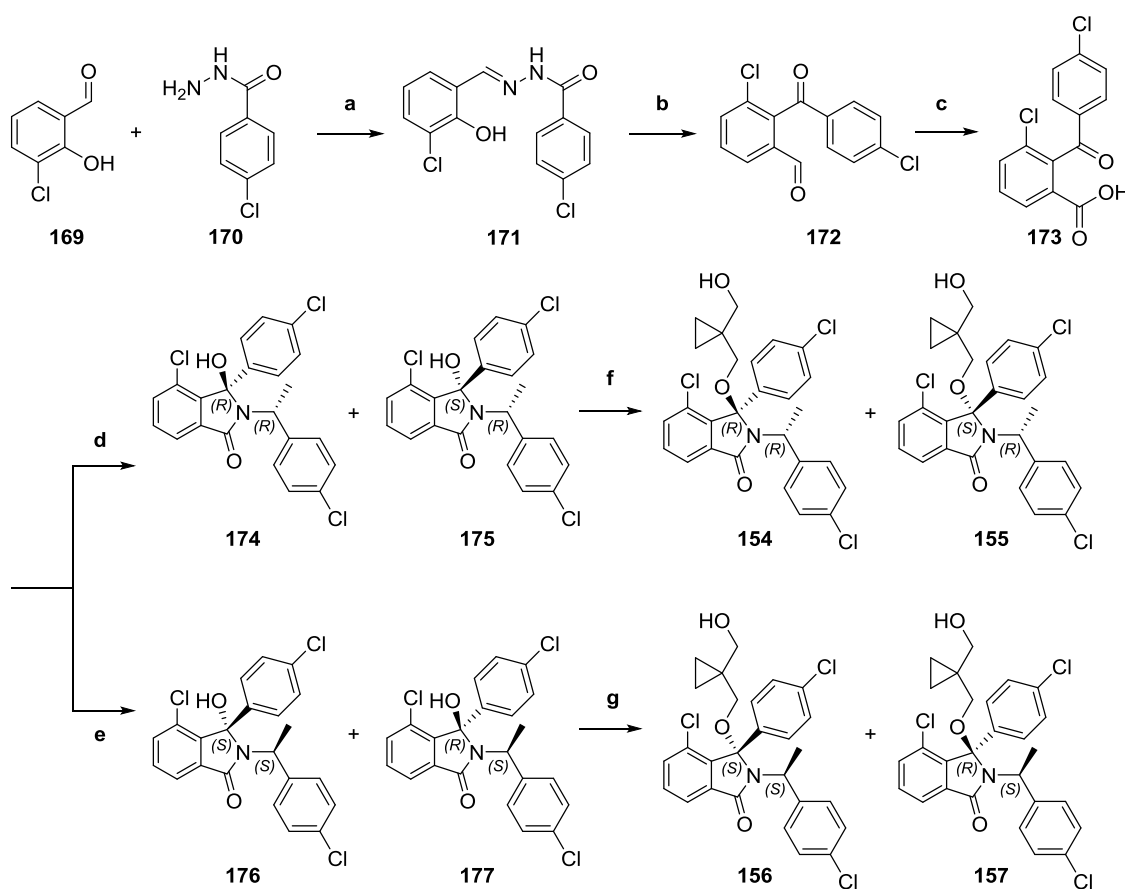


Figure 6.1 - Sequential chlorine deletion from the initial hit 153.

6.1.2 Synthetic route to the targets

The synthesis of the sixteen target isoindolinones was accomplished following the route previously used by Sarah Cully¹⁵⁶ and Bian Zhang¹⁵⁷ to obtain **157** and its diastereoisomers. This 5-step regiospecific synthetic pathway was developed within the MDM2:p53 inhibition project and is based on work of Jacq *et al.*¹⁵⁸ for the synthesis of 2-benzoylbenzoic acids.¹⁵⁹ As shown in Scheme 6.1, coupling of 3-chloro-2-hydroxybenzaldehyde **169** and 4-chlorobenzhydrazide **170** in acetic acid yielded the *N*-aroylhydrazone **171**.¹⁵⁸ A lead tetraacetate-mediated rearrangement¹⁵⁸ yielded the aldehyde **172**, which was oxidized to the corresponding carboxylic acid **173** following the Pinnick procedure.¹⁶⁰ The

formation of the isoindolinone core was performed *via* thionyl chloride-promoted formation of the acid chloride, followed by reaction with the appropriate enantiopure 4-chloro- α -methylbenzylamine: the (*R*)- α -methylbenzylamine yielded isoindolinones **174** and **175**, while the mirror image isoindolinones **176** and **177** were obtained using (*S*)- α -methylbenzylamine. Vilsmeier reagent was reacted *in situ* with each pair of intermediate 3-hydroxyisoindolinones to form the ether linkage between the (1-hydroxymethylcyclopropyl)methoxy side chain and to obtain the target compounds **154** and **155**, **156** and **157** (Scheme 6.1).¹⁵⁷ The diastereoisomers were separated by column chromatography on silica in the last step.



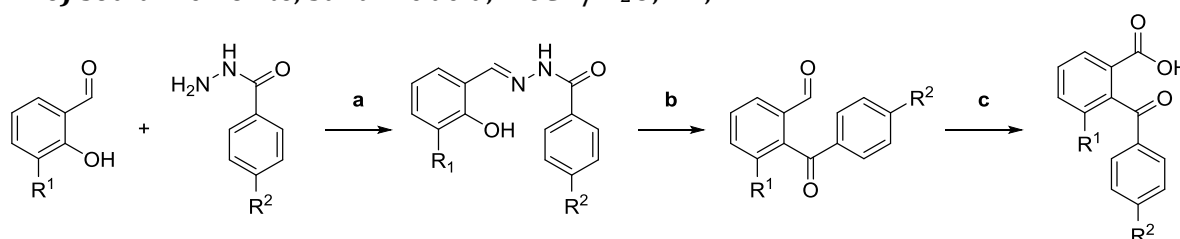
Scheme 6.1 - Synthesis of four isoindolinone diastereoisomers by B. Zhang.

Reagents and conditions: **a)** acetic acid, RT, 1 h, 97%; **b)** Pb(OAc)₄, THF, RT, 3 h, 79%; **c)** sodium chlorite, sulfamic acid, MeCN/H₂O, RT, 2 h, 94%; **d)** i) SOCl₂, cat. DMF, THF, RT, 4 h; ii) (*R*)-4-chloro- α -methylbenzylamine, DIPEA, THF, RT, 18 h, 61%; **e)** i) SOCl₂, cat. DMF, THF, RT, 4 h; ii) (*S*)-4-chloro- α -methylbenzylamine, DIPEA, THF, RT, 18 h, 35%; **f)** i) SOCl₂, cat. DMF, THF, RT, 4 h; ii) 1,1-bis(hydroxymethyl)cyclopropane, K₂CO₃, THF, RT, 18 h, **154** 6%, **155** 13%; **g)** i) SOCl₂, cat. DMF, THF, RT, 4 h; ii) 1,1-bis(hydroxymethyl)cyclopropane, K₂CO₃, THF, RT, 18 h, **156** 8%, **157** 32%.

During the synthesis of the abovementioned sixteen analogues, all steps were found to be highly reproducible. A higher yielding InBr_3 -promoted ether linkage formation optimized by Timothy Blackburn¹⁶¹ was used to add the side chain to the isoindolinone core. The *N*-aroylhydrazone did not require any purification and could be used directly in the second step. The desired carboxylic acid intermediates were obtained in very good to excellent yields (Table 6.1). The lower yield for compound **186** was due to poor recovery following recrystallization.

Table 6.1 - Summary of yields for the synthesis of benzoylbenzoic acids.

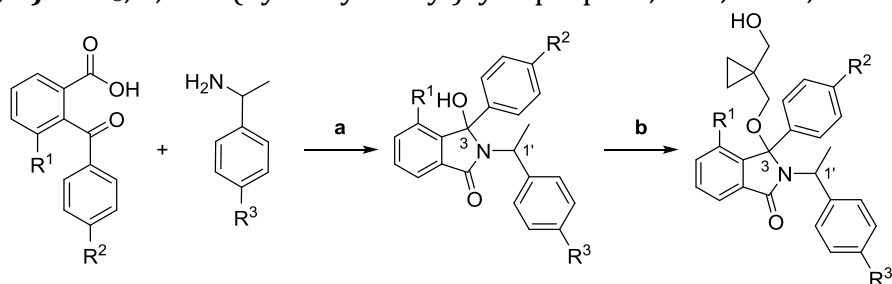
Reagents and conditions: **a)** acetic acid, RT, 1 h; **b)** $\text{Pb}(\text{OAc})_4$, THF, RT, 3 h; **c)** sodium chlorite, sulfamic acid, $\text{MeCN}/\text{H}_2\text{O}$, RT, 2 h.



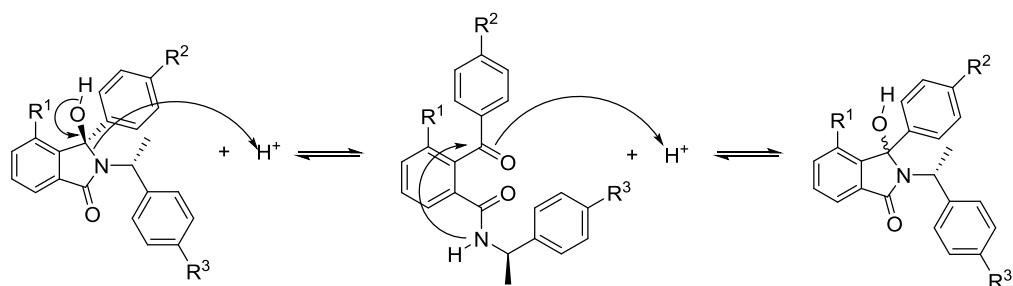
#	R ¹	R ²	Product (isolated yield %) Step a	Product (isolated yield %) Step b	Product (isolated yield %) Step c
1	Cl	Cl	178 (86)	179 (95)	180 (95)
2	Cl	H	181 (95)	182 (90)	183 (96)
3	H	Cl	184 (97)	185 (93)	186 (57)
4	H	H	187 (86)	188 (90)	189 (95)

The formation of the isoindolinone core was performed using the appropriate enantiopure α -methylbenzylamine (Table 6.2 – Step a). In some cases, the two isoindolinone diastereoisomers were separated at this stage, but epimerization was observed by polarimetry when compounds were solubilized in ethanol. To allow reliable optical rotation measurements, the compounds were dissolved in EtOAc. Ring-chain tautomerism occurring at the isoindolinone stereocentre with formation of a sp^2 (planar) carbon is probably responsible for this phenomenon (Scheme 6.2). Following this observation, the two diastereoisomers were taken to the next step without attempting any separation during the purification.

Table 6.2 - Summary of yields for the synthesis of the target isoindolinones.
Reagents and conditions: a) i) SOCl₂, cat. DMF, THF, RT, 4 h; ii) amine, DIPEA, THF, RT, 18 h; b) InBr₃, 1,1-bis(hydroxymethyl)cyclopropane, DCE, 80 °C, 18 h.



#	R ¹	R ²	R ³	(3,1')	Product (isolated yield %) step a	Product (isolated yield %) step b
1	Cl	Cl	H	<i>R,R</i>	190 (20)	191 (24)
2	Cl	Cl	H	<i>S,R</i>	192 (23)	193 (23)
3	Cl	Cl	H	<i>S,S</i>	194 (40)	195 (35)
4	Cl	Cl	H	<i>R,S</i>	196 (30)	197 (26)
5	Cl	H	Cl	<i>R,R</i>	198 (88)	159 (36)
6	Cl	H	Cl	<i>S,R</i>		199 (44)
7	Cl	H	Cl	<i>S,S</i>	200 (94)	201 (43)
8	Cl	H	Cl	<i>R,S</i>		202 (50)
9	H	Cl	Cl	<i>R,R</i>	203 (96)	204 (40)
10	H	Cl	Cl	<i>S,R</i>		205 (38)
11	H	Cl	Cl	<i>S,S</i>	206 (94)	207 (39)
12	H	Cl	Cl	<i>R,S</i>		208 (38)
13	H	H	H	<i>R,R</i>	209 (16)	210 (24)
14	H	H	H	<i>S,R</i>	211 (11)	212 (23)
15	H	H	H	<i>S,S</i>	213 (34)	214 (20)
16	H	H	H	<i>R,S</i>	215 (36)	216 (9)



Scheme 6.2 - Ring-chain tautomerism of isoindolinones in protic solvents.

With regard to the indium bromide-promoted addition of the side chain, the low yields for the unsubstituted isoindolinones **210**, **212**, **214**, and **216** (Scheme 6.2 – Step b – Entries 13-16) were caused by poor separation during purification on silica, due to similar retention factors probably caused by the absence of substituents reducing the difference in polarity of the two diastereoisomers.

6.1.3 Determination of the absolute configuration at the isoindolinone stereocentre

The absolute configuration of **155** had previously been unambiguously assigned by X-ray crystallography and was found to be (*S*) at the 3-position of the isoindolinone ring and confirmed to be (*R*) at the benzylic position, in agreement with the stereochemistry of the α -methylbenzylamine used for the synthesis. Once the absolute stereochemistry of **155** had been assigned, the configuration of the stereocentres of the remaining three diastereoisomers could be deduced by virtue of the stereochemical relationships among the four compounds (Figure 6.2 and Table 6.3). The isomer present in the same mixture, **154**, must have the opposite configuration at the isoindolinone stereocentre (*R*), while retaining the same configuration at the benzylic position (*R*). The other pair of diastereoisomers had been obtained using enantiopure (*S*)-4-chloro- α -methylbenzylamine, and were therefore expected to have (*S*) configuration at the benzylic position. By comparison of physicochemical properties such as polarity, optical rotation and $^1\text{H-NMR}$, **157** was found to be enantiomer of **155**, and **156** to be enantiomer of **154**.¹⁵⁷ Epimerization at the 3-position can be excluded after addition of the side chain.

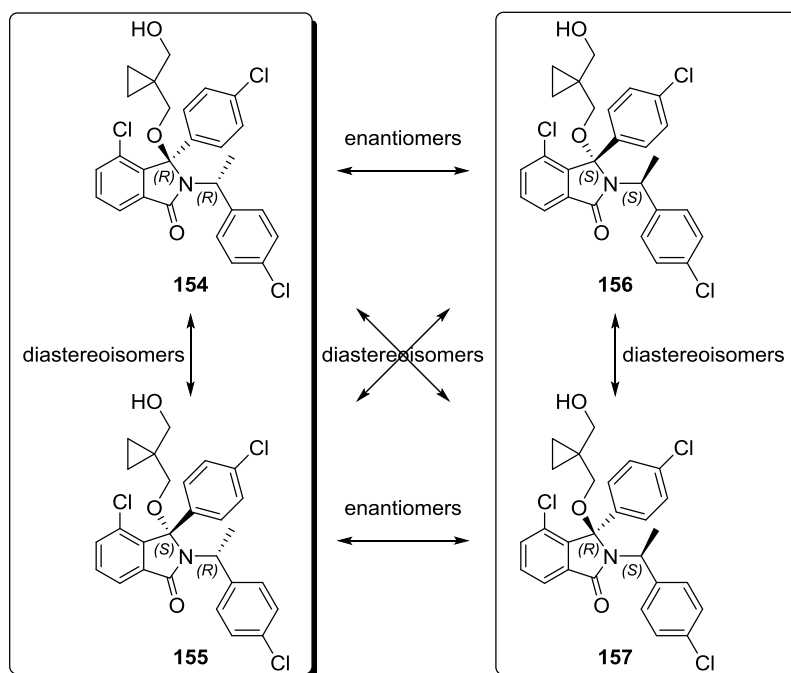


Figure 6.2 - Stereochemical relationship between the four diastereoisomers of 157.

Each framed pair of diastereoisomers was generated in the same reaction.

Initially, the absolute configuration of the isoindolinone stereocentre of the twelve dichloro- and the four *des*-chloro- analogues in Table 6.2 was arbitrarily assigned by comparison of their physicochemical properties, such as polarity and optical rotation data, with those of the trichloro-analogues **154-157**. The data available for **155** and its diastereoisomers, allowed two main observations to be made: a) the (3*R*,1'*R*) and (3*S*,1'*S*) isomers were more lipophilic and b) an (*R*) configuration at the benzylic stereocentre caused polarized light to rotate clockwise ($[\alpha] > 0^\circ$). The absolute configurations of the sixteen new isoindolinones were assigned on the basis of such evidence (Table 6.3). Subsequently, the stereochemistry predicted for compounds **199** and **208** was confirmed by X-ray crystallography (Figure 6.3 and Figure 6.4).

Table 6.3 - Table for the arbitrary assignment of the configuration at the two stereocentres of the compounds synthesized.

#	Compound	R_f	Optical rotation	(3,1')
1	154	0.54 (33% EtOAc/petrol)	$[\alpha]_D^{24} +60$ (c 0.100, EtOH)	<i>R,R</i>
2	155	0.37 (33% EtOAc/petrol)	$[\alpha]_D^{24} +59$ (c 0.100, EtOH)	<i>S,R</i>
3	156	0.54 (33% EtOAc/petrol)	$[\alpha]_D^{24} -65$ (c 0.100, EtOH)	<i>S,S</i>
4	157	0.37 (33% EtOAc/petrol)	$[\alpha]_D^{24} -56$ (c 0.100, EtOH)	<i>R,S</i>
5	159	0.25 (25% EtOAc/petrol)	$[\alpha]_D^{24} +118^\circ$ (c 0.764, EtOAc)	<i>R,R</i>
6	199	0.14 (25% EtOAc/petrol)	$[\alpha]_D^{24} +35^\circ$ (c 0.747, EtOAc)	<i>S,R</i>
7	201	0.25 (25% EtOAc/petrol)	$[\alpha]_D^{24} -115$ (c 0.745, EtOAc)	<i>S,S</i>
8	202	0.14 (25% EtOAc/petrol)	$[\alpha]_D^{24} -35$ (c 0.878, EtOAc)	<i>R,S</i>
9	204	0.17 (25% EtOAc/petrol)	$[\alpha]_D^{30} +105$ (c 0.502, EtOAc)	<i>R,R</i>
10	205	0.09 (25% EtOAc/petrol)	$[\alpha]_D^{30} +21^\circ$ (c 0.210, EtOAc)	<i>S,R</i>
11	207	0.17 (25% EtOAc/petrol)	$[\alpha]_D^{30} -105^\circ$ (c 0.477, EtOAc)	<i>S,S</i>
12	208	0.09 (25% EtOAc/petrol)	$[\alpha]_D^{30} +22^\circ$ (c 0.200, EtOAc)	<i>R,S</i>

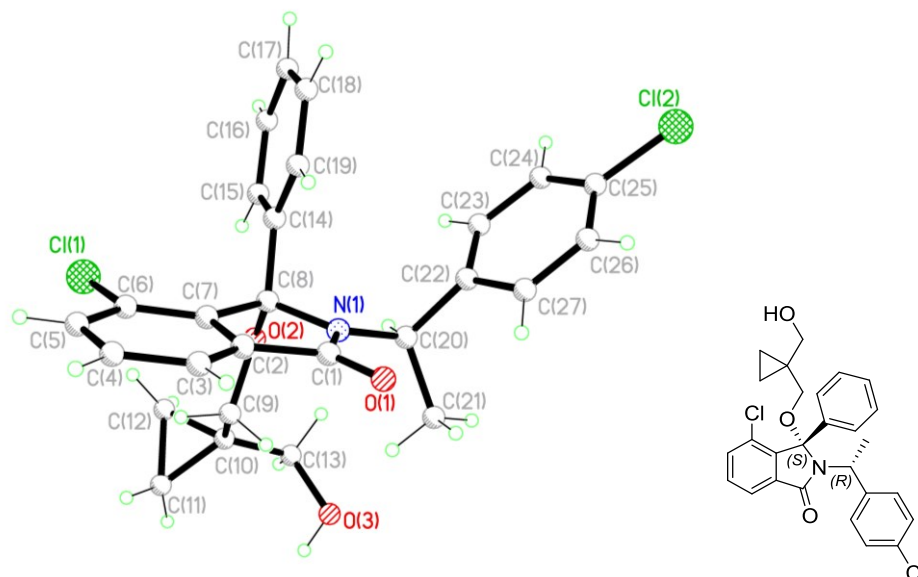


Figure 6.3 - X-ray crystal structure of the isoindolinone 199.

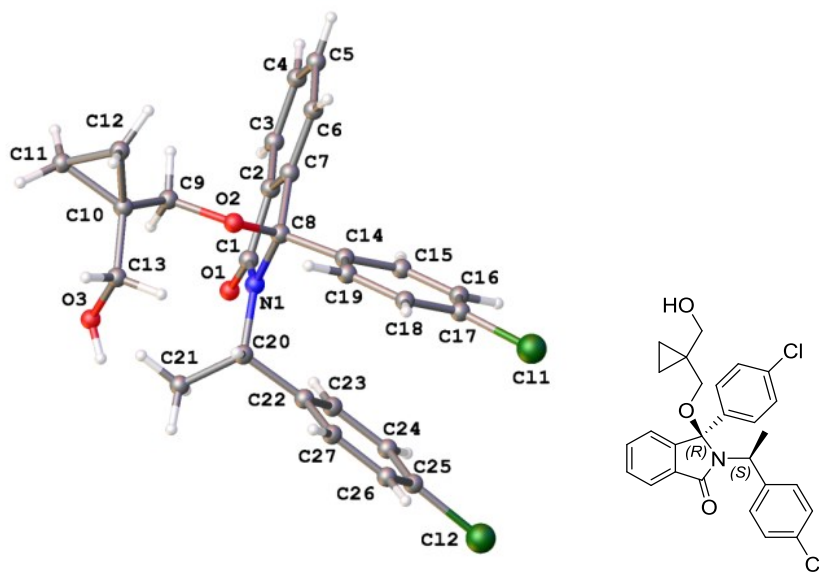


Figure 6.4 - X-ray crystal structure of the isoindolinone 208.

In the light of the X-ray data, the analysis of the ^1H -NMR of pairs of enantiomers allowed making a few interesting observations. Figure 6.6 shows the spectra for compounds **159** and **199** in CDCl_3 . The protons of the cyclopropyl ring are more shielded in the (3*R*,1'*R*) diastereoisomer **159** (−0.07–−0.04 and 0.14–0.25 ppm) than they are in the (3*S*,1'*R*) isomer **199** (0.51–0.71 ppm). The same applies to the two side chain methylene groups (double doublets between 2.89 and 3.75 ppm). In the aromatic region, the protons of the benzyl and the phenyl rings are more shielded in **199** ($\delta_{\text{H}} < 7.26$ ppm), in which both rings point in the same direction.

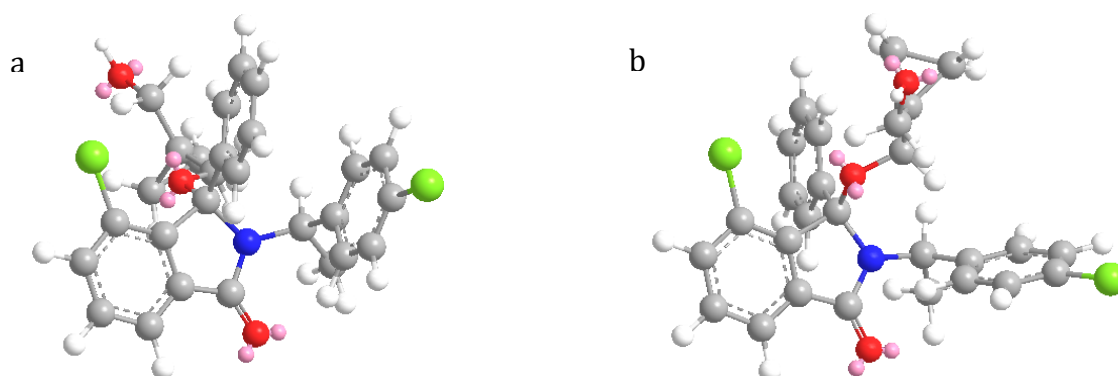


Figure 6.5 - Model of two isoindolinone stereoisomers.

Model of **159** (a) and **199** (b) obtained by iterative calculation of the minimum conformational energy using ChemBio3D Ultra.

The crystal structure of the (3*S*,1'*R*) diastereoisomer **199** shown in Figure 6.3 confirms the prediction obtained using ChemBio3D Ultra by iterative minimization of the conformational energy (Figure 6.5b) and suggests that the aromatic rings of

the benzyl and the phenyl form a π -stacking interaction which cannot be achieved with opposite configuration at the 3 stereocentre, as in (3*R*,1'*R*)-**159**, where they point away from each other as predicted by the model (Figure 6.5a). The establishment of such an interaction may be responsible for the shielding effect on the benzyl and phenyl protons observed in **199**.

The rotation of the phenyl ring was slow compared to the NMR time scale, resulting in a broad signal for its protons; this was more evident for diastereoisomer **199**. In support of this analysis, a variable temperature ^1H -NMR in DMSO- d_6 showed that when the temperature was raised, and therefore molecular mobility was increased allowing the phenyl to rotate, the peak at 7.12 ppm increased in intensity and became sharper (Figure 6.7). A similar trend for the (3*R*,1'*R*) and (3*R*,1'*S*) diastereoisomers (and their enantiomers) could be found in the ^1H -NMR of all the other compounds. In the light of the data shown here, it was considered reasonable to perform subsequent assignments of the configuration at the isoindolinone stereocentre on the basis of polarity, ^1H -NMR and optical rotation data.

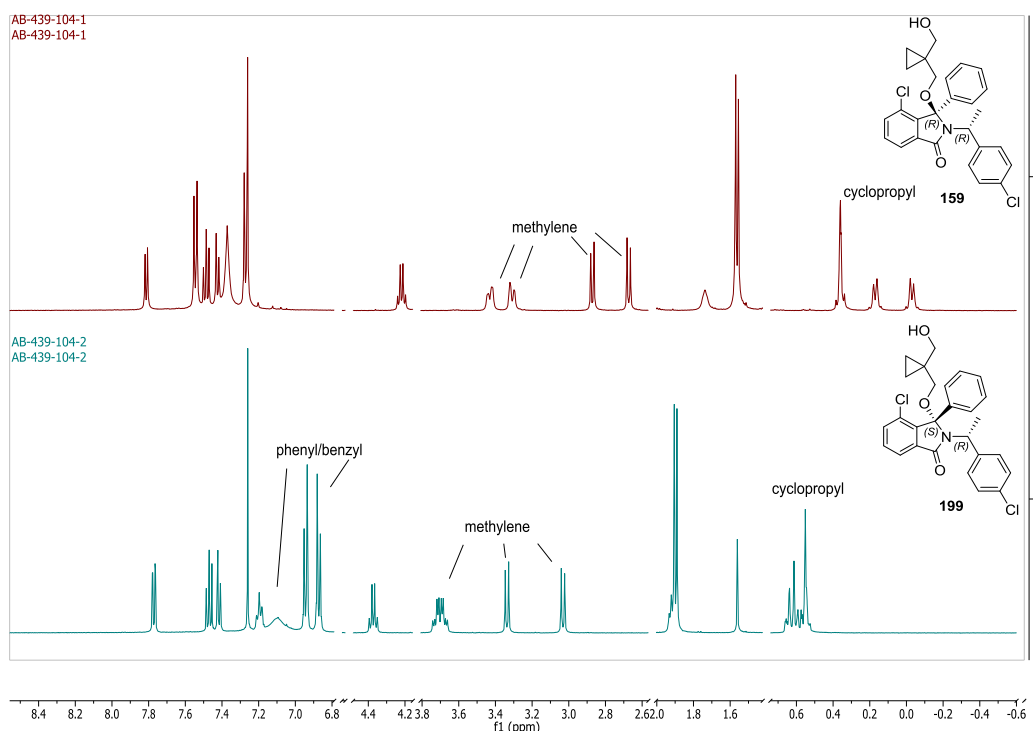


Figure 6.6 - NMR analysis of isoindolinone diastereoisomers.

Comparison between the ^1H -NMR of the (3*R*,1'*R*) isomer **159** (red) and the (3*S*,1'*R*) isomer **199** (blue).

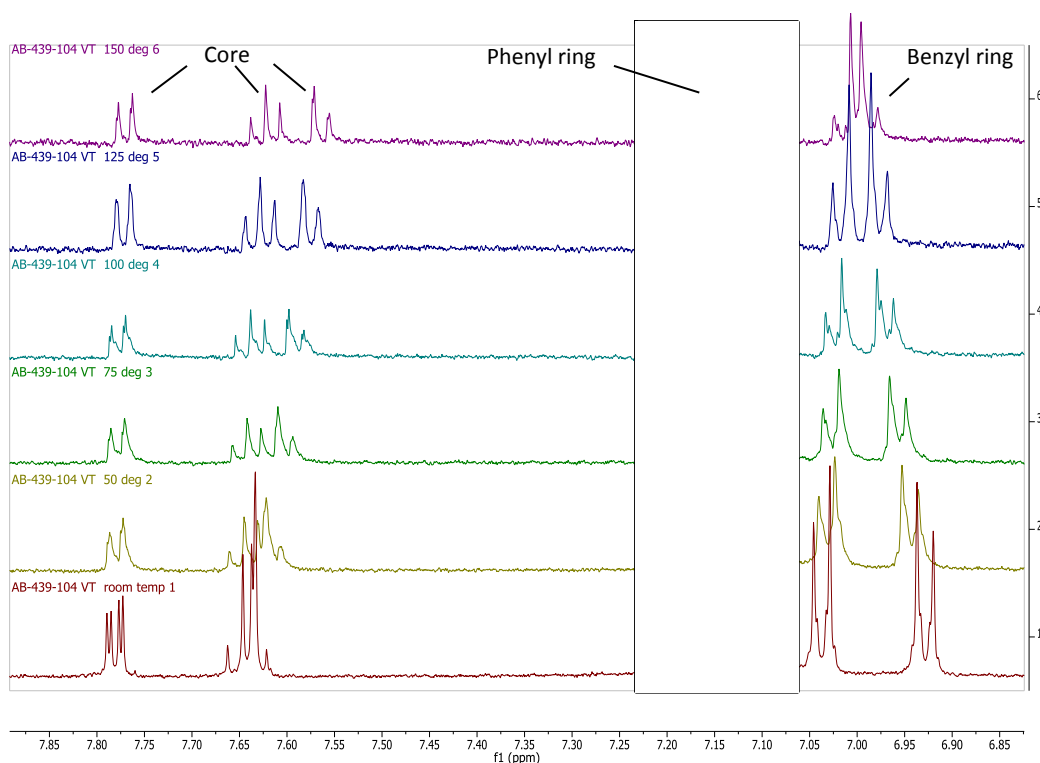


Figure 6.7 - Variable temperature ^1H -NMR of 199.
Aromatic region.

6.1.4 Biological evaluation

The activities of the sixteen isoindolinones were measured by Yan Zhao¹⁶² against both full length MDMX and full length MDM2 (produced by *in vitro* transcription/translation) in an ELISA assay format (Figure 6.8) using DMSO as negative control and AP-B peptide¹⁶³ as positive control. Unless otherwise stated, one replicate was performed for each inhibitor. As shown in Table 6.4, activities are reported either as percentage inhibition at 200 μM or as half maximal inhibitory concentration (IC_{50}) for compounds with percentage inhibition lower than 50%. For comparison, entries 1-4 report the IC_{50} values for the trichloro compounds synthesized by Bian Zhang.

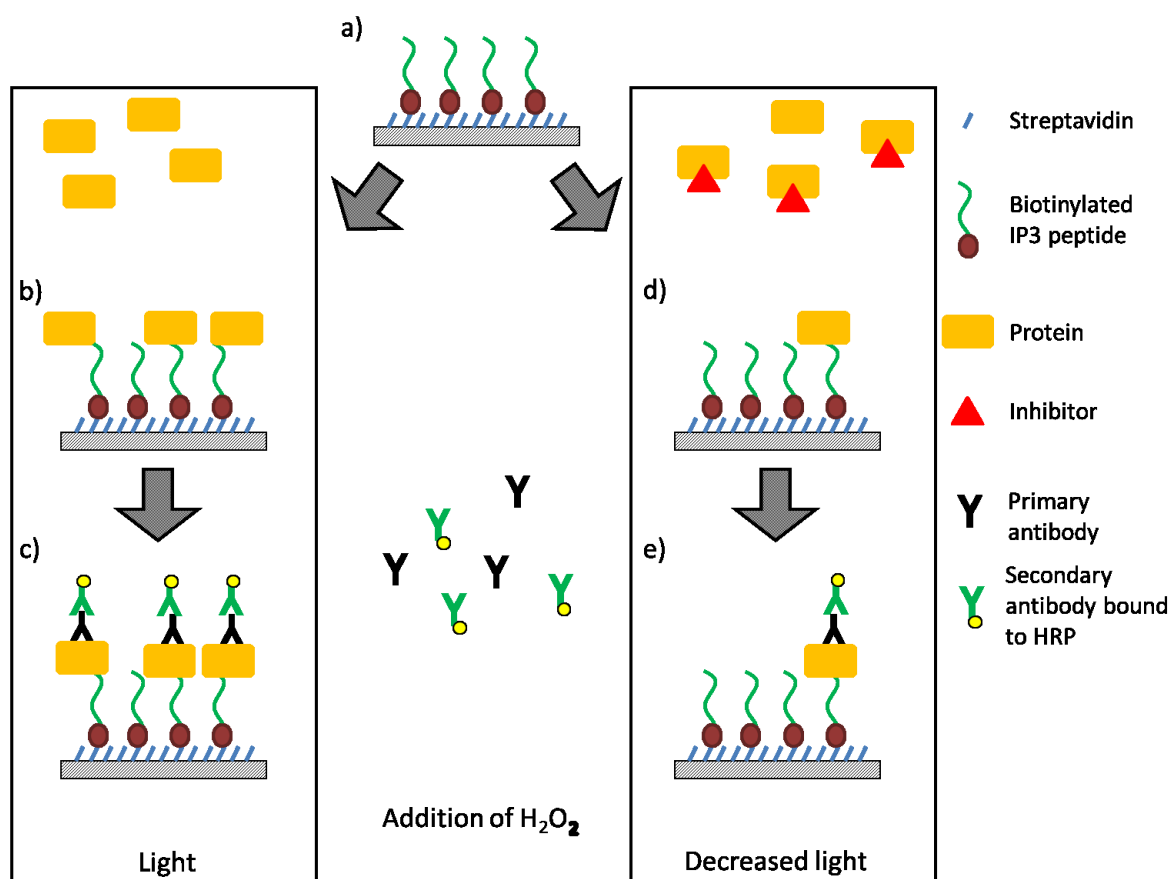


Figure 6.8 - Schematic representation of the ELISA for MDMX and MDM2.

a) Biotinylated IP3 peptide¹⁶⁴ is immobilized on a streptavidin-coated plate; **b)** protein (MDMX or MDM2) binds the the IP3 peptide; **c)** the target protein is recognized by a primary antibody to which a secondary antibody conjugated to horseradish peroxidase (HRP) binds. Addition of hydrogen peroxide causes oxidation of HRP and emission of light; **d)** in the presence of an inhibitor, only a fraction of protein binds to the IP3 peptide leading to **e)** decreased light emission. Adapted from Sarah Cully.¹⁶⁵

Removal of the chlorine from the benzyl group (Table 6.4 – Entries 5-8) did not lead to an increase in neither MDMX nor MDM2 activity. Removal of the chlorine from the chlorophenyl group (Table 6.4 – Entries 9-12) caused a significant drop in MDM2 activity, whereas the (3*R*,1'*R*) diastereoisomer **159** (entry 9) showed a 4-fold increase in the activity against MDMX ($IC_{50} = 25.9 \mu M$), which led to an inversion in the selectivity (MDMX/MDM2 0.14). The efficiency of the binding of **159** to MDMX, expressed as ligand efficiency (LE) was the highest in the isoindolinone series (LE = 0.19). Its enantiomer **201** (entry 11) also had a preference towards MDMX (MDMX/MDM2 0.86), although it was ~6-fold lower

than that of **159**. A possible explanation is that the 4-chlorophenyl is likely to make a favourable interaction with MDM2, *e.g.* halogen bond, and loss of the chloro-substituent results in reduced potency against this target. However, the relatively high potency observed for **202** (entry 12; IC₅₀ = 1.98 μM) is in contradiction with this theory. Nonetheless, it seems reasonable to postulate that a favourable interaction is formed when **159** interacts with MDMX. Replacement of the chlorine at the 4-position of the isoindolinone core with a hydrogen (Table 6.4 – Entries 13-16) also reduced affinity against MDM2, apart from the (3*S*,1'*R*) isomer, but did not seem to affect greatly MDMX binding. The simultaneous removal of the three chlorines (Table 6.4 – Entries 17-20) was overall detrimental to activity against both targets, with the only exception being the (3*S*,1'*S*) diastereoisomer **214**, which retained some activity against MDM2.

Table 6.4 - Results of the ELISA for the sequential chlorine deletion set of compounds.

#	R ¹	R ²	R ³	(3,1')	Compound	MDMX IC ₅₀ (μM)	MDM2 IC ₅₀ (μM)	MDMX % Inhibition at 200 μM	MDM2 % Inhibition at 200 μM
1	Cl	Cl	Cl	<i>R,R</i>	154	102 ^a	1.71±0.13 ^c		
2	Cl	Cl	Cl	<i>S,R</i>	155	132 ^a	1.15±0.32 ^c		
3	Cl	Cl	Cl	<i>S,S</i>	156	N/A	11.4±1.6 ^c	40%	
4	Cl	Cl	Cl	<i>R,S</i>	157	59.6 ^a	0.0394±0.0051 ^c		

#	R ¹	R ²	R ³	(3,1')	Compound	MDMX IC ₅₀ (μM)	MDM2 IC ₅₀ (μM)	MDMX % Inhibition at 200 μM	MDM2 % Inhibition at 200 μM
5	Cl	Cl	H	<i>R,R</i>	191	114 ^a	2.54 ^a		
6	Cl	Cl	H	<i>S,R</i>	193	N/A	22.4 ^a	37%	
7	Cl	Cl	H	<i>S,S</i>	195	N/A	95.3 ^a	47%	
8	Cl	Cl	H	<i>R,S</i>	197	N/A	0.880 ^a	46%	
9	Cl	H	Cl	<i>R,R</i>	159	25.9 ^a	180±10 ^b		
10	Cl	H	Cl	<i>S,R</i>	199	182 ^a	171±90 ^b		
11	Cl	H	Cl	<i>S,S</i>	201	173 ^a	202±23 ^b		
12	Cl	H	Cl	<i>R,S</i>	202	118 ^a	1.98±0.85 ^b		
13	H	Cl	Cl	<i>R,R</i>	204	82.2 ^a	57.9±0.2 ^b		
14	H	Cl	Cl	<i>S,R</i>	205	52.9 ^a	0.347±0.114 ^b		
15	H	Cl	Cl	<i>S,S</i>	207	56.6 ^a	85.0±27.5 ^b		
16	H	Cl	Cl	<i>R,S</i>	208	135 ^a	3.62±1.02 ^b		
17	H	H	H	<i>R,R</i>	210	N/A	N/A	24%	24%
18	H	H	H	<i>S,R</i>	212	N/A	N/A	3%	25%
19	H	H	H	<i>S,S</i>	214	N/A	40.5 ^a	41%	
20	H	H	H	<i>R,S</i>	216	N/A	N/A	7%	41%

^a n = 1; ^b n = 2; ^c n = 3.

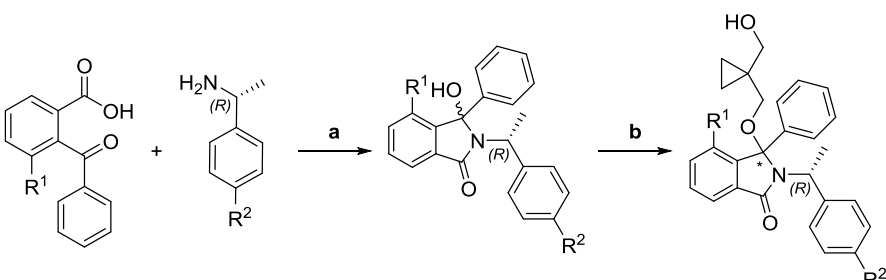
The ELISA was performed by Yan Zhao¹⁶² against full length MDMX and MDM2 using DMSO as negative control and active AP-B peptide (IC₅₀ = 5 nM)¹⁶³ (100 μM) as positive control. IC₅₀ values were measured when the percentage inhibition at 200 μM was less than 50% (if not measured, the field is marked as N/A, not available). Percentage inhibition is not reported for compounds whose IC₅₀ is available.

6.2 Sequential chlorine deletion from 159

To further investigate the role of the 4-chloro substituent on the isoindolinone core in binding, a second chlorine atom was replaced with hydrogen. Only the (3*R*,1'*R*) and the (3*S*,1'*R*) diastereoisomers were synthesized. The four target compounds were obtained using the general synthetic pathway described above using the appropriate benzoylbenzoic acid and amine to form the isoindolinone. Yields are reported in Table 6.5. Unfortunately, the biological evaluation for these compounds was not performed (see Chapter 7).

Table 6.5 - Summary of yields for the synthesis of the target isoindolinones with a second chlorine deletion.

Reagents and conditions: a) i) 183 or 189 SOCl₂, cat. DMF, THF, RT, 4 h; ii) amine, DIPEA, THF, RT, 18 h; b) InBr₃, 1,1-bis(hydroxymethyl)cyclopropane, DCE, 80 °C, 18 h.



#	R ¹	R ²	*	Product (isolated yield %) step a	Product (isolated yield %) step b
1	Cl	H	<i>R</i>	217 (87)	218 (20)
2	Cl	H	<i>S</i>		219 (21)
3	H	Cl	<i>R</i>	220 (85)	221 (33)
4	H	Cl	<i>S</i>		222 (21)

6.3 Structural minimization of the core structure

To provide information on the Phe19 binding pocket of MDMX and its interaction with the A-ring of isoindolinones, the core was minimized and replaced with either a 1,5-dihydropyrrol-2-one or a cyclohexene isoindolinone analogue (Figure 6.9). Both targets were obtained using a synthetic approach devised in the past by Anna Watson for the synthesis of analogues similar in structure.¹⁶⁶⁻¹⁶⁷

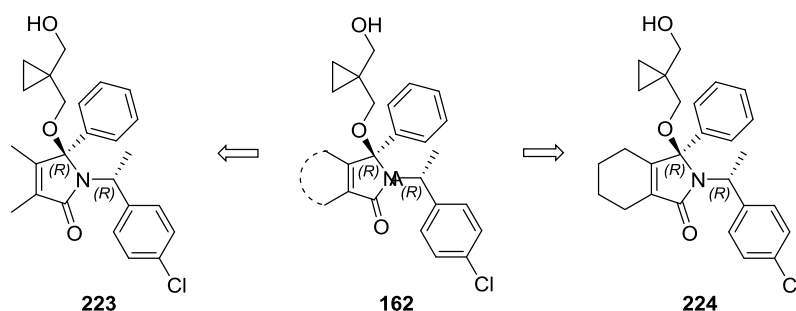
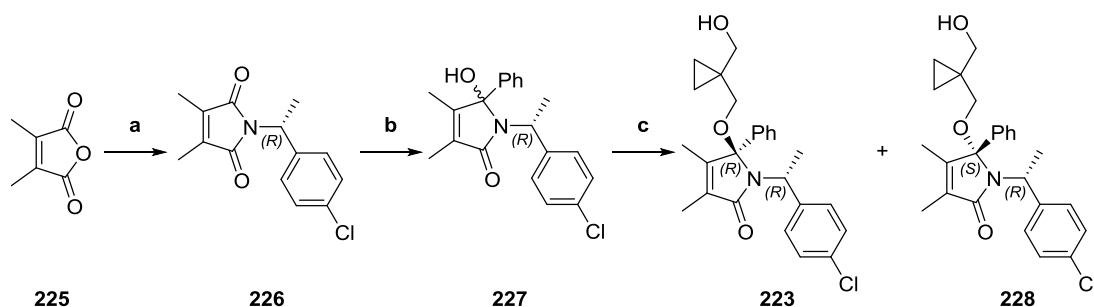


Figure 6.9 - Minimization of the isoindolinone core.

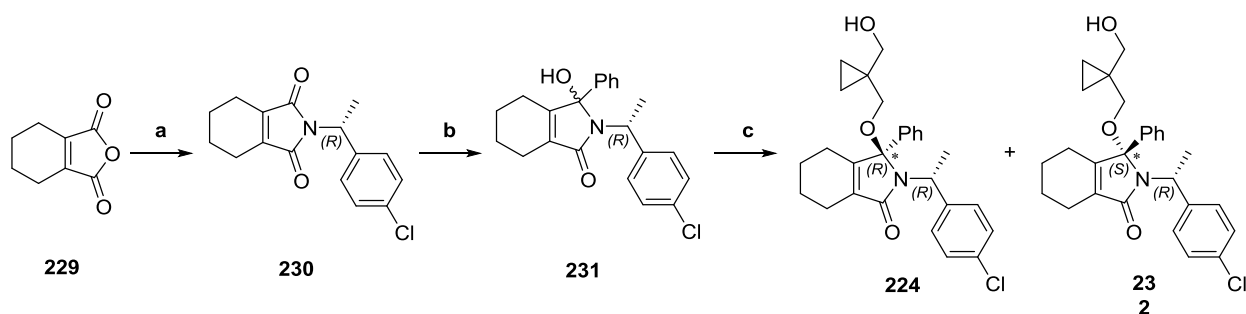
To synthesize the 1,5-dihydropyrrol-2-ones **223** and **228** (Scheme 6.3), the maleimide **226** was obtained from 2,3-dimethylmaleic anhydride **225** and (*R*)-4-chloro- α -methylbenzylamine according to the procedure described by Punniyamurthy *et al.*¹⁶⁸ Steric hindrance caused by the α -methyl group may be responsible for both the long reaction time and the modest yield of this step.



Scheme 6.3 - Synthesis of **223 and **228**.**

Reagents and conditions: **a**) (*R*)-4-chloro- α -methylbenzylamine, THF, reflux, 4 days, 59%; **b**) PhMgBr, THF, -78 °C to RT, 2 h, 54%; **c**) InBr₃, 1,1-bis(hydroxymethyl)cyclopropane, DCE, 80 °C, 18 h, **223** 38%; **228** 30%.

Addition of an excess of phenylmagnesium bromide to one of the imide carbonyls afforded the dihydropyrrolone **227**. The desired compound **223** and its diastereoisomer **228** were obtained upon formation of the ether linkage with 1,1-bis(hydroxymethyl)cyclopropane. Starting from 3,4,5,6-tetrahydrophthalic anhydride, a similar approach was used to synthesize the cyclohexene isoindolinone analogues **224** and **232** (Scheme 6.4).



Scheme 6.4 - Synthesis of 224 and 232.

Reagents and conditions: **a)** (*R*)-4-chloro- α -methylbenzylamine, THF, reflux, 37 h, 72%; **b)** PhMgBr, THF, -78 °C, 2 h, 71%; **c)** InBr₃, 1,1-bis(hydroxymethyl)cyclopropane, DCE, 80 °C, 18 h, **224** 28%; **232** 14%.

6.3.1 Biological evaluation

As summarized in Table 6.6, both dihydropyrrolones **223** and **228** were weakly active against MDM2 and MDMX in the ELISA. The cyclohexene isoindolinone analogues **224** and **232**, instead, showed a moderate inhibitory effect against both MDMX and MDM2. Interestingly, as previously observed for the benchmark compound **159**, the (3*R*,1'*R*) diastereoisomer **224** was more potent against MDMX (IC₅₀ = 55.2 μ M) than MDM2 (IC₅₀ = 192 μ M).

Table 6.6 - Results of the ELISA for the 1,5-dihydropyrrol-2-one and the cyclohexene isoindolinone analogues.

#	*	Compound	MDMX IC ₅₀ (μ M)	MDM2 IC ₅₀ (μ M)	MDMX % inhibition at 200 μ M	MDM2 % inhibition at 200 μ M
1	<i>R</i>	223	N/A	N/A	37%	39%
2	<i>S</i>	228	N/A	200	28%	
3	<i>R</i>	224	55.2	192		
4	<i>S</i>	232	117	51.3		

The ELISA was performed by Yan Zhao¹⁶² against full length MDMX and MDM2 using DMSO as negative control and active AP-B peptide (IC₅₀ = 5 nM)¹⁶³ (100 μ M) as positive control. IC₅₀ values were measured when the percentage inhibition at 200 μ M was less than 50% (if not measured, the field is marked as N/A, not available). Percentage inhibition is not reported for compounds whose IC₅₀ is available.

6.4 Variations at the 3-position

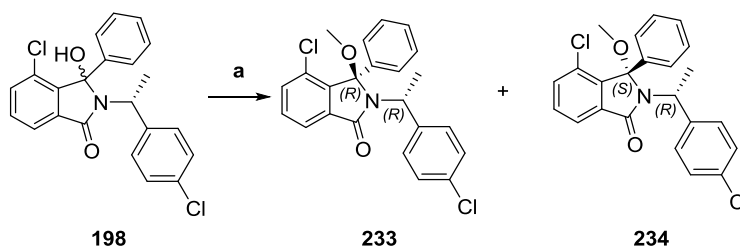
The next targets were designed to investigate the role of the side chain at the 3-position. Previously obtained structural data¹⁵⁶ showed that the cyclopropyl of the side chain interacts with a small lipophilic pocket on the outer surface of MDM2 while the terminal hydroxyl reaches out to solvent.

The main aims of the next phase of the study were: a) to probe whether the side chain was required for MDMX binding; b) to verify whether the cyclopropyl interacts with MDMX in a way similar to that observed for MDM2.

6.4.1 Removal of the side chain

As mentioned above (see Section 6.1.2), isoindolinones with a free OH at the 3-position undergo ring-chain tautomerism with consequent epimerization of the C-3 stereocentre. In order to assess purely the effect of the removal of the side chain, the hydroxyl- was replaced with a small methoxy-group whose presence prevents tautomerism.

The target compound **233** and its isomer **234** were obtained from the intermediate **198** following the indium bromide procedure and using MeOH to form the ether (Scheme 6.5).

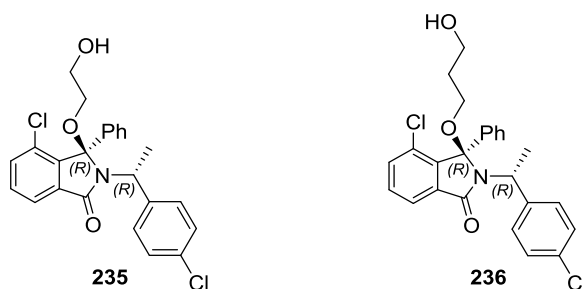


Scheme 6.5 - Synthesis of 233 and 234.

Reagents and conditions: a) InBr₃, MeOH, DCE, 80 °C, 1 h, 233 39%, 234 33%.

6.4.2 Removal of the cyclopropyl motif

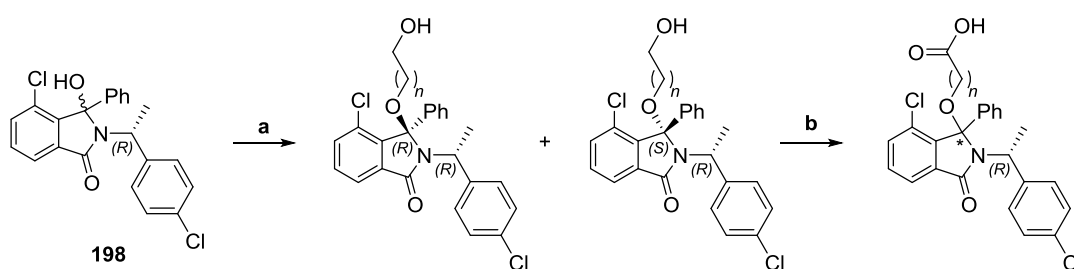
With a view to simplifying the molecule, it was envisaged that the cyclopropane motif would be removed and simple alkyl chains would be introduced. Propane-1,3-diol and ethane-1,2-diol were chosen to form the ether linkage at the isoindolinone 3-position to probe the area interacting with the side chain. Knowing from previous results (see Section 5.6) that a carboxylic acid moiety is beneficial to binding, biological evaluation of the carboxylic acid analogues was also desirable.



The alcohols **235** and **236** were obtained by reaction of the isoindolinone **198** with indium bromide and the appropriate diol, as shown in Table 6.7. At this stage, diastereoisomers were resolved and each of the alcohols was oxidised with sodium periodate and ruthenium chloride to afford the corresponding carboxylic acid. The yields for the reactions are summarized in Table 6.7.

Table 6.7 - Summary of yields for the synthesis of isoindolinones bearing carboxylic acid side chains.

Reagents and conditions: a) $\text{OH}(\text{CH}_2)_n\text{CH}_2\text{OH}$, InBr_3 , DCE, 80 °C, 4.5 h; b) NaIO_4 , RuCl_3 , $\text{MeCN}/\text{EtOAc}/\text{H}_2\text{O}$, RT, 15-20 min.



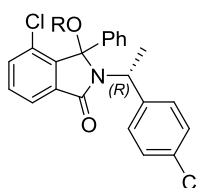
#	<i>n</i>	*	Product (isolated yield %) step a	Product (isolated yield %) step b
1	1	<i>R</i>	235 (50)	237 (53)
2	1	<i>S</i>	238 (45)	239 (70)
3	2	<i>R</i>	236 (49)	240 (61)
4	2	<i>S</i>	241 (37)	242 (58)

6.4.3 Biological evaluation

Both diastereoisomers **233** and **234** were weakly active against both targets, providing evidence for the need of a side chain at the 3-position (Table 6.8 – Entries 1-2). Among the alcohols, **235** ($n=2$, ($3R,1'R$) configuration) and **236** ($n=3$, ($3R,1'R$) configuration) retained some activity against MDMX. By virtue of its low

molecular weight, **235** is the isoindolinone with the highest ligand efficiency (LE = 0.20). All the alcohols were weakly active against MDM2. Activity against MDM2 was retrieved by oxidation of the hydroxyl to the correspondent carboxylic acid and was at maximum with $n=3$ and (3*S*,1'*R*) configuration of the stereocentres. Overall these results suggest that a) the side chain is a requirement for binding; b) the cyclopropyl motif is beneficial but not essential in isoindolinones with (3*R*,1'*R*) configuration; c) the carboxylic acid has to be at a certain distance from the core in order to contribute most effectively to the binding energy.

Table 6.8 - Results of the ELISA for isoindolinones bearing a range of simplified side chains.



#	R	* Compound	MDMX IC ₅₀ (μM)	MDM2 IC ₅₀ (μM)	MDMX % inhibition at 200 μM	MDM2 % inhibition at 200 μM
1	-Me	<i>R</i> 233	N/A	N/A	41%	6%
2	-Me	<i>S</i> 234	N/A	N/A	26%	25%
3	-(CH ₂) ₂ OH	<i>R</i> 235	42.9	N/A		44%
4	-(CH ₂) ₂ OH	<i>S</i> 238	N/A	N/A	36%	41%
5	-(CH ₂) ₃ OH	<i>R</i> 236	61.8	N/A		40%
6	-(CH ₂) ₂ OH	<i>S</i> 241	N/A	N/A	38%	44%
7	-CH ₂ CO ₂ H	<i>R</i> 237	N/A	185	31%	
8	-CH ₂ CO ₂ H	<i>S</i> 239	N/A	103	36%	
9	-(CH ₂) ₂ CO ₂ H	<i>R</i> 240	N/A	75.7	36%	
10	-(CH ₂) ₂ CO ₂ H	<i>S</i> 242	122	14.7		

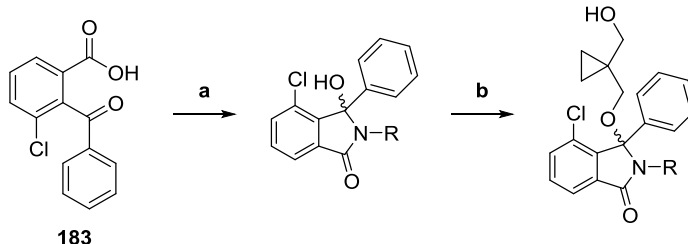
The ELISA was performed by Yan Zhao¹⁶² against full length MDMX and MDM2 using DMSO as negative control and active AP-B peptide (IC₅₀ = 5 nM)¹⁶³ (100 μM) as positive control. IC₅₀ values were measured when the percentage inhibition at 200 μM was less than 50% (if not measured, the field is marked as N/A, not available). Percentage inhibition is not reported for compounds whose IC₅₀ is available.

6.5 Structural minimization at the 2-position

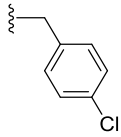
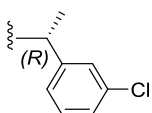
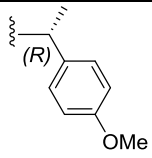
Finally, the interaction of the isoindolinone scaffold with the Leu26 binding pocket was assessed. A panel of amines was chosen to synthesize a variety of isoindolinones according to the general synthetic pathway described above. When only one stereocentre was present, the enantiomers were not resolved. The α -methylbenzyl moiety was initially replaced with an ethyl group (Table 6.9 – Entry 1). Subsequently, larger alkyl chains were introduced, such as isopropyl, cyclopropylmethyl and cyclohexylmethyl (Table 6.9 – Entries 2-4). Aromaticity was reintroduced with benzyl and 4-chlorobenzyl substituents lacking the second stereocentre (Table 6.9 – Entries 5-6). Finally, an analogue of **159** was synthesised in which the 4-chloro- α -methylbenzyl group was replaced by a 3-chloro- α -methylbenzyl.

Table 6.9 - Summary of yields for the synthesis of isoindolinones with a panel bearing a panel of R groups at the 2-position.

Reagents and conditions: **a**) i) SOCl_2 , THF, cat. DMF, RT, 4 h; ii) amine, THF, DIPEA, RT, 18 h; **b**) i) InBr_3 , 1,1-bis(hydroxymethyl)cyclopropane, DCE, 80 °C, 18 h.



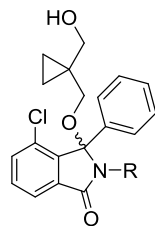
#	R	Configuration	Product (isolated yield %) step a	Product (isolated yield %) step b
1		(3 <i>RS</i>)	243 (54)	244 (76)
2		(3 <i>RS</i>)	245 (67)	246 (76)
3		(3 <i>RS</i>)	247 (55)	248 (85)
4		(3 <i>RS</i>)	249 (77)	250 (69)
5		(3 <i>RS</i>)	251 (90)	252 (69)

#	R	Configuration	Product (isolated yield %) step a	Product (isolated yield %) step b
6		(3 <i>RS</i>)	253 (74)	254 (70)
7		(3 <i>R</i> ,1' <i>R</i>)	255 (77)	256 (27)
		(3 <i>S</i> ,1' <i>R</i>)		257 (38)
8		(3 <i>R</i> ,1' <i>R</i>)	258 (93)	259 (30)
		(3 <i>S</i> ,1' <i>R</i>)		260 (20)

6.5.1 Biological evaluation

The results of the ELISA for the above compounds are summarized in Table 6.10. All the isoindolinones bearing an alkyl substituent only showed low activity against both MDM2 and MDMX (Table 6.10 – Entries 1-4). The same applied to **252**, bearing a simple benzyl group (Table 6.10 – Entry 5). The *N*-(4-chlorobenzyl) substituent resulted in the isoindolinone **254**, fairly active against MDM2 but still unable to inhibit the MDMX:p53 interaction (Table 6.10 – Entry 6). Reintroduction of the α -methyl motif in conjunction with the change of position of the chloro-group from the 4- to the 3-position resulted in partial recovery of the MDMX activity and selectivity (Table 6.10 – Entries 7-8).

Table 6.10 - Results of the ELISA for isoindolinones bearing a range of alkyl and benzyl chains at the 2-position.



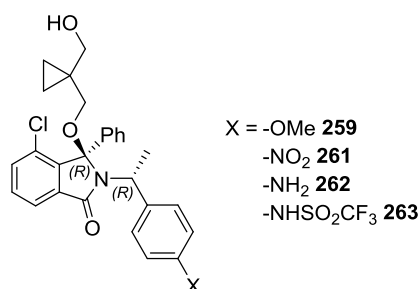
#	R	Configuration	Compound	MDMX IC ₅₀ (μ M)	MDM2 IC ₅₀ (μ M)	MDMX % inhibition at 200 μ M	MDM2 % inhibition at 200 μ M
1		(3 <i>RS</i>)	244	N/A	N/A	12%	34%
2		(3 <i>RS</i>)	246	N/A	N/A	15%	24%
3		(3 <i>RS</i>)	248	N/A	N/A	9%	35%
4		(3 <i>RS</i>)	250	N/A	140	45%	
5		(3 <i>RS</i>)	252	N/A	N/A	16%	37%
6		(3 <i>RS</i>)	254	N/A	1.75	38%	
7		(3 <i>R</i> ,1' <i>R</i>)	256	47.6	N/A		42%
8		(3 <i>S</i> ,1' <i>R</i>)	257	156	N/A		32%

The ELISA was performed by Yan Zhao¹⁶² against full length MDMX and MDM2 using DMSO as negative control and active AP-B peptide (IC₅₀ = 5 nM)¹⁶³ (100 μ M) as positive control. IC₅₀ values were measured when the percentage inhibition at 200 μ M was less than 50% (if not measured, the field is marked as N/A, not available). Percentage inhibition is not reported for compounds whose IC₅₀ is available.

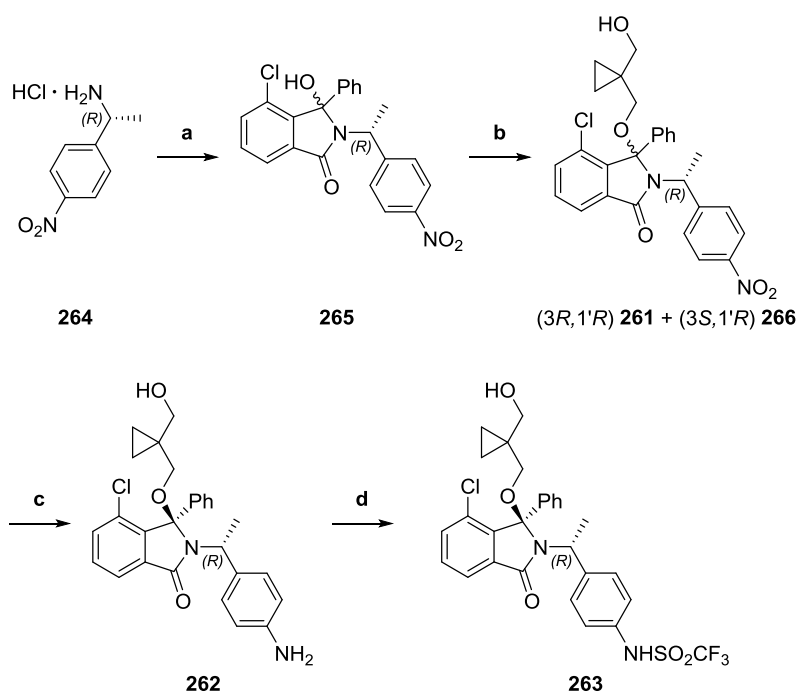
6.6 Introduction of a range of substituents at the 4-benzyl position

To probe further the Leu26 binding pocket, the replacement of the 4-chloro group with an array of substituent with diverse electronic and steric requirements

at the 4-position of the benzyl was desired. The availability of enantiopure starting materials and ease of synthesis were key to the choice of the replacement moieties shown below. The trifluoromethylsulfonamide **263** was of particular interest because in parallel series the -NHSO₂CF₃ group substantially improved potency.¹⁶⁹⁻¹⁷⁰ Molecular modelling by Martin Noble also suggests that mode of binding for this scaffold is such that the abovementioned group enters the Leu26 pocket with potential for interactions.¹⁷¹



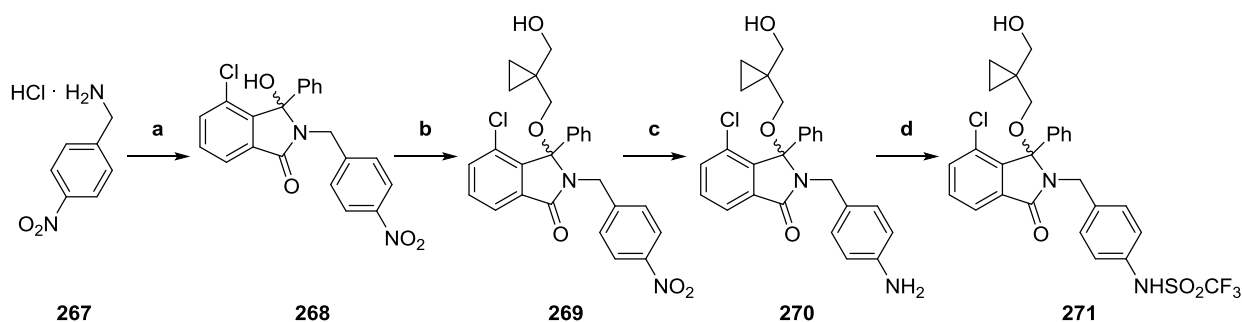
From the commercially available (*R*)-4-methoxy- α -methylbenzylamine, the target isoindolinone **259** and its diastereoisomer **260** were synthesized starting from **183** following the general synthetic pathway, as described in Table 6.9. In this case, the polarities of the two diastereoisomers **259** and **260** was very similar, therefore, after purification on silica was attempted few times in different conditions, HPLC was used to obtain the pure products. Similarly, the 4-nitro compound **261** could be obtained from the appropriate enantiopure α -methylbenzylamine. Once **261** was available, the aniline **262** could be accessed by catalytic hydrogenation. Subsequent trifluoromethylsulfonylation (triflation) of the NH₂ led to the trifluoromethylsulfonamide **263** (Scheme 6.6). Further optimization is required for the last step, as the use of triflic anhydride in the presence of DIPEA resulted in low isolated yield. This could be explained as a consequence of competition of the free hydroxyl in the triflation, although no bis-triflated side product was isolated. Optimization could be achieved by: a) lowering the temperature to ensure that the only group reacting is the more nucleophilic aniline; b) changing the base (*e.g.* Et₃N is commonly used in this kind of reaction); c) using a different triflating agent, such as *N*-phenylbis(trifluoromethylsulfonimide), successfully used in the Sulf2 project described above (see Chapter 3).



Scheme 6.6 - Synthesis of 263.

Reagents and conditions: **a)** (i) **183**, SOCl_2 , cat. DMF, THF, RT, 4 h; (ii) DIPEA, THF, RT, 18 h, 87%; **b)** InBr_3 , 1,1-bis(hydroxymethyl)cyclopropane, DCE, 80 °C, **261** 37%; **266** 54%; **c)** H_2 , Pd/C, RT, 3 h, 99%; **d)** $(\text{CF}_3\text{SO}_2)_2\text{O}$, DIPEA, DCM, 0 °C to RT, 1 h then NaOH, MeOH, 30 min, 16% (impurity present).

To enable a matched pair comparison, the *des*-methyl analogues were also obtained following a similar route. The trifluoromethylsulfonamide **271** was obtained in low yield following the same procedure described above (Scheme 6.7).



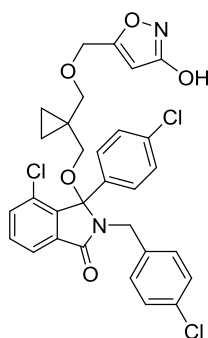
Scheme 6.7 - Synthesis of 271.

Reagents and conditions: **a)** (i) **183**, SOCl_2 , cat. DMF, THF, RT, 4 h; (ii) DIPEA, THF, RT, 18 h, 74%; **b)** InBr_3 , 1,1-bis(hydroxymethyl)cyclopropane, DCE, 80 °C, 82%; **c)** H_2 , Pd/C, RT, 3.5 h, 60%; **d)** $(\text{CF}_3\text{SO}_2)_2\text{O}$, DIPEA, DCM, 0 °C to RT, 1 h then NaOH, MeOH, 30 min, 21%.

Unfortunately, the biological evaluation for this set of compounds was not performed (see Chapter 7).

6.7 Introduction of a 5-hydroxyisoxazole moiety

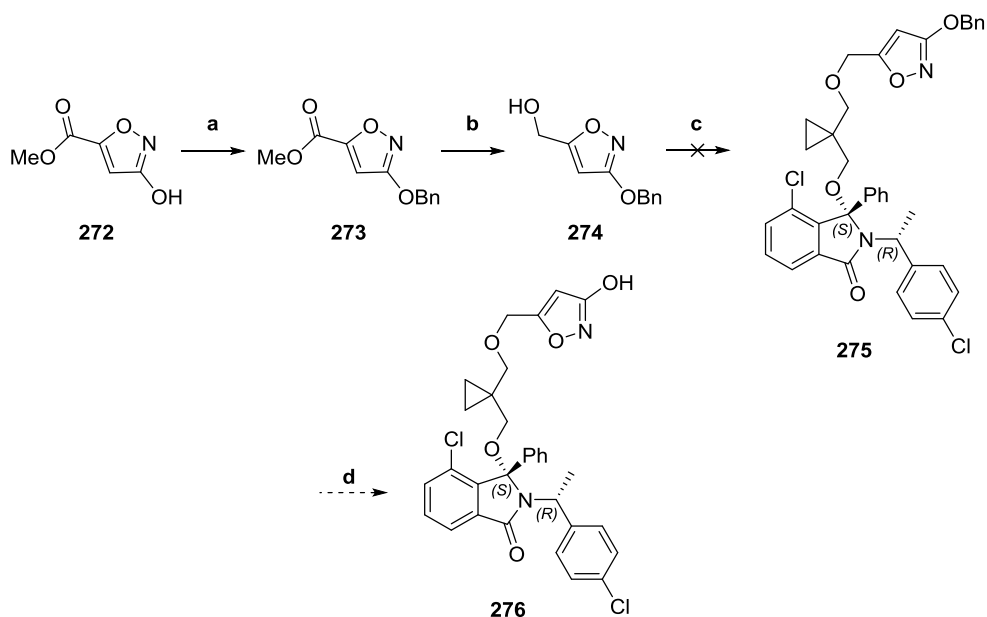
As shown in Chapter 5, the most potent compound in the isoindolinone series against MDMX is **148**, which features a 3-hydroxyisoxazole motif linked to the terminal hydroxyl of the side chain. One of the main aims of this project was to synthesize **164**, an analogue of **148** based on the substituent pattern and stereochemical configuration of the benchmark compound **159**, and its (3*S*,1'*R*) diastereoisomer **276**.



148

MDMX IC₅₀ 6.2 μM (LE 0.18)
MDM2 IC₅₀ 0.218 μM (LE 0.22)
MDMX/MDM2 28.9

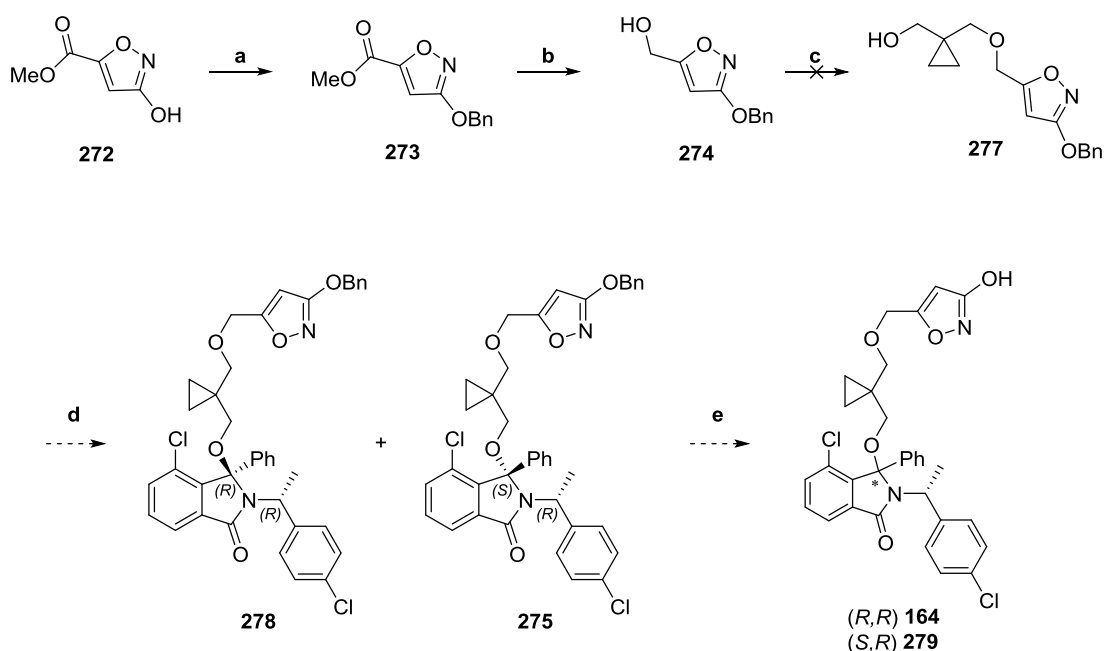
It was envisaged to obtain the target compound in four steps by slightly modifying the approach used by Sarah Cully for her synthesis of **148**.¹⁵⁶ Using a literature procedure,¹⁷² the free hydroxyl of the commercially available isoxazole **272** would be protected by benzylation followed by reduction of the ester moiety using sodium borohydride to obtain the alcohol **274**. The next steps would involve a Williamson synthesis between the pre-formed mesylate of alcohol **274** and the appropriate isoindolinone and subsequent removal of the benzyl to yield the target compound. Alcohol **274** was obtained as previously described by Sarah Cully. The Williamson etherification was attempted using the (3*S*,1'*R*) diastereoisomer **199**, but did not yield the desired isoindolinone **275** and a mixture of the mesylate and the alcohols **274** and **199** was recovered (Scheme 6.8).



Scheme 6.8 - Proposed route to the synthesis of 276.

Reagents and conditions: **a)** BnBr, K₂CO₃, MeCN, 0 °C then 70 °C, 5 h, 84% **b)** NaBH₄, MeOH, 0 °C, 18 h, 92%; **c)** i) methanesulfonyl chloride, Et₃N, DCM, RT, 15 min; ii) **199**, NaH, DCM, 0-65 °C, 16 h; **d)** Pd(OAc)₂, Et₃SiH, Et₃N, DCM.

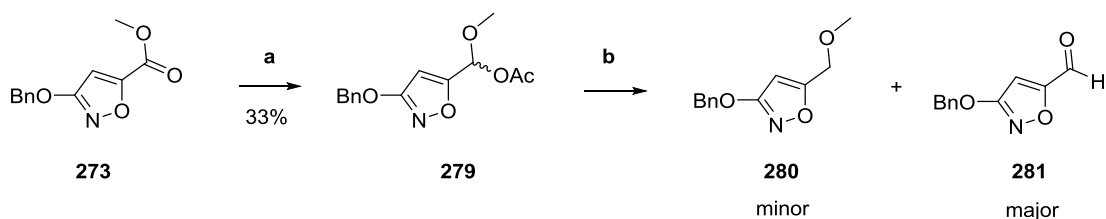
It was then decided to follow the same synthetic scheme used for the synthesis of **148** from **274** by Williamson reaction with 1,1-bis(hydroxymethyl)cyclopropane to give the alcohol **277**. At this stage, the side chain **277** could be introduced on the isoindolinone **198** using the InBr₃ protocol and, upon separation of the diastereoisomers and removal of the benzyl, the target compounds **164** and **276** could be obtained in parallel. Unfortunately, the Williamson reaction was again unsuccessful. Although the reported yield for this exact step was 23%, the reaction was difficult to reproduce. An attempt to replace sodium hydride with potassium bis(trimethylsilyl)amide as base and dichloromethane with tetrahydrofuran as solvent led to the formation of the desired product **277** in 10% yield, but this step was not reproducible. The low yields and poor reproducibility of this reaction are probably due to the steric hindrance around the hydroxyl moiety in bis(hydroxymethyl)cyclopropane.



Scheme 6.9 - Attempted route for the synthesis of 164 and 276.

Reagents and conditions: **a)** BnBr, K₂CO₃, MeCN, 0 °C then 70 °C, 5 h, 84%; **b)** NaBH₄, MeOH, 0 °C, 18 h, 92%; **c)** i) methanesulfonyl chloride, Et₃N, DCM, RT, 15 min; ii) 1,1-bis(hydroxymethyl)cyclopropane, NaH, DCM, 0 to 65 °C, 16 h; **d)** **198**, InBr₃, DCE, 80 °C; **e)** Pd(OAc)₂, Et₃SiH, Et₃N, DCM, RT.

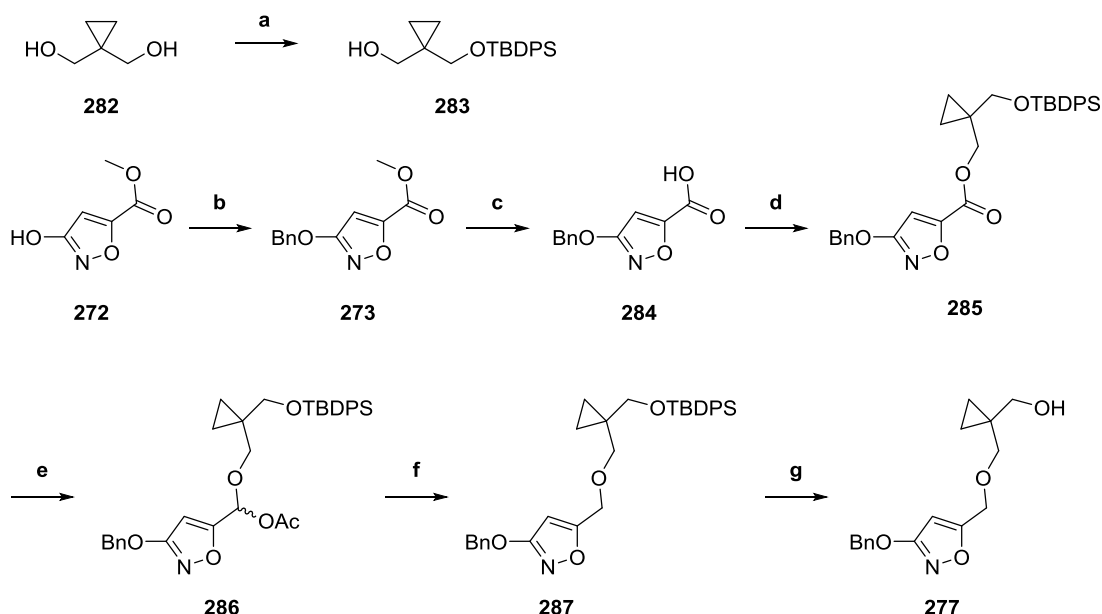
At this stage, it was clear that a new reliable approach to the synthesis of **277** was needed. Rychnovsky and co-workers¹⁷³⁻¹⁷⁵ proposed a new route to the synthesis of ethers from hindered alcohols, such as *t*-butanol. This was achieved in a 2-step net deoxygenation *via* reductive acetylation of an ester to an α -acetoxyether, which was reduced to an ether with triethylsilane in the presence of boron trifluoride. This sequence was attempted using **273** as model system and led to the formation of the desired ether **280** and the aldehyde **281** (Scheme 6.10).



Scheme 6.10 - Reductive acetylation using 273 as model system.

Reagents and conditions: **a)** i) DIBALH (2 equiv.), DCM, -78 °C, 45 min; ii) pyridine, DMAP, Ac₂O, DCM, -78 °C for 14 h then 0 °C for 30 min, 33%; **b)** BF₃ · Et₂O, Et₃SiH, DCM, -78 °C, **280** 20%, **281** 38%.

Although requiring a certain degree of optimization to favor the formation of the desired ether over the aldehyde side product, this approach was considered promising and, therefore, a new route to the synthesis of **164** and **276** was devised (Scheme 6.11).



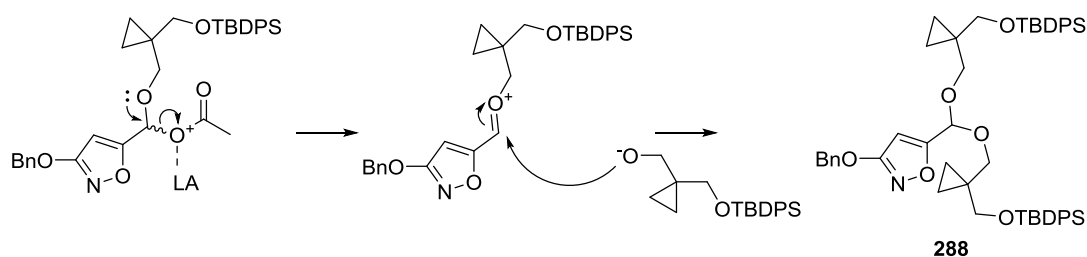
Scheme 6.11 - Synthesis of alcohol 277.

Reagents and conditions: **a**) TBDPS-Cl, Et₃N, DCM, 0 °C to RT, 2 h, 99%; **b**) BnBr, K₂CO₃, MeCN, 0 °C then 70 °C, 5 h, 84%; **c**) LiOH, H₂O/THF, RT, 30 min, quant.; **d**) i) SOCl₂, cat. DMF, THF, RT, 4 h; ii) **283**, DIPEA, THF, RT, 16 h, 72%; **e**) i) DIBALH (3 equiv.), DCM, -78 °C, 45 min; ii) pyridine, DMAP, Ac₂O, DCM, -78 °C for 14 h then 0 °C for 30 min, quant.; **f**) cat. TMSOTf, Et₃SiH, DCM, 0 °C, 30 min, 69%; **g**) TBAF, THF, 0 °C to RT, 10 h, 98%.

Monoprotection of the diol **282** with TBDPS following a literature procedure¹⁷⁶ yielded alcohol **283**, easier to handle than the starting material by virtue of its higher molecular weight and better UV absorption. The benzyl-protected isoxazole **273** was obtained as earlier described and underwent saponification to obtain the carboxylic acid **284**, which was treated with Vilsmeier reagent followed by addition of the alcohol **283** to give ester **284**. The latter was subjected to reductive acetylation by treatment with DIBAL followed by pyridine, DMAP and acetic anhydride to yield quantitatively the α -acetoxyether **277**.

In the light of the results obtained with the model system **273** and after an unsuccessful attempt with **277**, the deacetoxylation step was optimized.

Replacement of boron trifluoride with other Lewis acids, such as InBr_3 , ZnCl_2 and CuI , led to either no conversion or degradation of the starting material. Variation of the number of equivalents of either triethylsilane or boron trifluoride did not improve the LC-MS profile of the reaction. Interestingly, when 10 equiv. of triethylsilane were used, the isoxazole **288** was isolated as major product (35% compared of 6% of desired product **287**) probably originating from the addition of a side chain alkoxide to the oxonium ion formed after departure of the acetoxy group (Scheme 6.12).

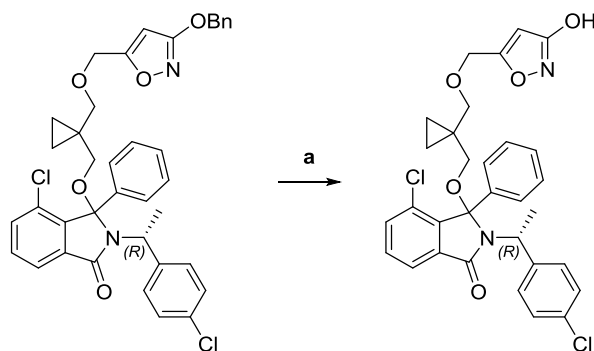


Scheme 6.12 - Proposed mechanism for the formation of 288.

In the attempt to obtain ether **287** from the by-product **288**, a procedure by Noyori was followed, which uses catalytic amounts of TMSOTf and trimethylsilane to generate ethers from benzaldehyde acetals. Under these conditions, ether **287** was formed from **288** in 18% yield. An even more satisfying yield of 69% was obtained when the α -acetoxyether **286** was used as starting material allowing completion of the scheme (Scheme 6.11). With **287** accessible *via* a reproducible and good yielding synthetic pathway, the desired side chain **277** was easily obtained through removal of the TBDPS protecting group using TBAF. Despite the number of steps required to obtain **277**, this route is made advantageous by its high reproducibility and its good overall yield (40% over seven steps). As previously done in the synthesis of **148**,¹⁵⁶ the benzyl protection was removed under mild catalytic conditions *via* the Birkofer reaction, according to a literature procedure,¹⁷⁷ in order to avoid dechlorination and ring-opening of the cyclopropane. Yields are reported in Table 6.11.

Unfortunately, the compounds could not be tested in the ELISA.

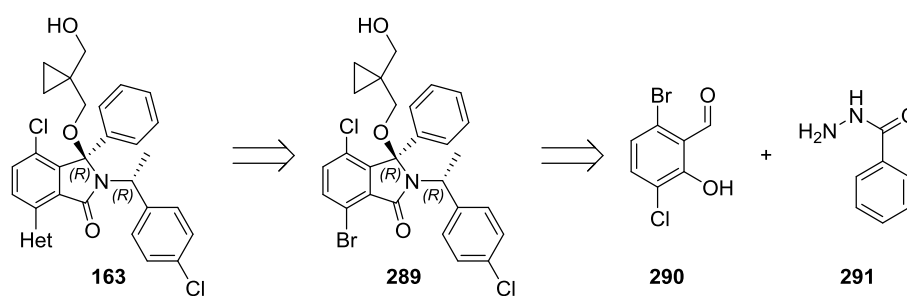
Table 6.11 - Summary of yields for the removal of the benzyl protection.
Reagents and conditions: a) Pd(OAc)₂, Et₃SiH, Et₃N, DCM, RT, 18 h.



#	Configuration	Starting material	Product (isolated yield %) step a
1	(3 <i>R</i> ,1' <i>R</i>)	278	164 (26)
2	(3 <i>S</i> ,1' <i>R</i>)	275	276 (73)

6.8 Introduction of nitrogen containing heteroaromatics at the 7-position

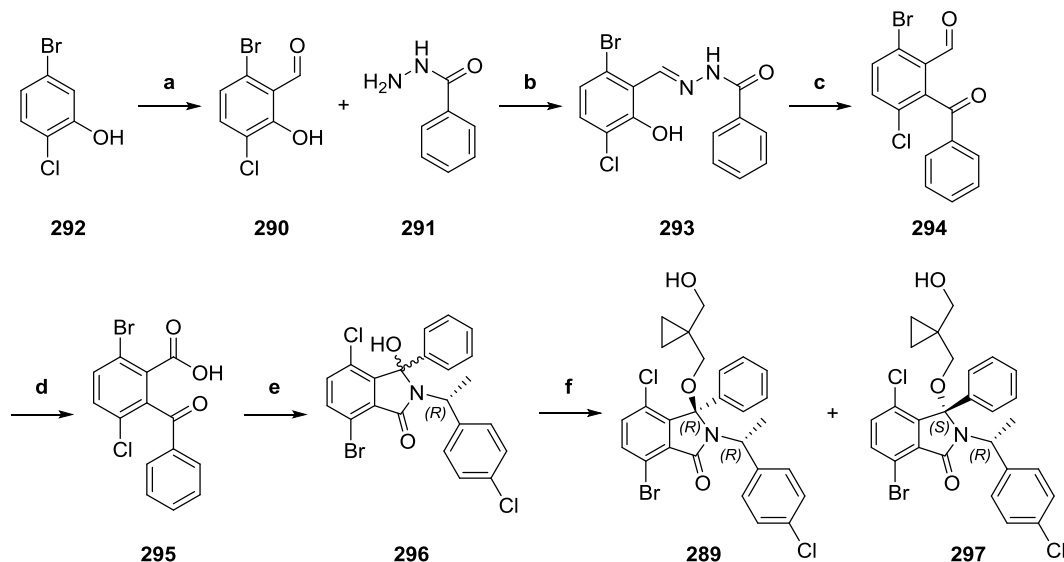
The final aim of this work was to introduce a range of heterocycles at the 7-position of the isoindolinone core following the route devised by Benoit Carbain¹⁶⁰ for the synthesis of **150**, the second most potent compound in the isoindolinone series against MDMX (see Section 5.6).



Scheme 6.13 - Retrosynthetic scheme for the 7-heteroaromatic compounds.

Envisaging exploitation of Suzuki chemistry to introduce heterocycles at the desired position, a bromo-substituent was needed at the 7-position of the isoindolinone core. The non-commercially available hydroxybenzaldehyde **290**

required to generate the desired bromo-intermediate **289** was obtained *via* Reimer-Tiemann reaction in 25% yield, in line with what reported for this reaction using halophenols.¹⁷⁸ The general route was then followed to obtain **289** (Scheme 6.14).

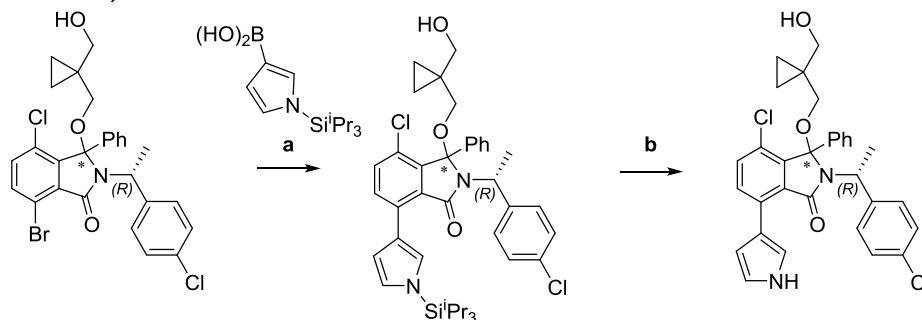


Scheme 6.14 - Synthesis of 7-bromo isoindolinone 289.

Reagents and conditions: **a)** CHCl_3 , NaOH , H_2O , $75\text{ }^\circ\text{C}$, 3 h, 25%; **b)** acetic acid, RT, 1 h, 81%; **c)** $\text{Pb}(\text{OAc})_4$, THF, RT, 3 h, 81%; **d)** sodium chlorite, sulfamic acid, $\text{MeCN}/\text{H}_2\text{O}$, RT, 2 h, 97%; **e)** (i) SOCl_2 , THF, cat. DMF, RT, 4 h; (ii) (*R*)-4-chloro- α -methylbenzylamine, DIPEA, THF, RT, 18 h, 98%; **f)** InBr_3 , 1,1-bis(hydroxymethyl)cyclopropane, DCE, $80\text{ }^\circ\text{C}$, 18 h, **289** 41%, **297** 44%.

The pyrrole targets **299** and **301** were obtained in good overall yield by Suzuki reaction of each of the intermediates **289** and **297** with silyl-protected pyrrole boronic acid followed by deprotection with TBAF following the procedure previously used by Benoit Carbain (Table 6.12).¹⁶⁰

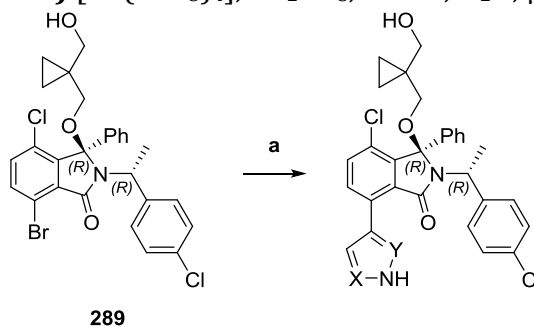
Table 6.12 - Summary of yields for the synthesis of 7-pyrroloisindolinones.
Reagents and conditions: a) [Pd(PPh₃)₄], Na₂CO₃, MeCN, H₂O, 85 °C, 6 h; b) TBAF, THF, 0 °C to RT, 3h.



#	*	Product (isolated yield %) step a	Product (isolated yield %) step b
1	<i>R</i>	298 (67)	299 (77)
2	<i>S</i>	300 (59)	301 (74)

The pyrazolo-regioisomers were prepared only in the (3*R*,1'*R*) configuration. The isoindolinone **289** was coupled with either 1*H*-pyrazol-3-yl boronic acid or 1*H*-pyrazole-4-boronic acid to obtain in good yield the target compounds **302** and **303**, respectively. Microwave heating was required for these reactions to go to completion (Table 6.13).

Table 6.13 - Summary of yields for the synthesis of 7-pyrazoloisindolinones.
Reagents and conditions: a) [Pd(PPh₃)₄], Na₂CO₃, MeCN, H₂O, μ W 120 °C, 1 h.



#	X	Y	Product (isolated yield %) step a
1	N	CH	302 (76)
2	CH	N	303 (59)

The ^1H -NMR of **302** in DMSO showed two exchangeable protons at 13.1 and 14.2 ppm. This could be explained by considering that pyrazole **302** can exist in two non-equivalent tautomeric forms, **302A** and **302B**, one of which can, in theory, form an intramolecular hydrogen bond with the carbonyl group of the isoindolinone core. The same phenomenon was not observed with **303**, whose tautomers are structurally equivalent upon rotation about a 180° angle along the C7-C4''' axis (Figure 6.10).

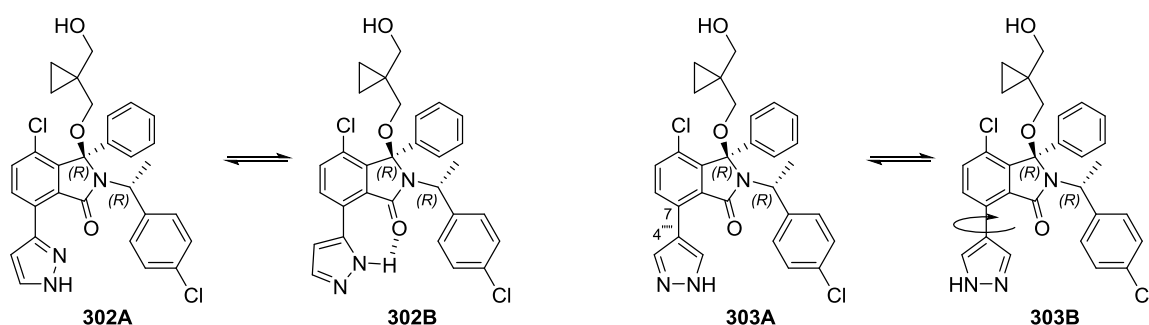
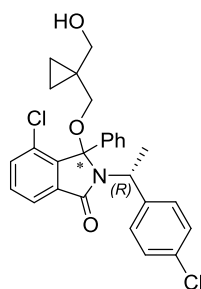


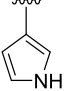
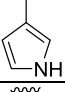
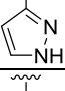
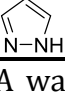
Figure 6.10 - Tautomerism of the pyrazole targets 302 and 303.

6.8.1 Biological evaluation

The 7-substituted isoindolinones described above were tested against MDM2 and MDMX and they all showed moderate activity against MDMX with IC_{50}s ranging from 31 to 56 μM . The most active compounds were the pyrazoles **302** and **303**, which were almost equipotent to the benchmark compound **159**, although with ligand efficiency lowered by the presence of the additional heterocycle ($\text{LE} = 0.16$). While **303** also inhibited MDM2, **302** was only weakly active against this target (Table 6.14).

Table 6.14 - Results of the ELISA for 7-substituted isoindolinones.

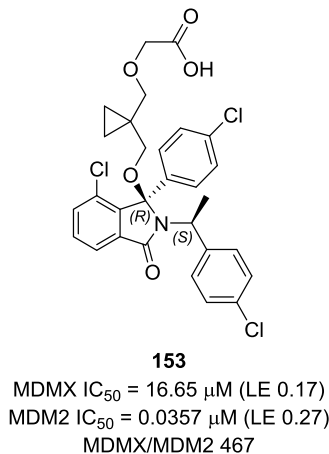


#	R	*	Compound	MDMX IC ₅₀ (μM)	MDM2 IC ₅₀ (μM)
1	-Br	<i>R</i>	289	40.1	124
2	-Br	<i>S</i>	297	41.7	65.9
3		<i>R</i>	299	56.4	78.1
4		<i>S</i>	301	44.1	26.8
5		<i>R</i>	302	30.8	200
6		<i>R</i>	303	34.2	13.3

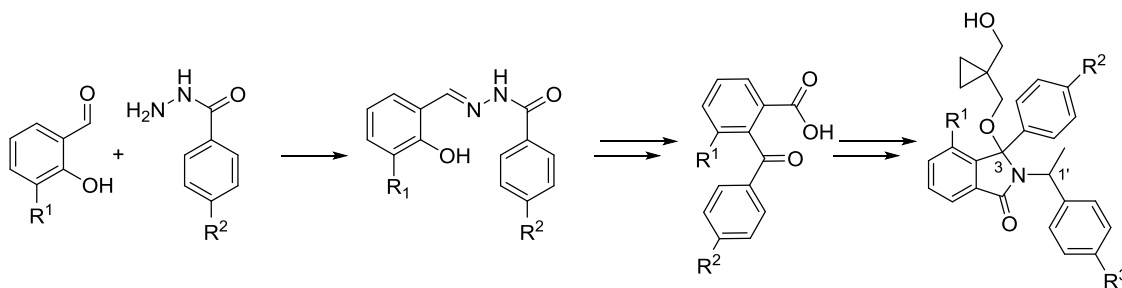
The ELISA was performed by Yan Zhao¹⁶² against full length MDMX and MDM2 using DMSO as negative control and active AP-B peptide (IC₅₀ = 5 nM)¹⁶³ (100 μM) as positive control. IC₅₀ values were measured when the percentage inhibition at 200 μM was less than 50% (if not measured, the field is marked as N/A, not available). Percentage inhibition is not reported for compounds whose IC₅₀ is available.

6.9 Conclusions

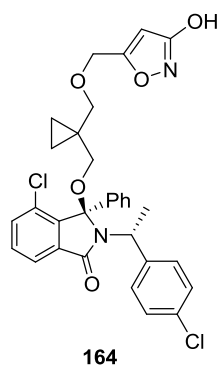
The α -methyl isoindolinone **153** (MDMX IC_{50} = 16.65 μ M) was selected as a starting point for SAR investigations aiming to achieve dual inhibitors of MDM2/MDMX or selective MDMX inhibitors.



Using the 5-step route developed within the research group for the synthesis of isoindolinones (Scheme 6.15), a number of analogs were synthesized using enantiopure α -methylbenzylamines and the diastereoisomers were separated by chromatography. The absolute configuration of the initial sets of compounds was assigned by solving the X-ray structure of at least one diastereoisomer. Once a considerable amount of data was available, the stereochemistry was predicted after careful analysis of the physicochemical properties (polarity, specific rotation, $^1\text{H-NMR}$).



Scheme 6.15 - Synthetic route to isoindolinones.



The synthesis of **164**, the α -methyl analog of **148**, was undertaken and a high yielding and reliable method to form the 3-hydroxyisoxazole side chain **277** was devised (7 steps; 40% yield). The desired compound **164** was obtained in 3% yield over a total of 13 steps.

A minimization approach was used to investigate what parts of the core are necessary for binding. Finally, modifications at the 7-position and at the 4''-benzyl position were performed by introducing nitrogen-containing heterocycles and moieties with a variety of stereoelectronic properties, respectively. The SAR for the library of compounds synthesized is summarized in Figure 6.11.

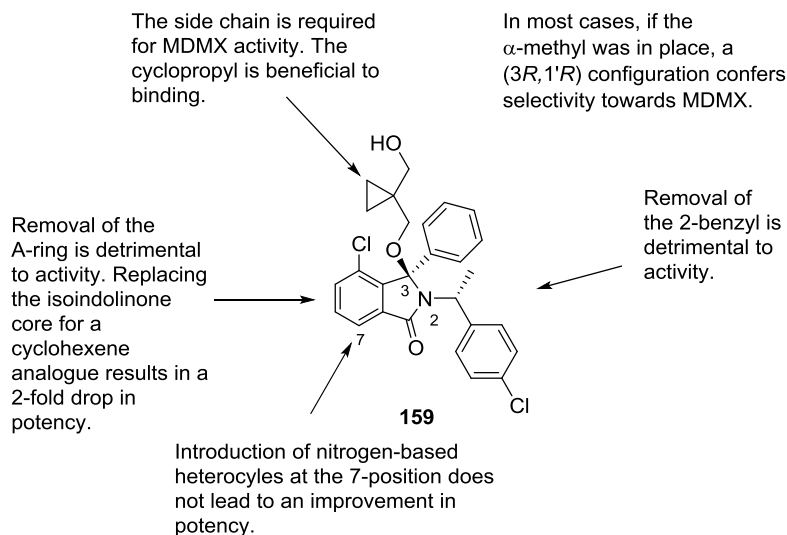
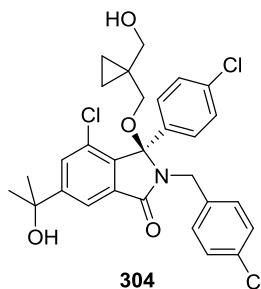


Figure 6.11 - Summary of the SAR of the isoindolinone library synthesized for the MDMX project.

CHAPTER 7. STRUCTURAL BIOLOGY INVESTIGATIONS WITH MDMX AND MDM2

7.1 Aims

In line with literature results,¹⁴⁸ the MDMX structure-activity relationship data around the isoindolinone series highlight the difficulty of obtaining sub-micromolar selective inhibitors of MDMX or dual MDM2/MDMX inhibitors. Although MDMX selectivity was achieved to some extent with compound **159** (IC_{50} MDMX/ IC_{50} MDM2 = 0.14), any modification performed around this structure did not lead to an increase in potency against the desired target. To enable a deeper understanding of the reasons underlying the large MDM2 selectivity, a co-crystal structure of an isoindolinone bound to MDMX was highly desired. Previous studies by Sarah Cully¹⁵⁶ had resulted in the solution of the structure of an isoindolinone, **304**, bound to MDM2 but, despite efforts,¹⁷⁹ no structural data of MDMX with an inhibitor from the isoindolinone series had been obtained. A 3-month placement in Structural Biology at the Northern Institute for Cancer Research was therefore undertaken aiming at obtaining a co-crystal structure of an isoindolinone with MDMX.



7.2 Protein crystallography and its challenges

Structural data represent an extremely powerful tool in drug discovery that can greatly accelerate the identification of clinical candidates through structure-based drug design. Unfortunately, despite the scientific and technical advances of the last decades, protein crystallography is still limited by the high number of variables influencing crystallization and an empirical approach to protein production is still required. The molecule of interest must be organized into a highly ordered three-

dimensional lattice to result in interpretable X-ray diffraction data. However, proteins are large biopolymers characterized by a certain degree of flexibility and micro-heterogeneities (*i.e.* conformation variability, post-translational modifications) and therefore crystallization can prove difficult. When varying the conditions of the environment, protein degradation or denaturation can occur in a population of biomolecules, interfering with crystal growth.¹⁸⁰ Additionally, some proteins may be intrinsically less prone to crystallization. Derewenda¹⁸¹ showed that in some cases large, flexible and hydrophilic side chains on the surface of the protein prevent molecules from packing. Their engineered mutation to smaller and more hydrophobic residues may enhance crystal formation (surface entropy reduction).

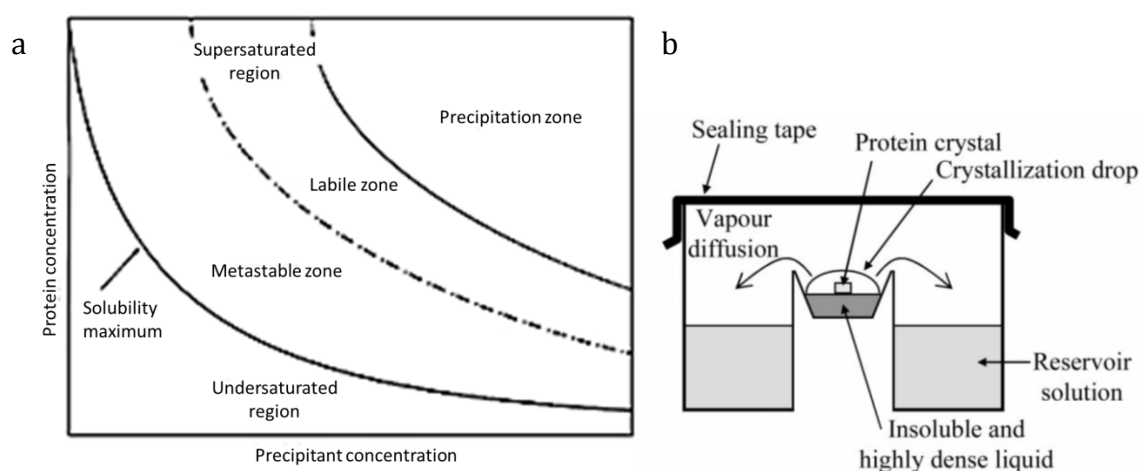


Figure 7.1

a) Crystallization phase diagram. Reproduced from McPherson, 2009.¹⁸² **b)** Sitting drop vapour diffusion crystallization method. Reproduced from Adachi, 2003.¹⁸³

Figure 7.1a shows the phase diagram for the crystallization process. In the undersaturated region, all the protein is soluble and no crystals will form. At equilibrium, molecules dynamically exchange from the aqueous solution (usually buffer) to the solid phase, preventing the formation of crystallization nuclei. At higher solute concentration, in the supersaturated phase, nucleation and growth may occur to generate crystals. As the concentration of protein increases, the further the system is from equilibrium, then the faster nucleation and growth take place, eventually resulting in the formation of precipitates. To allow the growth of suitable-sized and high-quality crystals, the system needs to be within the supersaturated region but relatively close to the equilibrium, in the so-called labile

zone.¹⁸² A number of techniques are available to reach the supersaturation conditions required for crystallization, such as the commonly used vapor diffusion method. Using automation for both sample preparation and monitoring, the preferred set-up for our studies was the sitting drop (Figure 7.1b), which involves a drop of solution, containing both the protein and a precipitating agent, sitting in a small well and equilibrating with a reservoir of precipitant at a higher concentration. In these conditions, water diffuses away from the droplet, thus increasing the concentration of protein and promoting the shift to a supersaturated state.

Considering the size and quality requirements for the crystals and given that the near-native conformation of the protein needs to be preserved, several parameters can be varied in the attempt to establish optimum conditions for nucleation and crystal growth, including temperature, pH, ionic strength of the solution, nature of the precipitant, volume of samples. Thanks to the advances in genetic engineering rendering larger scale protein production more efficient and to the availability of accurate automated systems for the preparation and monitoring of samples, the high-throughput screening of thousands of conditions on a micro- or nano-litre scale can be performed. Unfortunately, this is often not enough to lead to success and many systems have yet to be crystallized.

7.2.1 Selection of protein constructs for crystallization trials

To allow a comparison of the binding mode adopted by isoindolinones to MDMX and MDM2, crystallization trials with both proteins were deemed most desirable. Full length MDMX and MDM2 contain intrinsically disordered regions that would decrease the chances of crystal formation.¹⁸⁴ Additionally, the presence of the autoinhibitory domain on MDMX competing for the binding site¹²² (see Section 5.1.2) is not desirable for obtaining a homogenous population of protein-inhibitor complex molecules. In line with other work reported in the literature,^{153-154,185} the present study was focused on the expression and purification of the *N*-terminal p53-binding domain of MDMX and MDM2 to be co-crystallized with inhibitors, whose binding promotes partial order in the *N*-terminal domain. Three constructs of the MDMX p53-binding domain encoding up to amino acid residue 111 were

selected in which the disordered *N*-terminal loop (residues 1-19) was not included and the sequences started from residues 18, 22 and 26, respectively (Appendix C). With regards to MDM2, three previously optimized constructs were selected lacking the *N*-terminal loop and bearing surface entropy mutations to remove long hydrophilic side chains from the protein surface. These MDM2 constructs, MDM2^{K51A}₁₇₋₁₂₅, MDM2^{E69K70A}₁₇₋₁₀₈ and MDM2^{E69K70A}₁₇₋₁₂₅, are known to be prone to crystallization with inhibitors from the isoindolinone series.¹⁸⁶

7.2.2 Expression and purification

To produce a recombinant protein, *Escherichia coli* cells are transformed by the introduction of a vector bearing the appropriate DNA sequence coding for that protein. The vector also includes an antibiotic resistance gene that allows for the selection of the cell strain of interest and the minimization of contaminant strains by addition of antibiotics to the cultures. It also bears a sequence encoding for an *N*-terminal 3C (PreScission protease)-cleavable glutathione *S*-transferase (GST) tag to allow affinity purification. To increase protein yield, expression is induced in the exponential phase of cell growth (optical density at $\lambda = 600$ nm, OD₆₀₀, of 0.6-1.0) by addition of a non-hydrolysable lactose analogue, isopropyl β -D-1-thiogalactopyranoside (IPTG). This effector molecule activates the *lac* operon on the vector and triggers expression of the desired protein, which is present downstream on the plasmid.

To express MDMX and MDM2, the plasmid pGEX-6P-1 (Figure 7.2) was used as a vector for transformation. The plasmid was introduced into competent cells (RosettaTM BL21 (DE3) pLysS *E. coli* for the expression of all three MDMX constructs, BL21 (DE3) pLysS *E. coli* for MDM2^{E69K70A}₁₇₋₁₀₈, and *E. coli* BL21 (DE3) for MDM2^{K51A}₁₇₋₁₂₅ and MDM2^{E69K70A}₁₇₋₁₂₅) by heat shock and colonies were grown on Luria-Bertani broth (LB)-agar plates with selection from ampicillin (and chloramphenicol for pLysS-containing strains). Expression of the *N*-terminal tagged GST-fusion recombinant protein was induced by addition of 0.2 mM IPTG to cultures (1 L) originating from those colonies.

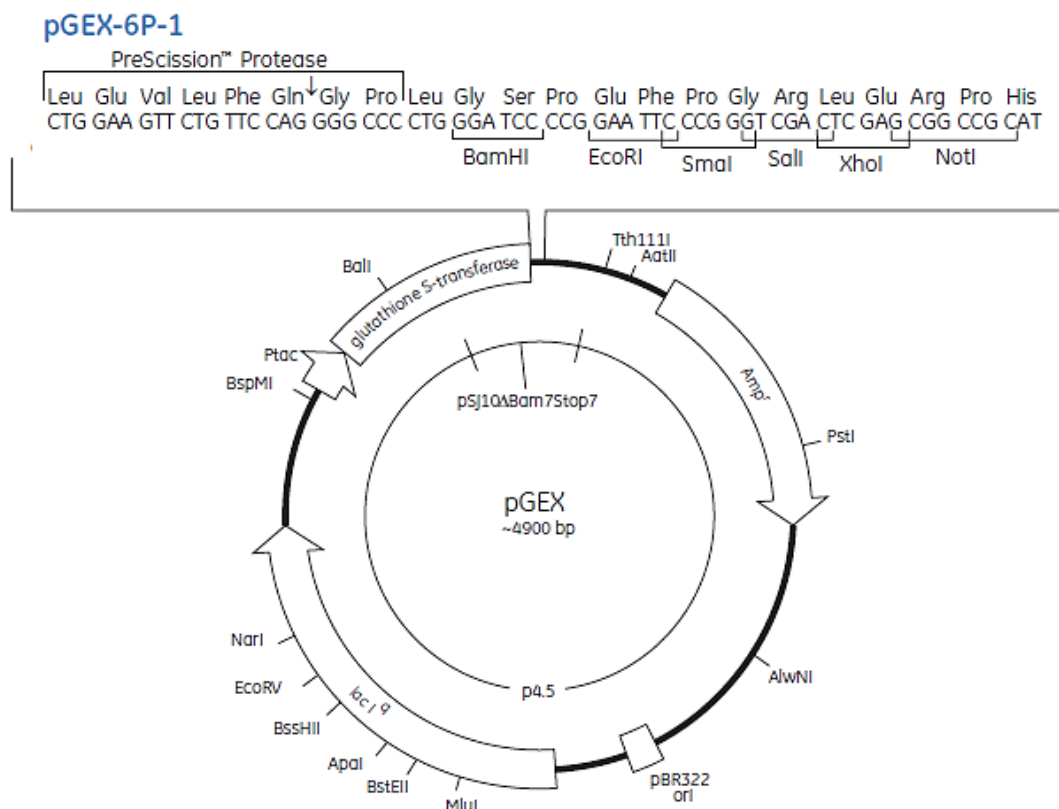


Figure 7.2 - Vector map of the pGEX-6P-1 expression vector.

The vector map highlights the ampicillin resistance gene (*amp^r*), the *lac* operon (*lac I^q*) and the *N*-terminal 3C (PreScission protease)-cleavable glutathione *S*-transferase (GST) tag. Reproduced from GE Life Sciences.¹⁸⁷

The GST tag was exploited to perform an affinity chromatography and separate GST-tagged protein of interest from other substances present in the lysate (Figure 7.3a) before being cleaved by 3C protease. A second purification by size-exclusion chromatography yielded the pure protein (Figure 7.3b and Figure 7.4).

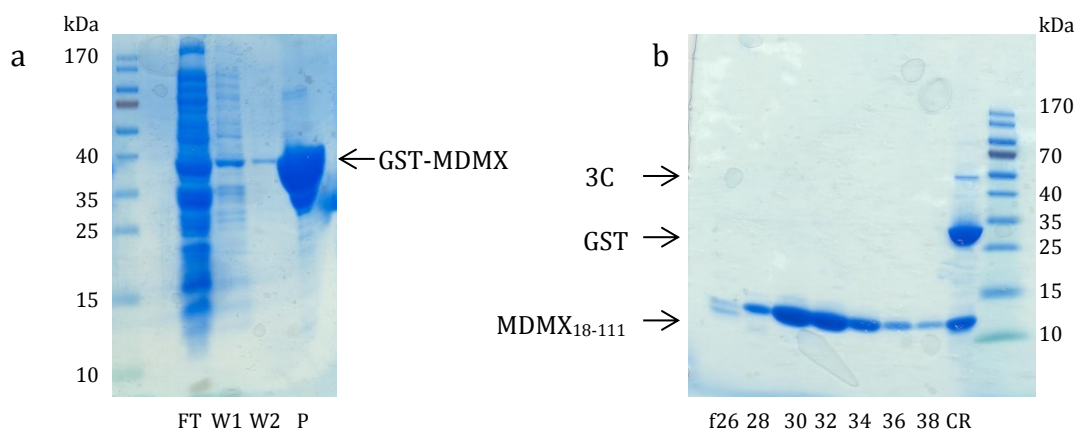


Figure 7.3 - Expression and purification of MDMX₁₈₋₁₁₁

a) Sodium dodecyl sulfate-polyacrylamide gel electrophoresis (SDS-PAGE) of GST-MDMX₁₈₋₁₁₁ following expression in *E. coli* and purification by GST affinity chromatography (FT: flow-through; W1 & W2: wash 1 and wash 2; P: purified GST-MDMX₁₈₋₁₁₁); **b)** SDS-PAGE of 3C cleaved purified MDMX₁₈₋₁₁₁ (CR: crude) and gel filtration fractions.

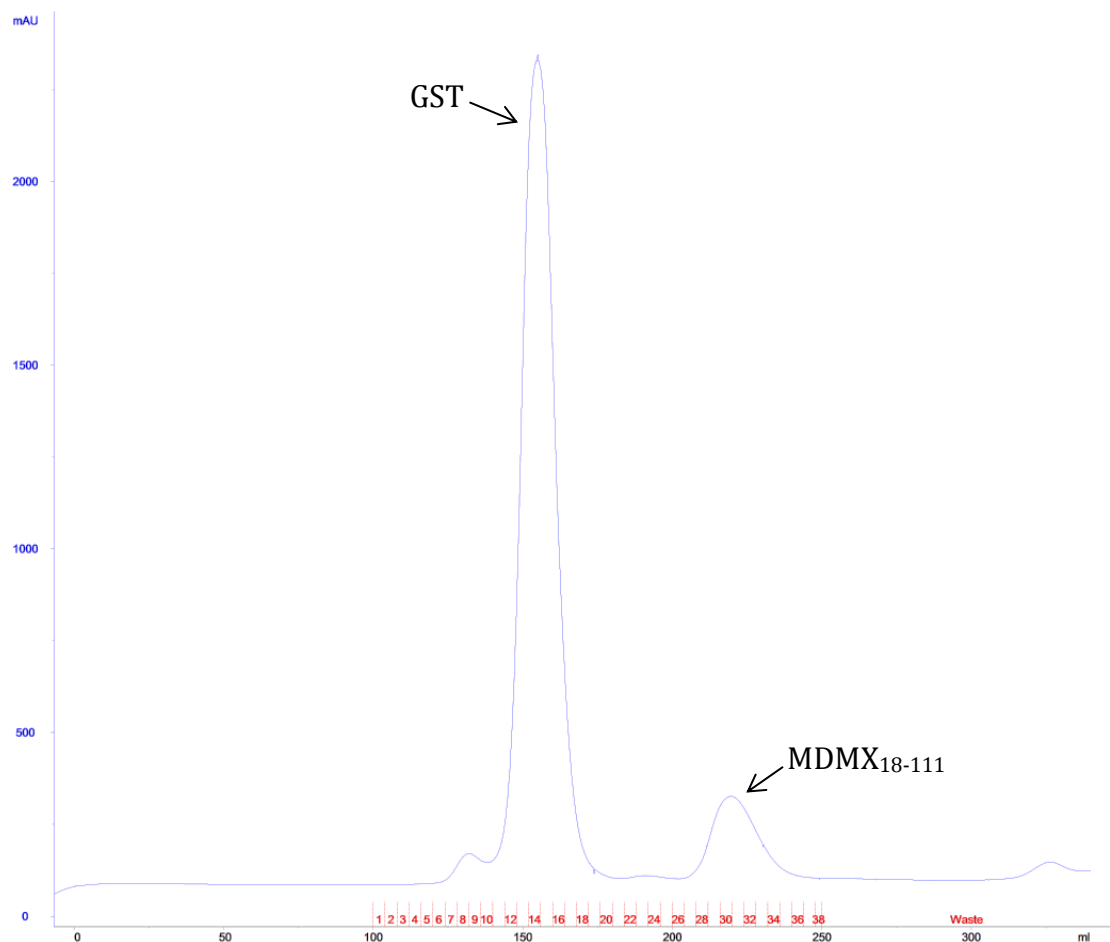


Figure 7.4 - Size-exclusion chromatogram of MDMX₁₈₋₁₁₁.

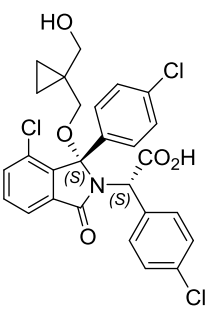
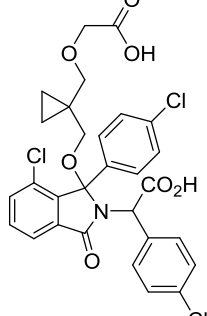
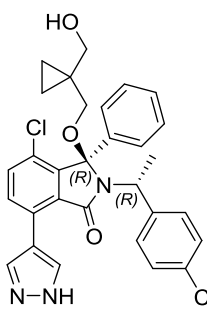
7.2.3 Crystallization trials

The three MDMX constructs expressed well under the conditions described above (MDMX₁₈₋₁₁₁ ~9.5 mg/L culture; MDMX₂₂₋₁₁₁ ~9.9 mg/L; MDMX₂₆₋₁₁₁ ~13.6 mg/L). As expected from previous observations,¹⁸⁶ two MDM2 constructs were obtained in good to moderate yield (MDM2^{K51A}₁₇₋₁₂₅ ~8.9 mg/L; MDM2^{E69K70A}₁₇₋₁₂₅ ~6.8 mg/L), while the final amount of MDM2^{E69K70A}₁₇₋₁₀₈ was extremely poor (0.32 mg/L).

Compounds from both the MDMX and the MDM2 projects were chosen within the isoindolinone series for the crystallization studies according to several parameters. Isoindolinones from the MDMX and the MDM2 projects with suitable activity against MDMX (IC₅₀ < 35 µM) were selected according to their availability. Also, because of known solubility issues in aqueous systems with this series, compounds which had a range of clogD values were selected to maximize the chance of success (Table 7.1).

Table 7.1 - Isoindolinone MDMX inhibitors selected for crystallization trials with MDMX.

Structure				
Compound	148	159	305	306
MDMX IC ₅₀ (LE)	6.2 µM (0.18)	26 µM (0.19)	20 µM (0.17)	26 µM (0.17)
MDM2 IC ₅₀ (LE)	0.218 µM (0.22)	181 µM (0.16)	0.007 µM (0.30)	0.034 µM (0.28)
MDMX/MDM2	28.9	0.14	2953	773
clogD	6.13	5.87	5.61	3.29
Crystallization trial with	MDMX MDM2	MDMX MDM2	MDMX	MDMX MDM2

Structure			
Compound	307	308	303
MDMX IC₅₀ (LE)	25 μM (0.18)	110 μM (0.14)	34 μM (0.16)
MDM2 IC₅₀ (LE)	0.745 μM (0.23)	0.061 μM (0.25)	13 μM (0.18)
MDMX/MDM2	33	1809	2.57
clogD	2.86	1.92	5.76
Crystallization trial with	MDMX MDM2	MDMX MDM2	MDM2

The isoindolinones selected for co-crystallization with MDMX included the most potent in the series, **148**, and the most MDMX selective, **159**. Compound **305** (synthesized by Ruth Bawn within the MDM2 project)¹⁸⁸ was chosen because it bears two groups whose interaction with MDMX was considered worth investigating: the methyl group on the benzylic position and the carbinol group at the 6-position. The presence of the side chain carboxylic acid, which lowers the clogD, was the reason behind the choice of **306** (synthesized by Sarah Cully within the MDM2 project)¹⁵⁶ and **307** (synthesized by Ruth Bawn within the MDM2 project).¹⁸⁸ The dicarboxylic acid **308** (synthesized by Ruth Bawn within the MDM2 project)¹⁸⁸ was included in the crystallization trials despite its low activity against MDMX (IC₅₀ = 110 μM) because it stood out in a parallel study performed by Santosh Adhikari¹⁵² as one of the few isoindolinones giving a dose-response curve in the homogenous time-resolved fluorescence (HTRF) assay (see Section 7.3), probably by virtue of its low clogD. To enable a comparison between the binding modes in the two protein homologs, the same compounds were used for crystallization trials with MDM2, with the exception of the 6-carbinol **305**, for which a co-crystal structure with MDM2^{E69K70A₁₇₋₁₀₈} was already available. Within the α-methyl series, the pyrazole **303** was therefore selected as an additional

compound with clogD and MDMX IC₅₀ comparable to those of **305**. The Roche compound RO-2443 was used as a positive control in trials with both proteins.

The purified proteins were incubated with a 1.5× molar excess of selected inhibitor overnight at 4 °C to allow binding before being concentrated to the concentration required for crystallization trials (5-10 mg/mL). A difference in behaviour could be observed between the two proteins. Achieving higher concentrations proved challenging with MDMX and protein precipitation was observed in the presence of the isoindolinones **148**, **159** and **308** with all constructs at concentrations higher than 2-3 mg/mL. Precipitation was also observed with MDMX₂₆₋₁₁₁ bound to RO-2443. However, when concentrating any of the MDM2 constructs, the process was quicker and precipitation did not occur, suggesting a more stable complex was formed.

The protein:inhibitor complexes were mixed with two commercial screens (ninety-six precipitants per screen) in an attempt to find conditions suitable for crystallization. The AmSO4 Suite from Qiagen and the JCSG+ screen from Molecular Dimensions were used for the trials with all constructs of both proteins. In a 96-well plate, a Mosquito liquid handling system (TTP Labtech) accurately dispensed the crystallization solution from the pre-pipetted reservoir and mixed it with the protein:inhibitor solution, generating two drops with ratios of 1:1 and 1:2. Approximately 6,900 conditions were screened for each protein.

7.2.4 Crystal formation and data collection

Upon preparation of the samples, the crystallization trays were incubated at 4 °C for up to five weeks and monitored periodically using an automated imaging system (Minstrel, Rigaku). Unfortunately, none of the three MDMX constructs crystallized in any of the conditions screened with any of the compounds selected, including the positive control RO-2443 and the formation of precipitates was mostly observed. However MDMX₂₆₋₁₁₁ in the presence of isoindolinones **307** and **308** generated small spheroidal masses of crystals called spherulites (Figure 7.5a and b), which may represent a starting point for further optimization of the crystallization conditions.

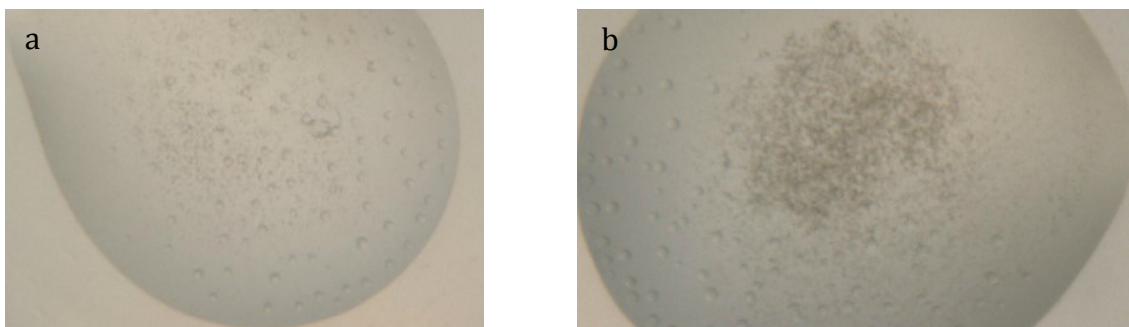


Figure 7.5 - Crystallization trials with MDMX₂₆₋₁₁₁.

Co-presence of spherulites and precipitate in drops containing MDMX₂₆₋₁₁₁ with **a)** isoindolinone **307** and **b)** isoindolinone **308**, both using JCSG+ screen, 0.2 M lithium sulfate, 50 v/v polyethylene glycol 400, 0.1 M sodium acetate, 200+100 nL precipitant:protein.

As expected, crystallization trials with MDM2 were more satisfactory and a few conditions proved successful. Both MDM2^{K51A}₁₇₋₁₂₅ and MDM2^{E69K70A}₁₇₋₁₀₈ formed crystals with **306** (Figure 7.6) and though diffraction data were obtained, a co-crystal structure could not be obtained from these samples due to crystal twinning (lattice points shared among two crystals).

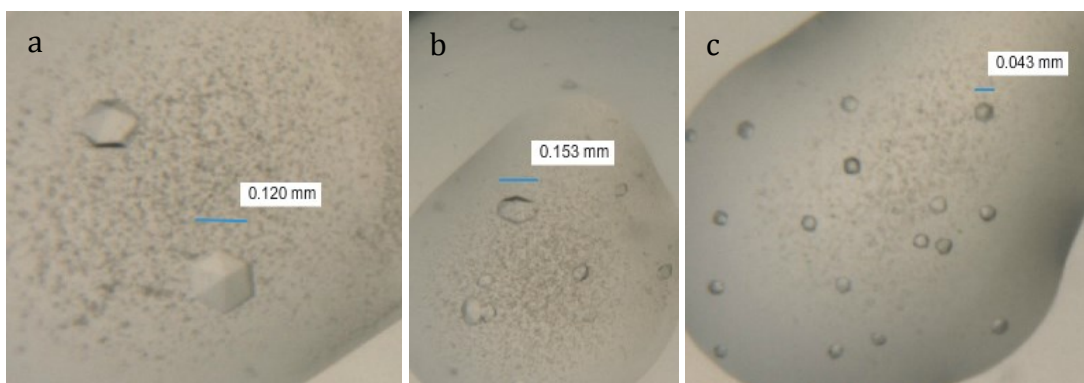


Figure 7.6 - Crystals of MDM2 with 306 (AmS04 Suite screen).

a) MDM2^{K51A}₁₇₋₁₂₅ with **306**, 0.2 M ammonium iodide, 2.2 M ammonium sulfate, 200+100 nL precipitant:protein; **b)** MDM2^{K51A}₁₇₋₁₂₅ with **306**, 0.2 M lithium sulfate, 2.2 M potassium thiocyanate, 200+100 nL precipitant:protein; **c)** MDM2^{E69K70A}₁₇₋₁₀₈ with **306**, 0.2 M potassium iodide, 2.2 M ammonium sulfate, 100+100 nL precipitant:protein.

To our delight, crystals of MDM2^{K51A}₁₇₋₁₂₅ and the MDMX-selective isoindolinone **159** were also grown (Figure 7.7), offering the chance to understand the reasons underlying the selectivity shown by this compound. The crystals were transferred in an appropriate cryo-protecting solution (reservoir supplemented with 30%

ethylene glycol) and flash-cooled in liquid nitrogen. Diffraction data were collected at the Diamond Light Source.



Figure 7.7 - Crystals of MDM2^{K51A}₁₇₋₁₂₅ with 159.

Crystallization conditions: AmSO₄ Suite screen, 0.2 M potassium iodide, 2.2 M potassium nitrate, 100+100 nL precipitant:protein.

7.2.5 Highlights of the X-ray structure of 159 bound to MDM2

The data collected for MDM2^{K51A}₁₇₋₁₂₅ with **159** were processed by Martin Noble and Judith Reeks. The solved co-crystal structure was obtained at 2.5 Å resolution. In each asymmetric unit, six molecules of protein were found but only three of them were in complex with the inhibitor. The remaining three sites were occupied by peptide from the *N*-terminal region of other MDM2 molecules. The three molecules of **159** were present at low occupancy, probably due to the low potency of the ligand against MDM2 (IC₅₀ = 181 μM), manifesting as poor but interpretable electron density. As observed for other isoindolinones, the A-ring of **159** enters the Phe19 pocket while the phenyl ring at the 3-position interacts with the Trp23 pocket of MDM2. The Leu26 pocket is not occupied in this structure, apparently because of the stereochemistry of the ligand. In the (3*R*,1'*R*) configuration, the steric hindrance pushes the phenyl substituent at the 3-position and the 4-chlorobenzyl at the 2-position in different directions, with the former entering the Trp23 pocket and the latter rotating outwards and away from the Leu26 pocket (Figure 7.8).

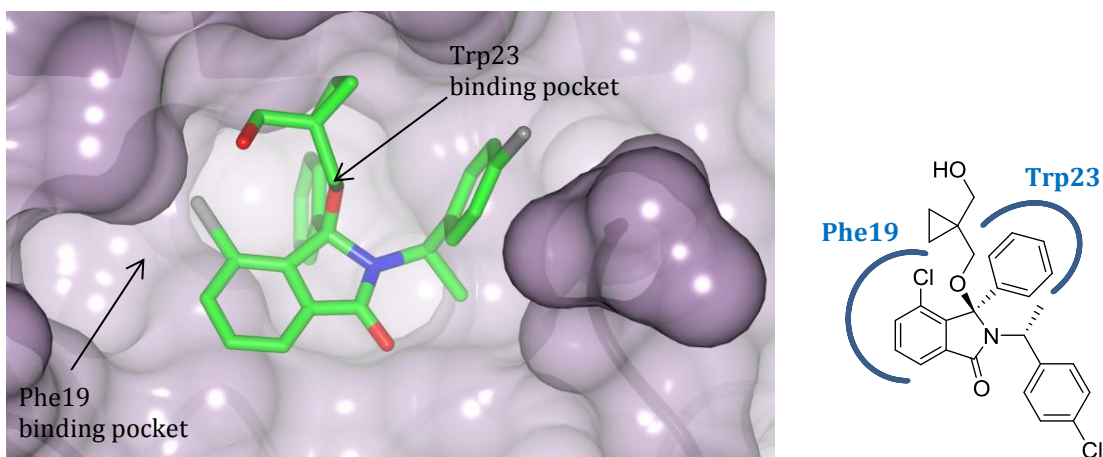


Figure 7.8 - Crystal structure of 159 bound to MDM2^{K51A}₁₇₋₁₂₅.

The stereochemistry at the benzylic stereocentre forces the aromatic ring into a conformation that prevents it from entering the Leu26 binding pocket.

Superposition of the structure of **305** with that of **159** (Figure 7.9) shows that with the α -methyl group in the opposite configuration (*S*) the benzyl enters the Leu26 pocket, while the (*R*) configuration leads to steric hindrance between the two aromatic rings forcing the benzyl out of the binding pocket. The conformation adopted by **305** upon binding to MDM2 is comparable to the low-energy conformation adopted by (3*R*,1'*S*)-**208** in the small-molecule crystal structure shown in Section 6.1.3. The *N*-terminal region of MDM2^{K51A}₁₇₋₁₂₅, which is normally disordered in MDM2-isoindolinone structures, is ordered in the **159** structure and interacts with the 4-chlorobenzyl. However, it is not certain whether this interaction would be biologically relevant in a native system, because the *N*-terminus of the protein construct MDM2^{K51A}₁₇₋₁₂₅ still possesses six non-native amino acid residues belonging to the cleaved GST tag. In the co-crystal structure, the isoindolinone core is substantially shifted outwards, resulting in a non-optimal occupancy of the Phe19 and Trp23 binding pockets by the isoindolinone A-ring and the phenyl ring, thus contributing to the low potency shown by **159** towards MDM2. This shift is also observed when comparing the structures of **159** with that of another isoindolinone analogue not bearing the carbinol moiety at the 6-position as well as with an analogue with fluorine in the 4-position (data not shown). This suggests that the (*R*)- α -methyl group is the cause of the alternative binding mode.

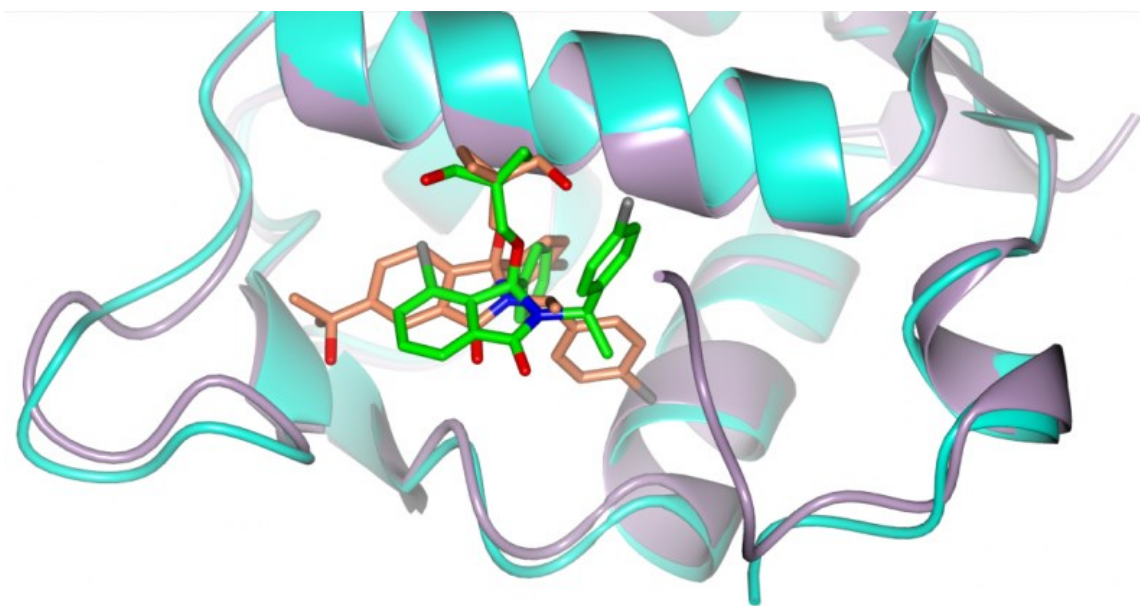


Figure 7.9 - Superposition of the crystal structure obtained from the 6-carbinol isoindolinone 305 (orange) bound to MDM2^{E69K70A}₁₇₋₁₀₈ with that of 159 (green) bound to MDM2^{K51A}₁₇₋₁₂₅.

The image shows the alternative binding modes of the benzyl group dictated by the stereochemistry of the α -methyl. Figure provided by Judith Reeks.

The MDM2^{K51A}₁₇₋₁₂₅:**159** co-crystal structure was superposed with an MDMX crystal structure available from the Protein Data Bank (PDB 3U15),¹⁵⁰ as shown in Figure 7.10. The model suggests that a mode of binding comparable to that observed with MDM2 is also plausible with MDMX. The 4-chlorobenzyl would be in proximity to the side chain of Lys50 (Lys51 in MDM2, mutated to alanine in the construct that co-crystallized with **159**) in the flexible loop, where a stabilizing interaction could potentially be established.

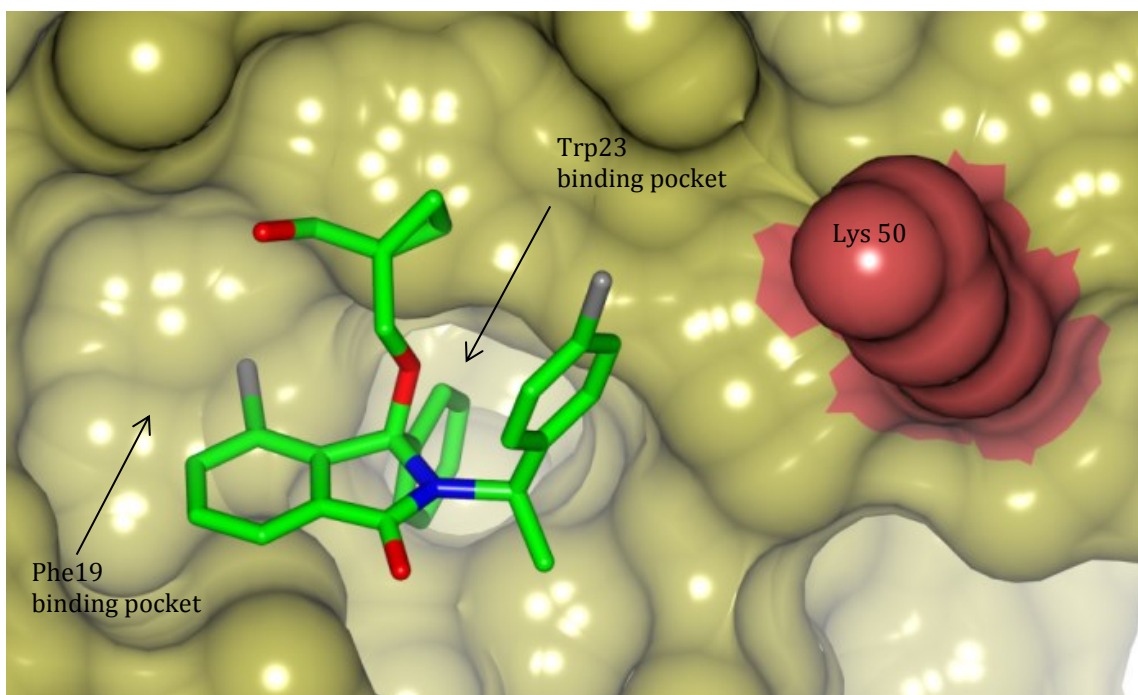


Figure 7.10 - Superposition of the MDM2:159 co-crystal structure to one of the MDMX crystal structures available in the PDB (PDB code 3U15).¹⁵⁰

The image suggests a potential interaction between the 4-chlorobenzyl group of **159** and the side chain of Lys50 (Lys51 in MDM2). Figure provided by Judith Reeks.

Although no definite conclusions can be drawn in the absence of a crystal structure of **159** in complex with MDMX, the data available suggest that for this inhibitor the interaction with MDM2 is compromised in three ways: a) the interaction of the 4-chlorobenzyl with the Leu26 pocket is abolished due to the steric hindrance originating from the stereochemical configuration of the isoindolinone forcing the phenyl and the benzyl groups in opposite directions; b) the interaction of the phenyl ring with the residues in the Trp23 pocket is weak due to the absence of the 4-chloro substituent; c) a putative interaction of the 4-chlorobenzyl with a flexible loop causes a shift of the whole isoindolinone core, ultimately resulting in sub-optimal interactions between the inhibitor and the two occupied pockets of MDM2. The data suggest that the binding mode adopted by **159** with MDMX is likely to be similar to that observed with MDM2. Therefore, it is reasonable to assume that either the lack of the 4-chloro substituent on the phenyl ring or the isoindolinone core shift, or a synergy of the two, are better tolerated by MDMX.

7.3 HTRF Assay

Fluorescence resonance energy transfer, FRET, is a physical phenomenon first described by the German physical chemist Theodor Förster in 1948. FRET involves the transfer of energy from an excited fluorophore (donor) to another suitable fluorophore (acceptor). The emission spectrum of the donor must overlap with the absorbance spectrum of the acceptor. FRET is a distance-dependent, non-radiative energy transfer and, for it to occur, the donor and acceptor must be in close proximity to one another (10-80 Å).¹⁸⁹⁻¹⁹¹

FRET is the basis of the high-throughput HTRF assay developed by Judith Reeks and Santosh Adhikari to evaluate the potency of compounds against the MDMX:p53 and the MDM2:p53 protein-protein interactions as a replacement for the ELISA. The need for an alternative way to measure the IC₅₀ of the compounds synthesized stemmed from the anti-MDMX antibody used in the ELISA being discontinued by the manufacturer. As shown in Figure 7.11a, addition of fluorescein-labelled IP3 peptide¹⁶⁴ to GST-tagged MDMX leads to the formation of an MDMX:IP3 complex. A terbium-labelled anti-GST antibody is added which binds to the GST-tag, bringing the terbium in close proximity to the fluorescein fluorophore. FRET excitation of terbium (donor) at a specific wavelength (320 nm) results in emission of energy from fluorescein (acceptor) at a different wavelength (520 nm). The presence of an inhibitor (Figure 7.11b) prevents the formation of the MDMX:IP3 complex and, consequently, FRET does not occur.

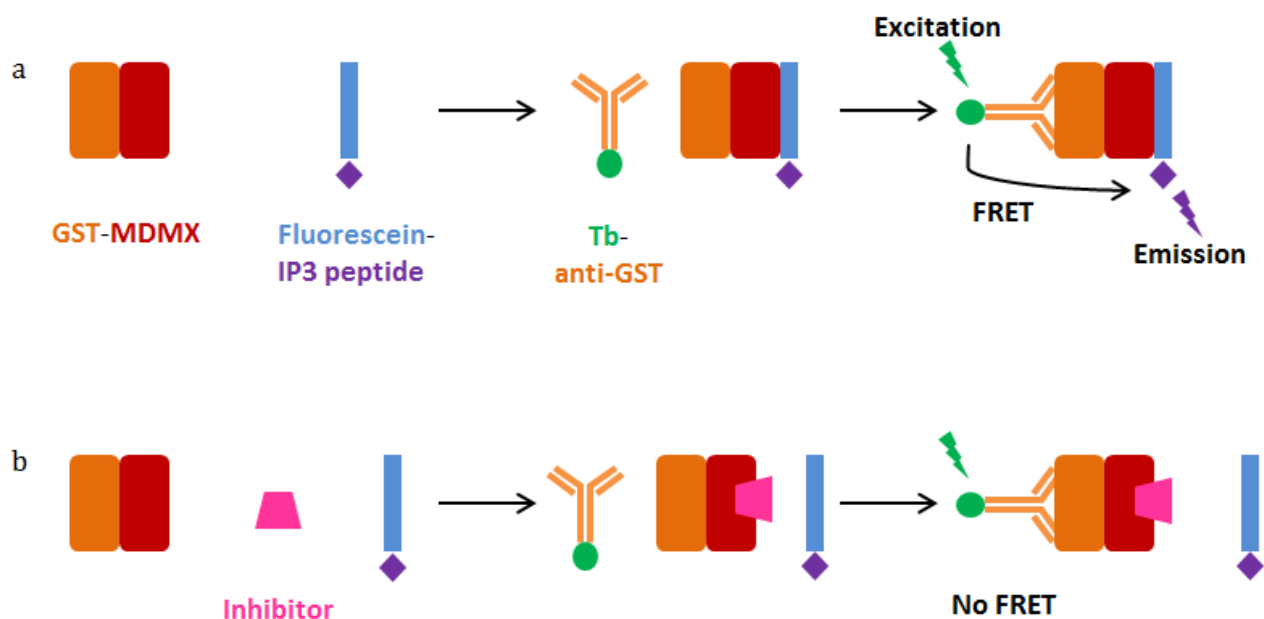


Figure 7.11 - Cartoon representing the principle behind the HTRF assay

a) The interaction between MDMX and IP3 brings the two fluorophores in close proximity and, upon excitation of the donor (Tb), the acceptor (fluorescein) fluoresces at a different wavelength (FRET); **b)** the presence of an inhibitor prevents the formation of the MDMX:IP3 complex and FRET does not occur. Adapted from Judith Reeks.

Validation of the HTRF assay for MDMX required a panel of compounds from the isoindolinone series with a range of potencies and clogD. Reportedly, solubility represented the main hurdle in the evaluation of the potency of compounds with both MDMX and MDM2.^{152,186} In addition to the seven compounds used for the crystallization studies (Table 7.1), six other isoindolinones were selected for HTRF validation (Table 7.2). Among these, the carboxylic acids **242** and **310** (synthesized by Sarah Cully within the MDM2 project)¹⁵⁶ were chosen because of their low clogD (2.53 and 2.66, respectively) and their alcohol analogues **236** and **309** (synthesized by Anna Watson within the MDM2 project)¹⁶⁶ were tested to verify the hypothesis that clogD is a key parameter to obtain meaningful results in the conditions required by the HTRF assay. In addition to the pyrazole **303** that was already included in the study (Table 7.1), the regioisomer **302** was also selected to compare the results obtained from the assay using equipotent close analogues. The α -methyl analogue of **148**, **164**, was included in the study as a sample compound with no measured IC₅₀.

Table 7.2 - Isoindolinones selected for HTRF assay evaluation.

Structure			
Compound	242	236	302
MDMX IC₅₀ (LE)	123 μ M (0.18)	62 μ M (0.19)	31 μ M (0.16)
MDM2 IC₅₀ (LE)	15 μ M (0.21)	Not active	200 μ M (0.13)
MDMX/MDM2	8.4	-	0.15
clogD	2.53	5.47	5.76

Structure			
Compound	309	310	164
MDMX IC₅₀ (LE)	114 μ M (0.15)	29 μ M (0.16)	N/A
MDM2 IC₅₀ (LE)	0.044 μ M (0.29)	0.057 μ M (0.25)	N/A
MDMX/MDM2	2562	500	-
clogD	4.99	2.67	6.14

For the experiment, a number of positive controls were used, including two p53 peptides, p53₁₇₋₂₇ (provided by Pamela Williams, Astex) and p53^{N30F}₁₇₋₃₀ (provided by David Lane, A*Star, Singapore), alongside two literature small molecule-inhibitors, RO-2443 and WK298 (Figure 7.12). The measured IC₅₀s were 9.33 μ M for the p53₁₇₋₂₇ peptide and 1.33 μ M for the p53^{N30F}₁₇₋₃₀ peptide. The dose-response curve generated for the small-molecule inhibitor RO-2443 corresponds to an IC₅₀

of 4.31 μM (literature 0.041 μM ;¹⁵⁰ in-house ELISA 13.7 μM) and the one for WK298 to 13.9 μM , (literature 19.7 μM).¹⁴⁸

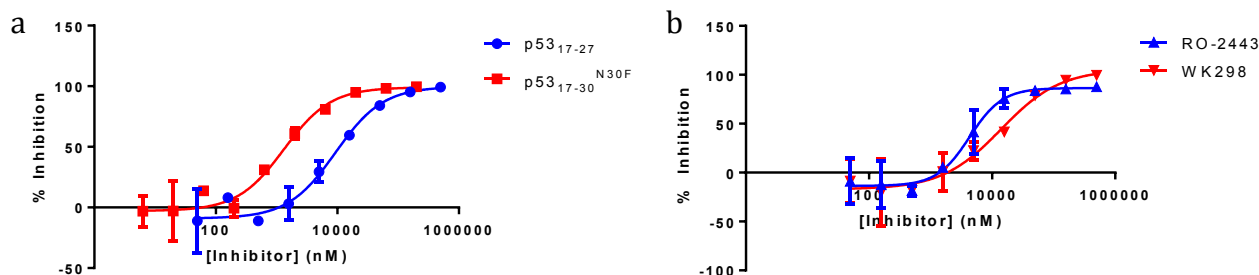


Figure 7.12 - HTRF dose-response curves for GST-MDMX₂₂₋₁₁₁ using positive controls.

a) Peptides p53₁₇₋₂₇ and p53₁₇₋₃₀^{N30F}; **b)** literature small-molecule inhibitors RO-2443 and WK298.

Suitable dose-response curves were obtained for the acids **310** (HTRF IC₅₀ = 37.5 μM ; ELISA IC₅₀ = 28.5 μM) and **242**, although extrapolation of the IC₅₀ for the latter compound was not possible because of the low potency of the compound (a plateau was not reached within the concentration range examined). The lipophilic alcohol analogues **310** and **236**, instead, hit a solubility threshold in the assay conditions and did not reach 50% inhibition (Figure 7.13).

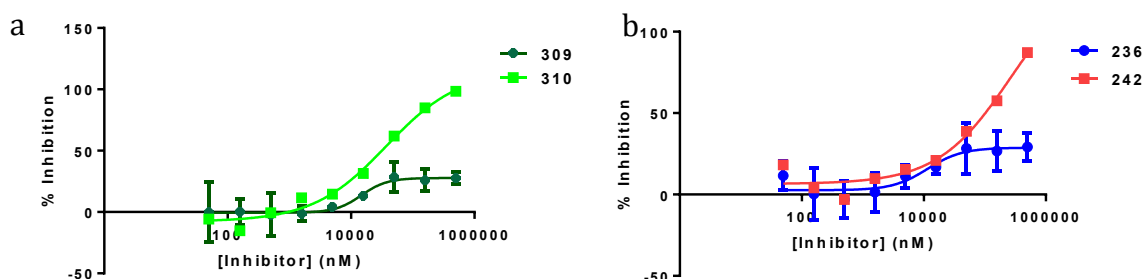


Figure 7.13 - HTRF curves for GST-MDMX₂₂₋₁₁₁.

a) 4-nitrobenzyl isoindolinones **309** and **310**; **b)** *des*-cyclopropyl isoindolinones **236** and **242**.

A dose-response curve was observed with the soluble carboxylic acids **306** (HTRF IC₅₀ = 40.2 μM ; ELISA IC₅₀ = 26.0 μM) and **307** (HTRF IC₅₀ = 90.1 μM ; ELISA IC₅₀ = 24.9 μM). An IC₅₀ value could not be extrapolated for isoindolinones **305**, **164**, **148**, **302**, **303** and **159** (Figure 7.14).

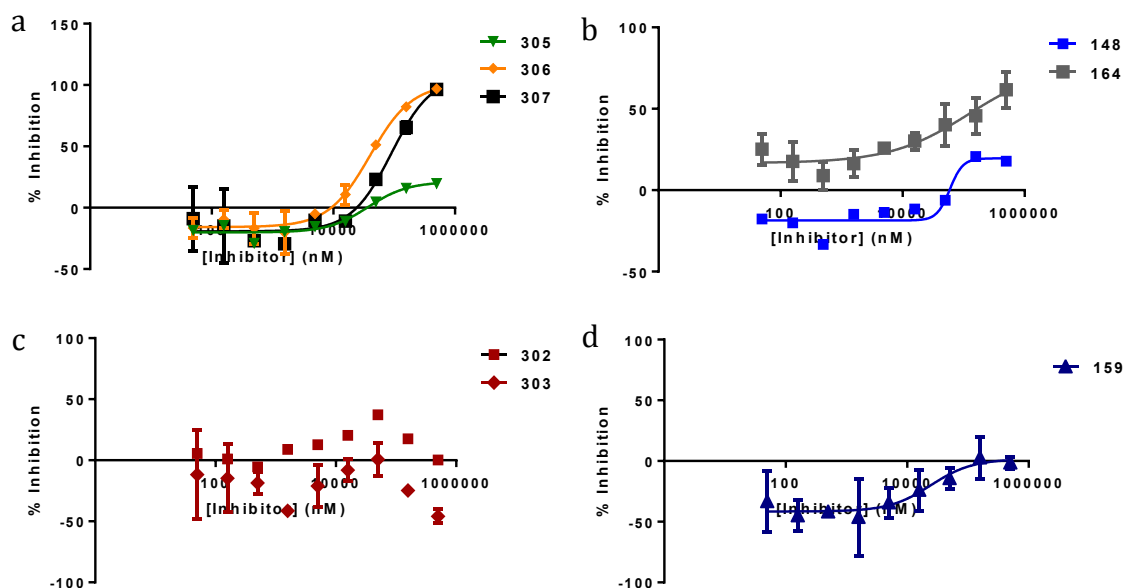


Figure 7.14 - HTRF curves for GST-MDMX₂₂₋₁₁₁.

a) Dose-response curves for the carboxylic acids **306** and **307**. The 6-carbinol isoindolinone **305** hits a solubility threshold at higher concentrations. **b)** The isoxazole compound **148** and its α -methyl analogue **164** did not give a dose-response curve. **c)** Data obtained for the pyrazole compounds **302** and **303** show an anomalous behavior and could not be fitted. **d)** The curve corresponding to the benchmark compound **159** is entirely at negative values of inhibition.

7.4 Differential scanning fluorimetry (DSF)

The isoindolinones synthesized within the MDMX project, together with those used for the structural biology studies and HTRF validation, were all screened against the three MDMX constructs using differential scanning fluorimetry, DSF. The screen was performed in set conditions to identify compounds that are effective in stabilizing the protein constructs. Each protein, or protein construct, is characterized by a distinct melting temperature, T_m , at which 50% of the protein is unfolded due to the denaturing effect of a temperature increase. By measuring the difference between the T_m of the apo protein and that of the protein bound to an inhibitor (thermal shift, ΔT_m), it is possible to evaluate whether the presence of the ligand has a stabilizing or a destabilizing effect on the protein. DSF experiments are performed with a temperature gradient in the presence of a dye (SYPRO orange) that binds to the hydrophobic sites of the protein that are exposed as a result of unfolding. The increasing fluorescence is proportional to the fraction of bound dye and is used to evaluate the stage of protein denaturation. Allowing for the

screening of a large number of compounds at the same time, DSF is a highly time-efficient, inexpensive and informative technique.¹⁹²

The imidazo-indole WK298 **143**, the indolyl-hydantoins RO-2443 **146** and RO-5963 **147** and the p53^{N30F}₁₇₋₃₀ peptide were included in the experiments as positive controls. Negative controls encompassed systems lacking of a) inhibitor, to determine the T_m of the apo protein; b) protein and inhibitor, to exclude the possibility of fluorescent contaminants; c) inhibitor and dye, to verify the absence of an interaction between the two compounds that would affect the fluorescence. Every condition was run in triplicate and average values and standard deviations were calculated. Example DSF curves are shown in Figure 7.15. The results of the experiments performed with the compound library using all three purified MDMX constructs are summarized in Figures 7.16–18.

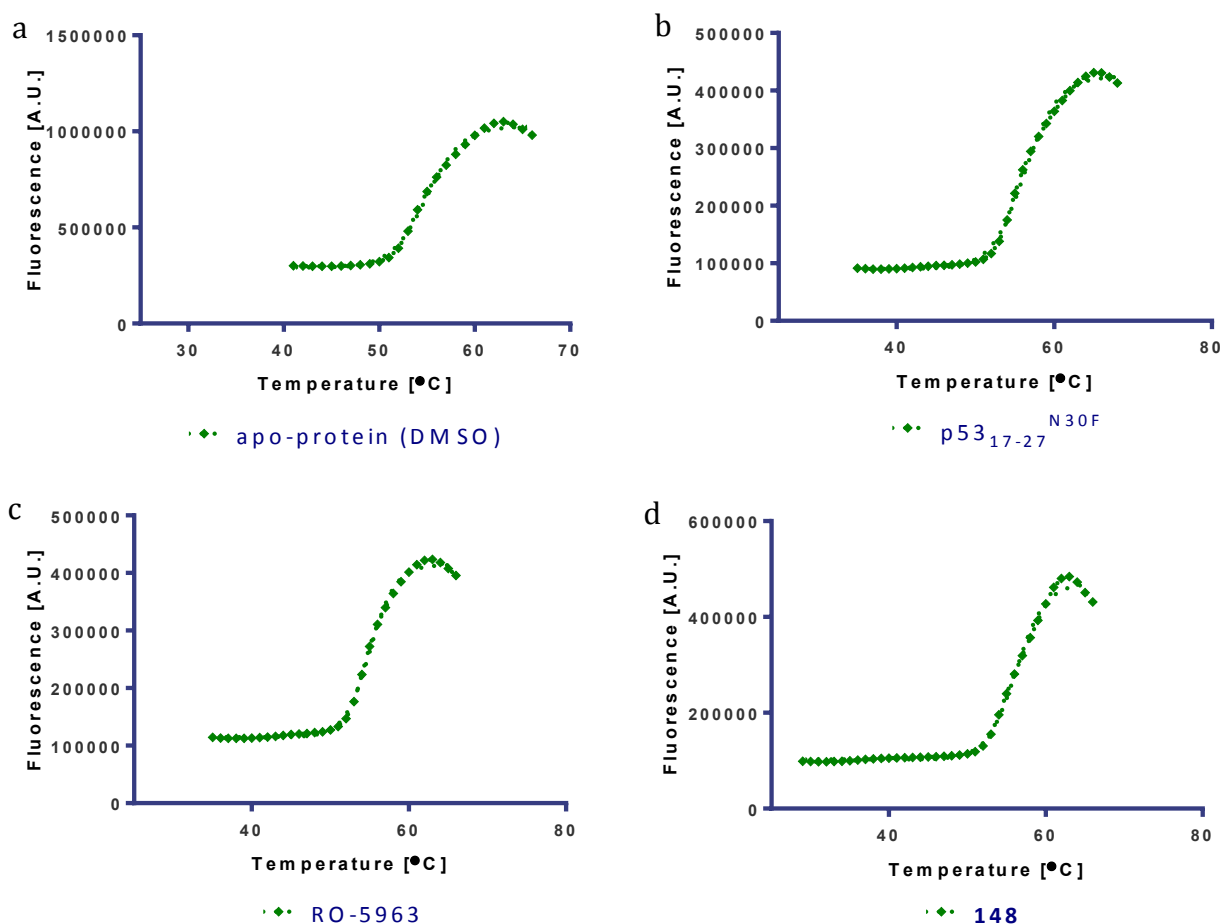


Figure 7.15 - Example of thermal denaturation curves with MDMX₂₂₋₁₁₁.

a) Apo protein ($T_m = 55.0$ °C); **b)** p53^{N30F}₁₇₋₃₀ peptide ($T_m = 57.0$ °C); **c)** RO-5963 ($T_m = 55.6$ °C); **d)** **148** ($T_m = 55.3$ °C).

The p53 peptide stabilized all three constructs by 1.5-2.0 °C. Among the literature compounds, the greatest effect was observed with the presence of WK298, especially with MDMX₂₂₋₁₁₁ and MDMX₂₆₋₁₁₁ ($\Delta T_m = +2.19 \pm 0.09$ and $+1.32 \pm 0.71$ °C, respectively). With the only exception of **248** bound to MDMX₂₂₋₁₁₁, all the isoindolinones synthesized within the project destabilized all three constructs. However, the result obtained with **248** must be interpreted with caution, due to the considerable error associated with the data ($\Delta T_m = +0.33 \pm 1.09$ °C). Among the other isoindolinones included in the study, the 4-nitrobenzyl carboxylic acid **310** induced a stabilization of 0.44 ± 0.09 °C with construct MDMX₁₈₋₁₁₁, 1.06 ± 0.19 °C with construct MDMX₂₂₋₁₁₁ and 0.98 ± 0.27 °C with MDMX₂₆₋₁₁₁. The dicarboxylic acid **308** also had a favorable effect on protein stability, especially with MDMX₂₂₋₁₁₁ ($\Delta T_m = 1.56 \pm 0.26$). The isoindolinones **306** and **305** also showed a mild stabilizing effect on MDMX upon binding.

7.5 Conclusions drawn from the structural biology studies on MDMX

Crystallization trials were set up with a selection of ligands using three constructs of each protein aimed at achieving a clearer understanding of the differences between the mode of binding of isoindolinones to MDMX and to MDM2. Unfortunately, crystals of MDMX were not obtained. However, the structure of the MDMX-selective **159** in complex with MDM2^{K51A}₁₇₋₁₂₅ was solved and exhibited a peculiar mode of binding triggered by the conformation adopted by the ligand as a result of its (3*R*,1'*R*) stereochemistry. The crystal structure showed that the 4-chlorobenzyl group at the 2-position of the isoindolinone core does not have access to the Leu26 binding pocket, but seems to interact with the flexible *N*-terminal of the protein. An outward shift of the core is also observed, which reduces the extent of the interaction of the A-ring and the phenyl group with the Phe19 and Trp23 pockets, respectively. Superposition of the structure obtained with a MDMX structure available in the PDB suggests that a similar mode of binding is plausible to MDMX, although it is not possible to determine the reasons underlying the selectivity of **159** towards this target. Similarly to what was

previously achieved with MDM2, a surface entropy mutation approach could be attempted to promote the crystallization of MDMX.

As a consequence of withdrawal from the market of the anti-MDMX antibody used for the ELISA, an HTRF assay was developed. A panel of isoindolinones was selected to validate it. The attainment of meaningful results was strongly dependent on the solubility of the ligands and only isoindolinones with $\text{clogD} < 3$ were likely to show a dose-response curve. These findings suggest that most of the MDMX-active isoindolinones are not amenable for HTRF assay because of their low solubility. A library of isoindolinones was screened to measure the thermal shift induced on three MDMX constructs. Only the soluble carboxylic acids **308** and **310** significantly stabilized the protein ($\Delta T_m \geq 1\text{ }^{\circ}\text{C}$) while **305** and **306** showed a moderate stabilizing effect. Taken together, these findings highlight the relevance of solubility as a parameter to be considered prior to the synthesis of any target molecule.

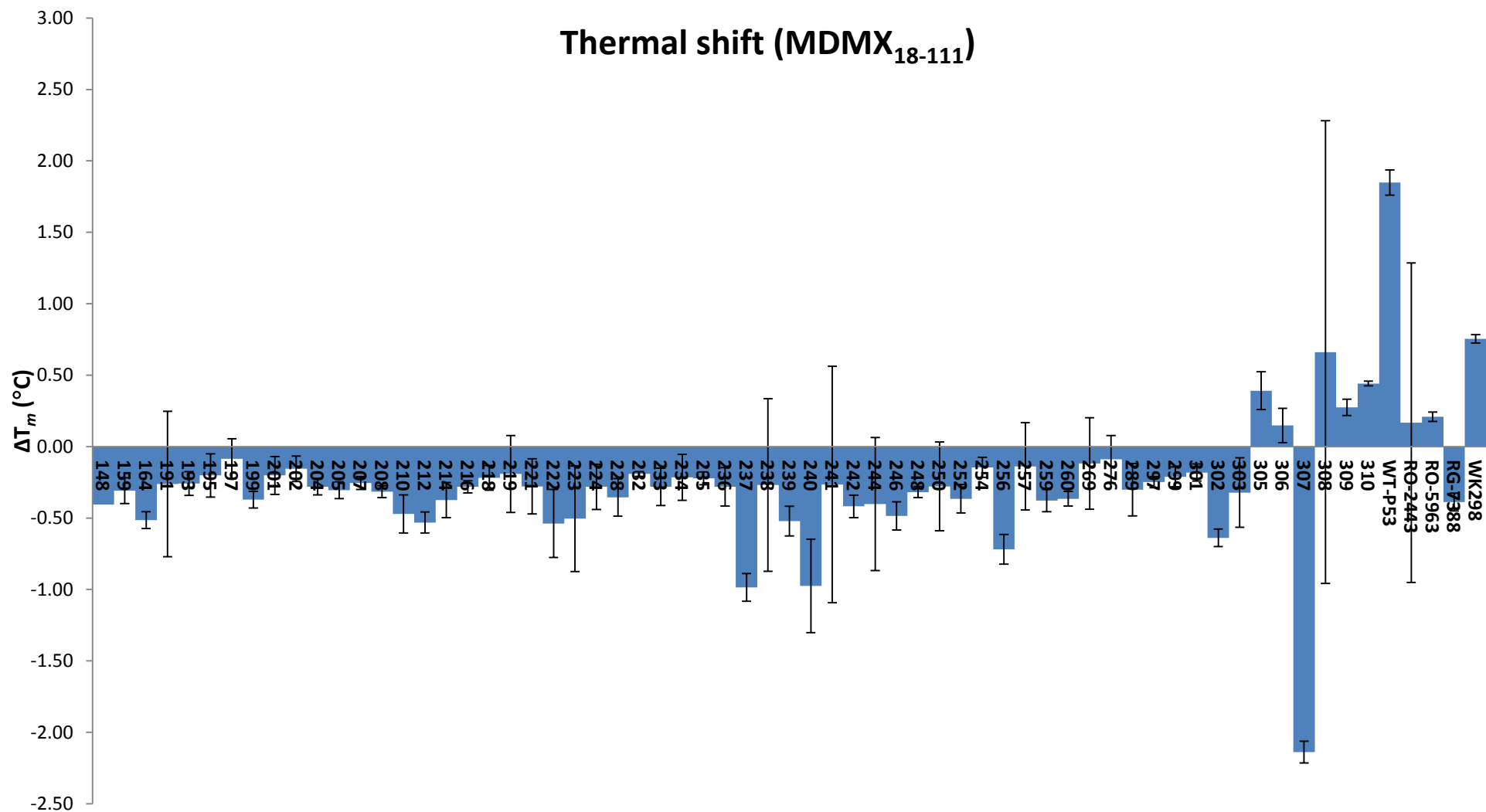


Figure 7. 16
Thermal shift for a selection of isoindolinones and MDMX₁₈₋₁₁₁.

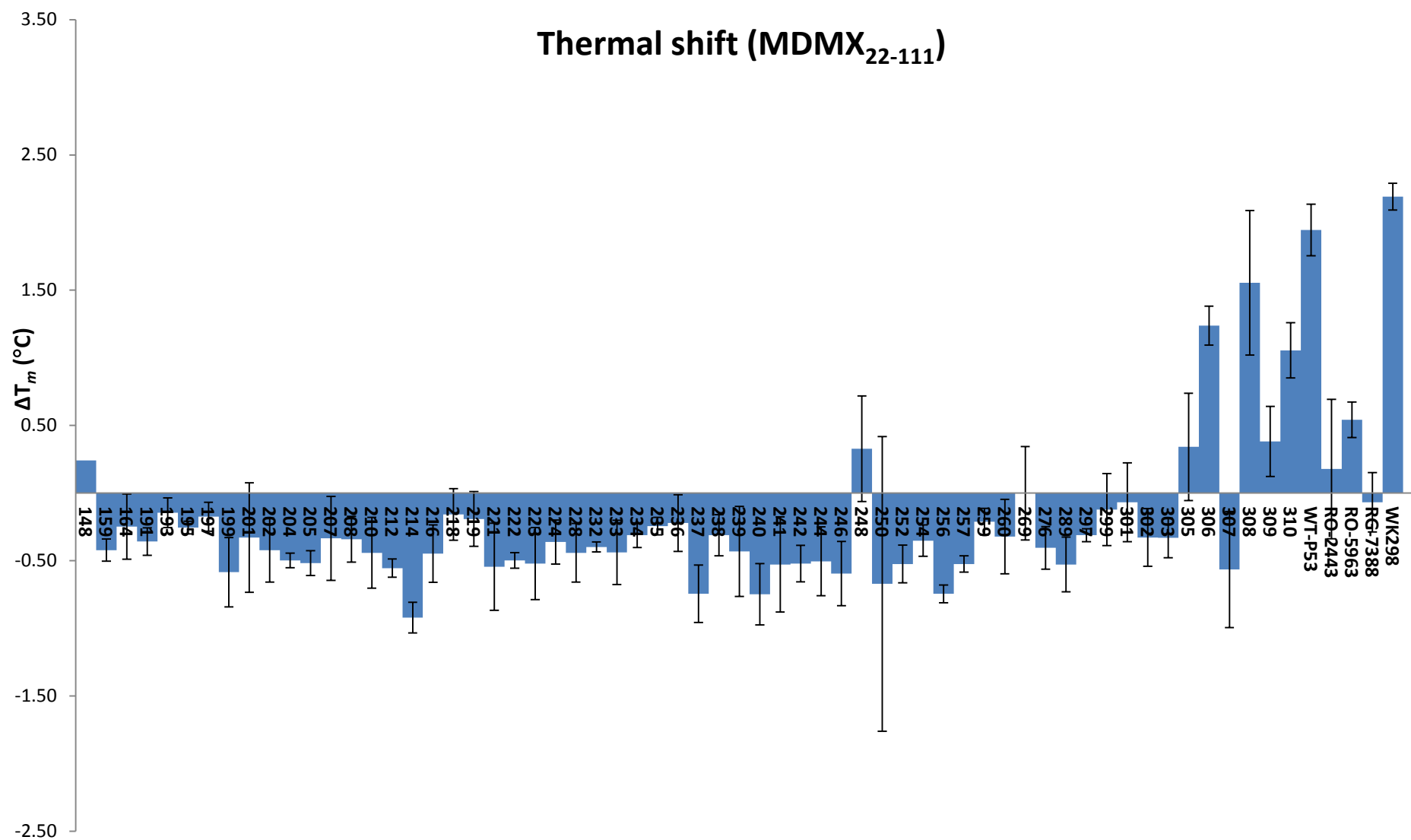


Figure 7.17
Thermal shift for a selection of isoindolinones and MDMX₂₂₋₁₁₁.

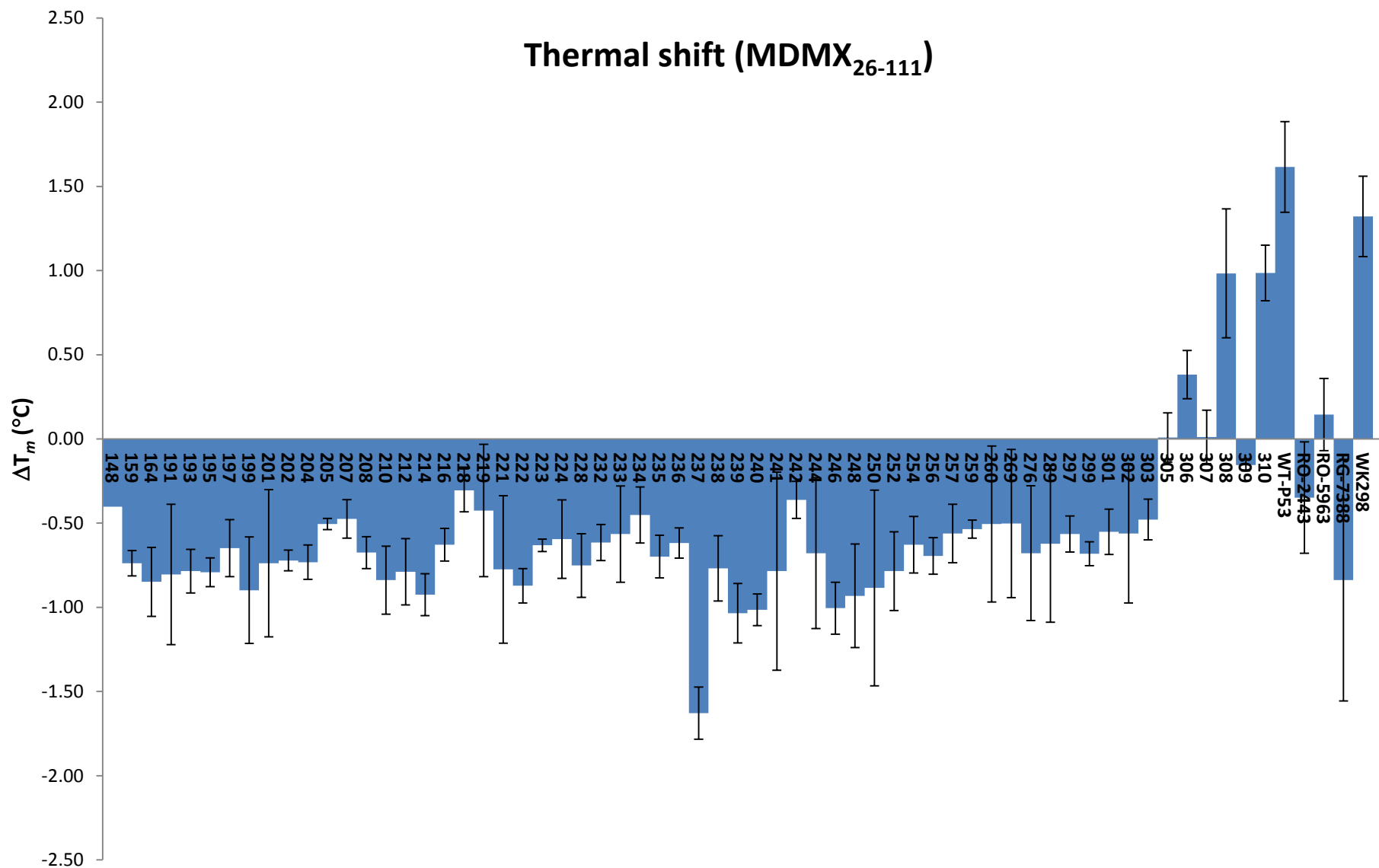


Figure 7.18
Thermal shift for a selection of isoindolinones and MDMX₂₆₋₁₁₁.

CHAPTER 8. CONCLUSIONS

Validation studies were undertaken on two different target classes potentially implicated in cancer survival and development, a sulfatase enzyme and a protein-protein interaction. In both cases, chemical tools of suitable potency were required, prompting the initiation of medicinal chemistry projects at the Northern Institute of Cancer Research.

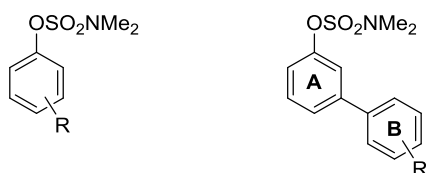
8.1 The Sulf2 project

Up-regulation of the endosulfatase Sulf2 in hepatocellular carcinoma corresponds to a more aggressive tumor phenotype, with lower survival rate for patients and higher tumor recurrence after excision. The interplay between Sulf2 and its homologue Sulf1 is still not completely understood, as the two enzymes appear to have non-redundant functions and different substrate specificity *in vivo*.⁵⁶ Additionally, Sulf1 may act either as a tumor suppressor or as an oncogene depending on the cellular context, making it difficult to evaluate whether a specific Sulf2 inhibitor would be desirable or if dual Sulf1 and Sulf2 inhibition would be preferred. Nonetheless, specificity could prove difficult to achieve with small-molecules due to the high degree of homology in the catalytic domains of the two enzymes.

Aiming to develop tool compounds for further target validation and rationalize interactions with the enzyme, three series of compounds were synthesized featuring either a tertiary or a primary sulfamate group on an aromatic template.

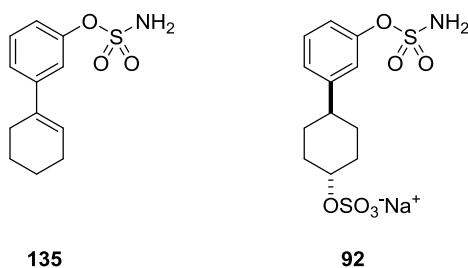
The first series designed, including diversely substituted monocyclic aromatic tertiary phenylsulfamates, was essentially inactive in a biochemical assay against Sulf2, but more encouraging results were obtained with a tertiary biphenylsulfamate template. The second aromatic ring (B-ring) was introduced *via* an optimized Suzuki-Miyaura cross-coupling to allow exploration of substitution with polar functionalities (carboxylic acid, amine, aminosulfate)

which were appended to the B-ring aiming to mimic the position of polar groups on the disaccharide unit of heparan sulfate, the endogenous substrate. Polar substituents, such as aminosulfates, carboxylic acids and sulfated hydroxymethyl, as well as the electron-withdrawing cyano- showed some level of activity (up to ~30% inhibition at 1 mM), which tend to be higher with a 3'- or 4'- substitution pattern.

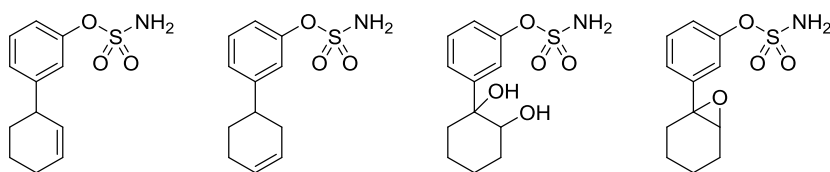


The third series of compounds featured a non-aromatic B-ring aiming to explore an area of space not accessible using a planar aromatic B-ring. The cyclohexene primary sulfamate **135** (49% inhibition at 1 mM) was more potent than its tertiary sulfamate counterpart (<5% inhibition at 1 mM) supporting the superiority of the non-alkylated primary sulfamate group.

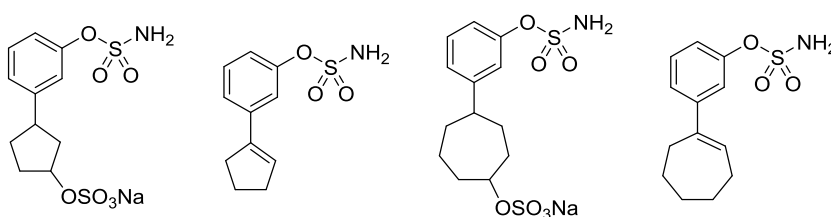
The *trans*-4-cyclohexylsulfate **92** (35% inhibition at 1 mM) was more potent than both the *cis*-isomer and the unsubstituted alcohol precursor.



Due to difficulties in the scale-up of production of pure Sulf2 enzyme, the project was down-prioritized and the studies aiming at the identification of tool molecules are currently on hold. Nonetheless, the synthesis of the 2- and 3-cyclohexene isomers of **135** would be required to investigate the preferred position of unsaturation. Further elaboration of the alkene of **135** would be desirable (*e.g.* dihydroxylation, epoxidation).



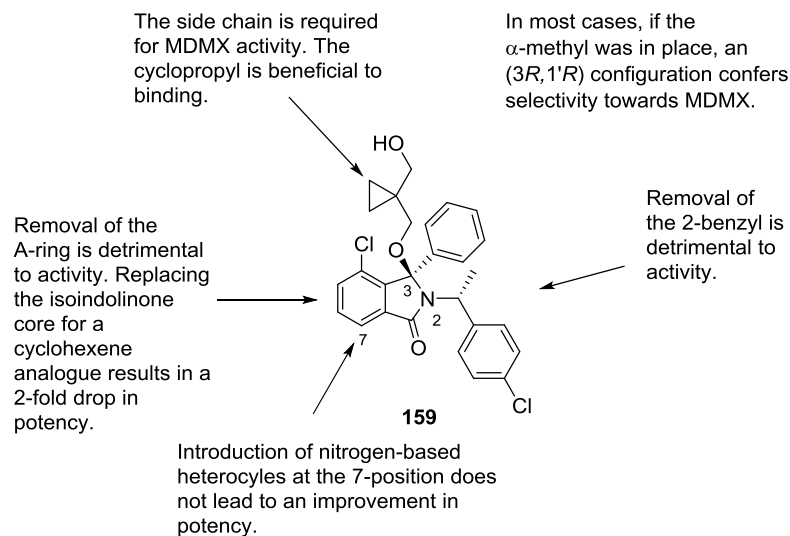
Also, different sizes of the B-ring could be explored, either in conjunction with the double bond or with the sulfate group. In the light of the results obtained by Tristan Reuillon, the introduction of an ether linkage as a spacer between the A- and B-rings would be worth investigating to generate more potent compounds.



8.2 The MDMX:p53 protein-protein interaction project

One of the most common ways adopted by cancer cells to evade apoptosis is to subvert the p53 pathway. When wild-type p53 is retained, this subversion is achieved through either amplification or overexpression of the two negative regulators MDM2 and MDMX. Although a number of candidates have reached the clinic as modulators of the MDM2:p53 protein-protein interaction, *in vitro* and *in vivo* studies indicate that in some cell-lines (low MDM2, high MDMX cellular levels) MDMX provides a mechanism of resistance to MDM2:p53 inhibitors, thus raising interest in the search for MDMX:p53-selective or dual MDM2/MDMX:p53 inhibitors. Despite the effort, only one series has been reported, which showed potencies in the low nanomolar range, although these results were not replicated by the in-house ELISA. Following the low micromolar activity measured with ELISA against MDMX:p53 for isoindolinone **153** ($IC_{50} = 16.7 \mu M$), a series of 2-(α -methyl)benzylisoindolinones was investigated. Serial deletion of the chloro- substituents and analysis of the pure diastereoisomers led to the identification of **159**, a selective low micromolar MDMX inhibitor (MDMX $IC_{50} = 25.9 \mu M$; MDM2 $IC_{50} = 180 \mu M$), with (3*R*,1'*R*)

configuration and lacking the 4-chloro-substituent at the 3-phenyl group. **159** was chosen as the benchmark compound for further SAR studies.

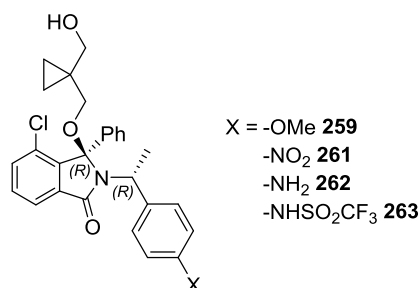


A structural minimization approach was used, with removal or simplification of the 2-benzyl substituent, the side chain at the 3-position or the isoindolinone core. Each one of the three elements examined proved to be necessary for binding, but the SAR confirmed that, for almost all compounds, the (3*R*,1'*R*) configuration at the stereocenters confers selectivity towards MDMX versus MDM2.

A panel of 7-substituted isoindolinones bearing nitrogen-based heterocycles was synthesized, ultimately resulting in potency to be either retained or slightly decreased (up to 2-fold). For 7-substituted compounds, the *R* and *S* configurations at the 3-stereocenter were almost equipotent against MDMX; only in the case of the 3-pyrazole **303**, was MDM2-selectivity observed with an (3*R*,1'*R*) configuration.

By analogy with the most potent compound in the isoindolinone series against MDMX, a 5-hydroxyisoxazole moiety was introduced at the free end of the side chain of **159** after a new reliable route to the ether linkage was devised. Unfortunately, the resulting compound **164** could not be tested by ELISA to compare the activities.

To investigate the Leu26 binding pocket, variations at the 4-benzyl position were introduced by replacement of the chloro- substituent with a methoxy- (**259**), nitro- (**261**), amino- (**262**) or trifluoromethylsulfonamide (**263**) group. Again, the compounds were not tested.



To understand the reasons behind the apparent difficulties in obtaining sub-micromolar IC₅₀ values against MDMX with the isoindolinone scaffold, crystallization trials were set up with both proteins. These trials used different constructs, two commercial screens (the AmSO4 Suite and JCSG+ screen) and six isoindolinones with suitable potency against MDMX (preferably < 35 μM) and in a range of clogD values. None of the trials with the MDMX constructs gave a co-crystal structure, but the complex formed by MDM2^{K51A}₁₇₋₁₂₅ with **159** resulted in a 2.5 Å-resolution structure revealing a peculiar mode of binding. The (3*R*,1'*R*) configuration forces the 2-benzyl out of the Leu26 binding pocket and makes it likely to induce an ordered structure of the *N*-terminal region of MDM2, which contains residues from the GST-tag used for protein purification. The isoindolinone core is shifted outwards and leads to sub-optimal occupation of the Phe19 and Trp23 binding pockets. This mode of binding may be adopted by **159** bound to MDMX and may lead to the formation of a stabilizing interaction with either the protein surface or *N*-terminal residues that would justify the selectivity observed towards this target. In light of these results, further investigation of the substitution pattern on the benzyl ring would be highly desirable.

The validation of a new assay format (HTRF) was attempted using a selection of isoindolinones, but results were only obtained for compounds with clogD < 3.3, highlighting solubility issues in the assay conditions.

A library of isoindolinones, including all the compounds whose synthesis has been described herein, was screened against three MDMX constructs using differential scanning fluorimetry to measure the thermal shift induced. Only the soluble carboxylic acids **308** and **310** significantly stabilized the protein ($\Delta T_m \geq 1$ °C) while **305** and **306** showed a moderate stabilizing effect. The remaining compounds, including the potent 5-hydroxyisoxazole **148** and the selective **159**, destabilized the protein upon binding.

Due to the lack of progress in achieving sub-micromolar potency against the target, the difficulties in obtaining structural data of isoindolinones bound to MDMX and the lack of a suitable assay to measure the activity against the target protein-protein interaction, the project was discontinued.

CHAPTER 9. EXPERIMENTAL

9.1 Summary of generic synthetic, analytical and chromatographic conditions

9.1.1 Chemicals and solvents

All commercial reagents were purchased from Acros, Alfa-Aesar, Avocado, BDH, Fluka, Lancaster, Sigma-Aldrich or Strem Chemicals at a degree of purity higher than 95%, unless otherwise stated. Anhydrous solvents were purchased from Sigma-Aldrich or Acros Organics. The solvents were enclosed in SureSeal™ or AcroSeal™ bottles and were handled under dry nitrogen whenever required. Microwave-assisted reactions were performed in a Biotage Initiator Sixty apparatus.

9.1.2 Synthesis

All water- and/or oxygen-sensitive reactions were carried out under strict anhydrous conditions with oven-dried glassware cooled under nitrogen. Metal catalyzed reactions were degassed by bubbling nitrogen through the reaction mixture prior to addition of the catalyst.

Microwave assisted synthesis was performed using an Initiator Sixty Biotage apparatus. Hydrogenation reactions were carried out using a Thales H-cube® continuous-flow hydrogenation reactor.

Thiol-functionalized polymer cartridges (Agilent Thiol MP SPE) were used to remove all traces of palladium-based catalysts.

The risk of each reaction was assessed in agreement with Newcastle University guidelines and a Control of Substances Hazardous to Health (COSHH) form was completed before performing any new reaction.

9.1.3 Chromatography

Thin Layer Chromatography (TLC) monitoring of reactions was performed using Merck silica gel-coated (Silica Gel 60 F₂₅₄, Silica Gel 60 RP-18 F₂₅₄S or NH₂F₂₅₄S) plates aluminium-backed. Compounds were visualized by UV light (254 and 298 nm) or by use of potassium permanganate or 2,4-

dinitrophenylhydrazine stains, as stated for each compound. LC-MS analyses were performed on a Waters Acquity UPLC system with PDA, and ELSD coupled with a Waters SQD with ESCi source in ES mode equipped with an Acquity UPLC BEH C18 column (17 μ m, 2.1 \times 50 mm) as the stationary phase. The samples were eluted using either a 2.0 or a 2.5 min gradient with a flow rate of 0.6 mL/min, and the mobile phase was 0.1% v/v formic acid (aq.)/MeCN.

All purifications were accomplished by medium pressure liquid chromatography (MPLC) using either a Biotage SP4 or a Varian 971-FP automated system, and the progress of the purification was followed by UV detection (collection wavelength: 254 nm). Varian silica pre-packed (Si50 or SF) cartridges were used, respectively, for normal phase and reverse phase purification. When semi-preparative HPLC was required, compounds were purified on Agilent 1200 Modular Preparative HPLC system using an ACE 5 Phenyl 150 \times 21.2 mm column.

Purities of compounds were measured by analytical HPLC using either Waters XTerra RP18 5 μ M, 150 \times 4.6 mm or Waters Xselect CSH C18 3.5 μ M, 4.6 \times 100 mm with a flow rate of 1 mL/min using up to three eluents (0.1% formic acid/MeCN, 0.1% ammonia/MeCN or water/MeCN). For bioassay, purities >95% were required. In some cases a discrepancy between acidic and basic eluents was ascribed to *e.g.* oxidative degradation or decomposition of the primary sulfamate moiety.

9.1.4 Analytical techniques

All melting points were measured with a Stuart Automatic Melting Point Apparatus Model SMP40 and are uncorrected. UV spectra were determined in ethanolic solution on a Hitachi U-2800A spectrophotometer (400 to 200 nm); unless reported, the extinction coefficient ϵ was not measured. Optical rotations were determined on an Optical Activity PolAAR 3001 polarimeter with a path length of 0.25 dm. $[\alpha]_D$ values are given in 10⁻¹ deg cm² g⁻¹. FTIR spectra were recorded as neat samples using a Bio-Rad FTS 3000MX diamond ATR or an Agilent Cary 630 FTIR. ¹H, ¹³C and ¹⁹F nuclear magnetic resonance (NMR) spectra were obtained using a Bruker Avance III 500 spectrometer (operating

at 500 MHz, 125 MHz and 75 MHz, respectively) using CDCl₃, DMSO-*d*₆ or CD₃OD as the solvent. Chemical shifts (δ) are reported in parts per million (ppm) and coupling constants (*J*) in Hertz. Homonuclear and heteronuclear two-dimensional NMR experiments were used where appropriate to facilitate assignment of chemical shifts. HR-MS spectra were determined by the ESPRC National Mass Spectrometry Service, University of Wales Swansea, Singleton Park, Swansea, SA2 8PP, using a Thermofisher LTQ Orbitrap XL coupled to an Advion TriVersa NanoMate or a Thermofisher DSQ-II coupled to a Trace GC Ultra gas chromatograph with Tri-plus auto-sampler and generating a list of possible elemental formulae. Data were compared with literature data for compounds which had been previously reported.

Measurements of pH values were carried out at room temperature using a SevenEasy pH Mettler Toledo pH-meter equipped with a InLab® Expert Pro pH combination electrode (reference system: ARGENTHAL™; reference electrolyte: XEROLYT® Polymer).

9.2 SULF2 project experimental procedures

9.2.1 Sulfatase Biological Assay Protocols

The sulfatase biological assays were performed by Dr Gary Beale and Dr Sari Alhasan (Northern Institute for Cancer Research, Paul O’Gorman Building, Framlington Place, Newcastle upon Tyne, Tyne and Wear NE2 4AD).

Sulf-2 assay protocol

Compounds were screened using 4-MUS as a substrate for Sulf-2 according to a protocol described by Morimoto-Tomita *et al.*³⁹ Briefly, 293T cells were transiently transfected with pcDNA3.1/Myc-His(-)-HSulf-2 DNA (Addgene) and TransIT-LT1 Transfection Reagent (Mirus) using a transfection mixture at the ratio 1:3 (μ g DNA: μ L transfection reagent) in Opti-MEM I reduced serum medium (Gibco). Conditioned medium containing Sulf-2 was collected after 3 days and bound to HIS-Select Nickel affinity gel (Sigma) overnight at 4 °C. Beads were washed three times with washing buffer containing 50 mM HEPES (pH 7.5), 300 mM NaCl, 0.05% Tween 20, followed by washing once with washing

buffer containing no Tween. Beads were suspended in 50 mM Hepes (pH 7.5) and used in inhibition assays. 20 μ L of bead slurry was incubated with 1 mM compound (in DMSO) plus 10X reaction buffer (500 mM HEPES pH 7.5, 100 mM CaCl₂) for 1 h at 37 °C. The reaction was started by the addition of 20 μ L of 20 mM 4-MUS (final concentration of 8 mM) and incubated at 37 °C for 1 h. The reaction was stopped with 100 μ L 1 M Tris buffer (pH 10.4) and read at 460 nm following excitation at 355 nm in FLUOstar Omega plate reader (BMG Labtech) using Omega data analysis software.

ARSA and ARSB assay protocols

Compounds were screened in a 96-well black plate (Sterilin) using 4-MUS as a substrate, using 50 μ L reaction mixture containing 40 ng of the commercially available enzymes (ARSA or ARSB from R & D Systems), 50 mM HEPES (pH = 4.5), 10 mM CaCl₂, 1 mM test compound (dissolved in DMSO; final concentration of DMSO in reaction = 2%), and H₂O (45 μ L). The assay mixture was incubated for 1 h at 37 °C, followed by addition of 5 μ L of 4-MUS (K_m = 1.6 mM for ARSA and 612 μ M for ARSB), and incubation for a further 1 h at 37 °C. The reaction was stopped with 100 μ L of 1 M Tris (pH = 10.5) and read at 460 nm following excitation at 355 nm in FLUOstar Omega plate reader (BMG Labtech) using Omega data analysis software.

9.2.2 General synthetic procedures

General procedure A - Synthesis of *N,N*-dimethylsulfamates from phenols

A mixture of the phenol (1.5 equiv.) and Cs₂CO₃ (1.7 equiv.) in dry acetonitrile (3 mL per mmol of phenol) was stirred at room temperature for 1 h. A solution of *N,N*-dimethylsulfamoyl chloride (1.0 equiv.) in dry acetonitrile (1.1 mL/mmol) was added dropwise to the mixture at 0 °C under nitrogen atmosphere. After complete conversion, the reaction mixture was filtered over Celite and the solvent was removed *in vacuo*. The residue was dissolved in diethyl ether, washed with water, and the aqueous layer was extracted twice with Et₂O. The combined organic phases were dried (MgSO₄), filtered and evaporated. The crude product was purified by MPLC on C18 reversed phase

SiO₂ with gradient elution, 20-80% acetonitrile/water, formic acid 0.1%, unless otherwise stated.

General procedure B - Suzuki-Miyaura cross-coupling of *N,N*-dimethyl 3-bromophenyl sulfamates with boronic acids⁷²

A 2.0 M aqueous solution of sodium carbonate (2.0 equiv.) was added to a solution of the sulfamate (1.0 equiv.) in 1,2-dimethoxyethane (4.0 mL/mmol), and the mixture was stirred and nitrogen was bubbled through it. The boronic acid (1.0 equiv.) and tetrakis(triphenylphosphine)palladium (0.05 equiv.) were added in one portion under an inert atmosphere. The mixture was heated at reflux overnight. Upon completion of the reaction, the solvent was removed *in vacuo*, water was added and the product was extracted with ethyl acetate. The combined organic layers were dried (MgSO₄), filtered, and evaporated. The crude product was purified by MPLC as described for each compound.

General procedure C - Acetylation of anilino-phenylsulfamates⁸⁰

The aniline was dissolved in dichloromethane (2.8 mL/mmol) under an inert atmosphere, and acetic anhydride (1.2 equiv.) was added. The solution was stirred overnight at RT before being diluted with DCM, and washed with a saturated aqueous NaHCO₃ solution. The aqueous layer was extracted with DCM; the combined organic phases were dried (MgSO₄), filtered and the solvent was removed *in vacuo*. Purification was performed by MPLC (gradient elution, 0-100% EtOAc/petrol) to obtain the desired compounds.

General procedure D - Preparation of sodium sulfate salts⁷⁹

Method 1 - Under an inert atmosphere, the aniline or phenol was dissolved in DMF (18 mL/mmol) and sulfur trioxide pyridine complex (3.0 equiv.) was added in one portion. The resulting solution was stirred at RT for 45 min. NaOH (2 M aq., 20 equiv.) was added, and the solution was stirred for 1.5 h. The solvent was removed under high vacuum, and the residue was dissolved in methanol and filtered through Celite. The crude product was purified by MPLC as described for each compound.

Method 2 - The alcohol (1.0 equiv.) was dissolved in DMF (2.7 mL/mmol) and $\text{SO}_3 \cdot \text{pyridine}$ complex (2.0 equiv.) was added in one portion. The solution was stirred at RT for 1 h before removing the solvent *in vacuo*. The residue was dissolved in Milli-Q[®] water and charged on an ion exchange column (Dowex 50WX2/ Na^+ form; pH adjusted to 7-8 by Milli-Q[®] flushing). The crude product was purified by MPLC (gradient elution, 0-10% MeOH/EtOAc) to yield the desired compounds.

General procedure E - Microwave-assisted Suzuki-Miyaura cross-coupling

Under an inert atmosphere, the appropriate boronic acid or ester (1.0 equiv.) was added to a solution of the *N,N*-dimethyl 3-bromophenylsulfamate (1.0 equiv.) in DME (2.8 mL/mmol). Following addition of Na_2CO_3 (2 M aq., 2 equiv.) and [1,1'-bis(diphenylphosphino)ferrocene]dichloropalladium(II) DCM complex (0.05 equiv.), the reaction mixture was heated under microwave irradiation at 80 °C for 10-20 min.

General procedure F - Ketone deprotection

A solution of the acetal (1.0 equiv.) was dissolved in a mixture of THF (7 mL/mmol), water (21mL/mmol) and acetic acid (43 mL/mmol). The solution was stirred for 4.5 hours at 40 °C. After removal of the solvents *in vacuo*, the residue was dissolved in EtOAc (40 mL) and washed with sat. aq. NaHCO_3 (40 mL). The aqueous layer was extracted with EtOAc (2 × 40 mL); the combined organic layers were washed with brine, dried (MgSO_4), filtered and evaporated. If required, the crude product was purified by MPLC as specified for each compound.

General procedure G - Sulfamate deprotection^{79,93}

The appropriate protected sulfamate (1.0 equiv.) was dissolved in a 10% (v/v) solution of TFA in DCM (10 mL/mmol). The reaction mixture was stirred at RT until complete conversion was reached. The solvent was removed *in vacuo* and the residue was dissolved in EtOAc (20 mL) and washed with aq. NaHCO_3 (10% v/v, 10 mL). The aqueous layer was extracted with EtOAc (2 × 20

mL); the combined organic layers were dried (MgSO₄), filtered, and evaporated. The crude product was purified by MPLC as described for each compound.

General procedure H - Synthesis of vinyl triflate from a ketone

A solution of KHMDS in toluene (0.5 M, 1.3 equiv.) was added dropwise to a solution of the appropriate ketone (1.0 equiv.) at -78 °C and *N*-phenyl bis(trifluoromethanesulfonamide) (1.3 equiv.) in THF (10 mL/mmol) and the resulting mixture was stirred for 3 h. Water (40 mL) was added and the product was extracted with Et₂O (3 × 40 mL). The combined organic layers were washed with aq. Na₂CO₃ (10% v/v, 40 mL) and brine (40 mL), dried (MgSO₄), filtered and evaporated. The crude product was purified by MPLC using the conditions as described below for each compound.

General procedure I - Miyaura borylation

Under an inert atmosphere, bis(pinacolato)diboron (1.2 equiv.), Pd(dppf)Cl₂ · DCM (0.03 equiv.), and potassium acetate (3.0 equiv.) were added to a solution of the vinyl triflate/halide (1.0 equiv.) in 1,4-dioxane (5.0 mL/mmol). The reaction mixture was heated at 80 °C overnight. Upon completion of the reaction, water (20 mL) was added and the product was extracted with EtOAc (3 × 30 mL). The combined organic layers were washed with brine, dried (MgSO₄), filtered and the solvent was removed *in vacuo*. The residue was dissolved in ethyl acetate and filtered through a Thiol MP SPE cartridge. The crude product was purified by MPLC according to the conditions described below.

Procedure for assessment of stability by HPLC analysis

Anhydrous basic conditions

NaBH₄ (3 mg, 79 μmol) was added to 4-(trifluoromethyl)phenyl dimethylsulfamate **51** (5 mg, 19 μmol) in EtOH (0.5 mL) and the resulting solution was stirred at RT. After 2, 24, and 96 h a sample was taken, diluted with MeOH (0.75 mL) and assayed by HPLC.

Aqueous basic conditions

NaOH (2 M aq., 0.5 mL, 1 mmol) was added to 4-(trifluoromethyl)phenyl dimethylsulfamate **51** (5 mg, 19 μ mol) in EtOH (0.5 mL) and the resulting solution was stirred at RT. After 2, 24, and 96 h a sample was taken, diluted with MeOH (0.75 mL) and assayed by HPLC.

Reductive conditions

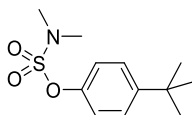
NaH (60% dispersion in mineral oil, 3 mg, 75 μ mol) was added to 4-(trifluoromethyl)phenyl dimethylsulfamate **51** (5 mg, 19 μ mol) in THF (0.5 mL) and the resulting solution was stirred at RT. After 2, 24, and 96 h a sample was taken, diluted with MeOH (0.75 mL) and assayed by HPLC.

Anhydrous acidic conditions

TFA (0.5 mL, 2.9 mmol) was added to 4-(trifluoromethyl)phenyl dimethylsulfamate **51** (5 mg, 19 μ mol) and the resulting solution was stirred at RT. After 2, 24 and 72 h a sample was taken, diluted with MeOH (0.75 mL) and assayed by HPLC. The sample taken at 72 h was filtered before HPLC analysis due to the formation of a precipitate.

9.2.3 SULF2 project - Synthesized compounds

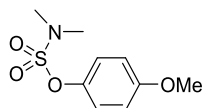
4-(*tert*-Butyl)phenyl dimethylsulfamate (41)



4-*t*-Butylphenol (100 mg, 0.67 mmol) was dissolved in acetonitrile (2.0 mL) under an inert atmosphere and a solution of *N,N*-dimethylsulfamoyl chloride (143 mg, 0.11 mL, 1.0 mmol) in acetonitrile (0.5 mL) was added dropwise at 0 °C followed by addition of potassium carbonate (143 mg, 1.0 mmol) in one portion. The reaction mixture was allowed to reach ambient temperature and stirred for 5.5 h. Water (3.0 mL) was added to quench the unreacted sulfamoyl chloride and the mixture was stirred at ambient temperature overnight. After addition of brine (3.0 mL), the mixture was neutralized by addition of HCl (aq., 1 M), diluted with water and extracted with ethyl acetate (3 \times 25 mL). The combined organic layers were dried over MgSO₄, filtered and the solvent was

removed *in vacuo* to afford the desired sulfamate **41** as a white solid without further purification (41 mg, 24%). R_f 0.30 (50% MeCN (0.1% formic acid)/H₂O); m.p. 77.2-78.2 °C; λ_{\max} (EtOH)/nm 261; $\nu_{\max}/\text{cm}^{-1}$ (neat) 1148 and 1176 (s, SO₂^{sy}), 1198 (m, C-O), 1356 (s, SO₂^{as}), 2871, 2926 and 2956 (w, aliphatic C-H stretching, *t*-Bu); ¹H NMR (500 MHz; CDCl₃) δ_H 1.31 (9H, s, C(CH₃)₃), 2.97 (6H, s, 2 × N-CH₃), 7.18-7.21 (2H, m, H-2 and H-6), 7.37-7.40 (2H, m, H-3 and H-5); ¹³C NMR (125 MHz; CDCl₃) δ_C 31.5 (3 × C-CH₃), 34.7 (C-CH₃), 38.9 (2 × N-CH₃), 121.3 (C-2 and C-6), 126.8 (C-3 and C-5), 148.0 (C-4), 149.9 (C-1); LRMS (ES⁺) m/z 258.2 [M+H]⁺; HRMS calcd for C₁₂H₂₀NO₃S [M+H]⁺ 258.1158, found 258.1163; HPLC 97.9% in 0.1% formic acid (aq.)/MeCN (R_t 12.9 min); 97.9% in 0.1% ammonia (aq.)/MeCN (R_t 12.9 min).

4-Methoxyphenyl dimethylsulfamate (42)

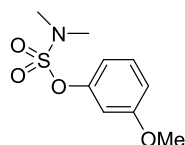


4-Methoxyphenol (100 mg, 0.81 mmol) was dissolved in acetonitrile (2.4 mL) and potassium carbonate (167 mg, 1.21 mmol) was added. The mixture was stirred for 1 h at ambient temperature (18-20 °C). A solution of *N,N*-dimethylsulfamoyl chloride (77 mg, 0.06 mL, 0.54 mmol) in acetonitrile (0.26 mL) was added dropwise to the mixture at 0 °C. The system was allowed to reach ambient temperature and was stirred for 19 h. The mixture was filtered through Celite and acetonitrile was removed *in vacuo*. The residue was dissolved in diethyl ether and washed with water. The aqueous layer was extracted with diethyl ether (30 mL) and with DCM (30 mL). The combined organic phases were dried (MgSO₄), filtered and evaporated. Purification by MPLC (C18 reversed phase SiO₂ with gradient elution, 20-80% acetonitrile/water, formic acid 0.1%) yielded the title compound **42** as a yellow oil (92 mg, 74%). R_f 0.34 (50% MeCN (0.1% formic acid)/H₂O); λ_{\max} (EtOH)/nm 276; $\nu_{\max}/\text{cm}^{-1}$ (neat) 1147 and 1164 (s, SO₂^{sy}), 1193 (m, C-O), 1249 (m, C-O-C^{as}), 1364 (s, SO₂^{as}), 1501 (s, C=C ring stretch); ¹H NMR (500 MHz; CDCl₃) δ_H 2.96 (6H, s, 2 × N-CH₃), 3.80 (3H, s, OCH₃), 6.86-6.90 (2H, m, H-2 and H-6), 7.18-7.26 (2H, m, H-3 and H-5); ¹³C NMR (125 MHz; CDCl₃) δ_C 38.8 (2 × N-CH₃), 55.7

(O-CH₃), 114.8 (C-2 and C-6), 123.0 (C-3 and C-5), 143.7 (C-4), 158.2 (C-1); LRMS (ES⁺) *m/z* 232.1 [M+H]⁺; HRMS calcd for C₉H₁₄O₄NS [M+H]⁺ 232.0638, found 232.0640; HPLC 96.9% in 0.1% formic acid (aq.)/MeCN (*R*_t 10.7 min); 96.2% in 0.1% ammonia (aq.)/MeCN (*R*_t 10.7 min).

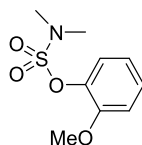
NMR data match those previously reported for this compound.⁷⁰

3-Methoxyphenyl dimethylsulfamate (43)



The sulfamate **43** was synthesized and purified as described in general procedure A, using 3-methoxyphenol (200 mg, 0.161 mmol.), cesium carbonate (578 mg, 1.77 mmol), *N,N*-dimethylsulfamoyl chloride (154 mg, 0.12 mL, 1.07 mmol) and acetonitrile (5.0 and 1.2 mL). The desired compound was obtained as a colorless oil (157 mg, 64%). *R*_f 0.29 (50% MeCN (0.1% formic acid)/H₂O); λ_{max} (EtOH)/nm 271, 276; ν_{max}/cm⁻¹ (neat) 1119 (s, SO₂^{sy}), 1175 (s, C-O), 1261 and 1285 (m, C-O-C^{as}), 1365 (s, SO₂^{as}), 1607 and 1588 (m, C=C ring stretch); ¹H NMR (500 MHz; CDCl₃) δ_H 2.90 (6H, s, 2 × N-CH₃), 3.74 (3H, s, OCH₃), 6.84 (1H, ddd, *J* = 0.8, 2.4, 8.1 Hz, *H*-6), 6.86 (1H, app. t, *J* = 2.4 Hz, *H*-2), 6.89 (1H, ddd, *J* = 0.8, 2.4, 8.1 Hz, *H*-4), 7.30 (1H, t, *J* = 8.1 Hz, *H*-5); ¹³C NMR (125 MHz; CDCl₃) δ_C 38.9 (2 × N-CH₃), 55.7 (OCH₃), 107.8 (C-2), 112.7 (C-6), 113.8 (C-4), 130.2 (C-5), 151.3 (C-1), 160.8 (C-3); LRMS (ES⁺) *m/z* 232.2 [M+H]⁺; HRMS calcd for C₉H₁₄O₄NS [M+H]⁺ 232.0638, found 232.0640; HPLC 99.3% in 0.1% formic acid (aq.)/MeCN (*R*_t 10.9 min); 99.4% in 0.1% ammonia (aq.)/MeCN (*R*_t 10.8 min).

2-Methoxyphenyl dimethylsulfamate (44)

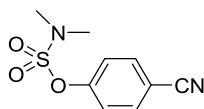


General procedure A was followed to synthesize and purify compound **44**, using 2-methoxyphenol (200 mg, 0.161 mmol), cesium carbonate (578 mg, 1.77 mmol), *N,N*-dimethylsulfamoyl chloride (154 mg, 0.12 mL, 1.07 mmol) and acetonitrile (5.0 and 1.2 mL). The desired sulfamate was obtained as a white

solid (108 mg, 43%). R_f 0.30 (50% MeCN (0.1% formic acid)/H₂O); m.p. 45.0-45.6 °C (lit.¹⁹³ 38-42 °C); λ_{max} (EtOH)/nm 271; ν_{max}/cm^{-1} (neat) 1109 (s, SO₂^{sy}), 1147 (s, C-O), 1281 (s, C-O-C^{as}), 1370 (s, SO₂^{as}), 1580 and 1602 (w, C=C ring stretch); ¹H NMR (500 MHz; CDCl₃) δ_H 2.97 (6H, s, 2 × N-CH₃), 3.89 (3H, s, OCH₃), 6.95 (1H, m, *H*-5), 6.98 (1H, dd, *J* = 1.6 and 8.0 Hz, *H*-3), 7.22 (1H, ddd, *J* = 1.6, 7.7, 8.0 Hz, *H*-4), 7.36 (1H, dd, *J* = 1.6 and 8.0 Hz, *H*-6); ¹³C NMR (125 MHz; CDCl₃) δ_C 38.8 (2 × N-CH₃), 56.1 (OCH₃), 113.0 (*C*-3), 121.1 (*C*-5), 123.9 (*C*-6), 127.7 (*C*-4), 139.5 (*C*-2), 151.7 (*C*-1); LRMS (ES⁺) *m/z* 232.2 [M+H]⁺; HRMS calcd for C₉H₁₄O₄NS [M+H]⁺ 232.0638, found 232.0640; HPLC 99.5% in 0.1% formic acid (aq.)/MeCN (R_t 10.6 min); 99.7% in 0.1% ammonia (aq.)/MeCN (R_t 10.5 min).

NMR data match those previously reported for this compound.⁷⁰

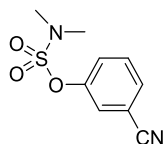
4-Cyanophenyl dimethylsulfamate (45)



Acetonitrile (2.5 mL) was added to 4-cyanophenol (96 mg, 0.806 mmol) and cesium carbonate (289 mg, 0.887 mmol) and the resulting mixture was stirred at RT for 1 h before adding a solution of *N,N*-dimethylsulfamoyl chloride (77 mg, 0.06 mL, 0.537 mmol) in acetonitrile (0.6 mL) pre-cooled to 0 °C under an inert atmosphere. The mixture was allowed to reach ambient temperature and was stirred overnight. The temperature was maintained at RT for 24 h before addition of further sulfamoyl chloride (0.03 mL in 0.3 mL acetonitrile) and stirring overnight. Additional phenolate (1.7 equiv. of phenol and 2.4 equiv. of base in 2.6 mL acetonitrile) was added in two portions to the reaction mixture at 0 °C in order to react with the excess sulfamoyl chloride. The mixture was stirred at RT and then at 30 °C for 36 h before filtering through Celite. The filtrate was evaporated and the residual oil was dissolved in diethyl ether. The ethereal solution was washed with water. The aqueous layer was extracted twice with Et₂O, the combined organic phases were dried (MgSO₄), filtered and the solvent was removed *in vacuo*. The crude product was purified by MPLC

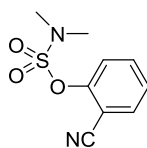
yielding the title compound as a light blue solid (129 mg, 71%). R_f 0.40 (50% MeCN (0.1% formic acid)/H₂O); m.p. 74.2-75.4 °C; λ_{max} (EtOH)/nm 232; ν_{max}/cm^{-1} (neat) 1150 and 1173 (s, SO₂^{sy}), 1199 (s, C-O), 1363 (s, SO₂^{as}), 2237 (m, C≡N); ¹H NMR (500 MHz; CDCl₃) δ_H 3.03 (6H, s, 2 × N-CH₃), 7.39-7.44 (2H, m, H-2 and H-6), 7.70-7.75 (2H, m, H-3 and H-5); ¹³C NMR (125 MHz; CDCl₃) δ_C 38.9 (2 × N-CH₃), 110.7 (-CN), 118.0 (C-4), 122.5 (C-2 and C-6), 134.2 (C-3 and C-6), 153.6 (C-1); LRMS (ES⁺) m/z 268.2 [M + MeCN + H]⁺; HRMS calcd for C₉H₁₀N₂O₃S [M+H]⁺ 226.0407, found 226.0407; HPLC >99.9% in 0.1% formic acid (aq.)/MeCN (R_t 10.4 min); >99.9% in 0.1% ammonia (aq.)/MeCN (R_t 10.3 min).

3-Cyanophenyl dimethylsulfamate (46)



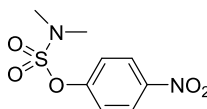
General procedure A was followed to synthesize and purify compound **46**, using 3-cyanophenol (192 mg, 0.161 mmol), cesium carbonate (578 mg, 1.77 mmol), *N,N*-dimethylsulfamoyl chloride (154 mg, 0.12 mL, 1.07 mmol) and acetonitrile (5.0 and 1.2 mL). The desired sulfamate was obtained as an oil (142 mg, 58%). R_f 0.31 (50% MeCN (0.1% formic acid)/H₂O); λ_{max} (EtOH)/nm 221, 274; ν_{max}/cm^{-1} (neat) 1171 (s, SO₂^{sy}), 1224 (m, C-O), 1361 (s, SO₂^{as}), 2235 (w, C≡N); ¹H NMR (500 MHz; CDCl₃) δ_H 3.37 (6H, s, 2 × N-CH₃), 7.82-7.95 (4H, m, H-Ar); ¹H NMR (500 MHz; DMSO-*d*₆) δ_H 2.93 (6 H, s, 2 × N-CH₃), 7.67-7.73 (2H, m, H-Ar), 7.83-7.87 (1H, m, H-Ar), 7.88-7.89 (1H, m, H-Ar); ¹³C NMR (125 MHz; CDCl₃) δ_C 38.9 (2 × N-CH₃), 114.1 (-CN), 117.6 (C-3), 125.5 (C-Ar), 126.7 (C-Ar), 130.4 (C-Ar), 131.0 (C-Ar), 150.5 (C-1); LRMS (ES⁺) m/z 268.1 [M + MeCN + H]⁺; HRMS calcd for C₉H₁₄N₃O₃S [M+NH₄]⁺ 244.0570, found 244.0573; HPLC >99.9% in 0.1% formic acid (aq.)/MeCN (R_t 10.4 min); >99.9% in 0.1% ammonia (aq.)/MeCN (R_t 10.4 min).

2-Cyanophenyl dimethylsulfamate (47)



The sulfamate **47** was synthesized and purified as described in general procedure A, using 2-cyanophenol (192 mg, 0.161 mmol), cesium carbonate (578 mg, 1.77 mmol), *N,N*-dimethylsulfamoyl chloride (154 mg, 0.12 mL, 1.07 mmol) and acetonitrile (5.0 and 1.2 mL). The title compound was obtained as colorless crystals (224 mg, 92%). R_f 0.32 (50% MeCN (0.1% formic acid)/H₂O); m.p. 70.1-71.0 °C (lit.⁷⁴ 70-71 °C); λ_{max} (EtOH)/nm 225, 276; ν_{max}/cm^{-1} (neat) 1164 (s, SO₂^{sy}), 1182 (m, C-O), 1368 (s, SO₂^{as}), 2235 (w, C≡N); ¹H NMR (500 MHz; CDCl₃) δ_H 3.10 (6H, s, 2 × N-CH₃), 7.32-7.39 (1H, m, H-4), 7.55-7.60 (1H, m, H-6), 7.61-7.70 (2H, m, H-5 and H-3); ¹³C NMR (125 MHz; CDCl₃) δ_C 39.1 (2 × N-CH₃), 107.1 (-CN), 115.1 (C-2), 122.7 (C-6), 126.8 (C-4), 133.8 (C-3), 134.6 (C-5), 151.3 (C-1); LRMS (ES⁺) m/z 227.1 [M+H]⁺; HRMS calcd for C₉H₁₄N₃O₃S [M+NH₄]⁺ 244.0570, found 244.0573; HPLC 99.1% in 0.1% formic acid (aq.)/MeCN (R_t 10.4 min); 99.3% in 0.1% ammonia (aq.)/MeCN (R_t 10.4 min).

4-Nitrophenyl dimethylsulfamate (48)

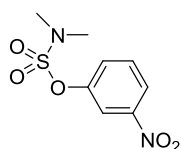


Compound **48** was synthesized and purified according to general procedure A, using 4-nitrophenol (224 mg, 0.161 mmol), cesium carbonate (578 mg, 1.77 mmol) in acetonitrile (5.0 mL) and *N,N*-dimethylsulfamoyl chloride (154 mg, 0.12 mL, 1.07 mmol) in acetonitrile (1.2 mL). The title compound was obtained as pale yellow crystals (129 mg, 49%). R_f 0.27 (50% MeCN (0.1% formic acid)/H₂O); m.p. 122.2-123.9 °C (lit.¹⁹⁴ 124 °C); λ_{max} (EtOH)/nm 267; ν_{max}/cm^{-1} (neat) 1144 (s, C-O), 1172 and 1197 (s, SO₂^{sy}), 1344 (s, SO₂^{as}), 1361 (m, NO^{sy}), 1521 (m, NO^{as}); ¹H NMR (500 MHz; CDCl₃) δ_H 3.04 (6H, s, 2 × N-CH₃), 7.41-7.47 (2H, m, H-2 and H-6), 8.26-8.32 (2H, m, H-3 and H-5); ¹³C NMR (125 MHz; CDCl₃) δ_C 38.9 (2 × CH₃), 122.2 (C-2 and C-6), 125.7 (C-3 and C-5), 155.1 (C-1). One quaternary carbon not detected; LRMS (ES⁺) m/z 247.2 [M+H]⁺; HRMS

calcd for $C_8H_{10}O_5N_2S$ $[M]^+$ 246.0305, found 246.0308; HPLC 98.6% in 0.1% formic acid (aq.)/MeCN (R_t 11.1 min); 98.8% in 0.1% ammonia (aq.)/MeCN (R_t 11.0 min).

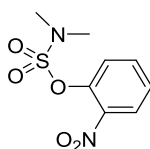
NMR and IR data match those previously reported for this compound.^{76,195}

3-Nitrophenyl dimethylsulfamate (49)



The sulfamate **49** was synthesized as described in general procedure A, using 3-nitrophenol (224 mg, 0.161 mmol), cesium carbonate (578 mg, 1.77 mmol), *N,N*-dimethylsulfamoyl chloride (154 mg, 0.12 mL, 1.07 mmol) and acetonitrile (5.0 and 1.2 mL). The crude product was purified by MPLC (gradient elution, 0-50% DCM/petrol) to yield the desired product as a white solid (297 mg, >99%). R_f 0.26 (50% MeCN (0.1% formic acid)/H₂O); m.p. 84.6-85.2 °C (lit.¹⁹³ 85 °C); λ_{max} (EtOH)/nm 256; ν_{max}/cm^{-1} (neat) 1167 (s, SO₂^{sy}), 1199 (s, C-O), 1352 (s, SO₂^{as}), 1528 (s, N=O^{as}); ¹H NMR (500 MHz; CDCl₃) δ_H 3.05 (6H, s, 2 × N-CH₃), 7.59 (1H, t, J = 8.2 Hz, H-5), 7.65 (1H, ddd, J = 1.0, 2.2 and 8.2 Hz, H-6), 8.12 (1H, t, J = 2.2 Hz, H-2), 8.16 (1H, ddd, J = 1.0, 2.2 and 8.2 Hz, H-4); ¹H NMR (500 MHz; CD₃OD) 3.05 (6H, s, 2 × N-CH₃), 7.71-7.78 (2H, m, H-Ar), 8.16-8.19 (1H, m, H-Ar), 8.21-8.28 (1H, m, H-Ar); ¹³C NMR (125 MHz; CDCl₃) δ_C 38.9 (2 × N-CH₃), 117.5 (C-2), 121.6 (C-4), 128.1 (C-6), 130.6 (C-5), 149.1 (C-Ar), 150.7 (C-Ar); LRMS (ES⁺) m/z 288.1 $[M + MeCN + H]^+$; HRMS calcd for $C_8H_{10}N_2O_5S$ $[M]^+$ 246.0305, found 246.0305; HPLC 97.9% in 0.1% formic acid (aq.)/MeCN (R_t 10.9 min); 97.9% in 0.1% ammonia (aq.)/MeCN (R_t 10.9 min).

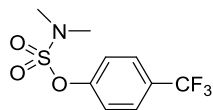
2-Nitrophenyl dimethylsulfamate (50)



General procedure A was followed to synthesize compound **50**, using 2-nitrophenol (224 mg, 0.161 mmol), cesium carbonate (578 mg, 1.77 mmol), *N,N*-dimethylsulfamoyl chloride (154 mg, 0.12 mL, 1.07 mmol) and acetonitrile

(5.0 and 1.2 mL). Purification by MPLC (gradient elution, 0-50% EtOAc/petrol) gave the title product as a yellow oil (250 mg, 94%). R_f 0.32 (50% MeCN (0.1% formic acid)/H₂O); λ_{\max} (EtOH)/nm 251; $\nu_{\max}/\text{cm}^{-1}$ (neat) 1171 (s, SO₂^{sy}), 1207 (m, C-O), 1351 (s, SO₂^{as}), 1523 (s, NO^{as}); ¹H NMR (500 MHz; CDCl₃) δ_H 3.06 (6H, s, 2 × N-CH₃), 7.40 (1H, m, H-Ar), 7.64 (2H, m, H-Ar), 7.97 (1H, m, H-Ar); ¹³C NMR (125 MHz; CDCl₃) δ_C 38.9 (2 × N-CH₃), 124.4 (C-Ar), 125.9 (C-Ar), 126.9 (C-Ar), 134.4 (C-Ar), 142.8 (C-Ar); LRMS (ES⁺) m/z 247.1 [M+H]⁺; HRMS calcd for C₈H₁₁O₅N₂S [M+H]⁺ 247.0390, found 247.0387; HPLC 97.7% in 0.1% formic acid (aq.)/MeCN (R_t 10.7 min); 97.7% in 0.1% ammonia (aq.)/MeCN (R_t 10.7 min).

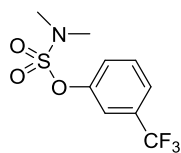
4-(Trifluoromethyl)phenyl dimethylsulfamate (**51**)



General procedure A was used to synthesize and purify compound **51**, using 4-(trifluoromethyl)phenol (261 mg, 0.161 mmol), cesium carbonate (578 mg, 1.77 mmol) in acetonitrile (5.0 mL) and *N,N*-dimethylsulfamoyl chloride (154 mg, 0.12 mL, 1.07 mmol) in acetonitrile (1.2 mL). The desired sulfamate was obtained as a pale yellow solid (95 mg, 33%). R_f 0.19 (50% MeCN (0.1% formic acid)/H₂O); m.p. 38.8-40.9 °C; λ_{\max} (EtOH)/nm 258; $\nu_{\max}/\text{cm}^{-1}$ (neat) 1098 (s, C-O), 1151 (s, SO₂^{sy}), 1319 (s, C-F), 1366 (m, SO₂^{as}); ¹H NMR (500 MHz; CDCl₃) δ_H 3.02 (6 H, s, 2 × N-CH₃), 7.38-7.42 (2 H, m, H-2 and H-6), 7.64-7.71 (2 H, m, H-3 and H-5); ¹⁹F NMR (470 MHz; CDCl₃) δ_F -62.33; ¹³C NMR (125 MHz; CDCl₃) δ_C 38.9 (2 × N-CH₃), 122.1 (C-2 and C-6), 123.8 (q, J = 270.9 Hz, CF₃), 127.3 (q, J = 3.82 Hz, C-3 and C-5), 129.1 (C-4), 152.8 (q, J = 33.1, Hz, C-1); LRMS (ES⁺) m/z 311.2 [M + MeCN + H]⁺; HRMS calcd for C₉H₁₁O₃NF₃S [M+H]⁺ 270.0406, found 270.0400; HPLC 96.1% in 0.1% formic acid (aq.)/MeCN (R_t 12.0 min); 97.3% in 0.1% ammonia (aq.)/MeCN (R_t 12.0 min).

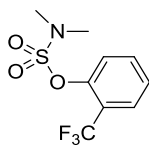
NMR data match those previously reported for this compound.⁷⁰

3-(Trifluoromethyl)phenyl dimethylsulfamate (52)



The sulfamate **52** was synthesized and purified as described in general procedure A, using 3-(trifluoromethyl)phenol (261 mg, 0.161 mmol), cesium carbonate (578 mg, 1.77 mmol), *N,N*-dimethylsulfamoyl chloride (154 mg, 0.12 mL, 1.07 mmol) and acetonitrile (5.0 and 1.2 mL). The desired product was obtained as a colorless oil (136 mg, 47%). R_f 0.15 (50% MeCN (0.1% formic acid)/H₂O); λ_{max} (EtOH)/nm 263; ν_{max}/cm^{-1} (neat) 1085 (m, C-O), 1171 (s, SO₂^{sy}), 1351 (s, C-F), 1363 (s, SO₂^{as}); ¹H NMR (500 MHz; CDCl₃) δ_H 3.02 (6H, s, 2 × N-CH₃), 7.46-7.57 (4H, m, H-Ar); ¹H NMR (500 MHz; DMSO-*d*₆) 2.94 (6H, s, 2 × N-CH₃), 7.75-7.79 (2H, m, H-Ar), 7.71-7.79 (2H, m, H-Ar); ¹H NMR (500 MHz; CD₃OD) 3.02 (6H, s, 2 × N-CH₃), 7.58-7.63 (2H, m, H-Ar), 7.65-7.70 (2H, m, H-Ar); ¹⁹F NMR (470 MHz; CDCl₃) δ_F -62.71; ¹³C NMR (125 MHz; CDCl₃) δ_C 38.9 (2 × NCH₃), 119.1 (q, J = 3.7 Hz, C-Ar), 123.5 (q, J = 272.6 Hz, CF₃), 123.6 (q, J = 3.4 Hz, C-Ar), 125.4 (C-Ar), 130.6 (C-Ar), 132.5 (q, J = 33.0 Hz, C-3), 150.5 (C-1); LRMS (ES⁺) m/z 270.1 [M+H]⁺; HRMS calcd for C₉H₁₀F₃NO₃S [M]⁺ 269.0328, found 269.0324; HPLC 99.4% in 0.1% formic acid (aq.)/MeCN (R_t 11.9 min); 99.8% in 0.1% ammonia (aq.)/MeCN (R_t 11.9 min).

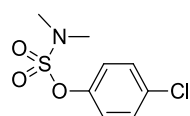
2-(Trifluoromethyl)phenyl dimethylsulfamate (53)



The sulfamate **53** was synthesized and purified as described in general procedure A, using 2-(trifluoromethyl)phenol (261 mg, 0.161 mmol), cesium carbonate (578 mg, 1.77 mmol), *N,N*-dimethylsulfamoyl chloride (154 mg, 0.12 mL, 1.07 mmol) and acetonitrile (5.0 and 1.2 mL). The title compound was obtained as a solid (152 mg, 52%). R_f 0.14 (50% MeCN (0.1% formic acid)/H₂O); m.p. 39.5-40.9 °C; λ_{max} (EtOH)/nm 264; ν_{max}/cm^{-1} (neat) 1111 and 1136 (s, C-O), 1162 (s, SO₂^{sy}), 1317 (s, C-F), 1376 (s, SO₂^{as}); ¹H NMR (500 MHz;

CDCl₃) δ_{H} 3.06 (6H, s, 2 \times N-CH₃), 7.29-7.36 (1H, m, H-Ar), 7.55-7.61 (1H, m, H-Ar), 7.64-7.69 (1H, m, H-Ar), 7.69-7.73 (1H, m, H-Ar); ¹⁹F NMR (470 MHz; CDCl₃) δ_{F} -60.69; ¹³C NMR (125 MHz; CDCl₃) δ_{C} 38.9 (2 \times NCH₃), 121.5 (C-Ar), 123.0 (q, J = 271.7, CF₃), 125.7 (C-Ar), 127.5 (q, J = 5.4 Hz, C-3), 133.7 (C-Ar). Two quaternary carbons were not visible; LRMS (ES⁺) m/z 270.2 [M+H]⁺; HRMS calcd for C₉H₁₀F₃NO₃S [M]⁺ 269.0328, found 269.0328; HPLC 98.1% in 0.1% formic acid (aq.)/MeCN (R_{t} 11.9 min); 99.0% in 0.1% ammonia (aq.)/MeCN (R_{t} 11.9 min).

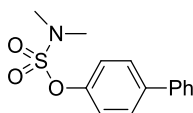
4-Chlorophenyl dimethylsulfamate (54)



Compound **54** was synthesized and purified according to the procedure described for the synthesis of compound **45**, using 4-chlorophenol (104 mg, 0.806 mmol) and cesium carbonate (289 mg, 0.887 mmol) in acetonitrile and *N,N*-dimethylsulfamoyl chloride (77 mg, 0.06 mL, 0.537 mmol), in acetonitrile (0.6 mL) to give the title compound as blue crystals (176 mg, 93%). R_{f} 0.19 (50% MeCN (0.1% formic acid)/H₂O); m.p. 48.1-49.5 °C (lit.¹⁹⁶ 46 °C); λ_{max} (EtOH)/nm 267, 274sh; ν_{max} /cm⁻¹ (neat) 1089 (m, C-Cl), 1146 (s, C-O), 1169 and 1188 (s, SO₂^{sy}), 1357 (s, SO₂^{as}); ¹H NMR (500 MHz; CDCl₃) δ_{H} 2.98 (6H, s, 2 \times N-CH₃), 7.19-7.25 (2H, m, H-2 and H-6), 7.33-7.38 (2H, m, H-3 and H-5); ¹³C NMR (125 MHz; CDCl₃) δ_{C} 38.9 (2 \times N-CH₃), 123.3 (C-2 and C-6), 130.0 (C-3 and C-5), 132.4 (C-4), 148.8 (C-1); LRMS (ES⁺) m/z 236.1 and 238.1 [M+H]⁺; HRMS calcd for C₈H₁₄O₃N₄³⁵ClS [M+NH₄]⁺ 253.0408, found 253.0412; HPLC 99.4% in 0.1% formic acid (aq.)/MeCN (R_{t} 11.7 min); 99.5% in 0.1% ammonia (aq.)/MeCN (R_{t} 11.7 min).

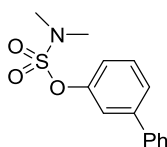
NMR data match those previously reported for this compound.⁷⁶

[1,1'-Biphenyl]-4-yl dimethylsulfamate (55)



Under an inert atmosphere, 4-phenylphenol (137 mg, 0.806 mmol) was dissolved in acetonitrile (2.4 mL) and potassium carbonate (167 mg, 1.21 mmol) was added. The mixture was stirred for 1 h at RT. A solution of *N,N*-dimethylsulfamoyl chloride (77 mg, 0.06 mL, 0.54 mmol) in acetonitrile (0.26 mL) was added dropwise to the mixture at 0 °C. The reaction was allowed to reach ambient temperature and stirred for 19 h. The mixture was filtered through Celite and acetonitrile was removed *in vacuo*. The residue was dissolved in diethyl ether (35 mL) and washed with water (20 mL). The aqueous layer was extracted with DCM (25 mL) and with diethyl ether (2 × 35 mL). The combined organic phases were dried (MgSO₄), filtered and evaporated. The crude product was purified by MPLC (gradient elution, 0-50% EtOAc/petrol) to afford title compound as a white solid (134 mg, 90%). *R*_f 0.17 (50% MeCN (0.1% formic acid)/H₂O); m.p. 110.4-111.8 °C (lit.¹⁹⁷ 105-107 °C); λ_{max} (EtOH)/nm 250; ν_{max}/cm⁻¹ (neat) 1149 (s, C-O), 1174 and 1187 (s, SO₂^{sy}), 1359 (s, SO₂^{as}); ¹H NMR (500 MHz; CDCl₃) δ_H 3.01 (6H, s, 2 × N-CH₃), 7.35-7.39 (3H, m, H-Ar), 7.42-7.47 (2H, m, H-Ar), 7.54-7.58 (2H, m, H-Ar), 7.58-7.63 (2H, m, H-Ar); ¹³C NMR (125 MHz; CDCl₃) δ_C 38.8 (2 × N-CH₃), 122.2 (C-3 and C-5), 127.3 (C-2' and C-6'), 127.7 (C-4'), 128.6 (C-2 and C-6), 129.0 (C-3' and C-5'), 139.9 (C-1 and C-1'), 149.8 (C-4); LRMS (ES⁺) *m/z* 278.2 [M+H]⁺; HRMS calcd for C₁₄H₁₆NO₃S [M+H]⁺ 278.0845, found 278.0850; HPLC 98.5% in 0.1% formic acid (aq.)/MeCN (*R*_t 12.8 min); 98.8% in 0.1% ammonia (aq.)/MeCN (*R*_t 12.8 min).

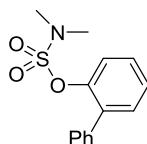
[1,1'-Biphenyl]-3-yl dimethylsulfamate (56)



Procedure 1 -Product **56** was obtained according to general procedure A using 3-phenylphenol (274 mg, 0.161 mmol), cesium carbonate (579 mg, 1.77 mmol), acetonitrile (5.0 mL) and *N,N*-dimethylsulfamoyl chloride (154 mg, 0.12 mL,

1.07 mmol) in acetonitrile (1.2 mL). Following MPLC, the desired product was obtained as a white solid (193 mg, 65%). *Procedure 2* - The biphenyl sulfamate **56** was also obtained following general procedure B, using 3-bromophenyl sulfamate (50 mg, 0.178 mmol), phenylboronic acid (22 mg, 0.178 mmol), sodium carbonate (2 M, aq., 1.0 mL), tetrakis(triphenylphosphine)palladium (10 mg, 8.92 μ mol) and DME (0.7 mL). Purification by MPLC (gradient elution, 0-20% EtOAc/petrol) yielded the desired product as a white solid (41 mg, 83%). R_f 0.14 (50% MeCN (0.1% formic acid)/H₂O); m.p. 51.1-54.6 °C; λ_{max} (EtOH)/nm 249; ν_{max}/cm^{-1} (neat) 1140 (s, SO₂^{sy}), 1178 (m, C-O), 1369 (s, SO₂^{as}); ¹H NMR (500 MHz; CDCl₃) δ_H 3.01 (6H, s, 2 \times N-CH₃), 7.26-7.29 (1H, m, H-Ar), 7.34-7.63 (8H, m, H-Ar); ¹³C NMR (125 MHz; CDCl₃) δ_C 38.8 (2 \times CH₃), 120.4 (C-Ar), 120.5 (C-Ar), 125.5 (C-Ar), 127.2 (2 \times C-Ar), 127.6 (C-Ar), 128.9 (2 \times C-Ar), 130.0 (C-Ar), 139.8 (C-Ar), 143.3 (C-Ar), 150.7 (C-Ar); LRMS (ES⁺) m/z 278.2 [M+H]⁺; HRMS calcd for C₁₄H₁₆NO₃S [M+H]⁺ 278.0845, found 278.0846; HPLC 99.6% in 0.1% formic acid (aq.)/MeCN (General procedure A; R_t 12.8 min); 99.7% in 0.1% ammonia (aq.)/MeCN (General procedure A; R_t 12.7 min).

[1,1'-Biphenyl]-2-yl dimethylsulfamate (**57**)

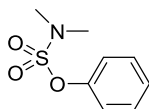


General procedure A was followed to synthesize and purify compound **57**, using 2-phenylphenol (274 mg, 0.161 mmol), cesium carbonate (578 mg, 1.77 mmol), *N,N*-dimethylsulfamoyl chloride (154 mg, 0.12 mL, 1.07 mmol) and acetonitrile (5.0 and 1.2 mL). The title compound was obtained as a white solid (213 mg, 72%). R_f 0.14 (50% MeCN (0.1% formic acid)/H₂O); m.p. 76.2-77.8 °C (lit.¹⁹³ 78 °C); λ_{max} (EtOH)/nm 240; ν_{max}/cm^{-1} (neat) 1153 (s, SO₂^{sy}), 1186 (s, C-O), 1356 (s, SO₂^{as}); ¹H NMR (500 MHz; CDCl₃) δ_H 2.53 (6H, s, 2 \times N-CH₃), 7.32-7.43 (4H, m, H-Ar), 7.43-7.48 (2H, m, H-Ar), 7.50-7.54 (2H, m, H-Ar), 7.56-7.60 (1H, m, H-Ar); ¹³C NMR (125 MHz; CDCl₃) δ_C 38.2 (2 \times N-CH₃), 122.9 (C-Ar), 126.9 (C-Ar), 127.8 (C-Ar), 128.4 (2 \times C-Ar), 128.9 (C-Ar), 129.9 (2 \times C-Ar), 131.3 (C-Ar), 135.1 (C-Ar), 137.3 (C-Ar), 147.4 (C-Ar); LRMS (ES⁺) m/z 278.2

[M+H]⁺; HRMS calcd for C₁₄H₁₆NO₃S [M+H]⁺ 278.0845, found 278.0849; HPLC 99.7% in 0.1% formic acid (aq.)/MeCN (*R*_t 12.6 min); 99.7% in 0.1% ammonia (aq.)/MeCN (*R*_t 12.5 min).

NMR data match those previously reported for this compound.⁷⁰

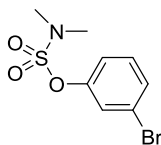
Phenyl dimethylsulfamate (58)



The sulfamate **58** was synthesized and purified as described in general procedure A, using phenol (152 mg, 0.161 mmol), cesium carbonate (578 mg, 1.77 mmol), *N,N*-dimethylsulfamoyl chloride (154 mg, 0.12 mL, 1.07 mmol) and acetonitrile (5.0 and 2.0 mL). The title compound (88 mg, 27%) was obtained as a brown oil. *R*_f 0.88 (10% MeOH/DCM); λ_{max} (EtOH)/nm 262; ν_{max}/cm⁻¹ (neat) 1145 (s, C-O), 1169 and 1193 (s, SO₂^{sy}), 1366 (s, SO₂^{as}); ¹H NMR (500 MHz; CDCl₃) δ_H 2.97 (6H, s, 2 × N-CH₃), 7.24-7.31 (3H, m, H-4, H-2 and H-6), 7.36-7.41 (2H, m, H-3 and H-5); ¹³C NMR (125 MHz; CDCl₃) δ_C 38.9 (2 × NCH₃), 121.9 (C-2 and C-6), 126.9 (C-4), 129.9 (C-3 and C-5), 150.4 (C-1); LRMS (ES⁺) *m/z* 202.2 [M+H]⁺; HRMS calcd for C₈H₁₁NO₃S [M+H]⁺ 202.0532, found 202.0539; HPLC 98.7% in 0.1% formic acid (aq.)/MeCN (*R*_t 10.5 min); 99.6% in 0.1% ammonia (aq.)/MeCN (*R*_t 10.5 min).

NMR data match those previously reported for this compound.⁷⁰

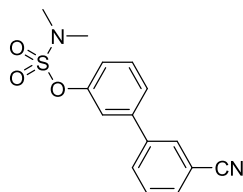
3-Bromophenyl dimethylsulfamate (59)



General procedure A was used to synthesize and purify compound **59**, using 3-bromophenol (2.00 g, 11.6 mol), cesium carbonate (4.14 g, 12.7 mmol) in acetonitrile (35 mL) and *N,N*-dimethylsulfamoyl chloride (1.11 g, 0.83 mL, 7.71 mmol) in acetonitrile (9 mL). The title compound was obtained as a colorless oil (1.58 g, 73%). *R*_f 0.16 (50% MeCN (0.1% formic acid)/H₂O); λ_{max} (EtOH)/nm 267; ν_{max}/cm⁻¹ (neat) 1062 (m, arom. C-Br), 1154 (s, C-O), 1165 and 1193 (s,

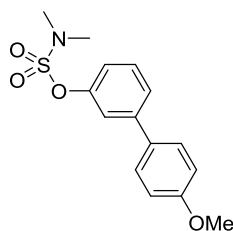
SO₂^{sy}), 1368 (s, SO₂^{as}); ¹H NMR (500 MHz; CDCl₃) δ_H 2.99 (6H, s, 2 × N-CH₃), 7.21-7.30 (2H, m, H-Ar), 7.39-7.44 (1H, m, H-Ar), 7.44-7.48 (1H, m, H-Ar); ¹³C NMR (125 MHz; CDCl₃) δ_C 38.9 (2 × NCH₃), 120.62 (C-Ar), 120.7 (C-3), 125.3 (C-Ar), 130.0 (C-Ar), 130.9 (C-Ar), 150.8 (C-1); LRMS (ES⁺) *m/z* 280.1 and 282.1 [M+H]⁺; HRMS calcd for C₈H₁₄⁷⁹BrN₂O₃S [M+NH₄]⁺ 296.9903, found 296.9908; HPLC 99.3% in 0.1% formic acid (aq.)/MeCN (*R*_t 11.8 min); 99.2% in 0.1% ammonia (aq.)/MeCN (*R*_t 11.8 min).

3'-Cyano-[1,1'-biphenyl]-3-yl dimethylsulfamate (81)



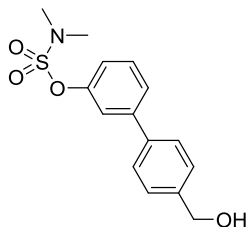
The title compound **81** was synthesized according to general procedure B using dimethyl 3-bromophenylsulfamate (120 mg, 0.428 mmol), 3-cyanophenylboronic acid (63 mg, 0.428 mmol), sodium carbonate (2 M aq., 0.42 mL), tetrakis(triphenylphosphine)palladium (25 mg, 21.4 μmol) and DME (1.7 mL). Purification by MPLC (gradient elution, 0-40% EtOAc/petrol) afforded the desired product as a colorless oil which solidified upon storage at RT (49 mg, 38%). *R*_f 0.11 (50% MeCN (0.1% formic acid)/H₂O); m.p. 73.8-75.0 °C; λ_{max} (EtOH)/nm 250, 350; ν_{max}/cm⁻¹ (neat) 1150 (s, SO₂^{sy}), 1176 (m, C-O), 1363 (s, SO₂^{as}), 2238 (m, C≡N); ¹H NMR (500 MHz; CDCl₃) δ_H 3.03 (6H, s, 2 × N-CH₃), 7.31-7.36 (1H, m, H-Ar), 7.44-7.52 (3H, m, H-Ar), 7.53-7.59 (1H, m, H-Ar), 7.63-7.68 (1H, m, H-Ar), 7.78-7.83 (1H, m, H-Ar), 7.84-7.87 (1H, m, H-Ar); ¹³C NMR (125 MHz; CDCl₃) δ_C 39.0 (2 × NCH₃), 113.4 (-CN), 118.7 (C-3'), 120.6 (C-Ar), 121.7 (C-Ar), 125.5 (C-Ar), 129.9 (C-Ar), 130.6 (C-Ar), 130.9 (C-Ar), 131.5, (C-Ar) 131.7 (C-Ar), 141.0 and 141.2 (C-1 and C-1'), 151.0 (C-3); LRMS (ES⁺) *m/z* 344.2 [M+MeCN+H]⁺; HRMS calcd for C₁₅H₁₈N₃O₃S [M+NH₄]⁺ 320.1063, found 320.1068; HPLC 97.6% in 0.1% formic acid (aq.)/MeCN (*R*_t 12.1 min); 96.6% in 0.1% ammonia (aq.)/MeCN (*R*_t 12.1 min).

4'-Methoxy-[1,1'-biphenyl]-3-yl dimethylsulfamate (82)



The title compound **82** was synthesized according to general procedure B using dimethyl 3-bromophenylsulfamate (120 mg, 0.428 mmol), 4-methoxyphenylboronic acid (65 mg, 0.428 mmol), sodium carbonate (2 M aq., 0.42 mL), tetrakis(triphenylphosphine)palladium (25 mg, 21.4 μ mol) and DME (1.7 mL). Purification by MPLC (gradient elution, 0-30% EtOAc/petrol) yielded the desired product as a yellow oil which solidified upon storage at RT (83 mg, 63%). R_f 0.11 (50% MeCN (0.1% formic acid)/H₂O); m.p. 75.3-76.0 °C; λ_{max} (EtOH)/nm 264, 350; ν_{max}/cm^{-1} (neat) 1141 (s, SO₂^{sy}), 1179 (s, C-O), 1244 (m, C-O-C^{as}), 1359 (s, SO₂^{as}), 2845 (w, CH₃^s), 2928 (w, CH₃^{as}); ¹H NMR (500 MHz; CDCl₃) δ_H 3.00 (6H, s, 2 \times N-CH₃), 3.86 (3H, s, -OCH₃), 6.96-7.01 (2H, m, H'-2 and H'-6), 7.20-7.24 (1H, m, H-Ar), 7.39-7.44 (1H, m, H-Ar), 7.45-7.49 (2H, m, H-Ar), 7.50-7.55 (2H, m, H'-3 and H'-5); ¹³C NMR (125 MHz; CDCl₃) δ_C 38.9 (2 \times N-CH₃), 55.5 (-OCH₃), 114.5 (C'-2 and C'-6), 119.8 (C-Ar), 120.1 (C-Ar), 125.1 (C-Ar), 128.4 (C'-3 and C'-5), 130.1 (C-Ar), 132.4 (C-Ar), 143.0 (C-Ar), 150.8 (C-Ar), 159.8 (C-Ar); LRMS (ES⁺) m/z 308.2 [M+H]⁺; HRMS calcd for C₁₅H₂₁N₂O₄S [M+NH₄]⁺ 325.1217, found 325.1222; HPLC 99.5% in 0.1% formic acid (aq.)/MeCN (R_t 12.6 min); 98.6% in 0.1% ammonia (aq.)/MeCN (R_t 12.5 min).

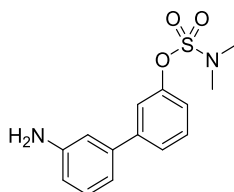
4'-(Hydroxymethyl)-[1,1'-biphenyl]-3-yl dimethylsulfamate (83)



General procedure B was followed using dimethyl 3-bromophenylsulfamate (120 mg, 0.428 mmol), 4-hydroxymethylphenylboronic acid (63 mg, 0.428 mmol), sodium carbonate (2 M aq., 0.42 mL), tetrakis(triphenyl-

phosphine)palladium (25 mg, 21.4 μmol) and DME (1.7 mL). After purification by MPLC (gradient elution, 0-100% EtOAc/petrol), the desired product was obtained as a colorless oil which solidified upon storage at RT (49 mg, 37%). R_f 0.54 (50% EtOAc/petrol); m.p. 50.5-51.7 $^{\circ}\text{C}$; λ_{max} (EtOH)/nm 253, 350; $\nu_{\text{max}}/\text{cm}^{-1}$ (neat) 1141 (s, SO_2^{sy}), 1178 (s, C-O), 1356 (s, SO_2^{as}), 2868 (w, CH_2^{s}), 2932 (w, CH_2^{as}), 3357 (w, O-H); ^1H NMR (500 MHz; CDCl_3) δ_{H} 1.68 (1H, br, OH), 3.01 (6H, s, $2 \times \text{N-CH}_3$), 1.71 (1H, t, $J = 6.0$ Hz, OH), 4.76 (2H, d, $J = 6.0$ Hz, CH_2), 7.25-7.30 (1H, m, H-Ar), 7.43-7.48 (3H, m, H-Ar), 7.49-7.53 (2H, m, H-Ar), 7.57-7.60 (2H, m, H-Ar); ^{13}C NMR (125 MHz; CDCl_3) δ_{C} 39.0 ($2 \times \text{NCH}_3$), 65.1 (CH_2), 120.5 (C-Ar), 120.5 (C-Ar), 125.5 (C-Ar), 127.5 ($2 \times \text{C-Ar}$), 127.6 ($2 \times \text{C-Ar}$), 130.2 (C-Ar), 139.3 (C-Ar), 140.8 (C-Ar), 143.0 (C-Ar), 150.8 (C-Ar); LRMS (ES^+) m/z 290.2 $[\text{M-H}_2\text{O}+\text{H}]^+$; HRMS calcd for $\text{C}_{15}\text{H}_{21}\text{N}_2\text{O}_4\text{S}$ $[\text{M}+\text{NH}_4]^+$ 325.1217, found 325.1222; HPLC 98.9% in 0.1% formic acid (aq.)/MeCN (R_t 10.8 min); 98.6% in 0.1% ammonia (aq.)/MeCN (R_t 10.7 min).

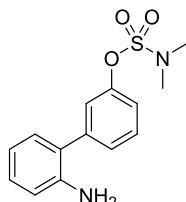
3'-Amino-[1,1'-biphenyl]-3-yl dimethylsulfamate (70)



General procedure B was followed using dimethyl 3-bromophenylsulfamate (60 mg, 0.214 mmol), 3-aminophenylboronic acid (30 mg, 0.214 mmol), sodium carbonate (2 M aq., 0.5 mL), tetrakis(triphenylphosphine)palladium (13 mg, 10.7 μmol) and 1,2-dimethoxyethane (0.5 mL). After purification by MPLC (gradient elution, 0-10% MeOH/DCM), the title compound was obtained as a brown oil (22 mg, 35%). R_f 0.67 (10% MeOH/DCM); λ_{max} (EtOH)/nm 235; $\nu_{\text{max}}/\text{cm}^{-1}$ (neat) 1139 (s, SO_2^{sy}), 1174 (s, C-O), 1356 (s, SO_2^{as}), 3372 (m, N-H), 3477 (m, N-H); ^1H NMR (500 MHz; CDCl_3) δ_{H} 2.92 (6H, s, $2 \times \text{N-CH}_3$), 3.63 (2H, br, - NH_2), 7.31-7.36 (1H, m, H-Ar), 7.49-7.55 (1H, m, H-Ar), 7.57-7.63 (1H, m, H-Ar), 7.83-7.91 (2H, m, H-Ar), 8.03-8.08 (1H, m, H-Ar), 8.09-8.13 (2H, m, H-Ar); ^{13}C NMR (125 MHz; CDCl_3) δ_{C} 38.9 ($2 \times \text{NCH}_3$), 114.0 (C-2'), 114.8 (C-4'), 117.7 (C-6'), 120.4 (C-Ar), 120.5 (C-Ar), 125.5 (C-Ar), 129.9 (C-Ar), 130.0 (C-5'), 141.1

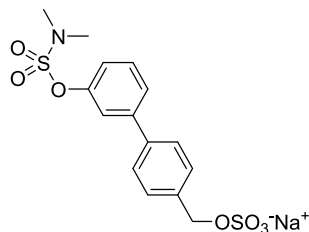
and 143.6 (C-1 and C-1'), 147.0 (C-3'), 150.7 (C-3); LRMS (ES⁺) m/z 293.1 [M+H]⁺; HRMS calcd for C₁₄H₁₇N₂O₃S [M+H]⁺ 293.0954, found 293.0957; HPLC 99.4% in 0.1% formic acid (aq.)/MeCN (R_t 10.4 min); 97.2% in 0.1% ammonia (aq.)/MeCN (R_t 11.7 min).

2'-Amino-[1,1'-biphenyl]-3-yl dimethylsulfamate (69)



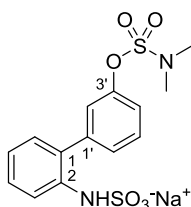
The title compound was synthesized according to general procedure B using dimethyl 3-bromophenylsulfamate (500 mg, 1.78 mmol), 2-aminophenylboronic acid pinacol ester (391 mg, 1.78 mmol), sodium carbonate (2 M aq., 1.8 mL), tetrakis(triphenylphosphine)palladium (103 mg, 89.2 μ mol) and DME (4.2 mL). Purification by MPLC (gradient elution, 0-10% MeOH/DCM) yielded the desired product as a brown oil (518 mg, >99%). R_f 0.78 (10% MeOH/DCM); λ_{max} (EtOH)/nm 226, 253sh; ν_{max}/cm^{-1} (neat) 1139 (s, SO₂^{sy}), 1180 (s, C-O), 1364 (s, SO₂^{as}), 3383 (m, N-H), 3468 (m, N-H); ¹H NMR (500 MHz; CDCl₃) δ_H 3.00 (6H, s, 2 \times N-CH₃), 3.70 (2H, br, NH₂), 6.75 (1H, dd, J = 0.9 and 8.0 Hz, H-3'), 6.82 (1H, td, J = 0.9 and 7.6 Hz, H-5'), 7.12 (1H, dd, J = 1.6, 7.6 Hz, H-6'), 7.15-7.19 (1H, m, H-4'), 7.28 (1H, ddd, J = 1.3, 2.4, 8.3 Hz, H-6), 7.37-7.41 (2H, m, H-4 and H-2), 7.44-7.49 (1H, m, H-5); ¹³C NMR (125 MHz; CDCl₃) δ_C 38.9 (2 \times N-CH₃), 116.0 (C-3'), 118.9 (C-5'), 120.5 (C-6), 122.5 (C-2), 126.2 (C-2'), 127.6 (C-4), 129.1 (C-4'), 130.3 (C-5), 130.5 (C-6'), 141.6 and 143.5 (C-1 and C-1'), 150.6 (C-3); LRMS (ES⁺) m/z 293.1 [M+H]⁺; HRMS calcd for C₁₄H₁₇N₂O₃S [M+H]⁺ 293.0954, found 293.0957; HPLC 99.5% in 0.1% formic acid (aq.)/MeCN (R_t 11.9 min); 99.3% in 0.1% ammonia (aq.)/MeCN (R_t 12.0 min).

Sodium (3'-((*N,N*-dimethylsulfamoyl)oxy)-[1,1'-biphenyl]-4-yl)methyl sulfate (84**)**



Compound **84** was synthesized according to general procedure D (method 1) using the benzyl alcohol **83** (125 mg, 0.407 mmol), sulfur trioxide pyridine complex (194 mg, 1.22 mmol), NaOH (2 M aq., 4.1 mL, 8.2 mmol) and *N,N*-dimethylformamide (8.0 mL). After purification by MPLC (gradient elution, 0-10% MeOH/DCM), the desired sulfate was obtained as yellow crystals (55.3 mg, 33%). R_f 0.40 (10% MeOH/DCM); not clear m.p. (dec. 163-187) λ_{\max} (EtOH)/nm 252; ν_{\max} /cm⁻¹ (neat) 1143 (s, SO₂^{sy}), 1178 (s, C-O), 1212 (s, sulfate SO₂^{as}), 1362 (s, sulfamate SO₂^{as}); ¹H NMR (500 MHz; CD₃OD) δ_H 2.98 (6H, s, 2 × N-CH₃), 5.07 (2H, s, CH₂), 7.27-7.31 (1H, m, H-Ar), 7.48-7.55 (4H, m, H-Ar), 7.58-7.65 (3H, m, H-Ar); ¹³C NMR (125 MHz; CD₃OD) δ_C 39.1 (2 × NCH₃), 70.3 (CH₂), 121.3 (C-Ar), 121.7 (C-Ar), 126.4 (C-Ar), 128.0 (2 × C-Ar), 129.7 (2 × C-Ar), 131.3 (C-Ar), 137.9 (C-Ar), 140.8 (C-Ar), 144.2 (C-Ar), 150.4 (C-3'); LRMS (ES⁻) m/z 386.1 [M-Na]⁻; HRMS calcd for C₁₅H₁₆NO₇S₂ [M-Na]⁻ 386.0374, found 386.0367; HPLC 99.5% in 0.1% formic acid (aq.)/MeCN (R_t 8.6 min); 99.7% in 0.1% ammonia (aq.)/MeCN (R_t 6.5 min).

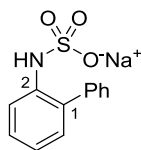
Sodium {3'-[(*N,N*-dimethylsulfamoyl)oxy]-[1,1'-biphenyl]-2-yl}sulfamate (72**)**



General procedure D (method 1) was followed to obtain the sulfate **72** using the aniline **69** (125 mg, 0.428 mmol), sulfur trioxide pyridine complex (204 mg, 1.28 mmol), NaOH (2 M aq., 4.3 mL, 8.6 mmol) and *N,N*-dimethylformamide (8.6

mL). After purification by MPLC (gradient elution, 0-10% MeOH/DCM), the desired sulfate was obtained as a yellow solid (123 mg, 73%). R_f 0.17 (10% MeOH/DCM); m.p. 90-123 °C (dec.); λ_{\max} (EtOH)/nm 251sh, 293; $\nu_{\max}/\text{cm}^{-1}$ (neat) 1142 (s, SO_2^{sy}), 1180 (s, C-O), 1363 (s, SO_2^{as}), 3524 (m, N-H); ^1H NMR (500 MHz; CD_3OD) δ_{H} 2.94 (6H, s, $2 \times \text{N-CH}_3$), 7.02 (1H, td, $J = 1.2, 7.6$ Hz, H-5'), 7.16 (1H, dd, $J = 1.8, 7.6$ Hz, H-6'), 7.28-7.32 (1H, m, H-4'), 7.33-7.38 (2H, m, H-2 and H-4), 7.40-7.45 (1H, m, H-5), 7.55 (1H, dt, $J = 0.5, 7.8$ Hz, H-6), 7.74 (1H, dd, $J = 1.2, 8.3$ Hz, H-2'); ^{13}C NMR (125 MHz; CD_3OD) δ_{C} 39.1 ($2 \times \text{N-CH}_3$), 120.0 (C-3), 122.2 (C-4'), 122.8 (C-5), 123.9 (C-2'), 129.0 (C-5'), 129.7 (C-4), 130.9 (C-2), 131.0 (C-6), 131.5 (C-6'), 139.5 and 142.3 (C-1 and C-1'), 152.2 (C-3'); LRMS (ES⁻) m/z 371.1 [M-Na]⁻; HRMS calcd for $\text{C}_{14}\text{H}_{15}\text{N}_2\text{O}_6\text{S}_2$ [M-Na]⁻ 371.0377, found 371.0372 (R_t 8.0 min); HPLC 96.8% in 0.1% formic acid (aq.)/MeCN; 96.2% in 0.1% ammonia (aq.)/MeCN (R_t 6.5 min).

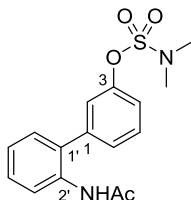
Sodium [1,1'-biphenyl]-2-ylsulfamate (87)



General procedure D (method 1) was followed to synthesize compound **87** using 2-aminobiphenyl (108 mg, 0.6376 mmol), sulfur trioxide pyridine complex (307 mg, 1.93 mmol), NaOH (2 M aq., 6.4 mL, 12.8 mmol) and *N,N*-dimethylformamide (12.0 mL). The crude product was purified by MPLC (gradient elution, 0-10% MeOH/DCM) to afford the product as a light brown solid (114 mg, 66%). R_f 0.29 (10% MeOH/DCM); m.p. 54-82 °C (dec.); λ_{\max} (EtOH)/nm 224, 289; $\nu_{\max}/\text{cm}^{-1}$ (neat) 1194 (s, SO_2^{sy}), 1481 (s, SO_2^{as}), 3358 (m, N-H); ^1H NMR (500 MHz; CD_3OD) δ_{H} 7.00 (1H, td, $J = 1.2, 7.5$ Hz, H-5), 7.12-7.16 (1H, m, H-6), 7.27 (ddd, $J = 1.6, 7.5$ and 8.3 Hz, H-4), 7.36-7.41 (1H, m, H-4'), 7.41-7.45 (1H, m, H-Ar), 7.45-7.50 (1H, m, H-Ar), 7.71 (ddd, $J = 0.3, 1.2$ and 8.3 Hz, H-3); ^{13}C NMR (125 MHz; CD_3OD) δ_{C} 119.3 (C-3), 122.6 (C-5), 128.6 (C-4'), 129.1 (C-4), 130.0 ($2 \times \text{C-Ar}$), 130.3 ($2 \times \text{C-Ar}$), 130.9 (C-6), 132.1 (C-2), 139.3 and 140.0 (C-1 and C1'); LRMS (ES⁻) m/z 247.8 [M-Na]⁻; HRMS calcd for

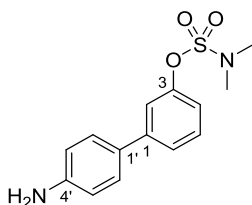
C₁₂H₁₂NO₃S [M-Na]⁻ 248.0387, found 248.0382; HPLC 99.5% in 0.1% formic acid (aq.)/MeCN (*R*_t 7.2 min); 99.4% in 0.1% ammonia (aq.)/MeCN (*R*_t 5.3 min).

2'-Acetamido-[1,1'-biphenyl]-3-yl dimethylsulfamate (75)⁸⁰



The title compound was obtained following general procedure C using the aniline **69** (125 mg, 0.428 mmol), dichloromethane (1.2 mL), acetic anhydride (52 mg, 0.05 mL, 0.513 mmol) and NaHCO₃ (sat. aq., 10 mL). Purification by MPLC afforded the title compound as a yellow oil (144 mg, >99%). *R*_f 0.20 (50% EtOAc/petrol); λ_{max} (EtOH)/nm 250sh; ν_{max}/cm⁻¹ (neat) 1143 (s, SO₂^{sy}), 1182 (s, C-O), 1366 (s, SO₂^{as}), 1663 (m, C=O); ¹H NMR (500 MHz; CDCl₃) δ_H 2.07 (3H, s, CH₃), 3.03 (6H, s, 2 × N-CH₃), 7.15 (1H, br, NH), 7.17-7.22 (1H, m, H-Ar), 7.24-7.26 (1H, m, H-Ar), 7.29-7.33 (2H, m, H-Ar), 7.33-7.36 (1H, m, H-Ar), 7.36-7.42 (1H, m, H-Ar), 7.48-7.55 (1H, m, H-Ar), 8.20-8.26 (1H, m, H-Ar); ¹³C NMR (125 MHz; CDCl₃) δ_C 24.6 (CH₃), 38.9 (2 × N-CH₃), 121.4 (C-Ar), 122.5 (C-Ar), 123.0 (C-Ar), 124.7 (C-Ar), 127.9 (C-Ar), 129.1 (2 × C-Ar), 130.1 (C-Ar), 130.7 (C-Ar), 134.8 and 140.2 (C-1 and C-1'), 150.4 (C-3), 168.7 (C=O); LRMS (ES⁺) *m/z* 335.2 [M+H]⁺; HRMS calcd for C₁₆H₁₉N₂O₄S [M+H]⁺ 335.1060, found 335.1064; HPLC 99.8% in 0.1% formic acid (aq.)/MeCN (*R*_t 10.5 min); 99.8% in 0.1% ammonia (aq.)/MeCN (*R*_t 10.5 min).

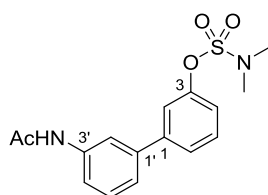
4'-Amino-[1,1'-biphenyl]-3-yl dimethylsulfamate (71)



General procedure B was followed to synthesize compound **71** using dimethyl 3-bromophenylsulfamate **59** (400 mg, 1.43 mmol), 4-aminophenylboronic acid pinacol ester (313 mg, 1.43 mmol), sodium carbonate (2 M aq., 1.4 mL),

tetrakis(triphenylphosphine)palladium (82 mg, 71 μmol), and DME (3.3 mL). Purification by MPLC (gradient elution, 0-10% MeOH/DCM) yielded the desired product as a red solid (339 mg, 81%). R_f 0.79 (10% MeOH/DCM); m.p. 82.4-83.1 $^{\circ}\text{C}$; λ_{max} (EtOH)/nm 290; $\nu_{\text{max}}/\text{cm}^{-1}$ (neat) 1134 (s, SO_2^{sy}), 1177 (s, C-O), 1361 (s, SO_2^{as}), 1476, 1627 (m, N-H bending), 3382 (m, N-H), 3480 (m, N-H); ^1H NMR (500 MHz; CDCl_3) δ_{H} 2.99 (6H, s, $2 \times \text{N-CH}_3$), 3.77 (2H, br, NH_2), 6.73-6.77 (2H, m, H-2' and H-6'), 7.16-7.20 (1H, m, H-Ar), 7.36-7.42 (3H, m, H-Ar, H-3' and H-5'), 7.43-7.46 (2H, m, H-Ar); ^{13}C NMR (125 MHz; CDCl_3) δ_{C} 39.0 ($2 \times \text{N-CH}_3$), 115.5 (C-2' and C-6'), 119.4 (C-Ar), 119.6 (C-Ar), 124.7 (C-Ar), 128.2 (C-3' and C-5'), 130.0 (C-Ar), 146.6 (C-Ar), 150.8 (C-3). Two carbons not detected; LRMS (ES^+) m/z 293.3 [$\text{M}+\text{H}$] $^+$; HRMS calcd for $\text{C}_{14}\text{H}_{17}\text{N}_2\text{O}_3\text{S}$ [$\text{M}+\text{H}$] $^+$ 293.0954, found 293.0957; HPLC 98.9% in 0.1% formic acid (aq.)/MeCN (R_t 10.5 min); 97.2% in 0.1% ammonia (aq.)/MeCN (R_t 11.6 min).

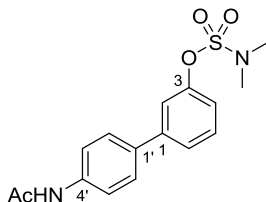
3'-Acetamido-[1,1'-biphenyl]-3-yl dimethylsulfamate (76)



Compound **76** was synthesized according to general procedure C using the aniline **70** (100 mg, 0.342 mmol) and acetic anhydride (42 mg, 0.04 mL, 0.410 mmol) in DCM (0.92 mL, 2.7 mL/mmol). Purification by MPLC afforded the desired product as a colorless oil (79 mg, 69%). R_f 0.43 (50% EtOAc/petrol); λ_{max} (EtOH)/nm 242; $\nu_{\text{max}}/\text{cm}^{-1}$ (neat) 1141 (s, SO_2^{sy}), 1178 (s, C-O), 1365 (s, SO_2^{as}), 1548 (s, N-H bending + C-N stretching or amide II band), 1667 (m, C=O or amide I band), 3300 (w, N-H); ^1H NMR (500 MHz; CDCl_3) δ_{H} 2.21 (3H, s, CH_3), 3.01 (6H, s, $2 \times \text{N-CH}_3$), 7.26-7.34 (3H, m, $2 \times \text{H-Ar}$, NH), 7.36-7.41 (1H, m, H-Ar), 7.42-7.46 (1H, m, H-Ar), 7.47-7.51 (2H, m, H-Ar), 7.51-7.55 (1H, m, H-Ar), 7.71-7.74 (1H, m, H-Ar); ^{13}C NMR (125 MHz; CDCl_3) δ_{C} 24.8 (CH_3), 39.0 ($2 \times \text{N-CH}_3$), 118.7 (C-Ar), 119.4 (C-Ar), 120.5 (C-Ar), 120.8 (C-Ar), 123.2 (C-Ar), 125.7 (C-Ar), 129.8 (C-Ar), 130.3 (C-Ar), 138.6 (C-Ar), 140.8 (C-Ar), 142.9 (C-Ar), 150.8 (C-3), 168.5 (C=O); LRMS (ES^+) m/z 335.2 [$\text{M}+\text{H}$] $^+$; HRMS calcd for $\text{C}_{16}\text{H}_{19}\text{N}_2\text{O}_4\text{S}$

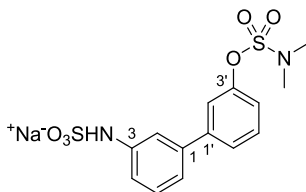
[M+H]⁺ 335.1060, found 335.1063; HPLC >99.9% in 0.1% formic acid (aq.)/MeCN (*R*_t 11.3 min); >99.9% in 0.1% ammonia (aq.)/MeCN (*R*_t 11.2 min).

4'-Acetamido-[1,1'-biphenyl]-3-yl dimethylsulfamate (77)



Compound **77** was synthesized according to general procedure C using the aniline **71** (100 mg, 0.342 mmol) and acetic anhydride (42 mg, 0.04 mL, 0.410 mmol) in DCM (0.92 mL, 2.7 mL/mmol). Purification by MPLC afforded the desired product as a white solid (95 mg, 83%). *R*_f 0.41 (50% EtOAc/petrol); m.p. 119.2-120.2 °C; λ_{max} (EtOH)/nm 275; ν_{max}/cm⁻¹ (neat) 1143 (s, SO₂^{sy}), 1181 (s, C-O), 1364 (s, SO₂^{as}), 1528 (s, N-H bending + C-N stretching or amide II band), 1665 (m, C=O or amide I band), 3314 (w, N-H); ¹H NMR (500 MHz; CDCl₃) δ_H 2.20 (3H, s, CH₃), 3.01 (6H, s, 2 × N-CH₃), 7.23-7.26 (1H, m, H-Ar), 7.27-7.30 (1H, br, NH), 7.41-7.50 (3H, m, H-Ar), 7.51-7.56 (2H, m, H-Ar), 7.56-7.61 (2H, m, H-Ar); ¹³C NMR (125 MHz; CDCl₃) δ_C 24.8 (CH₃), 39.0 (2 × N-CH₃), 120.2 (C-Ar), 120.3 (2 × C-Ar), 125.2 (C-Ar), 127.8 (2 × C-Ar), 130.2 (C-Ar), 135.7 (C-Ar), 137.9 (C-Ar), 142.7 (C-Ar), 150.8 (C-3), 168.4 (C=O); LRMS (ES⁺) *m/z* 335.3 [M+H]⁺; HRMS calcd for C₁₆H₁₉N₂O₄S [M+H]⁺ 335.1060, found 335.1063; HPLC >99.9% in 0.1% formic acid (aq.)/MeCN (*R*_t 11.2 min); >99.9% in 0.1% ammonia (aq.)/MeCN (*R*_t 11.2 min).

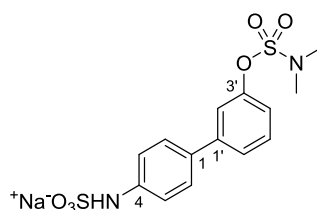
Sodium {3'-[(*N,N*-dimethylsulfamoyl)oxy]-[1,1'-biphenyl]-3-yl}sulfamate (73)



Compound **73** was synthesized according to general procedure D (method 1) using the aniline **70** (100 mg, 0.342 mmol), sulfur trioxide pyridine complex

(163 mg, 1.03 mmol), DMF (6.8 mL, 18 mL/mmol), and NaOH (2 M aq., 3.4 mL, 6.84 mmol). Purification by MPLC (gradient elution, 0-20% MeOH/DCM) afforded the desired product as a yellow solid (103 mg, 76%). R_f 0.01 (10% MeOH/DCM); m.p. 92-182 °C (dec.); λ_{\max} (EtOH)/nm 236; $\nu_{\max}/\text{cm}^{-1}$ (neat) 1142 (s, SO₂^{sy}), 1365 (m, SO₂^{as}), 1604 (m, N-H bending), 3247 (N-H stretching); ¹H NMR (500 MHz; CD₃OD) δ_H 2.97 (6H, s, 2 × N-CH₃), 7.12-7.16 (1H, m, H-Ar), 7.20 (1H, ddd, J = 0.9, 2.2, 8.1 Hz, H-Ar), 7.26 (1H, ddd, J = 0.8, 2.4, 8.1, H-Ar), 7.30 (1H, app. t, J = 7.6 Hz, H-Ar), 7.47 (1H, app. t, J = 7.9 Hz, H-Ar), 7.49-7.52 (2H, m, H-Ar), 7.55-7.59 (1H, m, H-Ar); ¹³C NMR (125 MHz; CD₃OD) δ_C 39.1 (2 × N-CH₃), 117.4 (C-Ar), 118.5 (C-Ar), 120.6 (C-Ar), 121.4 (C-Ar), 121.6 (C-Ar), 126.6 (C-Ar), 130.3 (C-Ar), 131.1 (C-Ar), 141.5 and 143.7 (C-1 and C-1'), 144.8 (C-3), 152.1 (C-3'); LRMS (ES⁻) m/z 371.1 [M-Na]⁻; HRMS calcd for C₁₄H₁₅N₂O₆S₂ [M-Na]⁻ 371.0377, found 371.0373; HPLC 95.6% in 0.1% formic acid (aq.)/MeCN (R_t 8.6 min); 95.5% in 0.1% ammonia (aq.)/MeCN (R_t 5.4 min).

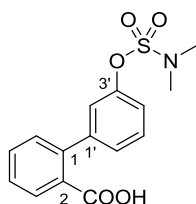
Sodium {3'-[(*N,N*-dimethylsulfamoyl)oxy]-[1,1'-biphenyl]-4-yl}sulfamate (74)



General procedure D (method 1) was used for the synthesis of compound **74** using the aniline **71** (100 mg, 0.342 mmol), sulfur trioxide pyridine complex (163 mg, 1.03 mmol), DMF (6.8 mL, 18 mL/mmol) and aq. NaOH (2 M, 3.4 mL, 6.84 mmol). Purification by MPLC (gradient elution, 0-20% MeOH/DCM) afforded the desired product as a brown amorphous solid (79 mg, 58%). R_f 0.10 (10%/MeOH/DCM); m.p. 66-105 °C (dec.); λ_{\max} (EtOH)/nm 284; $\nu_{\max}/\text{cm}^{-1}$ (neat) 1141 (s, SO₂^{sy}), 1180 (s, C-O), 1365 (m, SO₂^{as}), 1608 (m, N-H bending), 3226 (N-H stretching); ¹H NMR (500 MHz; CD₃OD) δ_H 2.95 (3H, s, CH₃), 7.17-7.22 (1H, m, C-2'), 7.26-7.30 (2H, m, H-2 and H-6), 7.40-7.47 (2H, m, H-Ar), 7.47-7.53 (3H, m, H-3 and H-5); ¹³C NMR (125 MHz; CD₃OD) δ_C 39.0 (2 × N-CH₃),

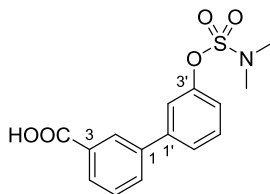
118.9 (C-2 and C-6), 120.5 (C-Ar), 120.7 (C-2'), 125.7 (C-Ar), 128.3 (C-3 and C-5), 131.1 (C-Ar), 133.2 (C-Ar), 143.2 (C-Ar), 144.3 (C-Ar), 152.2 (C-3'); LRMS (ES⁻) m/z 371.1 [M-Na]⁻; HRMS calcd for C₁₄H₁₅N₂O₆S₂ [M-Na]⁻ 371.0377, found 371.0370; HPLC 96.1% in 0.1% formic acid (aq.)/MeCN (R_t 8.5 min); 95.6% in 0.1% ammonia (aq.)/MeCN (R_t 5.4 min).

3'-[(*N,N*-Dimethylsulfamoyl)oxy]-[1,1'-biphenyl]-2-carboxylic acid (**63**)



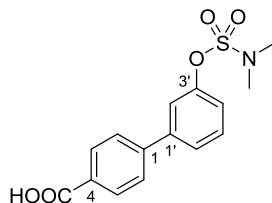
At RT, a solution of lithium hydroxide monohydrate (13.8 mg, 0.329 mmol) in water (1.0 mL, 3.3 mmol/mL) was added to a solution of the methyl ester **66** (70.4 mg 0.210 mmol) in THF (1.5 mL, 7 mL/mmol). The reaction mixture was heated at 50 °C for 3 days. Upon completion of the reaction, the mixture was acidified to pH 5-6 by addition of aq. HCl (1 M), and extracted with EtOAc (3 × 15 mL). The combined organic phases were washed with brine, dried (MgSO₄), filtered, and the solvent was removed *in vacuo*. The crude product was purified by MPLC (gradient elution, 0-10% MeOH/DCM) to afford the title compound as a pale yellow solid (68 mg, quant.). R_f 0.45 (10% MeOH/DCM); m.p. 151-162 °C (dec.); λ_{max} (EtOH)/nm 340; ν_{max}/cm^{-1} (neat) 1140 (s, SO₂^{sy}), 1179 (s, C-O), 1374 (m, SO₂^{as}), 1416 (m), 1681 (s, C=O), 1696 (s, C=O); ¹H NMR (500 MHz; CDCl₃) δ_H 2.93 (6H, s, 2 × N-CH₃), 7.22-7.25 (1H, m, H-6), 7.25-7.27 (1H, m, H-2), 7.28 (1H, ddd, J = 1.0, 2.4, 8.0 Hz, H-4), 7.33-7.36 (1H, m, H-6'), 7.39 (1H, app. t, J = 8.0 Hz, H-5), 7.46 (1H, td, J = 1.2, 7.6 Hz, H-4'), 7.57 (1H, td, J = 1.4, 7.6 Hz, H-5'), 7.96-8.00 (1H, m, H-3); ¹³C NMR (125 MHz; CDCl₃) δ_C 38.8 (2 × N-CH₃), 120.8 (C-4'), 122.3 (C-2'), 127.1 (C-6'), 128.0 (C-4), 129.1 (C-2), 129.6 (C-5'), 131.1 (C-3), 131.3 (C-6), 132.4 (C-5), 142.2 (C-1), 143.3 (C-1'), 150.0 (C-3'), 171.5 (-CO₂H); LRMS (ES⁻) m/z 320.2 [M-H]⁻; HRMS calcd for C₁₅H₁₄NO₅S [M-H]⁻ 320.0598, found 320.0590; HPLC 99.7% in 0.1% formic acid (aq.)/MeCN (R_t 11.0 min); N/A in 0.1% ammonia (aq.)/MeCN.

3'-[(*N,N*-Dimethylsulfamoyl)oxy]-[1,1'-biphenyl]-3-carboxylic acid (**64**)



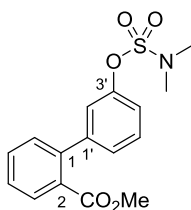
Compound **64** was synthesized following general procedure E using sulfamate **59** (152 mg, 0.54 mmol), 3-carboxyphenylboronic acid (90 mg, 0.54 mmol), aq. Na_2CO_3 (2 M, 0.54 mL, 1.1 mmol), $\text{Pd}(\text{dppf})\text{Cl}_2 \cdot \text{DCM}$ (22 mg, 0.024 mmol), and DME (1.3 mL). The reaction mixture was diluted with ethyl acetate and water, and filtered through Celite. The organic solvent was removed *in vacuo*, and the aqueous residue was extracted with EtOAc (50 mL). The aqueous layer was acidified by addition of a solution of 10% aqueous HCl, and extracted with ethyl acetate (3×50 mL). The combined organic layers were dried (MgSO_4), filtered, and evaporated. Purification by MPLC (gradient elution, 0-10% MeOH/DCM) afforded the product as a pale pink solid (113 mg, 66%). R_f 0.41 (10% MeOH/DCM); m.p. 130-147 °C (dec.); λ_{max} (EtOH)/nm 250 nm; $\nu_{\text{max}}/\text{cm}^{-1}$ (neat) 1144 (s, SO_2^{sy}), 1182 (s, C-O), 1364 (m, SO_2^{as}), 1448, 1678 (s, C=O); ^1H NMR (500 MHz; CDCl_3) δ_{H} 3.03 (6H, s, $2 \times \text{N-CH}_3$), 7.33 (1H, ddd, $J = 1.1, 2.4, 8.0$ Hz, H-Ar), 7.50 (1H, app. t, $J = 8.0$ Hz, H-5'), 7.52-7.55 (2H, m, H-Ar), 7.58 (1H, app. t, $J = 7.8$ Hz, H-5), 7.84 (1H, ddd, $J = 1.1, 1.7, 7.8$ Hz, H-6), 8.10-8.16 (1H, m, H-4), 8.31-8.35 (1H, m, H-2); ^{13}C NMR (125 MHz; CDCl_3) δ_{C} 39.0 ($2 \times \text{N-CH}_3$), 120.6 (C-Ar), 121.1 (C-Ar), 125.6 (C-Ar), 129.0 (C-2), 129.3 (C-5), 129.7 (C-4), 130.4 (C-5'), 132.5 (C-6), 140.4 and 142.1 (C-1 and C-1'), 150.9 (C-3'). Two carbons not detected; LRMS (ES^-) m/z 320.2 [M-H] $^-$; HRMS calcd for $\text{C}_5\text{H}_4\text{NO}_5\text{S}$ [M-H] $^-$ 320.0598, found 320.0594; HPLC 98.5% in 0.1% formic acid (aq.)/MeCN (R_t 11.4 min); N/A in 0.1% ammonia (aq.)/MeCN.

3'-[(*N,N*-Dimethylsulfamoyl)oxy]-[1,1'-biphenyl]-4-carboxylic acid (**65**)



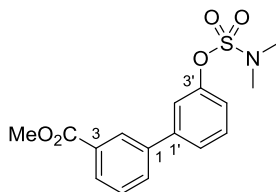
Compound **65** was synthesized following general procedure E using the sulfamate **59** (150 mg, 0.54 mmol), 4-carboxyphenylboronic acid (90 mg, 0.54 mmol), aq. Na₂CO₃ (2 M, 0.54 mL, 1.1 mmol), Pd(dppf)Cl₂ · DCM (22 mg, 0.024 mmol), and DME (1.3 mL). The reaction mixture was diluted with ethyl acetate and water, and filtered through Celite. The organic solvent was removed *in vacuo*, and the aqueous residue was extracted with EtOAc (50 mL). The aqueous layer was acidified by addition of HCl aqueous 10%, and extracted with ethyl acetate (3 × 50 mL). The combined organic layers were dried (MgSO₄), filtered, and evaporated. Purification by MPLC (gradient elution, 0-10% MeOH/DCM) afforded the product as a brown solid (118 mg, 68%). *R*_f 0.45 (10% MeOH/DCM); m.p. 100-180°C (dec.); λ_{max} (EtOH)/nm 262; ν_{max}/cm⁻¹ (neat) 1147(s, SO₂^{sy}), 1183 (s, C-O), 1361 (m, SO₂^{as}), 1419, 1680 (s, C=O); ¹H NMR (500 MHz; DMSO-*d*₆) δ_H 2.94 (6H, s, 2 × N-CH₃), 7.39 (1H, ddd, *J* = 0.8, 2.5, 8.1 Hz, H-4'), 7.61 (1H, app. t, *J* = 8.1 Hz, H-5'), 7.64-7.66 (1H, m, H-2'), 7.72-7.75 (1H, m, H-6'), 7.83 (2H, dt, *J* = 1.8, 8.4 Hz, H-2 and 6), 8.04 (2H, dt, *J* = 1.8, 8.4 Hz, H-3 and 5), 13.0 (1H, br, -CO₂H); ¹³C NMR (125 MHz; DMSO-*d*₆) δ_C 38.4 (2 × N-CH₃), 120.2 (C-2'), 121.5 (C-4'), 125.5 (C-6'), 127.1 (C-2 and C-6), 127.7 (C-4), 130.0 (C-3 and C-5), 130.7 (C-5'), 141.0 (C-1'), 142.7 (C-1), 150.4 (C-3'), 167.0 (-CO₂H); LRMS (ES⁻) *m/z* 320.2 [M-H]⁻; HRMS calcd for C₅H₁₄NO₅S [M-H]⁻ 320.0598, found 320.0594; HPLC >99.9% in 0.1% formic acid (aq.)/MeCN (*R*_t 11.4 min); N/A in 0.1% ammonia (aq.)/MeCN.

**Methyl 3'-[(*N,N*-dimethylsulfamoyl)oxy]-[1,1'-biphenyl]-2-carboxylate
(66)**



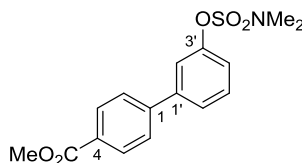
Compound **66** was synthesized according to general procedure E using sulfamate **59** (151 mg, 0.54 mmol), 2-methoxycarbonylphenylboronic acid (97 mg, 0.54 mmol), aq. Na₂CO₃ (2 M, 0.54 mL, 1.1 mmol), Pd(dppf)Cl₂ · DCM (22 mg, 0.024 mmol), and DME (1.3 mL). The reaction mixture was diluted with water, and extracted with EtOAc (3 × 50 mL). The combined organic layers were dried (MgSO₄), filtered, and evaporated *in vacuo*. The crude product was purified by MPLC (gradient elution, 0-50% EtOAc/petrol) to yield the title compound as a light brown oil (152 mg, 90%). *R*_f 0.71 (50% EtOAc/petrol); λ_{max} (EtOH)/nm 238sh, 279; ν_{max}/cm⁻¹ (neat) 1144 (s, SO₂^{sy}), 1182 (s, C-O), 1368 (m, SO₂^{as}), 1452 (m, CH₃ def), 1722 (s, C=O); ¹H NMR (500 MHz; CDCl₃) δ_H 2.99 (6H, s, 2 × N-CH₃), 3.66 (3H, s, CH₃), 7.23 (1H, m, H-6'), 7.20-7.25 (1H, m, H-2'), 7.30 (1H, ddd, *J* = 1.1, 2.3, 8.1 Hz, H-4'), 7.36 (1H, ddd, *J* = 0.5, 1.2, 7.6 Hz, H-6), 7.39-7.42 (1H, m, H-5'), 7.42-7.47 (1H, m, H-4), 7.55 (1H, td, *J* = 1.4, 7.6 Hz, H-5), 7.86 (1H, ddd, *J* = 0.5, 1.4, 7.8 Hz, H-3); ¹³C NMR (125 MHz; CDCl₃) δ_C 38.9 (2 × N-CH₃), 52.2 (-CH₃), 120.6 (C-4'), 122.4 (C-2'), 126.9 (C-6'), 127.9 (C-4), 128.6 (C-2), 129.4 (C-5'), 130.2 (C-3), 130.8 (C-6), 131.6 (C-5), 141.3 and 143.5 (C-1 and C-1'), 150.2 (C-3'); LRMS (ES⁺) *m/z* 336.2 [M+H]⁺; HRMS calcd for C₁₆H₂₁N₂O₅S [M+NH₄]⁺ 353.1166, found 353.1171; HPLC 99.6% in 0.1% formic acid (aq.)/MeCN (*R*_t 12.3 min); 99.7% in 0.1% ammonia (aq.)/MeCN (*R*_t 12.3 min).

**Methyl 3'-[(*N,N*-dimethylsulfamoyl)oxy]-[1,1'-biphenyl]-3-carboxylate
(67)**



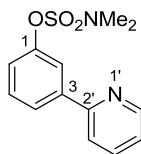
To a solution of **64** (68 mg, 0.212 mmol) in MeOH (1 mL, 4.7 mL/mmol), trimethylsilyl chloride (79 μ L, 92 mg, 0.847 mmol) was added in one portion, and the reaction mixture was stirred at room temperature for 40 h. After complete conversion, the solution was diluted with diethyl ether, and washed with sat. aq. NaHCO₃. The aqueous layer was extracted with Et₂O, and the combined organic layers were washed with brine, dried (MgSO₄), filtered, and evaporated *in vacuo*. Purification of the crude product by MPLC (gradient elution, 0-50% EtOAc/petrol) yielded the desired methyl ester (52 mg, 73%) as a colorless oil which solidified upon storage at room temperature giving an off-white solid. *R*_f 0.36 (33% EtOAc/petrol); m.p. 99.2-99.8 °C; λ_{max} (EtOH)/nm 254sh; ν_{max} /cm⁻¹ (neat) 1147 (s, SO₂^{sy}), 1360 (s, SO₂^{as}), 1455 (w, CH₃ def), 1715 (s, C=O); ¹H NMR (500 MHz; CDCl₃) δ_{H} 3.02 (6H, s, 2 \times N-CH₃), 3.96 (3H, s, CH₃), 7.31 (1H, ddd, *J* = 1.1, 2.4, 7.8 Hz, H-4'), 7.51 (1H, app. t, *J* = 7.8 Hz, H-5'), 7.51-7.57 (3H, m, H-Ar), 7.77 (1H, ddd, *J* = 1.2, 1.9, 7.8 Hz, H-4 or H-6), 7.98 (1H, m, H-4 or H-6), 8.19 (1H, m, H-2); ¹³C NMR (125 MHz; CDCl₃) δ_{C} 39.0 (2 \times N-CH₃), 52.4 (-CO₂CH₃), 120.6 (C-2' or C-6'), 121.0 (C-4'), 125.6 (C-2' or C-6'), 128.4 (C-2), 129.1 (C-4 or C-6), 129.2 (C-5), 130.3 (C-5'), 131.0 (C-3), 131.7 (C-4 or C-6), 140.2 (C-1), 142.3 (C-1'), 150.9 (C-3'), 167.0 (-CO₂Me); LRMS (ES⁺) *m/z* 336.3 [M+H]⁺; HRMS calcd for C₁₆H₁₈NO₅S [M+H]⁺ 336.0900, found 336.0908; HPLC 99.6% in 0.1% formic acid (aq.)/MeCN (*R*_t 8.7 min); 99.7% in 0.1% ammonia (aq.)/MeCN (*R*_t 8.7 min).

**Methyl 3'-[(*N,N*-dimethylsulfamoyl)oxy]-[1,1'-biphenyl]-4-carboxylate
(68)**



The acid **65** (40 mg, 0.124 mmol) was dissolved in methanol (0.2 mL, 1.6 mL/mmol), and a catalytic amount of conc. sulfuric acid was added (0.5 mg, 0.26 μ L, 5.1 μ mol). The reaction mixture was heated at 100 °C under microwave irradiation for 1.5 h. A solution of sat. aq. NaHCO₃ was added (0.5 mL), and the product was extracted with DCM (3 \times 5 mL). The combined organic layers were dried with MgSO₄, filtered, and the solvent was removed *in vacuo*. Purification by MPLC (gradient elution, 0-33% EtOAc/petrol) yielded the title compound as a colorless oil (24 mg, 57%), which solidified upon storage at room temperature. *R*_f 0.71 (50% EtOAc/petrol); m.p. 100.4-102.6 °C; λ_{max} (EtOH)/nm 268; ν_{max} /cm⁻¹ (neat) 1146 (m, SO₂^{sy}), 1179 (m, C-O), 1369 (s, SO₂^{as}), 1457 (w, CH₃ def), 1722 (s, C=O); ¹H NMR (500 MHz; CDCl₃) δ_{H} 3.02 (6H, s, 2 \times N-CH₃), 3.94 (3H, s, CH₃), 7.29-7.35 (1H, m, H-4'), 7.45-7.52 (1H, m, H-5'), 7.52-7.56 (2H, m, H-2' and H-6'), 7.65 (2H, d, *J* = 7.8 Hz, H-2 and H-6), 8.11 (2H, d, *J* = 7.8 Hz, H-3 and H-5); ¹³C NMR (125 MHz; CDCl₃) δ_{C} 39.0 (2 \times N-CH₃), 52.4 (-CO₂CH₃), 120.9 (C-2'), 121.4 (C-4'), 125.7 (C-6'), 127.3 (C-2 and C-6), 129.7 (C-4), 130.4 (C-3 and C-5), 130.5 (C-5'), 142.2 and 144.3 (C-1 and C-1'), 150.9 (C-3'), 167.0 (-CO₂Me); LRMS (ES⁺) *m/z* 336.3 [M+H]⁺; HRMS calcd for C₁₆H₁₈NO₅S [M+H]⁺ 336.0900, found 336.0907; HPLC 99.7% in 0.1% formic acid (aq.)/MeCN (*R*_t 12.9 min); >99.9% in 0.1% ammonia (aq.)/MeCN (*R*_t 12.9 min).

3-(Pyridin-2-yl)phenyl dimethylsulfamate (78)



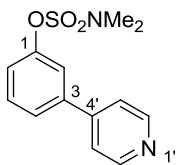
Potassium carbonate (259 mg, 1.87 mmol), copper(II) acetate (34 mg, 0.187 mmol), and 2-pyridyl MIDA boronate (131 mg, 0.56 mmol) were added to a solution of sulfamate **59** (105 mg, 0.375 mmol) in DMF (3.0 mL, 8 mL/mmol). After bubbling dry N₂ through the mixture for 2 min, Pd(dppf)Cl₂ · DCM (4.6 mg, 0.0056 mmol), and 2-propanol (0.75 mL, 2 mL/mmol) were added, and the mixture was heated at 100 °C for 40 min under microwave irradiation. The reaction mixture was diluted with aq. NaOH (1 M, 20 mL), and the product was extracted with Et₂O (3 × 30 mL). The combined organic phases were dried (MgSO₄), filtered, and the solvent was removed under high vacuum. The crude product was purified by MPLC (gradient elution, 0-50% EtOAc/petrol) to yield the title compound (51 mg, 48%) as a colorless oil giving a white solid upon storage at room temperature. *R_f* 0.53 (50% EtOAc/petrol); m.p. 57.9-59.7 °C; λ_{max} (EtOH)/nm 244, 275; ν_{max}/cm⁻¹ (neat) 1140 (s, SO₂^{sy}), 1173 (m, C-O), 1282 (m, ring def), 1366 (s, SO₂^{as}), 1450 (m, ring str); ¹H NMR (500 MHz; CDCl₃) δ_H 3.01 (6H, s, 2 × N-CH₃), 7.28 (1H, ddd, *J* = 1.1, 5.0, 7.5 Hz, H-3'), 7.36 (1H, ddd, *J* = 1.0, 2.3, 7.9 Hz, H-6), 7.50 (1H, app. t, *J* = 7.9 Hz, H-5), 7.75 (1H, m, H-5'), 7.78 (1H, m, H-4'), 7.92 (1H, m, H-4), 7.93 (1H, m, H-2), 8.71 (1H, m, H-6'); ¹³C NMR (125 MHz; CDCl₃) δ_C 39.0 (2 × N-CH₃), 120.5 (C-2), 121.0 (C-5'), 122.4 (C-6), 122.9 (C-3'), 125.3 (C-4), 130.2 (C-5), 137.3 (C-4'), 141.3 (C-3), 149.7 (C-6'), 150.9 (C-1), 155.9 (C-2'); LRMS (ES⁺) *m/z* 279.2 [M+H]⁺; HRMS calcd for C₁₃H₁₅N₂O₃S [M+H]⁺ 279.0798, found 279.0802; HPLC 99.6% in 0.1% formic acid (aq.)/MeCN (*R_t* 10.4 min); 98.4% in 0.1% ammonia (aq.)/MeCN (*R_t* 11.2 min).

3-(Pyridin-3-yl)phenyl dimethylsulfamate (79)



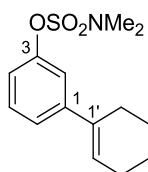
General procedure E was followed to synthesize compound **79** using the sulfamate **59** (150 mg, 0.54 mmol), pyridine 3-boronic acid (66 mg, 0.54 mmol), aq. Na₂CO₃ 2 M (0.54 mL, 1.0 mmol), Pd(dppf)Cl₂ · DCM (22 mg, 0.024 mmol), and DME (1.3 mL). Upon completion of the reaction, the mixture was partitioned between water and ethyl acetate. The aqueous layer was extracted with DCM (2 × 30 mL), and the combined organic layers were filtered through a Thiol MP SPE cartridge, dried (MgSO₄), filtered, and evaporated. The crude product was purified by MPLC (gradient elution, 0-100% EtOAc/petrol) to afford the desired compound (139 mg, 93%) as a colorless oil that solidified upon storage at room temperature to give a white solid. *R*_f 0.24 (75% EtOAc/petrol); m.p. 58.4-60.0 °C; λ_{max} (EtOH)/nm 244; ν_{max}/cm⁻¹ (neat) 1142 (s, SO₂^{sy}), 1178 (s, C-O), 1267 (m, ring def), 1360 (s, SO₂^{as}); ¹H NMR (500 MHz; CDCl₃) δ_H 3.02 (6H, s, 2 × N-CH₃), 7.30-7.36 (1H, m, H-6), 7.42 (1H, dd, *J* = 4.8, 7.9 Hz, H-5'), 7.48-7.53 (3H, m, H-2, H-4 and H-5), 7.91 (1H, ddd, *J* = 1.7, 2.4, 7.9 Hz, H-4'), 8.59-8.67 (1H, m, H-6'), 8.85 (1H, br, H-2'); ¹³C NMR (125 MHz; CDCl₃) δ_C 39.0 (2 × N-CH₃), 120.6 (C-2), 121.6 (C-6), 124.0 (C-5'), 125.5 (C-4), 130.7 (C-5), 135.2 (C-4'), 135.7 and 139.7 (C-3 and C-3'), 147.8 (C-6'), 148.6 (C-2'), 151.0 (C-1); LRMS (ES⁺) *m/z* 279.2 [M+H]⁺; HRMS calcd for C₁₃H₁₅N₂O₃S [M+H]⁺ 279.0798, found 279.0802; HPLC 99.9% in 0.1% formic acid (aq.)/MeCN (*R*_t 5.4 min); 99.9% in 0.1% ammonia (aq.)/MeCN (*R*_t 7.1 min).

3-(Pyridin-4-yl)phenyl dimethylsulfamate (80)



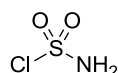
General procedure E was followed to synthesize compound **80** using sulfamate **59** (153 mg, 0.55 mmol), pyridine 4-boronic acid (67 mg, 0.55 mmol), aq. Na_2CO_3 2 M (0.54 mL, 1.0 mmol), $\text{Pd}(\text{dppf})\text{Cl}_2 \cdot \text{DCM}$ (22 mg, 0.024 mmol), and DME (1.3 mL). Upon completion of the reaction, the mixture was partitioned between water and ethyl acetate. The aqueous layer was extracted with EtOAc (2×30 mL); the combined organic layers were concentrated, and filtered through a Thiol MP SPE cartridge. The filtered solution was dried (MgSO_4), filtered, and evaporated. Purification by MPLC (DCM 100%) yielded the desired compound as a brown solid (72 mg, 49%). R_f 0.46 (10% MeOH/DCM); m.p. 55.8–57.1 °C; λ_{max} (EtOH)/nm 251; ν_{max} /cm $^{-1}$ (neat) 1143 (s, SO_2^{sy}), 1179 (s, C-O), 1361 (s, SO_2^{as}), 1460 (m, ring str), 1582 and 1592 (m, ring str); ^1H NMR (500 MHz; CDCl_3) δ_{H} 3.03 (6H, s, $2 \times \text{N-CH}_3$), 7.37 (1H, ddd, $J = 1.3, 2.3, 7.9$ Hz, H-6), 7.49–7.54 (3H, m, H-Ar, H-3' and H-5'), 7.54–7.57 (2H, m, H-2 and H-4), 8.69 (2H, d, $J = 3.7$ Hz, H-2' and H-6'); ^{13}C NMR (125 MHz; CDCl_3) δ_{C} 39.0 ($2 \times \text{N-CH}_3$), 120.5 (C-2), 121.8 (C-3' and C-5'), 122.3 (C-6), 125.4 (C-4), 130.7 (C-5), 140.3 and 147.2 (C-3 and C-4'), 150.5 (C-2' and C-6'), 151.0 (C-1); LRMS (ES^+) m/z 279.2 $[\text{M}+\text{H}]^+$; HRMS calcd for $\text{C}_{13}\text{H}_{15}\text{N}_2\text{O}_3\text{S}$ $[\text{M}+\text{H}]^+$ 279.0798, found 279.0802; HPLC 99.4% in 0.1% formic acid (aq.)/MeCN (R_t 4.6 min); 99.5% in 0.1% ammonia (aq.)/MeCN (R_t 7.1 min).

2',3',4',5'-Tetrahydro-[1,1'-biphenyl]-3-yl dimethylsulfamate (136)



Compound **136** was synthesized according to general procedure E using sulfamate **59** (138 mg, 0.50 mmol), 1-cyclohexen-1-yl boronic acid pinacol ester (103 mg, 0.50 mmol), aq. Na₂CO₃ (2 M, 0.50 mL, 1.1 mmol), [1,1'-bis(diphenylphosphino)ferrocene]dichloropalladium(II) · DCM complex (20 mg, 0.025 mmol), and DME (1.2 mL). The reaction mixture was diluted with water and EtOAc. The aqueous layer was extracted with EtOAc (3 × 25 mL). The combined organic layers were dried (MgSO₄), filtered, and the solvent was removed *in vacuo*. The crude product was purified by MPLC (gradient elution, 0-25% EtOAc/petrol) to afford the desired product (69 mg, 49%) as a colorless oil which solidified upon storage at room temperature to give a white solid. *R_f* 0.85 (50% EtOAc/petrol); m.p. 54.8-56.0 °C; λ_{max} (EtOH)/nm 249; ν_{max}/cm⁻¹ (neat) 1142 (s, SO₂^{sy}), 1178 (s, C-O), 1354 (s, SO₂^{as}), 1457 (w, CH₃ def), 1602 (w, C=C), 2938 (=C-H); ¹H NMR (500 MHz; CDCl₃) δ_H 1.66 (2H, m, -CH₂-), 1.78 (2H, m, -CH₂-), 2.21 (2H, m, -CH₂-), 2.38 (2H, m, -CH₂-), 2.97 (6H, s, 2 × N-CH₃), 6.16 (1H, m, -C=CH-), 7.12 (1H, dt, *J* = 2.2, 6.9 Hz, H-4), 7.25-7.33 (3H, m, H-5, H-2 and H-6); ¹³C NMR (125 MHz; CDCl₃) δ_C 22.2 (-CH₂-), 23.1 (-CH₂-), 26.0 (-CH₂-), 27.5 (-CH₂-), 38.9 (2 × N-CH₃), 118.4 (C-4), 119.6 (C-5), 123.3 (C-2), 126.4 (-C=CH-), 129.4 (C-6), 135.6 (C-1) 144.9 (-C=CH-), 150.5 (C-3); LRMS (ES⁺) *m/z* 282.3 [M+H]⁺; HRMS calcd for C₁₄H₂₀NO₃S [M+H]⁺ 282.1158, found 282.1162; HPLC 99.8% in 0.1% formic acid (aq.)/MeCN (*R_t* 13.9 min); 99.8% in 0.1% ammonia (aq.)/MeCN (*R_t* 14.0 min).

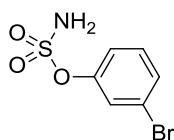
Sulfamoyl chloride (311)⁶⁵



Under an inert atmosphere, formic acid (0.55 g, 0.45 mL, 12 mmol) was added dropwise to neat chlorosulfonyl isocyanate (1.6 g, 1.0 mL, 12 mmol) at 0 °C with

gentle gas evolution. The resulting white slurry was stirred at room temperature for 3 h to give sulfamoyl chloride **311** as a white solid. Addition of anhydrous toluene (6.0 mL) yielded a solution (2 mmol/mL) of the reagent that was immediately used for the next step without further purification.

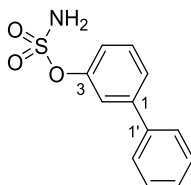
3-Bromophenyl sulfamate (**88**)¹⁹⁸



A freshly prepared solution of sulfamoyl chloride in toluene (6.0 mL, 12 mmol) was added dropwise to a solution of 3-bromophenol (1.0 g, 6.0 mmol) in DMA (6.0 mL, 1.0 mL/mmol) at 0 °C under an inert atmosphere. The resulting mixture was allowed to reach room temperature and stirred overnight. After careful addition of water (6.0 mL), the mixture was extracted with EtOAc (3 × 30 mL). The combined organic layers were washed with brine, dried (MgSO₄), filtered and the solvent was removed *in vacuo*. Purification by MPLC (gradient elution, 0-30% EtOAc/petrol) yielded the title compound as an off-white solid (1.31 g, 87%). *R*_f 0.30 (petrol/EtOAc 7:3); m.p. 89.1-90.5 °C (lit.¹⁹⁸ 90-91 °C); λ_{max} (EtOH)/nm 256sh, 267, 274sh ($\epsilon/\text{dm}^3 \text{ mol}^{-1} \text{ cm}^{-1}$ 600); $\nu_{\text{max}}/\text{cm}^{-1}$ (neat) 1164 (s, SO₂^{sy}), 1364 (s, SO₂^{as}), 1578 (m, NH₂ def), 3276 (m, NH₂^{sy}), 3374 (m, NH₂^{as}); ¹H NMR (500 MHz; CDCl₃) δ_{H} 4.98 (2H, br, -NH₂), 7.28-7.32 (2H, m, H-Ar), 7.45-7.49 (1H, m, H-Ar), 7.50-7.53 (1H, m, H-Ar); ¹³C NMR (125 MHz; CDCl₃) δ_{C} 121.0 (C-Ar), 125.56 (C-Ar), 130.7 (C-Ar), 131.1 (C-Ar), 150.3 (C-1). One quaternary carbon not detected; LRMS (ES⁻) *m/z* 250.0 and 252.0[M-H]⁻; HRMS calcd for C₆H₅⁷⁹BrNO₃S [M-H]⁻ 249.9179, found 249.9182.

NMR data match those previously reported for this compound.¹⁹⁸

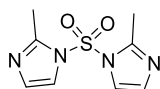
[1,1'-Biphenyl]-3-yl sulfamate (89)⁹³



Compound **41** was synthesized according to general procedure E using 3-bromophenyl sulfamate (53 mg, 0.210 mmol), phenyl boronic acid (24 mg, 0.20 mmol), Na₂CO₃ (2 M aq., 0.2 mL, 0.4 mmol), [1,1'-bis(diphenylphosphino)ferrocene]dichloropalladium(II) DCM complex (10 mg, 0.013 mmol), and DME (0.5 mL). The reaction mixture was diluted with water and EtOAc. The aqueous layer was extracted with DCM (2 × 20 mL). The combined organic layers were dried (MgSO₄), filtered, and the solvent was removed *in vacuo*. The crude product was purified by MPLC (gradient elution, 0-35% EtOAc/petrol) to afford the desired product (11 mg, 22%) as a white solid. *R*_f 0.78 (50% EtOAc/petrol); m.p. 88.9-93.6 °C (lit. 91-93 °C)⁶⁵; λ_{max} (EtOH)/nm 248 (ε /dm³ mol⁻¹ cm⁻¹ 49 000); ν_{max}/cm⁻¹ (neat) 1150 (s, SO₂^{sy}), 1364 (s, SO₂^{as}), 3311 (m, N-H), 3621 (m, N-H); ¹H NMR (500 MHz; CDCl₃) δ_H 5.01 (2H, s, -NH₂), 7.30 (1H, ddd, *J* = 1.2, 2.3, 8.1 Hz, H-Ar), 7.38 (1H, app. tt, *J* = 1.2, 6.5 Hz, H-Ar), 7.42-7.49 (3H, m, H-3', H-5' and H-Ar), 7.53-7.59 (4H, m, 2 × H-Ar, H-2' and H-6'); ¹³C NMR (125 MHz; CDCl₃) δ_C 120.8 (C-Ar), 120.9 (C-Ar), 126.1 (C-Ar), 127.3 (C-2' and C-6'), 128.2 (C-Ar), 129.1 (C-3' and C-5'), 130.3 (C-Ar), 139.7 and 143.6 (C-1 and C-1'), 150.6 (C-3); LRMS (ES⁻) *m/z* 248.2 [M-H]⁻; HPLC 98.6% in 0.1% formic acid (aq.)/MeCN (*R*_t 11.2 min); 98.8% in 0.1% ammonia (aq.)/MeCN (*R*_t 5.2 min).

NMR data match those previously reported for this compound.⁶⁵

1,1'-Sulfonylbis(2-methyl-1H-imidazole) (125)^{79,199}

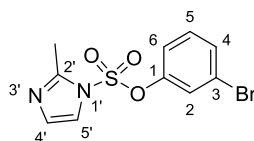


A solution of sulfonyl chloride (4.2 g, 31 mmol) in DCM (20 mL, 0.65 ml/mmol) was added dropwise at 0 °C to a suspension of 2-methylimidazole (10.2 g, 124

mmol) in DCM (50 mL, 0.4 mL/mmol). The resulting pale yellow solution was allowed to reach room temperature, and stirred for 24 h. At 0 °C, water was added to the reaction mixture, and the aqueous layer was extracted with DCM. The combined organic layers were washed with brine, dried (MgSO₄), filtered, and the solvent was removed *in vacuo*. Purification by MPLC (gradient elution, 0-10% MeOH/DCM) yielded the title compound (4.4 g, 63%) as an off-white solid. *R*_f 0.36 (5% MeOH/DCM); m.p. 87.9-92.6 °C (lit.¹⁹⁹ 90-91 °C); λ_{max} (EtOH) no maximum of absorption was detected; ν_{max}/cm⁻¹ (neat) 1147 (s, SO₂^{sy}), 1351 and 1378 (m, SO₂^{as}); ¹H NMR (500 MHz; CDCl₃) δ_H 2.53 (6H, s, -CH₃), 6.96 (2H, d, *J* = 1.8 Hz, C-4 or C-5), 7.39 (2H, d, *J* = 1.8 Hz, C-4 or C-5); ¹³C NMR (125 MHz; CDCl₃) δ_C 15.1 (-CH₃), 120.2 (C-4 or C-5), 128.7 (C-4 or C-5), 146.2 (-C-CH₃). LRMS (ES⁺) *m/z* 227.2 [M+H]⁺.

NMR data match those previously reported for this compound.¹⁹⁹

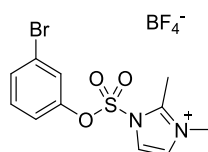
3-Bromophenyl 2'-methyl-1*H*-imidazole-1-sulfonate (**126**)^{79,93}



To a solution of the sulfonylbis(2-methyl-1*H*-imidazole) **125** (945 mg, 4.18 mmol) in acetonitrile (18.0 mL, 4.3 mL/mmol), 3-bromophenol (361 mg, 2.09 mmol), and cesium carbonate (748 mg, 2.30 mmol) were added in one portion at room temperature. The orange mixture was heated under microwave irradiation at 120 °C for 15 min. Upon completion of the reaction, the solvent was removed *in vacuo*, the residue was dissolved in saturated aqueous NH₄Cl, and extracted with EtOAc (3 × 45 mL). The combined organic layers were washed with water (20 mL), brine (20 mL), dried (MgSO₄), filtered, and evaporated. The crude product was purified by MPLC (gradient elution, 0-33% EtOAc/ petrol) to afford the desired compound (513 mg, 77%) as a pale yellow oil. *R*_f 0.63 (50% EtOAc/petrol); λ_{max} (EtOH)/nm 266; ν_{max}/cm⁻¹ (neat) 1150 (s, SO₂^{sy}), 1350 and 1384 (m, SO₂^{as}); ¹H NMR (500 MHz; CDCl₃) δ_H 2.51 (3H, s, -CH₃), 6.83 (1H, ddd, *J* = 0.9, 2.1, 8.3 Hz, H-4 or H-6), 6.91 (1H, d, *J* = 1.8 Hz, H-4'

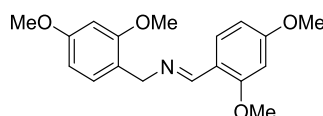
or H-5'), 7.14 (1H, d, $J = 1.8$ Hz, H-4' or H-5'), 7.18 (1H, t, $J = 2.1$ Hz, H-2), 7.24 (1H, t, $J = 8.3$ Hz, H-5), 7.51 (1H, ddd, $J = 0.9, 2.1, 8.3$ Hz, H-4 or H-6); ^{13}C NMR (125 MHz; CDCl_3) δ_{C} 15.1 (-CH₃), 120.3 (C-4 or C-6), 120.5 (C-4' or C-5'), 123.2 (C-3), 125.4 (C-2), 128.3 (C-4' or C-5'), 131.4 (C-5), 132.0 (C-4 or C-6), 146.9 (C-2'), 149.2 (C-1); LRMS (ES^+) m/z 317.1 and 319.1 $[\text{M}+\text{H}]^+$; HRMS calcd for $\text{C}_{10}\text{H}_{10}^{79}\text{BrN}_2\text{O}_3\text{S}$ $[\text{M}+\text{H}]^+$ 316.9596, found 316.9590.

1-[(3-Bromophenoxy)sulfonyl]-2,3-dimethyl-1*H*-imidazol-3-ium tetrafluoroborate (127)^{79,93}

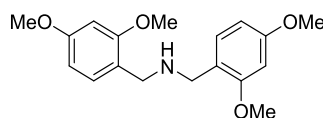


Trimethyloxonium tetrafluoroborate (278 mg, 1.88 mmol) was added in one portion to an iced cooled solution of the 2-methylimidazole sulfonate **59** (595 mg, 1.88 mmol) in dichloromethane (8.5 mL, 4.5 mL/mmol). The suspension was stirred at 0 °C for 1 h, and at room temperature overnight. Addition of cold petrol to the reaction mixture triggered the precipitation of the desired product as a white solid which was filtered and used for the subsequent step without further purification (yield assumed quantitative). LRMS (ES^+) m/z 331.1 and 333.1 $[\text{M}-\text{BF}_4]^+$.

bis(2,4-Dimethoxybenzyl)amine (131)^{79,93}



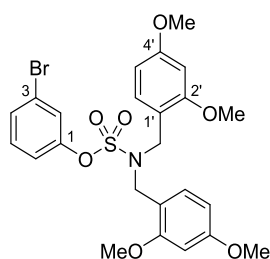
Under an inert atmosphere, 2,4-dimethoxybenzaldehyde (3.03 g, 18.0 mmol) was added in one portion to a solution of 2,4-dimethoxybenzylamine (3.00 g, 18.0 mmol) in EtOH (9.0 mL, 0.5 mL/mmol) together with MgSO_4 (a tip of a spatula). The mixture was stirred at 78 °C for 5 h; the reaction was monitored by TLC (5% MeOH/DCM + 2 drops of Et_3N).



The resulting imine was reduced by careful addition of sodium borohydride at 0 °C. The reaction mixture was stirred at room temperature for 2 d. The solvent was removed in vacuo, and the residue was partitioned between EtOAc (30 mL) and saturated aqueous NH₄Cl (20 mL). The aqueous layer was extracted with EtOAc (30 mL). The combined organic layers were washed with water (30 mL) and brine (30 mL), dried (MgSO₄), filtered, and the solvent was removed *in vacuo*. Purification by MPLC (gradient elution 0-10% MeOH/DCM) yielded the title compound (4.31, 75%) as a pale yellow oil which solidified upon storage at room temperature. *R*_f 0.33 (10% MeOH/DCM); λ_{max} (EtOH)/nm 276; ν_{max}/cm⁻¹ (neat) 1268 and 1286 (m, OCH₃), 2831 (w, C-H), 2937 (w, C-H); ¹H NMR (500 MHz; CDCl₃) δ_H 3.76 (4H, s, 2 × CH₂-), 3.79 (6H, s, 2 × -OCH₃), 3.82 (6H, s, 2 × -OCH₃), 6.41-6.45 (4H, m, 2 × H-3 and H-5), 7.20 (2H, d, *J* = 8.8 Hz, 2 × H-6); ¹³C NMR (125 MHz; CDCl₃) δ_C 48.1 (2 × -CH₂-), 55.4 (2 × -OCH₃), 55.5 (2 × -OCH₃), 98.6 (2 × C-3 or C-5), 103.9 (2 × C-3 or C-5), 130.8 (2 × C-6), 158.7 (2 × C-2 or C-4), 160.4 (2 × C-2 or C-4); LRMS (ES⁺) *m/z* 318.3 [M+H]⁺.

NMR data match those previously reported for this compound.²⁰⁰

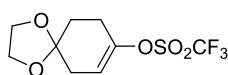
3-Bromophenyl bis(2',4'-dimethoxybenzyl)sulfamate (115)⁷⁹



A solution of the 2,3-dimethylimidazolium tetrafluoroborate **127** (701 mg, 1.7 mmol) in acetonitrile (10.0 mL) was added to a solution of the amine **131** (545 mg, 1.7 mmol) in acetonitrile (3.5 mL). The reaction mixture was stirred for 2 d at room temperature, and 17 h at 60 °C. The solvent was removed *in vacuo* to yield the crude product which was purified by MPLC (gradient elution 0-20%

EtOAc/petrol) to yield the title compound as a colorless oil (572 mg, 55% over two steps). R_f 0.16 (16% EtOAc/petrol; KMnO_4); λ_{max} (EtOH)/nm 276; $\nu_{\text{max}}/\text{cm}^{-1}$ (neat) 1154 (s, SO_2^{sy}), 1190 (s, C-O), 1260 and 1299 (m, OCH_3), 1371 (s, SO_2^{as}); ^1H NMR (500 MHz; CDCl_3) δ_{H} 3.75 (6H, s, $2 \times -\text{OMe}$), 3.81 (6H, s, $2 \times -\text{OMe}$), 3.93 (4H, s, $2 \times -\text{CH}_2$), 6.41 (2H, d, $J = 2.4$ Hz, H-Ar), 6.45 (2H, dd, $J = 2.4, 8.3$ Hz, H-Ar), 7.04 (1H, t, $J = 1.9$ Hz, H-Ar), 7.09 (1H, ddd, $J = 1.0, 2.4, 8.3$ Hz, H-Ar), 7.16 (1H, t, $J = 8.2$ Hz, H-Ar), 7.24-7.28 (1H, m, H-Ar), 7.33 (1H, ddd, $J = 1.0, 1.9, 8.0$ Hz, H-Ar); ^{13}C NMR (125 MHz; CDCl_3) δ_{C} 47.3 ($2 \times \text{N-CH}_2$), 55.3 ($2 \times \text{OCH}_3$), 55.6 ($2 \times \text{OCH}_3$), 98.4 ($2 \times \text{C-3'}$), 104.1 ($2 \times \text{C-5'}$), 116.68 ($2 \times \text{C-1'}$), 120.9 (C-Ar), 122.4 (C-3), 125.5 (C-Ar), 129.6 (C-Ar), 130.6 (C-Ar), 131.3 ($2 \times \text{C-6'}$), 150.9 (C-1), 158.6 ($2 \times \text{C-2'}$ or C-4'), 160.9 ($2 \times \text{C-2'}$ or C-4'); LRMS (ES^+) m/z 574.3 and 576.3 $[\text{M}+\text{Na}]^+$; HRMS calcd for $\text{C}_{24}\text{H}_{27}^{79}\text{BrNO}_7\text{S}$ $[\text{M}+\text{H}]^+$ 552.0686, found 552.0680.

1,4-Dioxaspiro[4.5]dec-7-en-8-yl trifluoromethanesulfonate (103)²⁰¹

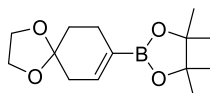


KHMDS (0.5 M soln. in toluene, 33.2 mL, 16.6 mmol) was added dropwise at -78 °C to a solution of 1,4-cyclohexanedione monoethylene acetal (2.00 g, 12.8 mmol) and *N*-phenyl-bis(trifluoromethylsulfonamide) (5.94 g, 16.6 mmol) in THF (128 mL, 10.0 mL/mmol), and the mixture was stirred at -78 °C for 3 h before cautious addition of water (50 mL). The phases were separated and the aqueous layer was extracted with diethyl ether (3×100 mL). The combined organic layers were washed with aq. 10% Na_2CO_3 (100 mL), dried (MgSO_4), filtered, and evaporated. Purification of the crude product by MPLC (gradient elution, 0-10% EtOAc/petrol) afforded the desired product (740 mg, 96%) as a light yellow oil. R_f 0.88 (Et_2O 100%; 2,4-DNP); λ_{max} (EtOH) no maximum of absorption was detected; $\nu_{\text{max}}/\text{cm}^{-1}$ (neat) 1210 (vs, C-F), 1417 (vs, SO_2^{str}), 1692 (w, C=C); ^1H NMR (500 MHz; CDCl_3) δ_{H} 1.88-1.93 (2H, m, $-\text{CH}_2-$), 2.38-2.44 (2H, m, CH_2-), 2.51-2.57 (2H, m, $-\text{CH}_2-$), 3.95-4.03 (4H, m, $2 \times -\text{O-CH}_2-$), 5.55-5.68 (1H, m, C=C-H); ^{13}C NMR (125 MHz; CDCl_3) δ_{C} 26.5 ($-\text{CH}_2-$), 31.2 ($-\text{CH}_2-$), 34.3 ($-\text{CH}_2-$),

64.8 (2 × O-CH₂-), 106.3 (O-C-O), 116.0 (C=C-H), 118.6 (-CF₃, *J* = 320 Hz), 148.3 (=C-OTf).

NMR data match those previously reported for this compound.²⁰²⁻²⁰³

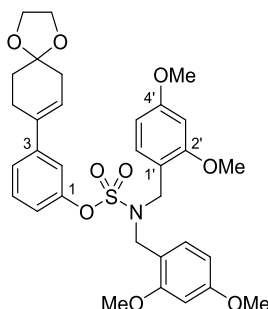
4,4,5,5-Tetramethyl-2-(1',4'-dioxaspiro[4'.5']dec-7'-en-8'-yl)-1,3,2-dioxaborolane (97)⁸⁹



Under an inert atmosphere, bis(pinacolato)diboron (585 mg, 2.30 mmol), Pd(dppf)Cl₂ · DCM (47 mg, 0.0576 mmol), 1,1'-(diphenylphosphino)ferrocene (32 mg, 0.0576 mmol), and potassium acetate (566 mg, 5.76 mmol) were added to a solution of the vinyl triflate **103** (553 mg, 1.92 mmol) in 1,4-dioxane (10.0 mL, 0.5 mL/mmol). The reaction mixture was heated at 80 °C overnight. Water (20 mL) was added, and the product was extracted with EtOAc (3 × 30 mL). The combined organic layers were washed with brine, dried (MgSO₄), filtered, and evaporated. The residue was dissolved in ethyl acetate and filtered through a Thiol MP SPE cartridge. The crude product was purified by MPLC (gradient elution, 0-100% Et₂O/petrol) to afford the desired boronic acid pinacol ester as a colorless oil (348 mg, 79%) which crystallized upon storage at room temperature. *R*_f 0.85 (Et₂O 100%; 2,4-DNP); m.p. 70.6-71.7 °C (lit.²⁰⁴ 58 °C); λ_{max} (EtOH) no maximum of absorption was detected; ν_{max}/cm⁻¹ (neat) 1250 and 1295 (m, O-C), 1368 and 1386 (s, B-O str.), 1415 (w, B-C str.), 1633 (m, C=C str), 2878 (CH₂^{as}), 2924 and 2986 (w, CH₂^{as}); ¹H NMR (500 MHz; CDCl₃) δ_H 1.25 (12H, s, 4 × CH₃), 1.71-1.76 (2H, m, -CH₂-), 2.32-2.41 (4H, m, 2 × -CH₂), 3.98 (4H, s, 2 × O-CH₂-), 6.47 (1H, s, C=C-H); ¹³C NMR (125 MHz; CDCl₃) δ_C 25.0 (4 × -CH₃), 25.9 (-CH₂-), 31.2 (-CH₂-), 37.2 (-CH₂-), 64.5 (O-CH₂-), 83.4 (2 × -C(CH₃)₂), 108.0 (O-C-O), 139.7 (C=C-H); LRMS (ES⁺) *m/z* 267.3 [M+H]⁺; HRMS calcd for C₁₄H₂₄BO₄ [M+H]⁺ 267.1762, found 267.1755.

NMR data match those previously reported for this compound.²⁰⁴

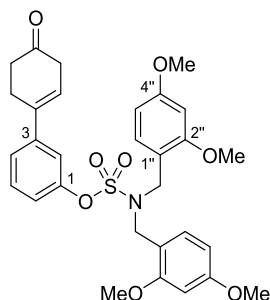
3-(1',4'-Dioxaspiro[4'.5']dec-7'-en-8'-yl)phenyl bis(2'',4''-dimethoxybenzyl)sulfamate (116)



The title compound was synthesized according to general procedure E using the 3-bromosulfamate **115** (572 mg, 1.04 mmol), boronic acid pinacol ester **97** (277 mg, 1.04 mmol), Na₂CO₃ (2 M aq., 1 mL, 2.0 mmol), Pd(dppf)Cl₂ · DCM (42 mg, 0.052 mmol) and DME (2.4 mL, 2.3 mL/mmol). The reaction mixture was diluted with water, and extracted with EtOAc (3 × 20 mL). The combined organic layers were washed with brine, dried (MgSO₄), filtered and the solvent was removed *in vacuo*. The crude product was purified by MPLC (gradient elution, 0-50% EtOAc/petrol) to afford the title compound (552 mg, >99%) as a colorless oil which solidified upon storage at room temperature to give a light brown solid. *R*_f 0.35 (50% EtOAc/petrol; UV 254 nm, KMnO₄ and 2,4-DNP); m.p. 102.9-104.5 °C; λ_{max} (EtOH) 279sh; ν_{max}/cm⁻¹ (neat) 1135 (m, SO₂^{sy}), 1252 and 1298 (m, OCH₃), 1353 and 1364 (m, SO₂^{as}), 1588 (m, C=C ar), 1612 (m, C=C aromatic str), 2946 (w, C-H and -CH₂- aliphatic); ¹H NMR (500 MHz; CDCl₃) δ_H 1.90 (2H, t, *J* = 6.4 Hz, -C(O-CH₂-CH₂-O)-CH₂-CH₂-), 2.44-2.49 (2H, m, -CH₂-CH=), 2.54-2.61 (2H, m, -C(O-CH₂-CH₂-O)-CH₂-CH₂-), 3.71 (6H, s, 2 × -OCH₃), 3.79 (6H, s, 2 × -OCH₃), 3.99-4.06 (4H, m, 2 × CH₂-O), 4.43 (4H, s, 2 × N-CH₂-), 5.92-5.97 (1H, m, C=C-H), 6.38 (2H, d, *J* = 2.3 Hz, 2 × H-3'), 6.43 (2H, dd, *J* = 2.3, 8.3 Hz, 2 × H-5'), 6.97-7.02 (2H, m, H-Ar), 7.19-7.25 (2H, m, H-Ar), 7.26-7.29 (2H, m, 2 × H-6'); ¹³C NMR (125 MHz; CDCl₃) δ_C 26.7 (-C(O-Et-O)-CH₂-CH₂-), 31.4 (-C(O-Et-O)-CH₂-CH₂-), 36.2 (-CH₂-CH=C), 46.9 (2 × N-CH₂-), 55.2 (2 × OCH₃), 55.5 (2 × -OCH₃), 64.6 (2 × CH₂-O), 98.3 (2 × C-3'), 104.1 (2 × C-5'), 107.7 (-O-C-O-), 116.8 (2 × C-1'), 118.8 (C-Ar), 120.3 (C-Ar), 122.8 (C=C-H), 123.2 (C-Ar), 129.2 (C-Ar),

131.1 (2 × C-6'), 135.3 (C-Ar), 143.2 (C-3), 150.6 (C-1), 158.6 (2 × C-2' or C-4'), 160.7 (2 × C-2' or C-4'); LRMS (ES⁺) *m/z* 634.4 [M+Na]⁺; HRMS calcd for C₃₂H₃₈NO₉S [M+H]⁺ 612.2262, found 612.2261.

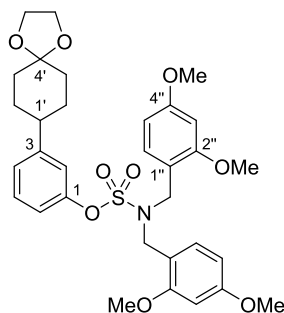
4'-Oxo-2',3',4',5'-tetrahydro-[1,1'-biphenyl]-3-yl bis(2'',4''-dimethoxybenzyl)sulfamate (117)



To a solution of the ketal **116** (152 mg, 0.248 mmol, 1 equiv.) in acetone (4 mL, 16 mL/mmol) and water (1 mL, 4 mL/mmol) was added *p*-toluenesulfonic acid (47 mg, 0.247 mmol, 1 equiv.) and the mixture was heated under microwave irradiation at 60 °C for 1 h. The solvent was removed *in vacuo* and the residue was dissolved in NaHCO₃ (aq., 5% v/v). The product was extracted with EtOAc (3 × 25 mL), and the combined organic layers were dried (MgSO₄), filtered, and evaporated. Purification by MPLC (gradient elution, 0-50% EtOAc/petrol) of the crude product yielded the title compound as a colorless oil (102 mg, 72%). *R*_f 0.36 (petrol/EtOAc; stain UV 254 nm); λ_{max} (EtOH)/nm 276; ν_{max}/cm⁻¹ (neat) 1130 (s, SO₂^{sy}), 1157 (s, C-O), 1265 and 1291(m, O-C), 1369 (s, SO₂^{as}), 1587 (m, C=C ar), 1611 (s, C=C aromatic str), 1686 (m, C=O), 2838, 2937 and 2957 (w, C-H and -CH₂- aliphatic); ¹H NMR (500 MHz; CDCl₃) δ_H 2.66 (2H, t, *J* = 6.9 Hz, -CO-CH₂-CH₂-), 2.83 (2H, m, -CO-CH₂-CH₂-), 3.09 (2H, m, -CH₂-CH=C), 3.75 (6H, s, 2 × OCH₃), 3.82 (6H, s, 2 × OCH₃), 4.48 (4H, s, 2 × N-CH₂), 6.07 (1H, m, =C-H), 6.42 (2H, d, *J* = 2.4 Hz, 2 × H-3''), 6.47 (2H, dd, *J* = 2.4, 8.3 Hz, 2 × H-5''), 7.04 (1H, app. t, *J* = 2.0 Hz, H-Ar), 7.07 (1H, ddd, *J* = 1.1, 2.4, 7.9 Hz, H-Ar), 7.27 (1H, m, H-Ar), 7.30 (1H, m, H-Ar), 7.30 (2H, t, *J* = 8.3 Hz, 2 × H-6''); ¹³C NMR (125 MHz; CDCl₃) δ_C 27.8 (-CO-CH₂-CH₂-), 38.7 (-CO-CH₂-CH₂-), 40.0 (-CH₂-CH=C), 46.9 (2 × N-CH₂), 55.2 (2 × OCH₃), 55.5 (2 × OCH₃), 98.3 (2 × C-3''), 104.1 (2 × C-5''), 116.6 (2 × C-1''), 118.9 (C-Ar), 120.9 (C-Ar), 122.2 (C=C-H), 123.2 (C-Ar), 129.6 (C-Ar),

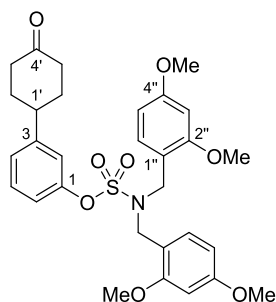
131.1 (2 × C-6'), 136.8 (C-1'), 142.4 (C-3), 150.7 (C-1), 158.6 (2 × C-2' or C-4'), 160.7 (2 × C-2' or C-4'), 209.7 (C=O); LRMS (ES⁺) *m/z* 590.4 [M+Na]⁺.

3-(1',4'-Dioxaspiro[4.5]decan-8-yl)phenyl bis(2'',4''-dimethoxybenzyl)sulfamate (132)



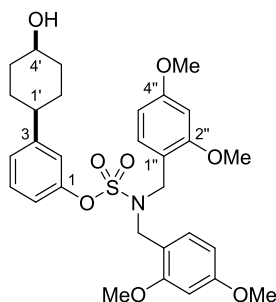
A solution of **116** (1.01 g, 1.65 mmol) in EtOH/THF 4:1 (66 mL, 40 mL/mmol) was hydrogenated over 10% Pd/C in a flow reactor (1.0 mL/min) for 5.5 h with recycling of the reaction mixture. Solvent was removed *in vacuo* to obtain compound **132**. The title compound (colorless oil; 0.97 g, 96%) was used in the following step without further purification. *R_f* 0.44 (50% EtOAc/petrol; 254 nm, KMnO₄, DNP); λ_{max} (EtOH)/nm 277, 283sh; ν_{max}/cm⁻¹ (neat) 1130 (s, SO₂^{sy}), 1158 (s, C-O), 1173 (s, C-O-C-O-C vib), 1267 and 1292 (m, O-C), 1374 (m, SO₂^{as}), 1612 (s, C=C aromatic str); ¹H NMR (500 MHz; CDCl₃) δ_H 1.62-1.68 (4H, m, cyclohexyl H^{ax}), 1.78-1.90 (4H, m, H^{eq}), 2.44-2.55 (1H, m, -CH-Ar), 3.71 (6H, s, 2 × OCH₃), 3.79 (6H, s, 2 × OCH₃), 3.98 (4H, s, -O-CH₂-CH₂-O-), 4.43 (4H, s, 2 × N-CH₂-), 6.39 (2H, d, *J* = 2.4 Hz, 2 × H-3''), 6.44 (2H, dd, *J* = 2.4, 8.5 Hz, 2 × H-5''), 6.82-6.87 (1H, m, H-Ar), 6.93-7.00 (1H, m, H-Ar), 7.06-7.13 (1H, m, H-Ar), 7.22 (1H, app. t, *J* = 8.0 Hz, H-5), 7.27 (2H, t, *J* = 8.5 Hz, 2 × H-6''); ¹³C NMR (125 MHz; CDCl₃) δ_C 31.5 (2 × CH₂), 35.3 (2 × CH₂), 43.3 (CH-Ar), 46.9 (2 × N-CH₂-), 55.2 (2 × -OCH₃), 55.5 (2 × -OCH₃), 64.4 (-O-CH₂-CH₂-O-), 98.4 (2 × C-3''), 104.1 (2 × C-5''), 108.5 (C-4'), 116.8 (2 × C-1''), 119.8 (C-Ar), 120.6 (C-Ar), 125.1 (C-Ar), 129.6 (C-Ar), 131.1 (2 × C-6''), 148.5 (C-Ar), 150.6 (C-1), 158.6 (2 × C-2'' or C-4''), 160.7 (2 × C-2'' or C-4''); LRMS (ES⁺) *m/z* 636.6 [M+Na]⁺; HRMS calcd for C₃₂H₄₀NO₉S [M+H]⁺ 614.2418, found 614.2412.

3-(4'-Oxocyclohexyl)phenyl bis(2'',4''-dimethoxybenzyl)sulfamate (**118**)



The ketone **118** was prepared according to general procedure F using the ketal **132** (0.87 g, 1.42 mmol), a mixture of THF (10 mL), water (30 mL) and acetic acid (60 mL). Purification by MPLC (gradient elution, 0-10% MeOH/DCM) yielded the title compound (0.70 g, 87%) as a pale yellow oil which solidified upon storage at RT to give a white solid. R_f 0.48 (50% EtOAc/petrol); m.p. 125.2-126.5 °C; λ_{max} (EtOH)/nm 278; ν_{max}/cm^{-1} (neat) 1125 (s, SO₂^{sy}), 1157 (s, C-O), 1371 (s, SO₂^{as}), 1710 (m, C=O), 2939 (w, C-H and -CH₂- aliphatic); ¹H NMR (500 MHz; CDCl₃) δ_H 1.72–1.88 (2H, m, 2 × CH^{eq}H^{ax}-CHAR), 2.09–2.20 (2H, m, 2 × CH^{eq}H^{ax}-CHAR), 2.42–2.55 (4H, m, 2 × CH₂-CO), 2.95 (1H, tt, J = 3.2, 12.1 Hz, CH-Ar), 3.72 (6H, s, 2 × -OCH₃), 3.80 (6H, s, 2 × -OCH₃), 4.42 (4H, s, 2 × N-CH₂-), 6.40 (2H, d, J = 2.4 Hz, 2 × H-3''), 6.45 (2H, dd, J = 2.4, 8.5 Hz, 2 × H-5''), 6.77 (1H, t, J = 1.9 Hz, H-Ar), 6.99–7.03 (1H, m, H-Ar), 7.07–7.12 (1H, m, H-Ar), 7.24 (1H, s, H-Ar), 7.29 (2H, t, J = 8.5 Hz, 2 × H-6''); ¹³C NMR (125 MHz; CDCl₃) δ_C 33.8 (2 × CH₂-CHAR), 41.3 (2 × CH₂-CO), 42.4 (CH-Ar), 46.9 (2 × N-CH₂), 55.2 (2 × OCH₃), 55.4 (2 × OCH₃), 98.2 (2 × C-3''), 104.1 (2 × C-5''), 116.5 (2 × C-1''), 120.2 (C-Ar), 120.4 (C-Ar), 125.0 (C-Ar), 129.7 (C-Ar), 131.0 (2 × C-6''), 146.6 (C-Ar), 150.7 (C-1), 158.5 (2 × C-2'' or C-4''), 160.7 (2 × C-2'' or C-4''), 210.7 (C=O); LRMS (ES⁺) m/z 592.5 [M+Na]⁺; HRMS calcd for C₃₀H₃₉N₂O₈S [M+NH₄]⁺ 587.2422, found 587.2391.

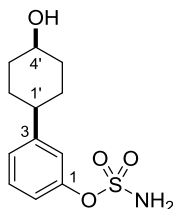
3-(*cis*-4'-Hydroxycyclohexyl)phenyl bis(2'',4''-dimethoxybenzyl)sulfamate (119)



A solution of lithium tri-*sec*-butylborohydride (1.0 M in THF, 0.73 mL, 0.73 mmol) was added dropwise to a solution of **119** (345 mg, 0.61 mmol) in THF (10 mL, 16 mL/mmol) at -78 °C. The solution was stirred at -78 °C for 1 h. The unreacted L-Selectride was quenched by addition of NH₄Cl (sat. aq., 2 mL) at 0 °C. The mixture was diluted with water (10 mL) and extracted with ethyl acetate (3 × 25 mL). The combined organic layers were washed with brine, dried (MgSO₄), filtered, and the solvent was removed *in vacuo*. Purification by MPLC (gradient elution, 0-75% EtOAc/petrol) yielded the title compound (240 mg, 69%) as a pale yellow oil (formation of the *trans*-diastereoisomer **118** was also observed even though the compound was not isolated). *R*_f 0.26 (50% EtOAc/petrol; KMnO₄, DNP); λ_{max} (EtOH)/nm 278; ν_{max}/cm⁻¹ (neat) 1127 (s, SO₂^{sy}), 1158 (s, C-O), 1267 and 1291 (m, O-C), 1369 (s, SO₂^{as}), 1588 (m, C=C ar), 1611 (s, C=C str), 2932 (w, C-H and -CH₂- aliphatic); ¹H NMR (500 MHz; CDCl₃) δ_H 1.52 (1H, br, O-H), 1.58–1.64 (2H, m, 2 × CH^{eq}H^{ax}-CHAr), 1.64–1.71 (2H, m, 2 × CH^{eq}H^{ax}-CHOH), 1.72–1.84 (2H, m, 2 × CH^{eq}H^{ax}-CHAr), 1.84–1.94 (2H, m, 2 × CH^{eq}H^{ax}-CHOH), 2.41–2.52 (1H, m CH-Ar), 3.71 (6H, s, 2 × OCH₃), 3.80 (6H, s, 2 × OCH₃), 4.09–4.14 (1H, m, CH-OH), 4.43 (4H, s, 2 × N-CH₂-), 6.41 (2H, d, *J* = 2.4 Hz, 2 × H-3''), 6.45 (2 H, dd, *J* = 2.4, 8.4 Hz, 2 × H-5''), 6.78 (1H, t, *J* = 2.0 Hz, H-Ar), 6.98 (1H, ddd, *J* = 1.1, 2.4, 8.1 Hz, H-Ar), 7.04–7.12 (1H, m, H-Ar), 7.22 (1H, t, *J* = 7.9 Hz, H-Ar), 7.28 (2H, d, *J* = 8.4 Hz, 2 × H-6''); ¹³C NMR (125 MHz; CDCl₃) δ_C 27.6 (2 × CH₂-CHAr), 33.1 (2 × CH₂-CHOH), 43.7 (CH-Ar), 46.8 (2 × N-CH₂), 55.2 (2 × OCH₃), 55.5 (2 × OCH₃), 65.6 (-CH-OH), 98.3 (2 × C-3''), 104.1 (2 × C-5''), 116.8 (2 × C-1''), 119.7 (C-Ar), 120.4 (C-Ar), 125.1 (C-Ar), 129.4 (C-Ar), 131.1 (2

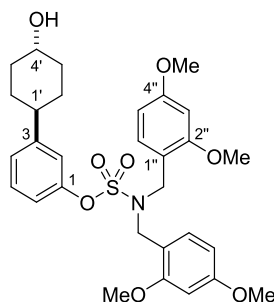
× C-6''), 149.3 (C-Ar), 150.7 (C-Ar), 158.6 (2 × C-2'' or C-4''), 160.6 (2 × C-2'' or C-4''); LRMS (ES⁺) *m/z* 572.5 [M+H]⁺; HRMS calcd for C₃₀H₃₈NO₈S [M+H]⁺ 572.2313, found 572.2305.

3-(*cis*-4'-Hydroxycyclohexyl)phenyl sulfamate (**110**)



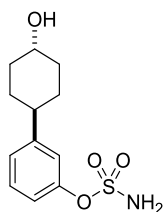
Compound **110** was synthesized according to general procedure G using the alcohol **119** (261 mg, 0.457 mmol), DCM (6.4 mL), and TFA (0.7 mL). Complete conversion was reached after 1 h. The pure product (pale brown solid, 65 mg, 53%) was obtained by MPLC (gradient elution, 0-50% EtOAc/petrol). *R_f* 0.23 (50% EtOAc/petrol; KMnO₄); m.p. 119.4-120.8 °C; λ_{max} (EtOH)/nm 261, 280sh; ν_{max}/cm⁻¹ (neat) 1176 (s, SO₂^{sy}), 1366 (s, SO₂^{as}), 1582 (m), 2952 (m), 3302 (m), 3519 (m); ¹H NMR (500 MHz; CD₃OD) δ_H 1.55 – 1.73 (4H, m, CH^{ax}), 1.81 – 1.98 (4H, m, CH^{eq}), 2.55-2.64 (1H, m, CH-Ar), 3.99 – 4.07 (1H, m, H-Ar), 7.12 (1H, ddd, *J* = 1.1, 2.4, 8.1 Hz, H-Ar), 7.20 (2H, m, H-Ar), 7.32 (1H, t, *J* = 8.1 Hz, H-5); ¹³C NMR (125 MHz; CD₃OD) δ_C 28.8 (2 × CH₂-CHAr), 33.6 (2 × CH₂-CHOH), 44.9 (CH-Ar), 66.2 (-CH-OH), 120.7 (C-Ar), 121.8 (C-Ar), 126.3 (C-Ar), 130.4 (C-5), 151.0 (C-Ar q), 152.1 (C-Ar q); LRMS (ES⁻) *m/z* 270.3 [M-H]⁻; HRMS calcd for C₁₂H₁₆NO₄S [M-H]⁻ 270.0806, found 270.0796; HPLC 96.6% in water/MeCN (*R_t* 6.1 min); 98.0% in 0.1% formic acid (aq.)/MeCN (*R_t* 6.1 min); 98.0% in 0.1% ammonia (aq.)/MeCN (*R_t* 3.8 min).

3-(*trans*-4'-Hydroxycyclohexyl)phenyl bis(2'',4''-dimethoxybenzyl)sulfamate (120)



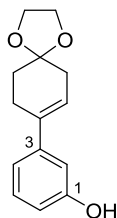
NaBH₄ (46 mg, 1.2 mmol) was added to a solution of **118** (345 mg, 0.61 mmol) in EtOH/THF 3:1 (28 mL), at -78 °C. The reaction mixture was stirred at -78 °C for 1.5 h and it was poured into iced saturated NH₄Cl (aq., 50 mL) to quench the unreacted sodium borohydride. The product was extracted with EtOAc (3 × 50 mL) and the combined organic layers were washed with brine, dried (MgSO₄), filtered and evaporated. Purification by MPLC (gradient elution, 0-75% EtOAc/petrol) yielded the desired compound (270 mg, 78%) as an oil which solidified to give a white amorphous solid (19 mg, 5.5% yield of the *cis*-diastereoisomer **119** were also obtained as an oil). *R*_f 0.15 (50% EtOAc/petrol); λ_{max} (EtOH)/nm 278; ν_{max}/cm⁻¹ (neat) 1127 (s, SO₂^{sy}), 1157 (s, C-O), 1370 (s, SO₂^{as}), 1586 (m, C=C ar), 1612 (s, C=C str), 2558 and 2931 (w, C-H and -CH₂-aliphatic); ¹H NMR (500 MHz; CDCl₃) δ_H 1.34–1.48 (4H, m, CH, 4 × CH^{eq}H^{ax}), 1.81–1.93 (2H, m, 2 × CH^{eq}H^{ax}), 2.04–2.13 (2H, m, 2 × CH^{eq}H^{ax}), 2.38–2.48 (1H, m, CH-Ar), 3.63–3.70 (1H, m, CHOH), 3.72 (6H, s, 2 × OCH₃), 3.80 (6H, s, 2 × OCH₃), 4.42 (4H, s, 2 × N-CH₂), 6.40 (2H, d, *J* = 2.4 Hz, 2 × H-3''), 6.45 (2H, dd, *J* = 2.4, 8.4 Hz, 2 × H-5''), 6.74–6.79 (1H, m, H-Ar), 6.97 (1H, ddd, *J* = 1.0, 2.4, 8.0 Hz, H-Ar), 6.95–7.00 (1H, m, H-Ar), 7.15 (1H, t, *J* = 8.0 Hz, H-5), 7.20 (1H, d, *J* = 8.4 Hz, 2 × H-6''); ¹³C NMR (125 MHz; CDCl₃) δ_C 32.2 (2 × CH₂-CHAr), 35.8 (2 × CH₂-CHOH), 43.1 (CH-Ar), 46.6 (2 × N-CH₂-), 55.1 (2 × -OCH₃), 55.4 (2 × -OCH₃), 70.4 (-CH-OH), 98.2 (2 × C-3''), 104.0 (2 × C-5''), 116.6 (2 × C-1''), 119.8 (C-Ar), 120.2 (C-Ar), 125.0 (C-Ar), 129.4 (C-Ar), 131.0 (2 × C-6''), 148.4 (C-Ar), 150.5 (C-Ar), 158.5 (2 × C-2'' or C-4''), 160.6 (2 × C-2'' or C-4''); LRMS (ES⁺) *m/z* 594.6 [M+Na]⁺; HRMS calcd for C₃₀H₃₈NO₈S [M+H]⁺ 572.2313, found 572.2301.

3-(*trans*-4'-Hydroxycyclohexyl)phenyl sulfamate (**111**)



Compound **111** was obtained according to general procedure G using the alcohol **120** (270 mg, 0.47 mmol), DCM (6.4 mL), and TFA (0.7 mL). The reaction mixture was stirred overnight at RT. The crude product was purified by MPLC (gradient elution, 0-50% EtOAc/petrol) to give the title compound (59 mg, 46%) as an oil which solidified to give an off-white solid. R_f 0.16 (50% EtOAc/petrol; KMnO_4); m.p. 136.4-136.7 °C; λ_{max} (EtOH)/nm 262; $\nu_{\text{max}}/\text{cm}^{-1}$ (neat) 1186 (s, SO_2^{sy}), 1360 (s, SO_2^{as}), 1585 (m, NH_2 def), 3303 (m, N-H); ^1H NMR (500 MHz; CD_3OD) δ_{H} 1.35–1.48 (2H, m, $\text{CHH}^{\text{ax}}\text{-CHOH}$), 1.49–1.64 (2H, m, $\text{CHH}^{\text{ax}}\text{-CHAr}$), 1.83–1.97 (2H, m, $\text{CHH}^{\text{eq}}\text{-CHAr}$), 1.98–2.12 (2H, m, $\text{CHH}^{\text{eq}}\text{-CHOH}$), 2.54 (1H, tt, $J = 3.4, 12.0$ Hz, CH-Ar), 3.60 (1H, tt, $J = 4.3, 11.0$ Hz, CH-OH), 7.12 (1H, m, H-Ar), 7.16–7.20 (2H, m, H-Ar), 7.29–7.34 (1H, m, H-5). ^{13}C NMR (125 MHz; CD_3OD) δ_{C} 33.5 ($2 \times \text{CH}_2\text{-CHAr}$), 36.5 ($2 \times \text{CH}_2\text{-CHOH}$), 44.7 (CH-Ar), 71.02 ($-\text{CH-OH}$), 120.8 (C-Ar), 121.8 (C-Ar), 126.2 (C-Ar), 130.5 (C-5), 150.2 (C-Ar q), 152.1 (C-Ar q); LRMS (ES^-) m/z 270.2 [M-H] $^-$; HRMS calcd for $\text{C}_{12}\text{H}_{16}\text{NO}_4\text{S}$ [M-H] $^-$ 270.0806, found 270.0796; HPLC 97.6% in water/MeCN (R_t 5.8 min); 98.0% in 0.1% formic acid (aq.)/MeCN (R_t 5.8 min); 98.7% in 0.1% ammonia (aq.)/MeCN (R_t 3.4 min).

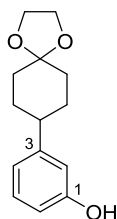
3-(1',4'-Dioxaspiro[4'.5']dec-7'-en-8'-yl)phenol (**106**)



Procedure 1: compound **106** was synthesized following general procedure E using the triflate **103** (219 mg, 0.76 mmol), the boronic ester **114** (167 mg, 0.76 mmol), sodium carbonate (2 M aq., 0.76 mL, 1.52 mmol), $[\text{Pd}(\text{dppf})\text{Cl}_2]$ (31 mg,

0.038 mmol) and DME (1.8 mL, 2.4 mL/mmol). Complete conversion was reached after 15 min. The crude product was purified by MPLC (gradient elution, 0-40% EtOAc/petrol) to yield the title compound (113 mg, 64%) as a yellow oil. *Procedure 2*: compound **106** was synthesized according to general procedure E using 3-bromophenol (250 mg, 1.44 mmol), the boronic ester **97** (383 mg, 1.44 mmol), sodium carbonate (2 M aq., 1.44 mL, 2.88 mmol), [Pd(dppf)Cl₂] (59 mg, 0.072 mmol) and DME (3.5 mL, 2.4 mL/mmol). The reaction mixture was heated under microwave irradiation for 45 min. The crude product was purified by MPLC (gradient elution, 0-40% EtOAc/petrol) to yield the title compound (95 mg, 28%) as a yellow oil. *R_f* 0.46 (40% EtOAc/petrol); λ_{max} (EtOH)/nm 246, 288; ν_{max} /cm⁻¹ (neat) 1282 (s, O-C), 1580 (s, C=C), 2888 and 2924 (m, C-H and -CH₂- aliphatic), 3339 (br, O-H); ¹H NMR (500 MHz; CDCl₃) δ_{H} 1.88–1.96 (2H, m, -CH₂-C-Ar), 2.41–2.50 (2H, m, -CH₂-CH=C), 2.58–2.69 (2H, m, -C(O-CH₂CH₂-O)-CH₂-CH₂-), 4.03 (4H, s, O-CH₂-CH₂-O), 5.95–5.99 (1H, m, CH=CAr), 6.67–6.72 (1H, m, H-Ar), 6.83–6.86 (1H, m, H-2), 6.94–6.99 (1H, m, H-Ar), 7.16 (1 H, t, *J* = 7.9 Hz, H-5); ¹³C NMR (125 MHz; CDCl₃) δ_{C} 26.9 (-C(O-CH₂CH₂-O)-CH₂-CH₂-), 31.5 (-CH₂-C-Ar), 36.3 (-CH₂-CH=C), 64.6 (O-CH₂-CH₂-O), 107.9 (O-C-O), 112.4 (C-2), 113.9 (C-Ar), 118.0 (C-Ar), 122.0 (CH=C-Ar), 129.5 (C-5), 136.1 (CH=C-Ar), 143.4 (C-Ar q), 155.6 (C-Ar q); LRMS (ES⁺) *m/z* 233.3 [M+H]⁺.

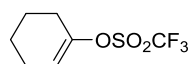
3-(1',4'-Dioxaspiro[4.5]decan-8'-yl)phenol (**107**)



A solution of **106** (387 mg, 1.65 mmol) in ethanol (56 mL, 34 mL/mmol) was passed over a 10% Pd/C catalyst cartridge embedded in a Thales H-cube. Flow rate, H₂ pressure, and temperature were set according to the manufacture instructions (full H₂ mode, 40 °C, 2 h 45 min). Upon completion of the reaction, the solvent was removed *in vacuo*. The product (white solid; 371 mg, 96%) was

used in the next step without further purification. R_f 0.30 (25% EtOAc/petrol); m.p. 97.8-98.9 °C; λ_{\max} (EtOH)/nm 273; $\nu_{\max}/\text{cm}^{-1}$ (neat) 1280 (s, O-C), 2932 (m, C-H and -CH₂- aliphatic), 3295 (m, O-H); ¹H NMR (500 MHz; CDCl₃) δ_H 1.62–1.90 (8H, m, 4 × CH₂), 2.51 (1H, tt, J = 3.4, 11.9 Hz, CH-Ar), 3.98 (4H, s, O-CH₂-CH₂-O), 6.66 (1H, ddd, J = 1.0, 2.5, 7.9 Hz, H-6), 6.69–6.74 (1H, m, H-2), 6.77–6.86 (1H, m, H-4), 7.15 (1H, t, J = 7.9 Hz, H-5); ¹³C NMR (125 MHz; CDCl₃) δ_C 31.6 (2 × CH₂), 35.2 (2 × CH₂), 43.3 (CH-Ar), 64.4 (-O-CH₂-CH₂-O-), 64.5 (-O-CH₂-CH₂-O-), 108.7 (O-C-O), 113.1 (C-Ar), 113.9 (C-2), 119.6 (C-Ar), 129.6 (C-5), 148.8 (C-Ar q), 155.7 (C-Ar q); LRMS (ES⁺) m/z 235.3 [M+H]⁺; HRMS calcd for C₁₄H₁₇O₃ [M-H]⁻ 233.1173, found 233.1173.

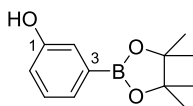
Cyclohex-1-en-1-yl trifluoromethanesulfonate (**105**)



Compound **105** was synthesized according to general procedure H using cyclohexanone (250 mg, 2.55 mmol), KHMDS 0.5 M in toluene (6.64 mL, 3.32 mmol), *N*-phenylbis(trifluoromethanesulfonamide) (1.18 g, 3.32 mmol) and THF (25.5 mL, 10 mL/mmol). Purification by MPLC (gradient elution, petrol 0-2% EtOAc/petrol) afforded the title compound (380 mg, 65%) as a colorless oil. R_f 0.60 (5% EtOAc/petrol; UV 254 nm, KMnO₄); λ_{\max} (EtOH)/nm 263; $\nu_{\max}/\text{cm}^{-1}$ (neat) 1199 (vs, C-F), 1413 (vs, SO₂^{str}), 1689 (w, C=C); ¹H NMR (500 MHz; CDCl₃) δ_H 1.56–1.64 (2H, m, =CHCH₂-CH₂), 1.74–1.81 (2H, m, CH₂CH₂C-OSO₂CF₃), 2.13–2.22 (2H, m, =CH-CH₂), 2.27–2.36 (2H, m, CH₂C-OSO₂CF₃), 5.75 (1H, tt, J = 1.6, 4.1 Hz, C=CHCH₂-); ¹³C NMR (125 MHz; CDCl₃) δ_C 21.1 (C=CH-CH₂-CH₂), 22.8 (CH₂CH₂C-OSO₂CF₃), 24.0 (C=CH-CH₂), 27.7 (CH₂C-OSO₂CF₃), 118.6 (CH₂C=CH), 118.7 (q, J = 320 Hz, CF₃), 149.5 (CH₂C=CH); ¹⁹F NMR (470 MHz; CDCl₃) δ_F -74.1; HRMS calcd for C₇H₁₀O₄F₃S [M+OH]⁺ 247.0246, found 247.0244.

NMR data match those previously reported for this compound.²⁰³

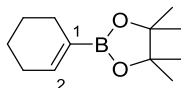
3-(4',4',5',5'-Tetramethyl-1',3',2'-dioxaborolan-2'-yl)phenol (**114**)



Compound **114** was obtained following general procedure I using 3-bromophenol (500 mg, 2.89 mmol), B₂pin₂ (881 mg, 3.47 mmol), [Pd(dppf)Cl₂] (71 mg, 0.0867 mmol), potassium acetate (852 mg, 8.67 mmol) and 1,4-dioxane (15 mL). The crude product was purified by MPLC (gradient elution, 0-25% EtOAc/petrol) to afford the title compound as a pale yellow oil, which solidified upon storage at RT (580 mg, 81%). *R*_f 0.45 (25% EtOAc/petrol; KMnO₄); m.p. 77.5-79.3 °C; λ_{max} (EtOH)/nm 249; ν_{max}/cm⁻¹ (neat) 2979, 3387 (m, OH); ¹H NMR (500 MHz; CDCl₃) δ_H 1.27 (12H, s, 4 × CH₃), 6.88 (1H, ddd, *J* = 1.1, 2.9, 8.0 Hz, H-6), 7.15 – 7.18 (1H, m, H-2), 7.18 – 7.22 (1H, m, H-5), 7.28 – 7.33 (1H, m, H-4); ¹³C NMR (125 MHz; CDCl₃) δ_C 25.0 (4 × CH₃), 84.1 (2 × C-(CH₃)₂), 118.6 (C-6), 121.2 (C-2), 127.2 (C-4), 129.4 (C-5), 155.2 (C-1). One quaternary carbon not detected; LRMS (ES⁻) *m/z* 219.3 [M-H]⁻; HRMS calcd for C₁₂H₁₆O₃B [M-H]⁻ 219.1198, found 219.1190.

NMR data match those previously reported for this compound.²⁰⁵

2-(Cyclohex-1-en-1-yl)-4,4,5,5-tetramethyl-1,3,2-dioxaborolane (**101**)

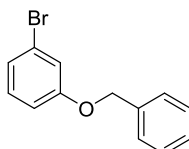


Compound **101** was synthesized according to general procedure I using the triflate **105** (1.52 g, 6.60 mmol), (Bpin)₂ (2.01 g, 7.92 mmol), [Pd(dppf)Cl₂] (162 mg, 0.198 mmol), potassium acetate (1.95 g, 19.8 mmol) and 1,4-dioxane (34 mL). The crude product was purified by MPLC (gradient elution, 0-3% EtOAc/petrol) to afford the title compound as a colorless oil (981 mg, 71%). *R*_f 0.68 (20% EtOAc/petrol; UV 254 nm, KMnO₄); λ_{max} (EtOH)/nm no max of absorption; ν_{max}/cm⁻¹ (neat) 1382 (s, B-O str.), 1447 (s, B-C str.), 1633 (m, C=C str), 2929 and 2977 (w, CH₂^{as}); ¹H NMR (500 MHz; CDCl₃) δ_H 1.25 (12H, s, 4 × CH₃), 1.52 – 1.66 (4H, m, 2 × CH₂), 2.01 – 2.16 (4H, m, 2 × CH₂), 6.52 – 6.61 (1H,

m, C=CHCH₂-); ¹³C NMR (125 MHz; CDCl₃) δ_C 22.3 (CH₂), 22.7 (CH₂), 24.9 (4 × CH₃), 26.2 (CH₂), 26.7 (CH₂), 83.1 (2 × C-(CH₃)₂), 143.1 (CH₂C=CH); LRMS (ES⁺) *m/z* 209.4 [M+H]⁺; HRMS calcd for C₁₂H₂₀¹⁰BO₂ [M-H]⁻ 206.1587, found 206.1587.

NMR data match those previously reported for this compound.²⁰⁶

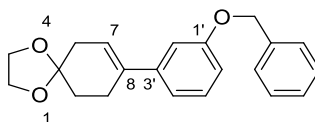
1-(Benzyloxy)-3-bromobenzene (112)



Potassium carbonate (799 mg, 5.78 mmol) and benzyl bromide (544 mg, 3.18 mmol) were added to a solution of 3-bromophenol (500 mg, 2.89 mmol) in acetone and the mixture was stirred at 57 °C for 3 h. The solvent was evaporated and the residue was dissolved in DCM (5 mL) and water (5 mL). The layers were separated and the aqueous phase was extracted with DCM (2 × 7.5 mL). The combined organic layers were dried (MgSO₄), filtered and evaporated *in vacuo*. Purification by MPLC (gradient elution, 0-1% EtOAc/petrol) yielded the title compound (680 mg, 89%) as an oil which solidified to give a white solid. *R*_f 0.50 (5% EtOAc/petrol); m.p. 61.4-62.6 °C (lit.²⁰⁷ 61-62 °C); λ_{max} (EtOH)/nm 249, 279; ν_{max}/cm⁻¹ (neat) 1237 (s, C-O-C^{as}), 2939 (aliphatic stretch), 3034, 3062, and 3103 (aromatic stretch); ¹H NMR (500 MHz; CDCl₃) δ_H 5.04 (2H, s, CH₂), 6.88–6.93 (1H, m H-Ar), 7.07–7.17 (3H, m, H-Ar), 7.31–7.48 (5H, m, H-Ar); ¹³C NMR (125 MHz; CDCl₃) δ_C 70.4 (CH₂), 114.0 (C-Ar), 118.3 (C-Ar), 123.0 (C-Ar q), 124.2 (C-Ar), 127.6 (C-Ar), 128.3 (C-Ar), 128.8 (C-Ar), 130.7 (C-Ar), 136.5 (C-Ar q), 159.7 (C-Ar q).

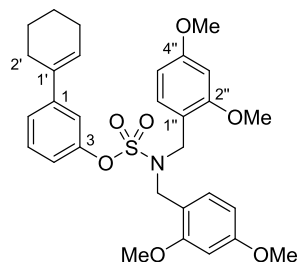
NMR data match those previously reported for this compound.²⁰⁷

8-[3'-(Benzyloxy)phenyl]-1,4-dioxaspiro[4.5]dec-7-ene (113)



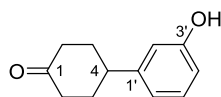
Compound **113** was synthesized according to general procedure E using boronic ester **97** (202 mg, 0.760 mmol), bromide **112** (200 mg, 0.760 mmol), Na_2CO_3 (2 M aq., 0.76 mL, 1.52 mmol), $[\text{Pd}(\text{dppf})\text{Cl}_2]$ (31 mg, 0.0380 mmol) and DME (1.8 mL). Purification by MPLC (gradient elution, 0-10% EtOAc/petrol) yielded the desired compound (183 mg, 75%) as a colorless oil. R_f 0.27 (10% EtOAc/petrol); λ_{max} (EtOH)/nm 246, 285; $\nu_{\text{max}}/\text{cm}^{-1}$ (neat) 1115, 1188 (m, C-O-C-O-C vib), 1267 and 1285 (m, O-C), 1576 (m, C=C ar), 1597, 1603 (m, C=C str), 2879, 2925 and 2947 (w, C-H and $-\text{CH}_2-$ aliphatic); ^1H NMR (500 MHz; CDCl_3) δ_{H} 1.77–1.90 (2H, m, C(O- CH_2 - CH_2 -O)- CH_2 - CH_2 -), 2.33–2.43 (2H, m, $-\text{CH}_2$ -CH=C), 2.58 (2H, tq, J = 6.3, 2.0 Hz, -C(O-Et-O)- CH_2 - CH_2 -), 3.95 (4H, s, O- CH_2 - CH_2 -O), 4.99 (2H, s, CH_2 -Ph), 5.89–5.93 (1H, m, C=C-H), 6.78 (1H, ddd, J = 1.0, 2.5, 8.2 Hz, H-Ar), 6.90–6.97 (2H, m, H-Ar), 7.14 (1H, app. t, J = 7.9 Hz, H-5'), 7.22–7.29 (1H, m, H-Ar), 7.29–7.34 (2H, m, H-Ar), 7.34–7.39 (2H, m, H-Ar); ^{13}C NMR (125 MHz; CDCl_3) δ_{C} 27.0 (-C(O-Et-O)- CH_2 - CH_2 -), 31.5 (-C(O-Et-O)- CH_2 - CH_2 -), 36.3 (- CH_2 -CH=C), 64.6 (O- CH_2 - CH_2 -O), 70.1 (CH_2 -Ph), 107.9 (-O-C-O-), 112.3 (C-Ar), 113.3 (C-Ar), 118.2 (C-Ar), 122.0 (C=C-H), 127.6 (2 \times C-Ar), 128.1 (C-Ar), 128.7 (2 \times C-Ar), 129.3 (C-5'), 136.3 (C q), 137.2 (C q), 143.2 (C-1'), 158.9 (C-Ar q); LRMS (ES^+) m/z 323.5 $[\text{M}+\text{H}]^+$; HRMS calcd for $\text{C}_{21}\text{H}_{23}\text{O}_3$ $[\text{M}+\text{H}]^+$ 323.1642, found 323.1645.

2',3',4',5'-tetrahydro-[1,1'-biphenyl]-3-yl bis(2'',4''-dimethoxybenzyl)sulfamate (121)



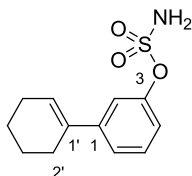
Compound **121** was synthesized according to general procedure E using boronic ester **101** (574 mg, 2.76 mmol), bromide **115** (1.52 g, 2.76 mmol), Na₂CO₃ (2 M aq., 2.76 mL, 5.52 mmol), [Pd(dppf)Cl₂] (113 mg, 0.138 mmol) and DME (6.6 mL). Complete conversion was reached after 75 min. Purification by MPLC (gradient elution, 0-20% EtOAc/petrol) yielded the desired compound (1.47 g, 96%) as a pale yellow oil. *R*_f 0.20 (10% EtOAc/petrol); λ_{max} (EtOH)/nm no maximum absorption observed; ν_{max}/cm⁻¹ (neat) 1133 (m, SO₂^{sy}), 1157 (m, C-O), 1369 (m, SO₂^{as}), 1588 (m, C=C ar), 2934 (w, C-H and -CH₂- aliphatic); ¹H NMR (500 MHz; CDCl₃) δ_H 1.61–1.70 (2H, m, =CHCH₂-CH₂), 1.72–1.82 (2H, m, CH₂CH₂C-Ar), 2.16–2.24 (2H, m, =CH-CH₂), 2.26–2.35 (2H, m, CH₂C-Ar), 3.72 (6H, s, 2 × OCH₃), 3.80 (6H, s, 2 × OCH₃), 4.45 (4H, s, 2 × N-CH₂-), 6.07 (1H, tt, *J* = 1.8, 3.9 Hz, =CHCH₂-), 6.38 (2H, d, *J* = 2.4 Hz, 2 × H-3''), 6.44 (2H, dd, *J* = 2.4, 8.4 Hz, 2 × H-5''), 6.96–7.02 (2H, m, H-Ar), 7.20–7.24 (2H, m, H-Ar), 7.25–7.31 (2H, m, 2 × H-6''); ¹³C NMR (125 MHz; CDCl₃) δ_C 22.2 (C=CHCH₂-CH₂), 23.1 (CH₂CH₂C-Ar), 26.0 (C=CH-CH₂), 27.4 (CH₂C-Ar), 46.9 (2 × N-CH₂), 55.2 (2 × OCH₃), 55.5 (2 × OCH₃), 98.3 (2 × C-3''), 104.1 (2 × C-5''), 116.8 (2 × C-1''), 118.6 (C-Ar), 120.0 (C-Ar), 122.9 (C-Ar), 126.0 (C=C-H), 129.2 (C-Ar), 131.1 (2 × C-6''), 135.7 (C q), 144.5 (C q), 150.6 (C-3), 158.6 (2 × C-2'' or C-4''), 160.7 (2 × C-2'' or C-4''); LRMS (ES⁺) *m/z* 576.5 [M+Na]⁺; HRMS calcd for C₃₀H₃₆NO₇S [M+H]⁺ 554.2207, found 554.2198.

4-(3'-Hydroxyphenyl)cyclohexanone (**109**)



Compound **109** was prepared according to general procedure F using ketal **107** (371 mg, 1.58 mmol), THF/H₂O 1:3 (44 mL, 28 mL/mmol) and acetic acid (68 mL, 42 mL/mmol). The crude product was purified by MPLC (gradient elution, 0-40% EtOAc/petrol) to yield the title compound as a white solid (230 mg, 77%). *R_f* 0.36 (33% EtOAc/petrol; UV 254 nm, KMnO₄); m.p. 132-134 °C; λ_{max} (EtOH)/nm 274, 380; ν_{max} /cm⁻¹(neat) 1689 (vs, C=O), 3386 (s, O-H); ¹H NMR (500 MHz; CDCl₃) δ_{H} 1.83–1.99 (2H, m, 2 × CH_{eq}H_{ax}), 2.15–2.27 (2H, m, 2 × CH_{eq}H_{ax}), 2.44–2.57 (4H, m, 2 × CH₂-C=O), 2.97 (1H, tt, *J* = 3.4, 12.1), 6.07 (1H, br, OH), 6.69–6.76 (2H, m, H-2' and H-4'), 6.77–6.82 (1H, m, H-6'), 7.15–7.21 (1H, m, H-5'); ¹³C NMR (125 MHz; CDCl₃) δ_{C} 34.0 (C-3 and C-5), 41.4 (C-2 and C-6), 42.7 (C-4), 113.7 and 113.8 (C-2' and C-4'), 119.1 (C-6'), 129.9 (C-5'), 146.7 (C-1'), 156.2 (C-3'), 212.7 (CO); LRMS (ES⁻) *m/z* 189.2 [M-H]⁻; HRMS calcd for C₁₂H₁₄O₂Na [M+Na]⁺ 213.0886, found 213.0887.

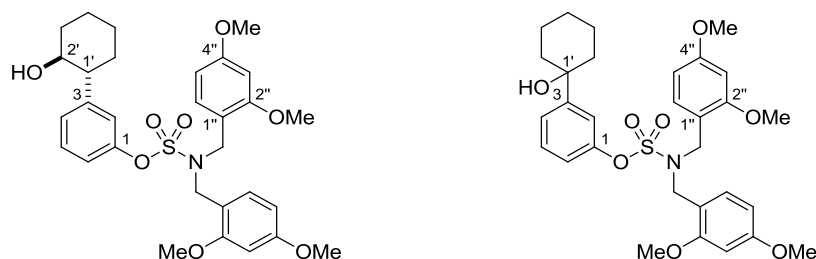
2',3',4',5'-Tetrahydro-[1,1'-biphenyl]-3-yl sulfamate (**135**)



Sulfamate **135** was prepared according to general procedure G using protected sulfamate **121** (256 mg, 0.462 mmol), DCM (5.4 mL) and TFA (0.6 mL.) Purification by MPLC (gradient elution, 0-40% EtOAc/petrol) yielded the desired compound as a white solid (87 mg; 74%). *R_f* 0.52 (50% EtOAc/petrol); m.p. 99.6-100.7 °C; λ_{max} (EtOH)/nm 248; ν_{max} /cm⁻¹ (neat) 1146 and 1178 (s, SO₂^{sy}), 1351 (s, SO₂^{as}), 1605 (m, C=C), 2933 (m, C-H and -CH₂- aliphatic), 3263 and 3365 (m, N-H str.); ¹H NMR (500 MHz; CDCl₃) δ_{H} 1.59–1.71 (2H, m, C=CHCH₂-CH₂), 1.71–1.82 (2H, m, CH₂CH₂C-Ar), 2.13–2.28 (2H, m, C=CH-CH₂), 2.34–2.30 (2H, tt, *J* = 2.5, 6.2 Hz, CH₂C-Ar), 5.05 (2H, s, NH₂), 6.14–6.18 (1H, m,

C=CHCH₂-), 7.13–7.19 (1H, m, H-Ar), 7.30–7.35 (3H, m, H-Ar); ¹³C NMR (125 MHz; CDCl₃) δ_C 22.1 (C=CHCH₂-CH₂), 23.0 (CH₂CH₂C-Ar), 26.0 (C=CH-CH₂), 27.4 (CH₂C-Ar), 118.6 (C-Ar), 119.9 (C-Ar), 123.9 (C-Ar), 126.7 (C=C-H), 129.6 (C-Ar), 135.4 (C q), 145.0 (C q), 150.3 (C-3); LRMS (ES⁻) *m/z* 252.2 [M-H]⁻; HRMS calcd for C₁₂H₁₄O₃NS [M-H]⁻ 252.0700, found 252.0689; HPLC 99.0% in water/MeCN (*R*_t 8.2 min); 99.3% in 0.1% formic acid (aq.)/MeCN (*R*_t 8.2 min); 99.2% in 0.1% ammonia (aq.)/MeCN (*R*_t 6.2 min).

3-(2'-Hydroxycyclohexyl)phenyl bis(2'',4''-dimethoxybenzyl)sulfamate (122) and 3-(1'-hydroxycyclohexyl)phenyl bis(2'',4''-dimethoxybenzyl)sulfamate (137)



To a solution of alkene **121** (1.01 g, 1.82 mmol) in THF (1.02 mL, 0.56 mL/mmol), BH₃ · THF complex (1.0 M, 1.82 mL, 1.82 mmol) was added dropwise at 0 °C and the mixture was stirred for 1 h at 0 °C and 3 h at RT. NaOH (3 M aq., 0.38 mL, 1.15 mmol) and H₂O₂ (aq. 30% w/v, 0.33 mL, 2.84 mmol) were added and the mixture was stirred overnight at RT. Water (30 mL) was added and the product was extracted with EtOAc (3 × 30 mL). The combined organic layers were washed with Na₂S₂O₃ (sat. aq.), brine, dried (MgSO₄), filtered and evaporated. Purification by MPLC (gradient elution, 0-40% EtOAc/petrol) yielded the desired compound **122** (570 mg, 55%) and the side product **137** (170 mg, 16%) as colorless oils.

122

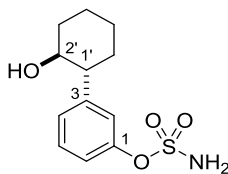
*R*_f 0.44 (50% EtOAc/petrol; UV 254 nm, KMnO₄); λ_{max} (EtOH)/nm 277; ν_{max}/cm⁻¹ (neat) 1128 (s, SO₂^{sy}), 1157 (s, C-O), 1375 (m, SO₂^{as}), 1587 (m, C=C ar), 2933 (w, C-H and -CH₂- aliphatic); ¹H NMR (500 MHz; CDCl₃) δ_H 1.20–1.40 (4H, m, CH^{ax}H^{eq}), 1.60–1.74 (2H, m, CH^{ax}H^{eq}), 1.74–1.83 (1H, m, CH^{ax}H^{eq}), 1.98–2.05 (1H,

m, CH^{ax}H^{eq}), 2.24–2.35 (1H, m, CH-Ar), 3.43 (1H, app. td, $J = 4.2, 10.1$ Hz, CHOH), 3.64 (6H, s, $2 \times$ -OCH₃), 3.72 (6H, s, $2 \times$ -OCH₃), 4.33 (4H, s, $2 \times$ N-CH₂-), 6.33 (2H, d, $J = 2.4$ Hz, $2 \times$ H-3''), 6.38 (2H, dd, $J = 2.4, 8.4$ Hz, $2 \times$ H-5''), 6.65 (1H, app. t, $J = 2.0$ Hz, H-2), 6.97 (1H, ddd, $J = 1.0, 2.3, 8.1$ Hz, H-Ar), 7.00–7.05 (1H, m, H-Ar), 7.18 (1H, app. t, $J = 8.1$ Hz, H-5), 7.22 (2H, d, $J = 8.1$ Hz, $2 \times$ H-6''); ¹³C NMR (125 MHz; CDCl₃) δ_C 25.0 (C-4'), 26.1 (C-5'), 33.3 (C-6'), 34.7 (C-3'), 46.7 ($2 \times$ N-CH₂-), 53.0 (C-1'), 55.2 ($2 \times$ -OCH₃), 55.5 ($2 \times$ -OCH₃), 74.1 (C-2'), 98.3 ($2 \times$ C-3''), 104.1 ($2 \times$ C-5''), 116.6 ($2 \times$ C-1''), 120.7 (C-Ar), 120.9 (C-2), 126.6 (C-Ar), 129.8 (C-5), 131.0 (C-6''), 145.5 (C-3), 150.9 (C-1), 158.5 ($2 \times$ C-2'' or C-4''), 160.7 ($2 \times$ C-2'' or C-4''); LRMS (ES⁺) m/z 594.6 [M+Na]⁺; HRMS calcd for C₃₀H₄₁O₈N₂S [M+NH₄]⁺ 589.2578, found 589.2553.

137

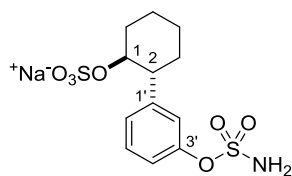
R_f 0.56 (50% EtOAc/petrol; UV 254 nm, KMnO₄); λ_{max} (EtOH)/nm 278; ν_{max}/cm^{-1} (neat) 1128 (s, SO₂^{sy}), 1157 (s, C-O), 1372 (m, SO₂^{as}), 1588 (m, C=C ar), 2934 (w, C-H and -CH₂- aliphatic); ¹H NMR (500 MHz; CDCl₃) δ_H 1.23–1.37 (1H, m, cyclohexyl CH), 1.54–1.83 (9H, m, $9 \times$ cyclohexyl CH), 3.71 (6H, s, $2 \times$ OCH₃), 3.80 (6H, s, $2 \times$ -OCH₃), 4.43 (4H, s, $2 \times$ N-CH₂-), 6.39 (2H, d, $J = 2.4$ Hz, $2 \times$ H-3''), 6.44 (2H, dd, $J = 2.4, 8.3$ Hz, $2 \times$ H-5''), 7.01–7.08 (2H, m, H-Ar), 7.23–7.32 (3H, m, H-Ar and $2 \times$ H-6''), 7.33–7.42 (1H, m, H-Ar); ¹³C NMR (125 MHz; CDCl₃) δ_C 22.2 ($2 \times$ CH₂), 25.5 (CH₂), 38.8 ($2 \times$ CH₂), 46.8 ($2 \times$ N-CH₂), 55.2 ($2 \times$ OCH₃), 55.5 ($2 \times$ OCH₃), 73.0 (C-1'), 98.3 ($2 \times$ C-3''), 104.1 ($2 \times$ C-5''), 116.7 ($2 \times$ C-1''), 118.5 (C-Ar), 120.4 (C-Ar), 122.7 (C-Ar), 129.4 (C-Ar), 131.0 ($2 \times$ C-6''), 150.6 (C-1), 151.7 (C-3), 158.6 ($2 \times$ C-2'' or C-4''), 160.7 ($2 \times$ C-2'' or C-4''); LRMS (ES⁺) m/z 594.6 [M+Na]⁺; HRMS calcd for C₃₀H₄₁O₈N₂S [M+NH₄]⁺ 589.2578, found 589.2569.

3-(*trans*-2'-Hydroxycyclohexyl)phenyl sulfamate (**123**)



Compound **123** was obtained according to general procedure G using protected sulfamate **122** (570 mg, 1.00 mmol) and 10% TFA/DCM (10 mL). Purification by MPLC (gradient elution, 0-50% EtOAc/petrol) yielded the desired racemic compound (94 mg, 35%) as an oil. R_f 0.26 (50% EtOAc/petrol; UV 254 nm, KMnO_4); λ_{max} (EtOH)/nm 261; $\nu_{\text{max}}/\text{cm}^{-1}$ (neat) 1135 (m, SO_2^{sy}), 1182 (s, C-O), 1372 (m, SO_2^{as}), 2930 (w, C-H and $-\text{CH}_2-$ aliphatic), 3358 (br, O-H); ^1H NMR (500 MHz; CDCl_3) δ_{H} 1.30–1.69 (5H, m, $5 \times$ cyclohexyl CH), 1.77–1.87 (1H, m, cyclohexyl CH), 1.89–2.02 (2H, m, $2 \times$ cyclohexyl CH), 2.13–2.20 (1H, m, CH-Ar), 2.71 (1H, ddd, $J = 12.6, 10.8, 3.8$ Hz, CH-OH), 5.07 (1H, td, $J = 4.5, 10.8$ Hz, OH), 6.63–6.72 (2H, m, H-Ar), 6.75 (1H, dt, $J = 7.7, 1.3$ Hz, H-Ar), 7.11–7.17 (1H, m, H-Ar); ^{13}C NMR (125 MHz; CDCl_3) δ_{C} 24.7 (CH_2), 25.5 (CH_2), 31.8 (CH_2), 33.1 (CH_2), 49.3 (CH-Ar), 81.0 (CH-OH), 114.1 (C-Ar), 114.5 (C-Ar), 120.0 (C-Ar), 129.8 (C-Ar), 143.4 (C-3), 155.8 (C-1); LRMS (ES^-) m/z 270.2 [M-H] $^-$; HRMS calcd for $\text{C}_{12}\text{H}_{21}\text{O}_7\text{N}_2\text{S}$ [$\text{M}+\text{NH}_4$] $^+$ 289.1217, found 289.1220; HPLC 97.0% in water/MeCN (R_t 6.3 min); 99.2% in 0.1% formic acid (aq.)/MeCN (R_t 6.5 min); 97.5% in 0.1% ammonia (aq.)/MeCN (R_t 3.8 min).

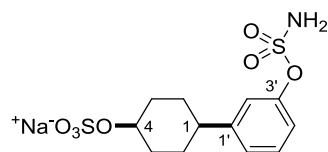
Sodium *trans*-2-[3-(sulfamoyloxy)phenyl]cyclohexyl sulfate (**93**)



Sulfate **93** was obtained following general procedure D (method 2) using alcohol **123** (45 mg, 0.166 mmol), sulfur trioxide pyridine complex (53 mg, 0.332 mmol) and DMF (0.45 mL). Purification by MPLC yielded the desired compound (20 mg, 32%) as a white solid. R_f 0.27 (10% MeOH/EtOAc; KMnO_4); m.p. 205–218 (dec.); λ_{max} (EtOH)/nm 260; $\nu_{\text{max}}/\text{cm}^{-1}$ (neat) 1198 (vs, SO_2^{sy}),

1382 (m, SO₂^{as}), 2926 (w, CH and CH₂ aliphatic), 3254 and 3346 (w, N-H); ¹H NMR (500 MHz; DMSO-*d*₆) δ_H 1.21 – 1.44 (4H, m, 4 × cyclohexyl CH), 1.60–1.69 (1H, m, cyclohexyl CH), 1.70–1.86 (2H, m, 2 × cyclohexyl CH), 2.52 (1H, m, cyclohexyl CH), 2.55–2.62 (1H, m, CH-Ar), 4.19–4.28 (1H, m, CH-OSO₃Na), 6.98–7.05 (1H, m, H-Ar), 7.19 (1H, app. d, *J* = 7.8 Hz), 7.22–7.26 (1H, m), 7.30 (1H, app. t, *J* = 7.8 Hz), 7.71 (2H, br, NH₂) ppm. One proton signal is covered by the DMSO signal (confirmed by COSY and HSQC); ¹³C NMR (125 MHz; DMSO-*d*₆) δ_C 24.4 (CH₂), 25.6 (CH₂), 32.9 (CH₂), 35.0 (CH₂), 49.6 (CH-Ar), 77.4 (CH-OSO₃Na), 119.6 (C-Ar), 120.9 (C-Ar), 126.3 (C-Ar), 129.0 (C-Ar), 146.4 (C-Ar), 149.9 (C-3'); LRMS (ES⁻) *m/z* 350.2 [M-Na]⁻; HRMS calcd for C₁₂H₁₆O₇NS₂ [M-Na]⁻ 350.0374, found 350.0367; HPLC 97.0% in water/MeCN (*R*_t 4.2 min); 96.5% in 0.1% formic acid (aq.)/MeCN (*R*_t 7.7 min); 92.5% in 0.1% ammonia (aq.)/MeCN (*R*_t 3.4 min).

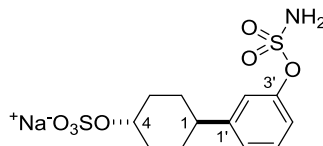
Sodium *cis*-4-[3'-(sulfamoyloxy)phenyl]cyclohexyl sulfate (**91**)



Sulfate **91** was obtained following general procedure D (method 2) using alcohol **110** (85 mg, 0.313 mmol), sulfur trioxide pyridine complex (200 mg, 1.25 mmol), and DMF (0.85 mL). Purification by MPLC yielded the desired compound (114 mg, 98%) as a white solid. *R*_f 0.10 (10% MeOH/EtOAc; KMnO₄); m.p. 144.6–146.0 °C; λ_{max} (EtOH)/nm 261; ν_{max}/cm⁻¹ (neat) 1195 (vs, SO₂^{sy}), 1380 (m, SO₂^{as}), 2861 and 2943 (w, C-H and -CH₂- aliphatic), 3108 and 3254 (w, N-H); ¹H NMR (500 MHz; DMSO-*d*₆) δ_H 1.43–1.62 (4H, m, CH^{ax}), 1.70 (2H, m, 2 × CH^{eq}), 2.03 (2H, m, 2 × CH^{eq}), 2.53–2.62 (1H, m, CH-Ar), 4.35–4.40 (1H, m, CH-OSO₃Na), 7.07–7.11 (1H, dd, *J* = 2.0, 7.9 Hz, H-Ar), 7.12 (1H, app. t, *J* = 2.0, H-2'), 7.19 (1H, app. d, *J* = 7.9, H-Ar), 7.37 (1H, app. t, *J* = 7.9, H-5'), 7.94 (2H, s, NH₂); ¹³C NMR (125 MHz; DMSO-*d*₆) δ_C 27.9 (2 × CH₂), 30.5 (2 × CH₂), 42.4 (CH-Ar), 69.8 (CH-OSO₃Na), 119.6 (C-Ar), 120.4 (C-Ar), 124.9 (C-Ar), 129.5 (C-Ar), 149.5 (C-Ar q), 150.2 (C-Ar q); LRMS (ES⁻) *m/z* 350.2 [M-Na]⁻; HRMS calcd for C₁₂H₁₆O₇NS₂ [M-Na]⁻ 350.0374, found 350.0368; HPLC 97.0% in water/MeCN

(R_t 3.6 min); 97.9% in 0.1% formic acid (aq.)/MeCN (R_t 7.0 min); N/A in 0.1% ammonia (aq.)/MeCN.

Sodium *trans*-4-[3'-(sulfamoyloxy)phenyl]cyclohexyl sulfate (**92**)



Compound **92** was obtained following general procedure D (method 2) using alcohol **111** (114 mg, 0.420 mmol), sulfur trioxide pyridine complex (134 mg, 0.840 mmol), and DMF (1.13 mL). Purification by MPLC yielded the desired compound (132 mg, 84%) as a colorless oil. R_f 0.10 (10% MeOH/EtOAc; KMnO_4); λ_{max} (EtOH)/nm 260; $\nu_{\text{max}}/\text{cm}^{-1}$ (neat) 1183 (vs, SO_2^{sy}), 1373 (s, SO_2^{as}), 2864 and 2938 (w, C-H and $-\text{CH}_2-$ aliphatic), 3089 and 3263 (w, N-H); ^1H NMR (500 MHz; $\text{DMSO}-d_6$) δ_{H} 1.29 – 1.40 (2H, m, CH^{ax}), 1.41–1.56 (2H, m, CH^{ax}), 1.74–1.85 (2H, m, CH^{eq}), 2.07–2.18 (2H, m, CH^{ax}), 3.99–4.11 (1H, m, $\text{CH}-\text{OSO}_3\text{Na}$), 7.09 (1H, dd, $J = 1.9, 8.0$ Hz, H-Ar), 7.14 (1H, app. t, $J = 1.9$ Hz, H-2'), 7.21 (1H, d, $J = 8.0$ Hz, H-Ar), 7.35 (1H, t, $J = 8.0$ Hz, H-5'), 7.91 (2H, br, NH_2). One proton signal (CH-Ar) is covered by the DMSO signal (confirmed by COSY and HSQC); ^{13}C NMR (125 MHz; $\text{DMSO}-d_6$) δ_{C} 32.0 (CH_2), 33.0 (CH_2), 42.4 (CH_2), 74.2 (CH_2), 119.6 (C-Ar), 120.5 (C-Ar), 124.8 (C-Ar), 129.4 (C-Ar), 148.7 (C-Ar q), 150.2 (C-Ar q); LRMS (ES^-) m/z 350.2 [$\text{M} - \text{Na}$] $^-$; HRMS calcd for $\text{C}_{12}\text{H}_{16}\text{O}_7\text{NS}_2$ [$\text{M}-\text{Na}$] $^-$ 350.0374, found 350.0367; HPLC 95.7% in water/MeCN (R_t 3.5 min); 97.0% in 0.1% formic acid (aq.)/MeCN (R_t 7.0 min); N/A in 0.1% ammonia (aq.)/MeCN.

9.3 MDMX project experimental procedures

9.3.1 MDMX and MDM2 biological assay protocols

ELISA

Biological testing of compounds was undertaken by Dr Yan Zhao at the Northern Institute for Cancer Research using an ELISA assay (details taken from Hardcastle *et al.*).²⁰⁸ The 96-well black and white high binding luminometry isoplates (Wallac, Cat N0 140-155) were coated by overnight incubation at 35 °C with 200 μL per well of 5 $\mu\text{g mL}^{-1}$ streptavidin (Chemicon International)

in coating buffer (0.1 M Na₂HPO₄·2 H₂O; 0.1 M citric acid; pH 5.0). The plates were washed five times in 1× dissociation enhanced lanthanide fluorescence immunoassay (DELFI) buffer (Wallac) and then incubated for 3 h at room temperature with saturation buffer (0.3 M D-sorbitol; 50 mM Tris; 150 mM NaCl; 0.1% BSA; 0.05% sodium azide; pH 7.0) to block nonspecific protein binding sites on the plate. After removal of the buffer from the plates, they were allowed to dry in a sterile laminar air flow hood at room temperature before incubation for 1 h at 4 °C with 200 µL per well of 100 µg/mL-1 biotinylated IP3 peptide (b-IP3: Ac-Met-Pro-Arg-Phe¹⁹-Met-Asp-Tyr-Trp-Glu-Gly-Leu²⁶-Asn-NH₂) dissolved in 0.05% DMSO-PBS, pH 7.4 buffer. After washing the wells three times with PBS, the plates were ready to use for MDM2 binding.

For initial testing, the compounds and controls were plated out in triplicate into clear 96-well plates (Nunc) in 10 µL aliquots to give final concentrations of 500 µM, 100 µM and 20 µM in the assay. Control samples consisted of 5% DMSO carrier alone as a negative control and 100 nM active peptide (AP-B: Ac-Phe¹⁹-Met-Aib-Pmp-6-Cl-Trp-Glu-Ac³-Leu²⁶-NH₂)¹⁶³ as a positive control peptide antagonist of the MDM2:p53 interaction (IC₅₀ = 5 nM). Compounds and controls aliquoted in 96-well plates were preincubated at 20° C for 20 min with 190 µL aliquots of optimized concentrations of in vitro translated MDM2, before transfer of the MDM2-compound mixture to the b-IP3 streptavidin plates, and incubation at 4 °C for 90 min. After washing three times with PBS to remove unbound MDM2, each well was incubated at 20 °C for 1 h with a TBS-Tween (50 mM Tris pH 7.5; 150 mM NaCl; 0.05% Tween 20 non-ionic detergent) buffered solution of primary mouse monoclonal anti-MDM2 antibody (Ab-5, Calbiochem, used at a 1/200 dilution), washed three times with TBS-Tween before incubation for 45 min at 20 °C with a goat-anti-mouse horseradish peroxidase (HRP) conjugated secondary antibody (Dako, used at 1/2000). The unbound secondary antibody was removed by washing three times with TBS-Tween. The bound HRP activity was measured by enhanced chemiluminescence (ECL, Amersham Biosciences) using the oxidation of the diacylhydrazide substrate, luminol, to generate a quantifiable light signal. The luminol substrate together with enhancer was automatically injected into each well and the relative

luminescence units (RLU) measured over 30 s using a Berthold MicroLumat-Plus LB 96 V microplate luminometer. The percentage MDM2 inhibition at a given concentration was calculated as the (RLU detected in the compound treated sample \div RLU of DMSO controls) \times 100. The IC₅₀ was calculated using a plot of % MDM2 inhibition vs concentration and is the average of three independent experiments.

The same procedure was used for measuring MDMX inhibition. Unless otherwise stated, only one measurement was performed.

9.3.2 General synthetic procedures

General procedure J: *N*-aroylhydrazone formation¹⁵⁸

Under an inert atmosphere, the benzaldehyde (1.0 equiv.) was dissolved in acetic acid (4.2 mL/mmol), and the appropriate hydrazide (1.1 equiv.) was added in one portion at RT. Upon completion of the reaction, the solution was cautiously poured into ice water. The white slurry was filtered, washed with a little cold water and triturated with petrol. The solid was dried overnight at 40 °C over P₂O₅. The product was used directly without further purification.

General procedure K: Pb(OAc)₄-mediated benzoylbenzaldehyde formation¹⁵⁸

At RT, lead tetraacetate (1.2 equiv.) was added in small portions to a solution of the hydrazone (1.0 equiv.) in THF (7.7 mL/mmol) and the mixture was stirred for 3 h. Upon completion of the reaction, the mixture was diluted with ethyl acetate, filtered through Celite, washed with sat. aq. NaHCO₃ and brine, dried, filtered and evaporated *in vacuo*. The crude product was purified by MPLC.

General procedure L: Pinnick oxidation

NaClO₂ (1.3 equiv. in water, 1.4 mL/mmol) and sulfamic acid (1.3 equiv. in water, 1.4 mL/mmol) were added to a solution of the benzaldehyde in acetonitrile in one portion and the yellow solution was stirred at RT for 2 h. The solvent was removed *in vacuo*, and the residue was dissolved in ethyl acetate

and washed with water and brine. The organic layer was dried, filtered and evaporated. Unless otherwise stated, further purification was not required.

General procedure M: isoindolinone formation

To a solution of the benzoylbenzoic acid (1.0 equiv.) in THF (1.2 mL/mmol), thionyl chloride (2.0 equiv.) was added followed by a catalytic amount of DMF (1-3 drops); the solution was stirred at RT for 4 h, and evaporated. The residue was redissolved in THF (1.2 mL/mmol), and the appropriate amine (1.1 equiv.) and DIPEA (1.1 equiv.) were added dropwise. The resulting solution was stirred at RT overnight. Ethyl acetate was added to the mixture and the layers were separated. The aqueous layer was extracted with EtOAc and the combined organic layers were dried (MgSO₄), filtered and the solvent was removed *in vacuo*. The crude product was purified by MPLC.

General procedure N: side chain addition

Under an inert atmosphere, the isoindolinone (1.0 equiv.) was dissolved in 1,2-dichloroethane. InBr₃ (0.20 equiv.) and 1,1-bis(hydroxymethyl)cyclopropane (5.0 equiv.) were added in one portion and the reaction mixture was stirred at 85 °C. Upon completion of the reaction, the solvent was removed *in vacuo*. The residue was dissolved in Et₂O (20 mL) and the resulting solution was washed with water (3 × 30 mL). The aqueous layer was back-extracted with Et₂O (2 × 30 mL). The combined organic layers were washed with brine, dried (MgSO₄), filtered and evaporated. Unless otherwise stated, the crude product was purified by MPLC.

General procedure O: Suzuki coupling of 7-bromoisindolinones

Under an inert atmosphere, the appropriate boronic acid (1.3 equiv.) and Na₂CO₃ (aq. 2M, 3.0 equiv.) were added to a solution of the 7-bromoisindolinone (1.0 equiv.) in acetonitrile (1.2 mL/mmol) and the mixture was degassed for 3-5 min before adding tetrakis(triphenylphosphine)palladium (0.10 equiv.). After further degassing, the reaction mixture was heated at 85 °C. Upon completion of the reaction, the mixture was diluted with EtOAc (10 mL) and water (10 mL); the layers were separated and the aqueous phase was

extracted with EtOAc (3 × 15 mL). The combined organic layers were washed with brine, dried (MgSO₄), filtered and evaporated. The residue was dissolved in MeOH and filtered through a Thiol MP SPE cartridge. The crude product was purified by MPLC.

General procedure P: TBAF deprotection

At 0 °C and under an inert atmosphere, TBAF (1 M in THF, 1.1 equiv.) was added dropwise to a solution of the silylated compound (1.0 equiv.) in THF (60 mL/mmol). The yellow solution was allowed to warm up to RT and stirred for 3 h. Upon completion of the reaction, the solvent was removed *in vacuo* and the crude product was purified by MPLC.

General procedure Q: phthalimide formation

At 0 °C, the amine (1.0 equiv.) was added to a solution of the anhydride (1.0 equiv.) in THF (0.5 mL/mmol). The suspension was refluxed until disappearance of the starting material. The solvent was removed *in vacuo* and the residue was taken up in EtOAc, washed with water (3 × 10 mL) and brine (10 mL). The organic layer was dried (MgSO₄), filtered and concentrated *in vacuo*. The crude product was purified by MPLC.

General procedure R: addition of a Grignard to a phthalimide

Under an inert atmosphere, phenylmagnesium bromide (3.0 equiv.) was added dropwise to a cooled solution (-78 °C) of the imide (1.0 equiv.) in THF (2.0 mL/mmol). The deep red reaction mixture was stirred for 1 h at 0 °C and 1 h at RT. Upon completion of the reaction, the mixture was quenched with NH₄Cl (sat. aq., 5 mL) and the product was extracted with EtOAc (3 × 15 mL). The combined organic layers were washed with brine (20 mL), dried (MgSO₄), filtered and evaporated. The crude product was purified by MPLC.

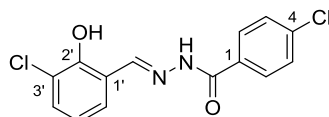
General procedure S: oxidation of a primary alcohol

The alcohol (1.0 equiv.) was dissolved in a mixture of EtOAc (1.43 mL/mmol), acetonitrile (1.43 mL/mmol) and water (2.5 mL/mmol). NaIO₄ (4.1 equiv.) was added at RT in one portion followed by RuCl₃ · H₂O. The mixture was stirred at RT for 20 min, diluted with EtOAc (1.2 mL) and filtered through a Celite

cartridge. The filtrate was washed with H₂O (2 mL) and the aqueous layer was back-extracted with EtOAc (2 × 2 mL). The combined organic layers were washed with brine (4 mL), dried (MgSO₄) and the solvent was removed *in vacuo*. The product was purified by MPLC as described for each compound.

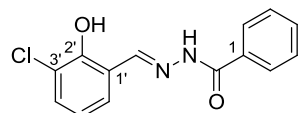
9.3.3 MDMX project - Synthesized compounds

(E)-4-Chloro-*N'*-(3'-chloro-2'-hydroxybenzylidene)benzohydrazide (**178**)



Compound **178** was synthesized according to general procedure J using 3-chloro-2-hydroxybenzaldehyde (1.00 g, 6.39 mmol), 4-chlorobenzhydrazide (1.09 g, 6.39 mmol) and acetic acid (27 mL). The crude product (off-white solid; 1.70 g, 86%) was used for the next step without further purification. *R_f* 0.58 (10% MeOH/DCM); m.p. 217.0-217.4 °C; λ_{max} (EtOH)/nm 292, 304, 330; ν_{max} /cm⁻¹ (neat) 1665 (s, C=O), 3074 (m, C-H str, aromatic), 3205 (m, N-H), 3348 (w, C=O, overtone), 3543 (m, O-H); ¹H NMR (500 MHz; DMSO-*d*₆) δ_{H} 6.98 (1H, app. t, *J* = 7.8 Hz, H-5'), 7.47-7.54 (2H, m, H-4' and H-6'), 7.63-7.68 (2H, m, H-3 and H-5), 7.94 – 8.01 (2H, m, H-2 and H-6), 8.61 (1H, s, CH=N), 12.36 and 12.45 (2 × 1H, br s, O-H and N-H); ¹³C NMR (125 MHz; DMSO-*d*₆) δ_{C} 119.6 (C-1' or C-3'), 120.1 (C-5'), 120.4 (C-1' or C-3'), 128.8 (C-3 and C-5), 129.6 (C-4' or C-6'), 129.7 (C-2 and C-6), 131.1 (C-4), 131.4 (C-4' or C-6'), 137.1 (C-1), 148.9 (CH=N), 153.3 (C-2'), 161.9 (C=O); LRMS (ES⁺) *m/z* 309.3 [M+H]⁺; HRMS calcd for C₁₄H₁₁O₂N₂³⁵Cl₂ [M+H]⁺ 309.0192, found 309.0191.

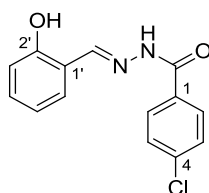
(E)-*N'*-(3'-Chloro-2'-hydroxybenzylidene)benzohydrazide (**181**)



Compound **181** was synthesized according to general procedure J using 3-chloro-2-hydroxybenzaldehyde (1.00 g, 6.39 mmol), benzohydrazide (0.87 g, 6.39 mmol) and acetic acid (27 mL). The crude product (off-white solid; 1.67 g,

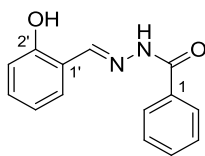
95%) was used for the next step without further purification. R_f 0.54 (10% MeOH/DCM); m.p. 190.5-191.1 °C; λ_{\max} (EtOH)/nm 291, 302, 329; $\nu_{\max}/\text{cm}^{-1}$ (neat) 1643 (s, C=O), 3197 (m, C-H str, aromatic), 3195 (m, N-H); ^1H NMR (500 MHz; DMSO- d_6) δ_{H} 6.97 (1H, t, J = 7.7 Hz, H-5'), 7.49 (2H, app. d, J = 7.7 Hz, H-4' and H-6'), 7.53-7.60 (2H, m, H-3 and H-5), 7.60-7.67 (1H, m, H-4), 7.92-8.00 (2H, m, H-2 and H-6), 8.62 (1H, s, CH=N), 12.39 and 12.44 (2 \times 1H, br s, O-H and N-H); ^{13}C NMR (125 MHz; DMSO- d_6) δ_{C} 119.6 (C-1' or C-3'), 120.0 (C-5'), 120.3 (C-1' or C-3'), 127.7 (C-2 and C-6), 128.6 (C-3 and C-5), 129.5 (C-4' or C-6'), 131.3 (C-4' or C-6'), 132.3 (C-4), 132.4 (C-1), 148.6 (CH=N), 153.3 (C-2'), 162.9 (C=O); LRMS (ES $^-$) m/z 273.2 [M-H] $^-$; HRMS calcd for C₁₄H₁₀O₂N₂³⁵Cl [M-H] $^-$ 273.0436, found 273.0435.

(E)-4-Chloro-*N'*-(2'-hydroxybenzylidene)benzohydrazide (184)



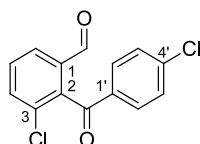
Compound **184** was synthesized according to general procedure J using salicylaldehyde (4.92 g, 40.3 mmol), 4-chlorobenzhydrazide (6.87 g, 40.3 mmol) and acetic acid (169 mL). The crude product (off-white solid; 10.77 g, 97%) was used in the following step without further purification. R_f 0.60 (10% MeOH/DCM); m.p. 220.1-220.3 °C; λ_{\max} (EtOH)/nm 287, 398, 330; $\nu_{\max}/\text{cm}^{-1}$ (neat) 1641 (s, C=O), 3068 (m, C-H str, aromatic), 3212 (m, N-H); ^1H NMR (500 MHz; DMSO- d_6) δ_{H} 6.90-6.97 (2H, m, H-4' and H-6'), 7.28-7.34 (1H, m, H-5'), 7.57 (1H, dd, J = 1.7, 7.6, H-3'), 7.60-7.67 (2H, m, H-3 and H-5), 7.93-8.01 (2H, m, H-2 and H-6), 8.64 (1H, s, CH=N), 11.22 and 12.17 (2 \times 1H, br s, O-H and N-H); ^{13}C NMR (125 MHz; DMSO- d_6) δ_{C} 116.4 (C-4), 118.7 (C-1'), 119.3 (C-6'), 128.6 (C-3 and C-5), 129.4 (C-3'), 129.5 (C-2 and C-6), 131.5 (C-5'), 131.5 (C-4), 136.8 (C-1), 148.4 (CH=N), 157.4 (C-2'), 161.7 (C=O); LRMS (ES $^-$) m/z 273.2 [M-H] $^-$; HRMS calcd for C₁₄H₁₀O₂N₂³⁵Cl [M-H] $^-$ 273.0436, found 273.0425.

(*E*)-*N'*-(2'-Hydroxybenzylidene)benzohydrazide (**187**)



Compound **187** was synthesized according to general procedure J using salicylaldehyde (5.00 g, 40.9 mmol), benzhydrazide (5.57 g, 40.9 mmol) and acetic acid (172 mL). The crude product (off-white solid; 1.70 g, 86%) was used for the next step without further purification. R_f 0.54 (10% MeOH/DCM); m.p. 171.2-171.5°C; λ_{\max} (EtOH)/nm 286, 297, 328; $\nu_{\max}/\text{cm}^{-1}$ (neat) 1671 (s, C=O), 3057 (w, C-H str, aromatic), 3264 (m, N-H); ^1H NMR (500 MHz; DMSO- d_6) δ_{H} 6.89–6.98 (2H, m, H-4' and H-6'), 7.27–7.34 (1H, m, H-5'), 7.52–7.58 (3H, m, H-3, H-3, and H-5), 7.59–7.64 (1H, m, H-4), 7.91–7.98 (2H, m, H-2 and H-6), 8.65 (1H, s, CH=N), 11.30 and 12.13 (2 \times 1H, br s, O-H and N-H); ^{13}C NMR (125 MHz; DMSO- d_6) δ_{C} 116.4 (C-4'), 118.7 (C-1'), 119.4 (C-6'), 127.7 (C-2 and C-6), 128.6 (C-3 and C-5), 129.5 (C-3'), 131.4 (C-5'), 132.0 (C-4), 132.8 (C-1), 148.3 (CH=N), 157.5 (C-2'), 162.8 (C=O); LRMS (ES $^+$) m/z 241.3 [M+H] $^+$; (ES $^-$) m/z 239.3 [M-H] $^-$; HRMS calcd for C₁₄H₁₁O₂N₂ [M-H] $^-$ 239.0826, found 239.0817.

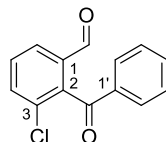
3-Chloro-2-(4'-chlorobenzoyl)benzaldehyde (**179**)



Compound **179** was synthesized according to general procedure K using benzohydrazide **178** (1.5 g, 4385 mmol), lead tetraacetate (2.58 g, 5.82 mmol) and THF (37 mL). The crude product was purified by MPLC (gradient elution, 0-25% EtOAc/petrol) to yield the title compound (1.29 g, 95%) as an orange oil which solidified upon storage at RT to give an orange solid. R_f 0.27 (20% EtOAc/petrol); m.p. 99.8-100.9 °C; λ_{\max} (EtOH)/nm 257; $\nu_{\max}/\text{cm}^{-1}$ (neat) 1669 (s, C=O ketone), 1695 (s, C=O aldehyde); ^1H NMR (500 MHz; CDCl₃) δ_{H} 7.40–7.47 (2H, m, H-3' and H-5'), 7.64 (1H, app. t, J = 7.8 Hz, H-5), 7.69–7.74 (3H, m, H-4, H-2' and H-6'), 7.90 (1H, dd, J = 7.8, 1.2 Hz, H-6), 9.88 (1H, s, CHO); ^{13}C NMR

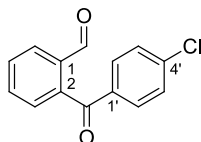
(125 MHz; CDCl₃) δ_c 129.3 (C-3' and C-5'), 130.4 (C-2' and C-6'), 130.5 (C-6), 130.8 (C-5), 132.4 (C-4'), 134.7 (C-3), 135.3 (C-4), 135.9 (C-1), 139.2 (C-2), 140.5 (C-1'), 189.4 (CHO), 193.1 (C=O); LRMS (ES⁺) m/z 279.2 [M+H]⁺; HRMS calcd for C₁₄H₉³⁵Cl₂O₂ [M+H]⁺ 278.9974, found 278.9977.

2-Benzoyl-3-chlorobenzaldehyde (**182**)



Compound **182** was synthesized according to general procedure K using benzohydrazide **181** (1.50 g, 5.46 mmol), lead tetraacetate (2.91 g, 6.55 mmol) and THF (42 mL). The crude product was purified by MPLC (gradient elution, 0-30% EtOAc/petrol) to yield the title compound (1.20 g, 90%) in form of yellow crystals. R_f 0.20 (20% EtOAc/petrol); m.p. 121.0-122.9 °C; λ_{max} (EtOH)/nm 248; ν_{max}/cm^{-1} (neat) 1666 (s, C=O ketone), 1697 (s, C=O aldehyde); ¹H NMR (500 MHz; DMSO-*d*₆) δ_H 7.48–7.56 (2H, m, H-2' and H-6'), 7.62–7.70 (3H, m, H-3', H-4', and H-5'), 7.84 (1H, app. t, J = 7.9 Hz, H-5), 7.95 (1H, dd, J = 7.9, 1.1 Hz, H-4), 8.15 (1H, dd, J = 7.9, 1.1 Hz, H-6), 9.91 (1H, s, CHO); ¹³C NMR (125 MHz; DMSO-*d*₆) δ_c 128.5 (C-3' and C-5'), 129.0 (C-2' and C-6'), 130.8 (C-3), 131.6 (C-5), 133.0 (C-6), 133.9 (C-4'), 135.2 (C-4), 135.7 (C-1'), 135.8 (C-1), 137.7 (C-2), 191.6 (CHO), 193.9 (C=O); LRMS (ES⁺) m/z 245.2 [M+H]⁺; HRMS calcd for C₁₄H₁₀³⁵ClO₂ [M+H]⁺ 245.0364, found 245.0365.

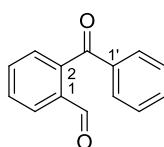
2-(4'-Chlorobenzoyl)benzaldehyde (**185**)



Compound **185** was synthesized according to general procedure K using benzohydrazide **184** (5.39 g, 19.6 mmol), lead tetraacetate (10.4 g, 23.5 mmol) and THF (150 mL). The crude product was purified by medium pressure liquid chromatography (gradient elution, 0-20% EtOAc/petrol) to yield the desired aldehyde (4.48 g, 93%) as an orange solid. R_f 0.29 (20% EtOAc/petrol);

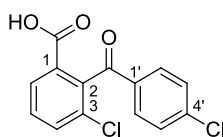
m.p. 102.8-107-1 °C; λ_{max} (EtOH)/nm 258; ν_{max} /cm⁻¹ (neat) 1664 (s, C=O ketone), 1689 (m, C=O aldehyde); ¹H NMR (500 MHz; CDCl₃) δ_{H} 7.41–7.45 (2H, m, H-3' and H-5'), 7.46–7.51 (1H, m, H-Ar), 7.67–7.78 (4H, m, 2 × H-Ar, H-2' and H-6'), 7.97–8.06 (1H, m, H-Ar), 10.01 (1H, s, CHO); ¹³C NMR (125 MHz; CDCl₃) δ_{C} 128.8 (C-Ar), 129.1 (C-3' and C-5'), 130.9 (C-Ar), 130.9 (C-Ar), 131.3 (C-2' and C-6'), 133.7 (C-Ar), 135.4 (C-Ar), 135.5 (C-Ar), 140.3 (C-Ar), 140.8 (C-Ar), 190.7 (CHO), 195.5 (C=O); LRMS (ES⁺) m/z 245.2 [M+H]⁺; HRMS calcd for C₁₄H₁₀³⁵ClO₂ [M+H]⁺ 245.0364, found 245.0365.

2-Benzoylbenzaldehyde (**188**)



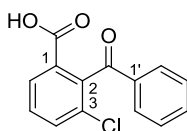
Compound **188** was synthesized according to general procedure K using benzohydrizide **187** (4.50 g, 18.7 mmol), lead tetraacetate (9.93 g, 22.4 mmol), and THF (145 mL). The crude product was purified by MPLC (gradient elution, petrol to petrol/EtOAc 4:1) to yield the title compound (3.58 g, 90%) as an orange solid. R_f 0.39 (20% EtOAc/petrol); m.p. 65.4-65.9 °C; λ_{max} (EtOH)/nm 251; ν_{max} /cm⁻¹ (neat) 1664 (s, C=O ketone), 1682 (m, C=O aldehyde); ¹H NMR (500 MHz; CDCl₃) δ_{H} 7.44–7.50 (2H, m, H-2' and H-6'), 7.50–7.54 (1H, m, H-Ar), 7.58–7.65 (1H, m, H-4'), 7.65–7.73 (2H, m, H-3' and H-5'), 7.77–7.83 (2H, m, 2 × H-Ar), 8.00–8.07 (1H, m, H-Ar), 10.03 (1H, s, CHO); ¹³C NMR (125 MHz; CDCl₃) δ_{C} 128.8 (C-2' and C-6'), 129.0 (C-Ar), 130.1 (C-3' and C-5'), 130.2 (C-Ar), 130.8 (C-Ar), 133.5 (C-Ar), 133.8 (C-4'), 135.6 (C-Ar), 137.2 (C-Ar), 141.6 (C-Ar), 190.7 (CHO), 196.6 (C=O); LRMS (ES⁺) m/z 211.3 [M+H]⁺; HRMS calcd for C₁₄H₁₁O₂ [M+H]⁺ 211.0754, found 211.0755.

3-Chloro-2-(4'-chlorobenzoyl)benzoic acid (**180**)



Compound **180** was obtained following general procedure L using **179** (1.15 g, 4.12 mmol), sodium chlorite (485 mg, 5.36 mmol), sulfamic acid (520 mg, 5.36 mmol), acetonitrile (52 mL) and water (2×7.5 mL). The crude product (yellow solid; 1.15 g, 95%) was used in the following step without further purification. R_f 0.17 (10% MeOH/DCM); m.p. 179.7-180.0 °C; λ_{\max} (EtOH)/nm 257; $\nu_{\max}/\text{cm}^{-1}$ (neat) 1678 (s, C=O), 2543, 2661, and 2833 (m br, O-H, hydrogen bonded); ^1H NMR (500 MHz; CDCl_3) δ_{H} 7.37–7.45 (2H, m, H-3' and H-5'), 7.52 (1H, t, J = 8.0 Hz, H-5), 7.62–7.72 (3H, m, H-4, H-2' and H-6'), 8.02–8.09 (1H, m, H-6); ^{13}C NMR (125 MHz; CDCl_3) δ_{C} 129.2 (C-Ar), 129.2 (C-3' and C-5'), 129.9 (C-6), 130.4 (C-5, C-2' and C-6'), 132.1 (C-Ar), 135.0 (C-Ar), 135.2 (C-4), 140.1 (C-1'), 140.8 (C-2), 169.3 (CO_2H), 193.2 (C=O); LRMS (ES⁻) m/z 293.2 [M-H]⁻; HRMS calcd for $\text{C}_{14}\text{H}_7\text{O}_3^{35}\text{Cl}_2$ [M-H]⁻ 292.9778, found 292.9763.

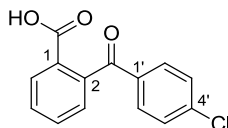
2-Benzoyl-3-chlorobenzoic acid (**183**)



Compound **183** was synthesized according to general procedure L using the aldehyde **182** (1.19 g, 4.86 mmol), sodium chlorite (572 mg, 6.32 mmol), sulfamic acid (614 mg, 6.32 mmol), acetonitrile (60 mL) and water (2×6.8 mL). The crude product (yellow solid; 1.22 g, 96%) was used in the following step without further purification. R_f 0.16 (10% MeOH/DCM); m.p. 231.7-232.3 °C; λ_{\max} (EtOH)/nm 245; $\nu_{\max}/\text{cm}^{-1}$ (neat) 1675 (s, C=O), 2548, 2661, and 2815 (m br, O-H, hydrogen bonded); ^1H NMR (500 MHz; $\text{DMSO}-d_6$) δ_{H} 7.52 (2H, m, H-2' and H-6'), 7.60–7.72 (4H, m, H-5, H-3', H-4', and H-5'), 7.82–7.91 (1H, m, H-4), 8.04 (1H, d, J = 7.9 Hz, H-6), 13.54 (1H, s, CO_2H); ^{13}C NMR (125 MHz; $\text{DMSO}-d_6$) δ_{C} 128.5 (C-3' and C-5'), 128.9 (C-2' and C-6'), 129.2 (C-6), 130.3 (C-Ar), 130.9 (C-5), 131.3 (C-Ar), 133.5 (C-4'), 133.9 (C-4), 136.3 (C-Ar), 139.8 (C-Ar), 165.6

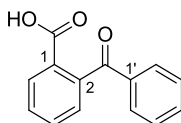
(CO₂H), 193.7 (C=O); LRMS (ES⁻) *m/z* 259.2 [M-H]⁻; HRMS calcd for C₁₄H₈O₃³⁵Cl [M-H]⁻ 259.0167, found 259.0169.

2-(4'-Chlorobenzoyl)benzoic acid (**186**)



Compound **186** was synthesized according to general procedure L using the aldehyde **185** (4.40 g, 18.0 mmol), sodium chlorite (2.12 g, 23.4 mmol), sulfamic acid (2.27 g, 23.4 mmol), MeCN (225 mL) and water (2 × 25 mL). Recrystallization from petrol/ethyl acetate yielded the title compound as a white solid (2.69 g, 57%). *R_f* 0.31 (10% MeOH/DCM); m.p. 151.5-152.1 °C; λ_{max} (EtOH)/nm 256; ν_{max}/cm⁻¹ (neat) 1670 (s, C=O), 2549, 2672, and 2835 (m br, O-H, hydrogen bonded); ¹H NMR (500 MHz; DMSO-*d*₆) δ_H 7.39–7.48 (1H, m, H-Ar), 7.54–7.59 (2H, m, H-3' and H-5'), 7.59–7.64 (2H, m, H-Ar), 7.67 (1H, td, *J* = 7.6, 1.3 Hz, H-Ar), 7.74 (1H, td, *J* = 7.6, 1.3 Hz, H-Ar), 7.97–8.03 (1H, m, H-Ar), 13.25 (1H, s, CO₂H); ¹³C NMR (125 MHz; DMSO-*d*₆) δ_C 127.4 (C-Ar), 128.9 (C-3' and C-5'), 129.8 (C-Ar), 129.9 (C-Ar), 130.0 (C-Ar), 130.6 (C-2' and C-6'), 132.6 (C-Ar), 135.8 (C-Ar), 138.0 (C-Ar), 141.0 (C-Ar), 166.8 (CO₂H), 195.4 (C=O); LRMS (ES⁻) *m/z* 259.2 [M-H]⁻; HRMS calcd for C₁₄H₈O₃³⁵Cl [M-H]⁻ 259.0167, found 259.0159.

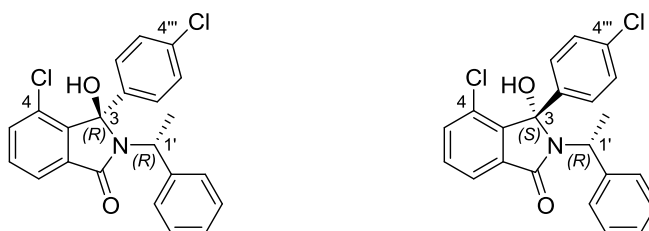
2-Benzoylbenzoic acid (**189**)



Compound **189** was obtained following general procedure L using aldehyde **188** (3.55 g, 16.9 mmol), sodium chlorite (1.99 g, 22.0 mmol), sulfamic acid (2.14 g, 22.0 mmol), MeCN (211 mL), and water (2 × 24 mL). The crude product (off-white solid; 3.65 g, 95%) was used for the following step without further purification. *R_f* 0.22 (10% MeOH/DCM); m.p. 117.7-119.7 °C; λ_{max} (EtOH)/nm 244; ν_{max}/cm⁻¹ (neat) 1675 (s, C=O), 2555, 2661, and 2825 (m br, O-H, hydrogen

bonded); ^1H NMR (500 MHz; $\text{DMSO-}d_6$) δ_{H} 7.38–7.46 (1H, m, H-3), 7.46–7.57 (2H, m, H-3' and H-5'), 7.58–7.65 (2H, m, H-2' and H-6'), 7.67 (1H, td, $J = 7.5, 1.3$ Hz, H-Ar), 7.74 (1H, td, $J = 7.5, 1.3$, H-Ar), 7.94–8.07 (1H, m, H-6), 13.18 (1 H, s, CO_2H); ^{13}C NMR (125 MHz; $\text{DMSO-}d_6$) δ_{C} 127.4 (C-3), 128.7 (C-3' and C-5'), 128.9 (C-2' and C-6'), 129.8 (C-6), 129.8 (C-Ar), 132.4 (C-Ar), 133.1 (C-Ar), 136.9 (C-Ar), 141.4 (C-Ar), 166.8 (CO_2H), 196.4 (C=O). One quaternary carbon not detected; LRMS (ES^-) m/z 225.2 $[\text{M-H}]^-$; HRMS calcd for $\text{C}_{14}\text{H}_9\text{O}_3$ $[\text{M-H}]^-$ 225.0557, found 225.0549.

(3*R*,1'*R*)-4-Chloro-3-(4'''-chlorophenyl)-3-hydroxy-2-(1'-phenylethyl)isoindolin-1-one (190) and (3*S*,1'*R*)-4-chloro-3-(4'''-chlorophenyl)-3-hydroxy-2-(1'-phenylethyl)isoindolin-1-one (192)



To a solution of the benzoylbenzoic acid **180** (550 mg, 1.86 mmol) in THF (2.2 mL, 1.2 mmol/mL), thionyl chloride (0.27 mL, 443 mg, 3.72 mmol) and a catalytic amount of DMF (1 drop) were added at room temperature. The solution was stirred for 2 h before removal of solvent and excess SOCl_2 *in vacuo*. THF (2.2 mL, 1.2 mmol/mL) was added to the residue, followed by (*R*)-(+)-methylbenzylamine (0.26 mL, 248 mg, 2.05 mmol) and diisopropylamine (0.36 mL, 260 mg, 2.57 mmol), and the reaction mixture was stirred overnight. Water (10 mL) and EtOAc (10 mL) were added, and the two layers were separated. The aqueous layer was extracted with EtOAc (20 mL). The combined organic layers were washed with brine, dried (MgSO_4), filtered and the solvent was removed *in vacuo*. The crude product was purified by MPLC (gradient elution, 0–25% EtOAc/petrol) to yield isoindolinones **190** (151 mg, 20%) and **192** (171 mg, 23%) as colorless oils which crystallized upon storage at RT. A mixture of the two diastereoisomers was also recovered (79 mg, 54% overall yield).

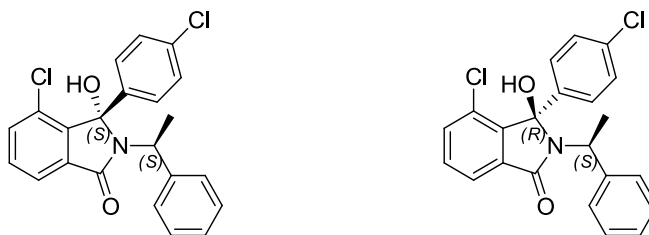
190

R_f 0.60 (33% EtOAc/petrol); m.p. 164.7-166.6 °C; $[\alpha]_D^{29} +161^\circ$ (c 0.511, EtOAc); λ_{\max} (EtOH)/nm 258; $\nu_{\max}/\text{cm}^{-1}$ (neat) 1588 (s, C-N amide), 1679 (s, C=O), 3244 (br, O-H); ^1H NMR (500 MHz; DMSO- d_6) δ_{H} 1.42 (3H, d, J = 7.2 Hz, CHCH₃), 4.40 (1H, q, J = 7.2 Hz, CHCH₃), 7.17-7.23 (1H, m, H-4'), 7.24-7.30 (2H, m, H-Ar), 7.37-7.49 (6H, br m, H-Ar), 7.52 (1H, s, OH), 7.56-7.62 (2H, m, H-Ar), 7.65-7.70 (1H, m, H-Ar); ^{13}C NMR (125 MHz; DMSO- d_6) δ_{C} 17.7 (CHCH₃), 50.3 (CHCH₃), 90.3 (C-3), 121.2 (C-Ar), 126.5 (C-Ar), 127.3 (C-Ar), 127.7 (2 × C-Ar), 128.2 (2 × C-Ar), 128.5 (C-Ar), 128.7 (2 × C-Ar), 129.5 (C-Ar), 131.7 (C-Ar), 133.8 (C-Ar), 134.2 (C-Ar), 135.5 (C-Ar), 142.2 (C-Ar), 143.4 (C-Ar), 165.8 (C-1); LRMS (ES⁻) m/z [M-H]⁻ 396.2; HRMS calcd for C₂₂H₁₆³⁵Cl₂NO₂ [M-H]⁻ 396.0564, found 396.0547; HPLC 96.9% in 0.1% formic acid (aq)/MeCN (R_t 9.7 min); 99.1% in 0.1% ammonia (aq)/MeCN (R_t 9.6 min); 97.5% in water/MeCN (R_t 9.8 min).

192

R_f 0.51 (33% EtOAc/petrol); m.p. 201.5-204.5 °C; $[\alpha]_D^{29} +58^\circ$ (c 0.542, EtOAc); λ_{\max} (EtOH)/nm 257; $\nu_{\max}/\text{cm}^{-1}$ (neat) 1589 (s, C-N amide), 1670 (s, C=O), 3127 (br, O-H); ^1H NMR (500 MHz; DMSO- d_6) δ_{H} 1.79 (3H, d, J = 7.0 Hz, CHCH₃), 4.48 (1H, q, J = 7.0 Hz, CHCH₃), 6.94-6.99 (2H, m, H-Ar), 7.01-7.09 (3H, m, H-Ar), 7.16-7.25 (4H, br, H-Ar), 7.49 (1H, s, OH), 7.57-7.62 (2H, m, H-Ar), 7.67-7.73 (1H, m, H-Ar); ^{13}C NMR (125 MHz; DMSO- d_6) δ_{C} 19.7 (CHCH₃), 51.0 (CHCH₃), 90.1 (C-3), 121.3 (C-Ar), 126.4 (C-Ar), 127.1 (2 × C-Ar), 127.5 (2 × C-Ar), 127.8 (2 × C-Ar), 128.4 (C-Ar), 128.6 (2 × C-Ar), 131.7 (C-Ar), 132.6 (C-Ar), 133.3 (C-Ar), 134.5 (C-Ar), 136.8 (C-Ar), 141.9 (C-Ar), 143.9 (C-Ar), 164.9 (C-1); LRMS (ES⁻) m/z [M-H]⁻ 396.2; HRMS calcd for C₂₂H₁₆³⁵Cl₂NO₂ [M-H]⁻ 369.0564, found 396.0546; HPLC 94.1% in 0.1% formic acid (aq)/MeCN (R_t 9.5 min); 99.4% in 0.1% ammonia (aq)/MeCN (R_t 9.6 min); 96.2% in water/MeCN (R_t 9.5 min).

(3*S*,1'*S*)-4-Chloro-3-(4'''-chlorophenyl)-3-hydroxy-2-(1'-phenylethyl)isoindolin-1-one (194) and (3*R*,1'*S*)-4-chloro-3-(4'''-chlorophenyl)-3-hydroxy-2-(1'-phenylethyl)isoindolin-1-one (196)



Isoindolinones **194** and **196** were synthesized according to general procedure M using benzybenzoic acid **180** (550 mg, 1.86 mmol), thionyl chloride (0.27 mL, 443 mg, 3.72 mmol), catalytic DMF (3 drops), THF (2 × 2.2 mL), (*S*)-(-)-methylbenzylamine (0.26 mL, 248 mg, 2.05 mmol) and DIPEA (0.36 mL, 265 mg, 2.05 mmol). The crude product was purified by MPLC (gradient elution, 0-75% EtOAc/petrol) to yield the desired compounds **194** (298 mg, 40%) and **196** (219 mg, 30%) as off-white solids.

194

R_f 0.60 (33% EtOAc/petrol); m.p. 164.5-168.1 °C; $[\alpha]_D^{29}$ -168° (c 0.513, EtOAc); λ_{max} (EtOH)/nm 259; ν_{max}/cm^{-1} (neat) 1587 (m, C-N amide), 1674 (vs, C=O), 3257 (br, O-H); 1H NMR (500 MHz; DMSO- d_6) δ_H 1.42 (3H, d, J = 7.1 Hz, CHCH₃), 4.39 (1H, q, J = 7.1 Hz, CHCH₃), 7.16–7.22 (1H, m, H-4'), 7.22–7.29 (2H, m, H-Ar), 7.33–7.49 (6H, m, H-Ar), 7.51 (1H, s, OH), 7.56–7.61 (2H, m, H-Ar), 7.64–7.69 (1H, m, H-Ar); ^{13}C NMR (125 MHz; DMSO- d_6) δ_C 17.7 (CHCH₃), 50.3 (CHCH₃), 90.3 (C-3), 121.2 (C-Ar), 126.5 (C-Ar), 127.3 (2 × C-Ar), 127.7 (2 × C-Ar), 128.1 (2 × C-Ar), 128.5 (C-Ar), 128.7 (2 × C-Ar), 131.6 (C-Ar), 132.8 (C-Ar), 133.3 (C-Ar), 134.2 (C-Ar), 137.1 (C-Ar), 141.7 (C-Ar), 143.8 (C-Ar), 164.4 (C-1); LRMS (ES⁻) m/z [M-H]⁻ 396.2; HRMS calcd for C₂₂H₁₆³⁵Cl₂NO₂ [M-H]⁻ 396.0562, found 396.0564.

196

R_f 0.51 (33% EtOAc/petrol); m.p. 202.7-203.9 °C; $[\alpha]_D^{29}$ -62° (c 0.568, EtOAc); λ_{max} (EtOH)/nm 257; ν_{max}/cm^{-1} (neat) 1589 (s, C-N amide), 1671 (s, C=O), 3155

(br, O-H); ^1H NMR (500 MHz; $\text{DMSO-}d_6$) δ_{H} 1.77 (3H, d, $J = 7.0$ Hz, CHCH_3), 4.48 (1H, q, $J = 7.0$ Hz, CHCH_3), 6.94-6.99 (2H, m, H-Ar), 7.02-7.09 (3H, m, H-Ar), 7.13-7.28 (4H, m, H-Ar), 7.49 (1H, s, OH), 7.57-7.62 (2H, m, H-Ar), 7.66-7.73 (1H, m, H-Ar); ^{13}C NMR (125 MHz; $\text{DMSO-}d_6$) δ_{C} 19.8 (CHCH_3), 51.0 (CHCH_3), 90.1 (C-3), 121.3 (C-Ar), 126.4 (C-Ar), 127.1 ($2 \times$ C-Ar), 127.5 ($2 \times$ C-Ar), 127.8 ($2 \times$ C-Ar), 128.4 (C-Ar), 128.6 ($2 \times$ C-Ar), 131.7 (C-Ar), 132.6 (C-Ar), 133.3 (C-Ar), 134.5 (C-Ar), 136.8 (C-Ar), 141.9 (C-Ar), 143.9 (C-Ar), 164.9 (C-1); LRMS (ES-) m/z $[\text{M-H}]^-$ 396.2; HRMS calcd for $\text{C}_{22}\text{H}_{16}^{35}\text{Cl}_2\text{NO}_2$ $[\text{M-H}]^-$ 396.0564, found 396.0564; HPLC 96.5% in 0.1% formic acid (aq)/MeCN (R_{t} 9.5 min); 99.6% in 0.1% ammonia (aq)/MeCN (R_{t} 9.6 min); 95.3% in water/ MeCN (R_{t} 9.5 min).

(3*R*,1'*R*)-3-Hydroxy-3-phenyl-2-(1'-phenylethyl)isoindolin-1-one (209)
and (3*R*,1'*R*)-3-Hydroxy-3-phenyl-2-(1'-phenylethyl)isoindolin-1-one (211)



Compounds **209** and **211** were synthesized according to general procedure M using benzoylbenzoic acid **189** (1.00 g, 4.42 mmol), thionyl chloride (1.72 mL, 1.05 g, 8.84 mmol), catalytic DMF (3 drops), THF (2×5.3 mL), (*R*)-(+)-methylbenzylamine (0.62 mL, 589 mg, 4.86 mmol) and DIPEA (0.85 mL, 628 mg, 4.86 mmol). The crude product was purified by MPLC (gradient elution, 0-24% EtOAc/petrol) to yield the desired compounds **209** (239 mg, 16%) and **211** (158 mg, 11%) as white solids. The total yield of the two diastereoisomers was 1.18 g (81%).

209

R_{f} 0.68 (50% EtOAc/petrol); m.p. 129.8-131.7°C; $[\alpha]_{\text{D}}^{30} +179^\circ$ (c 0.488, EtOAc); λ_{max} (EtOH)/nm 252; ν_{max} /cm $^{-1}$ (neat) 1670 (s, C=O), 3220 (br, O-H); ^1H NMR (500 MHz; $\text{DMSO-}d_6$) δ_{H} 1.46 (3H, d, $J = 7.1$ Hz, CHCH_3), 4.40 (1H, q, $J = 7.1$ Hz, CHCH_3), 7.15-7.22 (2H, m, H-Ar), 7.22-7.28 (3H, m, H-Ar), 7.29-7.43 (5H, m, H-

Ar and OH), 7.44-7.58 (4H, m, H-Ar), 7.64-7.72 (1H, m, H-Ar); ^{13}C NMR (125 MHz; DMSO- d_6) δ_{C} 17.8 (CHCH $_3$), 50.6 (CHCH $_3$), 91.1 (C-3), 122.2 (C-Ar), 122.9 (C-Ar), 126.3 (2 \times C-Ar), 126.4 (C-Ar), 127.4 (2 \times C-Ar), 127.7 (2 \times C-Ar), 128.1 (C-Ar), 128.3 (2 \times C-Ar), 129.2 (C-Ar), 131.4 (C-Ar), 132.4 (C-Ar), 140.1 (C-Ar), 142.3 (C-Ar), 149.0 (C-Ar), 166.0 (C-1); LRMS (ES $^-$) m/z [M-H] $^-$ 328.3; HRMS calcd for C $_{22}$ H $_{20}$ NO $_2$ [M+H] $^+$ 330.1489, found 330.1491; HPLC 95.2% in 0.1% formic acid (aq)/MeCN (R_{t} 8.7 min); 98.4% in 0.1% ammonia (aq)/MeCN (R_{t} 8.5 min); 93.7% in water/ MeCN (R_{t} 8.7 min).

211

R_{f} 0.63 (50% EtOAc/petrol); m.p. 172.1-174.4 $^{\circ}\text{C}$; $[\alpha]_{\text{D}}^{30}$ -34 $^{\circ}$ (c 0.536, EtOAc); λ_{max} (EtOH)/nm 252; ν_{max} /cm $^{-1}$ (neat) 1668 (s, C=O), 3211 (br, O-H); ^1H NMR (500 MHz; DMSO- d_6) δ_{H} 1.75 (3H, d, J = 7.2 Hz, CHCH $_3$), 4.52 (1H, q, J = 7.2 Hz, CHCH $_3$), 6.98-7.08 (5H, m, H-Ar), 7.14-7.23 (6H, m, H-Ar), 7.24 (1H, s, OH), 7.49-7.58 (2H, m, H-Ar), 7.67-7.72 (1H, m, H-Ar); ^{13}C NMR (125 MHz; DMSO- d_6) δ_{C} 19.7 (CHCH $_3$), 51.1 (CHCH $_3$), 90.9 (C-3), 122.2 (C-Ar), 122.8 (C-Ar), 126.3 (C-Ar), 126.4 (2 \times C-Ar), 127.3 (2 \times C-Ar), 127.5 (2 \times C-Ar), 127.9 (2 \times C-Ar), 127.9 (C-Ar), 129.3 (C-Ar), 131.5 (C-Ar), 132.4 (C-Ar), 139.7 (C-Ar), 142.2 (C-Ar), 149.2 (C-Ar), 166.4 (C-1); LRMS (ES $^-$) m/z [M-H] $^-$ 328.3; HRMS calcd for C $_{22}$ H $_{20}$ NO $_2$ [M+H] $^+$ 330.1489, found 330.1493; HPLC 95.2% in 0.1% formic acid (aq)/MeCN (R_{t} 8.5 min); 99.6% in 0.1% ammonia (aq)/MeCN (R_{t} 8.5 min); 94.5% in water/ MeCN (R_{t} 8.5 min).

(3*S*,1'*S*)-3-Hydroxy-3-phenyl-2-(1'-phenylethyl)isoindolin-1-one (213) and (3*R*,1'*S*)-3-hydroxy-3-phenyl-2-(1'-phenylethyl)isoindolin-1-one (215)



Compounds **213** and **215** were synthesized according to general procedure M using benzoylbenzoic acid **189** (1.00 g, 4.42 mmol), thionyl

chloride (1.72 mL, 1.05 g, 8.84 mmol), catalytic DMF (3 drops), THF (2×5.3 mL), (*S*)-(-)-methylbenzylamine (0.62 mL, 589 mg, 4.86 mmol) and DIPEA (0.85 mL, 628 mg, 4.86 mmol). The crude product was purified by MPLC (gradient elution, 3-20% EtOAc/petrol) to yield the desired compounds **213** (0.49 g, 34%) and **215** (0.53 g, 36%) as white solids. The total yield of the two diastereoisomers was 1.26 g (87%).

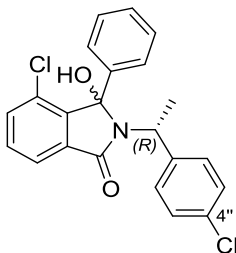
213

R_f 0.68 (50% EtOAc/petrol); m.p. 129.8-131.7°C; $[\alpha]_D^{30}$ -184° (c 0.424, EtOAc); λ_{max} (EtOH)/nm 252; ν_{max}/cm^{-1} (neat) 1665 (s, C=O), 3224 (br, O-H); 1H NMR (500 MHz; DMSO- d_6) δ_H 1.47 (3H, d, J = 7.1 Hz, CHCH₃), 4.41 (1H, q, J = 7.1 Hz, CHCH₃), 7.15-7.22 (2H, m, H-Ar), 7.22-7.29 (3H, m, H-Ar), 7.30-7.42 (5H, m, H-Ar and OH), 7.46-7.58 (4H, m, H-Ar), 7.66-7.70 (1H, m, H-Ar); ^{13}C NMR (125 MHz; DMSO- d_6) δ_C 17.8 (CHCH₃), 50.5 (CHCH₃), 91.1 (C-3), 122.2 (C-Ar), 122.8 (C-Ar), 126.2 ($2 \times$ C-Ar), 126.4 (C-Ar), 127.3 ($2 \times$ C-Ar), 127.6 ($2 \times$ C-Ar), 128.0 (C-Ar), 128.3 ($2 \times$ C-Ar), 129.2 (C-Ar), 131.3 (C-Ar), 132.4 (C-Ar), 140.1 (C-Ar), 142.3 (C-Ar), 149.0 (C-Ar), 166.0 (C-1); LRMS (ES⁻) m/z 328.3 [M-H]⁻; HRMS calcd for C₂₂H₂₀NO₂ [M+H]⁺ 330.1489, found 330.1491; HPLC 95.3% in 0.1% formic acid (aq)/MeCN (R_t 8.6 min); 98.0% in 0.1% ammonia (aq)/MeCN (R_t 8.5 min); 94.8% in water/ MeCN (R_t 8.7 min).

215

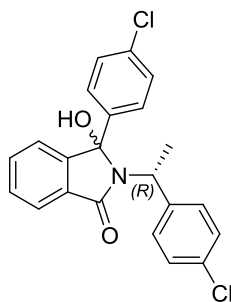
R_f 0.63 (50% EtOAc/petrol); m.p. 170.8-173.2 °C; $[\alpha]_D^{30}$ +51° (c 0.593, EtOAc); λ_{max} (EtOH)/nm 252; ν_{max}/cm^{-1} (neat) 1669 (s, C=O), 3216 (br, O-H); 1H NMR (500 MHz; DMSO- d_6) δ_H 1.76 (3H, d, J = 7.2 Hz, CHCH₃), 4.53 (1H, q, J = 7.2 Hz, CHCH₃), 6.99-7.09 (5H, m, H-Ar), 7.15-7.24 (6H, m, H-Ar), 7.25 (1H, s, OH), 7.51-7.59 (2H, m, H-Ar), 7.67-7.73 (1H, m, H-Ar); ^{13}C NMR (125 MHz; DMSO- d_6) δ_C 19.7 (CHCH₃), 51.0 (CHCH₃), 90.9 (C-3), 122.2 (C-Ar), 122.8 (C-Ar), 126.3 (C-Ar), 126.3 ($2 \times$ C-Ar), 127.3 ($2 \times$ C-Ar), 127.4 ($2 \times$ C-Ar), 127.9 ($2 \times$ C-Ar), 127.9 (C-Ar), 129.2 (C-Ar), 131.5 (C-Ar), 132.4 (C-Ar), 139.7 (C-Ar), 142.2 (C-Ar), 149.2 (C-Ar), 166.4 (C-1); LRMS (ES⁻) m/z 328.3 [M-H]⁻; HRMS calcd for C₂₂H₂₀NO₂ [M+H]⁺ 330.1489, found 330.1493.

(1'*R*)-4-Chloro-2-[1'-(4''-chlorophenyl)ethyl]-3-hydroxy-3-phenylisoindolin-1-one (198)



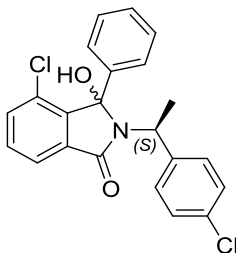
Compound **198** was synthesized according to general procedure M using acid **183** (600 mg, 2.30 mmol), thionyl chloride (0.33 mL, 547 mg, 4.60 mmol), catalytic DMF (3 drops), (*R*)-4-chloro- α -methylbenzylamine (0.35 mL, 394 mg, 2.53 mmol), DIPEA (0.44 mL, 327 mg, 2.53 mmol) and THF (2 \times 2.8 mL). The product was obtained as a mixture of diastereoisomers (cream-colored solid; 0.81 g, 88%) after purification by MPLC (gradient elution, 3-30% EtOAc/petrol). $R_{f(1)}$ 0.55; $R_{f(2)}$ 0.40 (25% EtOAc/petrol); no clear m.p. detected; λ_{\max} (EtOH)/nm 259; $\nu_{\max}/\text{cm}^{-1}$ (neat) 1660 and 1673 (vs, C=O), 3212 (br, O-H); ^1H NMR (500 MHz; DMSO- d_6) δ_{H} 1.36 (3H, d, J = 7.1 Hz, -CH₃), 1.75 (3H, d, J = 7.1 Hz, CH₃), 4.38 (1H, q, J = 7.1 Hz, CHCH₃), 4.50 (1H, q, J = 7.0 Hz, CHCH₃), 6.88 – 6.97 (2H, m, H-Ar), 7.03 – 7.15 (2H, m, H-Ar), 7.23 (5H, br, J = 14.5 Hz, H-Ar), 7.29 – 7.48 (8H, m, H-Ar), 7.48 – 7.54 (2H, m, H-Ar), 7.54 – 7.63 (3H, m, H-Ar), 7.67 (1H, dd, J = 5.3, 3.0 Hz, H-Ar), 7.70 (1H, dd, J = 5.2, 3.2 Hz, H-Ar); ^{13}C NMR (125 MHz; DMSO- d_6) δ_{C} 17.3 (CHCH₃), 19.4 (CHCH₃), 49.6 (CHCH₃), 50.1 (CHCH₃), 90.5 (C-3), 90.7 (C-3), 121.1 (C-Ar), 121.1 (C-Ar), 126.5 (C-Ar), 126.6 (C-Ar), 127.3 (C-Ar), 127.6 (C-Ar), 127.8 (C-Ar), 128.1 (C-Ar), 128.1 (C-Ar), 128.2 (C-Ar), 128.5 (C-Ar), 128.6 (C-Ar), 129.1 (C-Ar), 129.3 (C-Ar), 130.9 (C-Ar), 131.2 (C-Ar), 131.5 (C-Ar), 131.5 (C-Ar), 133.3 (C-Ar), 134.2 (C-Ar), 134.4 (C-Ar), 137.6 (C-Ar), 137.8 (C-Ar), 140.7 (C-Ar), 140.8 (C-Ar), 144.2 (C-Ar), 144.3 (C-Ar), 164.4 (C-Ar), 164.8 (C-Ar); LRMS (ES⁺) m/z 420.2 [M+Na]⁺; HRMS calcd for C₂₂H₁₈³⁵Cl₂NO₂ [M+H]⁺ 398.0709, found 398.0712.

(1'*R*)-3-(4-Chlorophenyl)-2-[1'-(4'''-chlorophenyl)ethyl]-3-hydroxyisoindolin-1-one (203)



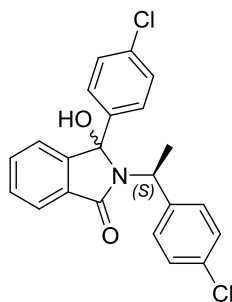
Compound **203** was synthesized according to general procedure M using acid **186** (600 mg, 2.30 mmol), thionyl chloride (0.33 mL, 547 mg, 4.60 mmol), catalytic DMF (3 drops), (*R*)-4-chloro- α -methylbenzylamine (0.35 mL, 394 mg, 2.53 mmol), DIPEA (0.44 mL, 327 mg, 2.53 mmol) and THF (2 \times 2.8 mL). The product was obtained as a mixture of diastereoisomers (white solid; 0.88 g, 96%) after purification by MPLC (gradient elution, 3-50% EtOAc/petrol). $R_{f(1)}$ 0.51; $R_{f(2)}$ 0.32 (25% EtOAc/petrol); no clear m.p. detected; λ_{\max} (EtOH)/nm 252sh; $\nu_{\max}/\text{cm}^{-1}$ (neat) 1672 (vs, C=O), 3265 (br, O-H); ^1H NMR (500 MHz; DMSO- d_6) δ_{H} 1.48 (3H, d, J = 7.1 Hz, CH₃), 1.74 (3H, d, J = 7.2 Hz, CH₃), 4.44 (1H, q, J = 7.1 Hz, CHCH₃), 4.54 (1H, q, J = 7.1 Hz, CHCH₃), 7.08 – 7.13 (2H, m, H-Ar), 7.13 – 7.18 (2H, m, H-Ar), 7.18 – 7.27 (5H, m, H-Ar), 7.28 – 7.34 (2H, m, H-Ar), 7.35 – 7.45 (5H, m, H-Ar), 7.46 – 7.51 (2H, m, H-Ar), 7.51 – 7.61 (4H, m, H-Ar), 7.66 – 7.70 (1H, m, H-Ar), 7.70 – 7.75 (1H, m, H-Ar); ^{13}C NMR (125 MHz; DMSO- d_6) δ_{C} 17.8 (CHCH₃), 19.9 (CHCH₃), 49.9 (CHCH₃), 50.6 (CHCH₃), 90.4 (C-3), 90.6 (C-3), 122.3 (C-Ar), 122.4 (C-Ar), 122.8 (C-Ar), 122.8 (C-Ar), 127.5 (C-Ar), 127.5 (C-Ar), 127.9 (C-Ar), 128.3 (C-Ar), 128.3 (C-Ar), 129.1 (C-Ar), 129. (C-Ar)₃, 129.4 (C-Ar), 129.5 (C-Ar), 131.0 (C-Ar), 131.0 (C-Ar), 131.1 (C-Ar), 131.2 (C-Ar), 132.6 (C-Ar), 132.7 (C-Ar), 132.7 (C-Ar), 132.8 (C-Ar), 138.7 (C-Ar), 139.1 (C-Ar), 141.0 (C-Ar), 141.4 (C-Ar), 148.6 (C-Ar), 148.7 (C-Ar), 166.0 (C-Ar), 166.5 (C-Ar); LRMS (ES⁺) m/z 420.2 [M+Na]⁺; HRMS calcd for C₂₂H₁₆³⁵Cl₂NO₂ [M-H]⁻ 396.0564, found 396.0564.

(1'S)-4-Chloro-2-[1'-(4'''-chlorophenyl)ethyl]-3-hydroxy-3-phenylisoindolin-1-one (200)



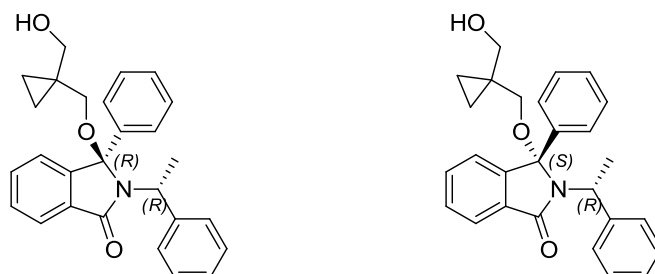
Compound **200** was synthesized according to general procedure M using acid **183** (538 mg, 2.06 mmol), thionyl chloride (0.30 mL, 490 mg, 4.12 mmol), catalytic DMF (3 drops), (*S*)-4-chloro- α -methylbenzylamine (0.32 mL, 353 mg, 2.27 mmol), DIPEA (0.40 mL, 293 mg, 2.27 mmol) and THF (2 \times 2.5 mL). The product was obtained as a mixture of diastereoisomers (off-white solid; 0.77 g, 94%) after purification by MPLC (gradient elution, petrol 0-25% EtOAc/petrol). $R_{f(1)}$ 0.52; $R_{f(2)}$ 0.35 (25% EtOAc/petrol); no clear m.p. detected; λ_{\max} (EtOH)/nm 259; $\nu_{\max}/\text{cm}^{-1}$ (neat) 1660 and 1673 (vs, C=O), 3215 (O-H); ^1H NMR (500 MHz; DMSO- d_6) δ_{H} 1.36 (3H, d, J = 7.1 Hz, -CH₃), 1.75 (3H, d, J = 7.2 Hz, CH₃), 4.38 (1H, q, J = 7.1 Hz, CHCH₃), 4.50 (1H, q, J = 7.0 Hz, CHCH₃), 6.88 – 6.97 (2H, m, H-Ar), 7.03 – 7.15 (2H, m, H-Ar), 7.23 (5H, br, J = 14.5 Hz, H-Ar), 7.29 – 7.48 (8H, m, H-Ar), 7.48 – 7.54 (2H, m, H-Ar), 7.54 – 7.63 (3H, m, H-Ar), 7.67 (1H, dd, J = 5.3, 3.0 Hz, H-Ar), 7.70 (1H, dd, J = 5.2, 3.2 Hz, H-Ar); ^{13}C NMR (125 MHz; DMSO- d_6) δ_{C} 17.3 (CHCH₃), 19.4 (CHCH₃), 49.6 (CHCH₃), 50.1 (CHCH₃), 90.5 (C-3), 90.7 (C-3), 121.1 (C-Ar), 121.1 (C-Ar), 126.5 (C-Ar), 126.6 (C-Ar), 127.3 (C-Ar), 127.6 (C-Ar), 127.8 (C-Ar), 128.1 (C-Ar), 128.1 (C-Ar), 128.2 (C-Ar), 128.5 (C-Ar), 128.6 (C-Ar), 129.1 (C-Ar), 129.3 (C-Ar), 130.9 (C-Ar), 131.2 (C-Ar), 131.5 (C-Ar), 131.5 (C-Ar), 133.3 (C-Ar), 134.2 (C-Ar), 134.4 (C-Ar), 137.6 (C-Ar), 137.8 (C-Ar), 140.7 (C-Ar), 140.8 (C-Ar), 144.2 (C-Ar), 144.3 (C-Ar), 164.4 (C-Ar), 164.8 (C-Ar); LRMS (ES⁺) m/z 420.1 [M+Na]⁺; HRMS calcd for C₂₂H₁₈³⁵Cl₂NO₂ [M+H]⁺ 398.0709, found 398.0714

(1'S)-3-(4''-Chlorophenyl)-2-[1'-(4'''-chlorophenyl)ethyl]-3-hydroxyisoindolin-1-one (206)



Compound **206** was synthesized according to general procedure M using acid **186** (600 mg, 2.30 mmol), thionyl chloride (0.33 mL, 547 mg, 4.60 mmol), catalytic DMF (3 drops), (*S*)-4-chloro- α -methylbenzylamine (0.35 mL, 394 mg, 2.53 mmol), DIPEA (0.44 mL, 327 mg, 2.53 mmol) and THF (2 \times 2.8 mL). The product was obtained as a mixture of diastereoisomers (white solid; 0.86 g, 94%) after purification by MPLC (gradient elution, 0-20% EtOAc/petrol). $R_{f(1)}$ 0.52; $R_{f(2)}$ 0.35 (25% EtOAc/petrol); no clear m.p. detected; λ_{\max} (EtOH)/nm 252sh; $\nu_{\max}/\text{cm}^{-1}$ (neat) 1673 (vs, C=O), 3265 (br, O-H); ^1H NMR (500 MHz; DMSO- d_6) δ_{H} 1.48 (3H, d, J = 7.1 Hz, CH₃), 1.74 (3H, d, J = 7.2 Hz, CH₃), 4.44 (1H, q, J = 7.1 Hz, CHCH₃), 4.54 (1H, q, J = 7.1 Hz, CHCH₃), 7.08 – 7.13 (2H, m, H-Ar), 7.13 – 7.18 (2H, m, H-Ar), 7.18 – 7.27 (5H, m, H-Ar), 7.28 – 7.34 (2H, m, H-Ar), 7.35 – 7.45 (5H, m, H-Ar), 7.46 – 7.51 (2H, m, H-Ar), 7.51 – 7.61 (4H, m, H-Ar), 7.66 – 7.70 (1H, m, H-Ar), 7.70 – 7.75 (1H, m, H-Ar); ^{13}C NMR (126 MHz, DMSO- d_6) δ_{C} 17.8 (CHCH₃), 19.9 (CHCH₃), 49.9 (CHCH₃), 50.6 (CHCH₃), 90.4 (C-3), 90.6 (C-3), 122.3 (C-Ar), 122.4 (C-Ar), 122.8 (C-Ar), 122.8 (C-Ar), 127.5 (C-Ar), 127.5 (C-Ar), 127.9 (C-Ar), 128.3 (C-Ar), 128.3 (C-Ar), 128.3 (C-Ar), 129.1 (C-Ar), 129.3 (C-Ar), 129.4 (C-Ar), 129.5 (C-Ar), 131.0 (C-Ar), 131.0 (C-Ar), 131.1 (C-Ar), 131.2 (C-Ar), 132.6 (C-Ar), 132.7 (C-Ar), 132.7 (C-Ar), 132.8 (C-Ar), 138.7 (C-Ar), 139.1 (C-Ar), 141.0 (C-Ar), 141.4 (C-Ar), 148.6 (C-Ar), 148.7 (C-Ar), 166.0 (C-Ar), 166.5 (C-Ar); LRMS (ES⁺) m/z 420.1 [M+Na]⁺; HRMS calcd for C₂₂H₁₆³⁵Cl₂NO₂ [M-H]⁻ 396.0564, found 396.0563.

(3*R*,1'*R*)-3-[[1'''-(Hydroxymethyl)cyclopropyl]methoxy]-3-phenyl-2-(1'-phenylethyl)isoindolin-1-one (210) and (3*S*,1'*R*)-3-[[1'''-(hydroxymethyl)cyclopropyl]methoxy]-3-phenyl-2-(1'-phenylethyl)isoindolin-1-one (212)



Alcohols **210** and **212** were obtained following general procedure N using isoindolinone **209** and **211** (341 mg, 1.03 mmol), indium tribromide (73 mg, 0.206 mmol), 1,1-bis(hydroxymethyl)cyclopropane (0.49 mL, 526 mg, 5.15 mmol), and DCE (10 mL, 10 mL/mmol). Purification by MPLC (gradient elution, 0-4% MeOH/DCM) yielded the pure diastereoisomers as white amorphous solids (**210**: 104 mg, 24%; **212**: 96 mg, 23%).

210

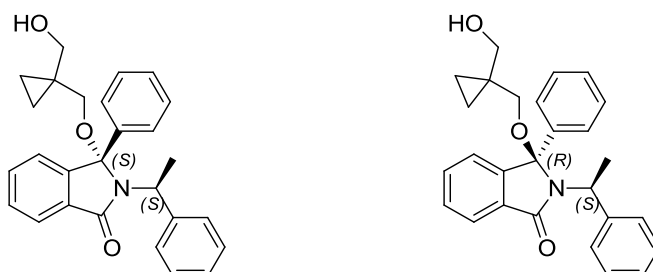
R_f 0.49 (4% MeOH/DCM); no clear m.p. detected; $[\alpha]_D^{30} +89^\circ$ (c 0.425, EtOAc); λ_{max} (EtOH)/nm 252; ν_{max}/cm^{-1} (neat) 1682 and 1697 (s, C=O), 2874, 2933 and 3059 (w, C-H and $-CH_2-$ aliphatic), 3400 (br, O-H); 1H NMR (500 MHz; $CDCl_3$) δ_H -0.12 – 0.05 (2H, m, cyclopropyl), 0.22 – 0.35 (2H, m, cyclopropyl), 1.48 – 1.56 (1H, ABXdd, $J_{AX} = 5.4$ Hz, $J_{BX} = 6.4$ Hz, O-H), 1.71 (3H, d, $J = 7.3$ Hz, $CHCH_3$), 2.53 (1H, d, $J_{AB} = 9.4$ Hz, CH_AH_BO-), 2.68 (1H, d, $J_{AB} = 9.4$ Hz, CH_AH_BO-), 3.23 and 3.31 (2H, ABX dq, $J_{AX} = 5.4$ Hz, $J_{BX} = 6.4$ Hz, $J_{AB} = 11.3$ Hz, CH_2OH), 4.22 (1H, q, $J = 7.3$ Hz, $CHCH_3$), 7.04 – 7.10 (1H, m, H-Ar), 7.21 – 7.26 (1H, m, H-Ar), 7.28 – 7.33 (2H, m, H-Ar), 7.33 – 7.41 (3H, m, H-Ar), 7.41 – 7.53 (4H, m, H-Ar), 7.59 – 7.66 (2H, m, H-Ar), 7.84 – 7.91 (1H, m, H-Ar); ^{13}C NMR (125 MHz; $CDCl_3$) δ_C 8.6 (CH_2 cyclopropyl), 8.7 (CH_2 cyclopropyl), 20.6 ($CHCH_3$), 22.2 (C q. cyclopropyl), 54.5 ($CHCH_3$), 68.1 (CH_2O-), 68.4 (CH_2OH), 96.8 (C-3), 122.9 (C-Ar), 123.4 (C-Ar), 126.6 (2 \times C-Ar), 127.4 (C-Ar), 128.1 (2 \times C-Ar), 128.6 (2 \times C-Ar), 128.8 (2 \times C-Ar), 129.8 (C-Ar), 132.8 (C-Ar), 132.8 (C-Ar), 139.2 (C-Ar q), 143.8 (C-Ar q),

145.3 (C-Ar q), 168.6 (C-1); LRMS (ES⁺) m/z 436.4 [M+Na]⁺; HRMS calcd for C₂₇H₂₈NO₃ [M+H]⁺ 414.2064, found 414.2066; HPLC 99.4% in 0.1% formic acid (aq)/MeCN (R_t 8.9 min); 99.7% in 0.1% ammonia (aq)/MeCN (R_t 8.9 min); 99.3% in isocratic 0.1% formic acid (aq)/MeCN (R_t 15.4 min).

212

R_f 0.41 (4% MeOH/DCM); m.p. 124.7-126.0 °C; $[\alpha]_D^{30}$ -61° (c 0.459, EtOAc); λ_{max} (EtOH)/nm 253; ν_{max}/cm^{-1} (neat) 1680 and 1697 (s, C=O), 2874 and 2926 (w, C-H and -CH₂- aliphatic), 3391 (br, O-H); ¹H NMR (500 MHz; CDCl₃) δ_H 0.32 – 0.44 (1H, m, cyclopropyl), 0.46 – 0.65 (3H, m, cyclopropyl), 1.85 (1H, ABX app. t, $J_{AX} = J_{BX} = 5.7$ Hz, OH), 1.90 (3H, d, $J = 7.3$ Hz, CHCH₃), 2.96 (1H, d, $J_{AB} = 9.5$ Hz, CH_AH_BO-), 3.28 (1H, d, $J_{AB} = 9.5$ Hz, CH_AH_BO-), 3.56 – 3.70 (2H, ABX m, $J_{AX} = J_{BX} = 5.7$ Hz, $J_{AB} = 11.4$ Hz, CH₂OH), 4.47 (1H, q, $J = 7.3$ Hz, CHCH₃), 6.97 – 7.08 (7H, m, H-Ar), 7.08 – 7.17 (4H, m, H-Ar), 7.44 – 7.53 (2H, m, H-Ar), 7.81 – 7.91 (1H, m, H-Ar); ¹³C NMR (125 MHz; CDCl₃) δ_C 9.0 (CH₂ cyclopropyl), 9.0 (CH₂ cyclopropyl), 20.2 (CHCH₃), 22.7 (C q. cyclopropyl), 53.0 (CHCH₃), 68.1 (CH₂O-), 68.5 (CH₂OH), 95.5 (C-3), 123.1 (C-Ar), 123.4 (C-Ar), 126.8 (C-Ar), 127.0 (C-Ar), 127.8 (C-Ar), 128.0 (C-Ar), 128.4 (C-Ar), 129.9 (C-Ar), 132.7 (C-Ar), 132.9 (C-Ar), 138.3 (C-Ar q), 142.7 (C-Ar q), 145.2 (C-Ar q), 168.3 (C-1); LRMS (ES⁺) m/z 436.4 [M+Na]⁺; HRMS calcd for C₂₇H₂₈NO₃ [M+H]⁺ 414.2064, found 414.2067; HPLC 97.5% in 0.1% formic acid (aq)/MeCN (R_t 8.8 min); 97.3% in 0.1% ammonia (aq)/MeCN (R_t 8.7 min); 95.9% in isocratic 0.1% formic acid (aq)/MeCN (R_t 14.8 min).

(3*S*,1'*S*)-3-[[1-(Hydroxymethyl)cyclopropyl]methoxy]-3-phenyl-2-(1-phenylethyl)isoindolin-1-one (214) and (3*R*,1'*S*)-3-[[1-(hydroxymethyl)cyclopropyl]methoxy]-3-phenyl-2-(1-phenylethyl)isoindolin-1-one (216)



Alcohols **214** and **216** were synthesized following general procedure N using isoindolinones **213** and **215** (255 mg, 0.774 mmol), indium tribromide (55 mg, 0.155 mmol), 1,1-bis(hydroxymethyl)cyclopropane (0.37 mL, 396 mg, 3.87 mmol) and DCE (8 mL, 10 mL/mmol). Purification by MPLC (gradient elution, 0–4% MeOH/DCM) yielded the two pure diastereoisomers as a colorless oil which solidified upon storage at RT (**214** 65 mg, 20%) and a amorphous solid (**216** 29 mg, 9%).

214

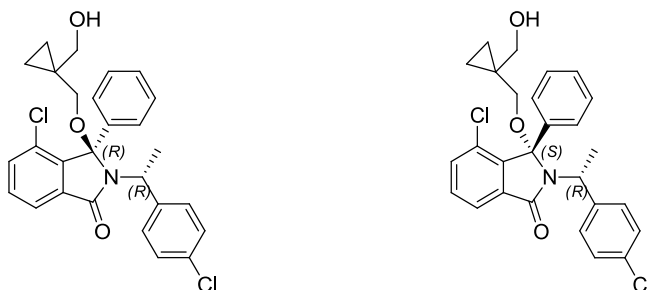
R_f 0.49 (4% MeOH/DCM); no clear m.p. detected; $[\alpha]_D^{30}$ -89° (c 0.443, EtOAc); λ_{max} (EtOH)/nm 252; ν_{max}/cm^{-1} (neat) 1682 and 1697 (s, C=O), 2876, 2933 and 3060 (s, C=O), 3400 (br, O-H); 1H NMR (500 MHz; $CDCl_3$) δ_H -0.11 – 0.04 (2H, m, cyclopropyl), 0.25 – 0.33 (2H, m, cyclopropyl), 1.48 – 1.56 (1H, ABXdd, J_{AX} = 5.4 Hz, J_{BX} = 6.4 Hz, O-H), 1.71 (3H, d, J = 7.3 Hz, $CHCH_3$), 2.53 (1H, d, J_{AB} = 9.4 Hz, CH_AH_BO-), 2.68 (1H, d, J_{AB} = 9.4 Hz, CH_AH_BO-), 3.23, 3.31 (2H, ABXdq, J_{AX} = 5.4 Hz, J_{BX} = 6.4 Hz, J_{AB} = 11.3 Hz, CH_2OH), 4.22 (1H, q, J = 7.3 Hz, $CHCH_3$), 7.04 – 7.10 (1H, m, H-Ar), 7.20 – 7.25 (1H, m, H-Ar), 7.28 – 7.33 (2H, m, H-Ar), 7.33 – 7.41 (3H, m, H-Ar), 7.41 – 7.53 (4H, m, H-Ar), 7.60 – 7.67 (2H, m, H-Ar), 7.84 – 7.91 (1H, m, H-Ar); ^{13}C NMR (125 MHz; $CDCl_3$) δ_C 8.6 (CH_2 cyclopropyl), 8.7 (CH_2 cyclopropyl), 20.6 ($CHCH_3$), 22.2 (C q. cyclopropyl), 54.5 ($CHCH_3$), 68.1 (CH_2O-), 68.4 (CH_2OH), 96.8 (C-3), 122.9 (C-Ar), 123.4 (C-Ar), 126.6 (2 \times C-Ar), 127.5 (C-Ar), 128.1 (2 \times C-Ar), 128.6 (2 \times C-Ar), 128.8 (2 \times C-Ar), 129.8 (C-Ar), 132.8 (C-

Ar), 132.8 (C-Ar), 139.2 (C-Ar q), 143.8 (C-Ar q), 145.3 (C-Ar q), 168.6 (C-1); LRMS (ES⁺) *m/z* 436.4 [M+Na]⁺; HRMS calcd for C₂₇H₂₈NO₃ [M+H]⁺ 414.2064, found 414.2065; HPLC 98.6% in 0.1% formic acid (aq)/MeCN (*R*_t 8.9 min); 98.0% in 0.1% ammonia (aq)/MeCN (*R*_t 8.9 min); 98.6% in isocratic 0.1% formic acid (aq)/MeCN (*R*_t 7.1 min).

216

*R*_f 0.41 (4% MeOH/DCM); no clear m.p. detected; [α]_D³⁰ +62° (*c* 0.502, EtOAc); λ_{max} (EtOH)/nm 253; ν_{max} /cm⁻¹ (neat) 1678 and 1697 (s, C=O), 2874 and 2932 (s, C=O), 3403 (br, O-H); ¹H NMR (500 MHz; CDCl₃) δ_{H} 0.32 – 0.44 (1H, m, cyclopropyl), 0.46 – 0.64 (3H, m, cyclopropyl), 1.85 (1H, ABX app. t, *J*_{AX} = *J*_{BX} = 5.7 Hz, OH), 1.90 (3H, d, *J* = 7.3 Hz, CHCH₃), 2.96 (1H, d, *J*_{AB} = 9.5 Hz, CH_AH_BO-), 3.28 (1H, d, *J*_{AB} = 9.5 Hz, CH_AH_BO-), 3.56 – 3.70 (2H, ABXm, *J*_{AX} = *J*_{BX} = 5.7 Hz, *J*_{AB} = 11.4 Hz, CH₂OH), 4.47 (1H, q, *J* = 7.3 Hz, CHCH₃), 6.97 – 7.07 (7H, m, H-Ar), 7.07 – 7.17 (4H, m, H-Ar), 7.44 – 7.54 (2H, m, H-Ar), 7.81 – 7.91 (1H, m, H-Ar); ¹³C NMR (125 MHz; CDCl₃) δ_{C} 9.0 (CH₂ cyclopropyl), 9.0 (CH₂ cyclopropyl), 20.2 (CHCH₃), 22.7 (C q. cyclopropyl), 53.0 (CHCH₃), 68.1 (CH₂O-), 68.5 (CH₂OH), 95.5 (C-3), 123.1 (C-Ar), 123.4 (C-Ar), 126.8 (C-Ar), 127.0 (C-Ar), 127.8 (C-Ar), 128.0 (C-Ar), 128.4 (C-Ar), 129.9 (C-Ar), 132.7 (C-Ar), 132.9 (C-Ar), 138.3 (C-Ar q), 142.7 (C-Ar q), 145.2 (C-Ar q), 168.3 (C-1); LRMS (ES⁺) *m/z* 436.4 [M+Na]⁺; HRMS calcd for C₂₇H₂₈NO₃ [M+H]⁺ 414.2064, found 414.2067; HPLC 96.6% in 0.1% formic acid (aq)/MeCN (*R*_t 8.9 min); 97.1% in 0.1% ammonia (aq)/MeCN (*R*_t 8.9 min); 98.5% in isocratic 0.1% formic acid (aq)/MeCN (*R*_t 6.8 min).

(3*R*,1'*R*)-4-Chloro-2-[1'-(4''-chlorophenyl)ethyl]-3-{[1'''-(hydroxymethyl)cyclopropyl]methoxy}-3-phenylisoindolin-1-one (159)
and (3*S*,1'*R*)-4-chloro-2-[1'-(4''-chlorophenyl)ethyl]-3-{[1'''-(hydroxymethyl)cyclopropyl]methoxy}-3-phenylisoindolin-1-one (199)



Compounds **159** and **199** were synthesized according to general procedure N using isoindolinone **198** as a mixture of (3*R*,1'*R*) and (3*S*,1'*R*) diastereoisomers (0.77 g, 1.9 mmol), InBr₃ (0.14 g, 0.38 mmol), 1,1-bis(hydroxymethyl)cyclopropane (0.91 mL, 0.97 g, 9.5 mmol) and DCE (19 mL). Purification of the crude product by MPLC (gradient elution, 0-22% EtOAc petrol) afforded the desired compounds **159** (0.33 g, 36%) and **199** (0.40 g, 44%), as white solids.

159

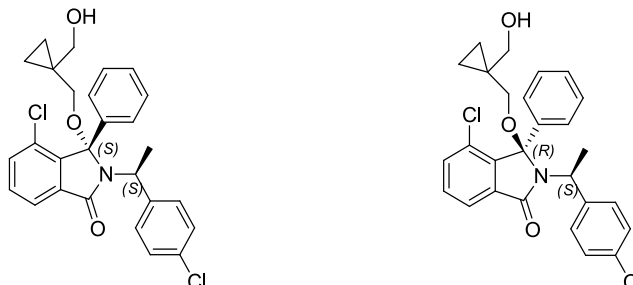
R_f 0.25 (25% EtOAc/petrol); m.p. 66-69 °C; $[\alpha]_D^{RT} +118^\circ$ (c 0.764, EtOAc); λ_{max} (EtOH)/nm 259; ν_{max}/cm^{-1} (neat) 1699 (s, C=O), 3439 (br, O-H); ¹H NMR (500 MHz; CDCl₃) δ_H -0.07-0.04 (1H, m, cyclopropyl), 0.14-0.25 (1H, m, cyclopropyl), 0.32-0.44 (2H, m, cyclopropyl), 1.58 (3H, d, $J = 7.2$ Hz, CHCH₃), 1.76 (1H, ABX br, OH), 1.69 (1H, d, $J_{AB} = 9.2$ Hz, CH_AH_BO-), 2.89 (1H, d, $J_{AB} = 9.2$ Hz, CH_AH_BO-), 3.27-3.37 and 3.40-3.50 (2H, ABX m, CH₂OH), 4.24 (1H, q, $J = 7.2$ Hz, CH-CH₃), 7.27-7.32 (2H, m, H-Ar), 7.35-7.43 (4H, br, H-Ar), 7.43-7.47 (1H, dd, $J = 0.9, 7.8$, H-Ar), 7.51 (1H, app. t, $J = 7.8$ Hz, H-6), 7.57 (2H, m, H-Ar), 7.83 (1H, dd, $J = 0.9, 7.8$ Hz, H-Ar); ¹³C NMR (125 MHz; CDCl₃) δ_C 8.6 (CH₂ cyclopropyl), 8.7 (CH₂ cyclopropyl), 20.1 (CHCH₃), 22.1 (C q cyclopropyl), 53.4 (CHCH₃), 68.4 (CH₂OH), 68.7 (CH₂O-), 96.4 (C-3), 122.0 (C-Ar), 127.1 (2 × C-Ar), 128.5 (2 × C-Ar), 128.7 (2 × C-Ar), 129.0 (C-Ar), 129.5 (2 × C-Ar), 129.6 (C-Ar q), 131.7 (C-Ar), 133.3 (C-Ar q), 133.8 (C-Ar), 135.2 (C-Ar q), 136.7 (C-Ar q), 140.8 (C-Ar q), 141.6 (C-Ar)

q), 167.0 (C-1); LRMS (ES⁺) m/z 504.4 [M+Na]⁺; HRMS calcd for C₂₇H₂₆³⁵Cl₂NO₃ [M+H]⁺ 482.1284, found 482.1285; HPLC 99.7% in 0.1% formic acid (aq.)/MeCN (R_t 9.7 min); 99.2% in 0.1% ammonia (aq.)/MeCN (R_t 9.7 min).

199

R_f 0.14 (25% EtOAc/petrol); m.p. 66-69 °C; $[\alpha]_D^{RT}$ +35° (c 0.747, EtOAc); λ_{max} (EtOH)/nm 260sh; ν_{max}/cm^{-1} (neat) 1693 (s, C=O), 3456 (w, O-H); ¹H NMR (500 MHz; CDCl₃) δ_H 0.51-0.71 (4H, m, 2 × CH₂ cyclopropyl), 1.92 (3H, d, J = 7.3 Hz, CH₃), 1.95 (1H, ABX app. t, $J_{AX} = J_{BX} = 5.6$ Hz, OH), 3.05 (1H, d, $J_{AB} = 9.4$ Hz, CH_AH_BO-), 3.36 (1H, d, $J_{AB} = 9.4$ Hz, CH_AH_BO-), 3.73 (2H, ABX dq, J = 5.6, 11.4 Hz, CH₂OH), 4.39 (1H, q, J = 7.3 Hz, CHCH₃), 6.90 (2H, m, H-Ar), 6.97 (2H, m, H-Ar), 7.02-7.29 (4H, br, H-Ar), 7.22 (1H, m, H-Ar), 7.44 (1H, dd, J = 1.0, 7.9 Hz, H-Ar), 7.50 (1H, m, H-Ar), 7.80 (1H, dd, J = 1.0, 7.4 Hz, H-Ar); ¹³C NMR (125 MHz; CDCl₃) δ_C 8.9 (CH₂ cyclopropyl), 9.1 (CH₂ cyclopropyl), 19.8 (CHCH₃), 22.7 (C q, cyclopropyl), 52.1 (CHCH₃), 68.3 (CH₂OH), 68.5 (CH₂O-), 95.2 (C-3), 121.9 (C-Ar), 127.1 (2 × C-Ar), 127.9 (2 × C-Ar), 128.1 (2 × C-Ar), 128.6 (C-Ar), 129.4 (2 × C-Ar), 129.8 (C-Ar q), 131.7 (C-Ar), 132.7 (C-Ar q), 133.6 (C-Ar), 135.4 (C-Ar q), 136.4 (C-Ar q), 140.6 (C-Ar q), 140.6 (C-Ar q), 166.5 (C-1); LRMS (ES⁺) m/z 482.4 [M+H]⁺; HRMS calcd for C₂₇H₂₆³⁵Cl₂NO₃ [M+H]⁺ 482.1284, found 482.1284; HPLC 98.8% in 0.1% formic acid (aq.)/MeCN (R_t 9.8 min); 98.4% in 0.1% ammonia (aq.)/MeCN (R_t 9.8 min).

(3*S*,1'*S*)-4-Chloro-2-[1'-(4''-chlorophenyl)ethyl]-3-{[1'''-(hydroxymethyl)cyclopropyl]methoxy}-3-phenylisoindolin-1-one (201)
and (3*R*,1'*S*)-4-chloro-2-[1'-(4''-chlorophenyl)ethyl]-3-{[1'''-(hydroxymethyl)cyclopropyl]methoxy}-3-phenylisoindolin-1-one (202)



Compounds **201** and **202** were synthesized according to general procedure N using isoindolinone **200** as a mixture of (3*S*,1'*S*) and (3*R*,1'*S*) diastereoisomers (0.70 g, 1.76 mmol), InBr₃ (0.12 g, 0.35 mmol), 1,1-bis(hydroxymethyl)cyclopropane (0.84 mL, 0.90 g, 8.8 mmol) and DCE (18 mL). Purification of the crude product by MPLC (gradient elution, 0-20% EtOAc/petrol) afforded the desired compounds **201** (0.36 g, 43%) and **202** (0.42 g, 50%), as colorless oils.

201

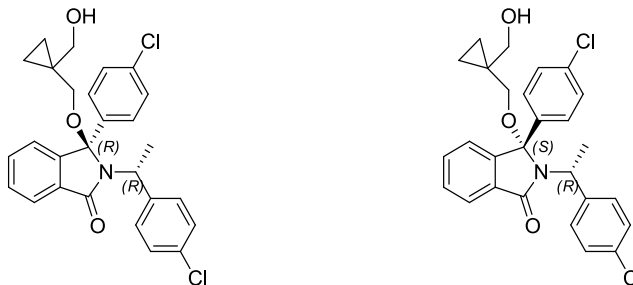
R_f 0.25 (25% EtOAc/petrol); $[\alpha]_D^{RT}$ -115° (c 0.745, EtOAc); λ_{max} (EtOH)/nm 259; ν_{max}/cm^{-1} (neat) 1699 (s, C=O), 3437 (br, O-H); ¹H NMR (500 MHz; CDCl₃) δ_H - 0.07-0.04 (1H, m, cyclopropyl), 0.14-0.25 (1H, m, cyclopropyl), 0.32-0.44 (2H, m, cyclopropyl), 1.58 (3H, d, J = 7.2 Hz, -CH₃), 1.76 (1H, ABXbr, OH), 1.69 and 2.89 (2H, ABq, J_{AB} = 9.2 Hz, CH₂O-), 3.27-3.37 and 3.40-3.50 (2H, ABXm, CH₂OH), 4.24 (1H, q, J = 7.2 Hz, CH-CH₃), 7.27-7.32 (3H, m, H-Ar), 7.35-7.43 (4H, br, H-Ar), 7.43-7.47 (1H, dd, J = 0.9, 8.0, H-Ar), 7.48-7.53 (1H, m, H-Ar), 7.57 (2H, m, H-Ar), 7.83 (1H, dd, J = 0.9, 7.5 Hz, H-Ar); ¹³C NMR (125 MHz; CDCl₃) δ_C 8.6 (CH₂ cyclopropyl), 8.7 (CH₂ cyclopropyl), 20.1 (CH₃), 22.1 (C q cyclopropyl), 53.4 (CHCH₃), 68.4 (CH₂OH), 68.7 (CH₂O-), 96.4 (C-3), 122.0 (C-Ar), 127.1 (2 × C-Ar), 128.5 (2 × C-Ar), 128.7 (2 × C-Ar), 129.0 (C-Ar), 129.5 (2 × C-Ar), 129.6 (C-Ar q), 131.7 (C-Ar), 133.3 (C-Ar q), 133.8 (C-Ar), 135.2 (C-Ar q), 136.7 (C-Ar q), 140.8 (C-Ar q), 141.6 (C-Ar q), 167.0 (C-1); LRMS (ES⁺) m/z 504.4 [M+Na]⁺; HRMS

calcd for $C_{27}H_{26}^{35}Cl_2NO_3$ $[M+H]^+$ 482.1284, found 482.1284; HPLC 97.7% in 0.1% formic acid (aq.)/MeCN (R_t 9.7 min); 97.6% in 0.1% ammonia (aq.)/MeCN (R_t 9.7 min).

202

R_f 0.14 (25% EtOAc/petrol); $[\alpha]_D^{RT}$ -35° (c 0.878, EtOAc); λ_{max} (EtOH)/nm 260sh; ν_{max}/cm^{-1} (neat) 1686 (s, C=O), 3416 (br, O-H); 1H NMR (500 MHz; $CDCl_3$) δ_H 0.51-0.71 (4H, m, $2 \times CH_2$ cyclopropyl), 1.92 (3H, d, $J = 7.3$, CH_3), 1.95 (1H, ABX app. t, $J_{AX} = J_{BX} = 5.6$ Hz, OH), 3.05 (1H, d, $J_{AB} = 9.4$ Hz, CH_AH_BO-), 3.36 (1H, d, $J_{AB} = 9.4$ Hz, CH_AH_BO-), 3.73 (2H, ABX dq, $J = 5.6, 11.4$ Hz, CH_2OH), 4.39 (1H, q, $J = 7.3$ Hz, $CHCH_3$), 6.90 (2H, m, H-Ar), 6.97 (2H, m, H-Ar), 7.02-7.29 (4H, br, H-Ar), 7.22 (1H, m, H-Ar), 7.44 (1H, dd, $J = 1.0, 7.9$ Hz, H-Ar), 7.50 (1H, m, H-Ar), 7.80 (1H, dd, $J = 1.0, 7.4$ Hz, H-Ar); ^{13}C NMR (125 MHz; $CDCl_3$) δ_C 8.9 (CH_2 cyclopropyl), 9.1 (CH_2 cyclopropyl), 19.8 ($CHCH_3$), 22.7 (C q, cyclopropyl), 52.1 ($CHCH_3$), 68.3 (CH_2OH), 68.5 (CH_2O-), 95.2 (C-3), 121.9 (C-Ar), 127.1 ($2 \times$ C-Ar), 127.9 ($2 \times$ C-Ar), 128.1 ($2 \times$ C-Ar), 128.6 (C-Ar), 129.4 ($2 \times$ C-Ar), 129.8 (C-Ar q), 131.7 (C-Ar), 132.7 (C-Ar q), 133.6 (C-Ar), 135.4 (C-Ar q), 136.4 (C-Ar q), 140.6 (C-Ar q), 140.6 (C-Ar q), 166.5 (C-1); LRMS (ES^+) m/z 482.4 $[M+H]^+$; HRMS calcd for $C_{27}H_{26}^{35}Cl_2NO_3$ $[M+H]^+$ 482.1284, found 482.1285; HPLC 95.4% in 0.1% formic acid (aq.)/MeCN (R_t 9.8 min); 95.6% in 0.1% ammonia (aq.)/MeCN (R_t 9.8 min).

(3*R*,1'*R*)-3-(4'''-Chlorophenyl)-2-[1'-(4''-chlorophenyl)ethyl]-3-{{1''''-(hydroxymethyl)cyclopropyl}methoxy}isoindolin-1-one (204**) and (3*S*,1'*R*)-3-(4'''-chlorophenyl)-2-[1'-(4''-chlorophenyl)ethyl]-3-{{1''''-(hydroxymethyl)cyclopropyl}methoxy}isoindolin-1-one (**205**)**



Compounds **204** and **205** were synthesized according to general procedure N using isoindolinone **203** as a mixture of (3*R*,1'*R*) and (3*S*,1'*S*) diastereoisomers (0.84 g, 2.1 mmol), InBr₃ (0.15 g, 0.42 mmol), 1,1-bis(hydroxymethyl)cyclopropane (1.00 mL, 1.07 g, 10.5 mmol) and DCE (21 mL). Purification of the crude product by MPLC (gradient elution, 3-22% EtOAc/petrol) afforded the desired compounds **204** (0.40 g, 40%) and **205** (0.38 g, 38%), as white solids.

204

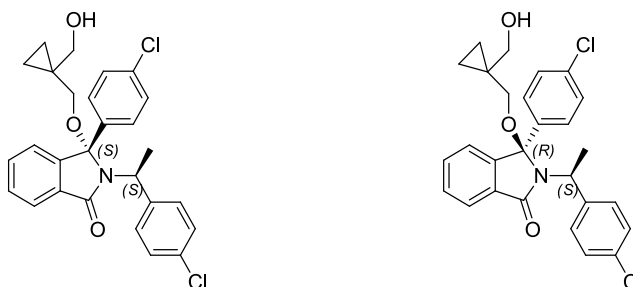
*R*_f 0.17 (25% EtOAc/petrol); m.p. 69-70 °C; [α]_D³⁰ +105° (*c* 0.502, EtOAc); λ_{max} (EtOH)/nm 258sh; ν_{max} /cm⁻¹ (neat) 1684 and 1698 (s, C=O), 3441 (br, O-H); ¹H NMR (500 MHz; CDCl₃) δ _H 0.00 (2H, m, cyclopropyl), 0.32 (2H, m, cyclopropyl), 1.46 (1H, ABX app. t, *J*_{AX} = *J*_{BX} = 5.0 Hz, OH), 1.64 (3H, d, *J* = 7.3 Hz, CH₃), 2.52 (1H, d, *J*_{AB} = 9.5 Hz, CH_AH_BO-), 2.71 (1H, d, *J*_{AB} = 9.5 Hz, CH_AH_BO-), 3.22 and 3.41 (2H, ABX dq, *J*_{AX} = *J*_{BX} = 5.0, *J*_{AB} = 11.3 Hz, CH₂OH), 4.21 (1H, q, *J* = 7.3 Hz, CH-CH₃), 7.01-7.07 (1H, m, H-Ar), 7.20-7.27 (3H, m, H-Ar), 7.28-7.39 (3H, m, H-Ar), 7.44-7.51 (2H, m, H-Ar), 7.51-7.56 (2H, m, H-Ar), 7.81-7.86 (1H, m, H-Ar); ¹³C NMR (125 MHz; CDCl₃) δ _C 8.7 (CH₂ cyclopropyl), 8.8 (CH₂ cyclopropyl), 20.1 (CH₃), 22.2 (C q cyclopropyl), 53.5 (CHCH₃), 68.1 (CH₂O-), 68.2 (CH₂OH), 96.2 (C-3), 122.9 (C-Ar), 123.6 (C-Ar), 128.1 (2 × C-Ar), 128.7 (2 × C-Ar), 129.0 (2 × C-Ar), 129.6 (2 × C-Ar), 130.6 (C-Ar), 132.5 (C-Ar q), 133.1 (C-Ar), 133.3 (C-Ar q), 134.8 (C-Ar q), 137.6 (C-Ar q), 141.7 (C-Ar q), 144.9 (C-Ar q), 168.4 (C-1); LRMS (ES⁺) *m/z* 482.4 [M+H]⁺; HRMS calcd for C₂₇H₂₆³⁵Cl₂NO₃ [M+H]⁺

482.1284, found 482.1283; HPLC 99.0% in 0.1% formic acid (aq.)/MeCN (R_t 10.0 min); 98.7% in 0.1% ammonia (aq.)/MeCN (R_t 9.9 min).

205

R_f 0.09 (25% EtOAc/petrol); m.p. 139-140 °C; $[\alpha]_D^{30} +21^\circ$ (c 0.210, EtOAc); λ_{max} (EtOH)/nm 258sh; ν_{max}/cm^{-1} (neat) 1680 (s, C=O), 3395 (br, O-H); 1H NMR (500 MHz; $CDCl_3$) δ_H 0.34-0.41 (1H, m, cyclopropyl), 0.45-0.50 (1H, m, cyclopropyl), 0.50-0.60 (2H, m, cyclopropyl), 1.65 (1H, ABX app.t, $J_{AX} = J_{BX} = 5.0$ Hz, OH), 1.89 (3H, d, $J = 7.3$ Hz, CH_3), 2.90 (1H, d, $J_{AB} = 9.5$ Hz, CH_AH_{BO-}), 3.27 (1H, d, $J_{AB} = 9.5$ Hz, CH_AH_{BO-}), 3.62 (2H, ABX app. d, $J_{AX} = J_{BX} = J_{AB} = 5.0$ Hz, CH_2OH), 4.33 (1H, q, $J = 7.3$ Hz, $CH-CH_3$), 6.95-7.09 (9H, m, H-Ar), 7.44-7.52 (2H, m, H-Ar), 7.79-7.85 (1H, m, H-Ar); ^{13}C NMR (125 MHz; $CDCl_3$) δ_C 8.9 (CH_2 cyclopropyl), 9.0 (CH_2 cyclopropyl), 20.2 (CH_3), 22.7 (C q cyclopropyl), 52.5 ($CHCH_3$), 67.8 (CH_2O-), 68.1 (CH_2OH), 95.0 (C-3), 123.0 (C-Ar), 123.5 (C-Ar), 128.1 ($2 \times$ C-Ar), 128.2 ($2 \times$ C-Ar), 128.4 ($2 \times$ C-Ar), 129.4 ($2 \times$ C-Ar), 130.2 (C-Ar), 132.7 (C-Ar q), 132.8 (C-Ar q), 132.9 (C-Ar), 134.6 (C-Ar q), 137.0 (C-Ar q), 141.3 (C-Ar q), 144.6 (C-Ar q), 168.1 (C-1); LRMS (ES^+) m/z 482.4 $[M+H]^+$; HRMS calcd for $C_{27}H_{26}^{35}Cl_2NO_3$ $[M+H]^+$ 482.1284, found 482.1284; HPLC 99.8% in 0.1% formic acid (aq.)/MeCN (R_t 9.9 min); 99.7% in 0.1% ammonia (aq.)/MeCN (R_t 9.9 min).

(3*S*,1'*S*)-3-(4'''-Chlorophenyl)-2-[1-(4-chlorophenyl)ethyl]-3-{[1'''-(hydroxymethyl)cyclopropyl]methoxy}isoindolin-1-one (207) and (3*R*,1'*S*)-3-(4'''-chlorophenyl)-2-[1-(4-chlorophenyl)ethyl]-3-{[1-(hydroxymethyl)cyclopropyl]methoxy}isoindolin-1-one (208)



Compounds **207** and **208** were synthesized according to general procedure N using isoindolinone **206** as a mixture of (3*S*,1'*S*) and (3*R*,1'*S*) diastereoisomers (0.79 g, 1.98 mmol), $InBr_3$ (0.14 g, 0.40 mmol), 1,1-bis(hydroxy-

methyl)cyclopropane (0.95 mL, 1.01 g, 9.9 mmol) and DCE (20 mL). The reaction mixture was heated at 80 °C for 3.5 days. Purification of the crude product by MPLC (gradient elution, 3-22% EtOAc/petrol) afforded the desired compounds **207** (0.37 g, 39%) and **208** (0.36 g, 38%), as white solids.

207

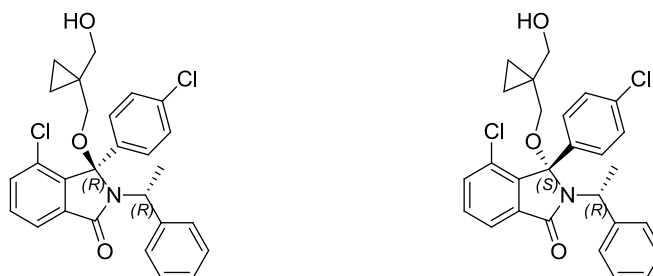
R_f 0.17 (25% EtOAc/petrol); m.p. 69-70 °C; $[\alpha]_D^{30}$ -105° (c 0.477, EtOAc); λ_{max} (EtOH)/nm 258sh; ν_{max}/cm^{-1} (neat) 1684 and 1698 (s, C=O), 3441 (br, O-H); 1H NMR (500 MHz; $CDCl_3$) δ_H 0.00 (2H, m, cyclopropyl), 0.32 (2H, m, cyclopropyl), 1.46 (1H, ABX app. t, $J_{AX} = J_{BX} = 5.7$ Hz, OH), 1.64 (3H, d, $J = 7.3$ Hz, CH_3), 2.52 (1H, d, $J_{AB} = 9.5$ Hz, CH_AH_BO-), 2.71 (1H, d, $J_{AB} = 9.5$ Hz, CH_AH_BO-), 3.22 and 3.41 (2H, ABX dq, $J_{AX} = J_{BX} = 6.2$, $J_{AB} = 11.3$ Hz, CH_2OH), 4.21 (1H, q, $J = 7.3$ Hz, $CH-CH_3$), 7.01-7.07 (1H, m, H-Ar), 7.20-7.27 (3H, m, H-Ar), 7.28-7.39 (3H, m, H-Ar), 7.44-7.51 (2H, m, H-Ar), 7.51-7.56 (2H, m, H-Ar), 7.81-7.86 (1H, m, H-Ar); ^{13}C NMR (125 MHz; $CDCl_3$) δ_C 8.7 (CH_2 cyclopropyl), 8.8 (CH_2 cyclopropyl), 20.1 (CH_3), 22.2 (C q cyclopropyl), 53.5 ($CHCH_3$), 68.1 (CH_2O-), 68.2 (CH_2OH), 96.2 (C-3), 122.9 (C-Ar), 123.6 (C-Ar), 128.1 ($2 \times$ C-Ar), 128.7 ($2 \times$ C-Ar), 129.0 ($2 \times$ C-Ar), 129.6 ($2 \times$ C-Ar), 130.2 (C-Ar), 132.5 (C-Ar q), 133.1 (C-Ar), 133.3 (C-Ar q), 134.8 (C-Ar q), 137.6 (C-Ar q), 141.7 (C-Ar q), 144.9 (C-Ar q), 168.4 (C-1); LRMS (ES^+) m/z 482.4 $[M+H]^+$; HRMS calcd for $C_{27}H_{26}^{35}Cl_2NO_3$ $[M+H]^+$ 482.1284, found 482.1282; HPLC 97.2% in 0.1% formic acid (aq.)/MeCN (R_t 10.0 min); 96.9% in 0.1% ammonia (aq.)/MeCN (R_t 10.0 min).

208

R_f 0.09 (25% EtOAc/petrol); m.p. 134-135 °C; $[\alpha]_D^{30}$ -22° (c 0.200, EtOAc); λ_{max} (EtOH)/nm 256sh; ν_{max}/cm^{-1} (neat) 1681 (s, C=O), 3441 (br, O-H); 1H NMR (500 MHz; $CDCl_3$) δ_H 0.34-0.41 (1H, m, cyclopropyl), 0.45-0.50 (1H, m, cyclopropyl), 0.50-0.60 (2H, m, cyclopropyl), 1.65 (1H, ABX app.t, $J_{AX} = J_{BX} = 5.0$ Hz, OH), 1.89 (3H, d, $J = 7.3$ Hz, CH_3), 2.90 (1H, d, $J_{AB} = 9.5$ Hz, CH_AH_BO-), 3.27 (1H, d, $J_{AB} = 9.5$ Hz, CH_AH_BO-), 3.61 (2H, ABX app. d, $J_{AX} = J_{BX} = J_{AB} = 5.0$ Hz, CH_2OH), 4.33 (1H, q, $J = 7.3$ Hz, $CH-CH_3$), 6.95-7.09 (9H, m, H-Ar), 7.44-7.52 (2H, m, H-Ar), 7.79-7.85 (1H, m, H-Ar); ^{13}C NMR (125 MHz; $CDCl_3$) δ_C 8.9 (CH_2 cyclopropyl), 9.0 (CH_2 cyclopropyl), 20.2 (CH_3), 22.7 (C q cyclopropyl), 52.5 ($CHCH_3$), 67.8 (CH_2O-),

68.1 (CH₂OH), 95.0 (C-3), 123.0 (C-Ar), 123.5 (C-Ar), 128.1 (2 × C-Ar), 128.2 (2 × C-Ar), 128.4 (2 × C-Ar), 129.4 (2 × C-Ar), 130.2 (C-Ar), 132.7 (C-Ar q), 132.8 (C-Ar q), 132.9 (C-Ar), 134.6 (C-Ar q), 137.0 (C-Ar q), 141.2 (C-Ar q), 144.6 (C-Ar q), 168.1 (C-1); LRMS (ES⁺) *m/z* 482.4 [M+H]⁺; HRMS calcd for C₂₇H₂₆³⁵Cl₂NO₃ [M+H]⁺ 482.1284, found 482.1283; HPLC 99.4% in 0.1% formic acid (aq.)/MeCN (*R*_t 9.9 min); 99.3% in 0.1% ammonia (aq.)/MeCN (*R*_t 9.9 min).

(3*R*,1'*R*)-4-chloro-3-(4'''-chlorophenyl)-3-[[1'''-(hydroxymethyl)cyclopropyl]methoxy]-2-(1'-phenylethyl)isoindolin-1-one (191) and (3*S*,1'*R*)-4-chloro-3-(4'''-chlorophenyl)-3-[[1'-(hydroxymethyl)cyclopropyl]methoxy]-2-(1'-phenylethyl)isoindolin-1-one (193)



Compounds **191** and **193** were obtained following general procedure N using isoindolinone **312** as a mixture of (3*R*,1'*R*) and (3*S*,1'*R*) diastereoisomers (456 mg, 1.14 mmol), InBr₃ (81 mg, 0.228 mmol), 1,1-bis(hydroxymethyl)cyclopropane (0.55 mL, 582 mg, 5.70 mmol) and DCE (11 mL). Purification of the crude product by MPLC (gradient elution, 3-18% EtOAc/petrol) afforded the desired compounds **191** (116 mg, 24%) and **193** (111 mg, 23%), as white amorphous solids.

191

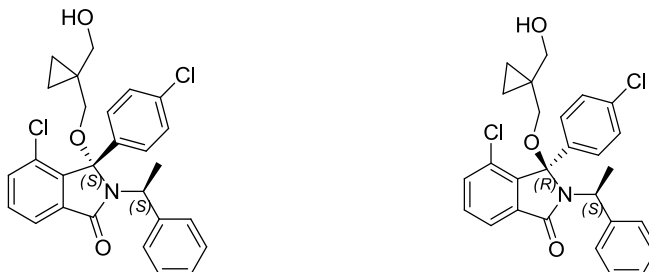
*R*_f 0.20 (25% EtOAc/petrol); no clear m.p. detected; [α]_D³⁰ +86° (*c* 0.600, EtOAc); λ_{max} (EtOH)/nm 258sh; ν_{max}/cm⁻¹ (neat) 1701 (s, CO=), 2873, 2922 and 2981 (w, C-H and -CH₂- aliphatic), 3400 (br, O-H); ¹H NMR (500 MHz; CDCl₃) δ_H -0.16 – -0.06 (1H, m, cyclopropyl), 0.08 – 0.17 (1H, m, cyclopropyl), 0.24 – 0.36 (2H, m, cyclopropyl), 1.43 (1H, ABX dd, *J*_{AX} = 5.4 Hz, *J*_{BX} = 6.9 Hz, OH), 1.63 (3H, d, *J* = 7.3 Hz, CH₃), 2.68 (1H, d, *J*_{AB} = 9.1 Hz, CH_AH_BO-), 2.79 (1H, d, *J*_{AB} = 9.1 Hz,

CH_AH_BO-), 3.21 – 3.38 (2H, ABX dq, $J_{AX} = 5.4$ Hz, $J_{BX} = 6.9$ Hz, $J_{AB} = 11.5$ Hz, CH₂OH), 4.19 (1H, q, $J = 7.3$ Hz, CHCH₃), 7.22 – 7.24 (1H, m, H-Ar), 7.26 – 7.40 (6H, m, H-Ar), 7.43 (1H, dd, $J = 1.0, 7.7$ Hz, H-Ar), 7.49 (1H, app. t, $J = 7.7$ Hz, H-6), 7.54 – 7.61 (2H, m, H-Ar), 7.83 (1H, dd, $J = 1.0, 7.7$ Hz, H-Ar); ¹³C NMR (125 MHz; CDCl₃) δ_C 8.5 (CH₂ cyclopropyl), 8.6 (CH₂ cyclopropyl), 20.7 (CH₃), 22.1 (C q cyclopropyl), 54.3 (CHCH₃), 68.1 (CH₂OH), 68.3 (CH₂O-), 96.1 (C-3), 122.2 (C-Ar), 127.6 (2 × C-Ar), 127.8 (2 × C-Ar), 128.7 (2 × C-Ar), 129.5 (2 × C-Ar), 131.9 (C-Ar), 133.7 (C-Ar), 134.9 (C-Ar q), 135.3 (C-Ar q), 135.7 (C-Ar q), 140.5 (C-Ar q), 143.3 (C-Ar q), 167.0 (C-1). Two quaternary carbons not detected; LRMS (ES⁺) m/z 504.4 [M+Na]⁺; HRMS calcd for C₂₇H₂₆³⁵Cl₂NO₃ [M+H]⁺ 482.1284, found 482.1284; HPLC 99.9% in 0.1% formic acid (aq)/MeCN (R_t 9.9 min); 99.9% in 0.1% ammonia (aq)/MeCN (R_t 9.9 min); 99.7% in isocratic 0.1% formic acid (aq)/MeCN (R_t 14.0 min).

193

R_f 0.14 (25% EtOAc/petrol); no clear m.p. detected; $[\alpha]_D^{30} +10^\circ$ (c 0.459, EtOAc); λ_{max} (EtOH)/nm 258sh; ν_{max}/cm^{-1} (neat) 1686 (s, C=O), 2874 and 2930 (w, C-H and -CH₂- aliphatic), 3400 br, O-H); ¹H NMR (500 MHz; CDCl₃) δ_H 0.49 – 0.68 (4H, m, cyclopropyl), 1.82 (1H, ABX app. t, $J_{AX} = J_{BX} = 5.9$ Hz, OH), 1.93 (3H, d, $J = 7.3$ Hz), 3.01 (1H, d, $J_{AB} = 9.0$ Hz, CH_AH_BO-), 3.32 (1H, d, $J_{AB} = 9.0$ Hz, CH_AH_BO-), 3.65 – 3.76 (2H, ABX dq, $J_{AX} = J_{BX} = 5.9$ Hz, $J_{AB} = 11.5$ Hz, CH₂OH), 4.36 (1H, q, $J = 7.3$ Hz, CHCH₃), 6.88 – 7.15 (9H, m, H-Ar), 7.41 (1H, dd, $J = 1.0, 7.7$ Hz, H-Ar), 7.47 (1H, app. t, $J = 7.7$ Hz, H-6), 7.79 (1H, dd, $J = 1.0, 7.7$ Hz, H-Ar); ¹³C NMR (125 MHz; CDCl₃) δ_C 8.9 (CH₂ cyclopropyl), 9.1 (CH₂ cyclopropyl), 20.2 (CH₃), 22.7 (C q cyclopropyl), 53.2 (CHCH₃), 68.1 (CH₂OH), 68.4 (CH₂O-), 94.7 (C-3), 122.1 (C-Ar), 127.0 (C-Ar), 127.8 (2 × C-Ar), 128.0 (2 × C-Ar), 128.0 (2 × C-Ar), 128.7 (2 × C-Ar), 129.6 (C-Ar q), 131.8 (C-6), 133.6 (C-Ar), 134.4 (C-Ar q), 135.6 (C-Ar q), 135.4 (C-Ar q), 140.3 (C-Ar q), 142.5 (C-Ar q), 166.6 (C-1); LRMS (ES⁺) m/z 482.4 [M+H]⁺; HRMS calcd for C₂₇H₂₆³⁵Cl₂NO₃ [M+H]⁺ 482.1284, found 482.1286; HPLC 98.5% in 0.1% formic acid (aq)/MeCN (R_t 9.8 min); 98.6% in 0.1% ammonia (aq)/MeCN (R_t 9.8 min); 98.6% in isocratic 0.1% formic acid (aq)/MeCN (R_t 12.7 min).

(3*S*,1'*S*)-4-chloro-3-(4'''-chlorophenyl)-3-[[1'''-(hydroxymethyl)cyclopropyl]methoxy]-2-(1-phenylethyl)isoindolin-1-one (195) and (3*R*,1'*S*)-4-chloro-3-(4'''-chlorophenyl)-3-[[1-(hydroxymethyl)cyclopropyl]methoxy]-2-(1-phenylethyl)isoindolin-1-one (197)



Compounds **195** and **197** were obtained following general procedure N using isoindolinone **313** as a mixture of (3*S*,1'*S*) and (3*R*,1'*S*) diastereoisomers (456 mg, 1.14 mmol), InBr₃ (81 mg, 0.228 mmol), 1,1-bis(hydroxymethyl)cyclopropane (0.55 mL, 582 mg, 5.70 mmol) and DCE (11 mL). The reaction mixture was heated at 80 °C for 4.5 days. Purification of the crude product by MPLC (gradient elution, 3-18% EtOAc/petrol) afforded the desired compounds **195** (191 mg, 35%) and **197** (142 mg, 26%), as white amorphous solids.

195

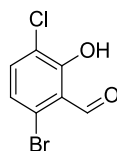
R_f 0.20 (25% EtOAc/petrol); no clear m.p. detected; $[\alpha]_D^{30}$ -83° (c 0.580, EtOAc); λ_{max} (EtOH)/nm 258sh; ν_{max}/cm^{-1} (neat) 1701 (s, C=O), 2873, 2927 and 2980 (w, C-H and -CH₂- aliphatic), 3400 (br, O-H); ¹H NMR (500 MHz; CDCl₃) δ_H -0.16 – -0.07 (1H, m, cyclopropyl), 0.08 – 0.16 (1H, m, cyclopropyl), 0.24 – 0.35 (2H, m, cyclopropyl), 1.43 (1H, ABX br, OH), 1.6363 (3H, d, J = 7.3 Hz, CH₃), 2.68 (1H, d, J_{AB} = 9.1 Hz, CH_AH_BO-), 2.79 (1H, d, J_{AB} = 9.1 Hz, CH_AH_BO-), 3.20 – 3.38 (2H, ABX m, J_{AB} = 11.5 Hz, CH₂OH), 4.1919 (1H, q, J = 7.3 Hz, CHCH₃), 7.22 – 7.25 (1H, m, H-Ar), 7.27 – 7.40 (6 H, m, H-Ar), 7.42 (1H, dd, J = 1.0, 7.7 Hz, H-Ar), 7.49 (1H, app. t, J = 7.7 Hz, H-6), 7.53 – 7.61 (2H, m, H-Ar), 7.8383 (1H, dd, J = 1.0, 7.7 Hz, H-Ar); ¹³C NMR (125 MHz; CDCl₃) δ_C 8.5 (CH₂ cyclopropyl), 8.6 (CH₂ cyclopropyl), 20.7 (CH₃), 22.1 (C q cyclopropyl), 54.3 (CHCH₃), 68.1 (CH₂OH), 68.3 (CH₂O-), 96.1 (C-3), 122.2 (C-Ar), 127.6 (2 × C-Ar), 127.8 (2 × C-Ar), 128.8

(2 × C-Ar), 129.50 (2 × C-Ar), 131.9 (C-Ar), 133.7 (C-Ar), 134.9 (C-Ar q), 135.3 (C-Ar q), 135.7 (C-Ar q), 140.5 (C-Ar q), 143.3 (C-Ar q), 167.0 (C-1). Two quaternary carbons not detected; LRMS (ES⁺) *m/z* 504.4 [M+Na]⁺; HRMS calcd for C₂₇H₂₆³⁵Cl₂NO₃ [M+H]⁺ 482.1284, found 482.1285; HPLC 99.5% in 0.1% formic acid (aq)/MeCN (*R*_t 9.9 min); >99.9% in 0.1% ammonia (aq)/MeCN (*R*_t 9.8 min); 99.4% in isocratic 0.1% formic acid (aq)/MeCN (*R*_t 14.0 min).

197

*R*_f 0.14 (25% EtOAc/petrol); no clear m.p. detected; [α]_D³⁰ -9° (*c* 0.594, EtOAc); λ_{max} (EtOH)/nm 258sh; ν_{max}/cm⁻¹ (neat) 1686 (s, C=O), 2874, 2930 and 2981 (w, C-H and -CH₂- aliphatic), 3400 (br, O-H); ¹H NMR (500 MHz; CDCl₃) δ_H 0.49 – 0.69 (4H, m, cyclopropyl), 1.85 (1H, ABX app. t, *J*_{AX} = *J*_{BX} = 5.9 Hz, OH), 1.93 (3H, d, *J* = 7.3 Hz), 3.00 (1H, d, *J*_{AB} = 9.0 Hz, CH_AH_BO-), 3.33 (1H, d, *J*_{AB} = 9.0 Hz, CH_AH_BO-), 3.64 – 3.78 (2H, ABX dq, *J*_{AX} = *J*_{BX} = 5.9 Hz, *J*_{AB} = 11.5 Hz, CH₂OH), 4.36 (1H, q, *J* = 7.3 Hz, CHCH₃), 6.90 – 7.15 (9H, m, H-Ar), 7.41 (1H, dd, *J* = 1.0, 7.7 Hz, H-Ar), 7.4747 (1H, app. t, *J* = 7.7 Hz, H-6), 7.79 (1H, dd, *J* = 1.0, 7.7 Hz, H-Ar); ¹³C NMR (125 MHz; CDCl₃) δ_C 8.9 (CH₂ cyclopropyl), 9.0 (CH₂ cyclopropyl), 20.2 (CH₃), 22.7 (C q cyclopropyl), 53.2 (CHCH₃), 68.1 (CH₂OH), 68.4 (CH₂O-), 94.7 (C-3), 122.1 (C-Ar), 127.0 (C-Ar), 127.8 (2 × C-Ar), 128.0 (2 × C-Ar), 128.0 (2 × C-Ar), 128.7 (2 × C-Ar), 129.6 (C-Ar q), 131.8 (C-6), 133.6 (C-Ar), 134.4 (C-Ar q), 135.1 (C-Ar q), 135.4 (C-Ar q), 140.3 (C-Ar q), 142.5 (C-Ar q), 166.6 (C-1); LRMS (ES⁺) *m/z* 482.4 [M+H]⁺; HRMS calcd for C₂₇H₂₆³⁵Cl₂NO₃ [M+H]⁺ 482.1284, found 482.1285; HPLC 99.0% in 0.1% formic acid (aq)/MeCN (*R*_t 9.8 min); 99.5% in 0.1% ammonia (aq)/MeCN (*R*_t 9.8 min); 97% in isocratic 0.1% formic acid (aq)/MeCN (*R*_t 12.7 min).

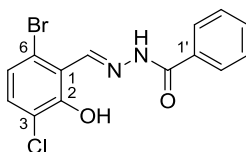
6-Bromo-3-chloro-2-hydroxybenzaldehyde (290)



The phenol (10.0 g, 48.2 mmol) was dissolved in chloroform (50 mL, 0.625 mol). Water (15 mL, 0.31 mL/mol) and NaOH (12.2 g, 0.304 mol) were added in

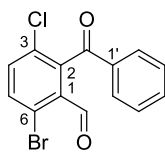
one portion and the pale pink mixture was stirred at 75 °C for 3 h. The reaction was quenched by addition of HCl (1 M aq.) and water (50 mL) until neutral pH was reached. DCM (50 mL) was added and the layers were separated. The aqueous layer was extracted with diethyl ether (2 × 50 mL). The combined organic layers were washed with 10 % aq. NaHCO₃ (50 mL), brine (50 mL), dried (MgSO₄), filtered and evaporated. Medium pressure liquid chromatography (gradient elution, 0-3% EtOAc/petrol) afforded the desired compound **290** (2.8 g, 25%) as a pale yellow solid. *R*_f 0.76 (17% EtOAc/petrol); m.p. 81.4-84.7 °C; λ_{max} (EtOH)/nm 271, 349; ν_{max}/cm⁻¹ (neat) 1640 (s, C=O); ¹H NMR (500 MHz; CDCl₃) δ_H 7.15 (1H, d, *J* = 8.4 Hz, H-5), 7.44 (1H, dd, *J* = 0.6, 8.4 Hz, H-4), 10.31 (1H, s, CHO), 12.52 (1H, br, OH); ¹³C NMR (125 MHz; CDCl₃) δ_C 118.5 (C-Ar q), 124.7 (C-5), 125.7 (C-3), 137.4 (C-4), 159.7 (C-2), 197.8 (CHO) ppm. One quaternary carbon not detected; LRMS (ES⁻) *m/z* 233.0 and 235.0 [M-H]⁻; HRMS calcd for C₇H₅⁸¹Br³⁵ClO₂ [M+H]⁺ 236.9129, found 236.9133.

(*E*)-*N'*-(6-Bromo-3-chloro-2-hydroxybenzylidene)benzohydrazide (293**)**



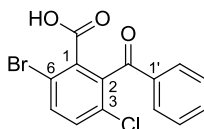
The hydrazide **293** was prepared following general procedure J using aldehyde **290** (2.50 g, 10.6 mmol), benzhydrazide (1.44 g, 10.6 mmol), and acetic acid (45 mL). The title compound was obtained (3.03 g, 81%) as an off-white solid. *R*_f 0.72 (50% EtOAc/petrol); m.p. 205.8-206.2 °C; λ_{max} (EtOH)/nm 301, 314, 341sh; ν_{max}/cm⁻¹ (neat) 1635 (s, C=O), 3060 (w, C-H str, aromatic), 3196 (br, OH), 3401 (br, N-H); ¹H NMR (500 MHz; DMSO-*d*₆) δ_H 7.25 (1H, d, *J* = 8.5 Hz, H-4), 7.44 (1H, d, *J* = 8.5 Hz, H-5), 7.56 – 7.61 (2H, m, H-3' and H-5'), 7.62 – 7.70 (1H, m, H-4'), 7.94 – 8.02 (2H, m, H-2' and H-6'), 9.02 (1H, s, C-H), 12.63 (1H, s, N-H), 13.54 (1H, s, O-H); ¹³C NMR (125 MHz; DMSO-*d*₆) δ_C 117.5 (C-Ar q), 120.4 (C-Ar q), 122.3 (C-Ar q), 124.0 (C-4), 127.7 (C-2' and C-6'), 128.7 (C-3' and C-5'), 132.1 (C-5), 132.5 (C-4'), 148.3 (C-1'), 154.9 (C-1), 162.8 (C=O). One quaternary carbon not detected; LRMS (ES⁺) *m/z* 353.2 and 355.2 [M+H]⁺; HRMS calcd for C₁₄H₁₁⁷⁹Br³⁵ClN₂O₂ [M+H]⁺ 352.9687, found 352.9695.

2-Benzoyl-6-bromo-3-chlorobenzaldehyde (**294**)



Compound **294** was prepared according to general procedure K using the hydrazide **293** (3.03 g, 8.57 mmol), lead tetraacetate (4.57 g, 10.3 mmol) and THF (65 mL). The crude product was purified by medium pressure liquid chromatography (gradient elution, 0-20% EtOAc/petrol) to yield the title compound (2.26 g, 81%) as an off-white solid. R_f 0.49 (20% EtOAc/petrol); m.p. 170.7-172.1 °C; λ_{max} (EtOH)/nm 248, 314; ν_{max}/cm^{-1} (neat) 1672 (vs, C=O); 1H NMR (500 MHz; DMSO- d_6) δ_H 7.49 – 7.55 (2H, m, H-3' and H-5'), 7.64 – 7.69 (1H, m, H-4'), 7.69 – 7.74 (2H, m, H-2' and H-6'), 7.85 (1H, d, J = 8.6 Hz, H-4), 8.01 (1H, d, J = 8.6 Hz, H-5), 10.15 (1H, s, CHO); ^{13}C NMR (125 MHz; DMSO- d_6) δ_C 125.8 (C-Ar q), 128.4 (C-2' and C-6'), 129.0 (C-3' and C-5'), 130.3 (C-Ar q), 132.5 (C-Ar q), 133.8 (C-4'), 135.6 (C-Ar q), 136.1 and 136.2 (C-4 and C-5), 140.3 (C-Ar q), 191.1 (CHO), 193.0 (C=O); LRMS (ES $^+$) m/z 289.2 and 291.2 [M+H] $^+$; HRMS calcd for C₁₄H₉⁸¹Br³⁵ClO₂ [M+H] $^+$ 324.9446, found 324.9447.

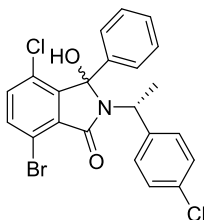
2-Benzoyl-6-bromo-3-chlorobenzoic acid (**295**)



Compound **295** was obtained following general procedure L using aldehyde **294** (2.26 g, 6.98 mmol), sodium chlorite (0.820 g, 9.07 mmol), sulfamic acid (0.880 g, 9.07 mmol), MeCN (87 mL) and water (2 × 10 mL). The crude product (yellow solid; 2.60 g, 97%) was used directly in the following step without further purification. R_f 0.28 (10% MeOH/DCM); m.p. 189.3-190.6 °C; λ_{max} (EtOH)/nm 292; ν_{max}/cm^{-1} (neat) 1747 (vs, C=O), 3375 (br s, O-H); 1H NMR (500 MHz; DMSO- d_6) δ_H 7.28-7.77 (6H, m, H-Ar), 7.85-7.97 (1H, m, H-Ar), 8.76 (1H, s, CO₂H); ^{13}C NMR (125 MHz; CDCl₃) δ_C 126.2 (C-Ar), 128.2 (C-Ar), 129.1 (C-Ar), 129.2 (C-Ar), 129.3 (C-Ar), 132.3 (C-Ar), 134.4 (C-Ar), 135.6 (C-Ar), 136.9

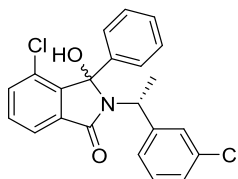
(C-Ar), 192.7 (C q). Two carbons not visible; LRMS (ES⁻) m/z 337.1 and 339.1 [M-H]⁻; HRMS calcd for C₁₄H₇⁷⁹Br³⁵ClO₃ [M-H]⁻ 336.9273, found 336.9264.

(1'*R*)-7-Bromo-4-chloro-2-[1'-(4''-chlorophenyl)ethyl]-3-hydroxy-3-phenylisoindolin-1-one (296)



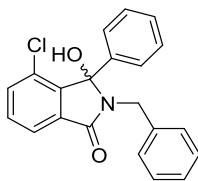
The isoindolinone **296** was obtained following general procedure M using acid **295** (2.30 g, 6.77 mmol), thionyl chloride (0.98 mL, 1.61 g, 13.54 mmol), catalytic DMF (3 drops), (*R*)-4-chloro- α -methylbenzylamine (1.05 mL, 1.16 g, 7.45 mmol), DIPEA (1.30 mL, 0.963 g, 7.45 mmol) and THF (2 \times 8.0 mL). The product was obtained as a mixture of diastereoisomers (dr 1:10; white powder; 2.56 g, 79%) after purification by MPLC (gradient elution, 0-25% EtOAc/petrol). $R_{f(1)}$ 0.70, $R_{f(2)}$ 0.57 (25% EtOAc/petrol); no clear m.p. detected; λ_{\max} (EtOH)/nm 252sh; $\nu_{\max}/\text{cm}^{-1}$ (neat) 1670 and 1682 (s, C=O), 3374 (m, O-H); ¹H NMR (500 MHz; DMSO-*d*₆) δ_{H} 1.33 (3H, d, J = 7.3 Hz, CHCH₃), 1.74 (3H, d, J = 7.2 Hz, CHCH₃), 4.36 (1H, q, J = 7.3 Hz, CHCH₃), 4.48 (1H, q, J = 7.2, CHCH₃), 6.84 – 6.90 (2H, m, H-Ar), 7.04 – 7.12 (2H, m, H-Ar), 7.13 – 7.31 (5H, m, H-Ar), 7.51 (1H, d, J = 8.5 Hz, H-5 or H-6), 7.75 (1H, d, J = 8.5 Hz, H-5 or H-6); ¹³C NMR (125 MHz; DMSO-*d*₆) δ_{C} 19.0 (CHCH₃), 50.2 (CHCH₃), 88.8 (C-3), 115.5 (C-Ar q), 126.6 (2 \times C-Ar), 127.4 (2 \times C-Ar), 128.0 (2 \times C-Ar), 128.1 (C-Ar), 128.3 (C-Ar), 129.2 (2 \times C-Ar), 130.6 (C-Ar q), 131.1 (C-Ar q), 134.7, 135.9, 137.2 (C-Ar q), 140.2 (C-Ar q), 146.7 (C-Ar q), 162.8 (C-1); LRMS (ES⁻) m/z 476.1 [M-H]⁻; HRMS calcd for C₂₂H₁₅⁷⁹Br³⁵Cl₂NO₂ [M-H]⁻ 473.9669, found 473.9674.

(1'*R*)-4-Chloro-2-[1'-(3''-chlorophenyl)ethyl]-3-hydroxy-3-phenylisoindolin-1-one (255)



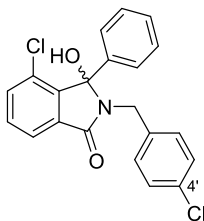
The isoindolinone **255** was obtained following general procedure M using acid **183** (290 mg, 1.11 mmol), thionyl chloride (0.16 mL, 264 mg, 2.22 mmol), catalytic DMF (3 drops), (*R*)-3-chloro- α -methylbenzylamine (0.18 mL, 190 mg, 1.22 mmol), DIPEA (0.21 mL, 158 mg, 1.22 mmol) and THF (2 \times 1.3 mL). The product was obtained as a mixture of diastereoisomers (cream-colored amorphous solid; 339 mg, 77%) after purification by MPLC (gradient elution, 0-33% EtOAc/petrol). $R_{f(1)}$ 0.69, $R_{f(2)}$ 0.54 (33% EtOAc/petrol); no clear m.p. detected; λ_{\max} (EtOH)/nm 259; ν_{\max} /cm⁻¹ (neat) 1669 (s, C=O), 3208 (br, O-H); ¹H NMR (500 MHz; DMSO-*d*₆) δ_{H} 1.36 (3H, d, J = 7.1 Hz, CH₃), 1.75 (3H, d, J = 7.1 Hz, CH₃), 4.38 (1H, q, J = 7.1 Hz, CHCH₃), 4.49 (1H, q, J = 7.1 Hz, CHCH₃), 6.82 (1H, t, J = 1.9 Hz, H-Ar), 6.88 (1H, dt, J = 7.6, 1.4 Hz, H-Ar), 7.06 (1H, t, J = 7.8 Hz, H-Ar), 7.10 (1H, ddd, J = 8.0, 2.1, 1.2 Hz, H-Ar), 7.12 – 7.28 (5H, m, H-Ar), 7.30 (1H, t, J = 7.7 Hz, H-Ar), 7.32 – 7.43 (6H, m, H-Ar), 7.48 (1H, s, H-Ar), 7.52 (1H, t, J = 1.8 Hz, H-Ar), 7.55 – 7.62 (4H, m, H-Ar), 7.64 – 7.72 (2H, m, H-Ar); ¹³C NMR (125 MHz; DMSO-*d*₆) δ_{C} 17.3 (CHCH₃), 19.1 (CHCH₃), 49.8 (CHCH₃), 50.2 (CHCH₃), 90.5 (C-3), 90.7 (C-3), 121.2 (C-Ar), 125.9 (C-Ar), 126.0 (C-Ar), 126.4 (C-Ar), 126.6 (C-Ar), 126.6 (C-Ar), 127.2 (C-Ar), 127.3 (C-Ar), 127.9 (C-Ar), 128.1 (C-Ar), 128.3 (C-Ar), 128.5 (C-Ar), 128.6 (C-Ar), 129.3 (C-Ar), 129.6 (C-Ar), 131.5 (C-Ar), 131.6 (C-Ar), 132.1 (C-Ar), 132.6 (C-Ar), 133.3 (C-Ar), 134.1 (C-Ar), 134.4 (C-Ar), 137.6 (C-Ar), 137.7 (C-Ar), 144.1 (C-Ar), 144.2 (C-Ar), 144.3 (C-Ar), 164.5 (C-1), 164.8 (C-1). One carbon not detected; LRMS (ES⁻) m/z 396.2 [M-H]⁻; HRMS calcd for C₂₂H₁₆³⁵Cl₂NO₂ [M-H]⁻ 396.0564, found 396.0564.

2-Benzyl-4-chloro-3-hydroxy-3-phenylisoindolin-1-one (251)



The isoindolinone **251** was obtained following general procedure M using benzoylbenzoic acid **183** (290 mg, 1.11 mmol), thionyl chloride (0.16 mL, 264 mg, 2.22 mmol), catalytic DMF (3 drops), benzylamine (0.13 mL, 131 mg, 1.22 mmol), DIPEA (0.21 mL, 158 mg, 1.22 mmol) and THF (2 × 1.3 mL). Purification by MPLC (gradient elution, 0-25% EtOAc/petrol) afforded title compound **251** as an off-white solid (349 mg, 90%). R_f 0.43 (33% EtOAc/petrol); m.p. 183.6-184.7 °C; λ_{max} (EtOH)/nm 258; ν_{max}/cm^{-1} (neat) 1656 (vs, C=O), 2850 and 2922 (w, C-H and -CH₂- aliphatic), 3194 (br, O-H); ¹H NMR (500 MHz; DMSO-*d*₆) δ_H 4.15 (1H, d, J_{AB} = 15.6 Hz, CH_AH_B), 4.38 (1H, d, J_{AB} = 15.6 Hz, CH_AH_B), 7.02 – 7.17 (5H, m, H-Ar), 7.18 – 7.34 (5H, m, H-Ar), 7.53 – 7.63 (2H, m, H-Ar), 7.70 – 7.79 (1H, m, H-Ar); ¹³C NMR (125 MHz; DMSO-*d*₆) δ_C 42.2 (CH₂), 90.3 (C-3), 121.4 (C-Ar), 126.4 (2 × C-Ar), 127.7 (C-Ar), 127.7 (2 × C-Ar), 127.8 (2 × C-Ar), 128.0 (2 × C-Ar), 128.7 (C-Ar), 131.5 (C-Ar), 133.5 (C-Ar), 137.7 (C-Ar q), 137.7 (C-Ar q), 165.4 (C-1). Three quaternary carbons not detected. LRMS (ES⁻) m/z 348.2 [M-H]⁻; HRMS calcd for C₂₁H₁₅³⁵ClNO₂ [M-H]⁻ 348.0797, found 348.0783.

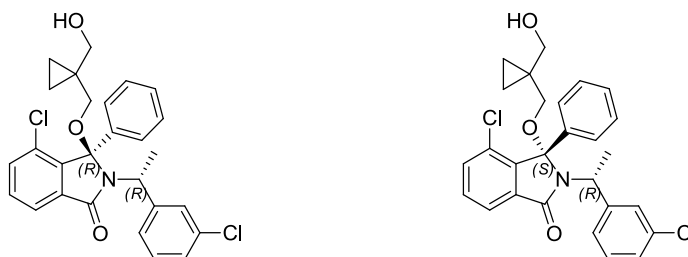
4-Chloro-2-(4'-chlorobenzyl)-3-hydroxy-3-phenylisoindolin-1-one (253)



General procedure M was used to synthesize the isoindolinone **253** using benzoylbenzoic acid **183** (290 mg, 1.11 mmol), thionyl chloride (0.16 mL, 264 mg, 2.22 mmol), catalytic DMF (3 drops), 4-chlorobenzylamine (0.15 mL, 173 mg, 1.22 mmol), DIPEA (0.21 mL, 158 mg, 1.22 mmol) and THF (2 × 1.3 mL). Purification by MPLC (gradient elution, 0-33% EtOAc/petrol) afforded the title

compound **253** as an off-white solid (317 mg, 74%). R_f 0.46 (33% EtOAc/petrol); m.p. 194.0-195.5 °C; λ_{\max} (EtOH)/nm 253; $\nu_{\max}/\text{cm}^{-1}$ (neat) 1655 (vs, C=O), 2924 (w, C-H and -CH₂- aliphatic), 3141 (br, O-H); ¹H NMR (500 MHz; DMSO-*d*₆) δ_H 4.16 (1H, d, J_{AB} = 15.7 Hz, CH_AH_B), 4.37 (1H, d, J_{AB} = 15.7 Hz, CH_AH_B), 7.08 – 7.15 (2H, m, H-Ar), 7.16 – 7.21 (2H, m, H-Ar), 7.21 – 7.29 (4H, m, H-Ar), 7.29 – 7.34 (1H, m, H-Ar), 7.57 – 7.61 (2H, m, H-Ar), 7.72 – 7.78 (1H, m, H-Ar); ¹³C NMR (125 MHz; DMSO-*d*₆) δ_C 41.5 (CH₂), 99.5 (C-3), 121.5 (C-Ar), 126.4 (2 × C-Ar), 127.7 (2 × C-Ar), 128.1 (2 × C-Ar), 129.7 (2 × C-Ar), 131.1 (C-Ar q), 131.6 (C-Ar), 133.3 (C-Ar q), 133.5 (C-Ar), 136.8 (C-Ar q), 165.3 (C-1). Four carbons not detected; LRMS (ES⁻) m/z 382.3 [M-H]⁻; HRMS calcd for C₂₁H₁₄³⁵Cl₂NO₂ [M-H]⁻ 382.0407, found 382.0397.

(3*R*,1'*R*)-4-Chloro-2-[1'-(3''-chlorophenyl)ethyl]-3-{[1''''-(hydroxymethyl)cyclopropyl]methoxy}-3-phenylisoindolin-1-one (256)
and (3*S*,1'*R*)-4-Chloro-2-[1'-(3''-chlorophenyl)ethyl]-3-{[1''''-(hydroxymethyl)cyclopropyl]methoxy}-3-phenylisoindolin-1-one (257)



Compounds **256** and **257** were obtained according to general procedure N using isoindolinone **255** (308 mg, 0.733 mmol), InBr₃ (55 mg, 0.155 mmol), 1,1-bis(hydroxymethyl)cyclopropane (0.37 mL, 395 mg, 3.87 mmol) and DCE (7.7 mL). Purification by MPLC (gradient elution, 0-20% EtOAc/petrol) yielded isoindolinones **256** (100 mg, 27%; white amorphous solid) and **257** (140 mg, 38%; white solid).

256

R_f 0.33 (33% EtOAc/petrol); no clear m.p. detected; $[\alpha]_D^{29} +90^\circ$ (*c* 0.706, EtOAc); λ_{\max} (EtOH)/nm 259; $\nu_{\max}/\text{cm}^{-1}$ (neat) 1343 (s), 1699 (vs, C=O), 3500 (br, O-H); ¹H NMR (500 MHz; CDCl₃) δ_H -0.07 – 0.00 (1H, m, cyclopropyl), 0.13 – 0.21 (1H,

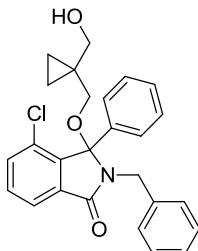
m, cyclopropyl), 0.31 – 0.40 (2H, m, cyclopropyl), 1.58 (3H, d, $J = 7.3$ Hz, $-\text{CH}_3$), 1.72 (1H, ABX br, -OH), 2.64 (1H, d, $J_{\text{AB}} = 9.1$ Hz, $\text{CH}_\text{A}\text{H}_\text{B}\text{O}-$), 2.94 (1H, d, $J_{\text{AB}} = 9.1$ Hz, $\text{CH}_\text{A}\text{H}_\text{B}\text{O}-$), 3.31 (1H, ABX app. d, $J_{\text{AB}} = 11.5$ Hz, $\text{CH}_\text{A}\text{H}_\text{B}\text{O}-\text{OH}$), 3.46 (1H, ABX app. d, $J_{\text{AB}} = 11.5$ Hz, $\text{CH}_\text{A}\text{H}_\text{B}\text{O}-\text{OH}$), 4.20 (1H, q, $J = 7.3$ Hz, $-\text{CHCH}_3$), 7.21 – 7.25 (2H, m, H-Ar), 7.30 – 7.41 (5H, m, H-Ar), 7.43 (1H, dd, $J = 7.7, 1.0$ Hz, H-5), 7.49 (1H, app. t, $J = 7.7$ Hz, H-6), 7.52 – 7.58 (2H, m, H-Ar), 7.83 (1H, dd, $J = 1.0, 7.7$ Hz, H-7); ^{13}C NMR (125 MHz; CDCl_3) δ_C 8.5 (CH_2 cyclopropyl), 8.5 (CH_2 cyclopropyl), 20.0 (CH_3), 22.1 (C q cyclopropyl), 53.6 (CHCH_3), 68.4 and 68.4 ($\text{CH}_2\text{O}-$ and CH_2OH), 96.4 (C-3), 122.1 (C-7), 126.3 (C-Ar), 127.7 (C-Ar), 128.2 (C-Ar), 128.5 (C-Ar), 129.0 (C-Ar), 129.6 (C-Ar q), 130.0 (C-Ar), 130.6 (C-Ar), 131.7 (C-6), 133.8 (C-5), 134.3 (C-Ar q), 135.2 (C-Ar q), 136.7 (C-Ar q), 140.8 (C-Ar q), 145.1 (C-Ar q), 167.0 (C-1); LRMS (ES^+) m/z 504.4 $[\text{M}+\text{Na}]^+$; HRMS calcd for $\text{C}_{27}\text{H}_{26}\text{Cl}_2\text{NO}_3$ $[\text{M}+\text{H}]^+$ 482.1284, found 482.1282; HPLC 98.4% in 0.1% formic acid (aq)/MeCN (R_t 9.7 min); 98.7% in 0.1% ammonia (aq)/MeCN (R_t 9.7 min); 98.7% in isocratic 0.1% formic acid (aq)/MeCN (R_t 12.5 min).

257

R_f 0.24 (33% EtOAc/petrol); m.p. 184.9-187.4 °C; $[\alpha]_\text{D}^{29} -3^\circ$ (c 0.702, EtOAc); λ_max (EtOH)/nm 259; $\nu_\text{max}/\text{cm}^{-1}$ (neat) 1684 (s, C=O), 2872 and 2921 (w, aliphatic C-H and $-\text{CH}_2-$), 3420 (br, O-H); ^1H NMR (500 MHz; CDCl_3) δ_H 0.51 – 0.67 (4H, m, cyclopropyl), 1.88 – 1.94 (4H, m, $-\text{CH}_3$ and -OH), 3.04 (1H, d, $J_{\text{AB}} = 9.2$ Hz, $\text{CH}_\text{A}\text{H}_\text{B}\text{O}-$), 3.32 (1H, d, $J_{\text{AB}} = 9.2$ Hz, $\text{CH}_\text{A}\text{H}_\text{B}\text{O}-$), 3.70 (2H, ABX dq, $J_{\text{AX}} = J_{\text{BX}} = 5.9$ Hz, $J_{\text{AB}} = 11.4$ Hz, CH_2OH), 4.35 (1H, q, $J = 7.3$ Hz, $-\text{CHCH}_3$), 6.70 (1H, app. t, $J = 1.9$ Hz, H-2'), 6.94 (1H, app. t, $J = 7.7$ Hz, H-5'), 7.00 (1H, m, H-Ar), 7.03 (1H, m, H-Ar), 7.10 (4H, br, H-Ar), 7.18 – 7.23 (1H, m, H-Ar), 7.42 (1H, dd, $J = 7.9, 1.1$ Hz, H-5), 7.47 (1H, dd, $J = 7.9, 7.4$ Hz, H-6), 7.78 (1H, dd, $J = 7.4, 1.1$ Hz, H-7); ^{13}C NMR (125 MHz; CDCl_3) δ_C 8.9 (CH_2 cyclopropyl), 9.1 (CH_2 cyclopropyl), 19.7 (CH_3), 22.7 (C q cyclopropyl), 52.3 (CHCH_3), 68.3 (CH_2OH), 68.5 (CH_2O), 95.1 (C-3), 122.0 (C-7), 126.1 (C-Ar), 127.1 ($2 \times$ C-Ar), 128.0 ($2 \times$ C-Ar), 128.2 (C-Ar), 128.8 (C-Ar), 129.1 (C-Ar), 129.8 (C-Ar q), 131.7 (C-6), 133.4 (C-Ar q), 133.6 (C-5), 135.4 (C-Ar q), 136.3 (C-Ar q), 140.6 (C-Ar q), 144.1 (C-Ar q), 166.5 (C-1). One carbon not detected; LRMS (ES^+) m/z 504.4 $[\text{M}+\text{Na}]^+$; HRMS calcd for

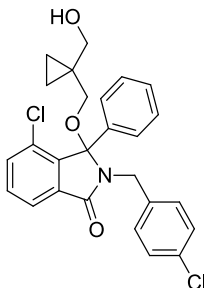
C₂₇H₂₆Cl₂NO₃ [M+H]⁺ 482.1284, found 482.1282; HPLC 99.8% in 0.1% formic acid (aq)/MeCN (*R*_t 9.7 min); >99.9% in 0.1% ammonia (aq)/MeCN (*R*_t 9.7 min); 99.2% in isocratic 0.1% formic acid (aq)/MeCN (*R*_t 12.0 min).

2-Benzyl-4-chloro-3-{{[1''''-(hydroxymethyl)cyclopropyl]methoxy}-3-phenylisoindolin-1-one (252)



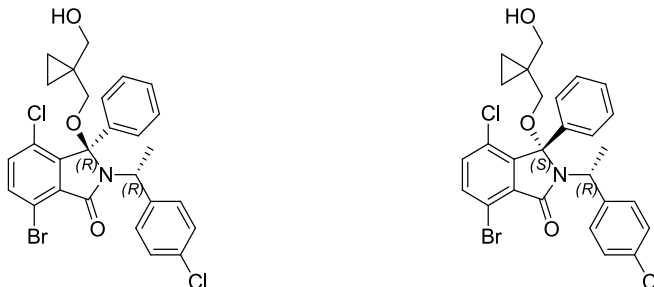
Compound **252** was obtained according to general procedure N using isoindolinone **251** (349 mg, 1.00 mmol), InBr₃ (71 mg, 0.20 mmol), 1,1-bis(hydroxymethyl)cyclopropane (0.48 mL, 511 mg, 5.0 mmol) and DCE (10 mL). Purification by MPLC (gradient elution, 0-30% EtOAc/petrol) yielded the title compound as a white amorphous solid (300 mg, 69%). *R*_f 0.19 (33% EtOAc/petrol); m.p. 132.0-132.8 °C; λ_{max} (EtOH)/nm 285; ν_{max}/cm⁻¹ (neat) 1389 (s), 1460 (m), 1687 (vs, C=O), 1704 (s), 2875 and 2922 (w, aliphatic CH and -CH₂-), 3417 (w, O-H); ¹H NMR (500 MHz; CDCl₃) δ_H -0.09 – 0.02 (1H, m, cyclopropyl), 0.15 – 0.26 (1H, m, cyclopropyl), 0.29 – 0.41 (2H, m, cyclopropyl), 1.69 (1H, ABX dd, *J*_{AX} = 5.7 Hz, *J*_{BX} = 6.5 Hz, -OH), 2.74 (1H, d, *J*_{AB} = 9.1 Hz, CH_AH_BO-), 2.88 (1H, d, *J*_{AB} = 9.1 Hz, CH_AH_BO-), 3.38 (2H, ABX m, , CH₂-OH), 3.93 (1H, d, *J*_{AB} = 15.0 Hz, CH_AH_B-Ph), 4.70 (1H, d, *J*_{AB} = 15.0 Hz, CH_AH_B-Ph), 7.13 – 7.24 (6H, m, H-Ar), 7.30 (4H, br, H-Ar), 7.42 – 7.46 (1H, m, H-5), 7.49 (1H, t, *J* = 7.7, H-6), 7.86 (1 H, dd, *J* 7.4, 1.0, H-7); ¹³C NMR (125 MHz; CDCl₃) δ_C 8.6 (CH₂ cyclopropyl), 8.7 (CH₂ cyclopropyl), 22.1 (C q cyclopropyl), 43.3 (CH₂-Ar) , 68.3 and 68.4 (CH₂O- and CH₂OH), 95.6 (C-3), 122.3 (C-7), 127.0 (2 × C-Ar), 127.5 (C-Ar), 128.4 (2 × C-Ar), 128.5 (2 × C-Ar), 128.8 (C-Ar), 129.2 (2 × C-Ar), 129.8 (C-Ar q), 131.7 (C-6), 133.9 (C-5), 134.5 (C-Ar q), 136.5 (C-Ar q), 137.6 (C-Ar q), 141.4 (C-Ar q), 167.0 (C-1); LRMS (ES⁺) *m/z* 456.4 [M+Na]⁺; HRMS calcd for C₂₆H₂₅ClNO₃ [M+H]⁺ 434.1517, found 434.1518; HPLC >99.9% in 0.1% formic acid (aq)/MeCN (*R*_t 8.9 min); 99.8% in 0.1% ammonia (aq)/MeCN (*R*_t 8.9 min).

4-Chloro-2-(4'-chlorobenzyl)-3-[[1'''-(hydroxymethyl)cyclopropyl]methoxy]-3-phenylisoindolin-1-one (254)



The title compound was obtained following general procedure N using isoindolinone **253** (317 mg, 0.825 mmol), InBr_3 (58 mg, 0.165 mmol), 1,1-bis(hydroxymethyl)cyclopropane (0.40 mL, 422 mg, 4.13 mmol) and DCE (8.3 mL). Purification by MPLC (gradient elution, 0-30% petrol/EtOAc) yielded the desired compound **254** (270 mg, 70%) as a white amorphous solid. R_f 0.19 (33% EtOAc/petrol); no clear m.p detected; λ_{max} (EtOH)/nm 252; $\nu_{\text{max}}/\text{cm}^{-1}$ (neat) 1704 (vs, C=O), 2874 and 2926 (w, aliphatic CH and $-\text{CH}_2-$), 3400 (br, O-H); ^1H NMR (500 MHz; CDCl_3) δ_{H} 0.11 (1H, m, cyclopropyl), 0.28 (1 H, m, cyclopropyl), 0.44 (2H, m, cyclopropyl), 1.78 (1H, ABX app. t, $J_{\text{AX}} = J_{\text{BX}} = 6.0$ Hz, -OH), 2.79 (1H, d, $J_{\text{AB}} = 9.1$ Hz, $\text{CH}_\text{A}\text{H}_\text{BO}$), 2.94 (1H, d, $J_{\text{AB}} = 9.1$ Hz, $\text{CH}_\text{A}\text{H}_\text{BO}$), 3.40 – 3.55 (2H, ABX m, CH_2OH), 4.12 (1H, d, $J_{\text{AB}} = 15.0$ Hz, $\text{CH}_\text{A}\text{H}_\text{B-Ar}$), 4.50 (1H, d, $J_{\text{AB}} = 15.0$ Hz, $\text{CH}_\text{A}\text{H}_\text{B-Ar}$), 7.02 – 7.15 (4H, m, H-Ar), 7.25 (5H, br, H-Ar), 7.45 (1H, m, H-5), 7.50 (1H, app. t, $J = 7.4$ Hz, H-6), 7.85 (1H, dd, $J = 1.1, 7.4$ Hz, H-7); ^{13}C NMR (125 MHz; CDCl_3) δ_{C} 8.8 (CH_2 cyclopropyl), 8.8 (CH_2 cyclopropyl), 22.2 (C q cyclopropyl), 42.5 ($\text{CH}_2\text{-Ar}$), 68.3 (CH_2OH), 68.4 ($\text{CH}_2\text{O-}$), 95.3 (C-3), 122.3 (C-7), 126.9 (C-Ar), 128.4 (C-Ar), 128.5 (C-Ar), 128.8 (C-Ar), 129.9 (C-Ar q), 130.6 (C-Ar), 131.8 (C-6), 133.3 (C-Ar q), 134.0 (C-5), 134.4 (C-Ar q), 135.8 (C-Ar q), 136.4 (C-Ar q), 141.3 (C-Ar q), 167.0 (C-1); LRMS (ES^+) m/z 490.3 [$\text{M}+\text{Na}$] $^+$; HRMS calcd for $\text{C}_{26}\text{H}_{24}\text{Cl}_2\text{NO}_3$ [$\text{M}+\text{H}$] $^+$ 468.1128, found 468.1127; HPLC 97.8% in 0.1% formic acid (aq)/MeCN (R_t 9.3 min); 97.7% in 0.1% ammonia (aq)/MeCN (R_t 9.3 min).

(3*R*,1'*R*)-7-Bromo-4-chloro-2-[1'-(4''-chlorophenyl)ethyl]-3-[[1'''-(hydroxymethyl)cyclopropyl]methoxy]-3-phenylisoindolin-1-one (289)
and (3*S*,1'*R*)-7-Bromo-4-chloro-2-[1'-(4''-chlorophenyl)ethyl]-3-[[1'''-(hydroxymethyl)cyclopropyl]methoxy]-3-phenylisoindolin-1-one (297)



The title compounds were obtained according to general procedure N using isoindolinone **296** (2.48 g, 5.20 mmol), InBr_3 (369 mg, 1.04 mmol), 1,1-bis(hydroxymethyl)cyclopropane (2.50 mL, 2.66 g, 26.0 mmol) and DCE (52mL). Purification by MPLC (gradient elution, 0-15% EtOAc/petrol) yielded isoindolinones **289** (1.19 g, 41%) and **297** (1.30 g, 44%) as white amorphous solids.

289

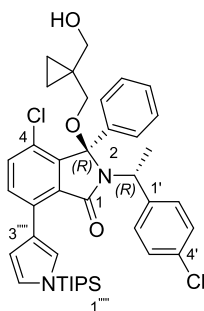
R_f 0.33 (25% EtOAc/petrol); no clear m.p. detected (melting range 78-105 °C; boils ~130 °C); $[\alpha]_D^{24} +75^\circ$ (c 0.722, EtOAc); λ_{max} (EtOH)/nm no maximum of absorption was detected; $\nu_{\text{max}}/\text{cm}^{-1}$ (neat) 1703 (vs, C=O), 2880, 2937 and 2984 (w, aliphatic CH and $-\text{CH}_2-$); ^1H NMR (500 MHz; CDCl_3) δ_{H} -0.03 – 0.05 (1H, m, cyclopropyl), 0.14 – 0.23 (1H, m, cyclopropyl), 0.33 – 0.41 (2H, m, cyclopropyl), 1.57 (3H, d, $J = 7.2$ Hz, CH_3), 1.64 (1H, ABX dd, $J_{\text{AX}} = 5.3$ Hz, $J_{\text{BX}} = 6.6$ Hz, -OH), 2.68 (1H, d, $J_{\text{AB}} = 9.1$ Hz, $\text{CH}_\text{A}\text{H}_\text{BO}-$), 2.85 (1H, d, $J_{\text{AB}} = 9.1$ Hz, $\text{CH}_\text{A}\text{H}_\text{BO}-$), 3.30 (1H, dd, $J_{\text{AX}} = 5.3$ Hz, $J_{\text{AB}} = 11.4$ Hz, $\text{CH}_\text{A}\text{H}_\text{BOH}$), 3.39 – 3.48 (1 H, dd, $J_{\text{AX}} = 6.6$ Hz, $J_{\text{AB}} = 11.4$ Hz, $\text{CH}_\text{A}\text{H}_\text{BOH}$), 4.19 (1H, q, $J = 7.2$ Hz, CHCH_3), 7.25-7.29 (3H, m, 2 \times H-Ar and H-5), 7.38 (5H, br, H-Ar), 7.54 – 7.58 (2H, m, H-Ar), 7.61 (1H, d, $J = 8.4$ Hz, H-6); ^{13}C NMR (125 MHz; CDCl_3) δ_{C} 8.6 (CH_2 cyclopropyl), 8.7 (CH_2 cyclopropyl), 19.9 (CH_3), 22.1 (C q cyclopropyl), 53.8 (CHCH_3), 68.3 (CH_2OH), 68.5 ($\text{CH}_2\text{-O}$), 94.8 (C-3), 117.2 (C-Ar q), 128.6 (2 \times C-Ar), 128.8 (2 \times C-Ar), 129.1 (C-Ar q), 129.2 (2 \times C-Ar), 129.7 (2 \times C-Ar), 131.6 (C-Ar q), 133.5 (C-Ar q), 134.6

(C-Ar), 136.3 (C-Ar q), 136.6 (C-Ar), 141.2 (C-Ar q), 143.2 (C-Ar q), 165.0 (C-1); LRMS (ES⁺) m/z 584.3 [M+Na]⁺; HRMS calcd for C₂₇H₂₅⁷⁹Br³⁵Cl₂NO₃ [M+H]⁺ 560.0389, found 560.0390; HPLC 96.7% in 0.1% formic acid (aq)/MeCN (R_t 10.1 min); 96.2% in 0.1% ammonia (aq)/MeCN (R_t 10.1 min).

297

R_f 0.23 (25% EtOAc/petrol); no clear m.p. detected; $[\alpha]_D^{24}$ -75° (c 0.774, EtOAc); λ_{max} (EtOH)/nm no maximum of absorption was detected; ν_{max}/cm^{-1} (neat) 1452 (s), 1493 (s), 1706 (s, C=O), 2875, 2938, and 2981 (w, aliphatic CH and -CH₂-); ¹H NMR (500 MHz; CDCl₃) δ_H 0.53 – 0.73 (4H, m, cyclopropyl), 1.86 (1H, ABX app. t, $J_{AX} = J_{BX} = 5.9$ Hz, -OH), 1.93 (3H, d, $J = 7.3$ Hz, CH₃), 3.02 (1H, d, $J_{AB} = 9.1$ Hz, CH_AH_BO-), 3.39 (1 H, d, $J_{AB} = 9.1$ Hz, CH_AH_BO-), 3.72 (2H, ABX m, CH₂OH), 4.38 (1H, q, $J = 7.3$ Hz, CHCH₃), 6.86 – 6.92 (2H, m, H-Ar), 6.94 – 6.99 (2H, m, H-Ar), 6.99 – 7.21 (4H, br, H-Ar), 7.24 (1H, m, H-Ar), 7.28 (1H, d, $J = 8.5$ Hz, H-5), 7.62 (1H, d, $J = 8.5$ Hz, H-6); ¹³C NMR (125 MHz; CDCl₃) δ_C 8.9 (CH₂ cyclopropyl), 9.1 (CH₂ cyclopropyl), 19.7 (CH₃), 22.7 (C q cyclopropyl), 52.4 (CHCH₃), 68.1 (CH₂-OH), 68.4 (CH₂OH), 93.5 (C-3), 117.2 (C-Ar q), 127.2 (2 × C-Ar), 127.9 (2 × C-Ar), 128.2 (2 × C-Ar), 128.8 (C-Ar), 129.2 (C-Ar q), 129.6 (2 × C-Ar), 131.7 (C-Ar q), 132.8 (C-Ar q), 134.4 (C-5), 136.0 (C-Ar q), 136.6 (C-6), 140.3 (C-Ar q), 143.0 (C-Ar q), 164.5 (C-1); LRMS (ES⁺) m/z 562.3 [M+H]⁺; HRMS calcd for C₂₇H₂₅⁷⁹Br³⁵Cl₂NO₃ [M+H]⁺ 560.0389, found 560.0389; HPLC 98.3% in 0.1% formic acid (aq)/MeCN (R_t 10.1 min); 97.6% in 0.1% ammonia (aq)/MeCN (R_t 10.1 min).

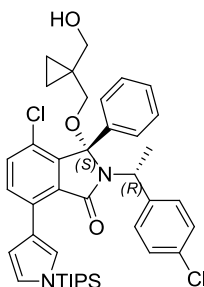
(3*R*,1'*R*)-4-Chloro-2-[1'-(4''-chlorophenyl)ethyl]-3-{[1'''-(hydroxymethyl)cyclopropyl]methoxy}-3-phenyl-7-(1^v-(triisopropylsilyl)-1^v*H*-pyrrol-3^v-yl)isoindolin-1-one (298)



Compound **298** was synthesized according to general procedure O using isoindolinone **289** (138 mg, 0.246 mmol), 1-(triisopropylsilyl)-1*H*-pyrrole-3-boronic acid (86 mg, 0.320 mmol), tetrakis(triphenylphosphine)palladium (29 mg, 0.025 mmol), Na₂CO₃ (2 M aq., 0.37 mL, 0.738 mmol) and acetonitrile (3.0 mL). The crude product was purified by MPLC (gradient elution, 0-25% EtOAc/petrol) and the title compound was obtained as a pale yellow solid (116 mg, 67%). *R*_f 0.68 (25% EtOAc/petrol); m.p. not clear melting point detected; λ_{max} (EtOH)/nm 276, 339; ν_{max}/cm⁻¹ (neat) 1365 (m, C=C and C=N in-plane vibs), 1696 (vs, C=O), 2866 and 2943 (w, aliphatic CH and -CH₂-, Si-R), 3460 (br, O-H); ¹H NMR (500 MHz; CDCl₃) δ_H -0.05 – 0.04 (1H, m, cyclopropyl), 0.15 – 0.24 (1H, m, cyclopropyl), 0.32 – 0.40 (2H, m, cyclopropyl), 1.14 – 1.23 (18H, m, 6 × CH₃), 1.49 – 1.57 (6H, m, CHCH₃ and 3 × CH(CH₃)₂), 1.93 (1H, ABX dd, *J*_{AX} = 5.6 Hz, *J*_{BX} = 6.7 Hz, OH), 2.74 (1H, d, *J*_{AB} = 9.2 Hz, CH_ACH_BO-), 2.93 (1H, d, *J*_{AB} = 9.2 Hz, CH_ACH_BO-), 3.38 (2H, ABX dq, *J*_{AX} = 5.6 Hz, *J*_{BX} = 6.7 Hz, *J*_{AB} = 11.4 Hz), 4.24 (1H, q, *J* = 7.3 Hz, CHCH₃), 6.85 (1H, dd, *J* = 2.1, 2.8 Hz, H-4'''' or H-5'''''), 6.87 (1H, dd, *J* = 1.5, 2.8 Hz, H-4'''' or H-5'''''), 7.20 – 7.25 (2H, m, H-Ar), 7.31 (1H, d, *J* = 8.4 Hz, H-5 or H-6), 7.35 (5H, br, H-Ar), 7.53 – 7.60 (3H, m, H-Ar), 7.79 (1H, dd, *J* = 1.5, 2.1 Hz, H-2'''''); ¹³C NMR (125 MHz; CDCl₃) δ_C 8.7 (2 × CH₂ cyclopropyl), 11.9 (3 × CH(CH₃)₂), 18.1 (6 × CH₃), 19.8 (CHCH₃), 22.1 (C q cyclopropyl), 53.2 (CHCH₃), 68.5 (CH₂O-), 68.8 (CH₂OH), 111.9 (C-4'''' or C-5'''''), 124.4 (C-4'''' or C-5'''''), 125.6 (C-Ar q), 127.4 (C-2'''''), 128.3 (C-Ar), 128.4 (C-Ar), 128.6 (C-Ar), 129.9 (C-Ar), 132.3 (C-Ar), 133.3 (C-Ar), 134.5 (C-Ar), 142.0 (C-Ar), 142.0 (C-

Ar). Five carbons not detected; LRMS (ES⁺) m/z 703.6 and 705.6 [M+H]⁺; HRMS calcd for C₄₀H₄₉³⁵Cl₂N₂O₃Si [M+H]⁺ 703.2884, found 703.2884.

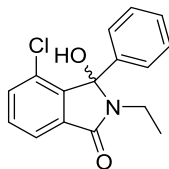
(3S1'R)-4-Chloro-2-[1'-(4''-chlorophenyl)ethyl]-3-{{1'''-(hydroxymethyl)cyclopropyl}methoxy}-3-phenyl-7-(1^v-(triisopropylsilyl)-1^vH-pyrrol-3^v-yl)isoindolin-1-one (300)



General procedure O was followed to prepare compounds **300** using isoindolinone **297** (150 mg, 0.267 mmol), 1-(triisopropylsilyl)-1H-pyrrole-3-boronic acid (93 mg, 0.347 mmol), tetrakis(triphenylphosphine)palladium (31 mg, 0.534 mmol), Na₂CO₃ (2 M aq., 0.27 mL, 0.738 mmol) and acetonitrile (3.2 mL). The crude product was purified by MPLC (gradient elution, 0-25% EtOAc/petrol) and the title compound was obtained as a pale yellow solid (111 mg, 59%). R_f 0.48 (25% EtOAc/petrol); no clear m.p. detected; λ_{\max} (EtOH)/nm 277, 339; ν_{\max} /cm⁻¹ (neat) 1696 (vs, C=O), 2866 and 2944 (w, aliphatic CH and -CH₂-, Si-R), 3464 (br, O-H); ¹H NMR (500 MHz; CDCl₃) δ_H 0.49 – 0.68 (4H, m, cyclopropyl), 1.18 (18H, dd, J = 2.2, 7.5 Hz, 6 × CH₃), 1.50 (3H, m, CH(CH₃)₂), 1.87 (3H, d, J = 7.3 Hz, CHCH₃), 2.10 (1H, ABX app. t, $J_{AX} = J_{BX} = 6.0$ Hz, OH), 3.11 (1H, d, $J_{AB} = 9.3$ Hz, CH_AH_BO-), 3.34 (1H, d, $J_{AB} = 9.3$ Hz, CH_AH_BO-), 3.69 (2H, qd, $J_{AX} = J_{BX} = 6.0$ Hz, $J_{AB} = 11.5$ Hz, CH₂OH), 4.36 (1H, q, J = 7.2 Hz, CHCH₃), 6.80 – 6.85 (2H, m, H-4'''' and H-5'''), 6.86 – 6.90 (2H, m, H-Ar), 6.90 – 6.95 (2H, m, H-Ar), 7.05 (4H, br, H-Ar), 7.16 – 7.22 (1H, m, H-Ar), 7.30 (1H, d, J = 8.4 Hz, H-5 or H-6), 7.55 (1H, d, J = 8.4 Hz, H-5 or H-6), 7.77 (1H, app. t, J = 1.8 Hz, H-2'''); ¹³C NMR (125 MHz; CDCl₃) δ_C 8.9 (CH₂ cyclopropyl), 9.1 (CH₂ cyclopropyl), 11.9 (3 × CH(CH₃)₂), 18.11 (6 × CH₃), 19.7 (CHCH₃), 22.7 (C q cyclopropyl), 52.0 (CHCH₃), 68.5 (CH₂O-), 68.7 (CH₂OH), 111.8 (C-4'''' or C-5'''), 121.2 (C-Ar q), 121.7 (C-Ar q), 124.3 (C-4'''' or C-5'''), 127.3 (C-Ar), 127.5 (C-Ar), 127.6 (C-Ar), 128.0 (C-

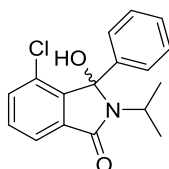
Ar), 128.4 (C-Ar), 129.1 (C-Ar), 129.8 (C-Ar), 132.3 (C-Ar), 133.1 (C-Ar), 137.4 (C-Ar), 140.9 (C-Ar), 166.7 (C-1). Two carbons not detected; LRMS (ES⁺) *m/z* 703.6 and 705.6 [M+H]⁺; HRMS calcd for C₄₀H₄₉³⁵Cl₂N₂O₃Si [M+H]⁺ 703.2884, found 703.2885.

4-Chloro-2-ethyl-3-hydroxy-3-phenylisoindolin-1-one (243)



Compound **243** was prepared according to general procedure M using benzoylbenzoic acid **183** (150 mg, 0.575 mmol), thionyl chloride (0.08 mL, 137 mg, 1.15 mmol), DMF (catalytic, 3 drops), ethylaminee hydrochloride (52 mg, 0.633 mmol), DIPEA (0.22 mL, 164 mg, 1.27 mmol) and THF (2 × 0.7 mL). Purification by MPLC (gradient elution, 0-20% EtOAc/petrol) yielded the title compound as a white solid (89 mg, 54%). *R_f* 0.36 (25% EtOAc/petrol); m.p. 176.1-177.0 °C; λ_{max} (EtOH)/nm 259; ν_{max}/cm⁻¹ (neat) 1667 (s, C=O), 1686 (vs, C=O), 2937 and 2985 (w, aliphatic CH and -CH₂-), 3253 (br, O-H); ¹H NMR (500 MHz; CDCl₃) δ_H 0.90 (3H, t, *J* = 7.2 Hz, CH₂CH₃), 2.93 – 3.06 (1H, m, CH_AH_BCH₃), 3.22 – 3.31 (1 H, m, CH_AH_BCH₃), 7.15 (1H, s, OH), 7.27 – 7.39 (5H, m, H-Ar), 7.53 – 7.60 (2H, m, H-Ar), 7.68 – 7.75 (1H, m, H-Ar); ¹³C NMR (125 MHz; CDCl₃) δ_C 13.8 (CH₃), 33.3 (CH₂), 90.1 (C-3), 121.2 (C-Ar), 126.3 (2 × C-Ar), 128.1 (2 × C-Ar), 128.5 (C-Ar q), 131.4 (C-Ar), 133.2 (C-Ar), 133.9 (C-Ar q), 138.1 (C-Ar q), 144.8 (C-Ar q), 164.7 (C-1). One carbon not detected; LRMS (ES⁺) *m/z* 288.3 [M+H]⁺; HRMS calcd for C₁₆H₁₅³⁵ClNO₂ [M+H]⁺ 288.0786, found 288.0790.

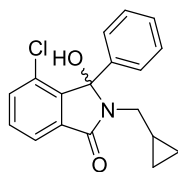
4-Chloro-3-hydroxy-2-isopropyl-3-phenylisoindolin-1-one (245)



General procedure M was followed to prepare isoindolinone **245** using benzoylbenzoic acid **183** (150 mg, 0.575 mmol), thionyl chloride (0.08 mL, 137

mg, 1.15 mmol), DMF (catalytic, 3 drops), isopropylamine (0.05 mL, 37 mg, 0.633 mmol), DIPEA (0.11 mL, 82 mg, 0.633 mmol) and THF (2 × 0.70 mL). Purification by MPLC (gradient elution, 0-25% EtOAc/petrol) yielded the desired compound as a white solid (116 mg, 67%). *R*_f 0.24 (25% EtOAc/petrol); m.p. 219.4-220.4 °C; λ_{max} (EtOH)/nm 259; ν_{max} /cm⁻¹ (neat) 1667 (vs, C=O), 1679 (s, C=O), 2935 and 2980 (w, aliphatic CH and -CH₂-), 3153 (br, O-H); ¹H NMR (500 MHz; CDCl₃) δ_{H} 1.02 (3H, d, *J* = 6.8 Hz, CH₃), 1.36 (3H, d, *J* = 6.8 Hz, CH₃), 3.39 (1H, m, CH(CH₃)₂), 7.16 (1H, s, OH), 7.26 – 7.40 (5H, m, H-Ar), 7.51 – 7.58 (2H, m, H-Ar), 7.67 (1H, dd, *J* = 2.2, 6.2 Hz, H-Ar); ¹³C NMR (125 MHz; CDCl₃) δ_{C} 19.4 (CH₃), 20.5 (CH₃), 43.5 (CH(CH₃)₂), 90.4 (C-3), 120.9 (C-Ar), 126.5 (2 × C-Ar), 127.9 (2 × C-Ar), 128.0 (C-Ar), 128.4 (C-Ar q), 131.3 (C-Ar), 133.0 (C-Ar), 134.7 (C-Ar q), 137.9 (C-Ar q), 144.5 (C-Ar q), 164.5 (C-1); LRMS (ES⁻) *m/z* 300.2 [M-H]⁻; HRMS calcd for C₁₇H₁₇³⁵ClNO₂ [M+H]⁺ 302.0942, found 302.0946.

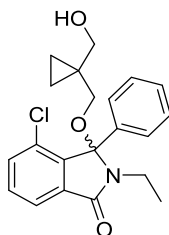
4-Chloro-2-(cyclopropylmethyl)-3-hydroxy-3-phenylisoindolin-1-one (247)



General procedure M was followed to synthesize isoindolinone **247** using benzoylbenzoic acid **183** (150 mg, 0.575 mmol), thionyl chloride (0.08 mL, 137 mg, 1.15 mmol), DMF (catalytic, 3 drops), cyclopropylmethylamine hydrochloride (68 mg, 0.633 mmol), DIPEA (0.22 mL, 164 mg, 1.27 mmol) and THF (2 × 0.70 mL). Purification by MPLC (gradient elution, 0-25% EtOAc/petrol) yielded the desired compound as a white solid (100 mg, 55%). *R*_f 0.33 (25% EtOAc/petrol); m.p. 197.0-198.5 °C; λ_{max} (EtOH)/nm 246; ν_{max} /cm⁻¹ (neat) 1667 and 1686 (s, C=O), 2924, 3232 (br, O-H); ¹H NMR (500 MHz; DMSO-*d*₆) δ_{H} -0.20 – -0.09 (1H, m, cyclopropyl), 0.06 – 0.20 (2H, m, cyclopropyl), 0.20 – 0.27 (1H, m, cyclopropyl), 0.62 – 0.77 (1H, m, CH cyclopropyl), 2.88 (1H, ABX dd, *J*_{AX} = 6.8 Hz, *J*_{AB} = 14.4 Hz, CH_AH_B), 3.05 (1H, ABX dd, *J*_{BX} = 7.3 Hz, *J*_{AB} = 14.4 Hz, CH_AH_B), 7.18 (1H, s, OH), 7.27 – 7.36 (5H, m, H-Ar), 7.54 – 7.59 (2H, m, H-Ar),

7.72 (1H, dd, J 5.2, 3.1, H-Ar); ^{13}C NMR (125 MHz; $\text{DMSO-}d_6$) δ_{C} 3.8 (CH_2 cyclopropyl), 4.4 (CH_2 cyclopropyl), 10.4 (CH cyclopropyl), 43.1 (CH_2), 89.9 (C-3), 121.3 (C-Ar), 126.5 ($2 \times$ C-Ar), 128.0 ($2 \times$ C-Ar), 128.5 (C-Ar), 131.4 (C-Ar), 133.3 (C-Ar), 133.7 (C-Ar q), 138.2 (C-Ar q), 144.8 (C-Ar q), 165.1 (C-1). One quaternary carbon was not observed by NMR; LRMS (ES^+) m/z 312.2 $[\text{M}+\text{H}]^+$; HRMS calcd for $\text{C}_{18}\text{H}_{17}^{35}\text{ClNO}_2$ $[\text{M}+\text{H}]^+$ 314.0942, found 314.0946.

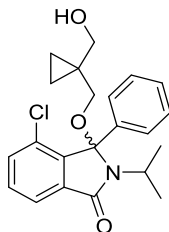
4-Chloro-2-ethyl-3-{[1'''-(hydroxymethyl)cyclopropyl]methoxy}-3-phenylisoindolin-1-one (244)



Compound **244** was obtained following general procedure N using isoindolinone **243** (80 mg, 0.278 mmol), indium tribromide (20 mg, 0.0556 mmol), 1,1-bis(hydroxymethyl)cyclopropane (0.13 mL, 142 mg, 1.39 mmol) and DCE (2.8 mL). Purification by MPLC (gradient elution, 0-33% EtOAc/ petrol) yielded the desired compound as a white solid (79 mg, 76%). R_f 0.09 (petrol/EtOAc 3:1); m.p. 130.0-130.7 °C; λ_{max} (EtOH)/nm 259; $\nu_{\text{max}}/\text{cm}^{-1}$ (neat) 1680 (vs, C=O), 2859 and 2921 (w, aliphatic CH and $-\text{CH}_2-$), 3421 (br, O-H); ^1H NMR (500 MHz; CDCl_3) δ_{H} 0.44 – 0.65 (4H, m, cyclopropyl), 0.95 (3H, t, J = 7.2 Hz, CH_2CH_3), 1.98 (1H, ABX app. t, $J_{\text{AX}} = J_{\text{BX}} = 6.0$ Hz, OH), 3.00 (1H, d, $J_{\text{AB}} = 9.1$ Hz, $\text{CH}_\text{A}\text{H}_\text{BO}-$), 3.12 (1H, d, $J_{\text{AB}} = 9.1$ Hz, $\text{CH}_\text{AH}_\text{BO}-$), 3.26 (2H, m, CH_2CH_3), 3.61 – 3.70 (2H, ABX m, CH_2OH), 7.30 – 7.35 (3H, m, H-Ar), 7.37 (2H, br, H-Ar), 7.43 (1H, dd, J = 1.1, 7.6 Hz, H-5), 7.48 (1H, app. t, J = 7.6 Hz, H-6), 7.81 (1 H, dd, J = 1.1, 7.6, H-7); ^{13}C NMR (125 MHz; CDCl_3) δ_{C} 8.9 (CH_2 cyclopropyl), 9.2 (CH_2 cyclopropyl), 13.5 (CH_2CH_3), 22.5 (C q cyclopropyl), 34.4 (CH_2CH_3), 68.4 ($\text{CH}_2\text{O}-$ and CH_2OH), 94.8 (C-3), 122.0 (C-7), 126.8 ($2 \times$ C-Ar), 128.4 ($2 \times$ C-Ar), 128.8 (C-Ar), 129.8 (C-Ar q), 131.7 (C-6), 133.6 (C-5), 135.0 (C-Ar q), 136.9 (C-Ar q), 141.2 (C-Ar q), 166.6 (C-1); LRMS (ES^+) m/z 394.4 $[\text{M}+\text{Na}]^+$; HRMS calcd for $\text{C}_{21}\text{H}_{23}^{35}\text{ClNO}_3$

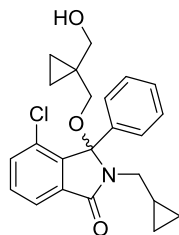
[M+H]⁺ 372.1361, found 372.1362; HPLC 98.5% in 0.1% formic acid (aq)/MeCN (*R*_t 8.0 min); 99.5% in 0.1% ammonia (aq)/MeCN (*R*_t 8.0 min).

4-Chloro-3-([1'''-(hydroxymethyl)cyclopropyl]methoxy)-2-isopropyl-3-phenylisoindolin-1-one (246)



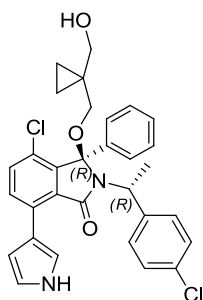
General procedure N was followed to synthesize compound **246** using isoindolinone **245** (110 mg, 0.365 mmol), indium tribromide (26 mg, 0.073 mmol), 1,1-bis(hydroxymethyl)cyclopropane (0.18 mL, 1.83 mmol) and DCE (3.7 mL). Purification by MPLC (gradient elution, 0-20% EtOAc/petrol) yielded the title compound (107 mg, 76%) as a white solid. *R*_f 0.15 (25% EtOAc/petrol); m.p. 128.5-129.2 °C; λ_{max} (EtOH)/nm 259; ν_{max}/cm⁻¹ (neat) 1682 (vs, C=O), 2878 and 2930 (w, aliphatic CH and -CH₂-), 3398 (br, O-H); ¹H NMR (500 MHz; CDCl₃) δ_H 0.48 – 0.64 (4H, m, cyclopropyl), 1.01 (3H, d, *J* = 6.9 Hz, CH₃), 1.48 (3H, d, *J* = 6.9 Hz, CH₃), 2.01 (1H, app. t, *J*_{AX} = *J*_{BX} = 6.0, OH), 3.01 (1H, d, *J*_{AB} = 9.2 Hz, CH_AH_BO-), 3.30 (1H, d, *J*_{AB} = 9.2 Hz, CH_AH_BO-), 3.42 – 3.56 (1H, m, CH(CH₃)₂), 3.66 (2H, d, *J*_{AX} = *J*_{BX} = 6.0, CH₂OH), 7.28 – 7.40 (5H, m, H-Ar), 7.42 (1H, dd, *J* = 1.1, 7.6 Hz, H-5), 7.47 (1H, app. t, *J* = 7.6 Hz, H-6), 7.77 (1H, dd, *J* = 1.1, 7.6 Hz, H-7); ¹³C NMR (125 MHz; CDCl₃) δ_C 8.9 (CH₂ cyclopropyl), 9.0 (CH₂ cyclopropyl), 19.5 (CH₃), 20.4 (CH₃), 22.6 (C q cyclopropyl), 44.7 (CH(CH₃)₂), 68.5 (CH₂O-), 68.6 (CH₂OH), 95.1 (C-3), 121.7 (C-7), 126.9 (2 × C-Ar), 128.3 (2 × C-Ar), 128.7 (C-Ar), 129.7 (C-Ar q), 131.6 (C-6), 133.3 (C-5), 135.8 (C-Ar q), 137.0 (C-Ar q), 140.8 (C-Ar q), 166.2 (C-1); LRMS (ES⁺) *m/z* 408.4 [M+Na]⁺; HRMS calcd for C₂₂H₂₅³⁵ClNO₃ [M+H]⁺ 386.1517, found 386.1519; HPLC 98.8% in 0.1% formic acid (aq)/MeCN (*R*_t 8.4 min); 99.2% in 0.1% ammonia (aq)/MeCN (*R*_t 8.4 min).

4-Chloro-2-(cyclopropylmethyl)-3-{{[1'''-(hydroxymethyl)cyclopropyl]methoxy}-3-phenylisoindolin-1-one (248)}



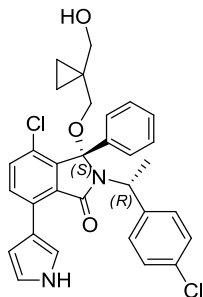
Compound **248** was obtained following general procedure N using isoindolinone **247** (94 mg, 0.300 mmol), indium tribromide (21 mg, 0.060 mmol), 1,1-bis(hydroxymethyl)cyclopropane (0.14 mL, 153 mg, 1.5 mmol), and DCE (3.0 mL). The crude product was purified by MPLC (gradient elution, 0-20% EtOAc/petrol) to afford the title compound as colorless crystals (101 mg, 85%). R_f 0.15 (25% EtOAc/petrol); m.p. 91.1-92.3 °C; λ_{max} (EtOH)/nm 259; ν_{max}/cm^{-1} (neat) 1683 (vs, C=O), 2865 and 2914 (w, aliphatic CH and -CH₂-), 3424 (br, O-H); ¹H NMR (500 MHz; CDCl₃) δ_H -0.09 – -0.00 (1H, m, cyclopropylmethyl), 0.18 – 0.27 (2H, m, cyclopropylmethyl), 0.29 – 0.39 (1H, m, cyclopropylmethyl), 0.43 – 0.64 (4H, m, cyclopropyl), 0.71 – 0.81 (1H, m, CH cyclopropylmethyl), 1.99 (1H, ABX app. t, J = 6.0 Hz, OH), 3.02 (1H, d, J_{AB} = 9.3 Hz, CH_AH_B-O), 3.03 – 3.13 (2H, m, CH₂CH), 3.22 (1H, d, J_{AB} = 9.3 Hz, CH_AH_B-O), 3.64 (2H, ABX m, CH₂OH), 7.32 (3H, m, H-Ar), 7.38 (2H, br, H-Ar), 7.43 (1H, dd, J = 1.1, 7.9 Hz, H-5), 7.48 (1H, dd, J = 7.2, 7.9 Hz, H-6), 7.81 (1H, dd, J = 1.1, 7.2 Hz, H-7); ¹³C NMR (125 MHz; CDCl₃) δ_C 4.5 (CH₂ cyclopropylmethyl), 4.7 (CH₂ cyclopropylmethyl), 8.8 (CH₂ cyclopropyl), 9.1 (CH₂ cyclopropyl), 10.3 (CH cyclopropylmethyl), 22.5 (C q cyclopropyl), 44.2 (CH₂CH), 68.4 (CH₂-O), 68.4 (CH₂OH), 94.3 (C-3), 122.1 (C-7), 127.0 (2 × C-Ar), 128.4 (2 × C-Ar), 128.7 (C-Ar), 129.8 (C-Ar q), 131.6 (C-6), 133.6 (C-5), 134.8 (C-Ar q), 137.0 (C-Ar q), 141.3 (C-9), 166.9 (C-1); LRMS (ES⁺) m/z 420.4 [M+Na]⁺; HRMS calcd for C₂₃H₂₅³⁵ClNO₃ [M+H]⁺ 398.1517, found 398.1520; HPLC 98.8% in 0.1% formic acid (aq)/MeCN (R_t 8.6 min); 99.2% in 0.1% ammonia (aq)/MeCN (R_t 8.5 min).

(3*R*,1'*R*)-4-Chloro-2-[1'-(4''-chlorophenyl)ethyl]-3-{[1'''-(hydroxymethyl)cyclopropyl]methoxy}-3-phenyl-7-(1'*H*-pyrrol-3-yl)isoindolin-1-one (299)



General procedure P was followed to synthesize compound **399** using isoindolinone **289** (101 mg, 0.144 mmol), tetrabutylammonium fluoride 1 M in THF (0.16 mL, 0.158 mmol) and THF (930 mL). The crude product was purified by MPLC (gradient elution, 0-5% MeOH/DCM) to afford the desired product (61 mg, 77%) as a pale yellow solid. R_f 0.67 (6% MeOH/DCM); no clear m.p. detected (dec. 116-162 °C); $[\alpha]_D^{26} +28$ (c 0.611, EtOAc); λ_{max} (EtOH)/nm 275, 339; ν_{max}/cm^{-1} (neat) 1396 (s, C=C and C=N in-plane vibs), 1682 (vs, C=O), 2871, 2928, and 2974 (w, aliphatic CH and -CH₂-), 3345 (br, O-H and N-H); ¹H NMR (500 MHz; CDCl₃) δ_H -0.09 – -0.02 (1H, m, cyclopropyl), 0.15 – 0.20 (1H, m, cyclopropyl), 0.32 – 0.39 (2H, m, cyclopropyl), 1.53 (3H, d, $J = 7.3$ Hz, CH₃), 1.81 – 1.92 (1H, ABX m, -OH), 2.72 (1H, d, $J_{AB} = 9.2$ Hz, CH_AH_BO-), 2.95 (1H, d, $J_{AB} = 9.2$ Hz, CH_AH_BO-), 3.28 – 3.46 (2H, ABX m, CH₂OH), 4.23 (1H, q, $J = 7.3$ Hz, CHCH₃), 6.71 (1H, td, $J = 1.6, 2.7$ Hz, H-4''' or H-5'''), 6.89 (1H, td, $J = 2.0, 2.7$ Hz, H-4''' or H-5'''), 7.22-7.26 (2H, m, H-Ar), 7.31 – 7.42 (6H, m, H-Ar), 7.53 – 7.59 (3H, m, H-Ar), 7.84 (1H, m, H-2'''), 8.45 (1H, br, NH); ¹³C NMR (125 MHz; CDCl₃) δ_C 8.7 (CH₂ cyclopropyl), 8.7 (CH₂ cyclopropyl), 20.1 (CH₃), 22.1 (C q cyclopropyl), 53.4 (CHCH₃), 68.5 (CH₂O-), 68.7 (CH₂OH), 109.7 (C-4''' or C-5'''), 118.2 (C-4''' or C-5'''), 119.2 (C-Ar q), 121.0 (C-2'''), 126.1 (C-Ar q), 128.4 (2 × C-Ar), 128.6 (2 × C-Ar), 128.7 (2 × C-Ar), 129.0 (C-Ar), 129.7 (2 × C-Ar), 132.5 (C-5 or C-6), 133.1 (C-Ar q), 133.5 (C-5 or C-6), 134.4 (C-Ar q), 137.4 (C-Ar q), 141.9 (C-Ar q), 142.0 (C-Ar q), 167.4 (C-1). Two carbons not detected; LRMS (ES⁻) m/z 545.3 [M-H]⁻; HRMS calcd for C₃₁H₂₇Cl₂N₂O₃ [M-H]⁻ 545.1404, found 545.1405; HPLC

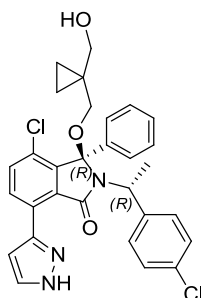
(3*S*,1'*R*)-4-Chloro-2-[1'-(4''-chlorophenyl)ethyl]-3-[[1'''-(hydroxymethyl)cyclopropyl]methoxy]-3-phenyl-7-(1*H*-pyrrol-3-yl)isoindolin-1-one (301)



294

detected; LRMS (ES⁺) m/z 547.4 [M+H]⁺; HRMS calcd for C₃₁H₂₉Cl₂N₂O₃ [M+H]⁺ 547.1550, found 547.1548; HPLC 96.5% in 0.1% formic acid (aq)/MeCN (R_t 9.9 min); 95.0% in 0.1% ammonia (aq)/MeCN (R_t 9.9 min).

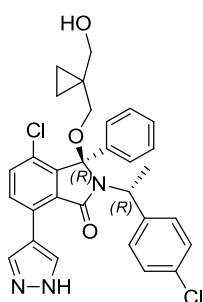
(3*R*,1'*R*)-4-Chloro-2-[1'-(4''-chlorophenyl)ethyl]-3-{[1'''-(hydroxymethyl)cyclopropyl]methoxy}-3-phenyl-7-(1'*H*-pyrazol-3'-yl)isoindolin-1-one (302)



General procedure O was followed to synthesize compound **302** using isoindolinone **289** (80 mg, 0.143), 1*H*-pyrazol-3-yl boronic acid hydrate (24 mg, 0.215 mmol), tetrakis(triphenylphosphine)palladium (17 mg, 0.0143 mmol), Na₂CO₃ (2 M aq., 0.64 mL, 1.29 mmol) and acetonitrile (1.7 mL). The crude product was purified by MPLC (gradient elution, 0-40% EtOAc/petrol) and the title compound was obtained as a white solid (59 mg, 76%). R_f 0.06 (25% EtOAc/petrol); m.p. 201.2-202.4 °C; $[\alpha]_D^{24}$ +30° (c 0.239, EtOAc); λ_{max} (EtOH)/nm 279, 322; ν_{max}/cm^{-1} (neat) 1676 (vs, C=O), 2873, 2927, and 2974 (w, aliphatic CH and -CH₂-), 3335 (br, O-H and N-H); ¹H NMR (500 MHz; CDCl₃) δ_H -0.15 – -0.24 (1H, m, cyclopropyl), 0.03 – -0.05 (1H, m, cyclopropyl), 0.21 – 0.12 (2H, m, cyclopropyl), 1.33 (3H, d, J = 7.2 Hz, CH₃), 1.45 (1H, ABX m, -OH), 2.52 (1H, d, J_{AB} = 9.1 Hz, CH_AH_BO-), 2.71 (1H, d, J_{AB} = 9.1 Hz, CH_AH_B-O), 3.12 (1H, dd, J_{AX} = 4.9 Hz, J_{AB} = 11.5 Hz, CH_AH_BOH), 3.24 (1H, dd, J_{AX} = 6.5 Hz, J_{AB} = 11.5 Hz, CH_AH_BOH), 4.08 (1H, q, J = 7.2 Hz, CHCH₃), 6.59 (1H, d, J = 2.0 Hz, H-4'''), 7.09 – 7.05 (2H, m, H-Ar), 7.17 (5H, br, H-Ar), 7.24 (1H, d, J = 8.5 Hz, H-5 or H-6), 7.37 – 7.32 (2H, m, H-Ar), 7.47 (1H, d, J = 2.0 Hz, H-5'''), 7.66 (1H, d, J = 8.5 Hz, H-5 or H-6), 14.47 (1 H, br, NH); ¹³C NMR (125 MHz; CDCl₃) δ_C 8.6 (CH₂ cyclopropyl), 8.7 (CH₂ cyclopropyl), 19.6 (CH₃), 22.1 (C q cyclopropyl), 53.8 (CHCH₃), 68.3 (CH₂O-), 68.5 (CH₂OH), 95.8 (C-3), 104.6 (C-4'''), 126.7 (C-Ar q), 128.5 (C-Ar),

128.6 (2 × C-Ar), 128.8 (2 × C-Ar), 129.0 (C-Ar), 129.2 (2 × C-Ar), 129.7 (2 × C-Ar), 130.6 (C-5 or C-6), 133.6 (C-Ar q), 134.5 (C-5 or C-6), 136.1 (C-Ar q), 139.4 (C-Ar q), 140.4 (C-Ar q), 140.6 (C-5'''), 142.5 (C-Ar q), 168.2 (C-1). One quaternary carbon not detected; LRMS (ES⁺) *m/z* 548.4 [M+H]⁺; HRMS calcd for C₃₀H₂₈Cl₂N₃O₃ [M+H]⁺ 548.1502, found 548.1500; HPLC 97.5% in 0.1% formic acid (aq.)/MeCN (*R*_t 9.9 min); 94.1% in 0.1% ammonia (aq.)/MeCN (*R*_t 9.9 min).

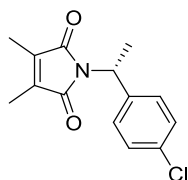
(*R*)-4-Chloro-2-((*R*)-1-(4-chlorophenyl)ethyl)-3-((1-(hydroxymethyl)cyclopropyl)methoxy)-3-phenyl-7-(1H-pyrazol-4-yl)isoindolin-1-one (303)



Compound **303** was obtained following general procedure O using isoindolinone **289** (80 mg, 0.143 mmol), 1*H*-pyrazole-4-boronic acid (24 mg, 0.215 mmol), tetrakis(triphenylphosphine)palladium (17 mg, 0.0143 mmol), Na₂CO₃ (2 M aq., 0.64 mL, 1.29 mmol) and acetonitrile (1.7 mL). The crude product was purified by reverse phase column chromatography (gradient elution, 0-70% acetonitrile/water +0.1% formic acid v/v) and the title compound was obtained as a cream-colored solid (111 mg, 59%). *R*_f 0.18 (33% EtOAc/petrol); 0.54 (MeCN + 0.1% formic acid v/v); m.p. 120.2-121.7 °C; [α]_D²⁴ +42° (*c* 0.228, EtOAc); λ_{max} (EtOH)/nm 267, 319; ν_{max} /cm⁻¹ (neat) 1694 (vs, C=O), 2875, 2935, and 2972 (w, aliphatic CH and -CH₂-), 3198 (br, O-H); ¹H NMR (500 MHz; CDCl₃) δ_{H} -0.04 – 0.04 (1H, m, cyclopropyl), 0.17 – 0.25 (1H, m, cyclopropyl), 0.34 – 0.42 (2H, m, cyclopropyl), 1.55 (3H, d, *J* = 7.3 Hz, CHCH₃), 2.75 (1H, d, *J*_{AB} = 9.1 Hz, CH_AH_BO-), 2.95 (1H, d, *J*_{AB} = 9.1 Hz, CH_AH_BO-), 3.34 (1H, d, *J*_{AB} = 11.5 Hz, CH_AH_BOH), 3.44 (1H, d, *J*_{AB} = 11.5 Hz, CH_AH_BOH), 4.25 (1H, q, *J* = 7.3 Hz, CHCH₃), 7.24 – 7.29 (2H, m, H-Ar), 7.38 (5H, br, H-Ar), 7.41 (1H, d, *J* = 8.3 Hz, H-5 or H-6), 7.51 – 7.56 (2H, m, H-Ar), 7.59 (1H, d, *J* = 8.3 Hz, H-5 or H-6),

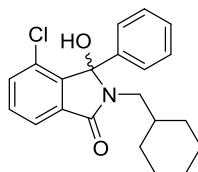
8.36 (2H, br, H-3'''' and H-5'''''); ^{13}C NMR (125 MHz; CDCl_3) δ_{C} 8.6 (CH_2 cyclopropyl), 8.7 (CH_2 cyclopropyl), 19.9 (CH_3), 22.1 (C q cyclopropyl), 53.4 (CHCH_3), 68.4 ($\text{CH}_2\text{O-}$), 68.5 (CH_2OH), 95.0 (C-3), 127.4 ($2 \times \text{C-Ar}$), 128.5 ($2 \times \text{C-Ar}$), 128.7 ($2 \times \text{C-Ar}$), 128.9 (C-Ar), 129.4 (C-Ar q), 129.6 ($2 \times \text{C-Ar}$), 132.0 (C-5 or C-6), 133.3 (C-Ar q), 133.8 (C-5 or C-6), 137.0 (C-Ar q), 141.5 (C-Ar q), 142.3 (C-Ar q), 167.1 (C-1). Four carbons not visible; LRMS (ES^+) m/z 548.5 $[\text{M}+\text{H}]^+$; HRMS calcd for $\text{C}_{30}\text{H}_{26}\text{Cl}_2\text{N}_3\text{O}_3$ $[\text{M}-\text{H}]^-$ 546.1357, found 546.1357; HPLC 94.8% in 0.1% formic acid (aq.)/MeCN (R_t 9.1 min); 94.8% in 0.1% ammonia (aq.)/MeCN (R_t 9.1 min).

(*R*)-1-(1-(4-Chlorophenyl)ethyl)-3,4-dimethyl-1H-pyrrole-2,5-dione
(226)



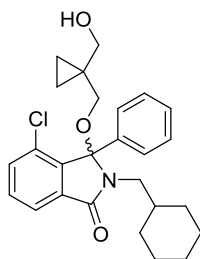
General procedure Q was used to synthesize compound **226** using 2,3-dimaleic anhydride (250 mg, 1.98 mmol), (*R*)-4-chloro- α -methylbenzylamine (308 mg, 1.98 mmol, 0.28 mL) and THF (1.0 mL). The reaction mixture was refluxed for 34 h. Medium pressure liquid chromatography (gradient elution, 0-20% EtOAc/petrol) afforded the desired compound as a colorless oil (311 mg, 59%). R_f 0.67 (25% EtOAc/petrol); λ_{max} (EtOH)/nm 247sh; $\nu_{\text{max}}/\text{cm}^{-1}$ (neat) 1696 (vs, C=O); ^1H NMR (500 MHz; CDCl_3) δ_{H} 1.78 (3H, d, $J = 7.3$ Hz, CHCH_3), 1.92 (6H, s, CH_3), 5.29 (1H, q, $J = 7.3$ Hz, CHCH_3), 7.24 – 7.30 (2H, m, H-Ar), 7.34 – 7.39 (2H, m, H-Ar); ^{13}C NMR (125 MHz; CDCl_3) δ_{C} 8.8 ($2 \times \text{CH}_3$), 17.8 (CHCH_3), 49.0 (CHCH_3), 128.7 ($2 \times \text{C-Ar}$), 128.9 ($2 \times \text{C-Ar}$), 133.5 (C-Ar q), 137.2 ($2 \times =\text{C-CH}_3$), 139.3 (C-Ar q), 172.0 ($2 \times \text{C=O}$).

4-Chloro-2-(cyclohexylmethyl)-3-hydroxy-3-phenylisoindolin-1-one (249)



General procedure M was followed to synthesize isoindolinone **249** using benzoylbenzoic acid **183** (85 mg, 0.326 mmol), thionyl chloride (0.05 mL, 78 mg, 0.652 mmol), catalytic DMF (3 drops), (aminomethyl)cyclohexane (0.05 mL, 41 mg, 0.359 mmol), DIPEA (0.06 mL, 46 mg, 0.359 mmol) and THF (2 × 0.4 mL). The crude product was purified by MPLC (gradient elution, 0-25% EtOAc/petrol) to obtain the racemic **249** as an off-white solid (89 mg, 77%). R_f 0.50 (33% EtOAc/petrol); m.p. 171.9-172.5 °C; λ_{\max} (EtOH)/nm 259; $\nu_{\max}/\text{cm}^{-1}$ (neat) 1673 (vs, C=O), 2848 and 2919 (w, aliphatic CH and -CH₂-), 3330 (br, O-H); ¹H NMR (500 MHz; DMSO-*d*₆) δ_H 0.65 – 1.09 (5H, m, H^{ax}), 1.15 – 1.30 (1H, m, CH-CH₂N), 1.43 – 1.62 (5H, m, H^{eq}), 2.72 (1H, ABX dd, J_{AB} = 13.8 Hz, J_{AX} = 7.8 Hz, CH_AH_B-cyclohexyl), 3.12 (1H, ABX dd, J_{AB} = 13.8 Hz, J_{AX} = 7.2 Hz, CH_AH_B-N), 7.15 (1H, s, OH), 7.24 – 7.37 (5H, m, H-Ar), 7.53 – 7.60 (2H, m, H-Ar), 7.71 (1H, m, H-Ar); ¹³C NMR (125 MHz; CDCl₃) δ_C (126 MHz, DMSO) 25.3 (CH₂), 25.4 (CH₂), 25.9 (CH₂), 30.5 (CH₂), 30.6 (CH₂), 36.2 (CHCH₂N), 44.7 (CH₂N), 90.2 (C-3), 121.3 (C-Ar), 126.2 (3 × C-Ar), 128.1 (2 × C-Ar), 128.5 (C-Ar q), 131.4 (C-Ar), 133.2 (C-Ar), 133.7 (C-Ar q), 138.3 (C-Ar q), 144.7 (C-Ar q), 165.4 (C-1); LRMS (ES⁻) m/z 354.4 [M-H]⁻; HRMS calcd for C₂₁H₂₁ClNO₂ [M-H]⁻ 354.1266, found 354.1252.

4-Chloro-2-(cyclohexylmethyl)-3-[[1'''-(hydroxymethyl)cyclopropyl]methoxy]-3-phenylisoindolin-1-one (250)



The desired compound **250** was obtained following a modified general procedure N and using isoindolinone **249** (80 mg, 0.225 mmol), InBr₃ (160 mg, 0.450 mmol, 2.0 equiv.), 1,1-bis(hydroxymethyl)cyclopropane (0.11 mL, 115 mg, 1.125 mmol), and DCE (2.25 mL). Purification by MPLC (gradient elution, 0-25% EtOAc/petrol) yielded the racemic isoindolinone **250** as a white amorphous solid (68 mg, 69%). *R*_f 0.31 (33% EtOAc/petrol); no clear m.p. detected; λ_{max} (EtOH)/nm 259; ν_{max}/cm⁻¹ (neat) 1686 (vs, C=O), 2849 and 2920 (m, aliphatic CH and -CH₂-), 3419 (br, OH); ¹H NMR (500 MHz; CDCl₃) δ_H 0.39 – 0.68 (4H, m, cyclopropyl), 0.73 – 1.13 (6H, m, CH^{ax}), 1.40 – 1.69 (5H, m, CH^{eq}), 2.01 (1H, app. t, *J*_{AX} = *J*_{BX} = 6.0 Hz, OH), 2.94 – 3.10 (4H, m, CH₂-N and CH₂O-), 3.57 – 3.72 (2H, m, CH₂OH), 7.32 (5H, br, H-Ar), 7.44 (dd, *J* = 1.2, 7.6 Hz, 1H, H-5), 7.48 (1H, app. t, *J* = 7.6 Hz, H-6), 7.80 (1H, dd, *J* = 1.2, 7.6 Hz, H-7); ¹³C NMR (125 MHz; CDCl₃) δ_C 8.8 (CH₂ cyclopropyl), 9.3 (CH₂ cyclopropyl), 22.5 (C q cyclopropyl), 25.8 (CH₂ cyclohexyl), 25.9 (CH₂ cyclohexyl), 26.4 (CH₂ cyclohexyl), 31.2 (CH₂ cyclohexyl), 31.5 (CH₂ cyclohexyl), 37.0 (CH-CH₂N), 45.6 (CH₂-C₆H₁₁), 68.5 (CH₂OH), 68.5 (CH₂O-), 95.0 (C-3), 122.1 (C-7), 126.6 (C-Ar), 128.4 (C-Ar), 128.8 (C-Ar), 129.8 (C-Ar q), 131.7 (C-6), 133.6 (C-5), 135.0 (C-Ar q), 137.4 (C-Ar q), 141.1 (C-Ar q), 167.2 (C-1); LRMS (ES⁺) *m/z* 462.5 [M+Na]⁺; HRMS calcd for C₂₆H₃₁ClNO₃ [M+H]⁺ 440.1987, found 440.1983; HPLC 99.0% in 0.1% formic acid (aq.)/MeCN (*R*_t 9.8 min); 99.3% in 0.1% ammonia (aq.)/MeCN (*R*_t 9.8 min).

(3*R*,1'*R*)-4-Chloro-2-[1'-(4''-chlorophenyl)ethyl]-3-methoxy-3-phenylisoindolin-1-one (233) and (3*S*,1'*R*)-4-Chloro-2-[1'-(4''-chlorophenyl)ethyl]-3-methoxy-3-phenylisoindolin-1-one (234)



Compounds **233** and **234** were obtained according to a modified general procedure N using isoindolinone **198** (98 mg, 0.246 mmol), InBr₃ (174 mg, 0.492 mmol), methanol (0.05 mL, 39 mg, 1.225 mmol) and DCE (2.5 mL). The reaction mixture was heated at 80 °C for 1 h. Purification by MPLC (gradient elution, 0-4% EtOAc/petrol) yielded isoindolinones **233** (40 mg, 39%; colorless oil) and **234** (33 mg, 33%; colorless oil).

233

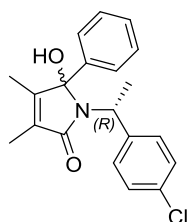
*R*_f 0.70 (25% EtOAc/petrol); [α]_D²⁴ +175° (*c* 0.410, EtOAc); λ_{max} (EtOH)/nm 259; ν_{max} /cm⁻¹ (neat) 1699 (vs, C=O), 2832, 2933, and 2973 (w, aliphatic CH and -CH₂-). ¹H NMR (500 MHz; CDCl₃) δ_{H} 1.61 (3H, d, *J* = 7.3 Hz, CHCH₃), 2.65 (3H, s, OCH₃), 4.22 (1H, q, *J* = 7.3 Hz, CHCH₃), 7.27 (2H, m, H-Ar), 7.32 – 7.38 (5H, m, H-Ar), 7.39 (1H, dd, *J* = 1.1, 7.7 Hz, H-5), 7.45 (1H, app. t, *J* = 7.7 Hz, H-6), 7.57 – 7.63 (2H, m, H-Ar), 7.77 (1H, dd, *J* = 1.1, 7.7 Hz, H-7); ¹³C NMR (125 MHz; CDCl₃) δ_{C} 18.7 (CHCH₃), 51.2 (OCH₃), 52.8 (CHCH₃), 96.7 (C-3), 121.8 (C-7), 127.3 (2 × C-Ar), 128.3 (2 × C-Ar), 128.5 (2 × C-Ar), 128.8 (C-Ar), 129.9 (C-Ar q), 130.0 (2 × C-Ar), 131.5 (C-6), 133.3 (C-Ar q), 133.5 (C-5), 135.5 (C-Ar q), 136.8 (C-Ar q), 140.5 (C-Ar q), 140.6 (C-Ar q), 166.8 (C-1); LRMS (ES⁺) *m/z* 412.4 [M+H]⁺; HRMS calcd for C₂₃H₂₀Cl₂NO₂ [M+H]⁺ 412.0866, found 412.0858; HPLC 99.6% in 0.1% formic acid (aq.)/MeCN (*R*_t 10.6 min); 99.6% in 0.1% ammonia (aq.)/MeCN (*R*_t 10.7 min).

234

*R*_f 0.62 (25% EtOAc/petrol); [α]_D²⁴ +71° (*c* 0.380, EtOAc); λ_{max} (EtOH)/nm 259sh; ν_{max} /cm⁻¹ (neat) 1699 (vs, C=O), 2831, 2933, and 2970 (w, aliphatic CH

and -CH₂-); ¹H NMR (500 MHz; CDCl₃) δ_H 1.84 (3H, d, *J* = 7.3 Hz, CHCH₃), 3.13 (3H, s, OCH₃), 4.45 (1H, q, *J* = 7.3 Hz, CHCH₃), 6.86 – 6.93 (2H, m, H-Ar), 6.94 – 7.01 (2H, m, H-Ar), 7.14 (4H, br, H-Ar), 7.19 – 7.25 (1H, m, H-Ar), 7.41 (1H, dd, *J* = 1.1, 7.6 Hz, H-5), 7.46 (1H, app. t, *J* = 7.6, H-6), 7.77 (1H, dd, *J* = 1.1, 7.3 Hz, H-7); ¹³C NMR (125 MHz; CDCl₃) δ_C 19.1 (CHCH₃), 51.2 (OCH₃), 51.6 (CHCH₃), 96.0 (C-3), 121.8 (C-7), 127.3 (2 × C-Ar), 127.8 (2 × C-Ar), 128.0 (2 × C-Ar), 128.6 (C-Ar), 129.6 (2 × C-Ar), 130.0 (C-Ar q), 131.6 (C-6), 132.7 (C-Ar q), 133.5 (C-5), 135.6 (C-Ar q), 136.6 (C-Ar q), 140.3 (C-Ar q), 140.5 (C-Ar q), 166.6 (C-1); LRMS (ES⁺) *m/z* 412.4 [M+H]⁺; HRMS calcd for C₂₃H₂₀Cl₂NO₂ [M+H]⁺ 412.0866, found 412.0856; HPLC 98.7% in 0.1% formic acid (aq.)/MeCN (*R*_t 10.4 min); 97.6% in 0.1% ammonia (aq.)/MeCN (*R*_t 10.5 min).

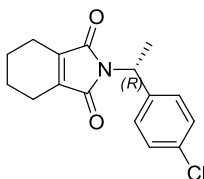
(1'*R*)-1-[1'-(4''-Chlorophenyl)ethyl]-5-hydroxy-3,4-dimethyl-5-phenyl-1*H*-pyrrol-2(5*H*)-one (227)



General procedure R was followed to prepare **227** using the imide **226** (114 mg, 0.432 mmol), phenylmagnesium bromide (1.0 M in THF, 1.30 mL, 1.30 mmol), and THF (0.9 mL). Purification by MPLC (gradient elution 0-26% EtOAc/petrol) yielded the desired product **227** (white solid; 80 mg, 54%) as a mixture of diastereoisomers. *R*_{f(1)} = 0.49 and *R*_{f(2)} = 0.23 (petrol/EtOAc 3:1; UV₂₅₄ nm, and KMnO₄); no clear m.p. detected; λ_{max} (EtOH)/nm 253; ν_{max}/cm⁻¹ (neat) 1655 (vs, C=O), 2581, 2919 and 2981 (w, aliphatic CH and -CH₂-), 3189 (br, O-H); ¹H NMR (500 MHz; CDCl₃) δ_H 1.57 – 1.61 (6H, m, CHCH₃ and CH₃-C=), 1.61 – 1.63 (3H, m, CH₃=), 1.64 (3H, d, *J* = 7.3 Hz, CHCH₃), 1.83 (3H, m, CH₃-C=), 1.83 – 1.86 (3H, m, CH₃), 1.87 (1H, s, OH), 2.02 – 2.07 (1H, m, OH), 4.33 (1H, q, *J* = 7.3 Hz, CHCH₃), 4.61 (1H, q, *J* = 7.3, CHCH₃), 6.95 – 7.01 (2H, m, H-Ar), 7.02 – 7.08 (2H, m, H-Ar), 7.18 – 7.25 (7H, m, H-Ar), 7.28 – 7.44 (5H, m, H-Ar), 7.44 – 7.49 (2H, m, H-Ar). ¹³C NMR (125 MHz; CDCl₃) δ_C 8.5 (CH₃-C=), 10.0 (CH₃-C=),

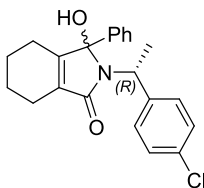
18.7 (CHCH₃), 19.8 (CHCH₃), 51.4 (CHCH₃), 52.2 (CHCH₃), 93.5 (C-3), 126.3 (C-Ar), 126.5 (C-Ar), 128.0 (C-Ar), 128.4 (C-Ar), 128.5 (C-Ar), 128.6 (C-Ar), 128.7 (C-Ar), 129.2 (C-Ar), 129.3 (C-Ar), 129.5 (C-Ar), 136.9 (C-Ar), 137.0 (C-Ar), 140.8 (C-Ar), 141.9 (C-Ar), 151.7 (C-Ar), 151.8 (C-Ar), 171.1 (C-3), 171.2 (C-3); LRMS (ES⁻) *m/z* 340.3 [M-H]⁻; HRMS calcd for C₂₀H₁₉³⁵ClNO₂ [M-H]⁻ 340.1110, found 340.1098.

(1'*R*)-2-[1'-(4''-Chlorophenyl)ethyl]-4,5,6,7-tetrahydro-1*H*-isoindole-1,3(2*H*)-dione (230)



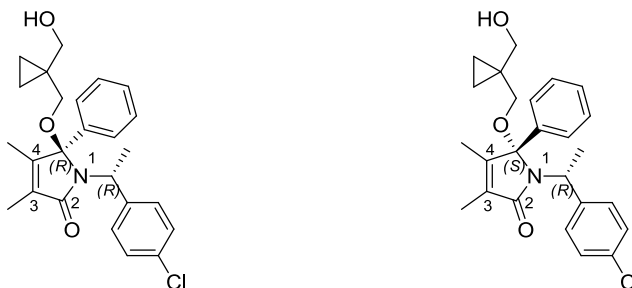
The imide **230** was obtained following general procedure Q using 3,4,5,6-tetrahydrophthalic anhydride (250 mg, 1.64 mmol), (*R*)-4-chloro- α -methylbenzylamine (0.23 mL, 255 mg, 1.64 mmol) and THF (0.8 mL). Purification by MPLC (gradient elution, 0-10% EtOAc/petrol) yielded the desired compound **230** (341 mg, 72%) as a pale yellow oil. *R_f* 0.76 (25% EtOAc/petrol); λ_{max} (EtOH)/nm 277sh; ν_{max} /cm⁻¹ (neat) 1697 (vs, C=O), 2936 (w, aliphatic CH and -CH₂-); ¹H NMR (500 MHz; CDCl₃) δ_{H} 1.76 (4H, m, 2 \times CH₂), 1.81 (3H, d, *J* = 7.3 Hz, CHCH₃), 2.31 (4H, m, 2 \times CH₂), 5.31 (1 H, q, *J* = 7.3 Hz, CHCH₃), 7.29 – 7.33 (2H, m, H-Ar), 7.37 – 7.42 (2H, m, H-Ar); ¹³C NMR (125 MHz; CDCl₃) δ_{C} 17.7 (CHCH₃), 19.9 (2 \times CH₂), 21.3 (2 \times CH₂), 48.6 (CHCH₃), 128.6 (2 \times C-Ar), 128.8 (2 \times C-Ar), 133.3 (C-Ar q), 139.3 (C-Ar q), 141.5 (2 \times CH₂C=), 170.9 (2 \times C=O).

(1'*R*)-2-[1-(4-Chlorophenyl)ethyl]-3-hydroxy-3-phenyl-2,3,4,5,6,7-hexahydro-1*H*-isoindol-1-one (231)



General procedure R was followed to synthesize **231** using the imide **230** (325 mg, 1.12 mmol), phenylmagnesium bromide 1.0 M in THF (3.4 mL, 3.36 mmol), and THF 2.2 mL). The crude product was purified by MPLC (gradient elution, 0-25% EtOAc/petrol) to afford the title compound (293 mg, 71%; white amorphous solid) as a mixture of diastereoisomers. $R_{f(1)} = 0.49$ and $R_{f(2)} = 0.23$ (25% EtOAc/petrol); no clear m.p. detected; λ_{max} (EtOH)/nm 253; ν_{max} /cm⁻¹ (neat) 1653 (vs, C=O), 2857 and 2931 (w, aliphatic CH and -CH₂-), 3230 (br, O-H); ¹H NMR (500 MHz; CDCl₃) δ_{H} 1.49 – 1.84 (16H, m, 2 × CH₃ and 5 × CH₂, 2 × OH), 2.09 – 2.14 (4H, m, 2 × CH₂), 2.14 – 2.38 (4H, m, 2 × CH₂), 4.38 (1H, q, $J = 7.3$ Hz, CHCH₃), 4.64 (1H, q, $J = 7.3$ Hz, CHCH₃), 6.99 – 7.04 (1H, m, H-Ar), 7.06 – 7.10 (1H, m, H-Ar), 7.22 – 7.26 (2H, m, H-Ar), 7.26 – 7.28 (2H, m, H-Ar), 7.35 – 7.47 (5H, m, H-Ar), 7.47 – 7.52 (2H, m, H-Ar); ¹³C NMR (125 MHz; CDCl₃) δ_{C} 18.8 (CHCH₃), 19.9 (CHCH₃), 19.9 (CH₂), 20.7 (CH₂), 22.0, 22.0 (CH₂), 22.1 (CH₂), 51.2 (CHCH₃), 51.9 (CHCH₃), 126.2 (C-Ar), 126.4 (C-Ar), 128.0 (C-Ar), 128.4 (C-Ar), 128.5 (C-Ar), 128.6 (C-Ar), 128.7 (C-Ar), 129.4 (C-Ar), 129.5 (C-Ar), 132.3 (C-Ar), 132.9 (C-Ar), 137.0 (C-Ar), 142.0 (C-Ar), 155.8 (C-Ar), 155.9 (C-Ar), 170.6 (C-Ar q); LRMS (ES⁻) m/z 366.3 [M-H]⁻; HRMS calcd for C₂₂H₂₁³⁵ClNO₂ [M-H]⁻ 366.1266, found 366.1255.

(3*R*,1'*R*)-1-[1'-(4''-Chlorophenyl)ethyl]-5-{{[1''''-(hydroxymethyl)cyclopropyl]methoxy}-3,4-dimethyl-5-phenyl-1*H*-pyrrol-2(5*H*)-one (223) and (3*S*,1'*R*)-1-[1'-(4''-Chlorophenyl)ethyl]-5-{{[1''''-(hydroxymethyl)cyclopropyl]methoxy}-3,4-dimethyl-5-phenyl-1*H*-pyrrol-2(5*H*)-one (224)



A modified general procedure N was used to synthesize compounds **223** and **224** using isoindolinone **227** (75 mg, 0.219 mmol), indium tribromide (155 mg, 0.438 mmol), 1,1-bis(hydroxymethyl)cyclopropane (0.11 mL, 112 mg, 1.095 mmol) and DCE (2.2 mL). Purification by MPLC (gradient elution, 0-26% EtOAc/petrol) yielded the desired isoindolinones **223** (35 mg, 38%; white amorphous solid) and **224** (28 mg, 30%; white solid).

223

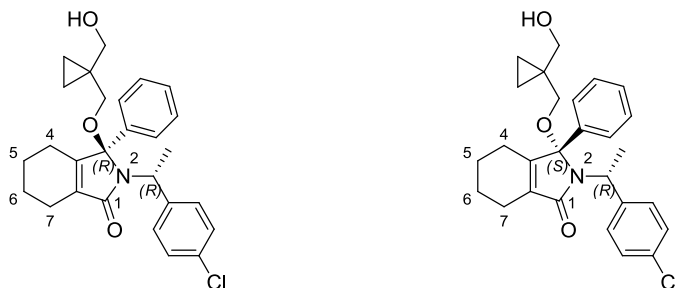
R_f 0.26 (25% EtOAc/petrol); no clear m.p. detected; $[\alpha]_D^{26} +108^\circ$ (c 0.434, EtOAc); λ_{max} (EtOH)/nm 258sh; ν_{max}/cm^{-1} (neat) 1673 and 1687 (vs, C=O), 2873, 2920, and 2973 (w, aliphatic CH and -CH₂-), 3407 (br, O-H) cm^{-1} ; ¹H NMR (500 MHz; CDCl₃) δ_H 0.03 – 0.21 (2H, m, cyclopropyl), 0.33 – 0.45 (2H, m, cyclopropyl), 1.51 – 1.59 (6H, m, =C-CH₃ and CHCH₃), 1.65 (1H, ABX m, OH), 1.89 (3H, m, =C-CH₃), 2.58 (1H, d, $J_{AB} = 9.5$ Hz, CH_AH_BO-), 2.99 (1H, d, $J_{AB} = 9.5$ Hz, CH_AH_BO-), 3.24 (1H, ABX dd, $J_{AX} = 4.0$ Hz, $J_{AB} = 11.2$ Hz, CH_AH_BOH), 3.48 (1H, ABX dd, $J_{BX} = 5.8$ Hz, $J_{AB} = 11.2$ Hz, CH_AH_BOH), 4.07 (1H, q, $J = 7.3$ Hz, CHCH₃), 7.19 – 7.25 (2H, m, H-Ar), 7.38 (5H, m, H-Ar), 7.44 – 7.51 (2H, m, H-Ar); ¹³C NMR (125 MHz; CDCl₃) δ_C 8.6 (CH₃), 8.7 (CH₂ cyclopropyl), 8.8 (CH₂ cyclopropyl), 10.3 (CH₃), 20.1 (CHCH₃), 22.2 (C q cyclopropyl), 53.4 (CHCH₃), 67.6 (CH₂O-), 68.6 (CH₂OH), 97.5 (C-3), 126.4 (2 × C-Ar), 128.6 (2 × C-Ar), 128.7 and 128.8 (3 × C-Ar), 129.4 (2 × C-Ar), 131.2 (C-3 or C-4), 133.0 (C-Ar q), 137.3 (C-Ar q),

142.4 (C-Ar q), 149.3 (C-3 or C-4), 172.0 (C-1); LRMS (ES⁺) *m/z* 448.5 [M +Na]⁺; HRMS calcd for C₂₅H₂₉³⁵ClNO₃ [M+H]⁺ 426.1830, found 426.1823; HPLC 94.1% in 0.1% formic acid (aq.)/MeCN (*R*_t 9.3 min); 95.0% in 0.1% ammonia (aq.)/MeCN (*R*_t 9.3 min).

224

*R*_f 0.16 (25% EtOAc/petrol); m.p. 131.6-133.0 °C; [α]_D²⁶ +10° (*c* 0.406, EtOAc); λ_{max} (EtOH)/nm 252sh; ν_{max} /cm⁻¹ (neat) 1671 (vs, C=O), 2874 and 2921 (w, aliphatic CH and -CH₂-), 3396 (m, O-H) cm⁻¹; ¹H NMR (500 MHz; CDCl₃) δ_{H} 0.48 – 0.69 (4H, m, cyclopropyl), 1.48 (3H, m, =C-CH₃), 1.78 (3H, d, *J* = 7.3 Hz, CHCH₃), 1.84 (1H, ABX m, OH), 1.86 – 1.93 (3H, m, =C-CH₃), 3.20 (1H, d, *J*_{AB} = 9.5 Hz, CH_AH_BO-), 3.30 (1H, d, *J*_{AB} = 9.5 Hz, CH_AH_BO-), 3.62 (1H, dd, *J*_{AX} = 5.0 Hz, *J*_{AB} = 11.3 Hz, CH_AH_BOH), 3.72 (1H, dd, *J*_{BX} = 5.5 Hz, *J*_{AB} = 11.3 Hz, CH_AH_BOH), 4.20 (1H, q, *J* = 7.3 Hz, CHCH₃), 6.86 – 6.92 (2H, m, H-Ar), 6.92 – 6.98 (2H, m, H-Ar), 7.09 (4H, br, H-Ar), 7.16 (1H, m, H-Ar); ¹³C NMR (125 MHz; CDCl₃) δ_{C} 8.5 (CH₃), 9.0 (CH₂ cyclopropyl), 9.1 (CH₂ cyclopropyl), 10.4 (CH₃), 20.1 (CHCH₃), 22.7 (C q cyclopropyl), 52.2 (CHCH₃), 67.4 (CH₂O-), 68.4 (CH₂OH), 96.1 (C-3), 126.5 (2 × C-Ar), 127.8 (2 × C-Ar), 128.2 (2 × C-Ar), 128.4 (C-Ar), 129.3 (2 × C-Ar), 131.5 (C-3 or C-4), 132.4 (C-Ar q), 136.7 (C-Ar q), 141.6 (C-Ar q), 148.8 (C-3 or C-4), 171.6 (C-1); LRMS (ES⁺) *m/z* 448.5 [M +Na]⁺; HRMS calcd for C₂₅H₂₉³⁵ClNO₃ [M+H]⁺ 426.1830, found 426.1821; HPLC 96.6% in 0.1% formic acid (aq.)/MeCN (*R*_t 9.3 min); 97.8% in 0.1% ammonia (aq.)/MeCN (*R*_t 9.3 min).

(3*R*,1'*R*)-2-[1'-(4''-Chlorophenyl)ethyl]-3-{{[1'''-(hydroxymethyl)cyclopropyl]methoxy}-3-phenyl-2,3,4,5,6,7-hexahydro-1*H*-isoindol-1-one (224) and (3*S*,1'*R*)-2-[1'-(4''-chlorophenyl)ethyl]-3-{{[1'''-(hydroxymethyl)cyclopropyl]methoxy}-3-phenyl-2,3,4,5,6,7-hexahydro-1*H*-isoindol-1-one (232)



A modified general procedure N was used to synthesize compounds **224** and **232** using isoindolinone **230** (108 mg, 0.294 mmol), indium tribromide (208 mg, 0.588 mmol), 1,1-bis(hydroxymethyl)cyclopropane (0.14 mL, 150 mg, 1.47 mmol) and DCE (2.9 mL). Purification by MPLC (gradient elution, 0-10% EtOAc/petrol) yielded the desired isoindolinones **224** (37 mg, 28%; colorless oil, solidified to a white solid) and **232** (18 mg, 14%; white amorphous solid).

224

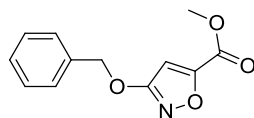
R_f 0.22 (25% EtOAc/petrol); m.p. 141.3-142.9 °C; $[\alpha]_D^{26} +86^\circ$ (c 0.454, EtOAc); λ_{max} (EtOH)/nm 252sh; ν_{max}/cm^{-1} (neat) 1669 (vs, C=O), 2883, 2942, and 2986 (w, aliphatic CH and -CH₂-), 3499 (m, O-H); ¹H NMR (500 MHz; CDCl₃) δ_H -0.04 – 0.07 (2H, m, cyclopropyl), 0.24 – 0.33 (2H, m, cyclopropyl), 1.45 (3H, d, $J = 7.3$ Hz, CH₃), 1.48 – 1.68 (6H, m, 5 × alkyl protons and OH), 1.81 – 1.92 (1H, m, alkyl proton), 2.12 – 2.30 (2H, m, alkyl protons), 2.48 (1H, d, $J_{AB} = 9.5$ Hz, CH_AH_BO-), 2.98 (1H, d, $J_{AB} = 9.5$ Hz, CH_AH_BO-), 3.15 (1H, ABX dd, $J_{AX} = 4.5$ Hz, $J_{AB} = 11.3$ Hz, CH_AH_BOH), 3.38 (1H, ABX dd, $J_{AX} = 6.5$ Hz, $J_{AB} = 11.3$ Hz, CH_AH_BOH), 3.99 (1H, q, $J = 7.3$ Hz, CHCH₃), 7.10 – 7.15 (2H, m, H-Ar), 7.22 – 7.33 (5H, m, H-Ar), 7.35 – 7.40 (2H, m, H-Ar); ¹³C NMR (125 MHz; CDCl₃) δ_C 8.7 (CH₂ cyclopropyl), 8.8 (CH₂ cyclopropyl), 20.1 (CH₃), 20.2 (CH₂), 21.3 (CH₂), 21.9 (CH₂), 22.0 (CH₂), 22.2 (C q cyclopropyl), 53.2 (CHCH₃), 67.8 (CH₂O-), 68.6 (CH₂OH), 97.1 (C-3), 126.3 (2 × C-Ar), 128.5 (2 × C-Ar), 128.7 and 128.8 (3 × C-Ar), 129.5 (2 × C-Ar), 133.0 (C-Ar)

q), 134.6 (C-5 or C-6), 137.3 (C-Ar q), 142.5 (C-Ar q), 153.4 (C-5 or C-6), 171.4 (C-1); LRMS (ES⁺) m/z 474.4 [M + Na]⁺; HRMS calcd for C₂₇H₃₁³⁵ClNO₃ [M+H]⁺ 452.1987, found 452.1976; HPLC 95.6% in 0.1% formic acid (aq.)/MeCN (R_t 9.7 min); 96.1% in 0.1% ammonia (aq.)/MeCN (R_t 9.7 min).

232

R_f 0.11 (25% EtOAc/petrol); no clear m.p. detected; $[\alpha]_D^{26} +16^\circ$ (c 0.205, EtOAc); λ_{max} (EtOH)/nm 252sh; ν_{max}/cm^{-1} (neat) 1669 and 1686 (vs, C=O), 2860 and 2928 (w, aliphatic CH and -CH₂-), 3383 (br, O-H); ¹H NMR (500 MHz; CDCl₃) δ_H 0.46 – 0.70 (4H, m, cyclopropyl), 1.57 – 1.76 (5H, m, 2 × CH₂ and -OH), 1.77 (3H, d, J = 7.3 Hz, CH₃), 1.82 – 2.04 (2H, m, CH₂), 2.25 – 2.35 (2H, m, CH₂), 3.22 – 3.36 (2H, AB q, J_{AB} = 9.5 Hz, CH₂O-), 3.61 (1H, d, J_{AB} = 11.3 Hz, CH_AH_BOH), 3.72 (1H, d, J_{AB} = 11.3 Hz, CH_AH_BOH), 4.22 (1H, q, J = 7.3 Hz, CHCH₃), 6.86 – 6.92 (2H, m, H-Ar), 6.92 – 6.98 (2H, m, H-Ar), 7.00 – 7.14 (4H, m, H-Ar), 7.14 – 7.20 (1H, m, H-Ar); ¹³C NMR (125 MHz; CDCl₃) δ_C 9.0 (CH₂ cyclopropyl), 9.1 (CH₂ cyclopropyl), 20.0 (CH₂), 20.1 (CH₃), 21.4 (CH₂), 21.9 (CH₂), 22.0 (CH₂), 22.7 (C q cyclopropyl), 51.9 (CHCH₃), 67.7 (CH₂O-), 68.5 (CH₂OH), 95.8 (C-3), 126.5 (2 × C-Ar), 127.8 (2 × C-Ar), 128.2 (2 × C-Ar), 128.4 (C-Ar), 129.3 (2 × C-Ar), 132.3 (C-Ar q), 134.9 (C-Ar q), 136.7 (C-Ar q), 141.7 (C-Ar q), 152.9 (C-Ar q), 171.0 (C-1); LRMS (ES⁺) m/z 452.5 [M+H]⁺; HRMS calcd for C₂₇H₃₁³⁵ClNO₃ [M+H]⁺ 452.1987, found 452.1977; HPLC 97.3% in 0.1% formic acid (aq.)/MeCN (R_t 9.7 min); 98.6% in 0.1% ammonia (aq.)/MeCN (R_t 9.7 min).

Methyl 3-(benzyloxy)isoxazole-5-carboxylate (273)

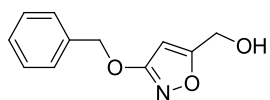


To a suspension of methyl 3-hydroxy-5-isoxazolecarboxylate (1.00 g, 7.00 mmol) in acetonitrile (19 mL, 2.7 mL/mmol), K₂CO₃ (1.93 g, 14.0 mmol) was added in one portion. The reaction mixture was stirred at 70 °C for 1 h and benzyl bromide (1.25 mL, 1.80 g, 10.5 mmol) was added portionwise over 30 min. The mixture was stirred at 70 °C for 3 hours and at RT overnight before being filtered through a Celite cartridge. The solvent was removed *in vacuo* and

the crude product was purified by MPLC (gradient elution, 0-20% EtOAc/petrol) to obtain the title compound (1.34 g, 82%) as a colorless oil which solidified upon storage at RT. R_f 0.64 (25% EtOAc/petrol); m.p. 37.4-37.7°C (lit.¹⁷² 43 °C); λ_{\max} (EtOH)/nm no maximum of absorption was observed; $\nu_{\max}/\text{cm}^{-1}$ (neat) 1736 (s, C=O); ^1H NMR (500 MHz; CDCl_3) δ_{H} 3.95 (3H, s, CH_3), 5.32 (2H, s, CH_2), 6.57 (1H, s, H-4), 7.34 – 7.43 (3H, m, H-Ar), 7.43 – 7.47 (2H, m, H-Ar); ^{13}C NMR (125 MHz; CDCl_3) δ_{C} 53.0 (CH_3), 72.3 (CH_2), 101.1 (C-4), 128.5 (C-Ar), 128.8 (C-Ar), 128.9 (C-Ar), 135.3 (C-Ar), 157.2 (C-3), 160.5 (C-5), 171.5 (CO_2CH_3); HRMS calcd for $\text{C}_{12}\text{H}_{12}\text{NO}_4$ $[\text{M}+\text{H}]^+$ 234.0761, found 234.0764.

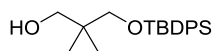
Spectral data are consistent with those reported in the literature.¹⁷²

[3-(Benzyloxy)isoxazol-5-yl]methanol (**274**)



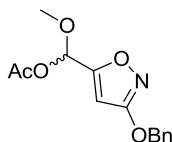
Sodium borohydride (168 mg, 4.45 mmol) was added carefully to a cooled (0 °C) solution of the ester **273** (416 mg, 1.78 mmol) in methanol (12.8 mL, 7.2 mL/mmol). The reaction mixture was allowed to warm up to RT, stirred overnight. HCl (1 M aq., 5 mL) and was stirred at RT for 30 min. The product was extracted with DCM (3 × 40 mL) and the combined organic layers were washed with brine (25 mL), dried (MgSO_4), filtered and evaporated. Purification by MPLC (0-40% EtOAc/petrol) yielded the title compound as a colorless oil (337 mg, 92%). R_f 0.24 (25% EtOAc/petrol); λ_{\max} (EtOH)/nm 257; $\nu_{\max}/\text{cm}^{-1}$ (neat) 3361 (O-H); ^1H NMR δ_{H} (500 MHz; CDCl_3) δ_{H} (500 MHz, CDCl_3) 1.94 (1H, br, OH), 4.67 (2H, s, CH_2OH), 5.27 (2H, s, CH_2O), 5.92 (1H, s, H-4), 7.32 – 7.48 (5H, m, H-Ar); ^{13}C NMR (125 MHz; CDCl_3) δ_{C} 57.1 (CH_2OH), 71.8 (CH_2O), 93.7 (C-4), 128.4 (2 × C-Ar), 128.7 (C-Ar), 128.8 (2 × C-Ar), 135.8 (C-Ar q), 171.8 (C-3), 172.2 (C-5); HRMS calcd for $\text{C}_{11}\text{H}_{12}\text{NO}_3$ $[\text{M}+\text{H}]^+$ 206.0812, found 206.0811.

{1-[[*tert*-Butyldiphenylsilyl]oxy]methyl}cyclopropyl}methanol (**283**)



Under an inert atmosphere, 1,1-bis(hydroxymethyl)cyclopropane (1.02 mL, 1.5 g, 14.7 mmol) was dissolved in DCM (15 mL, 1.0 mL/mmol) and triethylamine (1.23 mL, 0.89 g, 8.82 mmol) was added. The clear solution was cooled to 0 °C and a solution of TBDPSCl (1.91 mL, 2.02 g, 7.35 mmol) in DCM (2 mL) was added dropwise. The reaction mixture was allowed to warm up to RT and stirred for 2 h. Saturated NaHCO₃ (aq., 4 mL) was added to the reaction mixture and the layers were separated. The aqueous phase was extracted with DCM (2 × 30 mL) and the combined organic layers were washed with water (45 mL) and brine (45 mL), dried (MgSO₄) and the solvent was removed *in vacuo*. Purification by MPLC (gradient elution, 0-60% EtOAc/petrol) yielded the desired compound **283** (2.47 g, 99%) as a colorless oil. *R*_f 0.65 (25% EtOAc/petrol); λ_{max} (EtOH)/nm 264; ν_{max}/cm⁻¹ (neat) 2857 2930 and 3070 (w, aliphatic CH and -CH₂-), 3412 (br, O-H); ¹H NMR (500 MHz; CDCl₃) δ_H 0.32 – 0.39 (2H, m, cyclopropyl), 0.45 – 0.53 (2H, m, cyclopropyl), 1.07 (9H, s, 3 × CH₃), 2.56 (1H, ABX app. t, *J*_{AX} = *J*_{BX} = 5.6 Hz, OH), 3.57 – 3.66 (4H, m, 2 × CH₂), 7.34 – 7.49 (6H, m, H-Ar), 7.62 – 7.73 (4H, m, H-Ar); ¹³C NMR (125 MHz; CDCl₃) δ_C 8.9 (2 × CH₂ cyclopropyl), 19.3 (C(CH₃)₃), 24.2 (C q cyclopropyl), 27.0 (3 × CH₃), 69.5 (CH₂), 70.5 (CH₂), 127.9 (2 × C-Ar), 130.0 (C-Ar), 133.3 (C-Ar q), 135.8 (2 × C-Ar); HRMS calcd for C₂₁H₂₉O₂ [M+H]⁺ 341.1931, found 341.1936.

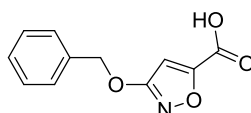
[3-(Benzyloxy)isoxazol-5-yl](methoxy)methyl acetate (**279**)



Under an inert atmosphere, DIBAL (1 M in cyclohexanes, 4.3 mL, 4.3 mmol) was added dropwise to a solution of **273** (250 mg, 1.07 mmol) in DCM (6.4 mL, 6.0 mL/mmol) cooled at -78 °C. The solution was stirred at -78 °C for 1.5 h. Pyridine (0.26 mL, 254 mg, 3.21 mmol), a solution of DMAP (261 mg, 2.14 mmol) in DCM (3.2 mL) and acetic anhydride (0.61 mL, 655 mg, 6.42 mmol) were added

sequentially dropwise. The reaction mixture was stirred at -78 °C for 15 h, at 0 °C for 30 min and quenched by addition of sat. aq. NH₄Cl (10 mL) and sat. aq. Rochelle salt solution (7.5 mL). The mixture was allowed to warm up to RT and stirred until the layers separated. The aqueous layer was extracted with DCM (4 × 10 mL); the combined organic layers were washed with ice-cooled potassium hydrogen sulfate (aq. 1 M, 2 × 10 mL), sat. aq. NaHCO₃ (3 × 10 mL) and brine (10 mL), dried (MgSO₄), filtered and evaporated. Purification on amine silica (gradient elution, 0-15% EtOAc/petrol) yielded the desired α -acetoxy ether **279** (99 mg, 33%) as a colorless oil. *R*_f 0.84 (50% EtOAc/petrol); λ_{max} (EtOH)/nm 257; ν_{max} /cm⁻¹ (neat) 1745 (m, C=O); ¹H NMR (500 MHz; CDCl₃) δ_{H} 2.21 (3H, s, O-CH₃), 3.57 (3H, s, CO-CH₃), 5.30 (2H, s, CH₂), 6.07 (1H, s, H-4), 6.70 (1H, s, O-CH-O), 7.33 – 7.52 (5H, m, H-Ar); ¹³C NMR (125 MHz; CDCl₃) δ_{C} 21.0 (OCH₃), 56.9(CO-CH₃), 71.9 (CH₂), 90.8 (O-CH-O), 94.9 (C-4), 128.4 (2 × C-Ar), 128.7 (C-Ar), 128.7 (2 × C-Ar), 135.7 (C-Ar q), 167.9 (C q), 170.0 (C q), 171.4 (C q); LRMS (ES⁺) *m/z* 300.2 [M+Na]⁺; HRMS calcd for C₁₄H₁₆N₁O₅ [M+H]⁺ 278.1023, found 278.1026.

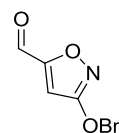
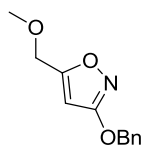
3-(Benzyloxy)isoxazole-5-carboxylic acid (**284**)



The ester **273** (620 mg, 2.66 mmol) was dissolved in THF (25 mL) and LiOH (aq. 2 M, 25 mL) was added in one portion. The reaction mixture was stirred for 45 min and acidified by addition of HCl (aq. 1 M) to pH 3. Ethyl acetate was added and the layers were separated. The aqueous layer was extracted with ethyl acetate (2 × 40 mL). The combined organic layers were washed with brine (30 mL), dried (MgSO₄), filtered and the solvent was removed in vacuo. The product (white solid; 0.56 mg, 96%) was used directly in the following step without further purification. *R*_f 0.01 (10% MeOH/petrol); m.p. 124.4-126.0 °C; λ_{max} (EtOH)/nm no maximum of absorption; ν_{max} /cm⁻¹ (neat) 1706 (s, C=O), 2900 (br, O-H); ¹H NMR (500 MHz; DMSO-*d*₆) δ_{H} 5.30 (2H, s, CH₂), 6.99 (1H, s, H-4), 7.27 – 7.60 (5H, m, H-Ar), 14.35 (1H, s, OH); ¹³C NMR (125 MHz; DMSO-*d*₆) δ_{C}

71.7 (CH₂), 100.3 (C-4), 128.4 (2 × C-Ar), 128.5 (2 × C-Ar), 128.5 (C-Ar), 135.5 (C-Ar q), 157.5 (C q), 161.6 (C q), 171.3 (CO₂H); LRMS (ES⁻) *m/z* 218.1 [M-H]⁻; HRMS calcd for C₁₁H₈NO₄ [M-H]⁻ 218.0459, found 218.0455.

3-(Benzyloxy)-5-(methoxymethyl)isoxazole (280) and 3-(benzyloxy)isoxazole-5-carbaldehyde (281)



Under an inert atmosphere, triethylsilane (0.07 mL, 52 mg, 0.450 mmol) was added to a solution of the α-acetoxyether **279** (50 mg, 0.180 mmol) in DCM (3.6 mL, 20 mL/mmol) cooled at -78 °C. Boron trifluoride etherate (0.06 mL, 64 mg, 0.450 mmol) was added dropwise and the mixture was stirred at -78 °C for 50 min. Upon completion of the reaction, the reaction mixture was partitioned between NaHCO₃ (sat. aq., 5 mL) and petrol (10 mL) and the aqueous layer was back-extracted with petrol (10 mL). The combined organic layers were dried (MgSO₄), filtered and evaporated. Purification by MPLC afforded the desired ether **280** (8 mg, 20%) and the aldehyde **281** (14 mg, 38%), both as colorless oils.

280

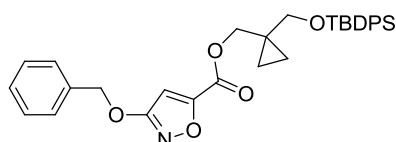
R_f 0.58 (25% EtOAc/petrol); λ_{max} (EtOH)/nm 257; ν_{max}/cm⁻¹ (neat) 2932 (w, aliphatic CH and -CH₂-); ¹H NMR (500 MHz; CDCl₃) δ_H 3.42 (3H, s, CH₃), 4.43 (2H, s, CH₂-OCH₃), 5.27 (2H, s, CH₂-Ph), 5.87 – 5.95 (1H, m, H-4), 7.30 – 7.54 (5H, m, H-Ar); ¹³C NMR (125 MHz; CDCl₃) δ_C 59.0 (CH₃), 65.8 (CH₂-OCH₃), 71.8 (CH₂-Ph), 94.7 (C-4), 128.4 (2 × C-Ar), 128.7 (C-Ar), 128.8 (2 × C-Ar), 135.9 (C-Ar q), 170.3 (C-3 or C-5), 171.8 (C-3 or C-5); LRMS (ES⁺) *m/z* 220.2 [M+H]⁺; HRMS calcd for C₁₂H₁₄NO₃ [M+H]⁺ 220.0968, found 220.0968.

281

R_f 0.53 (25% EtOAc/petrol); λ_{max} (EtOH)/nm 257sh; ν_{max}/cm⁻¹ (neat) 1703 (s, C=O); ¹H NMR (500 MHz; CDCl₃) δ_H 5.34 (2H, s, CH₂), 6.60 (1H, s, H-4), 7.31 –

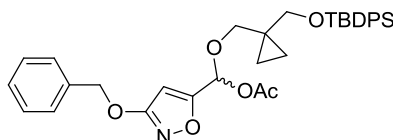
7.54 (5H, m, H-Ar), 9.84 (1H, s, CHO); ^{13}C NMR (125 MHz; CDCl_3) δ_{C} 72.6 (CH_2), 100.1 (C-4), 128.5 ($2 \times \text{C-Ar}$), 128.8 ($2 \times \text{C-Ar}$), 129.0 (C-Ar), 135.2 (C-Ar q), 166.0 (C-3 or C-5), 171.6 (C-3 or C-5), 178.8 (CHO); HRMS calcd for $\text{C}_{11}\text{H}_{10}\text{NO}_3$ $[\text{M}+\text{H}]^+$ 204.0655, found 204.0651.

{1-[[(*tert*-Butyldiphenylsilyl)oxy]methyl]cyclopropyl}methyl 3-(benzyloxy)isoxazole-5-carboxylate (284**)**



To a cooled (0 °C) solution of **284** (1.27 g, 5.79 mmol) in THF (4.6 mL, 0.8 mL/mmol), a solution of thionyl chloride (0.84 mL, 1.38 g, 11.6 mmol) in THF (2.3 mL, 0.4 mL/mmol) was added followed by a catalytic amount of DMF (1-3 drops); the solution was stirred at RT for 4 h and evaporated. The residue was redissolved in THF (5.8 mL, 1.2 mL/mmol), and **283** (2.17 g, 6.17 mmol) and DIPEA (1.11 mL, 0.82 g, 6.37 mmol) were added dropwise. The solution was stirred at RT overnight; Upon completion of the reaction, ethyl acetate (10 mL) was added to the mixture and the layers were separated. The aqueous layer was extracted with EtOAc (2×10 mL) and the combined organic layers were dried (MgSO_4), filtered and the solvent was removed *in vacuo*. The crude product was purified by MPLC (gradient elution, 0-6% EtOAc/petrol) to afford the desired product as a colorless oil (2.25 g, 72%). R_f 0.69 (17% EtOAc/petrol); $\nu_{\text{max}}/\text{cm}^{-1}$ (neat) 1733 (m, C=O), 2856, 2930 and 3069 (w, aliphatic CH and $-\text{CH}_2-$); ^1H NMR (500 MHz; CDCl_3) δ_{H} 0.45 – 0.64 (4H, m, cyclopropane), 1.05 (9H, s, $3 \times \text{CH}_3$), 3.59 (2H, s, $\text{CH}_2\text{-OTBDPS}$), 4.35 (2H, s, $\text{CH}_2\text{-OC=O}$), 5.33 (2H, s, $\text{CH}_2\text{-Ph}$), 6.46 (1H, s, H-4), 7.31 – 7.53 (11H, m, H-Ar), 7.59 – 7.70 (4H, m, H-Ar); ^{13}C NMR (125 MHz; CDCl_3) δ_{C} 9.0 (CH_2 cyclopropyl), 19.5 (C q), 22.0 (C q), 27.0 ($3 \times \text{CH}_3$), 66.6 ($\text{CH}_2\text{-OTBDPS}$), 69.8 ($\text{CH}_2\text{-OC=O}$), 72.2 ($\text{CH}_2\text{-Ph}$), 100.9 (C-4), 127.8 (C-Ar), 128.5 (C-Ar), 128.8 (C-Ar), 128.8 (C-Ar), 129.8 (C-Ar), 133.6 (C-Ar), 135.5 (C-Ar), 135.7 (C-Ar), 156.9 (C-3 or C-5), 160.7 (C-3 or C-5), 171.4 (CO_2R); HRMS calcd for $\text{C}_{32}\text{H}_{36}\text{NO}_5\text{Si}$ $[\text{M}+\text{H}]^+$ 542.2357, found 542.2350.

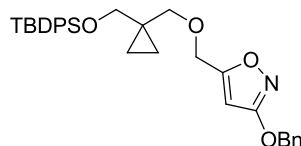
**[3-(Benzyloxy)isoxazol-5-yl]{1-[[(*tert*-butyldiphenylsilyl)oxy]methyl]cyclopropyl}methoxy}methyl acetate
(286)**



Under an inert atmosphere, DIBAL (1 M in cyclohexanes, 7.20 mL, 7.20 mmol) was added dropwise to a solution of **284** (1.30 g, 2.40 mmol) in DCM (14.4 mL, 6.0 mL/mmol) cooled at -78 °C. The solution was stirred at -78 °C for 1.5 h. Pyridine (0.58 mL, 570 mg, 7.20 mmol), a solution of DMAP (586 mg, 4.80 mmol) in DCM (7.2 mL) and acetic anhydride (1.36 mL, 1.47 g, 14.4 mmol) were added dropwise. The reaction mixture was stirred at -78 °C for 15 h, at 0 °C for 30 min and quenched by addition of sat. aq. NH₄Cl (20 mL) and sat. aq. Rochelle salt solution (15 mL). The mixture was allowed to warm up to RT and stirred until the layers separated. The aqueous layer was extracted with DCM (4 × 20 mL); the combined organic layers were washed with ice-cooled potassium hydrogen sulfate (aq. 1 M, 2 × 20 mL), sat. aq. NaHCO₃ (3 × 20 mL) and brine (20 mL), dried (MgSO₄), filtered and evaporated. Purification on previously neutralized silica (gradient elution, 0-30% EtOAc/petrol) yielded the desired α-acetoxyether **286** (1.40 g, quant.) as a colorless oil. *R*_f 0.56 (17% EtOAc/petrol); λ_{max} (EtOH)/nm 259; ν_{max}/cm⁻¹ (neat) 1750 (m, C=O), 2856, 2930 and 3070 (w, aliphatic CH and -CH₂-); ¹H NMR (500 MHz; CDCl₃) δ_H 0.37 – 0.53 (4H, m, cyclopropyl), 1.05 (9H, s, 3 × CH₃), 2.12 (3H, s, CH₃CO), 3.58 (2H, AB q, *J* = 10.2 Hz, CH₂OSi), 3.76 (2H, AB q, *J* = 9.6 Hz, CH₂C-OAc), 5.28 (2H, s, CH₂Ph), 5.97 (1H, s, H-4), 6.76 (1H, s, OCHOAc), 7.31 – 7.49 (11H, m, H-Ar), 7.65 (4H, m, H-Ar); ¹³C NMR (125 MHz; CDCl₃) δ_C 8.3 (CH₂ cyclopropyl), 8.6 (CH₂ cyclopropyl), 19.5 (C q cyclopropyl), 21.2 (CH₃CO), 22.4 (C(CH₃)₃), 27.0 (3 × CH₃), 66.4 (CH₂OSi), 71.9 (CH₂Ph), 73.7 (CH₂C-OAc), 90.0 (OCHOAc), 94.8 (C-4), 127.8 (2 × C-Ar), 127.8 (2 × C-Ar), 128.4 (2 × C-Ar), 128.7 (C-Ar), 128.7 (2 × C-Ar), 129.8 (C-Ar), 133.8 (2 × C-Ar), 133.8 (2 × C-Ar), 135.7 (C-Ar), 135.7 (C-Ar), 135.8 (C-Ar), 168.3 (OCO),

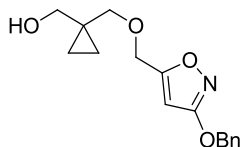
170.1 (C-5), 171.4 (C-3); LRMS (ES⁺) m/z 608.5 [M+Na]⁺; HRMS calcd for C₃₄H₄₀NO₆Si [M+H]⁺ 586.2619, found 586.2593.

3-(Benzyloxy)-5-{{[1-(((tert-butyl)diphenylsilyl)oxy)methyl]cyclopropyl}methoxy}methyl}isoxazole (287)



TMSOTf was dissolved in DCM; the solution was cooled to 0 °C and triethylsilane was added, followed by a solution of the acetal **286** in DCM. The reaction mixture was stirred for 30 min and quenched with saturated NaHCO₃ aq., extracted with Et₂O (3 × 20 mL), dried (MgSO₄) and the solvent was removed *in vacuo*. Purification on pre-neutralized silica (gradient elution 0-6% EtOAc/petrol) yielded the desired ether **287** (312 mg, 69%) as a colorless oil. R_f 0.80 (25% EtOAc/petrol); λ_{max} (EtOH)/nm 264; ν_{max}/cm^{-1} (neat) 2855, 2929 and 3069 (w, aliphatic CH and -CH₂-); ¹H NMR (500 MHz; CDCl₃) δ_H 0.44 (4H, s, cyclopropyl), 1.06 (9H, s, 3 × CH₃), 3.53 (2H, s, CH₂OSi), 3.61 (2H, s, CH₂OCH₂-isoxazole), 4.47 (2H, s, CH₂-isoxazole), 5.27 (2H, s, CH₂Ph), 5.89 (1H, s, H-4), 7.31 – 7.53 (11H, m, H-Ar), 7.61 – 7.73 (4H, m, H-Ar); ¹³C NMR (125 MHz; CDCl₃) δ_C 8.3 (CH₂-cyclopropyl), 19.5 (C q cyclopropyl), 22.5 (C(CH₃)₃), 27.0 (3 × CH₃), 64.2 (CH₂-isoxazole), 66.6 (CH₂OCH₂-isoxazole), 71.7 (CH₂Ph), 74.8 (CH₂OSi), 94.4 (C-4), 127.8 (4 × C-Ar), 128.3 (2 × C-Ar), 128.6 (C-Ar), 128.7 (2 × C-Ar), 129.7 (2 × C-Ar), 133.9 (C-Ar q), 135.7 (4 × C-Ar), 135.9 (C-Ar q), 170.8 (C-5), 171.8 (C-3); LRMS (ES⁺) m/z 482.4 [M+H]⁺; HRMS calcd for C₃₂H₃₈NO₄Si [M+NH₄]⁺ 528.2565, found 528.2560.

**{1-[(3-(Benzyloxy)isoxazol-5-yl)methoxy]methyl}cyclopropyl}methanol
(277)**



Compound **277** was obtained following general procedure P using isoxazole **287** (305 mg, 0.578 mmol), TBAF (1 M in THF, 0.87 mL, 0.87 mmol) and THF (23 mL). Purification by MPLC (gradient elution, 0-70% EtOAc/petrol) yielded the title compound as a yellow oil (164 mg, 98%). R_f 0.31 (50% EtOAc/petrol); λ_{\max} (EtOH)/nm 257; $\nu_{\max}/\text{cm}^{-1}$ (neat) 3432 (OH); ^1H NMR (500 MHz; CDCl_3) δ_{H} 0.44 – 0.65 (4H, m, cyclopropyl), 3.54 (2H, s, CH_2OH), 3.58 (2H, s, CH_2OCH_2 -isoxazole), 4.55 (2H, s, CH_2 -isoxazole), 5.29 (2H, s, CH_2Ph), 5.96 (1H, s, H-4), 7.32 – 7.55 (5H, m); ^{13}C NMR (125 MHz; CDCl_3) δ_{C} 9.0 (CH_2 cyclopropyl), 22.7 (C q cyclopropyl), 64.3 (CH_2 -isoxazole), 68.5 (CH_2OCH_2 -isoxazole), 71.8 (CH_2 benzylic), 76.9 (CH_2OH), 94.7 (C-4), 128.4 ($2 \times$ C-Ar), 128.7 (C-Ar), 128.8 ($2 \times$ C-Ar), 135.8 (C-Ar q), 170.2 (C-5), 171.8 (C-3); HRMS calcd for $\text{C}_{16}\text{H}_{23}\text{O}_4\text{N}_2$ $[\text{M}+\text{NH}_4]^+$ 307.1652, found 307.1656.

(3*R*,1'*R*)-4-Chloro-2-[1'-(4''-chlorophenyl)ethyl]-3-(2'''-hydroxyethoxy)-3-phenylisoindolin-1-one (235) and (3*S*,1'*R*)-4-chloro-2-[1'-(4''-chlorophenyl)ethyl]-3-(2'''-hydroxyethoxy)-3-phenylisoindolin-1-one (238)



Compounds **235** and **238** were synthesized following general procedure N using isoindolinone **198** (250 mg, 0.628 mmol), InBr_3 (45 mg, 0.126 mmol), 1,2-ethanediol (0.175 mL, 195 mg, 3.14 mmol) and dichloroethane (6.3 mL). Purification by MPLC (gradient elution, 0-40% EtOAc/petrol) yielded the two

diastereoisomers as white amorphous solids (**235** 139 mg, 50%; **238** 124 mg, 45%).

235

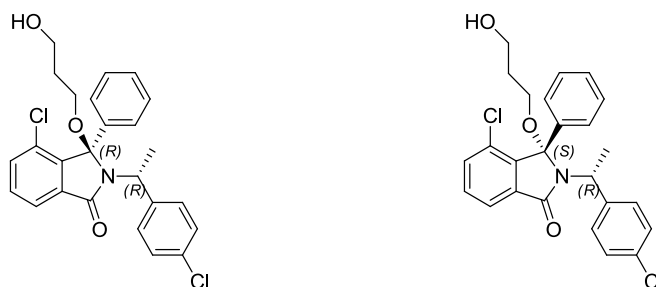
R_f 0.29 (25 %EtOAc/petrol); m.p. 136.8-137.6 °C; $[\alpha]^{24}_D +155^\circ$ (c 0.422, EtOAc); λ_{\max} (EtOH)/nm 259; $\nu_{\max}/\text{cm}^{-1}$ (neat) 1683 (s, C=O), 2932 (w, aliphatic CH₂), 3384 (br, O-H); ^1H NMR (500 MHz; CDCl₃) δ_{H} 1.61 (3H, d, J = 7.3 Hz, CH₃), 1.71 (1H, ABX dd, J = 4.4, 8.2 Hz, OH), 2.70 – 2.88 (2H, m, OCH₂CH₂OH), 3.35 – 3.54 (2H, ABX m, OCH₂CH₂OH), 4.21 (1H, q, J 7.3 Hz, CHCH₃), 7.26 – 7.29 (2H, m, H-Ar), 7.34 – 7.44 (6H, m, 5 × H-Ar and H-5), 7.48 (1H, app. t, J = 7.7 Hz, H-6), 7.55 – 7.61 (2H, m, H-Ar), 7.79 (1H, dd, J = 1.0, 7.7 Hz, H-7); ^{13}C NMR (125 MHz; CDCl₃) δ_{C} 19.4 (CHCH₃), 53.3 (ArCHCH₃), 61.4 (OCH₂CH₂OH), 65.0 (OCH₂CH₂OH), 96.3 (C-3), 122.0 (C-7), 128.5 (2 × C-Ar), 128.6 (C-Ar), 129.0 (C-Ar), 129.7 (2 × C-Ar), 129.7 (C-Ar q), 131.8 (C-6), 133.4 (C-Ar q), 133.8 (C-5), 135.2 (C-Ar q), 136.5 (C-Ar q), 140.6 (C-Ar q), 141.1 (C-Ar q), 166.8 (C-1). One carbon not detected; LRMS (ES⁺) m/z 442.3 [M+H]⁺; HRMS calcd for C₂₄H₂₂³⁵Cl₂NO₃ [M+H]⁺ 442.0971, found 442.0967; HPLC 96.4% in 0.1% formic acid (aq)/MeCN (R_t 9.1 min); 96.3% in 0.1% ammonia (aq)/MeCN (R_t 9.1 min).

238

R_f 0.09 (25 %EtOAc/petrol); m.p. 155.6-156.9 °C; $[\alpha]^{24}_D +56^\circ$ (c 0.674, EtOAc); λ_{\max} (EtOH)/nm 254; $\nu_{\max}/\text{cm}^{-1}$ (neat) 1681 (vs, C=O), 2870 and 2930 (w, aliphatic CH and -CH₂-), 3364 (br, O-H); ^1H NMR (500 MHz; CDCl₃) δ_{H} 1.87 (3H, d, J = 7.3 Hz, CHCH₃), 2.05 (1H, ABX dd, J = 5.5, 6.4 Hz, OCH₃), 3.10 – 3.21 (1H, m, OCH_AH_BCH₂OH), 3.44 – 3.55 (1H, m, OCH_AH_BCH₂OH), 3.77 – 3.95 (2H, m, OCH₂CH₂OH), 4.43 (1H, q, J = 7.3 Hz, CHCH₃), 6.82 – 6.92 (2H, m, H-Ar), 6.93 – 7.00 (2H, m, H-Ar), 7.13 (4H, br, H-Ar), 7.19 – 7.25 (1H, m, H-Ar), 7.42 (1H, dd, J = 1.1, 7.7 Hz, H-5), 7.48 (1H, app. t, J = 7.7 Hz, H-6), 7.78 (1H, dd, J = 1.1, 7.7, H-7); ^{13}C NMR (125 MHz; CDCl₃) δ_{C} 19.5 (CHCH₃), 52.0 (CHCH₃), 61.8 (OCH₂CH₂OH), 65.1 (OCH₂CH₂OH), 95.3 (C-3), 121.9 (C-7), 127.2 (2 × C-Ar), 127.9 (2 × C-Ar), 128.1 (2 × C-Ar), 128.7 (C-Ar), 129.5 (2 × C-Ar), 129.8 (C-Ar q), 131.8 (C-6), 132.7 (C-Ar q), 133.7 (C-5), 135.3 (C-Ar q), 136.2 (C-Ar q), 140.3 (C-Ar q), 140.5 (C-Ar q), 166.5 (C-1); LRMS (ES⁺) m/z 442.3 [M+H]⁺; HRMS calcd

for $C_{24}H_{22}^{35}Cl_2NO_3$ $[M+H]^+$ 442.0971, found 442.0967; HPLC 98.9% in 0.1% formic acid (aq)/MeCN (R_t 9.0 min); 99.1% in 0.1% ammonia (aq)/MeCN (R_t 9.0 min).

(3*R*,1'*R*)-4-Chloro-2-[1'-(4''-chlorophenyl)ethyl]-3-(3-hydroxypropoxy)-3-phenylisoindolin-1-one (236) and (3*S*,1'*R*)-4-chloro-2-[1-(4-chlorophenyl)ethyl]-3-(3'''-hydroxypropoxy)-3-phenylisoindolin-1-one (241)



Compounds **236** and **241** were synthesized following general procedure N using isoindolinone **198** (200 mg, 0.502 mmol), $InBr_3$ (35 mg, 0.100 mmol), 1,3-propanediol (0.18 mL, 191 mg, 2.51 mmol) and dichloroethane (5.0 mL). The two diastereoisomers were separated by MPLC (gradient elution, 0-45% EtOAc/petrol) to obtain **236** as a white amorphous solid (113 mg, 49%) and **241** as a white solid (84 mg, 37%).

236

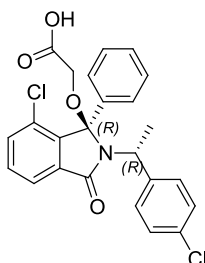
R_f 0.26 (25 %EtOAc/petrol); no clear m.p. detected; $[\alpha]^{24}_D +153^\circ$ (c 0.584, EtOAc); λ_{max} (EtOH)/nm 259; ν_{max}/cm^{-1} (neat) 1684 (s, C=O), 2878 and 2932 (w, aliphatic CH and CH_2), 3389 (br, O-H); 1H NMR (500 MHz; $CDCl_3$) δ_H 1.39 – 1.51 (1H, m, CH_AH_B), 1.52 – 1.68 (5H, m, CH_3 , CH_AH_B , and OH), 2.73 – 2.90 (2H, m, CH_2), 3.56 – 3.75 (2H, m, CH_2OH), 4.19 (1H, q, $J = 7.3$ Hz, $CHCH_3$), 7.26 – 7.30 (2H, m, H-Ar), 7.32 – 7.43 (6H, m, $5 \times$ C-Ar and C-5), 7.47 (1H, app. t, $J = 7.6$ Hz, H-6), 7.56 – 7.63 (2H, m, H-Ar), 7.79 (1H, dd, $J = 1.1, 7.5$ Hz, H-7); ^{13}C NMR (125 MHz; $CDCl_3$) δ_C 19.4 ($CHCH_3$), 31.7 ($OCH_2CH_2CH_2OH$), 53.2 ($CHCH_3$), 60.9 ($OCH_2CH_2CH_2OH$), 61.5 ($OCH_2CH_2CH_2OH$), 96.3 (C-3), 122.0 (C-7), 127.1 (C-Ar), 128.5 ($2 \times$ C-Ar), 128.6 ($2 \times$ C-Ar), 128.9 ($2 \times$ C-Ar), 129.6 (C-Ar q), 129.7 ($2 \times$ C-Ar), 131.6 (C-6), 133.3 (C-Ar q), 133.6 (C-5), 135.2 (C-Ar q), 136.7 (C-Ar q),

140.7 (C-Ar q), 141.3 (C-Ar q), 166.8 (C-1); LRMS (ES⁺) *m/z* 456.4 [M+H]⁺; HRMS calcd for C₂₅H₂₄³⁵Cl₂NO₃ [M+H]⁺ 456.1128, found 456.1125; HPLC 99.4% in 0.1% formic acid (aq)/MeCN (*R*_t 9.3 min); 99.4% in 0.1% ammonia (aq)/MeCN (*R*_t 9.3 min).

241

*R*_f 0.12 (25 %EtOAc/petrol); no clear m.p. detected; [α]_D²⁴ +54° (*c* 0.609, EtOAc); λ_{max} (EtOH)/nm 254; ν_{max}/cm⁻¹ (neat) 1684 (s, C=O), 2878 and 2933 (w, aliphatic CH and CH₂), 3405 (br, O-H); ¹H NMR (500 MHz; CDCl₃) δ_H 1.75 (1H, ABX app. t, *J* = 5.6 Hz, OH), 1.85 (3H, d, *J* = 7.3 Hz, CH₃), 1.87 – 2.04 (2H, m, CH₂), 3.17 (1H, m, CH_AH_B), 3.49 (1H, dt, m, CH_AH_B), 3.86 – 3.97 (2H, m, CH₂), 4.42 (1H, q, *J* = 7.3 Hz, CHCH₃), 6.84 – 6.91 (2H, m, H-Ar), 6.93 – 7.01 (2H, m, H-Ar), 7.13 (4H, br, H-Ar), 7.19 – 7.25 (1H, m, H-Ar), 7.42 (1H, dd, *J* = 1.1, 7.7 Hz, H-5), 7.47 (1H, app. t, *J* = 7.7 Hz, H-6), 7.77 (1H, dd, *J* = 1.1, 7.3 Hz, H-7); ¹³C NMR (125 MHz; CDCl₃) δ_C 19.4 (CHCH₃), 32.3 (OCH₂CH₂CH₂OH), 51.8 (CHCH₃), 60.8 (OCH₂CH₂CH₂OH), 61.3 (OCH₂CH₂CH₂OH), 95.4 (C-3), 121.9 (C-7), 127.2 (2 × C-Ar), 127.9 (2 × C-Ar), 128.1 (2 × C-Ar), 128.7 (C-Ar), 129.5 (2 × C-Ar), 129.8 (C-Ar q), 131.7 (C-6), 132.7 (C-Ar q), 133.5 (C-5), 135.4 (C-Ar q), 136.6 (C-Ar q), 140.3 (C-Ar q), 140.8 (C-Ar q), 166.5 (C-1); LRMS (ES⁺) *m/z* 456.4 [M+H]⁺; HRMS calcd for C₂₅H₂₄³⁵Cl₂NO₃ [M+H]⁺ 456.1128, found 456.1124; HPLC 97.4% in 0.1% formic acid (aq)/MeCN (*R*_t 9.2 min); 97.6% in 0.1% ammonia (aq)/MeCN (*R*_t 9.3 min).

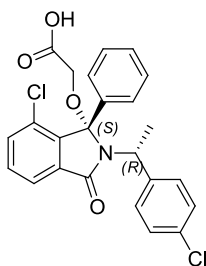
(3*R*,1'*R*)-2-[[7-Chloro-2-[1'-(4''-chlorophenyl)ethyl]-3-oxo-1-phenylisoindolin-1-yl]oxy}acetic acid (237)



General procedure S was followed to synthesize the acid **237** using the alcohol **235** (139 mg, 0.314 mmol), sodium periodate (276 mg, 1.29 mmol), RuCl₃ · H₂O

(6.5 mg, 0.0314), ethyl acetate (0.45 mL), acetonitrile (0.45 mL) and water (0.79 mL). Purification by MPLC (gradient elution, 1-25% EtOAc/petrol + 0.1% acetic acid) yielded the title compound as a white amorphous solid (76 mg, 53%). R_f 0.28 (33% EtOAc/petrol, 0.1% formic acid); no clear m.p. detected; $[\alpha]^{26}_D +180^\circ$ (c 0.543, EtOAc); λ_{max} (EtOH)/nm 259; ν_{max}/cm^{-1} (neat) 1667 (s, C=O), 1703 (s, C=O), 2932 (w, C-H), 3000 (br, O-H); 1H NMR (500 MHz; $CDCl_3$) δ_H 1.63 (3H, d, $J = 7.2$ Hz, CH_3), 3.28 (1H, d, $J_{AB} = 15.5$ Hz, CH_AH_B), 3.42 (1H, d, $J_{AB} = 15.5$ Hz, CH_AH_B), 4.27 (1H, q, $J = 7.2$ Hz, $CHCH_3$), 7.20 – 7.26 (2H, m, H-Ar), 7.34 – 7.46 (6H, m, H-Ar), 7.50 (1H, app. t, $J = 7.7$ Hz, H-6), 7.54 – 7.65 (2H, m, H-Ar), 7.81 (1H, dd, $J = 1.0, 7.7$ Hz, H-7); ^{13}C NMR (125 MHz; $CDCl_3$) δ_C 19.0 ($CHCH_3$), 53.2 ($CHCH_3$), 60.6 (OCH_2CO_2H), 96.1 (C-3), 122.2 (C-7), 127.2 ($2 \times$ C-Ar), 128.6 ($2 \times$ C-Ar), 128.8 ($2 \times$ C-Ar), 129.2 (C-Ar), 129.7 ($2 \times$ C-Ar), 130.0 (C-Ar q), 132.2 (C-6), 133.6 (C-Ar q), 134.0 (C-5), 135.0 (C-Ar q), 135.7 (C-Ar q), 139.7 (C-Ar q), 140.5 (C-Ar q), 166.7 (C-1), 172.4 (CO_2H); LRMS (ES^-) m/z 454.2 $[M-H]^-$; HRMS calcd for $C_{24}H_{18}^{35}Cl_2NO_4$ $[M-H]^-$ 454.0618, found 454.0603; HPLC 97.8% in 0.1% formic acid (aq)/MeCN (R_t 9.2 min); 99.0% in 0.1% ammonia (aq)/MeCN (R_t 4.7 min).

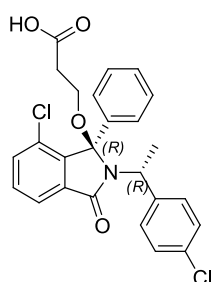
(3*S*,1'*R*)-2-[[7-Chloro-2-[1'-(4''-chlorophenyl)ethyl]-3-oxo-1-phenylisoindolin-1-yl]oxy}acetic acid (239**)**



General procedure S was followed to synthesize the acid **239** using the alcohol **238** (124 mg, 0.280 mmol), sodium periodate (246 mg, 1.15 mmol), $RuCl_3 \cdot H_2O$ (5.8 mg, 0.0280), ethyl acetate (0.40 mL), acetonitrile (0.40 mL) and water (0.70 mL). Purification by MPLC (gradient elution, 1-25% EtOAc/petrol + 0.1% acetic acid) yielded the title compound as a white amorphous solid (89 mg, 70%). R_f 0.23 (33% EtOAc/petrol + 0.1% formic acid); no clear m.p. detected; $[\alpha]^{26}_D +77^\circ$

(*c* 0.460, EtOAc); λ_{\max} (EtOH)/nm 252sh; $\nu_{\max}/\text{cm}^{-1}$ (neat) 1667 (s, C=O), 1702 (s, C=O), 2935 and 2977 (w, C-H), 3000 (br, O-H); ^1H NMR (500 MHz; CDCl_3) δ_{H} 1.79 (3H, d, $J = 7.3$ Hz, CHCH_3), 3.79 (1H, d, $J_{\text{AB}} = 15.7$ Hz, $\text{CH}_\text{A}\text{H}_\text{B}$), 3.91 (1H, d, $J_{\text{AB}} = 15.7$ Hz, $\text{CH}_\text{A}\text{H}_\text{B}$), 4.58 (1H, q, $J = 7.3$ Hz, CHCH_3), 6.86 – 6.94 (2H, m, H-Ar), 6.93 – 7.02 (2H, m, H-Ar), 7.16 (4H, br, H-Ar), 7.22 – 7.26 (1H, m, H-Ar), 7.45 (1H, dd, $J = 1.0, 7.7$ Hz, H-5), 7.52 (1H, app. t, $J = 7.7$ Hz, H-6), 7.81 (1H, dd, $J = 7.4$ Hz, 1.0, H-7); ^{13}C NMR (125 MHz; CDCl_3) δ_{C} 19.6 (CHCH_3), 52.0 (CHCH_3), 60.8 ($\text{OCH}_2\text{CO}_2\text{H}$), 95.5 (C-3), 122.2 (C-7), 127.2 ($2 \times \text{C-Ar}$), 128.0 ($2 \times \text{C-Ar}$), 128.3 ($2 \times \text{C-Ar}$), 129.0 (C-Ar), 129.5 ($2 \times \text{C-Ar}$), 130.0 (C-Ar q), 132.3 (C-6), 132.9 (C-Ar q), 134.0 (C-5), 135.1 (C-Ar q), 135.5 (C-Ar q), 139.7 (C-Ar q), 139.9, 166.6 (C-1), 172.3 (CO_2H); LRMS (ES^+) m/z 456.3 [$\text{M}+\text{H}$] $^+$; HRMS calcd for $\text{C}_{24}\text{H}_{18}^{35}\text{Cl}_2\text{NO}_4$ [$\text{M}-\text{H}$] $^-$ 454.0618, found 454.0602; HPLC 97.1% in 0.1% formic acid (aq)/MeCN (R_{t} 9.2 min); 97.8% in 0.1% ammonia (aq)/MeCN (R_{t} 4.8 min).

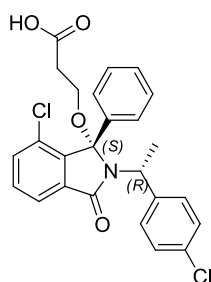
(3*R*,1'*R*)-3-[[7-Chloro-2-[1'-(4''-chlorophenyl)ethyl]-3-oxo-1-phenylisoindolin-1-yl]oxy}propanoic acid (240**)**



General procedure S was followed to synthesize the acid **240** using the alcohol **236** (13 mg, 0.248 mmol), sodium periodate (218 mg, 1.02 mmol), $\text{RuCl}_3 \cdot \text{H}_2\text{O}$ (5.0 mg, 0.0248), ethyl acetate (0.35 mL), acetonitrile (0.35 mL) and water (0.62 mL). Purification by MPLC (gradient elution, 1-25% EtOAc/petrol + 0.1% acetic acid) yielded the title compound as a white amorphous solid (71 mg, 61%). R_{f} 0.28 (33% EtOAc/petrol, 0.1% formic acid); no clear m.p. detected; $[\alpha]_{\text{D}}^{26} +161^\circ$ (*c* 0.595, EtOAc); λ_{\max} (EtOH)/nm 246; $\nu_{\max}/\text{cm}^{-1}$ (neat) 1688 (s, C=O), 1732 (s, C=O), 2937 (w, C-H), 3213 (br, O-H); ^1H NMR (500 MHz; CDCl_3) δ_{H} 1.62 (3H, d, $J = 7.3$ Hz, CH_3), 2.16 (1H, AA'BB' m, $\text{CH}_\text{A}\text{H}_\text{A'}$), 2.27 – 2.37 (1H, AA'BB' m, $\text{CH}_\text{A}\text{H}_\text{A'}$), 2.83 – 2.93 (1H, AA'BB' m, $\text{CH}_\text{B}\text{H}_\text{B'}$), 3.01 – 3.11 (1H, AA'BB' m, $\text{CH}_\text{B}\text{H}_\text{B'}$), 4.18 (1H,

q, $J = 7.3$ Hz, CHCH₃), 7.26 – 7.30 (2H, m, H-Ar), 7.35 (5H, br, H-Ar), 7.40 (1H, dd, $J = 1.0, 7.7$ Hz, H-5), 7.47 (1H, app. t, $J = 7.7$ Hz, H-6), 7.55 – 7.61 (2H, m, H-Ar), 7.79 (1H, dd, $J = 1.0, 7.7$ Hz, H-7); ¹³C NMR (125 MHz; CDCl₃) δ_c 19.5 (CHCH₃), 34.0 (OCH₂CH₂CO₂H), 53.3 (CHCH₃), 59.1 (OCH₂CH₂CO₂H), 96.3 (C-3), 121.9 (C-7), 127.1 (2 × C-Ar), 128.4 (2 × C-Ar), 128.7 (2 × C-Ar), 128.9 (C-Ar), 129.6 (2 × C-Ar), 130.0 (C-Ar q), 131.7 (C-6), 133.4 (C-Ar q), 133.8 (C-5), 135.1 (C-Ar q), 136.5 (C-Ar q), 140.5 (C-Ar q), 141.4 (C-Ar q), 167.0 (C-1), 175.9 (COOH); LRMS (ES⁺) m/z 470.3 [M+H]⁺; HRMS calcd for C₂₅H₂₀³⁵Cl₂NO₄ [M-H]⁻ 468.0775, found 468.0762; HPLC 98.2% in 0.1% formic acid (aq)/MeCN (R_t 9.2 min); 99.8% in 0.1% ammonia (aq)/MeCN (R_t 4.8 min).

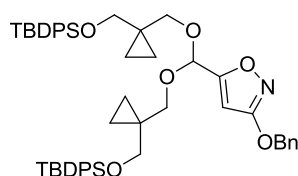
(3*S*,1'*R*)-3-[[7-Chloro-2-[1'-(4''-chlorophenyl)ethyl]-3-oxo-1-phenylisoindolin-1-yl]oxy}propanoic acid (242**)**



General procedure S was followed to synthesize the acid **242** using the alcohol **241** (84 mg, 0.184 mmol), sodium periodate (161 mg, 0.754 mmol), RuCl₃ · H₂O (4 mg, 0.0184), ethyl acetate (0.26 mL), acetonitrile (0.26 mL) and water (0.46 mL). Purification by MPLC (gradient elution, 1-25% EtOAc/petrol + 0.1% acetic acid) yielded the title compound as a white amorphous solid (50 mg, 58%). R_f 0.23 (33% EtOAc/petrol) 0.1% formic acid; m.p. 147.3-148.7 °C; $[\alpha]^{26}_D +44^\circ$ (c 0.543, EtOAc); λ_{max} (EtOH)/nm 247sh; ν_{max}/cm^{-1} (neat) 1659 (s, C=O), 1736 (s, C=O), 2922 (w, C-H), 3068 (br, O-H); ¹H NMR (500 MHz; CDCl₃) δ_H 1.81 (3H, d, $J = 7.2$ Hz, CH₃), 2.53 – 2.80 (2H, AA'BB' m, CH_AH_{A'}), 3.23 (1H, AA'BB' m, CH_BH_{B'}), 3.58 (1H, m, AA'BB', CH_BH_{B'}), 4.35 (1H, q, $J = 7.2$ Hz, CHCH₃), 6.77 – 6.86 (2H, m, H-Ar), 6.86 – 6.93 (2H, m, H-Ar), 7.01 (4H, br, H-Ar), 7.08 – 7.16 (1H, m, H-Ar), 7.33 (1H, dd, $J = 1.0, 7.7$ Hz, H-5), 7.40 (1H, app. t, $J = 7.7$ Hz, H-6), 7.71 (1H, dd, $J = 1.0, 7.7$ Hz, H-7); ¹³C NMR (125 MHz; CDCl₃) δ_c 19.6 (CHCH₃), 34.5

(OCH₂CH₂CO₂H), 52.0 (CHCH₃), 59.0 (OCH₂CH₂CO₂H), 95.3 (C-3), 121.9 (C-7), 127.2 (2 × C-Ar), 127.9 (2 × C-Ar), 128.0 (2 × C-Ar), 128.6 (C-Ar), 129.5 (2 × C-Ar), 130.0 (C-Ar q), 131.8 (C-6), 132.7 (C-Ar q), 133.7 (C-5), 135.3 (C-Ar q), 136.2 (C-Ar q), 140.4 (C-Ar q), 140.5 (C-Ar q), 166.6 (C-1), 175.8 (COOH); LRMS (ES⁺) *m/z* 470.3 [M+H]⁺; HRMS calcd for C₂₅H₂₀Cl₂NO₄ [M-H]⁻ 468.0775, found 468.0762; HPLC 99.2% in 0.1% formic acid (aq)/MeCN (*R*_t 9.2 min); 99.5% in 0.1% ammonia (aq)/MeCN (*R*_t 5.0 min).

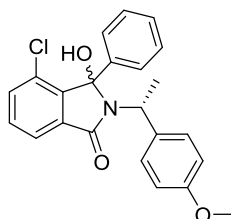
3-(Benzyloxy)-5-{bis{[1-(((*tert*-butyldiphenylsilyl)oxy)methyl]cyclopropyl)methoxy}methyl}isoxazole (288)



At -78 °C and under an inert atmosphere, triethylsilane was added to a solution of **286** in DCM. Boron trifluoride etherate was added dropwise and the solution was stirred at -78 °C for 20 min. Petrol (40 mL) was added at -78 °C followed by saturated NaHCO₃ (aq., 20 mL). The aqueous layer was extracted with DCM (40 mL). The combined organic layers were washed with brine (40 mL), dried (MgSO₄), filtered and evaporated. Purification by MPLC (gradient elution, 0→6→20% EtOAc/petrol) yielded the by-product **288** (colorless oil, 0.54 g, 35%), the aldehyde **281** (colorless oil, 210 mg, 58%) and the desired product **287** (colorless oil, 57 mg, 6%). *R*_f 0.21 (petrol); λ_{max} (EtOH)/nm 264; ν_{max}/cm⁻¹ (neat) 2856, 2930 and 3070 (w, aliphatic CH and -CH₂-); ¹H NMR (500 MHz; CDCl₃) δ_H 0.34 – 0.45 (8H, m, 4 × CH₂ cyclopropyl), 1.04 (18H, s, 6 × CH₃), 3.50 (4H, dd, *J* = 3.6, 10.2 Hz, 2 × CH₂OSi), 3.64 (4H, dd, *J* = 10.2, 19.5 Hz, CH₂OCH₂-isoxazole), 5.26 (2H, s, CH₂Ph), 5.56 (1H, s, OCHO), 5.91 (1H, s, H-4), 7.29 – 7.50 (17H, m, H-Ar), 7.58 – 7.70 (8H, m, H-Ar); ¹³C NMR (125 MHz; CDCl₃) δ_C 8.1 (2 × CH₂ cyclopropyl), 8.5 (2 × CH₂ cyclopropyl), 19.5 (2 × C q cyclopropyl), 22.3 (2 × C(CH₃)₃), 27.0 (6 × CH₃), 66.5 (CH₂OSi), 69.8 (CH₂O-CH-isoxazole), 71.7 (CH₂Ph),

94.8 (C-4), 95.4 (OCHO), 127.8 (6 × C-Ar), 128.3 (2 × C-Ar), 128.6 (C-Ar), 128.7 (2 × C-Ar), 129.7 (2 × C-Ar), 133.9 (C-Ar q), 135.7 (2 × C-Ar), 135.8 (2 × C-Ar), 136.0 (C-Ar q), 170.1 (C-5), 171.4 (C-3); HRMS calcd for C₅₃H₆₇N₂O₆Si₂ [M+NH₄]⁺ 883.4532, found 883.4534.

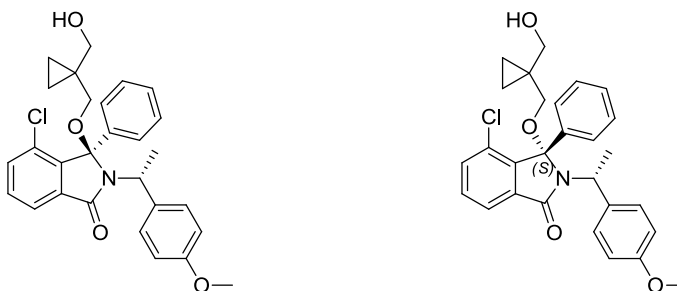
(1'*R*)-4-Chloro-3-hydroxy-2-[1'-(4''-methoxyphenyl)ethyl]-3-phenylisoindolin-1-one (258)



General procedure M was followed to synthesize isoindolinone **258** using the acid **183** (150 mg, 0.575 mmol), thionyl chloride (0.08 mL, 137 mg, 1.15 mmol), catalytic DMF (3 drops), (*R*)-(+)-1-(4-methoxyphenyl)ethylamine (0.09 mL, 96 mg, 0.633 mmol), DIPEA (0.22 mL, 164 mg, 1.27 mmol) and THF (2 × 0.7 mL). Purification by MPLC (gradient elution, 0-40% EtOAc/petrol) yielded the title compound (pale yellow oil, solidified upon storage at RT; 210 mg, 93%) as a mixture of diastereoisomers (dr 63:37). *R*_{f(1)} 0.30; *R*_{f(2)} 0.23 (25% EtOAc/petrol); m.p. 149.5-150.8; λ_{max} (EtOH)/nm 260; ν_{max}/cm⁻¹ (neat) 1671 (C=O), 3222 (br, O-H); ¹H NMR (500 MHz; CDCl₃) δ_H 1.56 (3H, d, *J* = 7.3 Hz), 1.75 (1H, d, *J* = 7.3 Hz), 3.01 (1H, s, OH), 3.06 (1H, s, OH), 3.71 (H, s, OCH₃), 3.76 (3H, s, OCH₃), 4.43 (1H, q, *J* = 7.3 Hz, CHCH₃), 4.70 (1H, q, *J* = 7.2 Hz, CHCH₃), 6.56 – 6.61 (2H, m, H-Ar), 6.74 – 6.82 (2H, m, H-Ar), 6.83 – 6.90 (2H, m, H-Ar), 7.24 (1H, m, H-Ar), 7.27 – 7.32 (2H, m, H-Ar), 7.34 – 7.45 (9H, m, H-Ar), 7.48 (2H, s, H-Ar), 7.52 – 7.57 (2H, m, H-Ar, H-Ar), 7.70 (2 H, m, H-Ar); ¹³C NMR (125 MHz; CDCl₃) δ_C 18.2 (CHCH₃), 19.6 (CHCH₃), 51.5 (CHCH₃), 52.0 (CHCH₃), 55.3 (OCH₃), 55.4 (OCH₃), 91.7 (C-3), 91.9 (C-3), 113.1 (C-Ar), 113.6 (C-Ar), 121.8 (C-Ar), 121.8 (C-Ar), 127.0 (C-Ar), 127.1 (C-Ar), 128.3 (C-Ar), 128.4 (C-Ar), 128.7 (C-Ar), 128.8 (C-Ar), 129.4 (C-Ar), 129.4 (C-Ar), 129.4 (C-Ar), 131.4 (C-Ar), 131.4 (C-Ar), 133.3 (C-Ar), 133.6 (C-Ar), 134.5 (C-Ar), 134.6 (C-Ar), 136.9 (C-Ar),

158.7 (C-Ar), 165.8 (C-Ar); LRMS (ES⁺) m/z 394.3 [M+H]⁺; HRMS calcd for C₂₃H₁₉³⁵ClNO₃ [M-H]⁻ 392.1059, found 392.1064.

(3*R*,1'*R*)-4-Chloro-3-{{1'''-(hydroxymethyl)cyclopropyl}methoxy}-2-[1'-(4''-methoxyphenyl)ethyl]-3-phenylisoindolin-1-one (259) and (3*S*,1'*R*)-4-chloro-3-{{1'''-(hydroxymethyl)cyclopropyl}methoxy}-2-[1'-(4''-methoxyphenyl)ethyl]-3-phenylisoindolin-1-one (260)



General procedure N was followed to obtain **259** and **260** using isoindolinone **258** (180 mg, 0.457 mmol), InBr₃ (32 mg, 0.0914 mmol), 1,1-bis(hydroxymethyl)cyclopropane (0.22 mL, 234 mg, 2.29 mmol) and DCE (4.6 mL). The reaction mixture was heated at 80 °C for 4 h. Purification by semi-preparative HPLC (55% MeCN/H₂O + 0.1% formic acid) yielded the desired compounds **259** (white amorphous solid; 66 mg, 30%) and **260** (colorless oil; 43 mg, 20%).

259

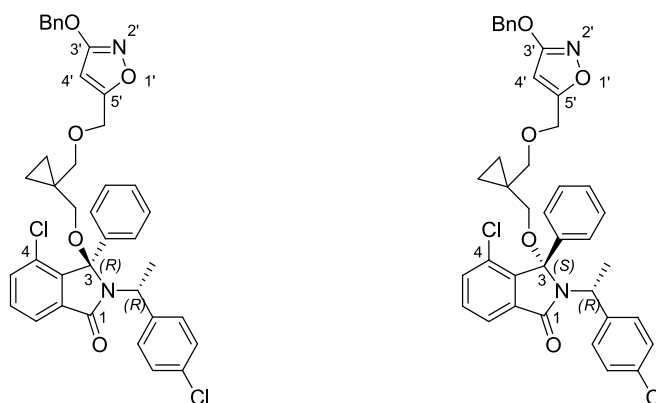
R_f 0.32 (50% EtOAc/petrol); no clear m.p. detected; $[\alpha]^{22}_D +122^\circ$ (c 0.643, EtOAc); λ_{max} (EtOH)/nm 260; ν_{max}/cm^{-1} (neat) 1686 and 1696 (s, C=O), 2874, 2932 and 3001 (w, aliphatic CH and -CH₂-), 3046 (br, O-H); ¹H NMR (500 MHz; CDCl₃) δ_H -0.01 – 0.08 (1H, m, cyclopropyl), 0.12 – 0.23 (1H, m, cyclopropyl), 0.29 – 0.41 (2H, m, cyclopropyl), 1.56 (3H, d, J = 7.3 Hz, CH₃), 1.72 (1H, ABX app. t, J = 5.5 Hz, OH), 2.72 (1H, d, J_{AB} = 9.1 Hz, CH_AH_BO-), 2.81 (1H, d, J_{AB} = 9.1 Hz, CH_AH_B-O), 3.33 (1H, dd, J_{AX} = 5.5 Hz, J_{AB} = 11.6 Hz, CH_AH_BOH), 3.38 (1H, dd, J_{BX} = 5.5 Hz, J_{AB} = 11.6 Hz, CH_AH_BOH), 3.78 (3H, s, OCH₃), 4.18 (1H, q, J = 7.3 Hz, CHCH₃), 6.80 – 6.87 (2H, m, H-Ar), 7.37 (5H, br, H-Ar), 7.41 (1H, d, J = 7.7 Hz, H-5), 7.47 (1H, t, J = 7.7 Hz, H-6), 7.51 – 7.57 (2H, m, H-Ar), 7.81 (1H, d, J = 7.7 Hz, H-7); ¹³C NMR (125 MHz; CDCl₃) δ_C 8.6 (CH₂ cyclopropyl), 8.7 (CH₂ cyclopropyl),

20.5 (CHCH₃), 22.1 (C q cyclopropyl), 53.5 (CHCH₃), 55.5 (OCH₃), 68.5 (CH₂OH), 68.6 (CH₂O-), 96.4 (C-3), 113.9 (2 × C-Ar), 121.9 (C-7), 127.2 (2 × C-Ar), 128.5 (2 × C-Ar), 128.9 (2 × C-Ar), 129.2 (2 × C-Ar), 129.5 (C-Ar q), 131.6 (C-6), 133.6 (C-5), 135.5 (C-Ar q), 135.5 (C-Ar q), 137.0 (C-Ar q), 140.9 (C-Ar q), 159.0 (C-Ar q), 166.9 (C-1); LRMS (ES⁺) *m/z* 500.4 [M+Na⁺]; HRMS calcd for C₂₈H₂₉ClNO₄ [M+H]⁺ 478.1780, found 478.1776; HPLC 99.4% in 0.1% formic acid (aq)/MeCN (*R*_t 9.2 min); 99.4% in 0.1% ammonia (aq)/MeCN (*R*_t 9.2 min).

260

*R*_f 0.32 (50% EtOAc/petrol); [α]_D²² +44° (*c* 0.562, EtOAc); λ_{\max} (EtOH)/nm 260; ν_{\max} /cm⁻¹ (neat) 1683 and 1694 (s, C=O), 2781, 2930 and 3069 (w, aliphatic CH and -CH₂-), 3407 (br, O-H); ¹H NMR (500 MHz; CD₃OD) δ _H 0.46 – 0.65 (4H, m, cyclopropyl), 1.88 (3H, d, *J* = 7.2 Hz, CHCH₃), 2.81 (1H, d, *J*_{AB} = 9.0, CH_AH_BO-), 3.50 (1H, d, *J*_{AB} = 11.1 Hz, CH_AH_BOH), 3.56 (1H, d, *J*_{AB} = 9.0 Hz, CH_AH_BO-), 3.66 (3H, s, OCH₃), 3.83 (1H, d, *J*_{AB} = 11.1 Hz, CH_AH_BOH), 4.43 (1H, q, *J* = 7.2 Hz, CHCH₃), 6.44 – 6.55 (2H, m, H-Ar), 6.79 – 6.88 (2H, m, H-Ar), 7.08 (4H, br, H-Ar), 7.13 – 7.22 (1H, m, H-Ar), 7.49 (1H, dd, *J* = 0.7, 7.7 Hz, H-5), 7.55 (1H, app. t, *J* = 7.7 Hz, H-6), 7.76 (1H, dd, *J* = 0.7, 7.7 Hz, H-7); ¹³C NMR (125 MHz; CDCl₃) δ _C 8.9 (CH₂ cyclopropyl), 9.1 (CH₂ cyclopropyl), 19.9 (CHCH₃), 22.7 (C q cyclopropyl), 52.1 (CHCH₃), 55.3 (OCH₃), 68.4 (CH₂OH), 68.6 (CH₂O-), 95.3 (C-3), 113.0 (2 × C-Ar), 121.9 (C-7), 127.3 (2 × C-Ar), 128.0 (2 × C-Ar), 128.5 (C-Ar), 129.3 (2 × C-Ar), 129.7 (C-Ar q), 131.6 (C-6), 133.4 (C-5), 134.3 (C-Ar q), 135.6 (C-Ar q), 136.5 (C-Ar q), 140.7 (C-Ar q), 158.4 (C-Ar q), 166.4 (C-1); LRMS (ES⁺) *m/z* 500.4 [M+Na]⁺; HRMS calcd for C₂₈H₂₉³⁵ClNO₄ [M+H]⁺ 478.1780, found 478.1775; HPLC 96.5% in 0.1% formic acid (aq)/MeCN (*R*_t 9.0 min); 97.4% in 0.1% ammonia (aq)/MeCN (*R*_t 9.0 min).

(3*R*,1'*R*)-3-{{1'''-[[[(3-(Benzyloxy)isoxazol-5-yl)methoxy]methyl]cyclopropyl}methoxy]-4-chloro-2-[1'-(4''-chlorophenyl)ethyl]-3-phenylisoindolin-1-one (278) and (*S*)-3-{{1'''-[[[(3-(benzyloxy)isoxazol-5-yl)methoxy]methyl]cyclopropyl}methoxy]-4-chloro-2-[1'-(4''-chlorophenyl)ethyl]-3-phenylisoindolin-1-one (275)



A modified general procedure N was followed to obtain **278** and **275** using the isoindolinone **198** (254 mg, 0.638 mmol), the alcohol **277** (277 mg, 0.957 mmol, 2.0 equiv.), InBr_3 (45 mg, 0.128 mmol) and DCE (2×3.2 mL). The reaction mixture was heated at 80 °C for 3 h. Purification by MPLC (gradient elution, 0-15% EtOAc/petrol) yielded the desired compounds **278** (156 mg, 37%) and **275** (180 mg, 42%) as colorless oils.

278

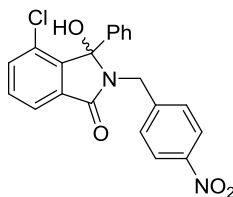
R_f 0.46 (25% EtOAc/petrol); λ_{max} (EtOH)/nm 258; ν_{max} /cm⁻¹ (neat) 1699 (vs, C=O), 2871, 2933 and 3064 (w, aliphatic CH and -CH₂-); ¹H NMR (500 MHz; CDCl₃) δ_H -0.02 – 0.05 (1H, m, cyclopropyl), 0.09 – 0.24 (1H, m, cyclopropyl), 0.24 – 0.41 (2H, m, cyclopropyl), 1.56 (3H, d, $J = 7.3$ Hz, CHCH₃), 2.50 (1H, d, $J_{AB} = 9.1$ Hz, CH_AH_BO-isoindolinone), 2.95 (1H, d, $J_{AB} = 9.1$ Hz, CH_ACH_BO-isoindolinone), 3.03 (1H, d, $J_{AB} = 9.6$ Hz, CH_AH_BOCH₂-isoxazole), 3.65 (1H, d, $J_{AB} = 9.6$ Hz, CH_AH_BOCH₂-isoxazole), 4.21 (1H, q, $J = 7.3$ Hz, CHCH₃), 4.29 – 4.41 (2H, AB q, $J_{AB} = 13.6$ Hz, CH₂-isoxazole), 5.25 (2H, s, CH₂Ph), 5.78 (1H, s, H-4'), 7.19 – 7.25 (2H, m, H-Ar), 7.29 – 7.47 (12H, m, H-Ar), 7.47 – 7.53 (2H, m, H-Ar), 7.78 (1H, dd, $J = 1.1, 7.4$ Hz, H-Ar); ¹³C NMR (125 MHz; CDCl₃) δ_C 8.1 (CH₂ cyclopropyl), 8.8 (CH₂ cyclopropyl), 19.9 (CHCH₃), 19.9 (C q cyclopropyl), 53.2

(CHCH₃), 64.0 (CH₂-isoxazole), 66.5 (CH₂O-isoindolinone), 71.7 (CH₂Ph), 74.9 (CH₂OCH₂-isoxazole), 94.5 (C-4'), 96.2 (C-3), 121.8 (C-Ar), 127.2 (C-Ar), 128.4 (C-Ar), 128.4 (C-Ar), 128.6 (C-Ar), 128.6 (C-Ar), 128.7 (C-Ar), 128.8 (C-Ar), 129.6 (C-Ar), 129.8 (C-Ar), 131.6 (C-Ar), 133.2 (C-Ar), 133.7 (C-Ar), 135.2 (C-Ar), 137.0 (C-Ar), 141.1 (C-Ar), 141.5 (C-Ar), 167.0 (C-1), 170.6 (C-5'), 171.7 (C-3'). One carbon not detected; LRMS (ES⁺) *m/z* 669.5 [M+H]⁺; HRMS calcd for C₃₈H₃₅³⁵Cl₂N₂O₅ [M+H]⁺ 669.1918, found 669.1917.

275

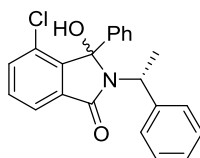
*R*_f 0.36 (25% EtOAc/petrol); λ_{max} (EtOH)/nm 258; ν_{max}/cm⁻¹ (neat) 1698 (vs, C=O), 2871, 2932, and 3064 (w, aliphatic CH and -CH₂-); ¹H NMR (500 MHz; CDCl₃) 0.46 – 0.68 (4H, m, cyclopropyl), 1.88 (3H, d, *J* = 7.3 Hz, CHCH₃), 2.86 (1H, d, *J*_{AB} = 9.1 Hz, CH_AH_BO-isoindolinone), 3.40 (1H, d, *J*_{AB} = 9.1 Hz, CH_AH_BO-isoindolinone), 3.55 (1H, d, *J*_{AB} = 9.7 Hz, CH_AH_BOCH₂-isoxazole), 3.70 (1H, d, *J*_{AB} = 9.7 Hz, CH_AH_BOCH₂-isoxazole), 4.35 (1H, d, *J* = 7.3 Hz, CHCH₃), 4.44 – 4.59 (2H, m, CH₂-isoxazole), 5.24 (2H, s, CH₂Ph), 5.88 (1H, s, H-4'), 6.84 – 6.91 (2H, m, H-Ar), 6.91 – 6.96 (2H, m, H-Ar), 7.08 (4H, br, H-Ar), 7.15 – 7.21 (1H, m, H-Ar), 7.31 – 7.48 (7H, m, H-Ar), 7.75 (1H, dd, *J* = 1.0, 7.5 Hz, H-Ar); ¹³C NMR (125 MHz; CDCl₃) δ_C 9.0 (CH₂ cyclopropyl), 9.1 (CH₂ cyclopropyl), 19.7 (CHCH₃), 20.5 (C q cyclopropyl), 52.1 (CHCH₃), 64.1 (CH₂-isoxazole), 66.8 (CH₂O-isoindolinone), 71.7 (CH₂Ph), 75.0 (CH₂OCH₂-isoxazole), 94.7 (C-4'), 94.9 (C-3), 121.8 (C-Ar), 127.3 (C-Ar), 127.8 (C-Ar), 128.0 (C-Ar), 128.4 (C-Ar), 128.5 (C-Ar), 128.7 (C-Ar), 128.7 (C-Ar), 129.4 (C-Ar), 129.5 (C-Ar), 129.8 (C-Ar), 131.6 (C-Ar), 132.6 (C-Ar), 133.5 (C-Ar), 135.4 (C-Ar), 135.8 (C-Ar), 136.6 (C-Ar), 140.7 (C-Ar), 140.8 (C-Ar), 166.5 (C-1), 170.5 (C-5'), 171.7 (C-3'); LRMS (ES⁺) *m/z* 669.5 [M+H]⁺; HRMS calcd for C₃₈H₃₅Cl₂N₂O₅ [M+H]⁺ 669.1918, found 669.1906.

4-Chloro-3-hydroxy-2-[1'-(4''-nitrophenyl)ethyl]-3-phenylisoindolin-1-one (268)



General procedure M was followed to obtain isoindolinone **268** using the acid **183** (223 mg, 0.855 mmol), thionyl chloride (0.12 mL, 203 mg, 1.71 mmol), catalytic DMF (3 drops), 4-nitrobenzylamine hydrochloride (177 mg, 0.941 mmol), DIPEA (0.33 mL, 243 mg, 1.88 mmol) and THF (2 × 1.0 mL). Purification by MPLC (gradient elution, 0-80% EtOAc/petrol) yielded the desired product **268** (0.26 g, 77%) as a pale yellow solid. R_f 0.14 (25% EtOAc/petrol); m.p. 210.1-211.4°C; λ_{\max} (EtOH)/nm 271; $\nu_{\max}/\text{cm}^{-1}$ (neat) 1510 (s, NO₂), 1660 and 1680 (s, C=O), 3206 (br, O-H); ¹H NMR (500 MHz; DMSO-*d*₆) δ_H 4.31 (1H, d, J_{AB} = 16.3 Hz, CH_ACH_B), 4.52 (1H, d, J_{AB} = 16.3 Hz, CH_ACH_B), 7.24 (5H, m, H-Ar), 7.34 – 7.41 (3H, m, H-Ar and OH), 7.59 – 7.64 (2H, m, H-Ar), 7.78 (1H, dd, J = 2.5, 5.9 Hz, H-Ar), 7.97 – 8.03 (2H, m, H-Ar); ¹³C NMR (125 MHz; DMSO-*d*₆) δ_C 41.6 (CH₂), 90.3 (C-3), 121.6 (C-Ar), 122.9 (2 × C-Ar), 126.4 (2 × C-Ar), 128.1 (2 × C-Ar), 128.2 (C-Ar), 128.7 (C-Ar), 128.8 (2 × C-Ar), 131.7 (C-Ar), 133.2 (C-Ar), 133.7 (C-Ar), 137.4 (C-Ar), 144.7 (C-Ar q), 145.8 (C-Ar q), 146.2 (C-Ar q), 165.5 (C-1); LRMS (ES⁻) m/z 393.2 [M-H]⁻; HRMS calcd for C₂₁H₁₄ClN₂O₄ [M-H]⁻ 393.0648, found 393.0639.

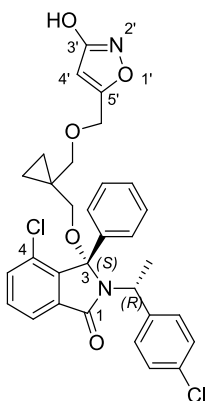
(1'*R*)-4-Chloro-3-hydroxy-3-phenyl-2-(1-phenylethyl)isoindolin-1-one (217)



General procedure M was followed to obtain isoindolinone **217** using the acid **183** (150 mg, 0.575 mmol), thionyl chloride (0.08 mL, 137 mg, 1.15 mmol), catalytic DMF (3 drops), (*R*)-(+)- α -methylbenzylamine (0.08 mL, 77 mg, 0.633

mmol), DIPEA (0.11 mL, 82 mg, 0.633 mmol) and THF (2×0.7 mL). Purification by MPLC (gradient elution, 0-10% EtOAc/petrol) yielded the desired product **217** (182 mg, 87%; dr 59:41) as a yellow oil which solidified upon storage at RT. $R_{f(1)}$ 0.47; $R_{f(2)}$ 0.39 (25% EtOAc/petrol); m.p. 133.0-133.8°C; λ_{\max} (EtOH)/nm 259; $\nu_{\max}/\text{cm}^{-1}$ (neat) 1669 (vs, C=O), 3218 (br, O-H); ^1H NMR (500 MHz; CDCl_3) δ_{H} 1.58 (3H, d, $J = 7.3$ Hz, CHCH_3), 1.80 (3H, d, $J = 7.3$ Hz, CHCH_3), 2.94 (1H, s, OH), 3.18 (1H, s, OH), 4.46 (1H, q, $J = 7.3$ Hz, CHCH_3), 4.74 (1H, q, $J = 7.3$ Hz, CHCH_3), 6.95 – 7.02 (2H, m, H-Ar), 7.03 – 7.11 (3H, m, H-Ar), 7.17 – 7.24 (3H, m, H-Ar), 7.24 – 7.32 (2H, m, H-Ar), 7.34 – 7.45 (9H, m, H-Ar), 7.48 (4H, br, H-Ar), 7.55 – 7.64 (2H, m, H-Ar), 7.68 – 7.76 (1H, m, H-Ar); ^{13}C NMR (125 MHz; CDCl_3) δ_{C} 18.2 (CH_3), 19.6 (CH_3), 52.1 (CHCH_3), 52.6 (CHCH_3), 91.7 (C-3), 91.9 (C-3), 121.8 (C-Ar), 121.9 (C-Ar), 126.9 (C-Ar), 127.0 (C-Ar), 127.1 (C-Ar), 127.4 (C-Ar), 127.9 (C-Ar), 128.0 (C-Ar), 128.1 (C-Ar), 128.2 (C-Ar), 128.4 (C-Ar), 128.4 (C-Ar), 128.7 (C-Ar), 128.8 (C-Ar), 129.4 (C-Ar), 129.5 (C-Ar), 131.4 (C-Ar), 133.6 (C-Ar), 133.7 (C-Ar), 134.4 (C-Ar), 134.4 (C-Ar), 136.8 (C-Ar), 136.9 (C-Ar), 141.3 (C-Ar), 142.4 (C-Ar), 143.8 (C-Ar), 165.9 (C-1); LRMS (ES^-) m/z 362.2 $[\text{M}-\text{H}]^-$; HRMS calcd for $\text{C}_{22}\text{H}_{17}\text{ClNO}_2$ $[\text{M}-\text{H}]^-$ 362.0953, found 362.0946.

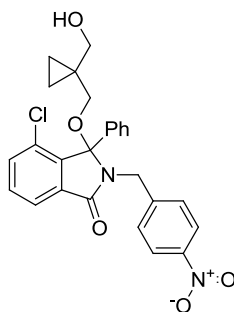
(3*S*,1'*R*)-4-Chloro-2-[1'-(4''-chlorophenyl)ethyl]-3-{{1'''-[[3-hydroxyisoxazol-5-yl)methoxy]methyl}cyclopropyl}methoxy]-3-phenylisoindolin-1-one (276)



Under an inert atmosphere, a solution of **275** (40 mg, 0.0597 mmol) in DCM (0.14 mL) was added to a suspension of $\text{Pd}(\text{OAc})_2$ (0.6 mg, 0.0030 mmol), triethylamine (0.01 mL, 8.5 mg, 0.0836 mmol) and triethylsilane (0.4 μL , 0.3 mg,

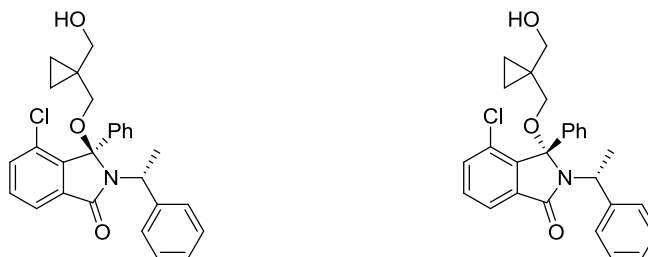
0.0030 mmol) in DCM (0.27 mL) and the mixture was stirred at RT for 18 h. Upon completion of the reaction, the mixture was quenched with saturated NH_4Cl (aq., 1.2 mL) and extracted with EtOAc (3×5 mL). The combined organic layers were washed with brine, filtered over a Thiol MP SPE cartridge, dried (MgSO_4) and concentrated *in vacuo*. Purification by MPLC (gradient elution, 0–88% EtOAc/petrol + 0.1% formic acid) yielded the desired product **276** (18 mg, 52%) as a colorless oil. R_f 0.51 (50% EtOAc/petrol + 0.1% formic acid); no clear m.p. detected; $[\alpha]_D^{22} +53$ (c 0.577, EtOAc); λ_{max} (EtOH)/nm 258; $\nu_{\text{max}}/\text{cm}^{-1}$ (neat) 1689 (s, C=O), 2627, 2799 and 2869 (w, aliphatic CH and $-\text{CH}_2-$), 3000 (br, O-H); ^1H NMR (500 MHz; CDCl_3) δ_{H} 0.50 – 0.66 (4H, m, cyclopropyl), 1.88 (3H, d, $J = 7.3$ Hz, CHCH_3), 2.90 (1H, d, $J_{\text{AB}} = 9.1$ Hz, $\text{CH}_\text{A}\text{H}_\text{B}\text{O}-$), 3.36 (1H, d, $J_{\text{AB}} = 9.1$ Hz, $\text{CH}_\text{A}\text{H}_\text{B}\text{O}-$), 3.58 (1H, d, $J_{\text{AB}} = 9.7$ Hz, $\text{CH}_\text{A}\text{H}_\text{B}-\text{OCH}_2$), 3.65 (1H, d, $J_{\text{AB}} = 9.7$ Hz, $\text{CH}_\text{A}\text{H}_\text{B}-\text{OCH}_2$), 4.33 (1H, q, $J = 7.3$ Hz, CHCH_3), 4.44 – 4.57 (2H, m, OCH_2 -isoxazole), 5.90 (1H, s, H-4'), 6.83 – 6.90 (2H, m, H-Ar), 6.90 – 6.96 (2H, m, H-Ar), 7.02 (4H, br, H-Ar), 7.15 – 7.21 (1H, m, H-Ar), 7.39 (1H, dd, $J = 1.0, 7.7$ Hz, H-5), 7.45 (1H, app. t, $J = 7.7$ Hz, H-6), 7.76 (1H, dd, $J = 1.0, 7.7$ Hz, H-7); ^{13}C NMR (125 MHz; CDCl_3) δ_{C} 8.9 (CH_2 cyclopropyl), 8.9 (CH_2 cyclopropyl), 19.5 (CHCH_3), 20.3 (C q cyclopropyl), 51.9 (CHCH_3), 63.9 (isoxazole- CH_2 -O), 66.6 ($\text{CH}_2\text{O}-$), 75.0 (CH_2 - OCH_2), 94.8 (C-4'), 95.1 (C-3), 121.7 (C-7), 127.1 ($2 \times$ C-Ar), 127.7 ($2 \times$ C-Ar), 127.8 ($2 \times$ C-Ar), 128.4 (C-Ar), 129.3 ($2 \times$ C-Ar), 129.7 (C-Ar q), 131.5 (C-6), 132.4 (C-Ar q), 133.4 (C-5), 135.2 (C-Ar q), 136.4 (C-Ar q), 140.6 (C-Ar q), 166.5 (C-1), 170.2 (C-5'), 170.8 (C-3') ppm. One quaternary carbon not detected; LRMS (ES^+) m/z 579.4 $[\text{M}+\text{H}]^+$; HRMS calcd for $\text{C}_{31}\text{H}_{29}^{35}\text{Cl}_2\text{N}_2\text{O}_5$ $[\text{M}+\text{H}]^+$ 579.1448, found 579.1444; HPLC 96.3% in 0.1% formic acid (aq)/MeCN (R_t 9.9 min); 96.5% in 0.1% ammonia (aq)/MeCN (R_t 5.8 min).

4-Chloro-3-{[1'''-(hydroxymethyl)cyclopropyl]methoxy}-2-(4''-nitrobenzyl)-3-phenylisoindolin-1-one (269)



General procedure N was followed to obtain **269** using the isoindolinone **186** (370 mg, 0.937 mmol), 1,1-bis(hydroxymethyl)cyclopropane (0.45 mL, 479 mg, 4.69 mmol.), InBr_3 (66 mg, 0.187 mmol) and DCE (9.5 mL). The reaction mixture was heated at 80 °C for 5 h. Purification on C18 silica (gradient elution, 5-90% MeCN/ H_2O + 0.1% formic acid) yielded the desired compound **269** (0.370 g, 82%) as a pale yellow oil. R_f 0.34 (5% MeOH/DCM); m.p. 174-176 °C; λ_{max} (EtOH)/nm 269; $\nu_{\text{max}}/\text{cm}^{-1}$ (neat) 1342 (vs, NO_2), 1699 (s, C=O), 2872, 2922 and 3077 (w, aliphatic CH and $-\text{CH}_2-$), 3419 (br, O-H); ^1H NMR (500 MHz; CDCl_3) δ_{H} 0.14 – 0.25 (1H, m, cyclopropyl), 0.31 – 0.44 (1H, m, cyclopropyl), 0.44 – 0.57 (2H, m, cyclopropyl), 1.76 (1H, t, $J = 5.4$ Hz, OH), 2.93 (1H, d, $J_{\text{AB}} = 9.1$ Hz, $\text{CH}_\text{A}\text{H}_\text{BO}-$), 2.96 (1H, d, $J_{\text{AB}} = 9.1$ Hz, $\text{CH}_\text{AH}_\text{BO}-$), 3.54 (2H, d, $J = 5.4$ Hz, CH_2OH), 4.44 (1H, d, $J_{\text{AB}} = 15.2$ Hz, $\text{CH}_\text{AH}_\text{B}-\text{Ar}$), 4.51 (1H, d, $J_{\text{AB}} = 15.2$ Hz, $\text{CH}_\text{AH}_\text{B}-\text{Ar}$), 7.19 (5H, m, H-Ar), 7.21 – 7.25 (2H, m, H-Ar), 7.48 (1H, dd, $J = 1.1, 7.7$ Hz, H-5), 7.53 (1H, t, $J = 7.7$ Hz, H-6), 7.86 (1H, dd, $J = 1.1, 7.7$ Hz, H-7), 7.92 – 7.98 (2H, m, H-Ar); ^{13}C NMR (125 MHz; CDCl_3) δ_{C} 8.8 (CH_2 cyclopropyl), 8.9 (CH_2 cyclopropyl), 22.4 (C q cyclopropyl), 42.2 (CH_2 -Ar), 68.1(CH_2OH), 68.3 ($\text{CH}_2\text{O}-$), 94.9 (C-3), 122.4 (C-7), 123.4 ($2 \times \text{C-Ar}$), 126.8 ($2 \times \text{C-Ar}$), 128.5 ($2 \times \text{C-Ar}$), 129.0 (C-Ar), 129.9 ($2 \times \text{C-Ar}$), 130.1 (C-Ar), 132.0 (C-6), 134.2 (C-5), 136.3 (C-Ar q), 141.1 (C-Ar q), 144.5 (C-Ar q), 147.1 (C-Ar q), 167.0 (C-1). One quaternary carbon not detected; LRMS (ES^-) m/z 477.3 [M-H] $^-$; HRMS calcd for $\text{C}_{26}\text{H}_{24}^{35}\text{ClN}_2\text{O}_5$ [M+H] $^+$ 479.368, found 479.1366; HPLC 96.3% in 0.1% formic acid (aq)/MeCN (R_t 8.7 min); 96.9% in 0.1% ammonia (aq)/MeCN (R_t 8.7 min).

(3*R*,1'*R*)-4-Chloro-3-[[1'''-(hydroxymethyl)cyclopropyl]methoxy]-3-phenyl-2-(1'-phenylethyl)isoindolin-1-one (218) and (3*S*,1'*R*)-4-chloro-3-[[1'''-(hydroxymethyl)cyclopropyl]methoxy]-3-phenyl-2-(1'-phenylethyl)isoindolin-1-one (219)



General procedure N was followed to obtain **218** and **219** using the isoindolinone **217** (160 mg, 0.440 mmol), 1,1-bis(hydroxymethyl)cyclopropane (0.21 mL, 225 mg, 2.20 mmol.), InBr₃ (31 mg, 0.0880 mmol) and DCE (4.4 mL). The reaction mixture was heated at 80 °C for 18 h. The diastereoisomers were separated by MPLC (gradient elution, 0-2% MeOH/DCM) to yield the desired compound **219** (42 mg, 21%) as white amorphous solid. The isoindolinone **218** was further purified on C18 silica (gradient elution, 10-80% MeCN/H₂O + 0.1% formic acid) to afford the pure compound (39 mg, 20%) as a colorless oil.

218

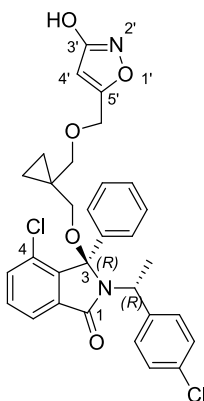
R_f 0.52 (5% MeOH/DCM); R_f 0.41 (80% MeCN/H₂O + 0.1% formic acid); $[\alpha]_D^{22} +105^\circ$ (c 0.474, EtOAc); λ_{max} (EtOH)/nm 258; ν_{max}/cm^{-1} (neat) 1689 and 1699 (s, C=O), 2873, 2933, 3002 and 3063 (w, aliphatic CH and -CH₂-), 3407 (br, O-H); ¹H NMR (500 MHz; CDCl₃) δ_H -0.15 – -0.06 (1H, m, cyclopropyl), 0.07 – 0.17 (1H, m, cyclopropyl), 0.30 (2H, m, cyclopropyl), 1.58 (1H, dd, J = 5.6, 6.8 Hz, OH), 1.61 (3H, d, J = 7.3 Hz, CHCH₃), 2.69 (1H, d, J_{AB} = 9.1 Hz, CH_AH_BO-), 2.81 (1H, d, J_{AB} = 9.1 Hz, CH_AH_BO-), 3.24 – 3.36 (2H, m, CH₂OH), 4.20 (1H, q, J = 7.3 Hz, CHCH₃), 7.22 – 7.25 (1H, m, H-Ar), 7.29 – 7.35 (2H, m, H-Ar), 7.38 (5H, br, H-Ar), 7.42 (1H, dd, J = 0.9, 7.7 Hz, H-5), 7.48 (1H, app. t, J = 7.7 Hz, H-6), 7.56 – 7.62 (2H, m, H-Ar), 7.83 (1 H, dd, J = 0.9, 7.7 Hz, H-7); ¹³C NMR (125 MHz; CDCl₃) δ_C 8.5 (CH₂ cyclopropyl), 8.6 (CH₂ cyclopropyl), 20.6 (CHCH₃), 22.1 (C q cyclopropyl), 54.3 (CHCH₃), 68.3 (CH₂OH), 68.4 (CH₂O-), 96.5 (C-3), 122.0 (C-7), 127.2 (2 × C-Ar), 127.5 (C-Ar), 127.9 (2 × C-Ar), 128.5 (2 × C-Ar), 128.7 (2 × C-

Ar), 128.9 (C-Ar), 129.6 (C-Ar q), 131.6 (C-6), 133.6 (C-5), 135.4 (C-Ar q), 137.0 (C-Ar q), 140.9 (C-Ar q), 143.5 (C-Ar q), 167.1 (C-1); LRMS (ES⁺) *m/z* 470.4 [M+Na]⁺; HRMS calcd for C₂₇H₂₇³⁵ClNO₃ [M+H]⁺ 448.1674, found 448.1665; HPLC 98.8% in 0.1% formic acid (aq)/MeCN (*R*_t 9.3 min); 98.7% in 0.1% ammonia (aq)/MeCN (*R*_t 9.3 min).

219

*R*_f 0.38 (5% MeOH/DCM); m.p. 183-185 °C; [α]_D²² -10° (*c* 0.464, EtOAc); λ_{max} (EtOH)/nm 259; ν_{max} /cm⁻¹ (neat) 1684 (vs, C=O), 2870 and 2914 (w, aliphatic CH and -CH₂-), 3509 (m sharp, O-H); ¹H NMR (500 MHz; CDCl₃) δ_{H} 0.46 – 0.70 (4H, m, cyclopropyl), 1.92 (3H, d, *J* = 7.3 Hz, CHCH₃), 1.94 – 1.99 (1H, m, OH), 3.05 (1H, d, *J*_{AB} = 9.2 Hz, CH_AH_BO-), 3.33 (1H, d, *J*_{AB} = 9.2 Hz, CH_AH_BO-), 3.64 – 3.79 (2H, m, CH₂OH), 4.43 (1H, q, *J* = 7.3 Hz, CHCH₃), 6.90 – 7.12 (9H, m, C-Ar), 7.13 – 7.19 (1H, m, C-Ar), 7.41 (1H, dd, *J* = 0.7, 7.6 Hz, H-5), 7.46 (1H, app. t, *J* = 7.6 Hz, H-6), 7.78 (1H, dd, *J* = 0.7, 7.6 Hz, H-7); ¹³C NMR (125 MHz; CDCl₃) δ_{C} 8.9 (CH₂ cyclopropyl), 9.1 (CH₂ cyclopropyl), 20.0 (CHCH₃), 22.7 (C q cyclopropyl), 52.9 (CHCH₃), 68.4 (CH₂OH), 68.6 (CH₂-O), 95.3 (C-3), 121.9 (C-7), 126.8 (2 × C-Ar), 127.2 (2 × C-Ar), 127.8 (2 × C-Ar), 127.9 (2 × C-Ar), 128.5 (C-Ar), 129.7 (C-Ar q), 131.6 (C-6), 133.5 (C-5), 135.5 (C-Ar q), 136.4 (C-Ar q), 140.7 (C-Ar q), 142.2 (C-Ar q), 166.6 (C-1). One quaternary carbon not detected; LRMS (ES⁺) *m/z* 448.3 [M+H]⁺; HRMS calcd for C₂₇H₂₇³⁵ClNO₃ [M+H]⁺ 448.1674, found 448.1672; HPLC 98.6% in 0.1% formic acid (aq)/MeCN (*R*_t 9.2 min); 99.0% in 0.1% ammonia (aq)/MeCN (*R*_t 9.2 min).

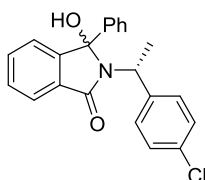
(3*R*,1'*R*)-4-Chloro-2-[1'-(4''-chlorophenyl)ethyl]-3-{{1-[[[(3-hydroxyisoxazol-5-yl)methoxy]methyl]cyclopropyl]methoxy}-3-phenylisoindolin-1-one (164)



Under an inert atmosphere, a solution of **278** (141 mg, 0.211 mmol) in DCM (0.49 mL) was added to a suspension of Pd(OAc)₂ (2.4 mg, 0.0106 mmol), triethylamine (0.04 mL, 29.9 mg, 0.295 mmol) and triethylsilane (1.6 μ L, 1.2 mg, 0.0106 mmol) in DCM (0.95 mL) and the mixture was stirred at RT for 7 h. Upon completion of the reaction, the mixture was quenched with saturated NH₄Cl (aq., 5 mL) and extracted with EtOAc (3 \times 15 mL). The combined organic layers were washed with brine, filtered over a Thiol MP SPE cartridge, dried (MgSO₄) and concentrated *in vacuo*. Purification by MPLC (gradient elution, 0-80% EtOAc/petrol + 0.1% formic acid) yielded the desired product **164** (32 mg, 26%) as a colorless oil. *R*_f 0.44 (50% EtOAc/petrol + 0.1% formic acid); no clear m.p. detected; $[\alpha]_D^{22} +104$ (*c* 0.341, EtOAc); λ_{\max} (EtOH)/nm 253; ν_{\max} /cm⁻¹ (neat) 1699 (s, C=O), 2867 and 2932 (w, aliphatic CH and -CH₂-), 3000 (br, OH); ¹H NMR (500 MHz; CDCl₃) δ _H -0.01 – 0.09 (1H, m, cyclopropyl), 0.12 – 0.22 (1H, m, cyclopropyl), 0.26 – 0.40 (2H, m cyclopropyl), 1.56 (3H, d, *J* = 7.3 Hz, CHCH₃), 2.47 (1H, d, *J*_{AB} = 9.2 Hz, CH_AH_B-O), 2.97 (1H, d, *J*_{AB} = 9.2 Hz, CH_AH_B-O), 3.00 (1H, d, *J*_{AB} = 9.6 Hz, CH_AH_B-OCH₂), 3.66 (1H, d, *J*_{AB} = 9.6 Hz, CH_AH_B-OCH₂), 4.21 (1H, q, *J* = 7.3 Hz, CHCH₃), 4.28 – 4.41 (2H, m, OCH₂-isoxazole), 5.79 (1 H, s, H-4 isoxazole), 7.20 – 7.25 (2 H, m, H-Ar), 7.35 (5 H, br, Ph), 7.39 (1 H, dd, *J* 7.9, 0.8, H-5), 7.46 (1 H, app. t, *J* 7.8, H-6), 7.47 – 7.54 (2 H, m, H-Ar), 7.80 (1 H, dd, *J* 7.5, 0.8, H-7); ¹³C NMR (125 MHz; CDCl₃) δ _C 8.1 (CH₂ cyclopropyl), 8.9 (CH₂ cyclopropyl), 19.9 (CHCH₃), 53.2 (CHCH₃), 63.9 (isoxazole-CH₂-O), 66.46 (CH₂-

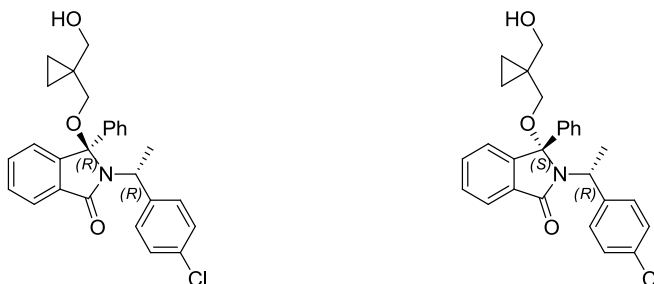
O), 75.1 (CH₂-OCH₂), 95.0 (C-4'), 96.2 (C-3), 121.9 (C-7), 127.2 (2 × C-Ar), 128.4 (2 × C-Ar), 128.6 (2 × C-Ar), 128.8 (C-Ar), 129.6 (2 × C-Ar), 129.8 (C-Ar), 131.6 (C-6), 133.2 (C-Ar q), 133.8 (C-5), 135.2 (C-Ar q), 137.0 (C-Ar q), 141.0 (C-Ar q), 141.5 (C-Ar q), 167.1 (C-1), 170.5 (C-5'), 170.9 (C-3 isoxazole). One quaternary carbon not detected; LRMS (ES⁺) *m/z* 579.4 [M+H]⁺; HRMS calcd for C₃₁H₂₉³⁵Cl₂N₂O₅ [M+H]⁺ 579.1448, found 579.1443; HPLC 95.9% in 0.1% formic acid (aq)/MeCN (*R*_t 9.9 min); 96.8% in 0.1% ammonia (aq)/MeCN (*R*_t 5.7 min).

(1'*R*)-2-[1'-(4''-chlorophenyl)ethyl]-3-hydroxy-3-phenylisoindolin-1-one (220)



General procedure M was followed to obtain isoindolinone **220** using the acid **189** (150 mg, 0.663 mmol), thionyl chloride (0.10 mL, 157 mg, 1.33 mmol), catalytic DMF (3 drops), (*R*)-4-chloro- α -methylbenzylamine (0.10 mL, 113 mg, 0.729 mmol), DIPEA (0.13 mL, 94 mg, 0.729 mmol) and THF (2 × 0.8 mL). Purification by MPLC (gradient elution, 0-25% EtOAc/petrol) yielded the desired product **220** (206 mg, 85%; dr 50:50) as a white solid. *R*_{f(1)} 0.71; *R*_{f(2)} 0.53 (33% EtOAc/petrol); m.p. 162.9-164.9 °C; λ_{max} (EtOH)/nm 253sh; ν_{max} /cm⁻¹ (neat) 1660 (vs, C=O), 3218 (br, O-H); ¹H NMR (500 MHz; DMSO-*d*₆) δ_{H} 1.45 (3H, d, *J* = 7.2 Hz, CHCH₃), 1.74 (3H, d, *J* = 7.1 Hz, CHCH₃), 4.41 (1H, q, *J* = 7.2 Hz, CHCH₃), 4.54 (1H, q, *J* = 7.1 Hz, CHCH₃), 7.01 – 7.06 (2H, m, H-Ar), 7.10 – 7.15 (2H, m, H-Ar), 7.21 – 7.25 (3H, m, H-Ar), 7.25 – 7.36 (6H, m, H-Ar), 7.38 (4H, m, H-Ar), 7.47 – 7.59 (7H, m, H-Ar), 7.65 – 7.73 (2H, m, H-Ar); ¹³C NMR (125 MHz; DMSO-*d*₆) δ_{C} 17.7 (CH₃), 19.7 (CH₃), 49.9 (CHCH₃), 50.5 (CHCH₃), 90.9 (C-3), 91.0 (C-3), 122.2 (C-Ar), 122.3 (C-Ar), 122.9 (C-Ar), 126.2 (C-Ar), 126.3 (C-Ar), 127.4 (C-Ar), 127.5 (C-Ar), 128.0 (C-Ar), 128.3 (C-Ar), 129.2 (C-Ar), 129.3 (C-Ar), 130.9 (C-Ar), 131.0 (C-Ar), 131.2 (C-Ar), 132.5 (C-Ar), 140.0 (C-Ar), 141.2 (C-Ar), 149.0 (C-Ar), 166.0 (C-1), 166.5 (C-1); LRMS (ES⁺) *m/z* 364.3 [M+H]⁺; HRMS calcd for C₂₂H₁₇³⁵ClNO₂ [M-H]⁻ 362.0953, found 362.0955.

(3*R*,1'*R*)-2-[1'-(4''-Chlorophenyl)ethyl]-3-{[1'''-(hydroxymethyl)cyclopropyl]methoxy}-3-phenylisoindolin-1-one (221)
and (3*S*,1'*R*)-2-[1'-(4''-chlorophenyl)ethyl]-3-{[1'''-(hydroxymethyl)cyclopropyl]methoxy}-3-phenylisoindolin-1-one (222)



General procedure N was followed to obtain **221** and **222** using the isoindolinone **220** (200 mg, 0.550 mmol), 1,1-bis(hydroxymethyl)cyclopropane (0.26 mL, 281 mg, 2.75 mmol.), InBr₃ (39 mg, 0.110 mmol) and DCE (5.5 mL). The reaction mixture was heated at 80 °C for 18 h. The diastereoisomers were separated by MPLC (gradient elution, 0-20% EtOAc/petrol) to yield the desired compounds **221** (81 mg, 33%) and **222** (51 mg, 21%) as white amorphous solids. A mixture of the two compounds was also recovered (57 mg, 23%).

221

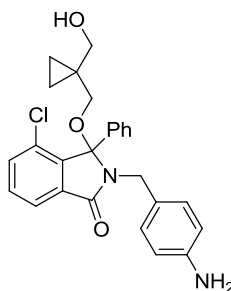
R_f 0.33 (33% EtOAc/petrol); no clear m.p. detected; $[\alpha]_D^{22} +102$ (c 0.694, EtOAc); λ_{max} (EtOH)/nm 253; ν_{max}/cm^{-1} (neat) 1681 and 1695 (vs, C=O), 2875, 2933, 2978 and 3060 (w, aliphatic CH and -CH₂-), 3396 (br, O-H); ¹H NMR (500 MHz; CDCl₃) δ_H -0.02 – 0.08 (2H, m, cyclopropyl), 0.27 – 0.41 (2H, m, cyclopropyl), 1.63 – 1.65 (1H, ABX m, OH), 1.66 (3H, d, $J = 7.2$ Hz, CHCH₃), 2.56 (1H, d, $J_{AB} = 9.5$ Hz, CH_AH_BO-), 2.74 (1H, d, $J_{AB} = 9.5$, CH_AH_B-O), 3.26 (1H, dd, $J_{AX} = 5.3$ hz, $J_{AB} = 11.3$ Hz, CH_AH_BOH), 3.41 (1H, dd, $J_{BX} = 6.1$ Hz, $J_{AB} = 11.3$ Hz, CH_AH_BOH), 4.24 (1H, q, $J = 7.3$ Hz, CHCH₃), 7.03 – 7.12 (1H, m, H-4), 7.22 – 7.29 (2H, m, H-Ar), 7.31 – 7.39 (3H, m, H-Ar), 7.43 (2H, br, H-Ar), 7.46 – 7.52 (2H, m, H-5 and H-6), 7.54 – 7.61 (2H, m, H-Ar), 7.85 (1H, m, H-7); ¹³C NMR (125 MHz; CDCl₃) δ_C 8.7 (CH₂ cyclopropyl), 8.7 (CH₂ cyclopropyl), 20.1 (CHCH₃), 22.2 (C q cyclopropyl), 53.6 (CHCH₃), 68.2 (CH₂-O), 68.4 (CH₂OH), 96.6 (C-3), 123.0 (C-7), 123.4 (C-4), 126.6 (CHCH₃), 128.4 (CH₂-O), 128.6 (2 × C-Ar), 128.8 (2 × C-Ar), 128.8 (C-Ar), 129.7 (2 × C-Ar),

129.9 (C-5 or C-6), 132.6 (C-Ar q), 132.9 (C-5 or C-6), 133.2 (C-Ar q), 138.9 (C-Ar q), 141.9 (C-Ar q), 145.3 (C-Ar q), 168.5 (C-1). One quaternary carbon not detected; HRMS calcd for $C_{27}H_{27}^{35}ClNO_3$ $[M+H]^+$ 448.1674, found 448.1667; HPLC 96.7% in 0.1% formic acid (aq)/MeCN (R_t 9.4 min); 96.4% in 0.1% ammonia (aq)/MeCN (R_t 9.4 min).

222

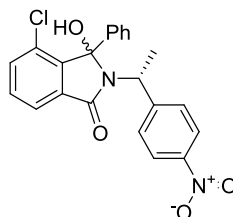
R_f 0.23 (33% EtOAc/petrol); no clear m.p. detected; $[\alpha]_D^{22}$ -5 (c 0.750, EtOAc); λ_{max} (EtOH)/nm 259; ν_{max}/cm^{-1} (neat) 1680 and 1695 (vs, C=O), 2873, 2928 and 3070 (w, aliphatic CH and $-CH_2-$), 3386 (br, O-H); 1H NMR (500 MHz; $CDCl_3$) δ_H 0.35 – 0.45 (1H, m, cyclopropyl), 0.47 – 0.53 (1H, m, cyclopropyl), 0.53 – 0.63 (2H, m, cyclopropyl), 1.82 (1H, t, $J = 5.7$ Hz, OH), 1.90 (3H, d, $J = 7.3$ Hz, $CHCH_3$), 2.96 (1H, d, $J_{AB} = 9.5$ Hz, CH_AH_BO-), 3.31 (1H, d, $J_{AB} = 9.5$ Hz, CH_AH_B-O), 3.64 (2H, d, $J = 5.7$ Hz, CH_2OH), 4.40 (1H, q, $J = 7.3$ Hz, $CHCH_3$), 6.89 – 7.00 (4H, m, H-Ar), 7.02 – 7.15 (5H, m, $4 \times$ H-Ph and H-4), 7.17 (1H, m, H-Ph), 7.44 – 7.52 (2H, m, H-5 and H-6), 7.79 – 7.89 (1H, m, H-7); ^{13}C NMR (125 MHz; $CDCl_3$) δ_C 8.9 (CH_2 cyclopropyl), 9.0 (CH_2 cyclopropyl), 20.0 ($CHCH_3$), 22.7 (C q cyclopropyl), 52.3 ($CHCH_3$), 68.0 (CH_2O-), 68.3 (CH_2OH), 95.4 (C-3), 123.1 (C-7), 123.4 (C-4), 127.0 ($2 \times$ C-Ar), 127.9 ($2 \times$ C-Ar), 128.1 ($2 \times$ C-Ar), 128.5 (C-Ar), 129.5 ($2 \times$ C-Ar), 130.0 (C-5 or C-6), 132.6 (C-Ar q), 132.8 (C-5 or C-6), 138.3 (C-Ar q), 141.2 (C-Ar q), 145.0 (C-Ar q), 168.2 (C-1). Two carbons not detected; HRMS calcd for $C_{27}H_{27}^{35}ClNO_3$ $[M+H]^+$ 448.1674, found 448.1671; HPLC 99.0% in 0.1% formic acid (aq)/MeCN (R_t 9.4 min); 98.1% in 0.1% ammonia (aq)/MeCN (R_t 9.4 min).

2-(4''-Aminobenzyl)-4-chloro-3-{{1'''-(hydroxymethyl)cyclopropyl}methoxy}-3-phenylisoindolin-1-one (270)



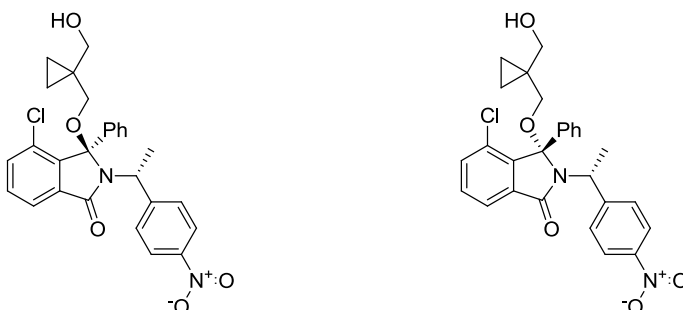
A solution of **269** (50 mg, 0.104 mmol) in ethanol (3.5 mL, 34 mL/mmol) and THF (1.6 mL, 15 mL/mmol) was passed over a 10% Pd/C catalyst cartridge embedded in a Thales H-cube. Flow rate, H₂ pressure, at RT (full H₂ mode, 2 h 45 min). Upon completion of the reaction, the solvent was removed *in vacuo*. The crude product was purified by MPLC (gradient elution on amine silica from .0-50% EtOAc/petrol) to obtain the title compound as an off-white solid (28 mg, 60%). *R_f* 0.32 (75% EtOAc/petrol); no clear m.p. detected; λ_{\max} (EtOH)/nm no maximum of absorption; ν_{\max} /cm⁻¹ (neat) 1685 (vs, C=O), 3356 (m, NH₂); ¹H NMR (500 MHz; CDCl₃) δ_{H} 0.06 – 0.15 (1H, m, cyclopropyl), 0.23 – 0.31 (1H, m, cyclopropyl), 0.34 – 0.42 (2H, m, cyclopropyl), 2.76 – 2.84 (2H, m, CH₂O-), 3.33 – 3.46 (2H, m, CH₂OH), 3.60 (2H, br, NH₂), 3.79 (1H, d, *J* = 14.9 Hz, CH_AH_B-Ar), 4.61 (1H, d, *J* = 14.9 Hz, CH_AH_B-Ar), 6.49 – 6.56 (2H, m, H-Ar), 6.98 – 7.06 (2H, m, H-Ar), 7.32 (5H, br, H-Ar), 7.42 (1H, dd, *J* = 7.7, 1.1 Hz, H-5), 7.47 (1H, d, *J* = 7.7 Hz, H-6), 7.84 (1 H, dd, *J* = 7.7, 1.1 Hz, H-7); ¹³C NMR (125 MHz; CDCl₃) δ_{C} 8.7 (CH₂ cyclopropyl), 8.8 (CH₂ cyclopropyl), 22.2 (C q cyclopropyl), 42.8 (CH₂-Ar), 68.4 (CH₂O- and CH₂OH), 95.6 (C-3), 114.9 (2 × C-Ar), 122.2 (C-7), 127.0 (2 × C-Ar), 127.4 (C-Ar), 128.4 (2 × C-Ar), 128.7 (2 × C-Ar), 129.7 (C-Ar q), 130.4 (2 × C-Ar), 131.6 (C-6), 133.7 (C-5), 134.7 (C-Ar q), 136.7 (C-Ar q), 141.4 (C-Ar q), 145.8 (C-Ar q), 166.92 (C-1); LRMS (ES⁺) *m/z* 471.1 [M+Na]⁺; HRMS calcd for C₂₆H₂₆³⁵ClN₂O₃ [M+H]⁺ 449.1626, found 449.1627; HPLC 96.2% in 0.1% formic acid (aq)/MeCN (*R_t* 6.1 min); 87.5% in 0.1% ammonia (aq)/MeCN (*R_t* 7.6 min).

(1'*R*)-4-Chloro-3-hydroxy-2-[1'-(4''-nitrophenyl)ethyl]-3-phenylisoindolin-1-one (265)



General procedure M was followed to synthesize isoindolinone **265** using the acid **183** (292 mg, 1.12 mmol), thionyl chloride (0.16 mL, 266 mg, 2.24 mmol), catalytic DMF (3 drops), (*R*)- α -methyl-4-nitrobenzylamine hydrochloride (250 mg, 1.23 mmol), DIPEA (0.43 mL, 318 mg, 2.46 mmol) and THF (2×1.3 mL). Purification by MPLC (gradient elution, 0-80% EtOAc/petrol) yielded the title compound (dr 53:47; 0.40 g, 87%) as an off-white solid. $R_{f(1)}$ 0.32; $R_{f(2)}$ 0.16 (25% EtOAc/petrol); m.p. 204.0-206.6 °C; λ_{\max} (EtOH)/nm 272; $\nu_{\max}/\text{cm}^{-1}$ (neat) 1514 (m, NO₂), 1658 and 1675 (m, C=O), 3213 (br, O-H); ¹H NMR (500 MHz; DMSO-*d*₆) δ_{H} 1.41 (3H, d, $J = 7.2$ Hz, CHCH₃), 1.79 (3H, d, $J = 7.2$ Hz, CHCH₃), 4.51 (1H, q, $J = 7.2$ Hz, CHCH₃), 4.66 (1H, q, $J = 7.2$ Hz, CHCH₃), 7.12 – 7.31 (7H, m, H-Ar), 7.31 – 7.46 (5H, m, H-Ar), 7.47 (1H, s, H-Ar), 7.52 (1H, s, H-Ar), 7.56 – 7.65 (4H, m, H-Ar), 7.68 (1H, dd, $J = 2.1, 6.4$ Hz, H-Ar), 7.70 – 7.78 (3H, m, H-Ar), 7.86 – 7.94 (2H, m, H-Ar), 8.09 – 8.17 (2H, m, H-Ar); ¹³C NMR (125 MHz; DMSO-*d*₆) δ_{C} 17.3 (CH₃), 19.3 (CH₃), 49.7 (CHCH₃), 50.2 (CHCH₃), 90.5 (C-3), 121.3 (C-Ar), 122.6 (C-Ar), 122.9 (C-Ar), 126.4 (C-Ar), 126.6 (C-Ar), 127.9 (C-Ar), 128.2 (C-Ar), 128.3 (C-Ar), 128.6 (C-Ar), 131.6 (C-Ar), 131.6 (C-Ar), 133.5 (C-Ar), 133.9 (C-Ar), 134.2 (C-Ar), 137.5 (C-Ar), 137.6 (C-Ar), 144.2 (C-Ar), 145.9 (C-Ar), 149.6 (C-Ar), 149.7 (C-Ar), 164.5 (C-1), 165.1 (C-1); LRMS (ES⁻) m/z 407.3 [M-H]⁻; HRMS calcd for C₂₂H₁₆ClN₂O₄ [M-H]⁻ 407.0804, found 407.0795.

(3*R*,1'*R*)-4-Chloro-3-{[1'''-(hydroxymethyl)cyclopropyl]methoxy}-2-[1'-(4''-nitrophenyl)ethyl]-3-phenylisoindolin-1-one (261) and (3*S*,1'*R*)-4-chloro-3-{[1-(hydroxymethyl)cyclopropyl]methoxy}-2-[1-(4-nitrophenyl)ethyl]-3-phenylisoindolin-1-one (266)



General procedure N was followed to obtain **261** and **266** using the isoindolinone **265** (342 mg, 0.837 mmol), 1,1-bis(hydroxymethyl)cyclopropane (0.40 mL, 428 mg, 4.19 mmol.), InBr_3 (59 mg, 0.167 mmol) and DCE (8.4 mL). The reaction mixture was heated at 80 °C for 18 h. The diastereoisomers were separated by MPLC (gradient elution, 0-30% EtOAc/petrol) to yield the desired compounds **261** (155 mg, 37%) and **266** (224 mg, 54%) as off-white amorphous solids.

261

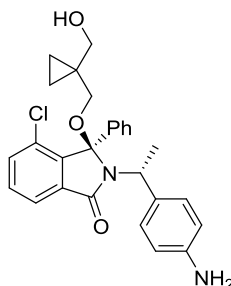
R_f 0.70 (50% EtOAc/petrol); no clear m.p. detected; $[\alpha]_D^{29} +128$ (c 0.434, EtOAc); λ_{max} (EtOH)/nm 269; $\nu_{\text{max}}/\text{cm}^{-1}$ (neat) 1519 (s, NO_2), 1698 (s, C=O), 2874, 2935 and 3002 (w, aliphatic CH and $-\text{CH}_2-$), 3408(br, O-H); ^1H NMR (500 MHz; CDCl_3) δ_{H} -0.05 – 0.04 (1H, m, cyclopropyl), 0.23 – 0.32 (1H, m, cyclopropyl), 0.37 – 0.54 (2H, m, cyclopropyl), 1.69 (3H, d, $J = 7.3$ Hz, CHCH_3), 1.80 (1H, br, OH), 2.80 (1H, d, $J = 9.1$ Hz, $\text{CH}_\text{A}\text{H}_\text{B}\text{O}-$), 3.00 (1H, d, $J = 9.1$ Hz, $\text{CH}_\text{A}\text{H}_\text{B}-\text{O}$), 3.41 (1H, d, $J = 11.5$ Hz, $\text{CH}_\text{A}\text{H}_\text{B}-\text{OH}$), 3.54 (1H, d, $J = 11.5$ Hz, $\text{CH}_\text{A}\text{H}_\text{B}-\text{OH}$), 4.51 (1H, q, $J = 7.3$ Hz, CHCH_3), 7.48 (5H, br, H-Ar), 7.55 (1H, dd, $J = 7.7, 1.1$ Hz, H-5), 7.61 (1H, app. t, $J = 7.7$, H-6), 7.82 – 7.89 (2H, m, H-Ar), 7.93 (1H, dd, $J = 7.7, 1.1$ Hz, H-7), 8.21 – 8.29 (2H, m, H-Ar); ^{13}C NMR (125 MHz; CDCl_3) δ_{C} 8.6 (CH_2 cyclopropyl), 8.7 (CH_2 cyclopropyl), 19.5 (CHCH_3), 22.2 (C q cyclopropyl), 53.1 (CHCH_3), 68.2 (CH_2 -OH), 68.6 (CH_2 -O), 96.4 (C-3), 122.2 (C-7), 123.8, 127.1 ($2 \times$ C-Ar), 128.6 ($2 \times$ C-

Ar), 129.1 (2 × C-Ar), 129.1 (C-Ar), 129.8 (C-Ar q), 131.9, 134.0 (C-5), 134.9 (C-Ar q), 136.5 (C-Ar q), 140.8 (C-Ar q), 147.3 (C-Ar q), 167.1 (C-1); LRMS (ES⁺) *m/z* 515.3 [M+Na]⁺; HRMS calcd for C₂₇H₂₆³⁵ClN₂O₅ [M+H]⁺ 493.1525, found 493.1522; HPLC 96.7% in 0.1% formic acid (aq)/MeCN (*R*_t 8.8 min); 96.7% in 0.1% ammonia (aq)/MeCN (*R*_t 8.8 min).

266

*R*_f 0.50 (50% EtOAc/petrol); no clear m.p. detected; [α]_D²⁹ +31 (*c* 0.462, EtOAc); λ_{max} (EtOH)/nm 271; ν_{max}/cm⁻¹ (neat) 1516 (s, NO₂), 1696 and 1698 (s, C=O), 2872, 2932 and 3002 (w, aliphatic CH and -CH₂-), 3395 (br, O-H); ¹H NMR (500 MHz; CDCl₃) δ_H: 0.48 – 0.60 (2H, m, cyclopropyl), 0.60 – 0.72 (2H, m, cyclopropyl), 1.84 (1H, app. t, *J* = 5.6 Hz, OH), 1.96 (3H, d, *J* = 7.2 Hz, CHCH₃), 3.02 (1H, d, *J* = 9.1 Hz, CH_AH_BO-), 3.39 (1H, d, *J* = 9.1 Hz, CH_AH_BO-), 3.67 (1H, dd, *J* = 11.4, 5.6 Hz, CH_AH_B-OH), 3.77 (1H, dd, *J* = 11.4, 5.6 Hz, CH_AH_B-OH), 4.49 (1H, q, *J* = 7.3 Hz, CHCH₃), 7.07 (4H, br, H-Ar), 7.10 – 7.15 (2H, m, H-Ar), 7.15 – 7.20 (1H, m, H-Ar), 7.45 (1H, dd, *J* = 7.7, 1.5 Hz, H-5), 7.50 (1H, app. t, *J* = 7.7 Hz, H-6), 7.80 (1H, dt, *J* = 7.7, 1.5 Hz, H-7), 7.81 – 7.86 (2 H, m, H-Ar); ¹³C NMR (125 MHz; CDCl₃) δ_C 8.9 (CH₂ cyclopropyl), 9.1 (CH₂ cyclopropyl), 19.6 (CHCH₃), 22.7 (C q cyclopropyl), 52.1 (CHCH₃), 68.1 (CH₂-OH), 68.4 (CH₂-O), 95.0 (C-3), 122.0 (C-7), 123.1 (2 × C-Ar), 127.0 (2 × C-Ar), 128.2 (2 × C-Ar), 128.8 (2 × C-Ar), 128.9 (C-Ar), 129.9 (C-Ar q), 131.9 (C-6), 133.8 (C-5), 135.1 (C-Ar q), 136.4 (C-Ar q), 140.4 (C-Ar q), 146.7 (C-Ar q), 149.6 (C-Ar q), 166.7 (C-1); LRMS (ES⁺) *m/z* 515.2 [M+Na]⁺; HRMS calcd for C₂₇H₂₆³⁵ClN₂O₅ [M+H]⁺ 493.1525, found 493.1520; HPLC 98.9% in 0.1% formic acid (aq)/MeCN (*R*_t 9.0 min); 99.1% in 0.1% ammonia (aq)/MeCN (*R*_t 9.0 min).

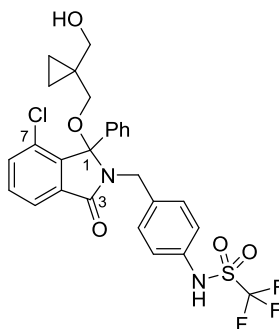
(3*R*,1'*R*)-2-[1'-(4''-Aminophenyl)ethyl]-4-chloro-3-{[1'''-(hydroxymethyl)cyclopropyl]methoxy}-3-phenylisoindolin-1-one (262)



A solution of **261** (72 mg, 0.146 mmol) in ethanol (5.0 mL, 34 mL/mmol) and THF (2.2 mL, 15 mL/mmol) was passed over a 10% Pd/C catalyst cartridge embedded in a Thales H-cube. Flow rate, H₂ pressure, at RT (full H₂ mode, 2 h 45 min). Upon completion of the reaction, the solvent was removed *in vacuo*. The crude product (white solid; 371 mg, 96%) was purified by MPLC (gradient elution on amine silica from .0-50% EtOAc/petrol) to obtain the title compound as a yellow oil (67 mg, 99%). *R*_f 0.16 (50% EtOAc/petrol); [α]_D²⁷ +122 (*c* 0.356, EtOAc); λ_{max} (EtOH)/nm no maximum of absorption; ν_{max} /cm⁻¹ (neat) 1684 (vs, C=O), 2871, 2927 and 3000 (w, aliphatic CH and -CH₂-), 3356 (m, NH₂); ¹H NMR (500 MHz; CDCl₃) δ_{H} -0.04 – 0.05 (1H, m, cyclopropyl), 0.11 – 0.17 (1H, m, cyclopropyl), 0.22 – 0.29 (2H, m, cyclopropyl), 1.45 (3H, d, *J* = 7.3 Hz, CHCH₃), 2.64 (1H, d, *J* = 9.1 Hz, CH_AH_BO-), 2.73 (1H, d, *J* = 9.1 Hz, CH_AH_BO-), 3.18 – 3.32 (2H, m, CH₂OH), 3.54 (2H, br, NH₂), 4.01 (1H, q, *J* = 7.3 Hz, CHCH₃), 6.48 – 6.58 (2H, m, H-Ar), 7.22 – 7.34 (8H, m, 7 × H-Ar, H-5), 7.34 – 7.41 (1H, app. t, *J* = 7.7 Hz, H-6), 7.71 (1H, dd, *J* = 7.7, 1.0 Hz, H-7); ¹³C NMR (125 MHz; CDCl₃) δ_{C} 8.6 (CH₂ cyclopropyl), 8.6 (CH₂ cyclopropyl), 20.5 (CHCH₃), 22.1 (C q cyclopropyl), 53.6 (CHCH₃), 68.3 (CH₂-OH and CH₂O-), 96.3 (C-3), 114.9 (2 × C-Ar), 121.8 (C-Ar), 127.0 (2 × C-Ar), 128.3 (2 × C-Ar), 128.7 (C-Ar), 128.9 (2 × C-Ar), 129.4 (C-Ar q), 131.4 (C-Ar), 133.2 (C-Ar q), 133.4 (C-Ar), 135.5 (C-Ar q), 136.9 (C-Ar q), 140.8 (C-Ar q), 145.6 (C-Ar q), 166.8 (C-1); LRMS (ES⁺) *m/z* 482.4 [M+Na]⁺ 485.4; HRMS calcd for C₂₇H₂₈³⁵ClN₂O₃ [M+H]⁺ 463.1783, found 463.1781; HRMS calcd for C₂₆H₂₆³⁵ClN₂O₃ [M+H]⁺ 449.1626, found 449.1627; HPLC 95.7% in

0.1% formic acid (aq)/MeCN (R_t 6.6 min); 90.1% in 0.1% ammonia (aq)/MeCN (R_t 7.5 min).

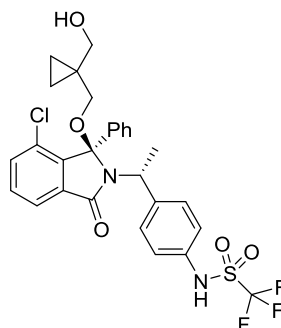
***N*-{4-[[7-Chloro-1-[(1''''-(hydroxymethyl)cyclopropyl)methoxy]-3-oxo-1-phenylisoindolin-2-yl]methyl]phenyl}-1,1,1-trifluoromethanesulfonamide (271)**



Aniline **270** (45 mg, 0.100 mmol) was dissolved in DCM (0.4 mL, 4mL/mmol) and DIPEA (0.05 mL, 39 mg, 0.300 mmol) was added at 0 °C followed by Tf₂O (25.5 μ L, 42 mg, 0.150 mmol). The mixture was stirred at 0 °C for 10 min and at RT for 45 min. A solution of NaOH in MeOH (2.5 M, 0.2 mL) and the solution was stirred for 30 min at RT. The mixture was partitioned between DCM (5 mL) and HCl (aq., 1 M, 2 mL). The aqueous layer was extracted with DCM (5 mL) and the combined organic layers were washed with HCl (aq., 1 M, 2 mL), brine (5 mL), dried (MgSO₄) and the solvent was removed *in vacuo*. The crude product was purified by MPLC (gradient elution on amine silica from .0-55% EtOAc/petrol) to obtain the title compound as a yellow oil (12 mg, 21%). R_f 0.30 (50% EtOAc/petrol); λ_{max} (EtOH)/nm no maximum of absorption; ν_{max}/cm^{-1} (neat) 1210 (s, C-F), 1375 (s, SO₂^{str}), 1683 (s, C=O), 2780, 2876 and 2921 (w, aliphatic CH and -CH₂-), 3495 (br, O-H); ¹H NMR (500 MHz; CDCl₃) δ_H -0.03 – 0.05 (1H, m, cyclopropyl), 0.14 – 0.20 (1H, m, cyclopropyl), 0.27 – 0.34 (2H, m, cyclopropyl), 1.67 (1H, br, OH), 2.72 (1H, d, J = 9.1 Hz, CH_AH_BO-), 2.79 (1H, d, J = 9.1 Hz, CH_AH_BO-), 3.31 (1H, d, J = 11.5 Hz, CH_AH_BOH), 3.37 (1H, d, J = 11.5 Hz, CH_AH_BOH), 4.09 (1H, d, J = 15.1 Hz, CH_AH_B-Ar), 4.33 (1H, d, J = 15.1 Hz, CH_AH_B-Ar), 6.87 – 6.93 (2H, m, H-Ar), 6.96 – 7.02 (2H, m, H-Ar), 7.05 – 7.12 (5H, m, H-Ar), 7.32 (1H, dd, J = 7.7, 1.0 Hz, H-5), 7.37 (1H, d, J 7.7 Hz, H-6), 7.72 (1H, dd, J

7.7, 1.0 Hz, H-7).; ^{13}C NMR (125 MHz; CDCl_3) δ_{C} 8.7 (CH_2 cyclopropyl), 8.7 (CH_2 cyclopropyl), 22.2 (C q cyclopropyl), 42.5 ($\text{CH}_2\text{-Ar}$), 68.2 (CH_2OH), 68.4 ($\text{CH}_2\text{O-}$), 95.4 (C-3), 118.7, 121.3, 122.4, 123.4, 126.8, 128.5, 129.0, 130.0, 130.1, 132.0, 133.5, 134.1, 136.1, 141.2, 167.4 (C-1); LRMS (ES^-) m/z 579.3 [M-H] $^-$; HRMS calcd for $\text{C}_{27}\text{H}_{24}\text{ClF}_3\text{N}_2\text{O}_5\text{S}$ [$\text{M}+\text{NH}_4$] $^+$ 598.1385, found 598.1371; HPLC 95.9% in 0.1% formic acid (aq)/MeCN (R_t 8.9 min); 97.7% in 0.1% ammonia (aq)/MeCN (R_t 5.4 min).

(3*R*,1'*R*)-*N*-{4-{1-[7-chloro-1-[(1-(hydroxymethyl)cyclopropyl)methoxy]-3-oxo-1-phenylisoindolin-2-yl]ethyl}phenyl}-1,1,1-trifluoromethanesulfonamide (263)



Aniline **262** (40 mg, 0.0864 mmol) was dissolved in DCM (0.35 mL, 4mL/mmol) and DIPEA (44 μL , 33 mg, 0.259 mmol) was added at 0 $^\circ\text{C}$ followed by Tf_2O (35 μL , 60 mg, 0.216 mmol). The mixture was stirred at 0 $^\circ\text{C}$ for 10 min and at RT for 45 min. A solution of NaOH in MeOH (2.5 M, 0.2 mL) and the solution was stirred for 30 min at RT. The mixture was partitioned between DCM (5 mL) and HCl (aq., 1 M, 2 mL). The aqueous layer was extracted with DCM (5mL) and the combined organic layers were washed with HCl (aq., 1 M, 2 mL), brine (5 mL), dried (MgSO_4) and the solvent was removed *in vacuo*. The crude product was purified by MPLC (gradient elution on amine silica from .0-55% EtOAc/petrol) to obtain the title compound as a yellow oil (8 mg, 16%). R_f 0.34 (50% EtOAc/petrol); λ_{max} (EtOH)/nm no maximum of absorption; $\nu_{\text{max}}/\text{cm}^{-1}$ (neat) 1213 (s, C-F), 1374 (s, SO_2^{str}), 1677 (s, C=O), 2930 (w, aliphatic CH and $-\text{CH}_2-$), 3030 (br, O-H); ^1H NMR (500 MHz; CDCl_3) δ_{H} -0.04 – 0.04 (1H, m, cyclopropyl), 0.13 – 0.23 (1H, m, cyclopropyl), 0.29 – 0.40 (2H, m, cyclopropyl), 1.53 (3H, d, *J*

= 7.2 Hz, CHCH₃), 2.75 (1H, d, *J* = 9.1 Hz, CH_AH_BO-), 2.91 (1H, d, *J* = 9.1 Hz, CH_AH_BO-), 3.28 (1H, d, *J* = 11.5 Hz, CH_AH_BOH), 3.43 (1H, d, *J* = 11.5 Hz, H_AH_BOH), 4.28 (1H, q, *J* = 7.2 Hz, CHCH₃), 7.20 – 7.25 (2H, m, H-Ar), 7.29 – 7.40 (5H, m, H-Ar), 7.44 (1H, dd, *J* = 7.7, 1.0 Hz, H-5), 7.50 (1H, d, *J* = 7.7 Hz H-6), 7.54 – 7.59 (2H, m, H-Ar), 7.87 (1H, dd, *J* = 7.7, 1.0 Hz, H-7); ¹³C NMR (125 MHz; CDCl₃) δ_C 8.4 (CH₂ cyclopropyl), 8.5 (CH₂ cyclopropyl), 19.9 (CHCH₃), 22.0 (CHCH₃), 53.2 (CHCH₃), 68.3 (CH₂-OH), 68.4 (CH₂-O), 96.6 (C-3), 122.2 (C-7), 123.6 (2 × C-Ar), 127.1 (2 × C-Ar), 128.6 (2 × C-Ar), 129.1 (C-Ar q), 129.2 (2 × C-Ar), 129.7, 131.9 (C-6), 133.6 (C-Ar q), 134.0 (C-5), 134.9 (C-Ar q), 136.4 (C-Ar q), 140.8 (C-Ar q), 141.7 (C-Ar q), 167.4 (C-1); LRMS (ES⁻) *m/z* 593.3 [M-H]⁻; HRMS calcd for C₂₇H₂₄ClF₃N₂O₅S [M+NH₄]⁺ 612.1541, found 612.1538.

9.4 Structural biology experimental

9.4.1 General procedures

Media supplementation

All cultures were supplemented with an antibiotic, according to the antibiotic selectivity of the pGEX-6P-1 vector and *E. coli* strain used during recombinant protein expression. During IPTG-based induction of protein expression, the lactose analogue IPTG was added to the culture to induce protein expression. Appropriate amounts of IPTG (200 mM) and ampicillin (50 mg/mL) were dissolved in sterile 18.2 MΩ/cm H₂O, before storing at -20 °C until required. Chloramphenicol (34 mg/mL) was dissolved in 100% ethanol and stored at -20 °C.

mHBS buffer

To prepare the mHBS buffer, 20 mL of aq. NaCl (5 M), 5 mL of aq. DTT (1 M) and 20 mL of aq. HEPES (1 mM, pH 7.4) were used in 1 L of solution and the pH was brought to 7.4 by addition of aq. NaOH (10 M). The buffer was filtered and degassed before use and, if required, stored at 4 °C for no longer than one week.

Glutathione elution buffer

To prepare the glutathione elution buffer, glutathione (0.123g) was dissolved in mHBS (20 mL) and the pH was brought to 7.4 by addition of aq. NaOH (10 M). The buffer was stored at 4 °C and used immediately after preparation.

Polyacrylamide gel electrophoresis

SDS-PAGE was used for protein identification and semi-quantitative analysis. Pre-cast 12-well acrylamide gels (RunBlue; 12% for GST-MDMX/GST-MDM2 and 16% for MDMX/MDM2) were used with SDS run buffer (RunBlue). Samples were mixed with SDS loading buffer (RunBlue) and denatured at 100 °C for 5 min before being loaded onto the gel. PageRuler pre-stained protein ladder (10-170 kDa, Thermo Scientific) was used. Electrophoresis was carried out at 180 V and gels were stained with InstantBlue™ protein stain.

9.4.2 Expression from MDMX and MDM2 gene constructs

Transformation of competent Rosetta™ BL21(DE3) pLysS *E. coli*

To allow protein expression, the pre-prepared pGEX-6P-1 plasmid encoding for the desired construct (provided by Jane Endicott and Martin Noble) was transformed into chemically competent Rosetta™ BL21 (DE3) pLysS *E. coli*. Competent cells were mixed with 1 µL of plasmid and incubated on ice for 30 min. The cells were transferred to a water bath at 42 °C for 30 sec, before incubating on ice for 2 min. The cells were recovered through aseptic addition of 200 µL super optimal broth with catabolite repression (SOC) medium and incubated at 37 °C, 200 rpm for 1 h. The recovered cells were aseptically plated onto LB-agar plates supplemented with ampicillin and chloramphenicol and incubated overnight at 37 °C to allow growth of transformed bacterial colonies.

Recombinant MDMX expression following IPTG induction

Transformed Rosetta™ BL21(DE3) pLysS *E. coli* colonies were used to inoculate starter cultures containing 10 mL of Terrific Broth (TB), supplemented with ampicillin (20 µL) and chloramphenicol (10 µL). The starter cultures were incubated overnight at 37 °C, 200 rpm before aseptic transfer of a 1% (v/v) inoculum into an appropriate volume of expression media, supplemented with

antibiotics. The culture was incubated at 37 °C, 160 rpm and the optical density (OD) of the culture was monitored by spectrometry during growth. Once an OD_{600 nm} of 0.6-1.0 was reached, 200 mM IPTG (1 mL) was added to the culture to induce protein expression. The culture was incubated at 20 °C, 160 rpm overnight.

Recombinant MDM2 expression following IPTG induction

BL21 (DE3) *E. coli* glycerol stocks for MDM2^{K51A}₁₇₋₁₂₅ and MDM2^{E69K70A}₁₇₋₁₂₅ were prepared previously by Judith Reeks and stored at -80 °C. A glycerol stock of BL21 (DE3) pLysS *E. coli* for MDM2^{E69K70A}₁₇₋₁₀₈ was prepared and stored similarly. Transformed BL21 *E. coli* cells were inoculated in starter cultures containing 10 mL of LB, supplemented with ampicillin (20 µL) (BL21 (DE3)) or ampicillin (20 µL) and chloramphenicol (10 µL) (BL21 (DE3) pLysS). The starter cultures were incubated overnight at 37 °C, 200 rpm, before aseptic transfer of a 1% (v/v) inoculum into an appropriate volume of expression media, supplemented with chloramphenicol (1 mL) and/or ampicillin (1 mL). The culture was incubated at 37 °C, 160 rpm, whilst the optical density of the culture was monitored during growth. Once an OD_{600 nm} of 0.6-1.0 was reached, 200 mM IPTG (1 mL) was added to the culture to induce protein expression. The culture was incubated at 20 °C, 160 rpm overnight.

Cell harvesting

Following culture, the *E. coli* cells were harvested by centrifugation (5000 × g, 15 min, 4°C) to give a pellet which was resuspended in mHBS supplemented with a protease inhibitor tablet (Roche; 1 tablet/40 mL), flash-frozen in dry ice and stored at -20 °C until further use.

9.4.3 Protein purification

The resuspended cell pellets were thawed under running water and lysozyme (400 µL of 25 mg/mL stock), RNAase A (200 µL of 10 mg/mL stock), DNAase I (200 µL of 2 mg/mL stock) and MgCl₂ (100 µL of 2 M stock) were added before sonication (30% amplitude; 20 sec on/40 sec off intervals for 15 min) whilst on ice. The lysed cells were centrifuged (45,000 × g, 60 min, 4°C) and the

supernatant (cell-free extract, CFE) was decanted from the pellet and retained. Diluted CFE samples were heated at 100 °C for 5 min and then analyzed by SDS-PAGE to establish whether the target protein had been overexpressed.

The supernatant was incubated overnight at 4 °C with glutathione Sepharose 4B resin (GE Healthcare, bed volume 2 mL). The mixture was loaded by gravity flow into a column and washed twice with mHBS (15 mL). The GST-MDMX (or GST-MDM2) was eluted with a fresh solution of glutathione in mHBS (20 mL). 3C protease (50:1 protein:3C protease by weight) was added to cleave MDMX or MDM2 from the GST tag and the mixture was incubated overnight at 4 °C. The desired protein was separated from the GST tag using gel filtration chromatography (Äkta Superdex 75 26/60, isocratic flow of mHBS, Äkta FPLC Chromatographic system, UV absorbance 280 nm).

The protein concentration was measured using a UV-vis spectrophotometer NanoDrop 2000 (Thermo Scientific).

9.4.4 Protein preparation for crystallography

The purified protein was incubated overnight at 4 °C with a 1.5× molar excess of inhibitor (20 mM stock in DMSO). Protein mixtures were concentrated using Amicon® Ultra-15 (Millipore) centrifugal filter devices (5000 × g, 4 °C) to a concentration between 5 and 10 mg/mL, if possible.

Crystallization trays were set up in 2-subwell 96-well plates by pipetting commercial screens (JCSG+ from Molecular Dimensions and the AmSO4 Suite from Qiagen) from deep well blocks prior to protein addition. Protein mixture and precipitant were mixed in the subwells by a Mosquito® robot (100 + 100 nL, 200 + 100 nL, precipitant:protein) using the sitting drop method. Plates were sealed and stored in the Minstrel (Rigaku) automated high-throughput monitoring system at 4 °C for up to five weeks. Crystals were transferred into a solution of 70% precipitant, 30% ethylene glycol, flash cooled in liquid nitrogen and shipped to Diamond Light Source (Oxford, UK) for data collection.

9.4.5 HTRF assay

The assay was set up and optimized by Judith Reeks and Santosh Adhikari.

The inhibitor solutions (20 mM solution in DMSO) were dispensed in an Echo qualified 384-well low dead volume microplate source plate using a multi-channel pipette.

Buffer A (50 mM Tris at pH 7.4, 100 mM NaCl, 100 µg/mL BSA, 1 mM DTT) and buffer B (50 mM Tris at pH 7.4, 100 mM NaCl, 100 µg/mL BSA) were prepared fresh. The inhibitors were dispensed into a 384-well black low-binding round bottom assay plate (Corning) using a Echo® Liquid Handler 550 (Labcyte), starting at 500 µM inhibitor (final assay concentration) and decreasing over a semi-log scale. Each well was backfilled with DMSO to a final volume of 250 nL and each condition was in duplicate.

IP3 peptide (300 µM in DMSO) was diluted in buffer A supplemented with 4.2 % DMSO to obtain a 500 nM solution and was added to all the wells on the assay plate (6 µL). GST-MDMX₂₂₋₁₁₁ (107 µM stock) was diluted with buffer A, first to 1.07 µM and subsequently to 25 nM and was added to the plate (4 µL). Positive (peptide, MDMX and DMSO; no inhibitor) and negative (peptide, buffer A and DMSO; no protein or inhibitor) controls were included. The plate was incubated on a shaking platform for 1 h. The final concentrations were as follows: 10 nM GST-MDMX, 300 nM IP3 peptide, 5 % DMSO. A solution of Tb-anti-GST-antibody (3.3 µM stock) was prepared in buffer B (20 nM) and added to each well (10 µL) of the assay plate followed by 45 min incubation on the shaker. The plate was read using PHERAstar FS (BMG Labtech) microplate reader.

9.4.6 Differential scanning fluorimetry (DSF)

The inhibitor solutions (20 mM solution in DMSO) were dispensed in an Echo Qualified 384-well low dead volume source plate using a multi-channel pipette. The inhibitors were dispensed in 45 nL aliquots in triplicate in a 384-well MicroAmp optical assay plate (Life Technologies) using the Echo® Liquid Handler 550 (Labcyte). Positive controls include known inhibitors (WT-p53, RO-2443, RO-5963, WK298). Negative controls include the absence of inhibitor (replaced by DMSO), the absence of protein (replaced by mHBS) and the absence of both (replaced by DMSO and mHBS). The plate was prepared by adding solutions of MDMX (final concentration 30 µM), SYPRO® Orange

(Invitrogen; 1:1000 dilution), 4% DMSO and mHBS to bring the reaction volume to 15 μ L per well. The final inhibitor concentration was 60 μ M. The plate was heated from 25 to 95 $^{\circ}$ C with a heating rate of 3 $^{\circ}$ C/min using a ViiATM 7 Real-Time PCR System (Applied Biosystems). The fluorescence intensity was measured and the melting points were calculated using an Excel-based DSF analysis transformation tool downloaded from <ftp://ftp.sgc.ox.ac.uk/pub/biophysics> (Frank H. Neisen, SGC, Oxford). Data were compiled using GraphPad Prism v6.

APPENDICES

Appendix A - Small molecule crystal structures

Crystal data and structure refinement for 199

Identification code	rjg130003		
Chemical formula (moiety)	C ₂₇ H ₂₅ Cl ₂ NO ₃		
Chemical formula (total)	C ₂₇ H ₂₅ Cl ₂ NO ₃		
Formula weight	482.38		
Temperature	120(2) K		
Radiation, wavelength	synchrotron, 0.6889 Å		
Crystal system, space group	monoclinic, P2 ₁		
Unit cell parameters	a = 8.718(5) Å	α = 90°	
	b = 13.802(7) Å	β	=
	c = 40.35(2) Å	γ = 90°	
Cell volume	4854(4) Å ³		
Z	8		
Calculated density	1.320 g/cm ³		
Absorption coefficient μ	0.274 mm ⁻¹		
F(000)	2016		
Crystal colour and size	colourless, 0.150 × 0.100 × 0.020 mm ³		
Reflections for cell refinement	9961 (θ range 2.3 to 26.4°)		
Data collection method	Rigaku Saturn 724+ on kappa		
diffractometer			
	wide-frame ω scans		
θ range for data collection	1.0 to 26.5°		
Index ranges	h -11 to 11, k -17 to 14, l -51 to 50		
Completeness to θ = 24.4°	99.2 %		
Reflections collected	37658		
Independent reflections	17481 (R _{int} = 0.0461)		
Reflections with F ² > 2σ	16747		
Absorption correction	none		
Structure solution	direct methods		
Refinement method	Full-matrix least-squares on F ²		
Weighting parameters a, b	0.0731, 28.8171		
Data / restraints / parameters	17481 / 1819 / 1191		
Final R indices [F ² > 2σ]	R1 = 0.1039, wR2 = 0.2652		
R indices (all data)	R1 = 0.1070, wR2 = 0.2679		
Goodness-of-fit on F ²	1.103		
Absolute structure parameter	0.07(2)		
Extinction coefficient	0.036(3)		
Largest and mean shift/su	0.000 and 0.000		
Largest diff. peak and hole	1.11 and -1.06 e Å ⁻³		

Crystal data and structure refinement for 208

Identification code	rjg130002		
Chemical formula (moiety)	C ₂₇ H ₂₅ Cl ₂ NO ₃ ·0.5CH ₂ Cl ₂		
Chemical formula (total)	C _{27.50} H ₂₆ Cl ₃ NO ₃		
Formula weight	524.84		
Temperature	150(2) K		
Radiation, wavelength	MoK α , 0.71073 Å		
Crystal system, space group	monoclinic, C2		
Unit cell parameters	a = 24.1233(10) Å	$\alpha = 90^\circ$	
	b = 11.1421(5) Å	β	=
	c = 11.1318(5) Å	$\gamma = 90^\circ$	
Cell volume	2734.8(2) Å ³		
Z	4		
Calculated density	1.275 g/cm ³		
Absorption coefficient μ	0.363 mm ⁻¹		
F(000)	1092		
Crystal colour and size	0.30 × 0.30 × 0.20 mm ³		
Reflections for cell refinement	15660 (θ range 3.7 to 28.6°)		
Data collection method	Xcalibur, Atlas, Gemini ultra		
	thick-slice ω scans		
θ range for data collection	3.1 to 28.6°		
Index ranges	h -31 to 31, k -14 to 14, l -14 to 14		
Completeness to $\theta = 25.0^\circ$	99.8 %		
Reflections collected	31840		
Independent reflections	6227 ($R_{\text{int}} = 0.0292$)		
Reflections with $F^2 > 2\sigma$	5891		
Absorption correction	semi-empirical from equivalents		
Min. and max. transmission	0.8988 and 0.9309		
Structure solution	direct methods		
Refinement method	Full-matrix least-squares on F^2		
Weighting parameters a, b	0.0602, 1.9405		
Data / restraints / parameters	6227 / 1 / 329		
Final R indices [$F^2 > 2\sigma$]	R1 = 0.0391, wR2 = 0.1027		
R indices (all data)	R1 = 0.0420, wR2 = 0.1057		
Goodness-of-fit on F^2	1.037		
Absolute structure parameter	-0.01(5)		
Largest and mean shift/su	0.001 and 0.000		
Largest diff. peak and hole	0.67 and -0.39 e Å ⁻³		

Appendix B - Crystallization conditions giving crystals

Summary of the selected crystals for attempted data collection.

<i>Construct</i>	<i>Inhibitor</i>	<i>Screen/conditions</i>
MDM2 c1	306	Ammonium sulfate suite A9 2:1 (0.2 M ammonium iodide, 2.2 M ammonium sulfate)
		Ammonium sulfate suite C10 2:1 (0.2 M Potassium thiocyanate, 2.2 M ammonium sulfate)
MDM2 c2		Ammonium sulfate suite C6 1:1 (0.2 M potassium iodide, 2.2 M ammonium sulfate)
MDM2 c1	159	C7 1:1 (0.2 M potassium nitrate, 2.2 M ammonium sulfate)

Appendix C - Construct sequences

Non-native amino acids recognized by 3C protease are highlighted in green.

Human MDMX₁₈₋₁₁₁ uncleaved

MSPILGYWKIKGLVQPTRLLEYLEEKYEEHLYERDEGDKWRNKKFELGLEFPNLP
YYIDGDVKLTQSMAIIRYIADKHNMLGGCPKERAEISMLEGAVLDIRYGVSRAYS
KDFETLKVDFLSKLPEMLKMFEDRLCHKTYLNGDHVTHPDFMLYDALDVVLYMDPM
CLDAFPKLVCFKKRIEAI PQIDKYLKSSKYIAWPLQGWQATFGGGDHPPKS **DLEVL**
FQGPLGSRISPGQINQVRPKLPLLKILHAAGAQQGEMFTVKEVMHYLGQYIMVKQLY
DQQEQHMYVYCGDLLGELLGRQSFVSKDPSPLYDMLRKNLVTLAT

Human MDMX₁₈₋₁₁₁ cleaved

GPLGSRISPGQINQVRPKLPLLKILHAAGAQQGEMFTVKEVMHYLGQYIMVKQLYDQ
QEQHMYVYCGDLLGELLGRQSFVSKDPSPLYDMLRKNLVTLAT

Molecular weight: 11070.9 Da

Extinction coefficient: 7450 M⁻¹ cm⁻¹

Human MDMX₂₂₋₁₁₁ uncleaved

MSPILGYWKIKGLVQPTRLLEYLEEKYEEHLYERDEGDKWRNKKFELGLEFPNLP
YYIDGDVKLTQSMAIIRYIADKHNMLGGCPKERAEISMLEGAVLDIRYGVSRAYS
KDFETLKVDFLSKLPEMLKMFEDRLCHKTYLNGDHVTHPDFMLYDALDVVLYMDPM
CLDAFPKLVCFKKRIEAI PQIDKYLKSSKYIAWPLQGWQATFGGGDHPPKS **DLEVL**
FQGPLGSGQINQVRPKLPLLKILHAAGAQQGEMFTVKEVMHYLGQYIMVKQLYDQQE
QHMYVYCGDLLGELLGRQSFVSKDPSPLYDMLRKNLVTLAT

Human MDMX₂₂₋₁₁₁ cleaved

GPLGSGQINQVRPKLP LLKILHAAGAQQGEMFTVKEVMHYLGQYIMVKQLYDQQEQH
MVYCGDLLGELLGRQSFSVKDPSPLYDMLRKNLVTLAT

Molecular weight: 10617.4 Da

Extinction coefficient: 7450 M⁻¹ cm⁻¹

Human MDMX₂₆₋₁₁₁ uncleaved

MSPILGYWKIKGLVQPTRLLLEYLEEKYEEHLYERDEGDKWRNKKFELGLEFPNLP
YYIDGDVKLTQSMAIIRYIADKHNM LGGCPKERA EISMLEGAVLDIRYGVSRIAYS
KDFETLKVDFLSKLP EMLKMFEDRLCHKTYLNGDHVTHPDFMLYDALDVVLYMDPM
CLDAFPKLVCFKKRIEAI PQIDKYLKSSKYIAWPLQGWQATFGGGDHPPKS DLEVL
FQGPLGSGQVRPKLP LLKILHAAGAQQGEMFTVKEVMHYLGQYIMVKQLYDQQEQH MV
YCGDLLGELLGRQSFSVKDPSPLYDMLRKNLVTLAT

Human MDMX₂₆₋₁₁₁ cleaved

GPLGSGQVRPKLP LLKILHAAGAQQGEMFTVKEVMHYLGQYIMVKQLYDQQEQH MVYC
GGDLLGELLGRQSFSVKDPSPLYDMLRKNLVTLAT

Molecular weight: 10204.9 Da

Extinction coefficient: 7450 M⁻¹ cm⁻¹

Human MDM2^{K51A}₁₇₋₁₂₅ uncleaved

MSPILGYWKIKGLVQPTRLLLEYLEEKYEEHLYERDEGDKWRNKKFELGLEFPNLP
YYIDGDVKLTQSMAIIRYIADKHNM LGGCPKERA EISMLEGAVLDIRYGVSRIAYS
KDFETLKVDFLSKLP EMLKMFEDRLCHKTYLNGDHVTHPDFMLYDALDVVLYMDPM
CLDAFPKLVCFKKRIEAI PQIDKYLKSSKYIAWPLQGWQATFGGGDHPPKS DLEVL
FQGPLGSSQIPASEQETLVRPKP LLLKLLKSVGAQKDTYTMAEVL FYLGQYIMTKR
LYDEKQQHIVYCSNDLLGDLFGVPSFSVKEHRKIYTMIYRNLVVVNQQESSDSGTS
VSEN

Human MDM2^{K51A}₁₇₋₁₂₅ cleaved

GPLGSSQIPASEQETLVRPKP LLLKLLKSVGAQKDTYTMAEVL FYLGQYIMTKR LY
DEKQQHIVYCSNDLLGDLFGVPSFSVKEHRKIYTMIYRNLVVVNQQESSDSGTS V
SEN

Molecular weight: 12874.7 Da

Extinction coefficient: 10430 M⁻¹ cm⁻¹

Human MDM2^{E69K70A}₁₇₋₁₀₈ uncleaved

MSPILGYWKIKGLVQPTRLLLEYLEEKYEEHLYERDEGDKWRNKKFELGLEFPNLP
YYIDGDVKLTQSMAIIRYIADKHNMLGGCPKERAIEISMLEGAVLDIRYGVSRIAYS
KDFETLKVDFLSKLPEMLKMFEDRLCHKTYLNGDHVTHPDFMLYDALDVVLYMDPM
CLDAFPKLVCFKKRIEAIPOIDKYLKSSKYIAWPLQGWQATFGGGDHPPKSDLEVL
FQGPLGSSQIPASEQETLVRPKPLLLKLLKSVGAQKDTYTMKEVLFYLGQYIMTKR
LYDAAQQQHIVYCSNDLLGDLFGVPSFSVKEHRKIYTMIRNVL

Human MDM2^{E69K70A}₁₇₋₁₀₈ cleaved

GPLGSSQIPASEQETLVRPKPLLLKLLKSVGAQKDTYTMKEVLFYLGQYIMTKRLY
DAAQQQHIVYCSNDLLGDLFGVPSFSVKEHRKIYTMIRNVL

Molecular weight: 11067.9 Da

Extinction coefficient: 10430 M⁻¹ cm⁻¹

Human MDM2^{E69K70A}₁₇₋₁₂₅ uncleaved

MSPILGYWKIKGLVQPTRLLLEYLEEKYEEHLYERDEGDKWRNKKFELGLEFPNLP
YYIDGDVKLTQSMAIIRYIADKHNMLGGCPKERAIEISMLEGAVLDIRYGVSRIAYS
KDFETLKVDFLSKLPEMLKMFEDRLCHKTYLNGDHVTHPDFMLYDALDVVLYMDPM
CLDAFPKLVCFKKRIEAIPOIDKYLKSSKYIAWPLQGWQATFGGGDHPPKSDLEVL
FQGPLGSSQIPASEQETLVRPKPLLLKLLKSVGAQKDTYTMKEVLFYLGQYIMTKR
LYDAAQQQHIVYCSNDLLGDLFGVPSFSVKEHRKIYTMIRNVLVVNQQESSDSGTS
VSEN

Human MDM2^{E69K70A}₁₇₋₁₂₅ cleaved

GPLGSSQIPASEQETLVRPKPLLLKLLKSVGAQKDTYTMKEVLFYLGQYIMTKRLY
DAAQQQHIVYCSNDLLGDLFGVPSFSVKEHRKIYTMIRNVLVVNQQESSDSGTSV
SEN

Molecular weight: 12816.7 Da

Extinction coefficient: 10430 M⁻¹ cm⁻¹

Sequence alignments for MDM2, MDM2^{K51A}₁₇₋₁₂₅ and MDMX

MDM2
MDM2^{K51A}₁₇₋₁₂₅
MDMX

MCNTNMSVPTDGAVTTSQIPASEQETLVRPKPLLLKLLKSVGAQKDTYTM 50
-----GPLGSSQIPASEQETLVRPKPLLLKLLKSVGAQKDTYTM 39
MTSFSTSAQCSTSDSACRISPG-QINQVRPKLPLLKILHAAGAQQGEMFTV 49

KEVLFYLGQYIMTKRLYDEKQQQHIVYCSNDLLGDLFGVPSFSVKEHRKIY 100
AEVLFYLGQYIMTKRLYDEKQQQHIVYCSNDLLGDLFGVPSFSVKEHRKIY 89
KEVMHYLGQYIMVKQLYDQQEQHVMVYCGDLLGELLGRQSFSVKDPSPLY 99

TMIYRNLVVN-----	111
TMIYRNLVVN-----	100
DMLRKNLVTLATATDAAQT-----	119

REFERENCES

1. Cancer Research UK; *All cancers combined Key Stats*; 2015.
2. World Cancer Report 2014. IARC: **2014**.
3. Bray, F.; Ren, J.-S.; Masuyer, E.; Ferlay, J., Global estimates of cancer prevalence for 27 sites in the adult population in 2008. *Int. J. Cancer* **2013**, *132*, 1133.
4. Ferlay, J.; Soerjomataram, I.; Dikshit, R.; Eser, S.; Mathers, C.; Rebelo, M.; Parkin, D. M.; Forman, D.; Bray, F., Cancer incidence and mortality worldwide: Sources, methods and major patterns in GLOBOCAN 2012. *Int. J. Cancer* **2015**, *136*, E359.
5. Bray, F.; Jemal, A.; Grey, N.; Ferlay, J.; Forman, D., Global cancer transitions according to the Human Development Index (2008–2030): a population-based study. *The Lancet Oncology* **2012**, *13*, 790.
6. Jemal, A.; Bray, F.; Center, M. M.; Ferlay, J.; Ward, E.; Forman, D., Global Cancer Statistics. *CA-Cancer J. Clin.* **2011**, *61*, 69.
7. Cancer Research UK; *Cancer Statistics Report: Cancer Incidence in the UK in 2011*; 2014.
8. Hanahan, D.; Weinberg, R. A., The hallmarks of cancer. *Cell* **2000**, *100*, 57.
9. Hanahan, D.; Weinberg, R. A., Hallmarks of cancer: the next generation. *Cell* **2011**, *144*, 646.
10. Hajdu, S. I., Greco-Roman thought about cancer. *Cancer* **2004**, *100*, 2048.
11. Sudhakar, A., History of Cancer, Ancient and Modern Treatment Methods. *J. Cancer Sci.Ther.* **2009**, *1*, 1.
12. Trinh, V. A.; Patel, S. P.; Hwu, W.-J., The safety of temozolomide in the treatment of malignancies. *Expert Opin. Drug Saf.* **2009**, *8*, 493.
13. Pecorino, L., Molecular biology of cancer. 3rd ed.; Oxford University Press: Oxford, **2012**.
14. Longley, D. B.; Harkin, D. P.; Johnston, P. G., 5-Fluorouracil: mechanisms of action and clinical strategies. *Nat. Rev. Cancer* **2003**, *3*, 330.
15. Pavet, V.; Portal, M. M.; Moulin, J. C.; Herbrecht, R.; Gronemeyer, H., Towards novel paradigms for cancer therapy. *Oncogene* **2011**, *30*, 1.

16. Olicio, R.; Rivero, M. B.; Seuanez, H. N., The paternal chromosome 9 and the maternal chromosome 22 are preferentially rearranged in chronic myeloid leukaemia. *Leukemia* **2004**, *18*, 1445.
17. Druker, B. J.; Guilhot, F.; O'Brien, S. G.; Gathmann, I.; Kantarjian, H.; Gattermann, N.; Deininger, M. W. N.; Silver, R. T.; Goldman, J. M.; Stone, R. M.; Cervantes, F.; Hochhaus, A.; Powell, B. L.; Gabrilove, J. L.; Rousselot, P.; Reiffers, J.; Cornelissen, J. J.; Hughes, T.; Agis, H.; Fischer, T.; Verhoef, G.; Shepherd, J.; Saglio, G.; Gratwohl, A.; Nielsen, J. L.; Radich, J. P.; Simonsson, B.; Taylor, K.; Baccarani, M.; So, C.; Letvak, L.; Larson, R. A., Five-Year Follow-up of Patients Receiving Imatinib for Chronic Myeloid Leukemia. *New Engl. J. Med.* **2006**, *355*, 2408.
18. Li, F.; Zhao, C.; Wang, L., Molecular-targeted agents combination therapy for cancer: Developments and potentials. *Int. J. Cancer* **2014**, *134*, 1257.
19. Hughes, J. P.; Rees, S.; Kalindjian, S. B.; Philpott, K. L., Principles of early drug discovery. *Br. J. Pharmacol.* **2011**, *162*, 1239.
20. Hanson, S. R.; Best, M. D.; Wong, C.-H., Sulfatases: structure, mechanism, biological activity, inhibition, and synthetic utility. *Angew. Chem. Int. Ed.* **2004**, *43*, 5736.
21. Dierks, T.; Lecca, M. R.; Schlotterhose, P.; Schmidt, B.; von Figura, K., Sequence determinants directing conversion of cysteine to formylglycine in eukaryotic sulfatases. *EMBO J.* **1999**, *18*, 2084.
22. Cleland, W. W.; Hengge, A. C., Enzymatic mechanism of phosphate and sulfate transfer. *Chem. Rev.* **2006**, *106*, 3252.
23. Spencer J., W., Sulfatase inhibitors: a patent review. *Expert Opin. Ther. Pat.* **2013**, *23*, 79.
24. Gosh, D., Human sulfatase: a structural perspective to catalysis. *Cell. Mol. Life Sci.* **2007**, *64*, 2013.
25. Waldow, A.; Schmidt, B.; Dierks, T.; von Bülow, R.; von Figura, K., Amino acid residues forming the active site of arylsulfatase A: role in catalytic activity and substrate binding. *J. Biol. Chem.* **1999**, *274*, 12284.
26. Bojarova, P.; Denehy, E.; Walker, I.; Loft, K.; De Souza, D. P.; Woo, L. W. L.; Potter, B. V. L.; McConville, M. J.; Williams, S. J., Direct evidence for ArO-S bond cleavage upon inactivation of *Pseudomonas aeruginosa* arylsulfamates by aryl sulfatase. *ChemBioChem* **2008**, *9*, 613.
27. Coughtrie, M. W. H.; Sharp, S.; Maxwell, K.; Innes, N. P., Biology and function of the reversible sulfation pathway catalysed by human sulfotransferases and sulfatases. *Chem.-Biol. Interact.* **1998**, *109*, 3.

28. Anzenbacher, P.; Zanger, U. M., Metabolism of Drugs and Other Xenobiotics. Wiley-VCH Verlag: Weinheim, **2012**.
29. Nussbaumer, P.; Billich, A., Steroid Sulfatase Inhibitors. *Med. Res. Rev.* **2004**, *24*, 529.
30. Poirier, D.; Ciobanu, L. C.; Maltais, R., Steroid sulfatase inhibitors. *Expert Opin. Ther. Pat.* **1999**, *9*, 1083.
31. Howarth, N. M.; Cooper, G.; Purhoit, A.; Duncan, L.; Reed, M. J.; Potter, B. V. L., Phosphonates and thiophosphonate as sulfate surrogates: synthesis of estrone 3-methylthiophosphonate, a potent inhibitor of estrone sulfatase. *Bioorg. Med. Chem. Lett.* **1993**, *3*, 313.
32. Howarth, N. M.; Purhoit, A.; Reed, M. J.; Potter, B. V. L., Estrone sulfonates as inhibitors of estrone sulfatase. *Steroids* **1997**, *62*, 346.
33. Howarth, N. M.; Purhoit, A.; Reed, M. J.; Potter, B. V. L., Estrone sulfamates: potent inhibitors of estrone sulfatase with therapeutic potential. *J. Med. Chem.* **1994**, *37*, 219.
34. Howarth, N. M.; Purhoit, A.; Robinson, J. J.; Vicker, N.; Reed, M. J.; Potter, B. V. L., Estrone 3-sulfate mimics, inhibitors of estrone sulfatase activity: homology model construction and docking studies. *Biochemistry* **2002**, *41*, 14801.
35. Reed, J. E.; Lawrence Woo, L. W.; Robinson, J. J.; Leblond, B.; Leese, M. P.; Purohit, A.; Reed, M. J.; Potter, B. V. L., 2-Difluoromethyloestrone 3-O-sulphamate, a highly potent steroid sulphatase inhibitor. *Biochem. Biophys. Res. Commun.* **2004**, *317*, 169.
36. Woo, L. W. L.; Jackson, T.; Putey, A.; Cozier, G.; Leonard, P.; Acharya, K. R.; Chander, S. K.; Purohit, A.; Reed, M. J.; Potter, B. V. L., Highly potent first examples of dual aromatase-steroid sulfatase inhibitors based on a biphenyl template. *J. Med. Chem.* **2010**, *53*, 2155.
37. Woo, L. W. L.; Lightowler, M.; Purohit, A.; Reed, M. J.; Potter, B. V. L., Heteroatom-substituted analogues of the active-site directed inhibitor estra-1,3,5(10)-trien-17-one-3-sulphamate inhibit estrone sulphatase by a different mechanism. *J. Steroid Biochem.* **1996**, *57*, 79.
38. Leese, M. P.; Leblond, B.; Smith, A.; Newman, S. P.; Di Fiore, A.; De Simone, G.; Supuran, C. T.; Purohit, A.; Reed, M. J.; Potter, B. V. L., 2-Substituted Estradiol Bis-sulfamates, Multitargeted Antitumor Agents: Synthesis, In Vitro SAR, Protein Crystallography, and In Vivo Activity. *J. Med. Chem.* **2006**, *49*, 7683.
39. Morimoto-Tomita, M.; Uchimura, K.; Werb, Z.; Hemmerich, S.; Rosen, S. D., Cloning and characterization of two extracellular heparin-degrading endosulfatases in mice and humans. *J. Biol. Chem.* **2002**, *277*, 49175.

40. Morimoto-Tomita, M.; Uchimura, K.; Rosen, S. D., Novel extracellular sulfatases: potential roles in cancer. *Trends. Glycosci. Glyc.* **2003**, *15*, 159.
41. Rosen, S. D.; Lemjabbar-Alaoui, H., Sulf-2: an extra-cellular modulator of cell signaling and a cancer target candidate. *Expert Opin. Ther. Tar.* **2010**, *14*, 935.
42. Yang, J. D.; Sun, Z.; Hu, C.; Lai, J.; Dove, R.; Nakamura, I.; Lee, J.-S.; Thorgeirsson, S. S.; Kang, K. J.; Chu, I.-S.; Roberts, L. R., Sulfatase 1 and sulfatase 2 in hepatocellular carcinoma: associated signaling pathways, tumor phenotypes, and survival. *Gene Chromosome Canc.* **2011**, *50*, 122.
43. Holst, C. R.; Bou-Reslan, H.; Gore, B. B.; Wong, K.; Grant, D.; Chalasani, S.; Carano, R. A.; Frantz, G. D.; Tessier-Lavigne, M.; Bolon, B.; French, D. M.; Ashkenazi, A., Secreted Sulfatases *Sulf1* and *Sulf2* Have Overlapping yet Essential Roles in Mouse Neonatal Survival. *PLoS ONE* **2007**, *2*, e575.
44. Milz, F.; Harder, A.; Neuhaus, P.; Breitzkreuz-Korff, O.; Walhorn, V.; Lübke, T.; Anselmetti, D.; Dierks, T., Cooperation of binding sites at the hydrophilic domain of cell-surface sulfatase Sulf1 allows for dynamic interaction of the enzyme with its substrate heparan sulfate. *Biochim. Biophys. Acta* **2013**, *1830*, 5287.
45. Sahota, A. P.; Dhoot, G. K., A novel SULF1 splice variant inhibits Wnt signalling but enhances angiogenesis by opposing SULF1 activity. *Exp. Cell Res.* **2009**, *315*, 2752.
46. Dhoot, G. K., Recent Progress and Related Patents on the Applications of SULF1/SULF2 Enzymes in Regenerative Medicine and Cancer Therapies. *Recent Pat. Regen. Med.* **2012**, *2*, 137.
47. Gill, R. B. S.; Day, A.; Barstow, A.; Liu, H.; Zaman, G.; Dhoot, G. K., Sulf2 gene is alternatively spliced in mammalian developing and tumour tissues with functional implications. *Biochem. Biophys. Res. Commun.* **2011**, *414*, 468.
48. Knelson, E. H.; Nee, J. C.; Blobe, G. C., Heparan sulfate signaling in cancer. *Trends Biochem. Sci.* **2014**, *39*, 277.
49. Staples, G. O.; Shi, X.; Zaia, J., Glycomics analysis of mammalian heparan sulfates modified by the human extracellular sulfatase HSulf2. *PLoS ONE* **2011**, *6*.
50. Malavaki, C. J.; Theocharis, A. D.; Lamari, F. N.; Kanakis, I.; Tsegenidis, T.; Tzanakakis, G. N.; Karamanos, N. K., Heparan sulfate: biological significance, tools for biochemical analysis and structural characterization. *Biomed. Chrom.* **2011**, *25*, 11.
51. Turnbull, J. E., Heparan sulfate glycomics: towards system biology strategies. *Biochem. Soc. Trans.* **2010**, *38*, 1356.

52. Pellegrini, L.; Burke, D. F.; von Delft, F.; Mulloy, B.; Blundell, T. L., Crystal structure of fibroblast growth factor receptor ectodomain bound to ligand and heparin. *Nature* **2000**, *407*, 1029.
53. Turnbull, J.; Powell, A.; Guimond, S., Heparan sulfate: decoding a dynamic multifunctional cell regulator. *Trends Cell Biol.* **2001**, *11*, 75.
54. Lai, J.-P.; Sandhu, D. S.; Yu, C.; Han, T.; Moser, C. D.; Jackson, K. K.; Guerrero, R. B.; Aderca, I.; Isomoto, H.; Garrity-Park, M. M.; Zou, H.; Shire, A. M.; Nagorney, D. M.; Sanderson, S. O.; Adjei, A. A.; Lee, J.-S.; Thorgeirsson, S. S.; Roberts, L. R., Sulfatase 2 up-regulates glypican 3, promotes fibroblast growth factor signaling, and decreases survival in hepatocellular carcinoma. *Hepatology* **2008**, *47*, 1211.
55. Goetz, R.; Mohammadi, M., Exploring mechanisms of FGF signalling through the lens of structural biology. *Nat Rev Mol Cell Biol* **2013**, *14*, 166.
56. Lai, J. P.; Thompson, J. R.; Sandhu, D. S.; Roberts, L. R., Heparin-degrading sulfatases in hepatocellular carcinoma: roles in pathogenesis and therapy targets. *Future Oncol.* **2008**, *4*, 803.
57. Uchimura, K.; Morimoto-Tomita, M.; Bistrup, A.; Li, J.; Lyon, M.; Gallagher, J.; Werb, Z.; Rosen, S., HSulf-2, an extracellular endoglucosamine-6-sulfatase, selectively mobilizes heparin-bound growth factors and chemokines: effects on VEGF, FGF-1, and SDF-1. *BMC Biochem.* **2006**, *7*, 2.
58. Chau, B. N.; Diaz, R. L.; Saunders, M. A.; Cheng, C.; Chang, A. N.; Warrenner, P.; Bradshaw, J.; Linsley, P. S.; Cleary, M. A., Identification of SULF2 as a novel transcriptional target of p53 by use of integrated genomic analyses. *Cancer Res.* **2009**, *69*, 1368.
59. Schelwies, M.; Brinson, D.; Otsuki, S.; Hong, Y.-H.; Lotz, M. K.; Wong, C.-H.; Hanson, S. R., Glucosamine-6-sulfamate analogues of heparan sulfate as inhibitors of endosulfatase. *ChemBioChem* **2010**, *11*, 2393.
60. Hassing, H. C.; Surendran, R. P.; Derudas, B.; Verrijken, A.; Francque, S. M.; Mooij, H. L.; Bernelot Moens, S. J.; Hart, L. M. t.; Nijpels, G.; Dekker, J. M.; Williams, K. J.; Stroes, E. S. G.; Van Gaal, L. F.; Staels, B.; Nieuwdorp, M.; Dallinga-Thie, G. M., SULF2 strongly prediposes to fasting and postprandial triglycerides in patients with obesity and type 2 diabetes mellitus. *Obesity* **2014**, *22*, 1309.
61. Alhasan, A. A.; Spielhofer, J.; Kusche-Gullberg, M.; Kirby, J. A.; Ali, S., Role of 6-O-sulfated heparan sulfate in chronic renal fibrosis. *J. Biol. Chem.* **2014**, *289*, 20295.
62. Hammond, E.; Khurana, A.; Shridhar, V.; Dredge, K., The role of heparanase and sulfatases in the modification of heparan sulfate proteoglycans within

the tumor microenvironment and opportunities for novel cancer therapeutics. *Frontiers in oncology* **2014**, *4*, 195.

63. Saad, O. M.; Ebel, H.; Uchimura, K.; Rosen, S. D.; Bertozzi, C. R.; Leary, J. A., Compositional profiling of heparin/heparan sulfate using mass spectrometry: assay for specificity of a novel extracellular human endosulfatase. *Glycobiology* **2005**, *15*, 818.
64. Hossain, M. M.; Hosono-Fukao, T.; Tang, R.; Sugaya, N.; van Kuppevelt, T. H.; Jenniskens, G. J.; Kimata, K.; Rosen, S. D.; Uchimura, K., Direct detection of HSulf-1 and HSulf-2 activities on extracellular heparan sulfate and their inhibition by PI-88. *Glycobiology* **2010**, *20*, 175.
65. Miller, D. C. Inhibitors of Sulf-2 and ERK5; modulators of cell signalling pathways, as potential cancer therapeutics. Ph. D. Thesis, Newcastle University, Newcastle upon Tyne, **2014**.
66. Beale, G., Unpublished work.
67. Alhasan, S. Biotechnology studies of sulfatase 2 as a novel target for the treatment of hepatocellular carcinoma. PhD thesis, Newcastle University, Newcastle Upon Tyne, **2014**.
68. Alhasan, S., Unpublished work.
69. Maltais, R.; Poirier, D., Steroid sulfatase inhibitors: A review covering the promising 2000-2010 decade. *Steroids* **2011**, *76*, 929.
70. Quasdorf, K. W.; Riener, M.; Petrova, K. V.; Garg, N. K., Suzuki-Miyaura coupling of aryl carbamates, carbonates and sulfamates. *J. Am. Chem. Soc.* **2009**, *131*, 17748.
71. Winum, J.-Y.; Vullo, D.; Casini, A.; Montero, J.-L.; Scozzafava, A.; Supuran, C. T., Carbonic anhydrase inhibitors. Inhibition of cytosolic isozymes I and II and transmembrane, tumor-associated isozyme IX with sulfamates including EMATE also acting as steroid sulfatase inhibitors. *J. Med. Chem.* **2003**, *46*, 2197.
72. Macklin, T. K.; Snieckus, V., Directed ortho metalation methodology. The *N,N*-dialkyl aryl *O*-sulfamate as a new directed metalation group and cross-coupling partner for Grignard reagents. *Org. Lett.* **2005**, *7*, 2519.
73. Knappke, C. E. I.; von Wangelin, A. J., A synthetic double punch: Suzuki-Miyaura cross-coupling with C-H functionalization. *Angew. Chem. Int. Ed.* **2010**, *49*, 3568.
74. Baghbanzadeh, M.; Pilger, C.; Kappe, C. O., Rapid nickel-catalyzed Suzuki-Miyaura cross-coupling of aryl carbamates and sulfamates utilising microwave heating. *J. Org. Chem.* **2011**, *76*, 1507.

75. Wang, Z.-Y.; Ma, Q.-N.; Li, R.-H.; Shao, L.-X., Palladium-catalyzed Suzuki-Miyaura coupling of aryl sulfamates with arylboronic acids. *Org. Biomol. Chem.* **2013**, *11*, 7899.
76. Molander, G. A.; Shin, I., Pd-catalyzed Suzuki-Miyaura cross-coupling reactions between sulfamates and potassium BOC-protected aminomethyltrifluoroborates. *Org. Lett.* **2013**, *15*, 2534.
77. Shalwitz, R. Compounds, compositions, and methods for preventing metastasis of cancer cells. WO2011005330, **2011**.
78. Attygalle, A. B.; Garcia-Rubio, S.; Ta, J.; Meinwald, J., Collisionally-induced dissociation mass spectra of organic sulfate anions. *J. Chem. Soc. Perk. Trans. 2* **2001**, 498.
79. Reuillon, T. Design of small-molecule inhibitors of sulfatase 2 and ERK5. Ph.D. Thesis, Newcastle University, Newcastle upon Tyne, **2015**.
80. Stuart, D. R.; Alsabeh, P.; Kuhn, M.; Fagnou, K., Rhodium(III)-catalyzed arene and alkene C-H bond functionalization leading to indoles and pyrroles. *J. Am. Chem. Soc.* **2010**, *132*, 18326.
81. Brook, M. A.; Chan, T. H., A simple procedure for the esterification of carboxylic acids. *Synthesis* **1983**, 1983, 201.
82. Di Raddo, P., A convenient method of esterification of fatty acids: An undergraduate organic laboratory experiment. *J. Chem. Educ.* **1993**, *70*, 1034.
83. Otera, J.; Nishikido, J., Esterification: methods, reactions, and applications. Wiley VCH Verlag: **2010**.
84. Knapp, D. M.; Gillis, E. P.; Burke, M. D., A general solution for unstable boronic acids: slow-release cross-coupling from air-stable MIDA boronates. *J. Am. Chem. Soc.* **2009**, *131*, 6961.
85. Dick, G. R.; Woerly, E. M.; Burke, M. D., A general solution for the 2-pyridyl problem. *Angew. Chem. Int. Ed.* **2012**, *51*, 2667.
86. Spillane, W. J.; O'Byrne, A.; McCaw, C. J. A., Elimination mechanisms in the aminolysis of sulfamate esters of the type $\text{NH}_2\text{SO}_2\text{OC}_6\text{H}_4\text{X}$ – models of enzyme inhibitors. *Eur. J. Org. Chem.* **2008**, 2008, 4200.
87. Wang, B.; Sun, H.-X.; Sun, Z.-H., A general and efficient Suzuki-Miyaura cross-coupling protocol using weak base and no water: the essential role of acetate. *Eur. J. Org. Chem.* **2009**, 2009, 3688.
88. Franke, D.; Lorbach, V.; Esser, S.; Dose, C.; Sprenger, G. A.; Halfar, M.; Thömmes, J.; Müller, R.; Takors, R.; Müller, M., (*S,S*)-2,3-Dihydroxy-2,3-

dihydrobenzoic acid: microbial access with engineered cells of *Escherichia coli* and application as starting material in natural-product synthesis. *Chem. Eur. J.* **2003**, *9*, 4188.

89. Kuntz, K.; Uehling, D. E.; Waterson, A. G.; Emmitte, K. A.; Steven, K.; Shotwell, J. B.; Smith, S. C.; Nailor, K. E.; Salovich, J. M.; Wilson, B. J.; Cheung, M.; Mook, R. A.; Baum, E. W.; Moorthy, G. Imidazopyridine kinase inhibitors. US2008300242 (A1), **2010**.
90. Jens, G.; Fernando Lopez, H.; Kai, L.; Frank, S. Industrially applicable process for the sulfamoylation of alcohols and phenols. US2003/171346 A1, **2003**.
91. Schmidt, B.; Riemer, M., Suzuki–Miyaura coupling of halophenols and phenol boronic acids: systematic investigation of positional isomer effects and conclusions for the synthesis of phytoalexins from pyrinae. *J. Org. Chem.* **2014**, *79*, 4104.
92. Freundlich, J. S.; Landis, H. E., An expeditious aqueous Suzuki–Miyaura method for the arylation of bromophenols. *Tet. Lett.* **2006**, *47*, 4275.
93. Reuillon, T.; Bertoli, A.; Griffin, R. J.; Miller, D. C.; Golding, B. T., Efficacious N-protection of O-aryl sulfamates with 2,4-dimethoxybenzyl groups. *Org. Biomol. Chem.* **2012**, *10*, 7610.
94. Brummond, K. M.; Lu, J.; Petersen, J., A rapid synthesis of hydroxymethylacylfulvene (HMAF) using the allenic Pauson–Khand reaction. A synthetic approach to either enantiomer of this illudane structure. *J. Am. Chem. Soc.* **2000**, *122*, 4915.
95. Miyano, M., Synthesis of aldosterone. *J. Org. Chem.* **1981**, *46*, 1846.
96. Karplus, M., Vicinal proton coupling in nuclear magnetic resonance. *J. Am. Chem. Soc.* **1963**, *85*, 2870.
97. Marine, J.-C.; Jochemsen, A. G., Mdmx and Mdm2: brothers in arms? *Cell Cycle* **2004**, *3*, 898.
98. Petitjean, A.; Mathe, E.; Kato, S.; Ishioka, C.; Tavtigian, S. V.; Hainaut, P.; Olivier, M., Impact of mutant p53 functional properties on TP53 mutation patterns and tumor phenotype: lessons from recent developments in the IARC TP53 database. *Human Mutation* **2007**, *28*, 622.
99. Lane, D. P., p53, guardian of the genome. *Nature* **1992**, *358*, 15.
100. Brown, C. J.; Lain, S.; Verma, C. S.; Fersht, A. R.; Lane, D. P., Awakening guardian angels: drugging the p53 pathway. *Nat Rev Cancer* **2009**, *9*, 862.
101. Brady, C. A.; Attardi, L. D., p53 at a glance. *J. Cell Sci.* **2010**, *123*, 2527.

102. Vogelstein, B., p53 : the most frequently altered gene in human cancers. *Nat. Educ.* **2010**, *3*.
103. Soussi, T., The history of p53. **2010**; Vol. 11, p 822.
104. Levine, A. J.; Oren, M., The first 30 years of p53: growing ever more complex. *Nat. Rev. Cancer* **2009**, *9*, 749.
105. Wang, X., p53 regulation: teamwork between RING domains of Mdm2 and MdmX. *Cell Cycle* **2011**, *10*, 4225.
106. Lavin, M. F.; Gueven, N., The complexity of p53 stabilization and activation. *Cell Death Differ* **2006**, *13*, 941.
107. McLure, K. G.; Lee, P. W. K., How p53 binds DNA as a tetramer. *EMBO J.* **1998**, *17*, 3342.
108. Khoury, K.; Popowicz, G. M.; Holak, T. A.; Domling, A., The p53-MDM2/MDMX axis - A chemotype perspective. *MedChemComm* **2011**, *2*, 246.
109. Hjortsberg, L.; Rubio-Nevado, J. M.; Hamroun, D.; Claustres, M.; Bérout, C.; Soussi, T., The p53 mutation handbook v2. 2008.
110. Follis, A. V.; Llambi, F.; Ou, L.; Baran, K.; Green, D. R.; Kriwacki, R. W., The DNA-binding domain mediates both nuclear and cytosolic functions of p53. *Nat Struct Mol Biol* **2014**, *21*, 535.
111. Stegh, A. H., Targeting the p53 signaling pathway in cancer therapy – the promises, challenges and perils. *Expert Opin. Ther. Tar.* **2012**, *16*, 67.
112. Migliorini, D.; Denchi, E. L.; Danovi, D.; Jochemsen, A.; Capillo, M.; Gobbi, A.; Helin, K.; Pelicci, P. G.; Marine, J.-C., Mdm4 (Mdmx) Regulates p53-Induced Growth Arrest and Neuronal Cell Death during Early Embryonic Mouse Development. *Mol. Cell. Biol.* **2002**, *22*, 5527.
113. Wade, M.; Wahl, G. M., Targeting Mdm2 and Mdmx in Cancer Therapy: Better Living through Medicinal Chemistry? *Mol. Cancer Res.* **2009**, *7*, 1.
114. Berg, J. M.; Tymoczko, J. L.; Stryer, L., Biochemistry. 5th ed.; W. H. Freeman and Company: New York, 2002.
115. Sadowski, M.; Sarcevic, B., Mechanisms of mono- and poly-ubiquitination: Ubiquitination specificity depends on compatibility between the E2 catalytic core and amino acid residues proximal to the lysine. *Cell Division* **2010**, *5*, 19.

116. Oliner, J. D.; Kinzler, K. W.; Meltzer, P. S.; George, D. L.; Vogelstein, B., Amplification of a gene encoding a p53-associated protein in human sarcomas. *Nature* **1992**, *358*, 80.
117. Blaydes, J., Cooperation between MDM2 and MDMX in the regulation of p53. In *p53*, Springer US: 2011; Vol. 1, pp 85.
118. Hock, A. K.; Vousden, K. H., The role of ubiquitin modification in the regulation of p53. *Biochim. Biophys. Acta* **2014**, *1843*, 137.
119. Macchiarulo, A.; Giacche, N.; Carotti, A.; Moretti, F.; Pellicciari, R., Expanding the horizon of chemotherapeutic targets: from MDM2 to MDMX (MDM4). *MedChemComm* **2011**, *2*, 455.
120. Marine, J.-C. W.; Dyer, M. A.; Jochemsen, A. G., MDMX: from bench to bedside. *J. Cell Sci.* **2007**, *120*, 371.
121. Wang, X.; Jiang, X., Mdm2 and MdmX partner to regulate p53. *FEBS Lett.* **2012**, *586*, 1390.
122. Bista, M.; Petrovich, M.; Fersht, A. R., MDMX contains an autoinhibitory sequence element. *PNAS* **2013**.
123. Popowicz, G.; Czarna, A.; Holak, T., Structure of the human Mdmx protein bound to the p53 tumor suppressor transactivation domain. *Cell Cycle* **2008**, *7*, 2441.
124. Popowicz, G. M.; Dömling, A.; Holak, T. A., The structure-based design of Mdm2/Mdmx-p53 inhibitors gets serious. *Angew. Chem. Int. Ed.* **2011**, *50*, 2680.
125. Yu, G. W.; Vaysburd, M.; Allen, M. D.; Settanni, G.; Fersht, A. R., Structure of human MDM4 N-terminal domain bound to a single-domain antibody. *J. Mol. Biol.* **2009**, *385*, 1578.
126. Mancini, F.; Di Conza, G.; Moretti, F., MDM4 (MDMX) and its transcript variants. *Curr. Genomics* **2009**, *10*, 42.
127. Wang, X.; Sheng, P.; Guo, X.; Wang, J.; Hou, L.; Hu, G.; Luo, C.; Dong, Y.; Lu, Y., Identification and expression of a novel MDM4 splice variant in human glioma. *Brain Res.* **2013**, *1537*, 260.
128. Rallapalli, R.; Strachan, G.; Tuan, R. S.; Hall, D. J., Identification of a domain within MDMX-S that is responsible for its high affinity interaction with p53 and high-level expression in mammalian cells. *J. Cell. Biochem.* **2003**, *89*, 563.
129. Honda, R.; Tanaka, H.; Yasuda, H., Oncoprotein MDM2 is a ubiquitin ligase E3 for tumor suppressor p53. *FEBS Lett.* **1997**, *420*, 25.

130. Stommel, J. M.; Wahl, G. M., A new twist in the feedback loop: stress-activated MDM2 destabilization is required for p53 activation. *Cell Cycle* **2005**, *4*, 411.
131. He, G.; Zhang, Y.-W.; Lee, J.-H.; Zeng, S. X.; Wang, Y. V.; Luo, Z.; Dong, X. C.; Viollet, B.; Wahl, G. M.; Lu, H., AMP-Activated protein kinase induces p53 by phosphorylating MDMX and inhibiting its activity. *Mol. Cell. Biol.* **2014**, *34*, 148.
132. Bernal, F.; Wade, M.; Godes, M.; Davis, T. N.; Whitehead, D. G.; Kung, A. L.; Wahl, G. M.; Walensky, L. D., A stapled p53 helix overcomes HDMX-mediated suppression of p53. *Cancer Cell* **2010**, *18*, 411.
133. Giaccia, A. J.; Kastan, M. B., The complexity of p53 modulation: emerging patterns from divergent signals. *Genes Dev.* **1998**, *12*, 2973.
134. Shvarts, A.; Steegenga, W. T.; Riteco, N.; van Laar, T.; Dekker, P.; Bazuine, M.; van Ham, R. C.; van der Houven van Oordt, W.; Hateboer, G.; van der Eb, A. J.; Jochemsen, A. G., MDMX: a novel p53-binding protein with some functional properties of MDM2. *EMBO J.* **1996**, *15*, 5349.
135. Chen, J., The roles of MDM2 and MDMX phosphorylation in stress signaling to p53. *Genes & Cancer* **2012**, *3*, 274.
136. Wade, M.; Li, Y.-C.; Wahl, G. M., MDM2, MDMX and p53 in oncogenesis and cancer therapy. *Nat Rev Cancer* **2013**, *13*, 83.
137. Gembarska, A.; Luciani, F.; Fedele, C.; Russell, E. A.; Dewaele, M.; Villar, S.; Zwolinska, A.; Haupt, S.; de Lange, J.; Yip, D.; Goydos, J.; Haigh, J. J.; Haupt, Y.; Larue, L.; Jochemsen, A.; Shi, H.; Moriceau, G.; Lo, R. S.; Ghanem, G.; Shackleton, M.; Bernal, F.; Marine, J.-C., MDM4 is a key therapeutic target in cutaneous melanoma. *Nat. Med.* **2012**, *18*, 1239.
138. Carrillo, A. M.; Bouska, A.; Arrate, M. P.; Eischen, C. M., Mdmx promotes genomic instability independent of p53 and Mdm2. *Oncogene* **2014**.
139. Hu, B.; Gilkes, D. M.; Farooqi, B.; Sebt, S. M.; Chen, J., MDMX overexpression prevents p53 activation by the MDM2 inhibitor Nutlin. *J. Biol. Chem.* **2006**, *281*, 33030.
140. Remington, J. P.; Beringer, P., The science and practice of pharmacy. 21st ed.; Lippincott Williams & Wilkins: Philadelphia, **2006**.
141. Clackson, T.; Wells, J., A hot spot of binding energy in a hormone-receptor interface. *Science* **1995**, *267*, 383.
142. Azzarito, V.; Long, K.; Murphy, N. S.; Wilson, A. J., Inhibition of [alpha]-helix-mediated protein-protein interactions using designed molecules. *Nat Chem* **2013**, *5*, 161.

143. Wilson, A. J., Inhibition of protein-protein interactions using designed molecules. *Chem. Soc. Rev.* **2009**, *38*, 3289.
144. Lipinski, C. A.; Lombardo, F.; Dominy, B. W.; Feeney, P. J., Experimental and computational approaches to estimate solubility and permeability in drug discovery and development settings. *Adv. Drug Delivery Rev.* **2001**, *46*, 3.
145. Zheng, G.-h.; Shen, J.-j.; Zhan, Y.-c.; Yi, H.; Xue, S.-t.; Wang, Z.; Ji, X.-y.; Li, Z.-r., Design, synthesis and *in vitro* and *in vivo* antitumour activity of 3-benzylideneindolin-2-one derivatives, a novel class of small-molecule inhibitors of the MDM2-p53 interaction. *Eur. J. Med. Chem.* **2014**, *81*, 277.
146. Tovar, C.; Graves, B.; Packman, K.; Filipovic, Z.; Xia, B. H. M.; Tardell, C.; Garrido, R.; Lee, E.; Kolinsky, K.; To, K.-H.; Linn, M.; Podlaski, F.; Wovkulich, P.; Vu, B.; Vassilev, L. T., MDM2 small-molecule antagonist RG7112 activates p53 signaling and regresses human tumors in preclinical cancer models. *Cancer Res.* **2013**, *73*, 2587.
147. Ding, Q.; Zhang, Z.; Liu, J.-J.; Jiang, N.; Zhang, J.; Ross, T. M.; Chu, X.-J.; Bartkovitz, D.; Podlaski, F.; Janson, C.; Tovar, C.; Filipovic, Z. M.; Higgins, B.; Glenn, K.; Packman, K.; Vassilev, L. T.; Graves, B., Discovery of RG7388, a Potent and Selective p53-MDM2 Inhibitor in Clinical Development. *J. Med. Chem.* **2013**, *56*, 5979.
148. Zak, K.; Pecak, A.; Rys, B.; Wladyka, B.; Dömling, A.; Weber, L.; Holak, T. A.; Dubin, G., Mdm2 and MdmX inhibitors for the treatment of cancer: a patent review (2011 – present). *Expert Opin. Ther. Pat.* **2013**, *23*, 425.
149. Vu, B.; Wovkulich, P.; Pizzolato, G.; Lovey, A.; Ding, Q.; Jiang, N.; Liu, J.-J.; Zhao, C.; Glenn, K.; Wen, Y.; Tovar, C.; Packman, K.; Vassilev, L.; Graves, B., Discovery of RG7112: a small-molecule MDM2 inhibitor in clinical development. *Med. Chem. Lett.* **2013**, *4*, 466.
150. Graves, B.; Thompson, T.; Xia, M.; Janson, C.; Lukacs, C.; Deo, D.; Di Lello, P.; Fry, D.; Garvie, C.; Huang, K.-S.; Gao, L.; Tovar, C.; Lovey, A.; Wanner, J.; Vassilev, L. T., Activation of the p53 pathway by small-molecule-induced MDM2 and MDMX dimerization. *PNAS* **2012**, *109*, 11788.
151. Bertoli, A.; Adhikari, S.; Harnor, S. J.; Myers, S. M.; Cano, C.; Golding, B. T.; Hardcastle, I. R.; Lunec, J.; Newell, D. R.; Tudhope, S.; Wedge, S. R.; Wittner, A.; Zhao, Y.; Griffin, R. J. In *Validation studies with small-molecule modulators of the MDM2/MDMX-p53 binding interaction*, 247th ACS National Meeting & Exposition, Dallas, TX, United States, March 16-20, **2014**; Dallas, TX, United States.
152. Adhikari, S., Unpublished work.

153. Popowicz, G. M.; Czarna, A.; Rothweiler, U.; Szwagierczak, A.; Krajewski, M.; Weber, L.; Holak, T. A., Molecular basis for the inhibition of p53 by Mdmx. *Cell Cycle* **2007**, *6*, 2386.
154. Popowicz, G. M.; Czarna, A.; Wolf, S.; Wang, K.; Wang, W.; Dömling, A.; Holak, T. A., Structures of low molecular weight inhibitors bound to MDMX and MDM2 reveal new approaches for p53-MDMX/MDM2 antagonist drug discovery. *Cell Cycle* **2010**, *9*, 1104.
155. Blackburn, T. J.; Ahmed, S.; Coxon, C. R.; Liu, J.; Lu, X.; Golding, B. T.; Griffin, R. J.; Hutton, C.; Newell, D. R.; Ojo, S.; Watson, A. F.; Zaytzev, A.; Zhao, Y.; Lunec, J.; Hardcastle, I. R., Diaryl- and triaryl-pyrrole derivatives: inhibitors of the MDM2-p53 and MDMX-p53 protein-protein interactions. *MedChemComm* **2013**, *4*, 1297.
156. Cully, S. J. Design and synthesis of isoindolinone MDM2-p53 inhibitors. PhD thesis, Newcastle University, Newcastle upon Tyne, **2014**.
157. Zhang, B., Unpublished work.
158. Jacq, J.; Einhorn, C.; Einhorn, J., A versatile and regiospecific synthesis of functionalized 1,3-diarylisobenzofurans. *Org. Lett.* **2008**, *10*, 3757.
159. Katritzky, A. R.; Harris, P. A.; Kotali, A., Mechanism of the replacement of phenolic hydroxyl by carbonyl on lead tetraacetate treatment of o-hydroxyaryl ketone acylhydrazones. *J. Org. Chem.* **1991**, *56*, 5049.
160. Carbain, B., Unpublished work.
161. Blackburn, T., Unpublished work.
162. Zhao, Y., Unpublished work.
163. Ahmed, S. U.; Hutton, C.; Lunec, J., Increased susceptibility of MDM2 amplified cell lines to MDM2-p53 inhibitors is associated with a high turnover of MDM2 and p53. *Cancer Res.* **2004**, *64*, 695.
164. Böttger, V.; Böttger, A.; S.F., H.; Picksley, S. M.; Chène, P.; Garcia-Echeverria, C.; Hochkeppel, H. K.; Lane, D. P., Identification of novel mdm2 binding peptides by phage display. *Oncogene* **1996**, *8-16*, 2141.
165. Cully, S. J., Unpublished work.
166. Watson, A. Structure-activity studies for inhibitors of two cancer targets: Tip60 histone acetyltransferase and MDM2-p53. PhD thesis, Newcastle University, Newcastle upon Tyne, **2010**.
167. Watson, A. F.; Liu, J.; Bennaceur, K.; Drummond, C. J.; Endicott, J. A.; Golding, B. T.; Griffin, R. J.; Haggerty, K.; Lu, X.; McDonnell, J. M.; Newell, D. R.; Noble,

- M. E. M.; Revill, C. H.; Riedinger, C.; Xu, Q.; Zhao, Y.; Lunec, J.; Hardcastle, I. R., MDM2-p53 protein-protein interaction inhibitors: A-ring substituted isoindolinones. *Bioorg. Med. Chem. Lett.* **2011**, *21*, 5916.
168. Punniyamurthy, T.; Katsuki, T., Asymmetric desymmetrization of meso-pyrrolidine derivatives by enantiotopic selective C-H hydroxylation using (salen)manganese(III) complexes. *Tetrahedron* **1999**, *55*, 9439.
 169. Bulatov, E. Identification and validation of p53-MDM2 and p53-MDMX protein-protein interaction inhibitors. MPhil thesis, Newcastle University, Newcastle upon Tyne, **2010**.
 170. Shouksmith, A. E. Design and Synthesis of Small Molecule Inhibitors Targeting the SCF^{SKP2} E3 Ligase and the MDMX-p53 Interaction for Cancer Therapy. PhD thesis, Newcastle University, Newcastle upon Tyne, **2015**.
 171. Noble, M. E. M., Observations.
 172. Riess, R.; Schön, M.; Laschat, S.; Jäger, V., Evaluation of protecting groups for 3-hydroxyisoxazoles – Short access to 3-alkoxyisoxazole-5-carbaldehydes and 3-hydroxyisoxazole-5-carbaldehyde, the putative toxic metabolite of muscimol. *Eur. J. Org. Chem.* **1998**, *1998*, 473.
 173. Kopecky, D. J.; Rychnovsky, S. D., Preparation of α -acetoxy ethers by the reductive acetylation of esters: *endo*-1-bornyloxyethyl acetate. *Organic Synthesis* **2003**, *80*.
 174. Sizemore, N.; Rychnovsky, S. D., Discussion addendum for: preparation of α -acetoxy ethers by the reductive acetylation of esters: *endo*-1-bornyloxyethyl acetate. *Organic Synthesis* **2012**, *89*, 143.
 175. Kopecky, D. J.; Rychnovsky, S. D., Improved procedure for the reductive acetylation of acyclic esters and a new synthesis of ethers. *J. Org. Chem.* **2000**, *65*, 191.
 176. Valot, G.; Regens, C. S.; O'Malley, D. P.; Godineau, E.; Takikawa, H.; Fürstner, A., Total synthesis of amphidinolide F. *Angew. Chem. Int. Ed.* **2013**, *52*, 9534.
 177. Coleman, R. S.; Shah, J. A., Chemoselective cleavage of benzyl ethers, esters, and carbamates in the presence of other easily reducible groups. *Synthesis* **1999**, 1399.
 178. Wynberg, H., The Reimer-Tiemann reaction. *Chem. Rev.* **1960**, *60*, 169.
 179. Jennings, C., Unpublished work.
 180. Giegé, R.; Mikol, V., Crystallogenes of proteins. *Trends Biotechnol.* **1989**, *7*, 277.

181. Derewenda, Z. S., Rational protein crystallization by mutational surface engineering. *Structure* **2004**, *12*, 529.
182. McPherson, A., Introduction to macromolecular crystallography. 2nd ed.; Wiley: Hoboken, **2009**.
183. Adachi, H.; Takano, K.; Morikawa, M.; Kanaya, S.; Yoshimura, M.; Mori, Y.; Sasaki, T., Application of a two-liquid system to sitting-drop vapour-diffusion protein crystallization. *Acta Crystallogr., Sect. D: Biol. Crystallogr.* **2003**, *59*, 194.
184. Robson, A. F.; Hupp, T. R.; Lickiss, F.; Ball, K. L.; Faulds, K.; Graham, D., Nanosensing protein allostery using a bivalent mouse double minute two (MDM2) assay. *PNAS* **2012**, *109*, 8073.
185. Kussie, P. H.; Gorina, S.; Marechal, V.; Elenbaas, B.; Moreau, J.; Levine, A. J.; Pavletich, N. P., Structure of the MDM2 Oncoprotein Bound to the p53 Tumor Suppressor Transactivation Domain. *Science* **1996**, *274*, 948.
186. Reeks, J., Observations.
187. GE Life Sciences; pGEX vectors, GST Gene Fusion System. <http://www.gelifesciences.com/> (accessed September 2014).
188. Bawn, R., Unpublished work.
189. Truong, K.; Ikura, M., The use of FRET imaging microscopy to detect protein-protein interactions and protein conformational changes in vivo. *Curr. Opin. Struct. Biol.* **2001**, *11*, 573.
190. Piston, D. W.; Kremers, G.-J., Fluorescent protein FRET: the good, the bad and the ugly. *Trends Biochem. Sci.* **32**, 407.
191. Hussain, S. A., An introduction to fluorescence resonance energy transfer (FRET). *Science Journal of Physics* **2012**, *1*.
192. Niesen, F. H.; Berglund, H.; Vedadi, M., The use of differential scanning fluorimetry to detect ligand interactions that promote protein stability. *Nat. Protocols* **2007**, *2*, 2212.
193. Corral, M., Anales de la Real Sociedad Espanola de Fisica y Quimica, Serie B: Quimica. **1964**, *60*, 341.
194. Williams, A.; Douglas, K. T., Hydrolysis of aryl *N*-methylaminosulphonates: evidence consistent with an E1cB mechanism. *J. Chem. Soc. Perk. Trans. 2* **1974**, 1972-1999, 1727.

195. King, J. F.; Mee-Ling Lee, T., Betylates. 1. Synthesis and reactions of an isolable [0]betylate, *N,N*-dimethyl-*N*-(phenoxysulfonyl)methanaminium fluorosulfate. *Can. J. Chem.* **1981**, *59*, 356.
196. Wegler, R.; Kukenthal, H. Derivatives of aminosulfonic acid. US 2839562 (A) **1954**.
197. Plant, A.; Marhold, A.; Grosser, R.; Erdelen, C.; Turberg, A.; Hansen, O. Delta 1-pyrrolines for use as pesticides. US2003220386 (A1); WO 0224644 (A1), **2003**.
198. Lo, Y. S.; Nolan, J.; Welsetad, J. W. J.; Walsh, D. A.; Shamblee, D. A.; Uwaydah, I. M. Compounds having one or more aminosulfaonyloxy radicals useful as pharmaceuticals. US5194446 (A), **1993**.
199. Beaudoin, S.; Kinsey, K. E.; Burns, J. F., Preparation of unsymmetrical sulfonylureas from *N,N'*-sulfuryldiimidazoles. *J. Org. Chem.* **2002**, *68*, 115.
200. Zakharian, T. Y.; Christianson, D. W., Design and synthesis of C60-benzenesulfonamide conjugates. *Tet. Lett.* **2010**, *51*, 3645.
201. Sünneemann, H. W.; Banwell, M. G.; de Meijere, A., Diversity-oriented synthesis of enantiomerically pure steroidal tetracycles employing Stille/Diels–Alder reaction sequences. *Chem. Eur. J.* **2008**, *14*, 7236.
202. Clasby, M. C.; Chackalamannil, S.; Czarniecki, M.; Doller, D.; Eagen, K.; Greenlee, W.; Kao, G.; Lin, Y.; Tsai, H.; Xia, Y.; Ahn, H.-S.; Agans-Fantuzzi, J.; Boykow, G.; Chintala, M.; Foster, C.; Smith-Torhan, A.; Alton, K.; Bryant, M.; Hsieh, Y.; Lau, J.; Palamanda, J., Metabolism-based identification of a potent thrombin receptor antagonist. *J. Med. Chem.* **2006**, *50*, 129.
203. Scheiper, B.; Bonnekessel, M.; Krause, H.; Fürstner, A., Selective iron-catalyzed cross-coupling reactions of Grignard reagents with enol triflates, acid chlorides, and dichloroarenes. *J. Org. Chem.* **2004**, *69*, 3943.
204. Coudert, G.; Lepifre, F.; Caignard, D.-H.; Renard, P.; Hickman, J.; Pierre, A.; Kraus-Berthier, L. Substituted benzo[e][1,4]oxazino[3,2-g]isoindole compounds **2003**.
205. Rudi, B.; Chengjung, L.; Changgeng, Q. Treatment of cancers having K-RAS mutations. US2013102595, **2013**.
206. Pennington, T. E.; Kardiman, C.; Hutton, C. A., Deprotection of pinacolyl boronate esters by transesterification with polystyrene–boronic acid. *Tet. Lett.* **2004**, *45*, 6657.
207. Kim, J.; Kim, Y. K.; Park, N.; Hahn, J. H.; Ahn, K. H., Synthesis of cage-type molecules with π -cavity and selective gas-phase cation complexation. *J. Org. Chem.* **2005**, *70*, 7087.

208. Hardcastle, I. R.; Ahmed, S. U.; Atkins, H.; Farnie, G.; Golding, B. T.; Griffin, R. J.; Guyenne, S.; Hutton, C.; Källblad, P.; Kemp, S. J.; Kitching, M. S.; Newell, D. R.; Norbedo, S.; Northen, J. S.; Reid, R. J.; Saravanan, K.; Willems, H. M. G.; Lunec, J., Small-molecule inhibitors of the MDM2-p53 protein-protein interaction based on an isoindolinone scaffold. *J. Med. Chem.* **2006**, *49*, 6209.